frontiers | Research Topics

Nutraceuticals and functional foods in chronic disease prevention and treatment

Edited by
Bwalya Angel Witika, Ntethelelo Sibiya,
Alina Kurylowicz and Pedzisai Makoni

Published in
Frontiers in Nutrition

FRONTIERS EBOOK COPYRIGHT STATEMENT

The copyright in the text of individual articles in this ebook is the property of their respective authors or their respective institutions or funders. The copyright in graphics and images within each article may be subject to copyright of other parties. In both cases this is subject to a license granted to Frontiers.

The compilation of articles constituting this ebook is the property of Frontiers.

Each article within this ebook, and the ebook itself, are published under the most recent version of the Creative Commons CC-BY licence. The version current at the date of publication of this ebook is CC-BY 4.0. If the CC-BY licence is updated, the licence granted by Frontiers is automatically updated to the new version.

When exercising any right under the CC-BY licence, Frontiers must be attributed as the original publisher of the article or ebook, as applicable.

Authors have the responsibility of ensuring that any graphics or other materials which are the property of others may be included in the CC-BY licence, but this should be checked before relying on the CC-BY licence to reproduce those materials. Any copyright notices relating to those materials must be complied with.

Copyright and source acknowledgement notices may not be removed and must be displayed in any copy, derivative work or partial copy which includes the elements in question.

All copyright, and all rights therein, are protected by national and international copyright laws. The above represents a summary only. For further information please read Frontiers' Conditions for Website Use and Copyright Statement, and the applicable CC-BY licence.

ISSN 1664-8714
ISBN 978-2-8325-7086-9
DOI 10.3389/978-2-8325-7086-9

Generative AI statement
Any alternative text (Alt text) provided alongside figures in the articles in this ebook has been generated by Frontiers with the support of artificial intelligence and reasonable efforts have been made to ensure accuracy, including review by the authors wherever possible. If you identify any issues, please contact us.

About Frontiers

Frontiers is more than just an open access publisher of scholarly articles: it is a pioneering approach to the world of academia, radically improving the way scholarly research is managed. The grand vision of Frontiers is a world where all people have an equal opportunity to seek, share and generate knowledge. Frontiers provides immediate and permanent online open access to all its publications, but this alone is not enough to realize our grand goals.

Frontiers journal series

The Frontiers journal series is a multi-tier and interdisciplinary set of open-access, online journals, promising a paradigm shift from the current review, selection and dissemination processes in academic publishing. All Frontiers journals are driven by researchers for researchers; therefore, they constitute a service to the scholarly community. At the same time, the *Frontiers journal series* operates on a revolutionary invention, the tiered publishing system, initially addressing specific communities of scholars, and gradually climbing up to broader public understanding, thus serving the interests of the lay society, too.

Dedication to quality

Each Frontiers article is a landmark of the highest quality, thanks to genuinely collaborative interactions between authors and review editors, who include some of the world's best academicians. Research must be certified by peers before entering a stream of knowledge that may eventually reach the public - and shape society; therefore, Frontiers only applies the most rigorous and unbiased reviews. Frontiers revolutionizes research publishing by freely delivering the most outstanding research, evaluated with no bias from both the academic and social point of view. By applying the most advanced information technologies, Frontiers is catapulting scholarly publishing into a new generation.

What are Frontiers Research Topics?

Frontiers Research Topics are very popular trademarks of the *Frontiers journals series*: they are collections of at least ten articles, all centered on a particular subject. With their unique mix of varied contributions from Original Research to Review Articles, Frontiers Research Topics unify the most influential researchers, the latest key findings and historical advances in a hot research area.

Find out more on how to host your own Frontiers Research Topic or contribute to one as an author by contacting the Frontiers editorial office: frontiersin.org/about/contact

Nutraceuticals and functional foods in chronic disease prevention and treatment

Topic editors

Bwalya Angel Witika — Sefako Makgatho Health Sciences University, South Africa

Ntethelelo Sibiya — Rhodes University, South Africa

Alina Kurylowicz — Mossakowski Medical Research Institute, Polish Academy of Sciences, Poland

Pedzisai Makoni — Sefako Makgatho Health Sciences University, South Africa

Citation

Witika, B. A., Sibiya, N., Kurylowicz, A., Makoni, P., eds. (2025). *Nutraceuticals and functional foods in chronic disease prevention and treatment*. Lausanne: Frontiers Media SA. doi: 10.3389/978-2-8325-7086-9

Table of contents

frontiers | Frontiers in Nutrition

TYPE Editorial
PUBLISHED 20 October 2025
DOI 10.3389/fnut.2025.1706190

Check for updates

OPEN ACCESS

EDITED AND REVIEWED BY
Barbara R. Cardoso,
Monash University, Australia

*CORRESPONDENCE
Alina Kurylowicz
akurylowicz@imdik.pan.pl

RECEIVED 15 September 2025
ACCEPTED 24 September 2025
PUBLISHED 20 October 2025

CITATION
Kurylowicz A (2025) Editorial: Nutraceuticals and functional foods in chronic disease prevention and treatment.
Front. Nutr. 12:1706190.
doi: 10.3389/fnut.2025.1706190

COPYRIGHT
© 2025 Kurylowicz. This is an open-access article distributed under the terms of the Creative Commons Attribution License (CC BY). The use, distribution or reproduction in other forums is permitted, provided the original author(s) and the copyright owner(s) are credited and that the original publication in this journal is cited, in accordance with accepted academic practice. No use, distribution or reproduction is permitted which does not comply with these terms.

Editorial: Nutraceuticals and functional foods in chronic disease prevention and treatment

Alina Kurylowicz[1,2]*

[1]Department of Human Eigenetics, Mossakowski Medical Research Centre, Polish Academy of Sciences, Warsaw, Poland, [2]Department of Internal Medicine and Geriatric Cardiology, Centre of Postgraduate Medical Education, Warsaw, Poland

KEYWORDS

nutraceuticals, functional foods, polyphenols, dietary fiber, trehalose, D-psicose, prebiotics

Editorial on the Research Topic
Nutraceuticals and functional foods in chronic disease prevention and treatment

In recent years, our understanding of the role nutraceuticals and functional foods play in the prevention and treatment of chronic diseases has increased significantly. By providing bioactive compounds and essential nutrients, nutraceuticals and functional foods modulate inflammation, improve metabolism, enhance immune function, and reduce risk factors associated with these diseases. This Research Topic of Frontiers in Nutrition collects original articles and meta-analyses on interventions using various natural and functional foods or compounds related to cardiovascular health, metabolic disorders, and associated conditions.

Cardiovascular diseases are currently the leading cause of death worldwide, and their prevention is a key element of health promotion strategies. In this Research Topic, Jia et al.'s meta-analysis clearly shows the beneficial effects of consuming polyphenol-rich seeds (e.g., Brazil nuts, almonds, and flaxseed) on lipid profiles and inflammatory parameters in patients with coronary heart disease (CHD). In turn, a meta-analysis by Arjmandfard et al. summarizes recent studies on the effects of apple cider vinegar on glycemic control and insulin sensitivity in patients with type 2 diabetes, showing that this intervention reduces fasting glucose and HbA1c levels and improves insulin secretion in a dose-dependent manner. A series of meta-analyses, conducted by Jangid et al., complements a study covering papers published over the past 60 years and highlights the potential of cranberry-derived bioactive compounds, particularly proanthocyanidins (PACs), in preventing and treatintg urinary tract infections.

The 21st century has brought about a pandemic of obesity and related complications; in addition to the meta-analyses mentioned above, the Research Topic includes several original papers evaluating the potential of nutritional interventions for various metabolic disorders. Liu et al. demonstrate the beneficial effect of black chokeberry (Aronia melanocarpa) on oxonic acid-induced hyperuricemia in mice, comparable in efficacy to allopurinol. Two studies on a mouse model with a high-fat diet (HFD) suggest the potential of Polygonatum sibiricum insoluble dietary fiber (PIDF) and the natural disaccharide trehalose to reduce hyperlipidemia, body weight, and improve carbohydrate

metabolism (Ma et al.; Yeh et al.). As one of the consequences of the obesity pandemic is an increasing frequency of steatotic liver disease, this Research Topic includes two original research studies by Tan et al. and Tang et al., who conducted experimental studies on the use of nutraceuticals in treating liver diseases. The first study utilized a mouse model of liver steatosis to demonstrate the potential of D-psicose (DPS), a sucrose substitute providing only 0.3% of sucrose's energy content, in reducing lipid accumulation, inflammation, and oxidative stress parameters in this organ. The second study found that the traditional Chinese herbal formula, Liuweizhiji Gegen-Sangshen Beverage (LGS), activates the SCFAs/GPR43/GLP-1 pathway, reducing liver damage in Alcoholic Liver Disease (ALD). Notably, both nutraceuticals exerted a beneficial effect on the microbiome. Subsequently, three consecutive articles in this Research Topic are devoted to dietary interventions that modulate gut microbiota. A study by Lian et al. demonstrates the beneficial, synergistic effect of cistanche polysaccharides and acteoside in regulating gut microbiota diversity and increasing the number of beneficial bacteria in rats. In turn, Wei et al. show in their work that restoring normal gut microbiota can be achieved through the use of a hawthorn postbiotic probiotic, which regulates intestinal water and sodium metabolism, maintains the intestinal barrier, promotes epithelial cell proliferation, reduces inflammatory responses, and improves short-chain fatty acid metabolism. Finally, the work by Bellomo et al. provides evidence of the potential of milk-based postbiotics from Lactobacillus plantarum to reduce gliadin peptide-induced inflammation *in vitro* and in intestinal organoids from patients with celiac disease.

We hope that these papers in this Research Topic will inspire future research on nutraceuticals and functional foods for the prevention and treatment of chronic diseases.

Author contributions

AK: Conceptualization, Writing – original draft, Writing – review & editing.

Conflict of interest

The author declares that the research was conducted in the absence of any commercial or financial relationships that could be construed as a potential conflict of interest.

Generative AI statement

The author(s) declare that no Gen AI was used in the creation of this manuscript.

Any alternative text (alt text) provided alongside figures in this article has been generated by Frontiers with the support of artificial intelligence and reasonable efforts have been made to ensure accuracy, including review by the authors wherever possible. If you identify any issues, please contact us.

Publisher's note

All claims expressed in this article are solely those of the authors and do not necessarily represent those of their affiliated organizations, or those of the publisher, the editors and the reviewers. Any product that may be evaluated in this article, or claim that may be made by its manufacturer, is not guaranteed or endorsed by the publisher.

frontiers | Frontiers in Nutrition

TYPE Systematic Review
PUBLISHED 19 November 2024
DOI 10.3389/fnut.2024.1493410

Check for updates

OPEN ACCESS

EDITED BY
Bwalya Angel Witika,
Sefako Makgatho Health Sciences University, South Africa

REVIEWED BY
David Katerere,
Tshwane University of Technology, South Africa
Lavina Prashar,
University of Zambia, Zambia

*CORRESPONDENCE
Qian Zhang
zhangqian@d.sxmu.edu.cn
Ruifang Zhu
ruifang.zhu@sxmu.edu.cn

RECEIVED 09 September 2024
ACCEPTED 06 November 2024
PUBLISHED 19 November 2024

CITATION
Jia Y, Wang H, Fan W, Lv J, Niu Q, Zhu R and Zhang Q (2024) Effects of polyphenol-rich seed foods on lipid and inflammatory markers in patients with coronary heart disease: a systematic review.
Front. Nutr. 11:1493410.
doi: 10.3389/fnut.2024.1493410

COPYRIGHT
© 2024 Jia, Wang, Fan, Lv, Niu, Zhu and Zhang. This is an open-access article distributed under the terms of the Creative Commons Attribution License (CC BY). The use, distribution or reproduction in other forums is permitted, provided the original author(s) and the copyright owner(s) are credited and that the original publication in this journal is cited, in accordance with accepted academic practice. No use, distribution or reproduction is permitted which does not comply with these terms.

Effects of polyphenol-rich seed foods on lipid and inflammatory markers in patients with coronary heart disease: a systematic review

Yatian Jia[1,2], Hui Wang[1,2], Wen Fan[1], Jie Lv[2], Qingmei Niu[1,2], Ruifang Zhu[3]* and Qian Zhang[1,2]*

[1]Nursing Department, Shanxi Bethune Hospital, Shanxi Academy of Medical Sciences, Third Hospital of Shanxi Medical University, Tongji Shanxi Hospital, Taiyuan, China, [2]School of Nursing, Shanxi University of Chinese Medicine, Yuci, China, [3]Editorial Office, First Hospital of Shanxi Medical University, Taiyuan, China

Background: Coronary heart disease (CHD) is a prevalent cardiovascular condition, with its incidence and mortality rates steadily rising over time, posing a significant threat to human health. Studies have indicated that polyphenols exhibit a certain degree of protective effect against coronary heart disease. However, the findings regarding the impact of polyphenol-rich seed foods on patients with CHD have yielded inconsistent results.

Objective: This study investigated the effects of polyphenol-rich seed foods on blood lipids and inflammatory markers in patients with coronary heart disease.

Methods: The China National Knowledge Network, China Science and Technology Journal Database, China Biomedical Literature Database, Wanfang Database, PubMed, Cochrane Library, Embase, and Web of Science were searched for articles from the self-built database until March 16, 2024. The quality of the included studies was assessed using Edition 2 of the Cochrane Randomized Trials Risk Bias Tool, and data analysis was conducted using RevMan 5.4.

Results: The study encompassed seven articles, with a total participation of 324 patients diagnosed with coronary heart disease. The study incorporated three seed foods abundant in polyphenols: Brazil nut, almond, and flaxseed. The meta-analysis findings revealed a significant reduction in triglyceride levels [MD = −20.03, 95% CI (−32.25, −17.44), $p < 0.00001$] among patients diagnosed with coronary heart disease who incorporated seed-based foods abundant in polyphenols into their diet regimen. Furthermore, a notable enhancement was observed in HDL cholesterol levels [MD = 3.14, 95% CI (1.55, 4.72), $p = 0.0001$]. Moreover, the type of intervention substance influenced the observed effects. The consumption of almonds has been demonstrated to significantly reduce total cholesterol [MD = −15.53, 95% CI (−21.97, −9.1), $p < 0.00001$] and LDL cholesterol [MD = −14.62, 95% CI (−20.92, −8.33), $p < 0.00001$] in patients diagnosed with coronary heart disease. Additionally, the incorporation of flaxseed into the diet has shown an enhanced effect on reducing C-reactive protein levels.

Conclusion: The consumption of polyphenol-rich seed foods can moderately improve TG and HDL-C levels in patients with coronary heart disease, while incorporating flaxseed into their diet can effectively improve inflammatory markers.

KEYWORDS

polyphenols, coronary heart disease, blood lipids, inflammatory markers, systematic review

Introduction

The prevalence and mortality of coronary atherosclerotic cardiopathy (CHD), commonly known as coronary heart disease, are progressively increasing year by year due to evolving lifestyle patterns, posing a significant threat to human health and life. The global health economy has been significantly burdened by this condition, which currently stands as the leading cause of mortality in the United States. It is estimated that 10.9% of adults aged 45 and above, along with 17.0% of adults aged 65 and above, are afflicted by coronary heart disease in the United States (1). According to the fifth China Health Service Survey in 2013, the prevalence rate of coronary heart disease among individuals aged 60 and above in China stands at 27.8‰, with a concomitant upward trend observed in mortality rates over time (2). The findings of several studies suggest that dyslipidemia and inflammation play a pivotal role in the pathogenesis of coronary heart disease (CHD) (3, 4). Currently, lifestyle modifications, pharmacotherapy, and revascularization procedures are the primary treatment modalities for CHD (5). Antiplatelet therapy serves as the cornerstone for secondary prevention of cardiovascular diseases; however, a subset of patients exhibit intolerance toward secondary prevention therapy, with up to 52.1% of individuals suffering from CHD displaying resistance to aspirin (6). Additionally, there exists a potential risk of bleeding (7). After revascularization, patients are required to adhere to a regimen of various medications, including antiplatelet and lipid-lowering agents, while still potentially encountering complications such as restenosis and postoperative depressive symptoms (8, 9). The occurrence of cardiovascular diseases is closely associated with diet and lifestyle (10), and the significance of "diet and lifestyle" as the fundamental aspect in preventing cardiovascular disease risk has been acknowledged by members of the European Atherosclerosis Society. Therefore, diet adjustment is essential for preventing and treating coronary heart disease. There is an urgent necessity to identify a safe and cost-effective dietary regimen for the management and treatment of coronary heart disease.

Polyphenols are a class of bioactive compounds widely distributed in plants, which contribute to the maintenance of health and exert preventive, delaying, or reducing effects on the occurrence and progression of certain chronic diseases. They are considered beneficial in combating degenerative conditions like atherosclerosis and central nervous system disorders (11), while also playing a preventive and therapeutic role in various medicinal and food homologous substances with favorable anti-inflammatory, antioxidant, and lipid-lowering properties (12). The impact of diet on cardiovascular disease development has been well-documented (13). Consequently, there is a growing interest among food and medical researchers in polyphenolic diets, necessitating the exploration of dietary plans that are not only safe and convenient but also highly compliant. Polyphenolic compounds have been found to be abundant in a diverse range of seed-based foods (14). Therefore, this study conducted a systematic review and meta-analysis of randomized controlled trials investigating the effects of polyphenol-rich seed foods on patients with coronary heart disease. The aim was to determine the efficacy of these foods in regulating blood lipids and inflammatory markers, providing valuable insights for future dietary management programs aimed at preventing cardiovascular diseases.

Methods

The present study has been duly registered with PROSPERO (registration number: CRD42024532025)[1] and adheres to the guidelines outlined in the Preferred Reporting Items for Systematic Reviews and Meta-Analyses (PRISMA) statement (15) within this paper.

The following inclusion and exclusion criteria were formulated to investigate the potential impact of seed foods rich in polyphenols on blood lipid levels and inflammatory status in patients with coronary heart disease.

Inclusion criteria

1. Patients aged ≥18 years diagnosed with coronary heart disease based on angiography or myocardial; 2. Patients provided with a dietary intervention involving any of the 22 seed foods listed in the Phenol Explorer Food Polyphenol Content Database[2] with no limitation to the grams, quantity, and duration of intervention seed food; 3 Control group for comparison with participants administered either the standard diet or a placebo.

Exclusion criteria

1. Patients who had additional comorbidities; 2. Patients where intervention incorporated additional active compounds or medications; 3. Patients taking seed food extracts; 4. Repeated published studies; 5. Articles such as research proposals, conference papers and abstracts that lack or be devoid of access to primary data.

Search strategy

The search was conducted independently by two researchers who systematically searched eight databases, including CNKI, VIP, Wanfang Data, China Biomedical Literature Database (CBM), PubMed, Cochrane Library, Embase, and Web of Science. The search period spanned from the inception of the database until March 16, 2024. Please refer to Annex 1 for the detailed search strategy.

Abbreviations: HDL-C, high-density lipoprotein cholesterol; LDL-C, low-density lipoprotein cholesterol; TC, total cholesterol; TG: triglyceride; CHD, coronary heart disease; CRP, C-reactive protein.

1 https://www.crd.york.ac.uk/PROSPERO/#recordDetails

2 http://phenol-explorer.eu/downloads

Literature screening and data extraction

Two researchers independently conducted a comprehensive literature search, importing the retrieved articles into EndNote20 literature management software for further analysis. Subsequently, the titles and abstracts were carefully reviewed to exclude irrelevant studies, followed by a thorough examination of the full texts to select relevant articles based on predefined inclusion and exclusion criteria. The extraction of data from selected studies was performed independently by both researchers, encompassing information such as the first author's name, publication year, participants involved, sample size, intervention measures employed, intervention duration, outcome indicators assessed, among others. In case of any discrepancies during this process, consultation with a third researcher was sought.

Literature quality assessment

The included literature was assessed by two investigators using the Cochrane Randomized Trial Bias Risk Assessment Tool, Edition 2 (RoB 2) (16) evaluation criteria. The evaluation encompassed the following aspects: randomization process, deviation from expected interventions, missing outcome data, outcome measures, and selection of reported outcomes. Based on the results obtained from The RoB 2 assessment tool, each article was categorized as "high risk," "some concern," or "low risk." In case of discrepancies during the above process, a third researcher would act as an arbitrator to facilitate consensus-building.

Evidence quality assessment

The certainty of the body of evidence was assessed using the Grading of Recommendations, Assessment, Development and Evaluations (GRADE) approach. The quality of evidence for RCTs was initially rated as high in this methodology, but it would be downgraded to medium, low, or very low if any limitations related to bias, inconsistency, directness, imprecision, or risk of publication bias were identified. The evidence, however, can be enhanced by incorporating significant effects and dose–response gradients. In the event of disagreement during the aforementioned process, a third researcher will serve as an arbitrator to ultimately reach a consensus.

Data analysis methods

The meta-analysis was conducted using RevMan 5.4 software. The mean square error (MD) combined effect size was utilized for the collection of quantitative data, and each point estimate of the effect size along with its corresponding 95% confidence interval (CI) was computed. According to the guidelines of the Cochrane Manual, I^2 values were utilized for assessing inter-study heterogeneity, with I^2 values ranging from 0 to 40%, 30 to 60%, 50 to 90%, and 75 to 100%, indicating no significant, low, medium, and high levels of heterogeneity, respectively (17). A random effects model was utilized, and further subgroup analysis was conducted based on potential sources of heterogeneity. Sensitivity analysis was employed to assess the stability and precision of the findings. A narrative analysis was performed for outcomes that exhibited excessive heterogeneity.

Results

Literature search results

After conducting an initial search of the database, a total of 1738 relevant literature sources were retrieved. Subsequently, by eliminating 521 duplicate sources, the final count amounted to 1,217 literature sources. After reviewing the title and abstract, a total of 1,205 literature sources that clearly did not meet the inclusion criteria were excluded, while 12 literature sources that potentially fulfilled the inclusion criteria were identified. The final selection comprised a total of seven relevant studies (18–24). The process and outcomes of the literature screening are illustrated in Figure 1.

Basic characteristics of the included studies

A total of seven articles (18–24) were included in this study, among which six were randomized controlled trials (18, 20–24), and one was a randomized cross-controlled trial (19). The study included two articles (22, 23) with 324 patients from Iran, Brazil, the United States, and Pakistan. Among the seed foods examined were Brazil nuts, almonds, and flaxseed. Notably, almonds were identified as a medicinal and food homologous substance. The duration of the intervention varied between 6 weeks and 3 months (Table 1).

Methodological quality of studies

The two researchers independently utilized the Cochrane Bias Risk Assessment tool (RoB 2) to evaluate the methodological quality of the included studies. Although all the included studies reported randomized controlled trials, there was evidence of bias in the randomization process, with only one study (24) providing detailed information on the randomization method and assignment concealment. The results of the assessment on the methodological quality of the included literature are presented in Figure 2.

Quality of evidence

According to the GRADE manual, TG and HDL-C have been assigned a low quality rating for evidence, while TC and LDL-C have been given a very low quality rating. The evaluation details are in Table 2.

Effect of polyphenol-rich seed foods on TC in patients with coronary heart disease

The effect of polyphenol-rich seed foods on total cholesterol (TC) in patients with coronary heart disease was investigated in six studies (18–22, 24). One study (21) included two intervention groups:

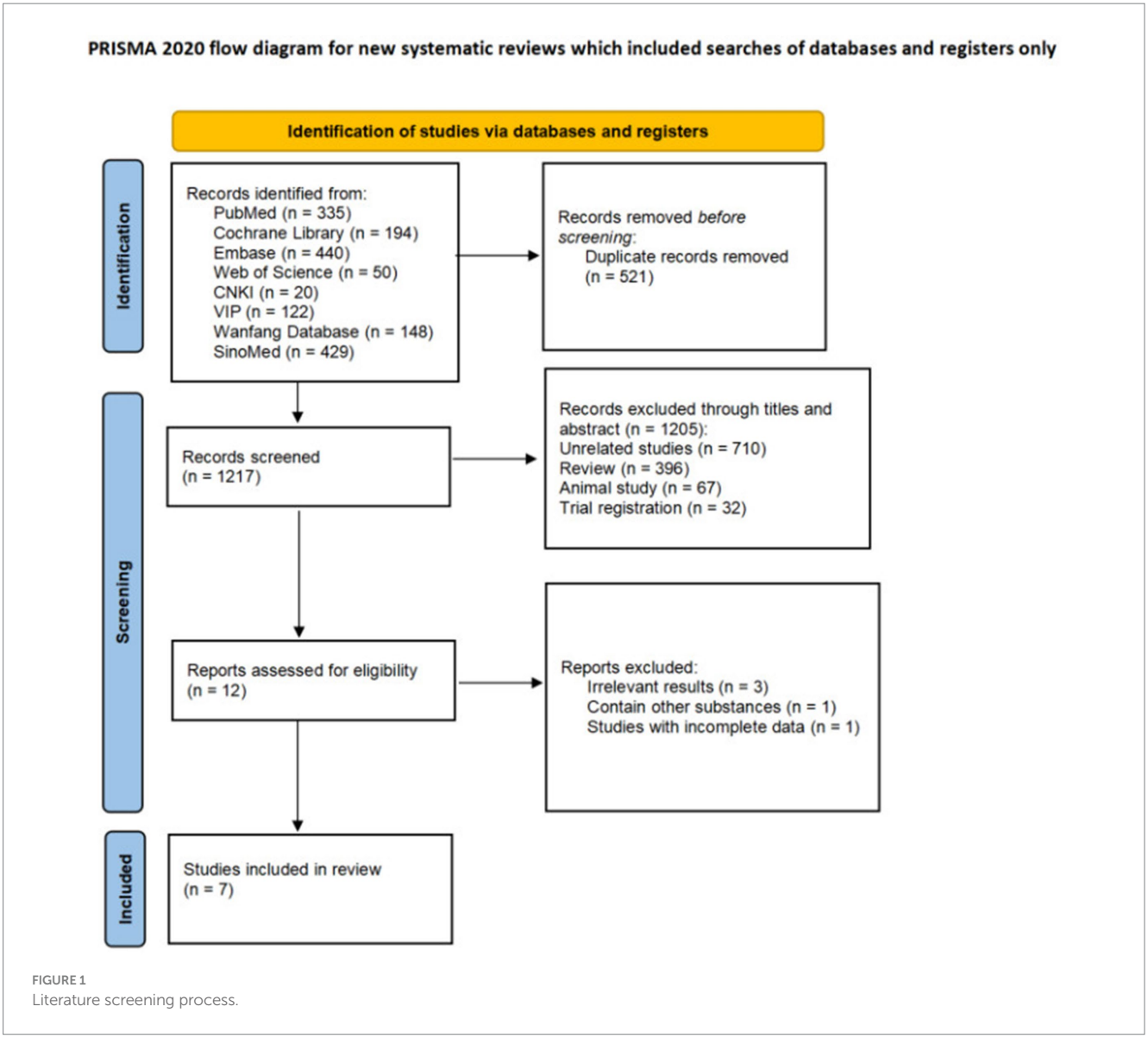

FIGURE 1
Literature screening process.

Pakistani almond and American almond. The heterogeneity test results revealed a significant level of heterogeneity, with $p = 0.007$ and $I^2 = 66\%$. Subgroup analysis based on intervention seed foods demonstrated that the almond group exhibited a significant reduction in TC among patients with CHD [MD = −15.53, 95%CI (−21.97, −9.1), $p < 0.00001$]. However, the impact of Brazil nut and flaxseed groups on total cholesterol (TC) in patients with coronary heart disease (CHD) did not yield statistically significant results. The overall findings from the meta-analysis indicate that the consumption of polyphenol-rich seed foods does not have a significant effect on TC levels in individuals with CHD [mean difference = −4.19, 95% confidence interval (−15.25, 6.87), $p = 0.46$]. See Figure 3.

Effect of polyphenol-rich seed foods on TG in patients with coronary heart disease

The effect of polyphenol-rich seed foods on TG in patients with coronary heart disease was investigated in six studies (18–22, 24). Heterogeneity test results demonstrated no significant heterogeneity ($p = 0.81$, $I^2 = 0\%$). Meta-analysis results revealed a statistically significant reduction in TG levels among patients with coronary heart disease who consumed polyphenol-rich seed foods [MD = −20.03, 95% CI (−32.25, −17.44), $p < 0.00001$]. See Figure 4.

Effect of polyphenol-rich seed foods on LDL-C in patients with coronary heart disease

The effect of polyphenol-rich seed foods on LDL-C in patients with coronary heart disease was investigated in six studies (18–22, 24). Heterogeneity test results revealed significant heterogeneity ($p < 0.00001$, $I^2 = 87\%$). Subgroup analysis based on intervention seed foods demonstrated a significant reduction in LDL-C among patients with coronary heart disease who consumed almonds [MD = −14.62, 95% CI (−20.92, −8.33), $p < 0.00001$]. However, no significant effects were observed for the Brazil nut and flaxseed

TABLE 1 Basic characteristics of the included literature.

First author, publication, year	Country	Study design	Patients	Age year	Sample size(T/C)	Sex (male/female) (T/C)	Intervention, time	Control condition	Dietary guidance	Outcomes	Time points of measurements	Outcome details
Cardozo (18)	Brazil	RCT	patient with CHD	T: 63.3 ± 6.7 C: 63.3 ± 8.0	42(25/17)	T:13/12 C:8/9	5 g Brazil nut a day, 3 months	Refrain from consuming any other types of nuts and maintain a daily nut-free diet, 3 months	Refrain from consuming any other types of nuts and adhere to the original dietary plan.	① a,b,c,d	after 3 months	The levels of TC, LDL-C, HDL-C, and TG did not show any significant changes.
Chen et al. (19)	America	Cross RCT	patient with CHD	61.8 ± 8.6	45	27/18	The National Cholesterol Education Program (NCEP) Step 1 Diet was supplemented with a daily intake of almonds (85 g/day), excluding other types of nuts, 6 weeks	The National Cholesterol Education Program (NCEP) Step 1 Diet, 6 weeks	Reinforce the implementation of the NCEP Step 1 diet, emphasizing a dietary pattern with reduced saturated fat and cholesterol intake.	① a,b,c,d ② CRP	after 6 weeks	The almond diet did not yield any significant impact on plasma lipid profiles or CRP levels.
Coutinho-Wolino et al. (20)	Brazil	RCT	patient with CHD	T: 62.7 ± 6.8 C: 63.7 ± 8.7	37(23/14)	T: 11/12 C: 6/8	One Brazil nut a day, 3 months	Refrain from consuming any other types of nuts and maintain a daily nut-free diet, 3 months	Refrain from consuming any other types of nuts and adhere to the original dietary plan.	① a,b,c,d ② CRP	after 3 months	The supplementation of Brazil nuts for a duration of 3 months did not result in any significant changes in TC, LDL-C, HDL-C, or TG levels in patients with CAD.

(Continued)

10.3389/fnut.2024.1493410

TABLE 1 (Continued)

First author, publication, year	Country	Study design	Patients	Age year	Sample size(T/C)	Sex (male/female) (T/C)	Intervention, time	Control condition	Dietary guidance	Outcomes	Time points of measurements	Outcome details
Jamshed et al. (21)	Pakistan	RCT	patient with CHD	32–86	113 T_1:T_2:C = (34/38/41)	113/37 (baseline)	T1: Consumption of 10 g/day Pakistani almonds, 12 weeks. T2: Consumption of 10 g/day American almonds, 12 weeks. (Soak the almonds overnight and consume them after peeling, before breakfast).	Refrain from consuming almonds and other nuts in your daily diet, 12 weeks	Refrain from consuming any other types of nuts and adhere to the original dietary plan.	① a,b,c,d	after 6、12 weeks	The consumption of almonds leads to a significant increase in HDL-C levels.
Khandouzi et al. (22)	Iran	RCT	patient with CHD	T: 56.67 ± 7.44 C: 56.22 ± 9.02	44(21/23)	T:16/5 C:21/2	Take a daily dosage of 30 g of flaxseed, 12 weeks	Receiving standard care, 12 weeks	Aim to consume a minimum of five servings of fruits and vegetables per day, while opting for foods that have reduced levels of saturated fat and cholesterol.	① a,b,c,d	after 12 weeks	The addition of flaxseed to the diet of patients with CHD did not result in any significant impact on plasma lipids.
Khandouzi et al. (23)	Iran	RCT	patient with CHD	T: 56.67 ± 7.44 C: 56.22 ± 9.02	44(21/23)	T:16/5 C:21/2	Take a daily dosage of 30 g of flaxseed, 12 weeks	Receiving standard care, 12 weeks	Aim to consume a minimum of five servings of fruits and vegetables per day, while opting for foods that have reduced levels of saturated fat and cholesterol.	② CRP	after 12 weeks	The inclusion of flaxseed in the diet of patients with CHD leads to an improvement in plasma inflammatory markers.

(Continued)

10.3389/fnut.2024.1493410

TABLE 1 (Continued)

First author, publication, year	Country	Study design	Patients	Age year	Sample size(T/C)	Sex (male/female) (T/C)	Intervention, time	Control condition	Dietary guidance	Outcomes	Time points of measurements	Outcome details
Saleh-Ghadimi et al. (24)	Iran	RCT	patient with CHD	T: 55.67 ± 6.9 C: 54.8 ± 7.80	40(21/19)	T: 19/2 C: 17/2	200 mL of sterilized milk with 1.5% fat content, supplemented with 2.5% flaxseed oil, 10 weeks	200 mL of sterilized milk with 1.5% fat content, 10 weeks	The participants adhered to a moderately calorie-restricted dietary regimen throughout the study.	① a,b,c,d	after 10 weeks	The consumption of flaxseed oil has been shown to effectively decrease triglyceride levels in patients with coronary heart disease (CHD).

① Blood lipids:a. LDL-C; b. TC; c. HDL-C; d.TG; ② Inflammatory biomarker: C-reactive protein (CRP); RCT: randomized controlled trial; T: treatment group; C: control group.

groups regarding CHD patients' LDL-C levels. Overall meta-analysis results indicated that the consumption of polyphenol-rich seed foods did not significantly affect LDL-C levels in patients with coronary heart disease [MD = −2.00, 95% CI (−11.31, 7.3), $p = 0.67$]. See Figure 5.

Effect of polyphenol-rich seed foods on HDL-C in patients with coronary heart disease

The effect of polyphenol-rich seed foods on HDL-C in patients with coronary heart disease was investigated in six studies (18–22, 24). Heterogeneity test results indicated no significant heterogeneity ($p = 0.42$, $I^2 = 0\%$). Meta-analysis revealed a significant positive impact of polyphenol-rich seed foods on HDL-C levels in patients with coronary heart disease [MD = 3.14, 95%CI (1.55, 4.72), $p = 0.0001$]. See Figure 6.

Effect of polyphenol-rich seed foods on CRP in patients with coronary heart disease

Three studies (19, 20, 23) examined the impact of polyphenol-rich seed foods on CRP levels in patients diagnosed with coronary heart disease. Among these studies, one (23) demonstrated a significant improvement in CRP levels through the incorporation of flaxseed into the diet, while no significant improvements were observed with almonds and Brazil nuts (19, 20).

Sensitivity analysis

The sensitivity analysis revealed no significant alterations in the combined findings, and no individual study was found to exert a substantial influence on the statistical outcomes, thereby indicating the relative stability of the meta-analysis results.

Discussion

Effects of polyphenol-rich seed foods on blood lipids and inflammatory markers in patients with coronary heart disease

In this study, it was observed that consumption of polyphenol-rich seed foods significantly improved the levels of triglycerides (TG) and high-density lipoprotein cholesterol (HDL-C) in patients diagnosed with coronary heart disease. The seed foods investigated in this study included almonds, Brazil nuts, and flaxseed. Notably, almond consumption demonstrated a significant reduction in total cholesterol (TC) and low-density lipoprotein cholesterol (LDL-C), while incorporating flaxseed into the diet resulted in decreased levels of the inflammatory marker C-reactive protein (CRP).

Almonds, among the foods examined in this study, are recognized as medicinal and food homologous substances according to traditional Chinese medicine theory. They possess dual properties of being both food and medicine, playing a

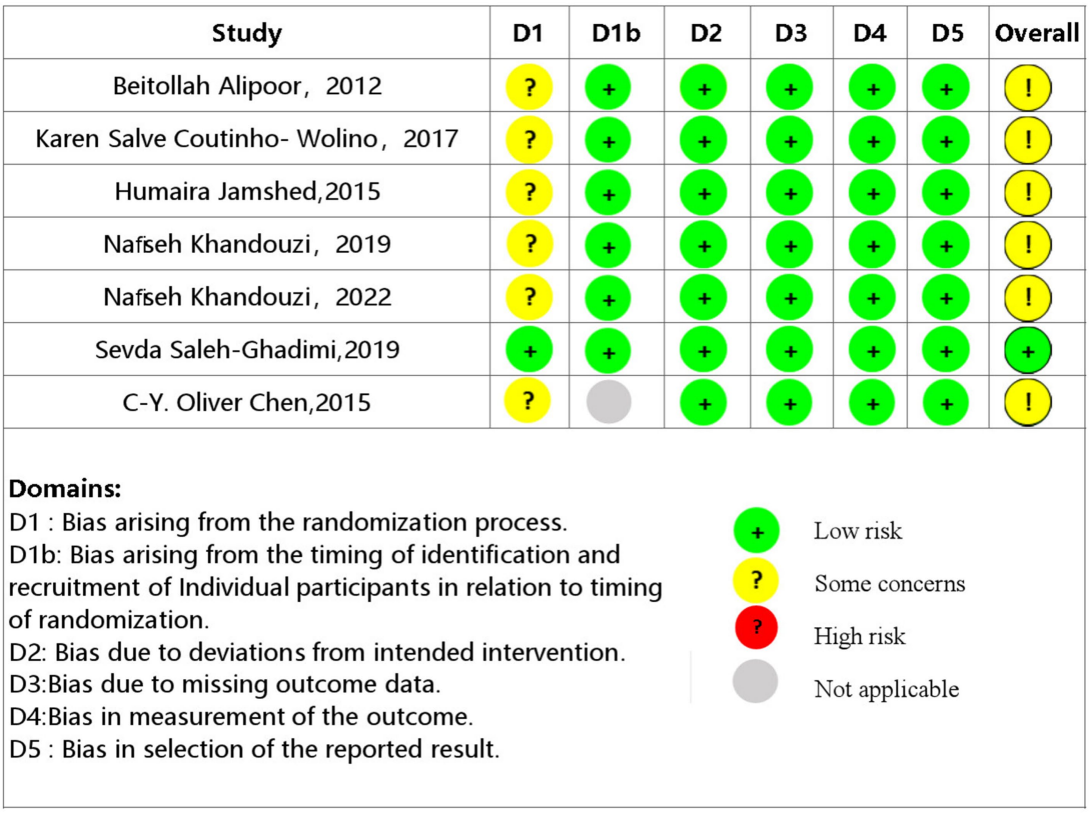

FIGURE 2
Results of methodological quality evaluation.

beneficial role in the prevention and management of various chronic diseases. The concept of "homologous medicine and food" aligns with the principles of natural, green, and healthy living, as well as resonates with the traditional Chinese medicine philosophy of disease prevention through holistic approaches (25, 26). In the process of foraging, human beings have systematically documented the inherent qualities and therapeutic potential of various types of sustenance, gradually recognizing that numerous edibles possess medicinal properties, blurring the distinction between food and medicine. The Qianjin Prescriptions, a traditional Chinese medicine text, states: "If one can utilize food to alleviate diseases and promote recovery, they can be deemed as an adept practitioner." Apart from providing essential nutrients for the human body, food also exerts influence on the equilibrium and regulation of human physiological functions. With prolonged adherence to this process, its effects become increasingly evident (27).

The medicinal and food homologous substances encompass a diverse range of polyphenols, particularly flavonoids, which serve as efficacious constituents in the reduction of blood lipids (28). Meanwhile, polyphenols in drug and food analogs have been scientifically proven to possess anti-inflammatory properties, primarily by inhibiting the metabolic pathway of prostaglandins (29). The lipid levels are closely associated with the development of coronary heart disease. An intervention study conducted on patients with hyperlipidemia demonstrated that incorporating almonds into their diet not only reduced lipid risk factors for coronary heart disease, but also significantly altered the relationship between these risk factors and susceptibility to lipid oxidation modification (30). A meta-analysis on almond consumption revealed significant improvements in blood lipid levels and inflammatory markers (31, 32), which aligns with the findings of this study. The study suggests that polyphenols, such as flavonoids, positively influence the cardiovascular system through their antioxidant and anti-inflammatory properties. These effects may enhance endothelial function through various molecular mechanisms, regulate vasodilation processes, and modulate nitric oxide (NO) levels by inhibiting NAD(P)H oxidase (33).

The findings of nutritional epidemiological studies often demonstrate a robust association between increased phenol intake and a decreased risk or incidence of non-communicable diseases (34). The studies have revealed a shared characteristic among chronic non-communicable diseases, namely the presence of low-grade, persistent, and systemic inflammation. Furthermore, oxidative stress and lipid abnormalities are also recognized as significant contributors to the development of chronic illnesses (35, 36). The previous research conducted by this research team (12) has concluded that various healthy diet patterns share commonalities and posits that non-nutrients present in food have the potential to promote health, prevent diseases, and aid in the treatment of chronic diseases through their anti-inflammatory, antioxidant, and metabolic regulatory properties. The research team simultaneously introduced a "theoretical model of family nurse diet therapy," in which oxidative stress, inflammation, and metabolic disorders in chronic illnesses form an equilateral triangle with non-nutrients at

TABLE 2 Quality assessment.

Quality assessment							Effect	Quality	Importance
No of studies	Design	Risk of bias	Inconsistency	Indirectness	Imprecision	Other considerations	Rate (95% CI)		
TC									
6	Randomized trials	Serious[1]	Serious[2]	No serious indirectness	Serious[3]	None	MD: −4.19 (−15.25 to 6.87)	ÂOOO VERY LOW	CRITICAL
TG									
6	Randomized trials	Serious[1]	no serious inconsistency	No serious indirectness	Serious[3]	None	MD: −20.03 (−32.25 to −17.44)	ÂÂOO LOW	CRITICAL
LDL-C									
6	Randomized trials	Serious[1]	Serious[2]	No serious indirectness	Serious[3]	None	MD: −2.00 (−11.31 to 7.3)	ÂOOO VERY LOW	CRITICAL
HDL-C									
6	Randomized trials	Serious[1]	No serious inconsistency	No serious indirectness	Serious[3]	None	MD: 3.14 (1.55 to 4.72)	ÂÂOO LOW	CRITICAL

HDL-C: high-density lipoprotein cholesterol; LDL-C: low-density lipoprotein cholesterol; TC: total cholesterol; TG: triglyceride; CHD: coronary heart disease; CRP: C-reactive protein.

its apex, creating a triangular pyramid structure. Nurses employ dietary prescriptions to prevent and manage chronic conditions while incorporating fundamental principles of wholesome eating patterns derived from both traditional Chinese medicine and contemporary medical perspectives (12). A cross-sectional study investigating the association between total nut consumption (including both tree nuts and peanuts) and metabolic health revealed a significant inverse relationship between higher nut intake and the incidence of hypertension, type 2 diabetes, and dyslipidemia. Moreover, an increased consumption of almonds was specifically associated with a reduced risk of developing hypertension. These findings suggest that incorporating nuts into one's diet may benefit metabolic status and prevent chronic diseases (37). The findings of a study demonstrated a correlation between the consumption of beverages rich in polyphenols and the presence of cardiovascular and metabolic risk factors. The consumption of polyphenol-rich beverages has been observed to be associated with higher intake of polyphenols, thereby reducing the risk of cardiovascular disease. It is worth noting that the Mediterranean diet places emphasis on consuming foods abundant in polyphenols, such as fruits, vegetables, whole grains, etc. (38). The study conducted by Zhang et al. revealed that the bioactive compounds present in medicinal and food homologous substances can effectively support the treatment of non-alcoholic fatty liver disease (39). A meta-analysis of lipids and apolipoproteins in nuts indicated that flavonoids may exert anti-inflammatory effects by attenuating LDL oxidation and modulating the expression of inflammatory genes in endothelial cells and macrophages (40).

The consumption of natural foods rich in polyphenols has been found to be safe for human consumption. Two studies (19, 21) included in the analysis reported no adverse reactions or safety concerns among patients. In the traditional Chinese diet, homologous substances of medicine and food are utilized as daily food ingredients, serving a specific role in health preservation. However, improper consumption of these substances may result in potential toxic side effects that can harm human health. The European Commission Regulation (EC) stipulates a maximum daily intake of 1,000 mg of polyphenol extract consumed by humans (41). The field of traditional Chinese medicine also acknowledges the interplay and potential contradictions between medicinal and food homologous substances (42). The content of non-nutrients in food intake should be carefully considered when supplementing non-nutrients in daily life, ensuring the appropriateness of food consumption.

Some of the included studies observed a lack of positive effects on patients, which may be attributed to variations in intervention timing, polyphenol content, and food preparation methods. The duration of intervention in the included studies varied from 6 to 12 weeks. Humaira Jamshed et al. demonstrated a significant increase in HDL-C levels among patients with coronary heart disease by incorporating almonds into their diet for a period of 12 weeks (21). Conversely, another study focusing on almonds observed no significant impact on the plasma lipid profile of patients after a 6-week intervention (19). In two studies investigating the impact of polyphenol-rich apples on patients with hyperlipidemia (43, 44), Athanasios Koutsos' study (43) utilized fresh apples containing polyphenols for a duration of 8 weeks, with an apple weight of 340 g. This intervention resulted in a significant improvement in blood lipid levels among individuals with

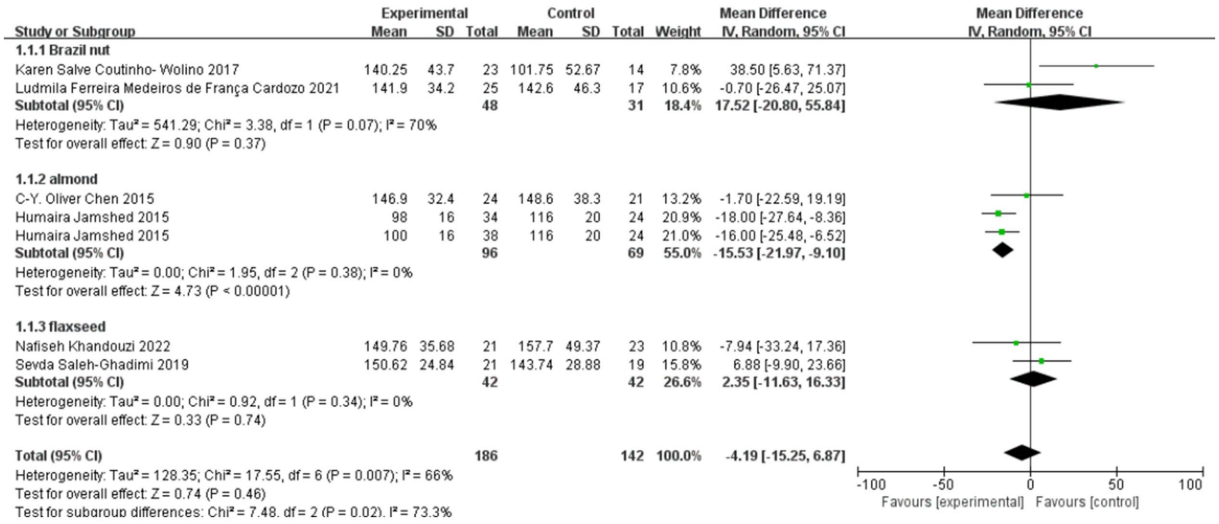

FIGURE 3
Effect of polyphenol-rich seed foods on TC in patients with CHD.

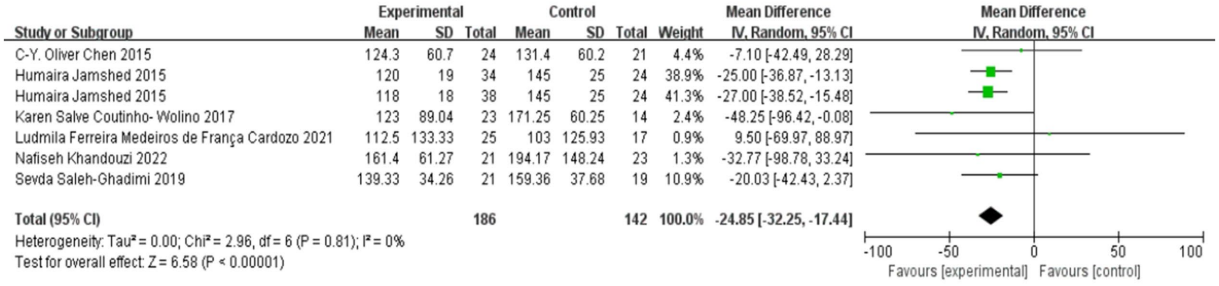

FIGURE 4
Effect of polyphenol-rich seed foods on TG in patients with CHD.

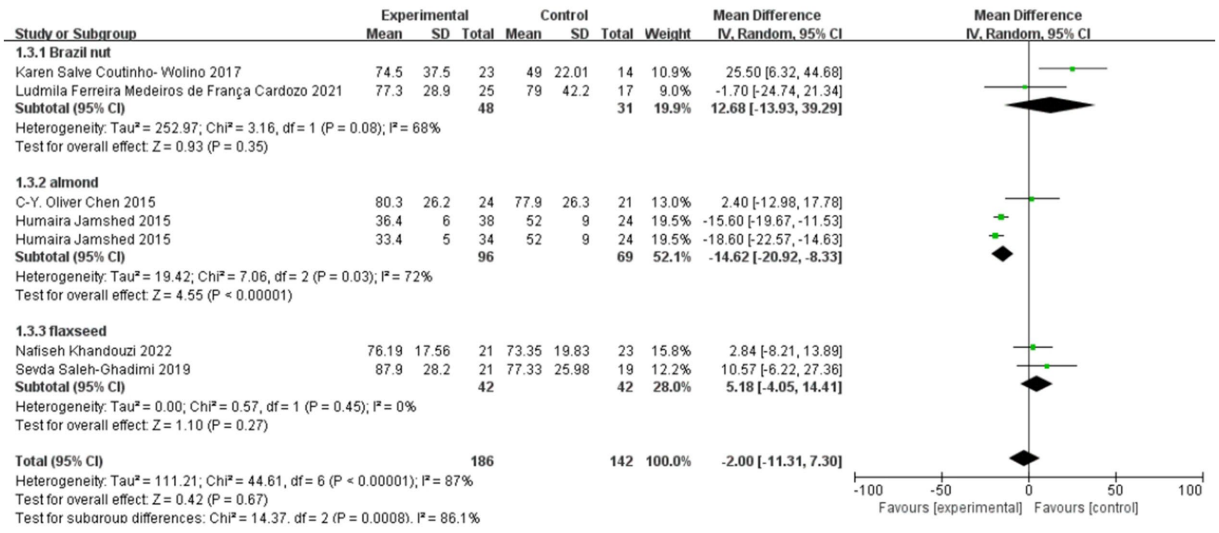

FIGURE 5
Effect of polyphenol-rich seed foods on LDL-C in patients with CHD.

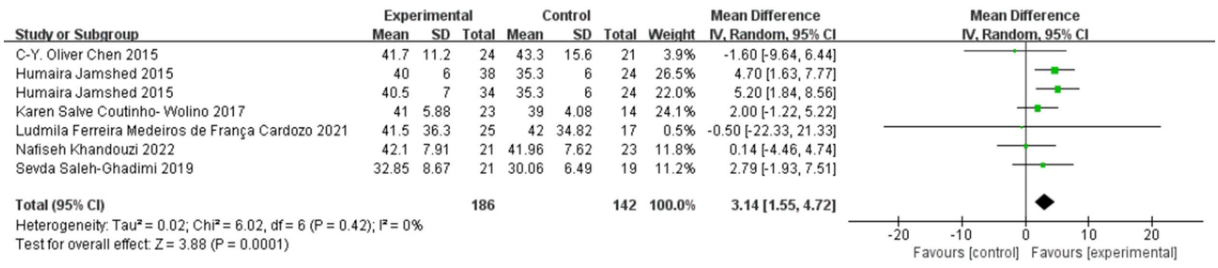

FIGURE 6
Effect of polyphenol-rich seed foods on HDL-C in patients with CHD.

hyperlipidemia. Conversely, one study (44) examined the effects of freeze-dried apples containing polyphenols over 4 weeks, equivalent to approximately 270 grams of fresh apples. However, no notable effect on blood lipids was observed among patients with hyperlipidemia. The study on the impact of almond consumption on adult inflammatory biomarkers revealed that when the daily intake of almonds was less than 60 g, it reduced serum CRP levels (31). Therefore, the duration and dosage of intervention may influence the efficacy of polyphenols in patients. Additionally, the food preparation method can also impact both the polyphenol content in food and its effects on individuals with coronary heart disease. Two studies on flaxseed have shown that dietary addition of flaxseed does not significantly affect plasma lipids, while consumption of flaxseed oil can effectively reduce triglycerides (TG) (22, 24). A study on cereal polyphenols (45) also reported that different processing methods of cereal impacted its polyphenol content. Therefore, in the process of managing diets for patients with coronary heart disease, it is recommended to encourage the consumption of seed foods as part of a healthy diet to help maintain healthy blood lipid levels, reduce inflammation levels and lower the risk of complications. Moreover, it is essential to consider the quantity and processing techniques of foods rich in polyphenols to optimize their potential benefits.

Practical implications

Studies (46) suggest that dietary adjustments can prevent and treat lifestyle-related diseases while promoting overall health. The concept of utilizing complementary medicine and food to enhance human well-being is evident as far back as the Chinese classical texts "Huangdi Neijing" and "Qianjin Prescription." With the advancement of an aging society, dietary management has gained momentum, and "prevention" and "maintenance" have gradually emerged as central themes in human health. The concept of medicinal food therapy represents the harmonious integration of traditional Chinese medicine's principles encompassing food therapy, medicinal diet, and health preservation. Non-nutrients found in medicinal and food homologs hold potential as adjunctive measures for preventing and treating chronic diseases, while the significance of a plant-based diet has been underscored in various dietary guidelines (12, 47, 48).

The implementation of dietary therapy is the optimal approach to support the prevention of chronic diseases. Consumption of polyphenols has been scientifically proven to exert favorable effects on health, thereby reducing the risk of cancer, cardiovascular diseases, neurodegenerative disorders, and other degenerative conditions through modulation of inflammatory capacity and improvement in metabolic dysregulation. Moreover, it can effectively impede the onset and progression of chronic ailments (49). The increasing awareness of healthcare among individuals has led to a growing focus on the theory of the homology between medicine and food. Homologs of medicine and food possess diverse characteristics, convenient sampling methods, and high safety standards, thereby offering extensive prospects for application in the field of biomedicine.

Strengths and limitations

The strength of this study lies in the inclusion of exclusively high-quality randomized controlled trials from four different countries, ensuring reliable results. However, certain limitations should be acknowledged. The search strategy employed in this study is limited to Chinese and English articles, potentially resulting in the omission of significant studies and impacting the overall analysis of results. Furthermore, due to the scarcity of included studies on the outcome indicator CRP and substantial heterogeneity among the included articles, a meta-analysis was not conducted.

Conclusion

The findings demonstrated that the consumption of polyphenol-rich seed-based foods significantly improved lipid profiles and reduced inflammatory markers among individuals diagnosed with coronary heart disease. The diverse array of foods rich in polyphenols provides a safe and effective complementary approach to preventing chronic diseases associated with diet, thereby promoting the prevention and management of cardiovascular conditions. Future research should investigate different dosages and durations of interventions to further elucidate the specific mechanisms underlying the lipid-lowering and anti-inflammatory effects of seed foods abundant in

polyphenols, as well as optimize intervention protocols involving these foods.

Data availability statement

The original contributions presented in the study are included in the article/Supplementary material, further inquiries can be directed to the corresponding author/s.

Author contributions

YJ: Methodology, Writing – original draft, Writing – review & editing. HW: Resources, Supervision, Writing – original draft, Writing – review & editing. WF: Data curation, Formal analysis, Writing – review & editing. JL: Methodology, Validation, Writing – review & editing. QN: Data curation, Formal analysis, Writing – review & editing. RZ: Funding acquisition, Visualization, Writing – review & editing. QZ: Conceptualization, Project administration, Supervision, Validation, Writing – review & editing.

Funding

The author(s) declare that financial support was received for the research, authorship, and/or publication of this article. This study was funded by "Shanxi Federation of Social Science key topic" no. SSKLZDKT2023209.

Conflict of interest

The authors declare that the research was conducted in the absence of any commercial or financial relationships that could be construed as a potential conflict of interest.

Publisher's note

All claims expressed in this article are solely those of the authors and do not necessarily represent those of their affiliated organizations, or those of the publisher, the editors and the reviewers. Any product that may be evaluated in this article, or claim that may be made by its manufacturer, is not guaranteed or endorsed by the publisher.

Supplementary material

The Supplementary material for this article can be found online at: https://www.frontiersin.org/articles/10.3389/fnut.2024.1493410/full#supplementary-material

References

1. Duggan JP, Peters AS, Trachiotis GD, Antevil JL. Epidemiology of coronary artery disease. *Surg Clin North Am*. (2022) 102:499–516. doi: 10.1016/j.suc.2022.01.007

2. Ma LY, Wang ZW, Fan J, Hu SS. Interpretation of report on cardiovascular health and diseases in China 2022. *Chin Gen Pract*. (2023) 26:3975–94. doi: 10.12114/j.issn.1007-9572.2023.0408

3. Drakopoulou M, Toutouzas K, Stathogiannis K, Synetos A, Trantalis G, Tousoulis D. Managing the lipid profile of coronary heart disease patients. *Expert Rev Cardiovasc Ther*. (2016) 14:1263–71. doi: 10.1080/14779072.2016.1221341

4. Li H, Sun K, Zhao R, Hu J, Hao Z, Wang F, et al. Inflammatory biomarkers of coronary heart disease. *Front Biosci (Schol Ed)*. (2018) 10:185–96. doi: 10.2741/s508

5. Lan Y, Luo FK, Yu Y, Wang XY, Wang PQ, Xiong XJ. Coronary heart disease: innovative understanding from traditional Chinese medicine and treatment by classic herbal formulas. *China J Chin Mater*. 2024, 49:3684–92. doi: 10.19540/j.cnki.cjcmm.20240326.501

6. Khan H, Kanny O, Syed MH, Qadura M. Aspirin resistance in vascular disease: a review highlighting the critical need for improved point-of-care testing and personalized therapy. *Int J Mol Sci*. (2022) 23:1317. doi: 10.3390/ijms231911317

7. Khadanga S, Beebe-Peat T. Optimal medical therapy for stable ischemic heart disease in 2024: focus on exercise and cardiac rehabilitation. *Med Clin North Am*. (2024) 108:509–16. doi: 10.1016/j.mcna.2023.11.005

8. Giustino G, Colombo A, Camaj A, Yasumura K, Mehran R, Stone GW, et al. Coronary in-stent restenosis: JACC state-of-the-art review. *J Am Coll Cardiol*. (2022) 80:348–72. doi: 10.1016/j.jacc.2022.05.017

9. Wang J, Zhang YL, Zhong Y, Liu ZW, Li WZ, Xia L, et al. Research advance of anxiety and depression in patient with percutaneous coronary intervention. *Chin Gen Pract*. (2020) 23:2938–43. doi: 10.12114/j.issn.1007-9572.2019.00.668

10. Trautwein EA, Catapano AL, Tokgözoğlu L. 'Diet and lifestyle' in the management of dyslipidaemia and prevention of CVD-understanding the level of knowledge and interest of European atherosclerosis society members. *Atheroscler Suppl*. (2020) 42:e9–e14. doi: 10.1016/j.atherosclerosissup.2021.01.003

11. Durazzo A, Lucarini M, Souto EB, Cicala C, Caiazzo E, Izzo AA, et al. Polyphenols: a concise overview on the chemistry, occurrence, and human health. *Phytother Res*. (2019) 33:2221–43. doi: 10.1002/ptr.6419

12. Han SF, Feng YQ, Gao WQ. Theoretical model of non-nutrient diet therapy for prevention and treatment of chronic diseases. *Chin Nurs Res*. (2023) 37:565–9. doi: 10.12102/j.issn.1009-6493.2023.04.001

13. Qorbani M, Mahdavi-Gorabi A, Khatibi N, Ejtahed HS, Khazdouz M, Djalalinia S, et al. Dietary diversity score and cardio-metabolic risk factors: an updated systematic review and meta-analysis. *Eat Weight Disord*. (2022) 27:85–100. doi: 10.1007/s40519-020-01090-4

14. Li H, Zou L, Li XY, Wu DT, Liu HY, Li HB, et al. Adzuki bean (*Vigna angularis*): chemical compositions, physicochemical properties, health benefits, and food applications. *Compr Rev Food Sci Food Saf*. (2022) 21:2335–62. doi: 10.1111/1541-4337.12945

15. Page MJ, McKenzie JE, Bossuyt PM, Boutron I, Hoffmann TC, Mulrow CD, et al. The PRISMA 2020 statement: an updated guideline for reporting systematic reviews. *J Clin Epidemiol*. (2021) 134:178–89. doi: 10.1016/j.jclinepi.2021.03.001

16. Cumpston M, Li T, Page MJ, Chandler J, Welch VA, Higgins JP, et al. Updated guidance for trusted systematic reviews: a new edition of the Cochrane handbook for systematic reviews of interventions. *Cochrane Database Syst Rev*. (2019) 10:ED000142. doi: 10.1002/14651858.ED000142

17. Higgins JPT, Thomas J, Chandler J, Cumpston M, Li T, Page MJ, et al. *Cochrane handbook for systematic reviews of interventions version 6.4 (updated august 2023). Cochrane* (2023).

18. Cardozo L, Mafra D, Silva ACT, Barbosa JE, da Cruz BO, Mesquita CT, et al. Effects of a Brazil nut-enriched diet on oxidative stress and inflammation markers in coronary artery disease patients: a small and preliminary randomised clinical trial. *Nutr Bull*. (2021) 46:139–48. doi: 10.1111/nbu.12495

19. Chen CY, Holbrook M, Duess MA, Dohadwala MM, Hamburg NM, Asztalos BF, et al. Effect of almond consumption on vascular function in patients with coronary artery disease: a randomized, controlled, cross-over trial. *Nutr J*. (2015) 14:61. doi: 10.1186/s12937-015-0049-5

20. Coutinho-Wolino KS, da Cruz BO, Cardozo L, Fernandes IA, Mesquita CT, Stenvinkel P, et al. Brazil nut supplementation does not affect trimethylamine-n-oxide plasma levels in patients with coronary artery disease. *J Food Biochem*. (2022) 46:e14201. doi: 10.1111/jfbc.14201

21. Jamshed H, Sultan FA, Iqbal R, Gilani AH. Dietary almonds increase serum HDL cholesterol in coronary artery disease patients in a randomized controlled trial. *J Nutr*. (2015) 145:2287–92. doi: 10.3945/jn.114.207944

22. Khandouzi N, Zahedmehr A, Firoozi A, Nasrollahzadehp J. Effects of flaxseed consumption on plasma lipids, lipoprotein-associated phospholipase a (2) activity and gut microbiota composition in patients with coronary artery disease. *Nutr Health*. (2022) 2022:1016. doi: 10.1177/02601060221091016

23. Khandouzi N, Zahedmehr A, Mohammadzadeh A, Sanati HR, Nasrollahzadeh J. Effect of flaxseed consumption on flow-mediated dilation and inflammatory biomarkers in patients with coronary artery disease: a randomized controlled trial. *Eur J Clin Nutr*. (2019) 73:258–65. doi: 10.1038/s41430-018-0268-x

24. Saleh-Ghadimi S, Kheirouri S, Golmohammadi A, Moludi J, Jafari-Vayghan H, Alizadeh M. Effect of flaxseed oil supplementation on anthropometric and metabolic indices in patients with coronary artery disease: a double-blinded randomized controlled trial. *J Cardiovasc Thorac Res*. (2019) 11:152–60. doi: 10.15171/jcvtr.2019.26

25. Li JH, Zhang YX, Gao F. Research on the development status and countermeasures of "medicine and food homology" food industry. *Food and Nutrition in China*. (2023) 29:5–11. doi: 10.19870/j.cnki.11-3716/ts.2023.09.002

26. Yu J. Catalogue of homologous raw materials of medicine and food (edition). *Oral Care Ind*. (2017) 27:24–8. doi: 10.3969/j.issn.2095-3607.2017.06.007

27. Hou Y, Jiang J-G. Origin and concept of medicine food homology and its application in modern functional foods. *Food Funct*. (2013) 4:1727–41. doi: 10.1039/c3fo60295h

28. Song DX, Jiang JG. Hypolipidemic components from medicine food homology species used in China: pharmacological and health effects. *Arch Med Res*. (2017) 48:569–81. doi: 10.1016/j.arcmed.2018.01.004

29. Lu Q, Li R, Yang Y, Zhang Y, Zhao Q, Li J. Ingredients with anti-inflammatory effect from medicine food homology plants. *Food Chem*. (2022) 368:130610. doi: 10.1016/j.foodchem.2021.130610

30. Jalali-Khanabadi BA, Mozaffari-Khosravi H, Parsaeyan N. Effects of almond dietary supplementation on coronary heart disease lipid risk factors and serum lipid oxidation parameters in men with mild hyperlipidemia. *J Altern Complement Med*. (2010) 16:1279–83. doi: 10.1089/acm.2009.0693

31. Fatahi S, Daneshzad E, Lotfi K, Azadbakht L. The effects of almond consumption on inflammatory biomarkers in adults: a systematic review and Meta-analysis of randomized clinical trials. *Adv Nutr*. (2022) 13:1462–75. doi: 10.1093/advances/nmab158

32. Phung OJ, Makanji SS, White CM, Coleman CI. Almonds have a neutral effect on serum lipid profiles: a meta-analysis of randomized trials. *J Am Diet Assoc*. (2009) 109:865–73. doi: 10.1016/j.jada.2009.02.014

33. Godos J, Vitale M, Micek A, Ray S, Martini D, Del Rio D, et al. Dietary polyphenol intake, blood pressure, and hypertension: a systematic review and meta-analysis of observational studies. *Antioxidants (Basel)*. (2019) 8:152. doi: 10.3390/antiox8060152

34. Xu Y, Le Sayec M, Roberts C, Hein S, Rodriguez-Mateos A, Gibson R. Dietary assessment methods to estimate (poly) phenol intake in epidemiological studies: a systematic review. *Adv Nutr*. (2021) 12:1781–801. doi: 10.1093/advances/nmab017

35. Geto Z, Molla MD, Challa F, Belay Y, Getahun T. Mitochondrial dynamic dysfunction as a Main triggering factor for inflammation associated chronic non-communicable diseases. *J Inflamm Res*. (2020) 13:97–107. doi: 10.2147/JIR.S232009

36. Seyedsadjadi N, Grant R. The potential benefit of monitoring oxidative stress and inflammation in the prevention of non-communicable diseases (NCDs). *Antioxidants (Basel)*. (2020) 10:10015. doi: 10.3390/antiox10010015

37. Micek A, Godos J, Cernigliaro A, Cincione RI, Buscemi S, Libra M, et al. Total nut, tree nut, and Peanut consumption and metabolic status in southern Italian adults. *Int J Environ Res Public Health*. (2021) 18:1847. doi: 10.3390/ijerph18041847

38. Micek A, Godos J, Cernigliaro A, Cincione RI, Buscemi S, Libra M, et al. Polyphenol-rich and alcoholic beverages and metabolic status in adults living in Sicily, southern Italy. *Food Secur*. (2021) 10:383. doi: 10.3390/foods10020383

39. Zhang Q, Jia Y, Zhang Y, Wang Y, Li X, Tian X, et al. The effects of medicinal and food homologous substances on blood lipid and blood glucose levels and liver function in patients with nonalcoholic fatty liver disease: a systematic review of randomized controlled trials. *Lipids Health Dis*. (2023) 22:137. doi: 10.1186/s12944-023-01900-5

40. Del Gobbo LC, Falk MC, Feldman R, Lewis K, Mozaffarian D. Effects of tree nuts on blood lipids, apolipoproteins, and blood pressure: systematic review, meta-analysis, and dose-response of 61 controlled intervention trials. *Am J Clin Nutr*. (2015) 102:1347–56. doi: 10.3945/ajcn.115.110965

41. Tenore GC, D'Avino M, Caruso D, Buonomo G, Acampora C, Caruso G, et al. Effect of Annurca apple polyphenols on intermittent claudication in patients with peripheral artery disease. *Am J Cardiol*. (2019) 123:847–53. doi: 10.1016/j.amjcard.2018.11.034

42. Yan LY, Cui W. Discussion on the Blend of Medicinal and Dietary Taboo Culture from the Perspective of "Avoiding Pork after Taking Rhizome of Chinese Goldthread". *Med Philos*. (2023) 44:55–9. doi: 10.12014/j.issn.1002-0772.2023.22.13

43. Auclair S, Chironi G, Milenkovic D, Hollman PC, Renard CM, Mégnien JL, et al. The regular consumption of a polyphenol-rich apple does not influence endothelial function: a randomised double-blind trial in hypercholesterolemic adults. *Eur J Clin Nutr*. (2010) 64:1158–65. doi: 10.1038/ejcn.2010.135

44. Koutsos A, Riccadonna S, Ulaszewska MM, Franceschi P, Trošt K, Galvin A, et al. Two apples a day lower serum cholesterol and improve cardiometabolic biomarkers in mildly hypercholesterolemic adults: a randomized, controlled, crossover trial. *Am J Clin Nutr*. (2020) 111:307–18. doi: 10.1093/ajcn/nqz282

45. Zhao GH, Zhang RF, Su DX, Dong LH, Liu L, Wei ZC, et al. Research progress of whole grain phenols and their antioxidant activities. *Chin Inst Food Sci*. (2017) 17:183–96. doi: 10.16429/j.1009-7848.2017.08.025

46. Roy F, Boye JI, Simpson BK. Bioactive proteins and peptides in pulse crops: pea, chickpea and lentil. *Food Res Int*. (2010) 43:432–42. doi: 10.1016/j.foodres.2009.09.002

47. Trautwein EA, McKay S. The role of specific components of a plant-based diet in Management of Dyslipidemia and the impact on cardiovascular risk. *Nutrients*. (2020) 12:2671. doi: 10.3390/nu12092671

48. Wu P. Research progress of homologous substances of medicine and food in China. *China Fruit Vegetable*. (2024) 44:1. doi: 10.3969/j.issn.1008-1038.2024.05.001

49. Quero J, Mármol I, Cerrada E, Rodríguez-Yoldi MJ. Insight into the potential application of polyphenol-rich dietary intervention in degenerative disease management. *Food Funct*. (2020) 11:2805–25. doi: 10.1039/D0FO00216J

frontiers | Frontiers in Nutrition

TYPE Original Research
PUBLISHED 13 December 2024
DOI 10.3389/fnut.2024.1495695

Check for updates

OPEN ACCESS

EDITED BY
Pedzisai Makoni,
Sefako Makgatho Health Sciences University, South Africa

REVIEWED BY
Palash Mandal,
Charotar University of Science and Technology, India
Qi Wang,
Yibin Vocational and Technical College, China

*CORRESPONDENCE
Guohui Xiao
✉ Xguohui88@163.com
Zhi Li
✉ lizhi_swmu@126.com

†These authors have contributed equally to this work

RECEIVED 13 September 2024
ACCEPTED 27 November 2024
PUBLISHED 13 December 2024

CITATION
Tang M, Zhao L, Huang F, Wang T, Wu X, Chen S, Fu J, Jiang C, Wei S, Zeng X, Zhang X, Zhou X, Wei M, Li Z and Xiao G (2024) Liuweizhiji Gegen-Sangshen beverage protects against alcoholic liver disease in mice through the gut microbiota mediated SCFAs/GPR43/GLP-1 pathway. *Front. Nutr.* 11:1495695. doi: 10.3389/fnut.2024.1495695

COPYRIGHT
© 2024 Tang, Zhao, Huang, Wang, Wu, Chen, Fu, Jiang, Wei, Zeng, Zhang, Zhou, Wei, Li and Xiao. This is an open-access article distributed under the terms of the Creative Commons Attribution License (CC BY). The use, distribution or reproduction in other forums is permitted, provided the original author(s) and the copyright owner(s) are credited and that the original publication in this journal is cited, in accordance with accepted academic practice. No use, distribution or reproduction is permitted which does not comply with these terms.

Liuweizhiji Gegen-Sangshen beverage protects against alcoholic liver disease in mice through the gut microbiota mediated SCFAs/GPR43/GLP-1 pathway

Mingyun Tang[1,2†], Long Zhao[1,2†], Fuchun Huang[1,2†], Tiangang Wang[1,2], Xu Wu[3], Shanshan Chen[1,2], Juan Fu[1,2], Chaoli Jiang[1,2], Shulin Wei[1,3], Xuseng Zeng[1,2], Xiaoling Zhang[1,2], Xin Zhou[1,2], Mei Wei[4], Zhi Li[1,2,5*] and Guohui Xiao[1,2*]

[1]Department of Spleen and Stomach Diseases, The Affiliated Traditional Chinese Medicine Hospital, Southwest Medical University, Luzhou, Sichuan, China, [2]The Key Laboratory of Integrated Traditional Chinese and Western Medicine for Prevention and Treatment of Digestive System Diseases of Luzhou City, The Affiliated Traditional Medicine Hospital, Southwest Medical University, Luzhou, Sichuan, China, [3]Cell Therapy and Cell Drugs of Luzhou Key Laboratory, Department of Pharmacology, School of Pharmacy, Southwest Medical University, Luzhou, Sichuan, China, [4]Department of Hepatobiliary Diseases, The Affiliated Traditional Chinese Medicine Hospital, Southwest Medical University, Luzhou, Sichuan, China, [5]School of Integrated Traditional Chinese and Western Clinical Medicine, North Sichuan Medical College, Nanchong, Sichuan, China

Introduction: Alcoholic liver disease (ALD) is a pathological state of the liver caused by longterm alcohol consumption. Recent studies have shown that the modulation of the gut microbiota and its metabolic products, specifically the short-chain fatty acids (SCFAs), exert a critical role in the evolution and progression of ALD. The Liuweizhiji Gegen-Sangshen beverage (LGS), as a functional beverage in China, is derived from a traditional Chinese herbal formula and has been clinically applied for ALD treatment, demonstrating significant efficacy. However, the underlying mechanisms of LGS for alleviating ALD involving gut microbiota regulation remain unknown.

Methods: In this study, an ALD murine model based on the National Institute on Alcohol Abuse and Alcoholism (NIAAA) method was established.

Results: The results showed that oral LGS treatment dose-dependently alleviated alcoholinduced liver injury and inflammation in mice through decreasing levels of ALT, AST and proinflammatory cytokines (TNF-α, IL-6, IL-1β). LGS significantly improved liver steatosis, enhanced activities of alcohol metabolizing enzymes (ALDH and ADH), and reduced the CYP2E1 activity. Notably, regarding most detected indices, the effect of LGS (particularly at medium and high dose) was comparable to the positive drug MTDX. Moreover, LGS had a favorable effect on maintaining intestinal barrier function through reducing epithelial injury and increasing expression of occludin. 16S rRNA sequencing results showed that LGS remarkably modulated gut microbiota structure in ALD mice via recovering alcohol-induced microbial changes and specifically mediating enrichment of several bacterial genera (*Alloprevotella*, *Monoglobus*, *Erysipelatoclostridium Parasutterella, Harryflintia*

and unclassified_c_Clostridia). Further study revealed that LGS increased production of SCFAs of hexanoic acid in cecum, promoted alcohol-mediated reduction of GRP43 expression in ileum, and increased serum GLP-1 level.

Discussion: Overall, LGS exerts a remarkable protective effect on ALD mice through the gut microbiota mediated specific hexanoic acid production and GPR43/GLP-1 pathway.

KEYWORDS

alcoholic liver disease, Liuweizhiji Gegen-Sangshen beverage, gut microbiota, SCFAs, GPR43, GLP-1

1 Introduction

Excessive drinking is a global issue that has a severe impact on human health. The liver, as the main organ for metabolism and detoxification, is the primary target organ for alcohol damage. Alcoholic liver disease (ALD) is a spectrum of diseases that begins with alcoholic fatty liver (AFL) and may progress to alcoholic steatohepatitis (ASH), alcoholic liver fibrosis (ALF), alcoholic cirrhosis (AC), and in some cases, alcohol-related liver cancer (ARLC). Approximately 90 percent of individuals with excessive alcohol consumption manifest primarily with hepatic steatosis (1), and it is one of the leading causes of illness and death from liver disease worldwide preventably (2).

The pathogenesis of ALD is complex, which is tightly associated with alcohol and its metabolites mediated liver injury, and the inflammatory response to injury. In recent years, with the development of omics study, research based on the gut-liver axis theory has revealed the impact of changes in the gut microbiota on ALD, becoming an important driving force in exploring the pathogenesis of the disease. The gut microbiota and its metabolites can penetrate the intestinal epithelial barrier and enter the portal vein, linking the connection between the gut and the entire body. The balance of the gut microbiota is characterized by a high abundance of essential beneficial bacteria and a low abundance of pathogenic or conditionally pathogenic bacteria. And the disruption of this balance is closely related to the development and severity of various diseases (3). Current research has confirmed that the dysregulation of the gut microbiota is a key factor in the occurrence and development of ALD (4). Bacterial products, including the short-chain fatty acids (SCFAs) and so on, mediate host response and plays an important roles in ALD pathogenesis (2). Regulating gut microbiota and the gut-liver axis has emerged as a promising strategy for ALD treatment.

Liuweizhiji Gegen-Sangshen beverage (LGS), a nutraceutical beverage composed of six medicinal and edible plants (*Puerariae lobatae* radix, *Hoveniae* semen, *Imperatae* rhizoma, *Crataegi* fructus, *Mori* fructus and *Canarli* fructus), is derived from Traditional Chinese Medicine, and has demonstrated significant clinical therapeutic effects and minimal side effects in the handling alcoholic symptoms and ALD (5, 6). In previous studies, it has been demonstrated that in ALD rats, LGS exerted protective effects through attenuating oxidative stress, alleviating insulin resistance and lipid metabolism, and enhancing alcohol metabolism (7–10). The involved signaling pathways included AMPK/SREBP-1, P2 × 7R/NLRP3, PPARα, Ras/ERK and IRS-1/PI3K/AKT (7–10). In HO2 cells, LGS enhanced the alcohol metabolism through increasing the activity of ADH1 and ALDH2, and reduced CYP2E1-induced oxidative stress (11). However, whether LGS has an impact on the gut microbiota and gut-liver axis remains unexplored. In our previous study, it was found that LGS mainly contained flavonoids, polyphenols and polysaccharides (5, 12). The *in vitro* incubation of LGS polysaccharides has demonstrated good prebiotic activity, which drew our attention to its potential for regulating the gut microbiota (12). Therefore, although LGS has shown considerable clinical benefit toward ALD, the mechanism of action remains unclear and requires further elucidation.

In this study, we hypothesized that LGS may impact the gut microbiota, trigger host response and alleviate ALD. An ALD murine model was established by using Lieber-DeCarli alcohol liquid diet, and the mice were treated with different doses of LGS to investigate the effects of LGS on ALD. The results of current study would reveal the potential mechanisms of LGS in treating ALD from the aspect of gut microbiota regulation and provide a scientific basis for the clinical application and development of related drugs.

Abbreviations: ALD, alcoholic liver disease; AFL, alcoholic fatty liver; AH, alcoholic hepatitis; AC, alcoholic cirrhosis; NAFLD, non-alcoholic fatty liver disease; NASH, non-alcoholic steatohepatitis, LGS, Liuweizhiji Gegen-Sangshen beverage; SCFAs, short-chain fatty acids; NIAAA, the national institute on alcohol abuse and alcoholism; GLP-1, glucagon-like peptide-1; ARLC, alcohol-related liver cancer; GC-MS, gas chromatography-mass spectrometry; HDACs, histone deacetylases; UPLC-Q-TOF-MS, ultra-performance liquid chromatography tandem quadrupole time-of-flight mass spectrometry; MTDX, metadoxine; AST, aspartate aminotransferase; ALT, alanine aminotransferase; TC, total cholesterol; TG, triglycerides; LDL-C, low-density lipoprotein cholesterol; HDL-C, high-density lipoprotein cholesterol; IL-6, interleukin-6; IL-1β, interleukin-1β; TNF-α, tumor necrosis factor-alpha; CYP2E1, hepatic tissue cytochrome P450 2E1; ADH, alcohol dehydrogenase; ALDH, aldehyde dehydrogenase; ELISA, enzyme-linked immunosorbent assay; H&E, hematoxylin and eosin; OCT, cutting temperature; ORO, oil red O; ZO-1, zonula occludens-1; qPCR, quantitative polymerase chain reaction; PE, paired-end; ASVs, amplicon sequence variants; PCoA, principal coordinate analysis; LEfSe, linear discriminant analysis effect size; ANOVA, one-way analysis of variance; F/B, the ratio of *Bacteroidetes* to *Firmicutes*; LDA, linear discriminant analysis; APN, adiponectin; AMPK, AMP-activated protein kinase; GPR43, G protein-coupled receptor 43; GPR41, G protein-coupled receptor 41; FDA, food and drug administration; PPARγ, peroxisome proliferator-activated receptor γ; PYY, pancreatic polypeptide; ROS, oxygen species; O2-, superoxide anion; ICP, Intrahepatic Cholestasis of Pregnancy; PBC, primary biliary cholangitis.

2 Materials and methods

2.1 Reagents and materials

LGS was provided by Sichuan Tongyou Life Health Technology Co., Ltd. (Sichuan, China). The chemical profile as well as quality control of LGS has been investigated thoroughly in our previous reports (5, 12). Metadoxine (MTDX) was purchased from MedChemExpress Co., Ltd. (New Jersey, US). Edible alcohol (95%) was acquired from Kelong Chemical Chemicals (Chengdu, China). Biochemical Assay Kits for TC, TG, ALT, AST, ADH and ALDH, Enzyme-linked immunosorbent assay (ELISA) kits for LDL-C, HDL-C, TNF-α, CYP2E1, and GLP-1 were provided by Quanzhou RuiXin Biotechnology Co., Ltd. (Fujian, China). 4% Paraformaldehyde from Sichuan Scientist Biotechnology Co., Ltd. (Sichuan, China). In histopathological examination and immunohistochemistry and immunofluorescence experiments, Hematoxylin (G1004) and Oil Red O stain (G1016) and Fixative were purchased from Wuhan Google Biotechnology Co., Ltd. (Wuhan, China). Primary Antibody, Occludin, ZO-1, and histological DAB Staining Kit purchased from Service Biotechnology Co., Ltd. (Wuhan, China). Secondary antibody, goat anti-rabbit IgG (Lianke Bio, GRA0072, 1:200, Hangzhou, China) were sourced from the respective suppliers. GPR43 polyclonal antibody (#19952-1-AP, 1:500) provided by Proteintech Group Co., Ltd. (Wuhan, China), and HRP conjugated affinipure goat anti-rabbit IgG (#BA1054) was provided by Boster Biological Technology Co., Ltd. (California, US). Anti-glyceraldehyde-3-phosphate dehydrogenase (GAPDH) antibody (AF2823) and Bicinchoninic acid (BCA) Protein Assay Kit was purchased from Beyotime Biotechnology Co., Ltd. (Shanghai China). The RIPA lysis buffer, protease inhibitor cocktail (100×), HRP-conjugated goat anti-mouse/Rabbit IgG (H + L) were sourced from Shanghai YaZi Bio-Pharmaceutical Technology Co., Ltd. (Shanghai China). Total RNA extraction kit was provided by TianGen Biochemical Technology Co, Ltd. (Beijing, China). The qRT-PCR kit was purchased from Vazyme Biotechnology Co., Ltd. (7E760L3, Nanjing, China). Primers were synthesized by Beijing Qingke Biotechnology Co., Ltd. (Beijing, China). FastPure Feces DNA Isolation Kit (YH-feces) was provided by Shanghai Major Yuhua Co., Ltd. (Shanghai, China). ECL luminescence detection kit was purchased from Affinity Biotech Co., Ltd. (Jiangsu, China).

2.2 Animals and experimental design

A total of 72 male C57BL/6J mice (specific pathogen free grade) aged between 6 to 8 weeks, with a body weight exceeding 20 grams, were provided by the Animal Center of Southwest Medical University (Sichuan, China). The experimental protocol was complied with the guidelines for the care and use of laboratory animals set forth by the National Institutes of Health, and has been rigorously reviewed and approved by the Experimental Animal Ethics Committee of Southwest Medical University, with the corresponding approval number: SWMU20230089. All mice were maintained at the Animal Center of Southwest Medical University, with a temperature of 23 ± 1°C, a humidity of 40–60%, and 12/12 h day/night turnover. The mice were subjected for adaptation for at least 1 week before experiment with free access to water and food.

Following the recommendations of the National Institute on Alcohol Abuse and Alcoholism (NIAAA) (13), we established a murine model of ALD (Figure 1A) using the Lieber-DeCarli alcoholic liquid diet (#TP4030D; Trophic Animal Feed High-Tech Co., Ltd., Jiangsu, China). The complete alcoholic liquid diet was prepared with food-grade 95% ethanol, with a final alcohol concentration of 5% (v/v), which was consisted of 28% calories from alcohol, 35% calories from fat, 18% calories from protein and 19% calories from alcohol carbohydrate. In the control liquid diet (#TP4020C; Trophic Animal Feed High-Tech Co., Ltd., Jiangsu, China), equal calories for alcohol were replaced by dextrin. All liquid diets were freshly prepared daily at a caloric density of 1 kcal/mL.

In the initial phase of the study, all mice were acclimated to the experimental environment for 1 week, followed by a 5-day period (days 1–5) of adaptation to liquid diet feeding. Then the mice were randomly assigned into six groups (n = 12 per group), comprising a control group (Ctrl), an ALD model group (ALD), a MTDX treatment group (MTDX), and three LGS treatment groups (LGS_L, LGS_M, LGS_H). The sample size was estimated by the free G*Power software (Universität Düsseldorf), with effect size setting at 0.25, α probability of 0.05 and power of 0.95.

From days 6 to 11, except for the Ctrl group which received control liquid diet, the remaining five groups were subjected to a graded transition feeding with the mixture of control liquid diet and alcoholic diet at the volume ratios of 2:1, 1:1, and 1:2 (each for 2 days). The Ctrl group was pair-fed according to the mean food intake of the ALD groups from the previous day, in order to ensure similar food intake for Ctrl and ALD mice. During days 12 to 21, the ALD, MTDX and LGS treatment groups were administered the complete alcoholic liquid diet, while the Ctrl group continued with pair-feeding for a total of 10 days.

Throughout this period, the Ctrl and ALD groups were daily gavage-fed with physiological saline, the MTDX group with metadoxine solution (200 mg/kg/day), and the LGS_L, LGS_M, and LGS_H groups with LGS at low, medium and high dosages of [6.15 mL (1.23 g solid content)/kg/day, 12.30 mL (2.46 g solid content)/kg/day, 24.60 mL (4.92 g solid content)/kg/day], with a gavage volume of 0.2 mL per mouse per day. The dosage of LGS used in mice was designed according to the human dose and cross-species dose conversion using body surface area scaling. Consequently, the dosages for LGS_L, LGS_M, and LGS_H corresponded to 0.5-fold, 1-fold and 2-fold of normal human daily dose. On the 21st day of the experiment, fresh fecal pellets from the mice were collected and stored at −80°C. On the 22nd day, the mice were euthanized for blood collection. After sacrifice of mice, liver and intestine tissues, as well as intestinal contents were collected for subsequent analysis. During the course of the study, each animal was weighed at 5-day intervals.

2.3 Biochemical analysis

Blood samples were centrifuged at 4°C, 4000 rpm for 20 min to collect the serum. Serum levels of liver function-related indicators (AST and ALT), blood lipids (TC, TG, LDL-C and

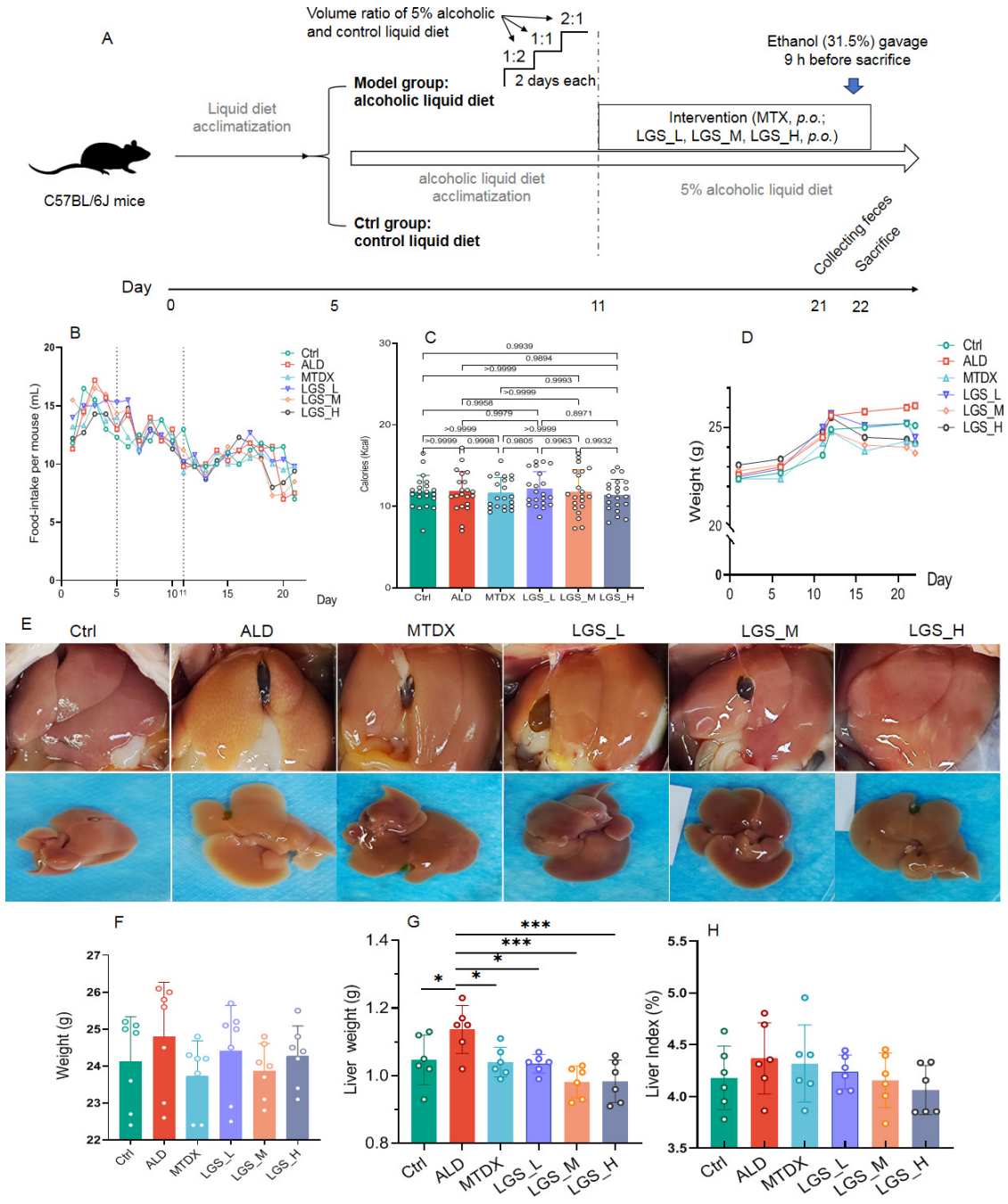

FIGURE 1
LGS ameliorates body and liver weight gain, and improves liver morphology in ALD mice. **(A)** Experimental procedure for animal studies. **(B)** Daily food intake of mice in each group. **(C)** Calories intake in each group. **(D)** The effect of LGS on the body weight of mice with ALD. **(E)** Trend of body weight change in each group. **(F)** Morphological presentation of liver images in each group. **(G)** Liver weight of mice. **(H)** Hepatic index (the ratio of liver weight to body weight) of mice. $^{*}P < 0.05$, $^{***}P < 0.001$ ($n = 6$). One-way ANOVA followed by Tukey test was employed to evaluate differences among multiple groups.

HDL-C), proinflammatory cytokines (IL-6, IL-1β and TNF-α), and alcohol metabolizing enzymes (CYP2E1, ADH, ALDH and GLP-1) concentrations were determined using the manufacturer's protocol with the respective ELISA or biochemical assay kits. The optical density (OD) of the plates was read at 450 nm for ELISA kits and 462 nm for biochemical assay kits, using a microplate reader, and the concentrations were calculated by standard curves.

2.4 Histopathological examination

The liver and intestinal tissues were fixed overnight in 4% paraformaldehyde and then embedded in paraffin. Sections of the liver and ileum were stained with hematoxylin and eosin (HE). To assess hepatic lipid accumulation, liver samples were frozen in optimal cutting temperature (OCT) compound and sectioned using a cryostat. After air-drying, the sections were fixed and stained with

oil red O (ORO) in propylene glycol, followed by counterstaining with hematoxylin to highlight lipid deposition and cell nuclei. Microscopic images were captured, and the area ratio of positive expression within the tissue was measured using Image-Pro Plus 6 software (Media Cybernetics, Inc, Rockville, MD, USA).

2.5 Immunohistochemical and immunofluorescence staining

Immunofluorescence staining was performed on colonic sections to detect tight junction proteins (Occludin and ZO-1). The tissue sections were incubated overnight with primary antibodies specific for Occludin (1:100) and ZO-1 (1:100) at 4°C. Subsequently, the sections were incubated with a secondary antibody, goat anti-rabbit IgG (GRA0072, 1:200), followed by a chromogenic reaction with 3,3′-diaminobenzidine (DAB, DA1016) for 45 min. Microscopic images were captured and analyzed using a digital pathology system (3DHIST ECH Kft Pannoramic SCAN II).

2.6 RNA isolation and real-time PCR analysis

RNA was isolated from liver and intestinal tissues using the total RNA Extraction Kit. Quantitative PCR (qPCR) was performed using a Roche fluorescence quantitative system (Life Science and Technology, Veriti 96-Well) to assess the mRNA expression of the gene encoding GPR43. Primer sequences were as follows: *GAPDH*, 5′-ACTGAGCAAGAGAGGCCCTA-3′ and 5′-CCCTAGGCCCCTCCTGTTAT-3′; *GPR43*, 5′-ATCC AACTTCCGCTGGTACC-3′ and 5′-GTAGCGTTCCATG CTGATGC-3′.

2.7 Western blot

According to the manufacturer's instructions, the ileal tissue (50 mg) was homogenized with RIPA lysis buffer and a 100 × protease inhibitor cocktail (v/v = 1:1) to obtain the ileal tissue lysate. Protein concentration was measured using the BCA Protein Assay Kit.

An equal amount of protein was separated by SDS-PAGE, and western blot analysis was performed using the specific primary antibody, GPR43 (1:1000), GAPDH (1:2000), and a horseradish peroxidase (HRP)-conjugated secondary antibody (rabbit pAb, 1:5000). The protein levels were quantified by densitometry scanning.

2.8 Gas chromatography-mass spectrometry (GC–MS) analysis

After re-suspending the cecal contents in a phosphate buffer, the supernatant was taken for analysis. Separation was performed using an Agilent DB-FFAP capillary column (30 m × 250 μm × 0.25 μm) and an Agilent 789B GC System. Nitrogen with flow at 1.0 mL/min as the carrier gas (Initial temperature was 90°C, raised to 160°C at 10°C /min, then raised to 240°C at 40°C /min, and held for 5 min). Subsequent mass spectrometry was conducted using an Agilent 5977B GC/MSD mass spectrometer (SCAN/SIM, inlet temperature 250°C, ion source temperature 230°C, transfer line temperature 250°C, quadrupole temperature 150°C, electron impact ionization (EI) source, electron energy 7 eV). The concentrations of SCFAs in the cecal contents were reported in milligrams per gram of feces (μg/g) by ChemStation software (Agilent Technologies, USA) on APT Cloud Platform.[1]

2.9 16S rRNA gene sequencing analysis

Total bacterial DNA was extracted using the FastPure Feces DNA Isolation Kit (YH-feces, Shanghai Major Yuhua). The quality of DNA extraction was verified by 1% agarose gel electrophoresis, and the quantity was determined using the QuantiFluor™ -ST Blue Fluorescence Quantitative System (Promega Corporation). Library preparation and sequencing were conducted at Majorbio Bio-pharm Technology Co. Ltd. (Shanghai, China). PCR amplification of the V3-V4 region was performed using the primers 338F (5′-ACTCCTACGGGAGGCAGCAG-3′) and 806R (5′-GGACTACHVGGGTWTCTAAT-3′) to prepare amplicons. The libraries were ultimately submitted for sequencing on the Illumina NextSeq 2000 PE300 platform (Illumina, San Diego, USA).

The paired-end (PE) reads obtained from Illumina sequencing were demultiplexed and subjected to quality control and filtering based on sequencing quality. The reads were then assembled based on the overlap between the paired-end reads to yield optimized data. Subsequently, the optimized data were processed using the sequence denoising method (DADA2) (14) to obtain amplicon sequence variants (ASVs) and their abundance information.

The raw paired-end reads from the Illumina platform were overlapped and merged using FLASH (v1.2.11) (15) with standard parameters. The merged reads were subjected to quality control using the QIIME2 platform. To minimize the impact of sequencing depth on subsequent alpha and beta diversity data analysis, all sample sequences were rarefied, and all data analyses were performed on the Majorbio Cloud Platform[2] based on the Silva 16S rRNA gene database (version 138). The ASVs were classified taxonomically using the Naive Bayes classifier in Qiime2. The composition of the microbial community, alpha diversity indices (Mothur v1.30.2) (16), and beta diversity (Bray-curtis) indices were calculated using QIIME2. The similarity of microbial communities between groups was determined by principal coordinate analysis (PCoA) (Vegan v2.4.3 package). The linear discriminant analysis (LDA) effect size (LEfSe)[3] was performed to identify the significantly abundant taxa (phylum to genera) of bacteria among the different groups (LDA score = 3.5, $P < 0.05$).

1 https://bio-cloud.aptbiotech.com/
2 https://cloud.majorbio.com
3 http://huttenhower.sph.harvard.edu/LEfSe

2.10 Statistical analysis

Statistical analysis was performed using GraphPad Prism version 8 (GraphPad Software Inc., USA) and SPSS version 20 (SPSS, USA). One-way analysis of variance (ANOVA) was employed to evaluate differences among multiple groups, and the unpaired student's *t*-test was used to assess the statistical significance between two groups. The results are presented as the mean ± the standard error of the mean (SD). Data were considered statistically significant when the *p*-value was less than 0.05.

3 Results

3.1 LGS protects against ALD in mice

In this study, we administered the LGS to a murine model of ALD for a 10-day treatment period to investigate the therapeutic effects of LGS on ALD. The experimental results are depicted in Figure 1. Throughout the study, body weight of mice was monitored. The liver morphology was observed, and liver indices were determined. Subsequently, the hepatic histopathological analysis, biochemical determinations, and ethanol metabolism assays were performed.

3.1.1 LGS ameliorates hepatic steatosis in ALD mice

In the initial 11 days of the experiment, corresponding to the liquid transition and alcohol acclimation period, there was a certain degree of fluctuation in the food intake of all groups. Despite a downward trend observed on the 5th–20th day, may be related to the alcohol intake, the food intake became more stable in general and with no difference between groups (Figure 1B). Moreover, to ensure that each group had similar calories intake, the amount of liquid diet supplied to the control group was given based on the amount of food consumed by the ALD group the day before. The results showed that there was no statistical difference in calories between the groups (Figure 1C).

As extrinsic indicator of obesity, the body weight of all groups showed an upward trend (Figure 1D), compared with Ctrl group, the ALD group having a higher average body weight. After intervention with LGS, the body weight of mice became lower. The MTDX group exhibited a loss of weight too (Figure 1F). Subsequently, we observed the *in vivo* and *ex vivo* images of the liver (Figure 1E). The livers of Ctrl and the medium and high dose LGS treatment groups (LGS_M, LGS_H) appeared red with sharp edges, in contrast, the livers of the ALD group were yellow, with blunt edges and a greasy texture. The MTDX group exhibited slight yellow areas with sharp edges. The livers of the LGS_L group were pale yellow with a few yellow areas, and the edges were slightly blunt. Further analysis revealed that, the ALD group mice had a larger liver weight ($p < 0.05$) (Figure 1F) and liver index (Figure 1G). After the treatment with LGS, the liver weight was reversed, with the liver index decreased. The improvement in the liver index showed a dose-dependent trend. The aforementioned findings indicate that LGS intervention apparently ameliorates body and liver weight gain, and improves liver morphology.

Furthermore, liver tissues were sectioned and stained with Oil Red O (Figure 2A). The results revealed that a significant aggregation of red lipid droplets was observed in the liver of ALD group mice. A moderate aggregation was observed in the liver of LGS_L group mice. A slight aggregation was noted in the liver of MTDX group mice, and minimal aggregation was seen in the liver of Ctrl group, LGS_M group, and LGS_H group mice. To demonstrate the fat content within tissues directly, the ratio of the area of positive Oil Red staining to the entire observed area (positive expression area ratio,%) was analyzed. It was found that, in comparison to the Ctrl group, the fat content in the ALD group elevated significantly, and the positive area ratio reduced after LGS treatment (Figure 2B). Noteworthy, the effect of LGS was markedly superior to that of MTDX, particularly in the medium and high-dose groups.

Further confirmation was provided by serum biochemical assays, showed that the lipid levels of TC (Figure 2C), TG (Figure 2D), and LDL-C (Figure 2E) in ALD group mice were significantly elevated compared to the normal group ($p < 0.05$). Blood lipids were reduced by both medium and high doses of LGS and MTDX ($p < 0.05$). However, the experiment did not reveal the alleviating effects of LGS and MTDX on HDL-C (Figure 2F).

These above findings indicate that LGS is capable of ameliorating hepatic steatosis in mice with ALD, and, in blood lipid reduction, the data endorsed the use of higher dosages more.

3.1.2 LGS protects against liver injury and inflammation in ALD mice

Hepatic histopathological analysis and biochemical assays of blood samples were subsequently conducted to evaluate the hepatoprotection of LGS (Figure 3).

Compared to the Ctrl group, the ALD group exhibited a disordered arrangement of hepatocytes, significant cell swelling, and scattered vacuole formation, which indicated the presence of liver inflammation. This suggested that the inflammatory damage was present in ALD, which confirmed by pathological scores among groups. After intervention with LGS or MTDX, the hepatocyte arrangement became tightly and orderly, the structure of the liver lobules was clear, the phenomenon of cell swelling was not obvious, and the number of vacuoles was correspondingly reduced (Figure 3A). Furthermore, the effect of medium and high doses of LGS was significantly superior to that of MTDX regarding the improvement in liver injury (Figure 3B) ($p < 0.05$).

Two enzymes, ALT and AST, are predominantly located within cells, especially the hepatocytes. Upon liver cell damage, those enzymes are released into the blood, resulting in abnormally elevated levels of serum ALT and AST, which are frequently utilized as clinical biomarkers for liver injury. The results demonstrated that the serum levels of ALT (Figure 3C) and AST (Figure 3D) were elevated significantly in ALD mice in contrast to the Ctrl group ($p < 0.05$). Inflammatory responses are usually accompanied by the production of inflammatory mediators. We further measured certain inflammatory cytokines in the serum, and the results showed that the levels of TNF-α (Figure 3E), IL-6 (Figure 3F), and IL-1β (Figure 3G) were increased ($p < 0.05$) in ALD mice. Notably, after treatment with LGS or MTDX, these serum indicators were all significantly improved, with LGS_M and LGS_H groups sowing the best efficacy.

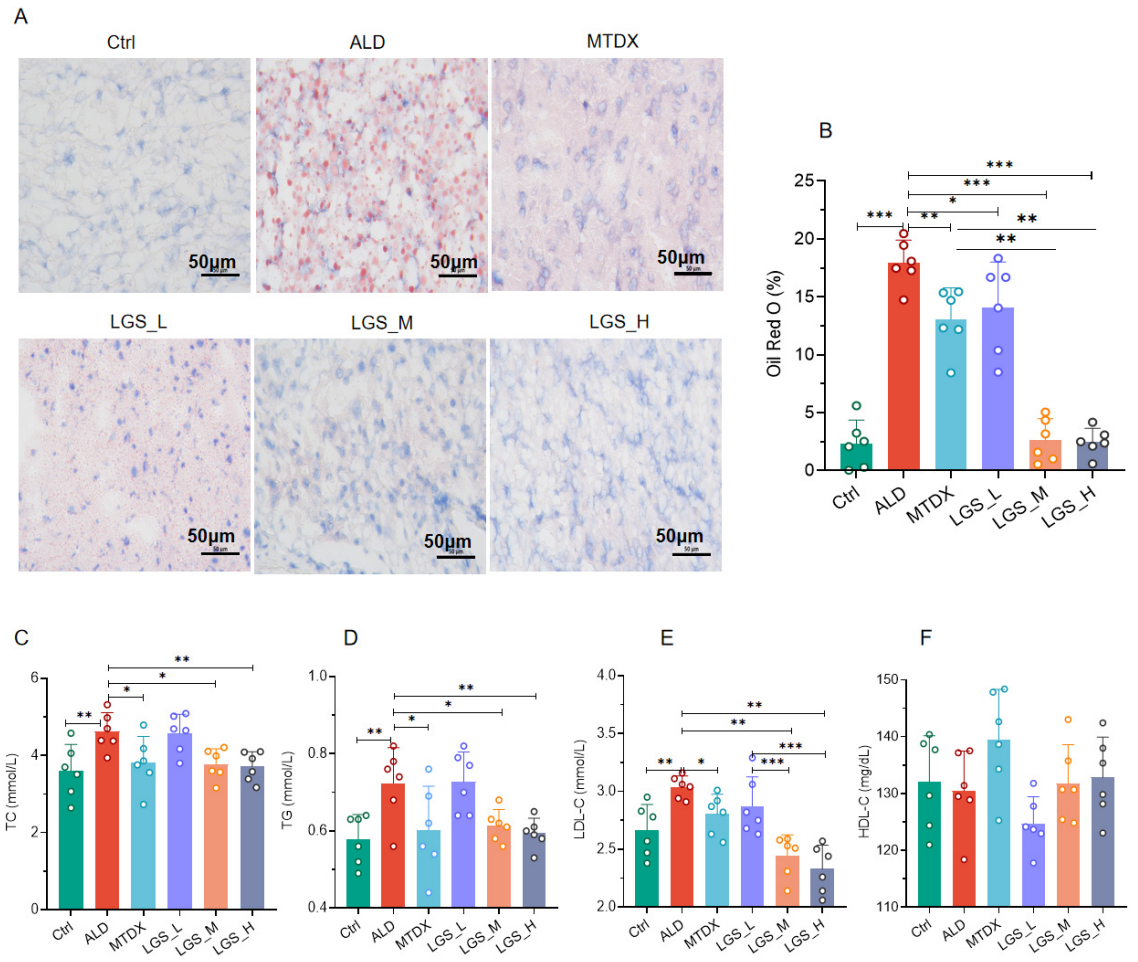

FIGURE 2
LGS ameliorates hepatic steatosis in ALD mice. **(A)** The effect of LGS on the Oil Red O staining of the livers of mice with ALD. **(B)** The proportion of the positive area of Oil Red O staining in the livers of mice in each group. **(C)** Serum TC of mice. **(D)** Serum TG of mice. **(E)** Serum LDL-C of mice. **(F)** Serum HDL-C of mice ($n = 6$, $^{*}P < 0.05$, $^{**}P < 0.01$, $^{***}P < 0.001$). One-way ANOVA followed by Tukey test was employed to evaluate differences among multiple groups.

Overall, LGS exerts a protective effect on liver injury and inflammation in ALD mice.

3.1.3 LGS enhances alcohol metabolism in ALD mice

The liver, as the primary metabolic organ, relies on the synergistic action of various enzymes. During the process of alcohol metabolism, three key enzymes (CYP2E1, ADH and ALDH) affect the rate of alcohol metabolism. In this study, we measured the activity of those enzymes related to alcohol metabolism to assess the impact of LGS on alcohol metabolism in Figure 4.

We detected the serum levels of CYP2E1 and observed that its activity was significant increased in ALD (Figure 4A) ($p < 0.05$), which was decreased by both MTDX and LGS ($p < 0.05$). This finding suggests that LGS may alleviate oxidative stress-induced damage caused by alcohol by inhibiting the activity of CYP2E1. Furthermore, In the ALD group, the activities of ADH (Figure 4B) and ALDH (Figure 4C) decreased significantly compared to the Ctrl group, and the intervention of the two drugs in the experiment could reverse this decline ($p < 0.05$) and this effect showed an increasing trend with the increase of LGS dosage. It was worth noted that for CYP2E1 and ALDH, the low-dose group also showed significant therapeutic effects, and LGS had better regulatory effects on the three enzymes above than MTDX, although there was no statistical difference. These results indicated that LGS may reduce the toxicity of alcohol to the liver by optimizing the enzyme catalysis in the metabolic process of alcohol.

In summary, our findings supported the potential application in promoting alcohol metabolism.

3.2 LGS maintains the intestinal epithelial barrier in ALD mice

The integrity of the intestinal barrier is crucial for preventing harmful substances and pathogens from entering the bloodstream. An analysis of the intestinal mucosal structure was conducted on mice from different groups using H&E and IHC staining, as depicted in Figure 5.

In the observation of intestinal tissue (H&E staining) (Figure 5A), the intestinal tissue structure of the Ctrl remained

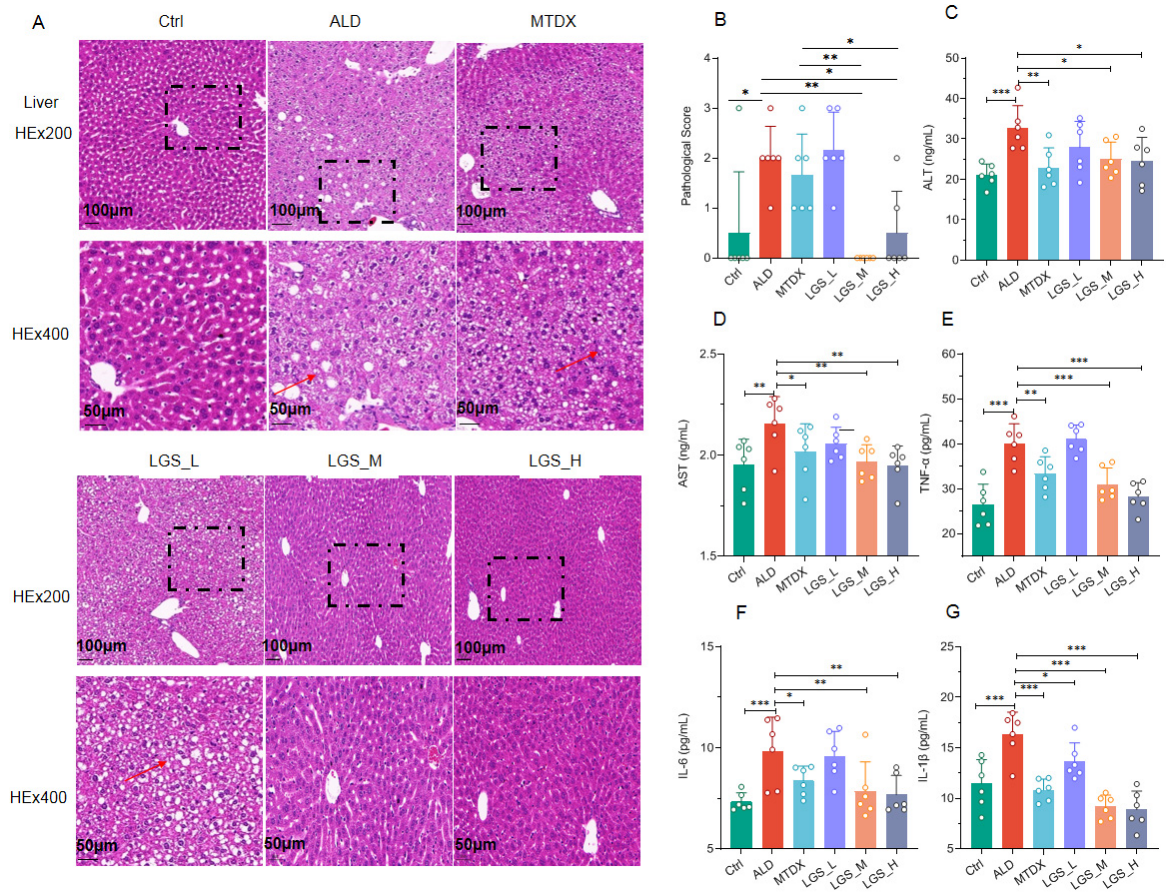

FIGURE 3
LGS ameliorates liver damage and inflammation in ALD mice. **(A)** Hematoxylin and Eosin (H&E) staining of mouse liver tissues at original magnifications of 200× and 400×. **(B)** Pathological scoring of H&E staining. **(C)** Serum ALT. **(D)** Serum AST. **(E)** Serum TNF-α in ALD mice. **(F)** Serum IL-6. **(G)** Serum IL-1β (n = 6, $^{*}P < 0.05$, $^{**}P < 0.01$, $^{***}P < 0.001$). One-way ANOVA followed by Tukey test was employed to evaluate differences among multiple groups.

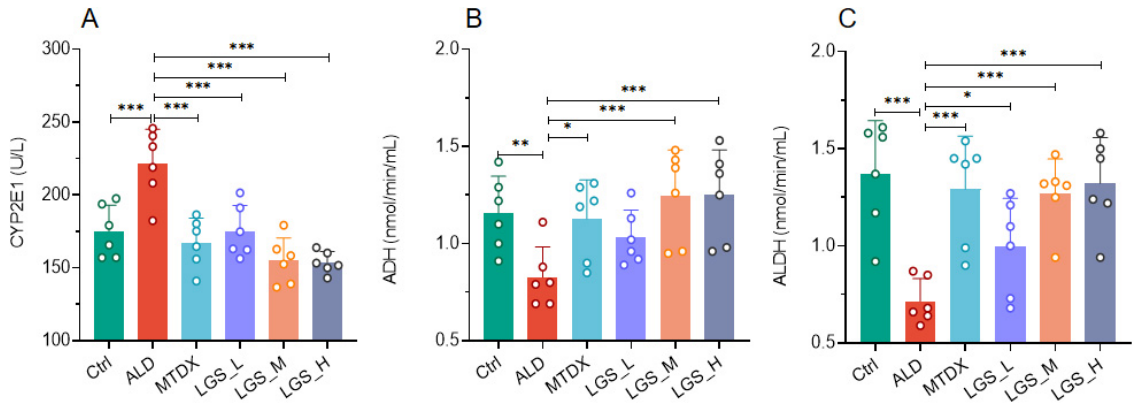

FIGURE 4
LGS enhances alcohol metabolism in a murine model of ALD. **(A)** The influence of LGS on CYP2E1 activity in ALD mice. **(B)** The influence of LGS on ADH activity in ALD mice. **(C)** The influence of LGS on ALDH activity in ALD mice (n = 6, $^{*}P < 0.05$, $^{**}P < 0.01$, $^{***}P < 0.001$). One-way ANOVA followed by Tukey test was employed to evaluate differences among multiple groups.

intact, including the mucosal layer, submucosal layer, muscular layer, and serosa, with no significant pathological changes observed. The intestinal mucosal layer and submucosal layer structures of the ALD group mice exhibited structural disruption, with localized involvement of the muscularis. In the mice of LGS_M and LGS_H, the intestinal tissue structure remained intact, with no significant pathological changes observed. The intestinal mucosal layer of the LGS_L group mice was damaged, and the crypt structure of

10.3389/fnut.2024.1495695

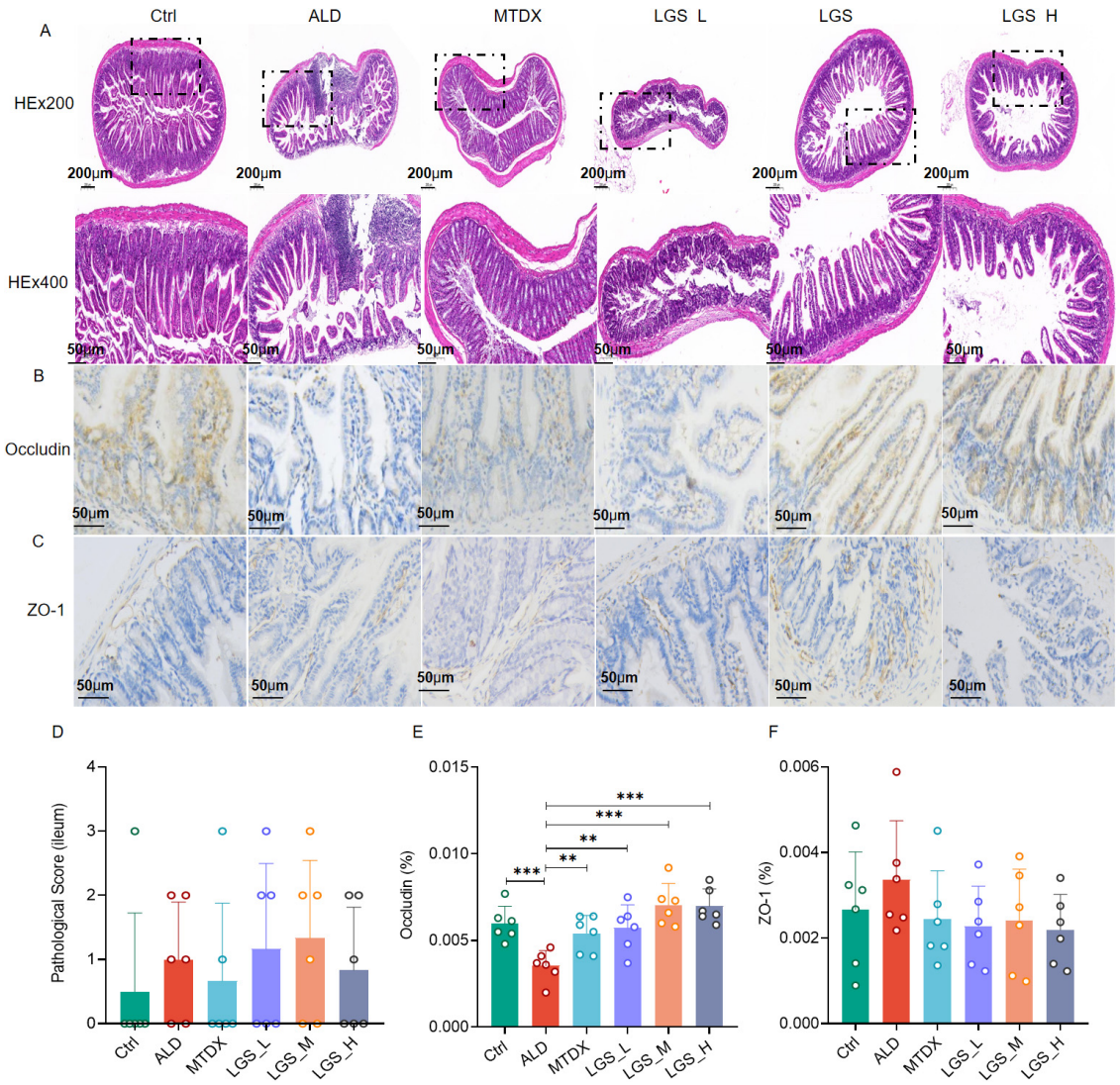

FIGURE 5
LGS ameliorates the intestinal epithelial barrier in ALD mice. **(A)** H&E staining of the ileum in mice at original magnifications of 100× and 400×. **(B)** Immunohistochemical staining for Occludin in the intestine at an original magnification of 400×. **(C)** Immunohistochemical staining for ZO-1 in the intestine at an original magnification of 400×. **(D)** Histopathological scoring of H&E staining in intestinal tissue. **(E)** Percentage of positive area expression for Occludin immunohistochemistry. **(F)** Percentage of positive area expression for ZO-1 immunohistochemistry ($n = 6$, $^{**}P < 0.01$, $^{***}P < 0.001$). One-way ANOVA followed by Tukey test was employed to evaluate differences among multiple groups.

the lamina propria showed disappearance or reduction. Further analysis of the expression of occludin (Figure 5B) and ZO-1 (Figure 5C) in the ileal tissue was performed, with the brown-yellow areas representing the positive expression areas. In Ctrl group, Occludin and ZO-1 distributed in the mucosa of the small intestine evenly, with a small amount in the submucosa. Compared with the Ctrl group, the brown-yellow area in the ALD group was reduced significantly, mainly in the mucosa. After LGS intervention, the area of Occludin positivity was increased and evenly distributed, while the changes of ZO-1 in each group were not obvious. These results indicated that the mucosal structure was damaged and the integrity of the mucosal barrier was affected in ALD mice. After LGS intervention, the expression of occludin at the top of the intestinal epithelium was increased. Although the H&E pathological scoring did not show a significant advantage of LGS in improving the intestinal barrier (Figure 5D), LGS significantly enhanced the expression of occludin in the ileal tissue of ALD mice (Figure 5E). During ALD, the expression level of ZO-1 in the intestine was not changed (Figure 5F).

These results suggest that the structural integrity of the intestine in ALD mice is damaged, and LGS may repair the intestinal epithelial barrier by upregulating the expression of the intestinal channel protein occludin.

3.3 LGS modulates gut microbiota structure in ALD mice

In order to investigate the impact of LGS on the gut microbiota of ALD mice, on the 21st day of the experiment, fecal samples were collected from mice in each group and subjected to 16S rRNA sequencing to observe the composition of fecal microorganisms. It

should be noted that the 16S sequencing depth can be represented by the coverage index in the Alpha diversity index (Supplementary Figure 1) or provided by the average sequencing data volume of the samples (Supplementary Table 1). The coverage for each sample is above 99.9%, indicating that the sequencing depth is sufficient for subsequent analysis. The analyzed results are presented in Figure 6.

The indices of α diversity, usually refer to the Chao index, the Shannon index, and the Simpson index, are paramount in quantifying the species richness and evenness within a population across various samples. β diversity, conversely, is an analytical approach grounded in the visual interpretation of distance matrices between samples, serving to assess the variances among groups. The closer the species composition, the shorter the distance, which is graphically represented in the PCoA plot, thereby revealing the clustering phenomena among different groups. Within the scope of this study, the curves of the Chao index, the Shannon, and the Simpson indices demonstrated saturation as the quantity of random sequencing increased (Supplementary Figure 2), the α diversity in the ALD group was significantly reduced when juxtaposed with the control group ($p < 0.05$). Comparatively, this reduction was reversed following intervention with LGS. The effects of the medium and high dosage groups were more pronounced than that of the low dosage group, with the medium dosage group exhibiting a more robust recovery (Figures 6A–C). The control group and the alcohol intervention group were distinctly separated in the PCoA plot (Figure 6D), indicating the differences in the gut microbiota structure among the groups (Figure 6E). These findings suggested a decrease in the gut microbiota diversity in ALD mice, and that LGS can, to a certain extent, restore the diversity of their gut microbiota.

This study conducted an in-depth analysis of the phylum-level microbial composition of the murine gut microbiota. The findings revealed that the gut microbiota of mice was predominantly composed of the phyla Firmicutes, Bacteroidetes, Verrucomicrobia, Actinobacteria, and Proteobacteria, with Firmicutes and Bacteroidetes occupying a dominant position (Figure 6F), which is consistent with previous research findings (1). At the phylum level, in comparison to Ctrl, the ALD exhibited an enrichment of Firmicutes (Figure 6G) ($p < 0.05$) and a relative reduction in Bacteroidetes (Figure 6H) ($p < 0.05$), resulting in an elevated F/B ratio ($p < 0.05$). Furthermore, Verrucomicrobia and Actinobacteria displayed an increasing trend, while the phylum Desulfurococcales showed a decreasing trend, although these differences were not statistically significant. These findings corroborate some current studies (17–19), yet contradict others (20, 21). Following the intervention with LGS and MTDX, a significant reduction in Firmicutes was observed in LGS_M and LGS_H groups, with a re-enrichment of Bacteroidetes across all groups, particularly in LGS_M and LGS_H groups ($p < 0.05$). Proteobacteria showed an enrichment (Figure 6I) ($p < 0.05$), and the F/B ratio was reduced (Figure 6J) ($p < 0.05$). The results of this study indicated that the dysbiosis in the gut microbiota of ALD mice primarily occurred in the phyla of Bacteroidetes and Firmicutes.

Further analysis revealed that within the Bacteroidetes (Supplementary Figure 3A), the genus *Muribaculaceae* and *Alloprevotella* were predominant, while within the *Firmicutes* (Supplementary Figure 3B), the genera *Faecalibaculum, Dubosiella, Monoglobus,* and *Lactobacillus* were the main constituents. The Ctrl group was characterized by the predominance of the genus *Muribaculaceae*, whereas the ALD group was dominated by the *Faecalibaculum*, which also maintained a considerable proportion in the alcohol-fed groups. Notably, the genus *Lactobacillus* was enriched in the Ctrl group but showed a decrease following alcohol intervention, suggested that it may be beneficial for ALD (22). Additionally, in the MTDX group, the genus *Dubosiella* was enriched. Those findings suggested that the gut microbiota of ALD mice was disordered, characterized by an increased abundance of Firmicutes, represented by *Faecalibaculum*, and a significant reduction of Bacteroidetes, represented by the *Muribaculaceae*. Moreover, LGS intervention ameliorated the gut microbiota dysbiosis in ALD mice.

To further investigate the impact of LGS on the microbial structure of mice in each group, the composition of the gut microbiota at the genus level, and LEfSe Analysis (LDA = 3.5, $n = 6$) were employed to compare the microbial structures among the groups in Figure 7.

The top 10 genera in abundance are shown in Figure 7A. Utilizing LEfSe analysis (LDA = 3.5, $n = 6$), we compared the microbial structures of different groups of mice, noticed potential biomarkers among groups (Figures 7B, C). In Ctrl, biomarkers mainly included *g_norank_f_Muribaculaceae*. Besides *g_Prevotellaceae_UCG-001, g_Lachnospiraceae_NK4A136_group* were abundant in the Ctrl group and may play a positive role in maintaining the balance of the gut microbiota and host health. Conversely, the *g_Faecalibacterium,* and *g_Enterococcus* were identified in the ALD group, which may be associated with the development of ALD. In the intervention groups, we found that *g_Dubosiella,* and *g_Romboutsia* in MTDX group, while the LGS_L was characterized by *g_Bacillus*. The biomarkers for the LGS_M included *g_Escherichia-Shigella,* and *g_Bacteroides*. The biomarkers for the LGS_H were *g_Alloprevotella,* and *g_Erysipelatoclostridium*.

A further comparison and analysis of the contents of various bacterial genera among the groups showed that LGS may against ALD by suppressing or enriching specific bacterial genera in Figure 8. We found some unique microbial genera, appeared only in specific groups, may play an important role in the microbial composition or have specific functions in Supplementary Table 2.

Initially, the *g_norank_f_Muribaculaceae* (Figure 8A) ($p < 0.05$), *g_Bacteroides* (Figure 8B), *g_Alistipes* (Figure 8C), *g_Prevotellaceae_UCG-001* (Figure 8D) ($p < 0.05$) decreased in the ALD compared with Ctrl group, which may be related to the imbalance of the gut microbiota in ALD mice. However, after LGS intervention, the abundance of these genera rebounded, indicated that LGS may restore the balance of the gut microbiota targeting these genera. Furthermore, the *g_Faecalibaculum* (Figure 8E), *g_Romboutsia* (Figure 8F), *g_norank_f_Eggerthellaceae* (Figure 8G), and *g_Enterococcus* (Figure 8H) were significantly enriched in the ALD group, and may be related to the pathogenesis of ALD. After LGS intervention, the abundance of these genera was reversed, indicating that LGS may alleviate the pathological process of ALD by regulating their abundance. Additionally, it was also noted that some unique genera appeared or became enriched in association with LGS, such as *Alloprevotella* (Figure 8I), *Monoglobus* (Figure 8J), *Erysipelatoclostridium* (Figure 8K), *Parasutterella* (Figure 8L), *Harryflintia* (Figure 8M), and *unclassified_c_Clostridia* (Figure 8N), which only increased after LGS intervention ($p < 0.05$), and these genera might have been specifically targeted by LGS.

10.3389/fnut.2024.1495695

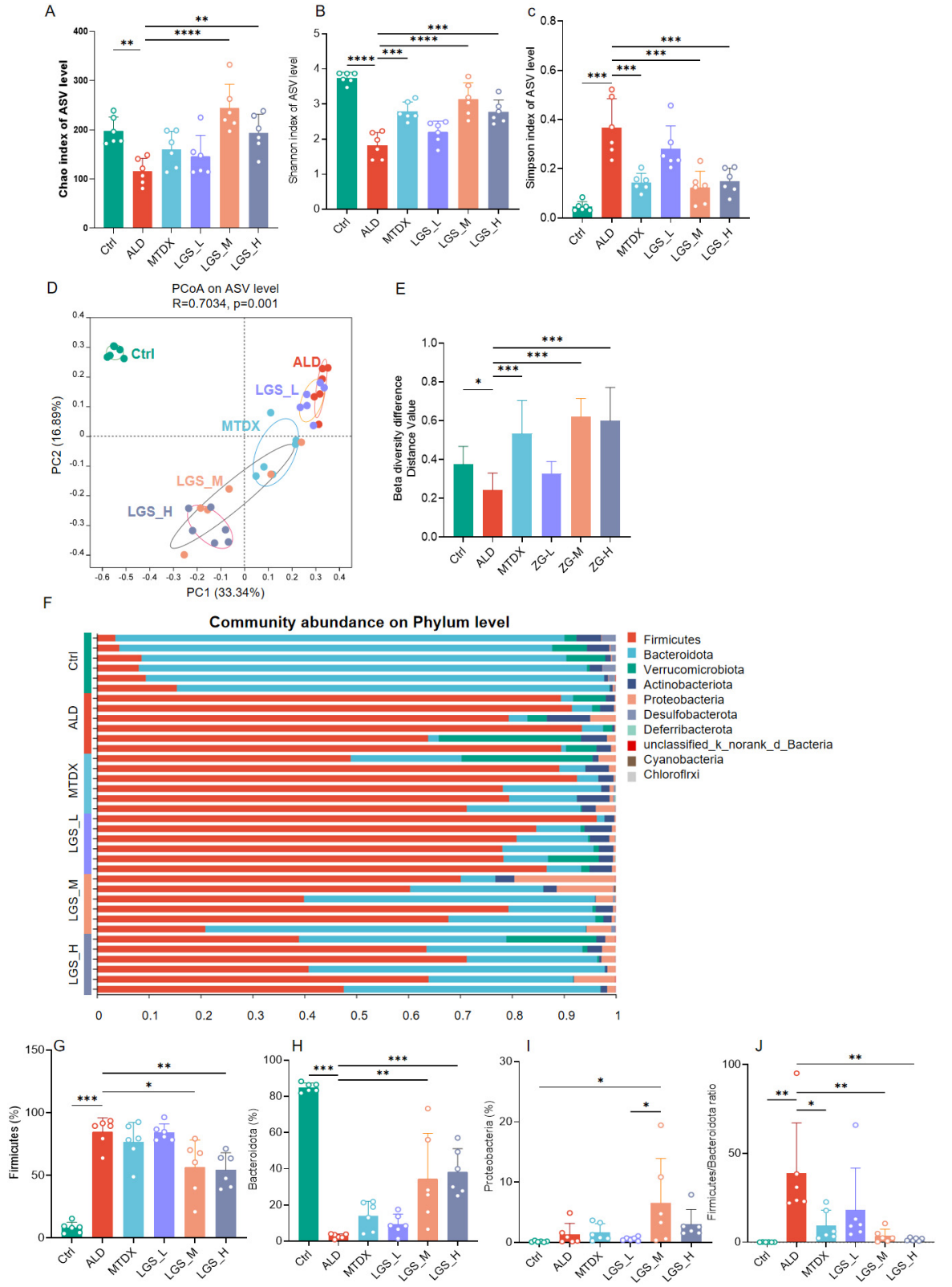

FIGURE 6

LGS improves the diversity of the gut microbiota in ALD mice and reduces the ratio of Firmicutes to Bacteroidetes. **(A)** Chao index. **(B)** Shannon index. **(C)** Simpson index. **(D)** Principal coordinates analysis (PCoA). **(E)** Differences in β diversity among groups. **(F)** Composition at the phylum level across groups (top ten abundance). **(G)** Differences of Firmicutes among groups. **(H)** Differences of Bacteroidetes among groups. **(I)** Differences of Proteobacteria among groups. **(J)** Differences of F/B (the ratio of Firmicutes to Bacteroidetes) among groups (n = 6, *P < 0.05, **P < 0.01, ***P < 0.001, ****P < 0.0001). One-way ANOVA followed by Tukey test was employed to evaluate differences among multiple groups.

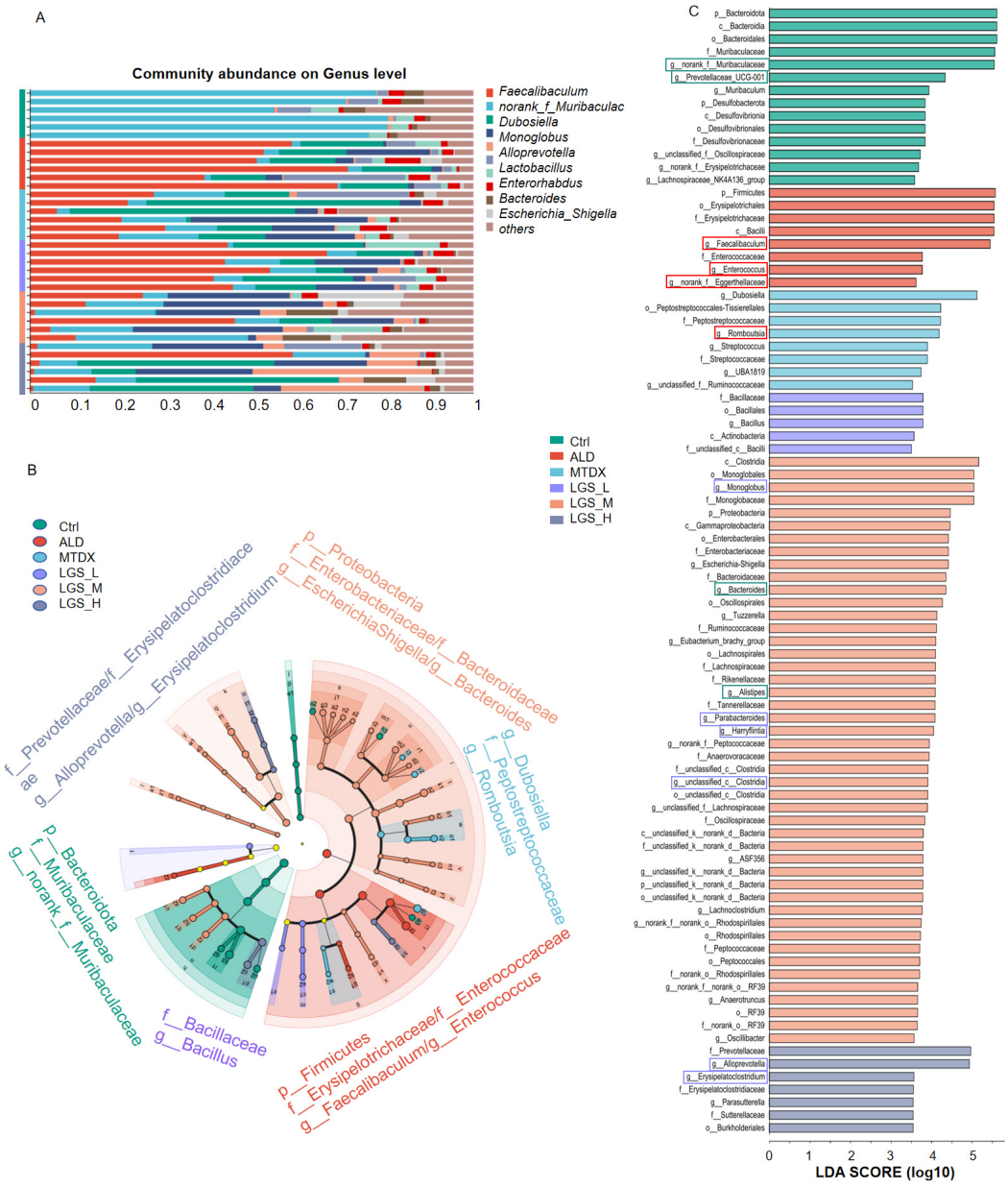

FIGURE 7
LGS improves the composition of the gut microbiota at the Genus Level in ALD mice. **(A)** Composition of the Intestinal Microbiota at the Genus Level among groups. **(B)** Multilevel Species Hierarchical Tree Diagram Linear Discriminant Analysis Effect Size (LDA = 3.5, n = 6). **(C)** LEfSe Analysis among groups. The green box indicates a decrease in ALD and an increase after LGS intervention, the red box indicates an enrichment in ALD and a decrease after LGS intervention, and the purple box indicates an increase only in the LGS group.

Overall, LGS regulated gut microbiota in mice through restoring ALD-mediated microbial changes and specifically inducing some gut microbes.

3.4 LGS promotes hexanoic acid production and regulates GPR43/GLP-1 pathway in ALD mice

SCFAs are the metabolic products of the gut microbiota and are closely related to ALD. In this study, the content and composition of SCFAs in the cecal contents of mice were determined by GC-MS in Figure 9.

In the study of SCFAs (Figures 9A–H), it was observed that the levels of various SCFAs in the cecum of mice in the ALD group were decreased. The administration of LGS restored the content of SCFAs in the cecal contents. Further analysis revealed that the levels of propionic acid (Figure 9B), butyric acid (Figure 9C), isobutyric acid (Figure 9D), and hexanoic acid (Figure 9G) were significantly reduced opposed to the Ctrl group ($p < 0.05$). After treatment, there was a certain degree of recovery in the levels of the aforementioned SCFAs, with a statistically significant improvement observed in the recovery of hexanoic acid ($p < 0.05$). The propionic

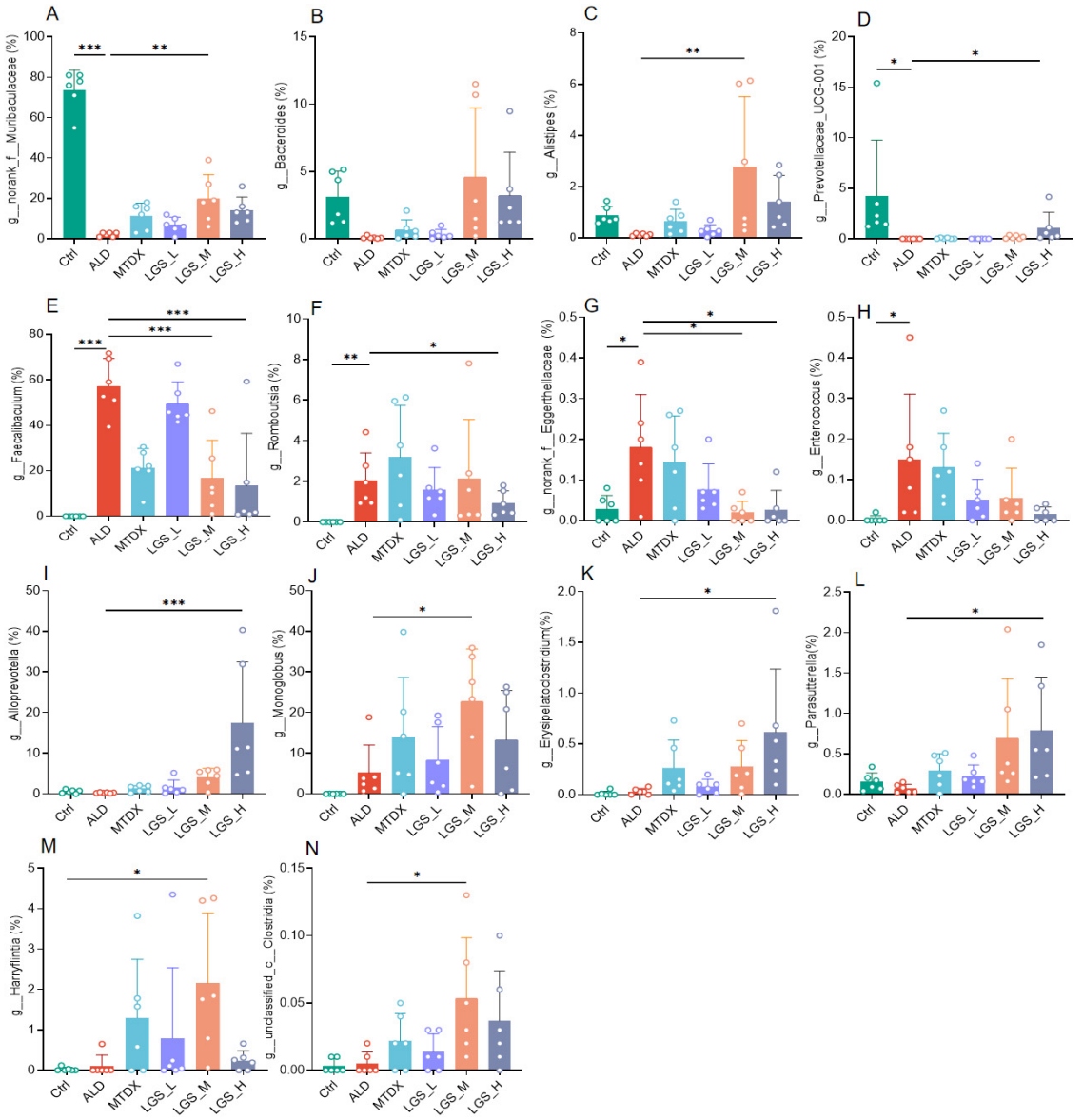

FIGURE 8
LGS intervention specifically alters gut microbes in ALD mice. **(A)** Differences of *g_norank_f_Muribaculaceae* among groups. **(B)** Differences of *g_Bacteroides* among groups. **(C)** Differences of *g_Alistipes* among groups. **(D)** Differences of *g_Prevotellaceae_UCG-001* among groups. **(E)** Differences of *g_Faecalibaculum* among groups. **(F)** Differences of *g_Romboutsia* among groups. **(G)** Differences of *g_norank_f_Eggerthellaceae* among groups. **(H)** Differences of *g_Enterococcus* among groups. **(I)** Differences of *g_Alloprevotella* among groups. **(J)** Differences of *g_Monoglobus* among groups. **(K)** Differences of *g_Erysipelatoclostridium* among groups. **(L)** Differences of *g_Parasutterella* among groups. **(M)** Differences of *g_Harryflintia* among groups. **(N)** Differences of *g_unclassified_c_Clostridia* among groups ($n = 6$, $^*P < 0.05$, $^{**}P < 0.01$, $^{***}P < 0.001$). One-way ANOVA followed by Tukey test was employed to evaluate differences among multiple groups.

acid content was also remarkably increased in LGS group, however, no statistical difference was found. The results suggested that LGS increased the total acid content in the intestinal tissue of ALD mice and restored the levels of various SCFAs, especially the hexanoic acid.

GLP-1 is an important target of SCFAs, and SCFAs can stimulate the release of GLP-1 from intestinal epithelial cells through the GPR43 pathway (23, 24), to improve liver fat deposition (25, 26). Western blot analysis in the ileal tissue showed a significant reduction in the expression of intestinal GPR43 in ALD mice (Figure 9J) ($p < 0.05$), which reversed by LGS ($p < 0.05$), which was confirmed again in PCR detection (Figures 9K, L). Concurrently, the detection of serum GLP-1 content showed changes consistent with GPR43 (Figure 9M), which was significantly reduced in the ALD group and could be increased by MTDX and LGS. However, the extent to which MTDX increased was similar to that of the low-dose LGS. The medium and high doses of LGS were able to restore the GLP-1 content to a level comparable to that of the Ctrl group, and the LGS_H group was superior to the MTDX group. Therefore, LGS may exert an anti-ALD effect through the hexanoic acid/GPR43/GLP-1 pathway.

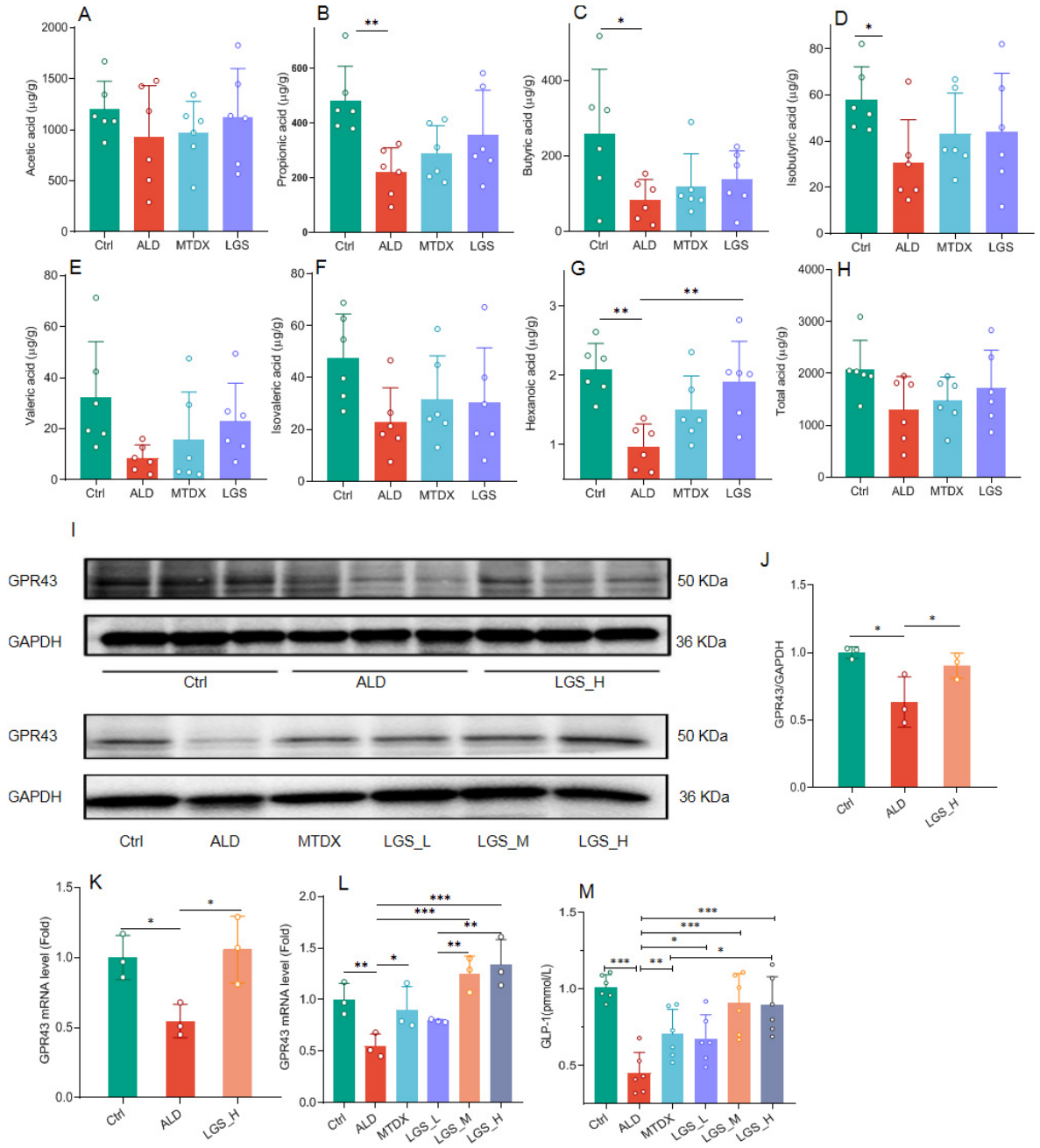

FIGURE 9
The influence of LGS on the SCFAs/GPR43/GLP-1 pathway in ALD mice. **(A)** The effect of LGS on the cecal content of acetic acid among groups. **(B)** The effect of LGS on the content of propionic acid among groups. **(C)** The effect of LGS on the content of butyric acid among groups. **(D)** The effect of LGS on the content of isobutyric acid among groups. **(E)** The effect of LGS on the content of valeric acid among groups. **(F)** The effect of LGS on the content of isovaleric acid among groups. **(G)** The effect of LGS on the content of hexanoic acid among groups. **(H)** The effect of LGS on the content of total acid among groups. **(I)** Detection of the expression of GPR43 in mouse ileal tissue by Western blot. **(J)** Semi-quantitative analysis of the expression of GPR43 in mouse ileal tissue of Western Blot. **(K,L)** Quantitative analysis of the expression of *GPR43* in mouse ileal tissue of qPCR. **(M)** The concentration of serum GLP-1 (n = 6, $^{*}P < 0.05$, $^{**}P < 0.01$, $^{***}P < 0.001$). One-way ANOVA followed by Tukey test was employed to evaluate differences among multiple groups.

4 Discussion

In this study, the anti-ALD effect of LGS and its possible mechanism was investigated by the ALD murine model mice treated with LGS. Our results highlight that LGS exerts a remarkable protective effect on ALD mice through the gut microbiota mediated hexanoic acid/GPR43/GLP-1 pathway (Figure 10).

The pathogenesis of ALD is complex, and has yet been fully understood (27). Chronic alcohol consumption can lead to the development of ALD, potentially driven by metabolic and immunologic factors induced by alcohol and its metabolites,

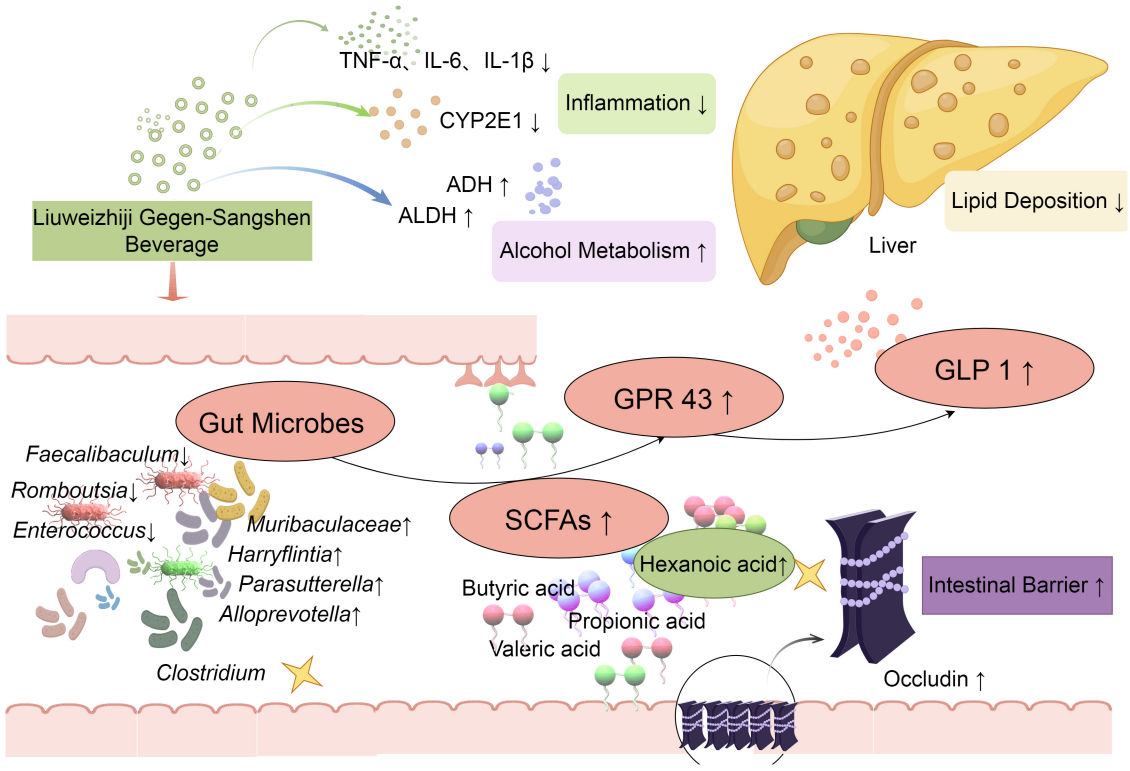

FIGURE 10
LGS protects against ALD in mice through the gut microbiota mediated SCFAs/GPR43/GLP-1 pathway. Levels of ALT, AST, TNF-$^{\alpha}$, IL-6, and IL-1β were decreased by LGS to mitigate alcoholic liver injury in mice. The activity of ethanol metabolism enzymes, ALDH and ADH, was enhanced, which improved the capacity for alcohol metabolism. The function of maintaining intestinal barrier was well preserved by LGS through reducing epithelial damage and increasing the expression of Occludin. Moreover, the structure of the gut microbiota in mice with alcoholic liver disease was significantly modulated by LGS, which restored alcohol-induced microbial alterations, specifically mediated the enrichment (*Muribaculaceae, Alloprevotella, Parasutterella, Harryflintia*), the suppression (*Faecalibaculum, Romboutsia, Enterococcus*), or the production (*Clostridium*). Further research indicated that the production of SCFA (hexanoic acid) in the cecum was increased by LGS, which promoted the increase of ethanol-mediated ileal GRP43 expression and increased the levels of serum GLP-1 to reduction of lipid deposition in the liver.

including reactive oxygen species (ROS) and proinflammatory cytokines (28). Specifically, alcohol exposure boosts the activity of the hepatic CYP2E1 enzyme, which increases ROS production, causing hepatic mitochondrial dysfunction, and stimulates *de novo* lipogenesis (28). Additionally, damage- and pathogen-associated molecular patterns activate specific receptors in non-parenchymal liver cells, such as Kupffer cells, hepatic stellate cells (HSCs), and lymphocytes, causing hepatocyte death and the infiltration of proinflammatory cells like neutrophils and macrophages into the liver (29). Various forms of hepatocyte death, including apoptosis, necroptosis, pyroptosis, and ferroptosis, have been reported to coexist in ALD (29). In severe cases, such as cirrhosis and severe alcohol-associated hepatitis, there is a significant hepatocyte degeneration. Liver sinusoidal endothelial cell dysfunction also contributes to ALD development. Furthermore, alcohol promotes global protein acetylation, disrupting clathrin-mediated endocytosis, a process that affects the uptake of macromolecules and the trafficking of receptor-ligand complexes, leading to metabolic imbalance (30).

Organ crosstalk has also emerged as a significant issue in ALD. Chronic alcohol intake disrupts the gut microbiome and its barrier function, allowing endotoxin leakage into the portal circulation and facilitating the transfer of triglycerides from adipose tissue to the liver through lipolysis (28). Notably, alterations in gut microbiota play a crucial role in the pathogenesis of ALD, as alcohol-induced changes in gut microbe compromise the intestinal epithelial barrier and trigger proinflammatory mediators.

Currently, no effective drugs for the treatment of ALD have been approved, highlighting the urgency of finding new therapeutic approaches (28). Some of drugs and therapies have been evaluated in clinical trials (Table 1), mainly targeting hepatocyte death and regeneration, inflammation and gut microbiome. In particular, fecal microbiota transplantation as well as some of probiotics have shown promising results in alleviating ALD in human. Therefore, targeting the gut microbiota presents new prospect in ALD treatment.

The present study focused on a Chinese medicine-derived herbal beverage, LGS. LGS, composed of six herbal components that are both edible and medicinal, was not observed to exhibit clear toxic side effects in previous clinical applications, offering a novel therapeutic choice for ALD. Previous studies (7–10) have demonstrated that LGS protected against ALD rats through alleviation of lipid metabolism and relief of inflammation in liver via regulating several signaling pathways. In LO-2 cells, LGS was found to inhibit ROS through regulating CYP2E1 and enhance alcohol metabolism through increasing ADH1 and ALDH2 expression (11). However, whether LGS had an impact on gut microbiota remains unexplored. Our previous report

TABLE 1 Ongoing trails for ALD and the targets.

Candidate drug	Targets	Status	References
IL-22 agonist (F-562)	Targeting hepatocyte death and regeneration	Ongoing phase IIb trials	(31)
IL-1R inhibitor	Antiinflammation	Ongoing phase II trial	(32)
Anti-LPS (hyperimmune bovine colostrum enriched with IgG)	Antiinflammation	Ongoing phase IIa clinical trial	NCT01968382
ASK-1 inhibitor (selonsertib GS-4997)	Targeting apoptosis	No benefits from a phase IIa trial	NCT02854631
Metadoxine	Anti-ROS	Short-term survival benefit	(33)
Microbiome and gut-liver axis	Healthy donor fecal microbiota transplantation (FMT)	A randomized clinical trial revealed survival benefit at 90 days in patients with severe alcoholic hepatitis	(34)
Microbiome and gut-liver axis	*Lactobacillus casei*	Improve lipid metabolism and regulate intestinal flora disorders in patients with alcoholic liver injury	(35)
Microbiome and gut-liver axis	*Lactobacillus subtilis/Streptococcus faecium*	Restoration of bowel flora and improvement of LPS in patients with alcoholic hepatitis	(36)
Microbiome and gut-liver axis, anti-ROS, improving alcohol metabolism	LGS	Improve lipid metabolism and inflammation	(7–10) and Current research

demonstrated that LGS mainly contained polyphenols, flavonoids and polysaccharides (12). Notably, the LGS polysaccharides have shown specific modulation *in vitro* on certain gut microbes that were potentially beneficial to health. Therefore, it is of our primary interests to investigate the impact of LGS on the gut microbiota and gut-liver axis.

As AFL and ASH were identified as the most prevalent clinical phase among patients with excessive alcohol consumption, and as the initial stage of ALD, recognized for its theoretical reversibility in treatment, the murine ALD model was established by the NIAAA method in our study to fit this stage of the disease. And we confirmed that in ALD mice, alcohol intake led to hepatic steatosis, elevated liver function tests, and serum inflammatory mediators. After the intervention of LGS, the aforementioned indicators were reversed, which confirmed the effectiveness of LGS for ALD via attenuating liver steatosis and injury (decreased AST, ALT, TC, TG and HDL-C, increased LDL-C, and alleviated histopathological scores in liver), relieving inflammation (decreased TNF-α, IL-6, and IL-1β) and enhancing alcohol metabolism (increased ADH and ALDH, and reduced CYP2E1 activity). These findings were consistent with previous reports based on rat ALD models.

Importantly, we newly found in the present study that LGS exerted a profound role in regulating the gut microbiota and the gut-liver axis. LGS effectively maintained the function of the intestinal barrier by reducing epithelial damage and increasing the expression of Occludin. In the analysis of the gut microbiota, it was observed that the F/B ratio in ALD mice significantly increased, which is consistent with the biological markers of obesity (37). The intervention of LGS not only reversed this change but also specifically mediated the enrichment of several bacterial genera, which have been proven to be associated with intestinal inflammation and lipid metabolism, potentially becoming the potential targets of LGS action. In particular, supplementation with LGS specifically mediated enrichment of several bacterial genera (*Alloprevotella, Monoglobus, Erysipelatoclostridium, Parasutterella, Harryflintia* and *unclassified_c_Clostridia*).

In the intestinal tract of mammals, the phyla Firmicutes and Bacteroidetes are identified as the two predominant bacterial phyla, the ratio of which, known as the F/B ratio, serves as an important indicator for assessing the balance of the gut ecosystem (1). Further analysis revealed that *Faecalibacterium* within the phylum Firmicutes and the *Bacteroidaceae* within the phylum Bacteroidetes are key microbial groups influencing the gut ecology. *Muribaculaceae* were found to be significant. Recent research has confirmed that both of them are known to produce SCFAs, and *Muribaculaceae* is negatively correlated with liver function abnormalities (38).

The *Alistipes* genus, which is negatively correlated with the occurrence of liver fibrosis and colitis (39). *Prevotellaceae_UCG-001* has been shown to improve colitis induced by *Clostridium* difficile (40), and its enrichment in the gut is associated with the significant improvement of abnormal liver lipid metabolism related to Type 2 Diabetes Mellitus by Jerusalem artichoke (41). *Alloprevotella*, which may play an important role in improvements of liver functions and reduction of colitis susceptibility (42). This suggested that they may alleviate pathological changes in ALD by regulating liver lipid metabolism and producing anti-inflammatory substances. In our experiments, these microbial communities were reduced in ALD, and notably increased following intervention with LGS, which corroborated their beneficial effects on alcoholic liver disease.

Regarding some of the genera that significantly enriched in ALD, they were notably suppressed following intervention with LGS or MTDX. The *Romboutsia*, a Gram-positive bacterium, has been identified as non-alcoholic steatohepatitis marker in the progression of non-alcoholic fatty liver disease (NAFLD) (43). Given the similarities between NAFLD and ALD in terms of liver fat accumulation and inflammation, *Romboutsia* may play a similar role in ALD. The *Eggerthellaceae* genus is positively correlated with the total gastrointestinal symptoms (including constipation) in children with autism spectrum disorder (44) and negatively correlated with the levels of Claudin 3 in patients with

cirrhosis (45). Cirrhosis is one of the severe complications of ALD, indicating that *Eggerthellaceae* may affect the progression of ALD by influencing the intestinal barrier function and liver inflammatory response. Furthermore, the *Enterococcus* genus may improve dextran sulfate sodium-induced colitis by increasing acetate production, reducing butyrate production, and regulating the expression of GPR43 (46). Overall, these genera may affect the progression of ALD by influencing the balance of gut microbiota, liver metabolism, and inflammatory responses through various mechanisms.

We have also noted some genera enriched in the LGS group, such as *Monoglobus* and *Erysipelatoclostridium*. *Monoglobus* is a pectin-degrading bacteria. LGS contained rich pectic polysaccharides, which may lead to enrichment of the pectin-degrading *Monoglobus*. It is reported that the *Erysipelatoclostridium* genus is associated with obesity (47) and is related to a lower risk of intrahepatic cholestasis of pregnancy (ICP) (48). The *Erysipelatoclostridium* plays a protective role in cirrhosis and primary biliary cholangitis (PBC) (49). Similarly, *Parasutterella, Harryflintia* and *Clostridia,* have been found to be negatively associated with ALD, sugar and fat metabolism, or intestinal inflammation (50–55). In terms of quantity, those genera only predominated after the LGS intervention.

Gut microbiota plays an important role in host health through generation of metabolites (56). The main microbial products include fermentation products (SCFAs, branched SCFAs), bile acid metabolites (secondary bile acids), amino acids degradants (indole), bacterial proteins and products (LPS, Amuc 1100), bioactive lipids (12-hydroxyeicosatetraenoic acid), and exosomes (57). These molecules can act on various host cell receptors, such as toll-like receptors (TLRs), peroxisome proliferator-activated receptor alpha (PPARα), aryl hydrocarbon receptor (AhR), G-protein-coupled receptors (e.g., GPR41/43/119 and TGR5), and endocannabinoid receptors, to regulate host signaling pathways and impact physiological functions such as the intestinal barrier, immune function, insulin resistance and host metabolism (57). Under conditions of gut barrier disruption, the bacteria can translocate into liver via portal vein and trigger host immune response.

The SCFAs, primarily comprising acetic acid, propionic acid, and butyric acid, have been identified as the principal end products of gut microbial fermentation. Indeed, they have been demonstrated to confer benefits not only to intestinal health but also to hepatic protection through modulation of energy metabolism, inflammatory responses, and lipid metabolism (58–60). However, the SCFAs were typically found in lower abundance in ALD, which was consistent with our experimental findings (61). After LGS intervention, the content of SCFAs increases, which is related to the enrichment of bacteria producing SCFAs in the gut microbiota, such as *Muribaculaceae, Alloprevotella, Parasutterella* and *Harryflintia* (62–65). In addition, *Romboutsia* was found to be potentially associated with the decrease in SCFAs, and it was inhibited after LGS intervention (66). The production of SCFAs required dietary fiber as a substrate, but *Enterococcus* population was reduced due to the decrease in dietary fiber (67). It is noteworthy that after the intervention of LGS, the levels of various SCFAs did not significantly rebound as we had expected, which may be related to the primary production by the *Firmicutes*, a phylum that enriched in the context of ALD. The improvement of hexanoic acid was not negligible, indicated that although valeric acid and hexanoic acid are present in low quantities among SCFAs, they are still worth further exploration and may play a pivotal role in certain aspects.

Valeric acid and hexanoic acid, strictly speaking, are medium-chain fatty acids, yet they appear in studies related to SCFAs. Valeric acid, is closely related to the body's energy metabolism as a direct form of energy storage. It has been demonstrated to ameliorate the impaired glucose homeostasis and insulin sensitivity in type 2 diabetes patients (68), showing a negative correlation with HDL-C (69). Hexanoic acid was produced by *Clostridium* (70, 71), which mainly utilized ethanol and glucose as substrates and grew anaerobically with ethanol and acetic acid as the only energy sources (72). Additionally, *norank_f_Muribaculaceae* (73), *Eubacterium*, *Ruminococcaceae*, and *Lachnospiraceae* (74) involved in the production of hexanoic acid (75). As the only saturated fatty acid that increases blood sugar levels (76), hexanoic acid has been confirmed that the inhibition of α-amylase activity is achieved, which has a clear effect on lowering postprandial blood glucose levels (77). On the one hand, it can promote appetite and weight gain; on the other hand, as a medium-chain fatty acid, it has a tendency to promote balanced metabolism, maintain optimal insulin sensitivity, and even promote the basal and insulin-dependent phosphorylation of the Akt-mTOR pathway (78). The deficiency of hexanoic acid was found to be associated with neurological disorders such as cognitive impairment (79–81). In studies related to SCFAs, some research suggests that low levels of hexanoic acid are associated with intestinal damage (74, 82). Oppositely, another study found that medium-chain fatty acids, represented by hexanoic acid, promote intestinal inflammatory responses, while SCFAs, represented by butyric acid, restore the intestinal barrier in pregnant women with diabetes (83).

GPR43 has been identified as one of the downstream receptors of SCFAs (23, 84, 85), and can be activated by hexanoic acid directly (86). Then activation of GPR43 is coupled with the downstream Gq/11 and Gi/G0 signaling pathway (87). The secretion of GLP-1 is triggered (23), which promotes glucose uptake and thereby improves glucose homeostasis within the body (24). The GPR43/GLP-1 axis has been recognized for its role in promoting insulin secretion and inhibiting glucagon secretion (88). Some studies also demonstrated that GPR43 specifically activated by SCFAs in the M2 macrophages facilitated the maintenance of gut barrier function (89). For the liver, GLP-1 has been found to inhibit the deposition of liver fat (90), and further research has confirmed that its antagonists may be beneficial for the treatment of NAFLD (91). In addition, GLP1/GLP1R were found to affect cell apoptosis (92), oxidative stress (93), inflammatory responses (94, 95), and even autophagy (96) and membrane transport (97) through multiple pathways, suggesting that LGS might influence the aforementioned mechanisms by modulating GLP1/GLP1R. It is showed that pre-treatment with liraglutide (a GLP-1 analog) significantly inhibited the M1 polarization of macrophages during liver ischemia-reperfusion injury (95). Combined with our experimental results, LGS has been shown to increase the content of SCFA (hexanoic acid) within the intestinal tract, along with enhanced expression of GPR43. The secretion of GLP-1 was also increased. Therefore, LGS treatment was able to specifically regulate gut microbiota (increased *Muribaculaceae, Alloprevotella, Parasutterella* and *Harryflintia*) to generate SCFA

(hexanoic acid) which activated GPR43. The activated GPR43 is believed to maintain gut barrier function and improve glucose homeostasis through GLP-1.

In summary, LGS exerts a significant protective effect on ALD mice through the gut microbiota-mediated production of hexanoic acid and activating GPR43/GLP-1 pathway, which might contribute to the maintenance of host glucose homeostasis and gut barrier function. Taken together with previous reports, LGS might be an effective treatment for ALD through multiple targets involving anti-inflammation, modulation of lipid and alcohol metabolism and gut microbiota, which may be attributable to its varied constituents of polyphenols, flavonoids and polysaccharides.

4.1 Research prospects and limitations

The model employed in this study was found to be more suitable for the early stages of AFL and AH in ALD. Although several targets within the gut-liver axis had been identified in the study, such as the gut microbiota (*Muribaculaceae, Alloprevotella, Parasutterella and Harryflintia*), SCFAs (*hexanoic acid*), and GPR43/GLP-1, the specific mechanisms, especially those delving into the cellular level, still required further research for validation. For instance, fecal transplantation can be performed to validate the role of gut microbiota regulation. GPR43 knockout mice can be used for validation of its role. The affected microbial strains can be further confirmed for ALD protection. In addition, the exploration of constituents of LGS would benefit for understanding the active fractions.

5 Conclusion

In summary, the findings of this study lead us to conclude that LGS has a definite protective effect on ALD mice. Consistent with previous reports, LGS alleviated liver steatosis, attenuated liver injury and inflammation and enhanced alcohol metabolism. It was newly found that LGS remarkably alleviated ALD-associated gut barrier function abnormality and gut dysbiosis. The attenuated gut dysbiosis was characterized as: (1) recovering the ALD-mediated alteration of microbial structure; (2) enriching some of unique microbial strains (*Alloprevotella, Monoglobus*, *Erysipelatoclostridium*, *Parasutterella*, *Harryflintia*, and *unclassified_c_Clostridia*). Moreover, Following LGS intervention, the microbial SCFA metabolite, hexanoic acid, was significantly increased, which was associated with activation of intestinal GPR43 and production of GLP-1. Therefore, the modulation of the gut microbiota and activation of the SCFAs/GPR43/GLP-1 signaling pathway may contribute to the anti-ALD effect of LGS.

Although this study has certain limitations, these discoveries provide a new perspective (particularly the modulation of gut microbiota) for further exploration of the application of LGS in the treatment of ALD. Future research should focus on the specific components of LGS, the affected microbial genera, and the types of SCFAs to gain a deeper understanding of the mechanisms of LGS. In addition, fecal transplantation or GPR43 inhibition should be performed to confirm their roles in ALD alleviation by LGS. These studies would provide a scientific basis for the development of new therapeutic strategies.

Data availability statement

The raw data supporting the conclusions of this article will be made available by the authors, without undue reservation.

Ethics statement

All animal experiments were approved by the Experimental Animal Ethics Committee of Southwest Medical University, with the approval number SWMU20230089. The study was conducted in accordance with local legislation and institutional requirements.

Author contributions

MT: Formal analysis, Validation, Writing – original draft. LZ: Formal analysis, Validation, Writing – original draft. FH: Formal analysis, Investigation, Validation, Writing – original draft. TW: Formal analysis, Validation, Writing – review and editing. XW: Conceptualization, Funding acquisition, Project administration, Writing – review and editing. SC: Formal analysis, Validation, Writing – review and editing. JF: Formal analysis, Validation, Writing – review and editing. CJ: Formal analysis, Validation, Writing – review and editing. SW: Formal analysis, Validation, Writing – review and editing. XsZ: Formal analysis, Validation, Writing – review and editing. XlZ: Formal analysis, Writing – review and editing. XZ: Resources, Writing – review and editing. MW: Methodology, Project administration, Resources, Supervision, Writing – review and editing. ZL: Conceptualization, Funding acquisition, Supervision, Writing – review and editing. GX: Conceptualization, Supervision, Writing – review and editing.

Funding

The author(s) declare that financial support was received for the research, authorship, and/or publication of this article. The present study was financially supported by the Sichuan Science and Technology Program, China (Grant Nos. 2022YFS0624 and 2024MS219), the Luzhou Science and Technology Program, China (Grant Nos. 2022YFS0624-B3, 2022YFS0 624-B1 and 2024SYF161), the grant from Sichuan Province Administration of Traditional Chinese Medicine (Grant No. 2023zd008).

Acknowledgments

We gratefully acknowledge the invaluable resource contributions made by Wei Mei and Professor Sun Tongqiao, which significantly supported our research endeavors. The following platforms provided technical support: Majorbio Cloud Platform (https://cloud.majorbio.com), Figdraw (https://www.figdraw.com), and APT Cloud Platform (https://bio-cloud.aptbiotech.com/).

Conflict of interest

The authors declare that the research was conducted in the absence of any commercial or financial relationships that could be construed as a potential conflict of interest.

Publisher's note

All claims expressed in this article are solely those of the authors and do not necessarily represent those of their affiliated organizations, or those of the publisher, the editors and the reviewers. Any product that may be evaluated in this article, or claim that may be made by its manufacturer, is not guaranteed or endorsed by the publisher.

Supplementary material

The Supplementary Material for this article can be found online at: https://www.frontiersin.org/articles/10.3389/fnut.2024.1495695/full#supplementary-material

References

1. Park JW, Kim SE, Lee NY, Kim JH, Jung JH, Jang MK, et al. Role of microbiota-derived metabolites in alcoholic and non-alcoholic fatty liver diseases. *Int J Mol Sci.* (2021) 23:426. doi: 10.3390/ijms23010426

2. Axley PD, Richardson CT, Singal AK. Epidemiology of alcohol consumption and societal burden of alcoholism and alcoholic liver disease. *Clin Liver Dis.* (2019) 23:39–50. doi: 10.1016/j.cld.2018.09.011

3. Lang S, Fairfied B, Gao B, Duan Y, Zhang X, Fouts DE, et al. Changes in the fecal bacterial microbiota associated with disease severity in alcoholic hepatitis patients. *Gut Microbes.* (2020) 12:1785251. doi: 10.1080/19490976.2020.1785251

4. Yan C, Hu W, Tu J, Li J, Liang Q, Han S. Pathogenic mechanisms and regulatory factors involved in alcoholic liver disease. *J Transl Med.* (2023) 21:300. doi: 10.1186/s12967-023-04166-8

5. Wei S, Jiang Y, Li M, Zhao L, Wang T, Wei M, et al. Chemical profiling and quality evaluation of Liuweizhiji Gegen-Sangshen oral liquid by UPLC-Q-TOF-MS and HPLC-diode array detector fingerprinting. *Phytochem Anal.* (2024) 35:860–72. doi: 10.1002/pca.3333

6. Wang S, Wei M, Yang G, Liang Y, Wang X, Yang H. Clinical efficacy of applying Gegen-sangshen beverage for treatment on patients with alcoholic liver disease. *J Chin Med Mater.* (2018) 41:2220–3.

7. Huang S, Gou S, Li B, Wang X, Liu Y, Li Z, et al. Exploring the protective effect and mechanism of serum containing Gegen-Sangshen beverage ameliorate ethanol-induced BRL-3A damage based on endoplasmic reticulum stress PERK/eIF2α/ATF4/CHOP pathway. *Modern Tradit Chin Med Materia Med World Sci Technol.* (2023) 25:3715–23.

8. Cai L, Liu Y, Li Z, Li B, Yang G, Wei M. Effect of Gegen-Sangshen beverage on lipid metabolism in rats with alcoholic liver disease. *World Sci Technol Modern Tradit Chin Med.* (2018) 20:929–34.

9. Gou S, Huang X, Li B, Wang X, Huang S, Wei M. Mechanism of Gegen-Sangshen beverage in preventing and treating alcoholic liver injury through Syk/Ras/ERK signal pathway. *Clin J Tradit Chin Med.* (2023) 35:1560–5. doi: 10.16448/j.cjtcm.2023.0823

10. Luo C, Li Z, liu R, Liu P. Study on the mechanism of Gegen-Sangshen beverage regulating lipid metabolism in rats with alcoholic liver disease based on PPARα-SREBP-1c-FAS pathway. *J Chin Med Mater.* (2024):1282–6. doi: 10.13863/j.issn1001-4454.2024.05.036

11. Li C, Wang X, Li B, Liu Y, Wei M. The effect of Gegen-Sangshen beverage medicated serum on the activity ofalcohol metabolizing enzymes in ethanol-induced injuried L-02Cells. *J Chin Med Mater.* (2019) 42:422–5. doi: 10.13863/j.issn1001-4454.2019.02.040

12. Wei S, Li M, Zhao L, Wang T, Wu K, Yang J, et al. Fingerprint profiling for quality evaluation and the related biological activity analysis of polysaccharides from Liuweizhiji Gegen-Sangshen beverage. *Front Nutr.* (2024) 11:1431518. doi: 10.3389/fnut.2024.1431518

13. Bertola A, Mathews S, Ki SH, Wang H, Gao B. Mouse model of chronic and binge ethanol feeding (the NIAAA model). *Nat Protoc.* (2013) 8:627–37. doi: 10.1038/nprot.2013.032

14. Callahan BJ, McMurdie PJ, Rosen MJ, Han AW, Johnson AJ, Holmes SP. DADA2: High-resolution sample inference from Illumina amplicon data. *Nat Methods.* (2016) 13:581–3. doi: 10.1038/nmeth.3869

15. Magoč T, Salzberg SL. FLASH: Fast length adjustment of short reads to improve genome assemblies. *Bioinformatics.* (2011) 27:2957–63. doi: 10.1093/bioinformatics/btr507

16. Schloss PD, Westcott SL, Ryabin T, Hall JR, Hartmann M, Hollister EB, et al. Introducing mothur: Open-source, platform-independent, community-supported software for describing and comparing microbial communities. *Appl Environ Microbiol.* (2009) 75:7537–41. doi: 10.1128/aem.01541-09

17. Fukui H. Gut microbiota and host reaction in liver diseases. *Microorganisms.* (2015) 3:759–91. doi: 10.3390/microorganisms3040759

18. Bull-Otterson L, Feng W, Kirpich I, Wang Y, Qin X, Liu Y, et al. Metagenomic analyses of alcohol induced pathogenic alterations in the intestinal microbiome and the effect of Lactobacillus rhamnosus GG treatment. *PLoS One.* (2013) 8:e53028. doi: 10.1371/journal.pone.0053028

19. Wang H, Yan Y, Yi X, Duan Y, Wang J, Li S, et al. Histopathological features and composition of gut microbiota in rhesus monkey of alcoholic liver disease. *Front Microbiol.* (2019) 10:165. doi: 10.3389/fmicb.2019.00165

20. Litwinowicz K, Gamian A. Microbiome alterations in alcohol use disorder and alcoholic liver disease. *Int. J Mol Sci.* (2023) 24:2461. doi: 10.3390/ijms24032461

21. Shao T, Zhao C, Li F, Gu Z, Liu L, Zhang L, et al. Intestinal HIF-1α deletion exacerbates alcoholic liver disease by inducing intestinal dysbiosis and barrier dysfunction. *J Hepatol.* (2018) 69:886–95. doi: 10.1016/j.jhep.2018.05.021

22. Li H, Shi J, Zhao L, Guan J, Liu F, Huo G, et al. Lactobacillus plantarum KLDS1.0344 and Lactobacillus acidophilus KLDS1.0901 mixture prevents chronic alcoholic liver injury in mice by protecting the intestinal barrier and regulating gut microbiota and liver-related pathways. *J Agric Food Chem.* (2021) 69:183–97. doi: 10.1021/acs.jafc.0c06346

23. Tolhurst G, Heffron H, Lam YS, Parker HE, Habib AM, Diakogiannaki E, et al. Short-chain fatty acids stimulate glucagon-like peptide-1 secretion via the G-protein-coupled receptor FFAR2. *Diabetes.* (2012) 61(2):364–71. doi: 10.2337/db11-1019

24. Yao Y, Yan L, Chen H, Wu N, Wang W, Wang D. Cyclocarya paliurus polysaccharides alleviate type 2 diabetic symptoms by modulating gut microbiota and short-chain fatty acids. *Phytomedicine.* (2020) 77:153268. doi: 10.1016/j.phymed.2020.153268

25. He J, Zhang P, Shen L, Niu L, Tan Y, Chen L, et al. Short-chain fatty acids and their association with signalling pathways in inflammation, glucose and lipid metabolism. *Int J Mol Sci.* (2020) 21:6356. doi: 10.3390/ijms21176356

26. Bu T, Sun Z, Pan Y, Deng X, Yuan G. Glucagon-like peptide-1: New regulator in lipid metabolism. *Diabetes Metab J.* (2024) 48:354–72. doi: 10.4093/dmj.2023.0277

27. Wu X, Fan X, Miyata T, Kim A, Cajigas-Du Ross CK, Ray S, et al. Recent advances in understanding of pathogenesis of alcohol-associated liver disease. *Annu Rev Pathol.* (2023) 18:411–38. doi: 10.1146/annurev-pathmechdis-031521-030435

28. Mackowiak B, Fu Y, Maccioni L, Gao B. Alcohol-associated liver disease. *J Clin Investig.* (2024) 134:e176345. doi: 10.1172/JCI176345

29. Mandrekar P, Mandal A. Pathogenesis of alcohol-associated liver disease. *Clin Liver Dis.* (2024) 28:647–61. doi: 10.1016/j.cld.2024.06.005

30. Schulze RJ, Schott MB, Casey CA, Tuma PL, McNiven MA. The cell biology of the hepatocyte: A membrane trafficking machine. *J Cell Biol.* (2019) 218:2096–112. doi: 10.1083/jcb.201903090

31. Arab JP, Sehrawat TS, Simonetto DA, Verma VK, Feng D, Tang T, et al. An open-label, dose-escalation study to assess the safety and efficacy of IL-22 agonist F-652 in patients with alcohol-associated hepatitis. *Hepatology.* (2020) 72:441–53. doi: 10.1002/hep.31046

32. Szabo G, Mitchell M, McClain CJ, Dasarathy S, Barton B, McCullough AJ, et al. IL-1 receptor antagonist plus pentoxifylline and zinc for severe alcohol-associated hepatitis. *Hepatology.* (2022) 76:1058–68. doi: 10.1002/hep.32478

33. Higuera-de la Tijera F, Servín-Caamaño A I, Cruz-Herrera J, Serralde-Zúñiga AE, Abdo-Francis JM, Gutiérrez-Reyes G, et al. Treatment with Metadoxine and its impact on early mortality in patients with severe alcoholic hepatitis. *Ann Hepatol.* (2014) 13:343–52. doi: 10.1016/S1665-2681(19)30863-4

34. Pande A, Sharma S, Khillan V, Rastogi A, Arora V, Shasthry S, et al. Fecal microbiota transplantation compared with prednisolone in severe alcoholic hepatitis patients: A randomized trial. *Hepatol Int.* (2023) 17:249–61. doi: 10.1007/s12072-022-10438-0

35. Li X, Liu Y, Guo X, Ma Y, Zhang H, Liang H. Effect of Lactobacillus casei on lipid metabolism and intestinal microflora in patients with alcoholic liver injury. *Eur J Clin Nutr.* (2021) 75:1227–36. doi: 10.1038/s41430-020-00852-8

36. Han SH, Suk KT, Kim DJ, Kim MY, Baik SK, Kim YD, et al. Effects of probiotics (cultured Lactobacillus subtilis/Streptococcus faecium) in the treatment of alcoholic hepatitis: Randomized-controlled multicenter study. *Eur J Gastroenterol Hepatol.* (2015) 27:1300–6. doi: 10.1097/meg.0000000000000458

37. de Sant'Ana LP, Ribeiro DJ, Martins AM, Dos Santos FN, Corrêa R, Almeida RD, et al. Absence of the caspases 1/11 modulates liver global lipid profile and gut microbiota in high-fat-diet-induced obese mice. *Front Immunol.* (2019) 10:2926. doi: 10.3389/fimmu.2019.02926

38. Yan F, Zhang Q, Shi K, Zhang Y, Zhu B, Bi Y, et al. Gut microbiota dysbiosis with hepatitis B virus liver disease and association with immune response. *Front Cell Infect Microbiol.* (2023) 13:1152987. doi: 10.3389/fcimb.2023.1152987

39. Parker BJ, Wearsch PA, Veloo AC, Rodriguez-Palacios A. The genus alistipes: Gut bacteria with emerging implications to inflammation, Cancer, and Mental Health. *Front Immunol.* (2020) 11:906. doi: 10.3389/fimmu.2020.00906

40. Dong D, Su T, Chen W, Wang D, Xue Y, Lu Q, et al. Clostridioides difficile aggravates dextran sulfate solution (DSS)-induced colitis by shaping the gut microbiota and promoting neutrophil recruitment. *Gut Microbes.* (2023) 15:2192478. doi: 10.1080/19490976.2023.2192478

41. Li J, Jia S, Yuan C, Yu B, Zhang Z, Zhao M, et al. Jerusalem artichoke inulin supplementation ameliorates hepatic lipid metabolism in type 2 diabetes mellitus mice by modulating the gut microbiota and fecal metabolome. *Food Funct.* (2022) 13:11503–17. doi: 10.1039/d2fo02051c

42. Song W, Wen R, Liu T, Zhou L, Wang G, Dai X, et al. Oat-based postbiotics ameliorate high-sucrose induced liver injury and colitis susceptibility by modulating fatty acids metabolism and gut microbiota. *J Nutr Biochem.* (2024) 125:109553. doi: 10.1016/j.jnutbio.2023.109553

43. Zhuge A, Li S, Lou P, Wu W, Wang K, Yuan Y, et al. Longitudinal 16S rRNA sequencing reveals relationships among alterations of gut microbiota and nonalcoholic fatty liver disease progression in mice. *Microbiol Spectr.* (2022) 10:e0004722. doi: 10.1128/spectrum.00047-22

44. Li H, Liu C, Huang S, Wang X, Cao M, Gu T, et al. Multi-omics analyses demonstrate the modulating role of gut microbiota on the associations of unbalanced dietary intake with gastrointestinal symptoms in children with autism spectrum disorder. *Gut Microbes.* (2023) 15:2281350. doi: 10.1080/19490976.2023.2281350

45. Efremova I, Maslennikov R, Medvedev O, Kudryavtseva A, Avdeeva A, Krasnov G, et al. Gut microbiota and biomarkers of intestinal barrier damage in cirrhosis. *Microorganisms.* (2024) 12:463. doi: 10.3390/microorganisms12030463

46. Dai J, Jiang M, Wang X, Lang T, Wan L, Wang J. Human-derived bacterial strains mitigate colitis via modulating gut microbiota and repairing intestinal barrier function in mice. *BMC Microbiol.* (2024) 24:96. doi: 10.1186/s12866-024-03216-5

47. Chen G, Peng Y, Huang Y, Xie M, Dai Z, Cai H, et al. Fluoride induced leaky gut and bloom of Erysipelatoclostridium ramosum mediate the exacerbation of obesity in high-fat-diet fed mice. *J Adv Res.* (2023) 50:35–54. doi: 10.1016/j.jare.2022.10.010

48. Li C, Li N, Liu C, Yin S. Causal association between gut microbiota and intrahepatic cholestasis of pregnancy: Mendelian randomization study. *BMC Pregn Childbirth.* (2023) 23:568. doi: 10.1186/s12884-023-05889-8

49. Xiao QA, Yang YF, Chen L, Xie YC, Li HT, Fu ZG, et al. The causality between gut microbiome and liver cirrhosis: A bi-directional two-sample Mendelian randomization analysis. *Front Microbiol.* (2023) 14:1256874. doi: 10.3389/fmicb.2023.1256874

50. Henneke L, Schlicht K, Andreani NA, Hollstein T, Demetrowitsch T, Knappe C, et al. A dietary carbohydrate - gut Parasutterella - human fatty acid biosynthesis metabolic axis in obesity and type 2 diabetes. *Gut Microbes.* (2022) 14:2057778. doi: 10.1080/19490976.2022.2057778

51. Ju T, Kong JY, Stothard P, Willing BP. Defining the role of Parasutterella, a previously uncharacterized member of the core gut microbiota. *ISME J.* (2019) 13:1520–34. doi: 10.1038/s41396-019-0364-5

52. Sprenger-Svačina A, Klein I, Svačina MK, Bobylev I, Kohle F, Schneider C, et al. Antibiotics-induced intestinal immunomodulation attenuates Experimental Autoimmune Neuritis (EAN). *J Neuroimmune Pharmacol.* (2024) 19:26. doi: 10.1007/s11481-024-10119-9

53. Qin S, Wang Y, Wang S, Ning B, Huai J, Yang H. Gut microbiota in women with gestational diabetes mellitus has potential impact on metabolism in pregnant mice and their offspring. *Front Microbiol.* (2022) 13:870422. doi: 10.3389/fmicb.2022.870422

54. Jo JK, Seo SH, Park SE, Kim HW, Kim EJ, Kim JS, et al. Gut microbiome and metabolome profiles associated with high-fat diet in mice. *Metabolites.* (2021) 11:482. doi: 10.3390/metabo11080482

55. Lee JY, Tiffany CR, Mahan SP, Kellom M, Rogers AW, Nguyen H, et al. High fat intake sustains sorbitol intolerance after antibiotic-mediated Clostridia depletion from the gut microbiota. *Cell.* (2024) 187:1191–205.e15. doi: 10.1016/j.cell.2024.01.029

56. Hou K, Wu Z-X, Chen X-Y, Wang J-Q, Zhang D, Xiao C, et al. Microbiota in health and diseases. *Signal Transduct Targeted Ther.* (2022) 7:135. doi: 10.1038/s41392-022-00974-4

57. de Vos WM, Tilg H, Van Hul M, Cani PD. Gut microbiome and health: Mechanistic insights. *Gut.* (2022) 71:1020–32. doi: 10.1136/gutjnl-2021-326789

58. Frost G, Sleeth ML, Sahuri-Arisoylu M, Lizarbe B, Cerdan S, Brody L, et al. The short-chain fatty acid acetate reduces appetite via a central homeostatic mechanism. *Nat Commun.* (2014) 5:3611. doi: 10.1038/ncomms4611

59. Li G, Yao W, Jiang H. Short-chain fatty acids enhance adipocyte differentiation in the stromal vascular fraction of porcine adipose tissue. *J Nutr.* (2014) 144:1887–95. doi: 10.3945/jn.114.198531

60. Nguyen TD, Prykhodko O, Hållenius FF, Nyman M. Monobutyrin reduces liver cholesterol and improves intestinal barrier function in rats fed high-fat diets. *Nutrients.* (2019) 11:308. doi: 10.3390/nu11020308

61. Ganesan R, Gupta H, Jeong J, Sharma SP, Won SM, Oh KK, et al. Characteristics of microbiome-derived metabolomics according to the progression of alcoholic liver disease. *Hepatol Int.* (2024) 18:486–99. doi: 10.1007/s12072-023-10518-9

62. Wang J, Han L, Liu Z, Zhang W, Zhang L, Jing J, et al. Genus unclassified_Muribaculaceae and microbiota-derived butyrate and indole-3-propionic acid are involved in benzene-induced hematopoietic injury in mice. *Chemosphere.* (2023) 313:137499. doi: 10.1016/j.chemosphere.2022.137499

63. Huang B, Yin T, Fu S, Liu L, Yang C, Zhou L, et al. Inflammation-oriented montmorillonite adjuvant enhanced oral delivery of anti-TNF-α nanobody against inflammatory bowel disease. *Proc Natl Acad Sci U S A.* (2024) 121:e2320482121. doi: 10.1073/pnas.2320482121

64. Chen HH, Wu QJ, Zhang TN, Zhao YH. Gut microbiome and serum short-chain fatty acids are associated with responses to chemo- or targeted therapies in Chinese patients with lung cancer. *Front Microbiol.* (2023) 14:1165360. doi: 10.3389/fmicb.2023.1165360

65. Dai X, Chen L, Liu M, Liu Y, Jiang S, Xu T, et al. Effect of 6-methoxybenzoxazolinone on the cecal microbiota of adult male Brandt's vole. *Front Microbiol.* (2022) 13:847073. doi: 10.3389/fmicb.2022.847073

66. Li X, Huang J, Yun J, Zhang G, Zhang Y, Zhao M, et al. d-Arabitol ameliorates obesity and metabolic disorders via the gut microbiota-SCFAs-WAT browning axis. *J Agric Food Chem.* (2023) 71:522–34. doi: 10.1021/acs.jafc.2c06674

67. Tomova A, Bukovsky I, Rembert E, Yonas W, Alwarith J, Barnard ND, et al. The effects of vegetarian and vegan diets on gut microbiota. *Front Nutr.* (2019) 6:47. doi: 10.3389/fnut.2019.00047

68. Zhang Y, Liu L, Wei C, Wang X, Li R, Xu X, et al. Vitamin K2 supplementation improves impaired glycemic homeostasis and insulin sensitivity for type 2 diabetes through gut microbiome and fecal metabolites. *BMC Med.* (2023) 21:174. doi: 10.1186/s12916-023-02880-0

69. Xu D, Feng M, Chu Y, Wang S, Shete V, Tuohy KM, et al. The prebiotic effects of oats on blood lipids, gut microbiota, and short-chain fatty acids in mildly hypercholesterolemic subjects compared with rice: A randomized, controlled trial. *Front Immunol.* (2021) 12:787797. doi: 10.3389/fimmu.2021.787797

70. Liu T, Li J, Hao X, Meng J. Efficient caproic acid production from lignocellulosic biomass by bio-augmented mixed microorganisms. *Bioresour Technol.* (2024) 399:130565. doi: 10.1016/j.biortech.2024.130565

71. Jin X, Yin X, Ling L, Mao H, Dong X, Chang X, et al. Adding glucose delays the conversion of ethanol and acetic acid to caproic acid in Lacrimispora celerecrescens JSJ-1. *Appl Microbiol Biotechnol.* (2023) 107:1453–63. doi: 10.1007/s00253-023-12378-7

72. Barker HA, Kamen MD, Bornstein BT. The synthesis of butyric and caproic acids from ethanol and acetic acid by clostridium kluyveri. *Proc Natl Acad Sci U S A.* (1945) 31:373–81. doi: 10.1073/pnas.31.12.373

73. Huang Y, Wang Z, Ye B, Ma JH, Ji S, Sheng W, et al. Sodium butyrate ameliorates diabetic retinopathy in mice via the regulation of gut microbiota and related short-chain fatty acids. *J Transl Med.* (2023) 21:451. doi: 10.1186/s12967-023-04259-4

74. Li B, Zhang J, Chen Y, Wang Q, Yan L, Wang R, et al. Alterations in microbiota and their metabolites are associated with beneficial effects of bile acid sequestrant on icteric primary biliary Cholangitis. *Gut Microbes.* (2021) 13:1946366. doi: 10.1080/19490976.2021.1946366

75. Han W, He P, Shao L, Lü F. Metabolic interactions of a chain elongation microbiome. *Appl Environ Microbiol.* (2018) 84:e01614-18. doi: 10.1128/aem.01614-18

76. Caster WO, Resureccion AV, Cody M, Andrews JW Jr., Bargmann R. Dietary effects of the esters of butyric, caproic, caprylic, capric, lauric, myristic, palmitic, and stearic acids on food intake, weight gain, plasma glucose, and tissue lipid in the male white rat. *J Nutr.* (1975) 105:676–87. doi: 10.1093/jn/105.6.676

77. Ghaedi N, Pouraboli I, Askari N. Antidiabetic properties of hydroalcoholic leaf and stem extract of levisticum officinale: An implication for α-amylase inhibitory activity of extract ingredients through molecular docking. *Iran J Pharm Res.* (2020) 19:231–50. doi: 10.22037/ijpr.2020.15140.12901

78. Rial SA, Ravaut G, Malaret TB, Bergeron KF, Mounier C. Hexanoic, octanoic and decanoic acids promote basal and insulin-induced phosphorylation of the Akt-mTOR axis and a balanced lipid metabolism in the HepG2 hepatoma cell line. *Molecules (Basel, Switzerland).* (2018) 23:2315. doi: 10.3390/molecules23092315

79. Gao C, Li B, He Y, Huang P, Du J, He G, et al. Early changes of fecal short-chain fatty acid levels in patients with mild cognitive impairments. *CNS Neurosci Ther.* (2023) 29:3657–66. doi: 10.1111/cns.14252

80. Fan X, Zhang Y, Song Y, Zhao Y, Xu Y, Guo F, et al. Compound Danshen dripping pills moderate intestinal flora and the TLR4/MyD88/NF-κB signaling pathway in alleviating cognitive dysfunction in type 2 diabetic KK-Ay mice. *Phytomedicine.* (2023) 111:154656. doi: 10.1016/j.phymed.2023.154656

81. Xiao-Hang Q, Si-Yue C, Hui-Dong T. Multi-strain probiotics ameliorate Alzheimer's-like cognitive impairment and pathological changes through the AKT/GSK-3β pathway in senescence-accelerated mouse prone 8 mice. *Brain Behav Immun.* (2024) 119:14–27. doi: 10.1016/j.bbi.2024.03.031

82. Huang Z, Wu H, Fan J, Mei Q, Fu Y, Yin N, et al. Colonic mucin-2 attenuates acute necrotizing pancreatitis in rats by modulating intestinal homeostasis. *FASEB J.* (2023) 37:e22994. doi: 10.1096/fj.202201998R

83. Gao Y, Chen H, Li J, Ren S, Yang Z, Zhou Y, et al. Alterations of gut microbiota-derived metabolites in gestational diabetes mellitus and clinical significance. *J Clin Lab Anal.* (2022) 36:e24333. doi: 10.1002/jcla.24333

84. Mei X, Li Y, Zhang X, Zhai X, Yang Y, Li Z, et al. Maternal phlorizin intake protects offspring from maternal obesity-induced metabolic disorders in mice via targeting gut microbiota to activate the SCFA-GPR43 pathway. *J Agric Food Chem.* (2024) 72:4703–25. doi: 10.1021/acs.jafc.3c06370

85. Tan JK, Macia L, Mackay CR. Dietary fiber and SCFAs in the regulation of mucosal immunity. *J Allergy Clin Immunol.* (2023) 151:361–70. doi: 10.1016/j.jaci.2022.11.007

86. Le Poul E, Loison C, Struyf S, Springael JY, Lannoy V, Decobecq ME, et al. Functional characterization of human receptors for short chain fatty acids and their role in polymorphonuclear cell activation. *J Biol. Chem.* (2003) 278:25481–9. doi: 10.1074/jbc.M301403200

87. Ang Z, Ding JL. GPR41 and GPR43 in obesity and inflammation - protective or causative? *Front Immunol.* (2016) 7:28. doi: 10.3389/fimmu.2016.00028

88. Holst JJ. The physiology of glucagon-like peptide 1. *Physiol Rev.* (2007) 87:1409–39. doi: 10.1152/physrev.00034.2006

89. Yao Y, Zhang Y, Song M, Fan J, Feng S, Li J, et al. Lactobacillus alleviates intestinal epithelial barrier function through GPR43-mediated M2 macrophage polarization. *Anim Dis.* (2024) 4:20. doi: 10.1186/s44149-024-00125-y

90. Matikainen N, Bogl LH, Hakkarainen A, Lundbom J, Lundbom N, Kaprio J, et al. GLP-1 responses are heritable and blunted in acquired obesity with high liver fat and insulin resistance. *Diabetes Care.* (2014) 37:242–51. doi: 10.2337/dc13-1283

91. Brunner K, Henneberg CJ, Wilechansky RM, Long MT. Nonalcoholic fatty liver disease and obesity treatment. *Curr Obes Rep.* (2019) 8:220–8. doi: 10.1007/s13679-019-00345-1

92. Bhalla S, Mehan S, Khan A, Rehman MU. Protective role of IGF-1 and GLP-1 signaling activation in neurological dysfunctions. *Neurosci Biobehav Rev.* (2022) 142:104896. doi: 10.1016/j.neubiorev.2022.104896

93. Luna-Marco C, Iannantuoni F, Hermo-Argibay A, Devos D, Salazar JD, Víctor VM, et al. Cardiovascular benefits of SGLT2 inhibitors and GLP-1 receptor agonists through effects on mitochondrial function and oxidative stress. *Free Radic Biol Med.* (2024) 213:19–35. doi: 10.1016/j.freeradbiomed.2024.01.015

94. Wong CK, McLean BA, Baggio LL, Koehler JA, Hammoud R, Rittig N, et al. Central glucagon-like peptide 1 receptor activation inhibits Toll-like receptor agonist-induced inflammation. *Cell Metab.* (2024) 36:130–43.e5. doi: 10.1016/j.cmet.2023.11.009

95. Li SL, Wang ZM, Xu C, Che FH, Hu XF, Cao R, et al. Liraglutide attenuates hepatic ischemia-reperfusion injury by modulating macrophage polarization. *Front Immunol.* (2022) 13:869050. doi: 10.3389/fimmu.2022.869050

96. Yaribeygi H, Maleki M, Santos RD, Jamialahmadi T, Sahebkar A. Glp-1 mimetics and autophagy in diabetic milieu: State-of-the-art. *Curr Diabetes Rev.* (2024) 20:e250124226181. doi: 10.2174/0115733998276570231222105959

97. Fang Z, Chen S, Manchanda Y, Bitsi S, Pickford P, David A, et al. Ligand-specific factors influencing GLP-1 receptor post-endocytic trafficking and degradation in pancreatic beta cells. *Int J Mol Sci.* (2020) 21:8404. doi: 10.3390/ijms21218404

frontiers | Frontiers in Nutrition

TYPE Systematic Review
PUBLISHED 30 January 2025
DOI 10.3389/fnut.2025.1528383

Check for updates

OPEN ACCESS

EDITED BY
Ntethelelo Sibiya,
Rhodes University, South Africa

REVIEWED BY
Jie Tu,
Jiangsu University of Science and Technology, China
Carol Johnston,
Arizona State University, United States
Asif Wali,
Karakoram International University, Pakistan

*CORRESPONDENCE
Zahra Sohrabi
✉ Zahra_2043@yahoo.com
Mohsen Mohammadi Sartang
✉ dr.mohamadi_nut@yahoo.com

†These authors have contributed equally to this work

RECEIVED 14 November 2024
ACCEPTED 10 January 2025
PUBLISHED 30 January 2025

CITATION
Arjmandfard D, Behzadi M, Sohrabi Z and Mohammadi Sartang M (2025) Effects of apple cider vinegar on glycemic control and insulin
sensitivity in patients with type 2 diabetes: A GRADE-assessed systematic review and dose–response meta-analysis of controlled clinical trials.
Front. Nutr. 12:1528383.
doi: 10.3389/fnut.2025.1528383

COPYRIGHT
© 2025 Arjmandfard, Behzadi, Sohrabi and Mohammadi Sartang. This is an open-access article distributed under the terms of the Creative Commons Attribution License (CC BY). The use, distribution or reproduction in other forums is permitted, provided the original author(s) and the copyright owner(s) are credited and that the original publication in this journal is cited, in accordance with accepted academic practice. No use, distribution or reproduction is permitted which does not comply with these terms.

Effects of apple cider vinegar on glycemic control and insulin sensitivity in patients with type 2 diabetes: A GRADE-assessed systematic review and dose–response meta-analysis of controlled clinical trials

Donya Arjmandfard[1], Mehrdad Behzadi[1], Zahra Sohrabi[2*†] and Mohsen Mohammadi Sartang[2*†]

[1]Student Research Committee, School of Nutrition and Food Sciences, Shiraz University of Medical Sciences, Shiraz, Iran, [2]Nutrition Research Center, School of Nutrition and Food Sciences, Shiraz University of Medical Sciences, Shiraz, Iran

Background and aims: Diabetes mellitus (DM) is a multifactorial metabolic disorder that affects the body's ability to regulate blood sugar levels. Apple cider vinegar (ACV) could possibly improve diabetes; nevertheless, evidences provide conflicting results. This study aimed to evaluate the effects of ACV on glycemic profile in type 2 diabetes patients (T2DM) in controlled trials (CTs) by systematically reviewing and dose–response meta-analysis.

Methods: The Scopus, PubMed, and Web of Science databases were searched until November 2024 according to a systematic approach. All CTs investigating ACV's effects on glycemic factors were included. We used a random-effects model to calculate WMDs and 95% confidence intervals (CIs). The present study assessed publication bias, sensitivity analysis, meta-regression, and heterogeneity based on standard methods. We assessed the bias risk of the included studies using Cochrane quality assessments and used GRADE (Grading of Recommendations Assessment, Development, and Evaluation) to calculate evidence certainty. We registered the study protocol at Prospero (no. CRD42023457493).

Results: Overall, we included seven studies in this meta-analysis. ACV significantly reduced fasting blood sugar (FBS) (WMD: −21.929 mg/dL, 95% CI: −29.19, −14.67, $p < 0.001$) and HbA1c (WMD: −1.53, 95% CI: −2.65, −0.41, $p = 0.008$) and increased insulin (WMD: 2.059 μu/ml, 95% CI: 0.26, 3.86, $p = 0.025$), while it did not affect hemostatic model assessment for insulin resistance (HOMA-IR). We observed linear and non-linear associations between ACV consumption and FBS levels ($p < 0.001$). Each 1 mL/day increase in ACV consumption was associated with a-1.255 mg/dL reduction in FBS. Moreover, greater effects on FBS were in dosages >10.

Conclusion: ACV had positive effects on FBS and HbA1c in T2DM patients.

Systematic Review Registration: The study protocol was registered at Prospero (no. CRD42023457493).

KEYWORDS

Apple cider vinegar, FBS, HbA1c, T2DM, meta-analysis

1 Introduction

Diabetes mellitus (DM) is a multifactorial metabolic disorder that affects the body's ability to regulate blood sugar levels (1). Type 2 diabetes mellitus (T2DM) is a condition characterized by hyperglycemia due to inadequate insulin secretion and insulin resistance (2). More than 500 million people worldwide suffer from diabetes, and by the year 2045, this number is expected to reach 783 million (3). About 90% of all diabetes patients have T2DM. There are several secondary complications associated with it, including cardiovascular disease, strokes, and diabetic retinopathy (4–6). A growing concern has been raised because an increase in T2DM prevalence will result in an increase in chronic and acute diseases in general. This will have profound effects on the quality of life, economic expenses and demand for health care services (7).

The treatment of T2DM relies on the long-term use of anti-diabetic drugs (8, 9), as there is no final cure for the disease (10, 11). It has been demonstrated that dietary modifications are crucial to successfully achieving and maintaining glycemic targets for people with type 2 diabetes mellitus (T2DM) and optimizing their health outcomes (12, 13). Therefore, it is imperative that new methods be explored that may delay or even reverse the progression of T2DM.

The use of plants and their derivatives in contemporary research and practice has gained much attention due to their beneficial effects on controlling glycemic control (14, 15). In this regard, vinegar is among the most commonly used plant derivatives. One of the most common types of vinegar is apple cider vinegar (ACV), which is made by fermenting apples (16). As a preservative agent and flavoring in foods, this acidic solution is used worldwide (17). There are several flavonoids in ACV, such as catechin, ferulic acid, caffeic acid and gallic acid which can improve glucose metabolism (18, 19). These components have been shown to play roles in glucose metabolism and possess anti-inflammatory and antioxidant properties. While acetic acid is indeed the primary active ingredient in all kinds of vinegar, the synergistic effects of these additional compounds present in ACV make it distinct and particularly relevant for investigating glycemic control in T2DM.

Animal studies have revealed that ACV has a number of pharmacological functions, including anti-inflammatory, anti-oxidant, anti-diabetic, anti-hyperlipidemic, and anti-hypertensive effects (20–23). There have been several randomized controlled trials (RCTs) conducted in this field. A contradictory effect was observed on glycemic indexes as a result of these interventions (24–30). In a meta-analysis conducted by Hadi et al., in 2021, on 9 RCTs, they almost reached positive conclusions about the effect of ACV on lipid and glycemic profiles in adults with various health conditions including diabetes, obesity, overweight, and the like (31).

Therefore, this systematic review and dose–response meta-analysis aimed to pool the results of various related controlled trials (CTs) assessing the effects of ACV on glycemic indices and insulin sensitivity in patients with T2DM.

2 Methods

2.1 Search strategy

The present study was conducted according to PRISMA guidelines (Preferred Reporting Items for Systematic Reviews and Meta-Analyses) (32). In addition, we used Prospero to register the study protocol (no. CRD42023457493). To identify relevant CTs that investigated whether ACV influenced the glycemic profile of T2DM patients, the current study conducted a comprehensive systematic search in the online databases Scopus, PubMed, and Web of Science until November 2024. No limitations were applied to the date or language of the studies. A detailed description of the database search strategy can be found in Table S1. Furthermore, we also reviewed relevant meta-analyses and reviews in addition to hand-searching reference lists. For notification of new publications, email alerts were also set up using PubMed's "My NCBI" (National Center for Biotechnology Information), Scopus, and Web of Science.

2.2 Study selection

Two independent investigators (DA and MB) reviewed the articles. To resolve discrepancies, discussions were held and conflicting opinions were resolved by consulting a third author (ZS) if the authors could not reach a consensus. We selected the studies for analysis according to the following criteria (Table 1): (1) controlled clinical trials featuring either a crossover or parallel design; (2) ACV's effect on glycemic profile could be extracted from the article (glycemic indices at baseline and follow-up were available with standard deviations (SD), standard errors (SEs), and 95% confidence intervals (CIs) for both control and intervention groups); (3) we distinguished the Control and intervention groups only by the ACV in a controlled study; (4) the intervention should last at least 2 weeks; (5) adults (18 years of age or older) with type 2 diabetes participated in the study.

Following is the list of exclusion criteria for studies: (i) the net effects of ACV could not be determined; (ii) the duration of intervention was <2 weeks; (iii) studies that were semi-experimental, cohort, case–control, and cross-sectional designs, review articles, and ecological studies; (iv) data on baseline and follow-up glycemic parameters were insufficient.

2.3 Data extraction

Two authors (DA and MB) selected the eligible articles independently by based on screening forms for inclusions and exclusions. We extracted the data using an Excel form for each article. This document has been revised to reflect the current title as well as the following abstracted information: It includes the first author's name, the location of the study, the publication year, the design of the study as parallel or crossover, the number of participants in each

TABLE 1 PICOS criteria for inclusion and exclusion of studies.

Parameter	Criteria
Participant	Type 2 diabetes mellitus patients
Intervention	Apple cider vinegar
Comparator	Placebo
Outcomes	FBS, HbA1c, HOMA-IR, Insulin
Study design	Controlled clinical trial

FBS, fasting blood sugar; HbA1c, glycated hemoglobin; HOMA-IR, homeostasis model assessment for insulin resistance.

group, dosages and types of intervention and control, durations of the interventions, the health status of the participants, and demographic information such as age and gender. Moreover, we extracted the mean values and standard deviations of glycemic parameters at baseline as well as at the end of the study. For trials that included multiple measurements, only the final values were considered for analysis.

2.4 Quality assessment

Two authors (MS and ZS) independently assessed the bias risk of the included studies using the last version of Cochrane quality assessment tools by Higgins that contain seven domains (33). We assigned a "high risk" score to every domain if there were methodological deficiencies that could have affected the results. In the case of no defects being found in those domains, the domain received a "low risk" score, and in the event of insufficient information available, it received an "unclear risk" score. Those studies that scored "low risk" in any of the domains were considered high-quality and had a completely low bias risk.

We used Grading of Recommendations Assessment, Development, and Evaluation (GRADE) to assess and summarize the total quality of the evidence of all studies. GRADE is a methodologically strong and clear approach for judging the strength of recommendations and the certainty of evidence. This method includes four key components: assessing the quality of evidence, evaluating the balance between benefits and harms, considering values and preferences, and making explicit judgments about the strength of recommendations (34).

2.5 Statistical analysis

This meta-analysis was conducted using Comprehensive Meta-Analysis (CMA) V3 software (35). When the probability value (*p*-value) was <0.05, it was considered statistically significant. For all parameters, we used a random effects model and assessed the effects of ACV on the following outcomes: (i) fasting blood sugar (FBS), (ii) parameter of insulin resistance including homeostasis model assessment for insulin resistance, (HOMA-IR), (iii) and quantitative insulin sensitivity checks index (QUICKI), (iv) serum insulin levels and (v) glycated hemoglobin (HbA1c). We expressed the effect sizes by weighted mean differences (WMD) and 95% CI. The mean and SD of glycemic values were calculated in both the ACV and control groups before and after the intervention to calculate net changes: Trial end value - trial baseline value. We also calculated the mean difference as follows: (final value in the ACV group – baseline value in the ACV group) - (final value in the control group - baseline value in the control group). If no SD was reported, it was calculated as follows: SD = square root [(SD pre-intervention)^2 + (SD post-intervention)^2 - (2 R × SD pre-intervention × SD post-intervention)] (36). We used the following formula for calculating SD from standard error of the mean (SEM) in some studies: SEM to SD. SDs = SEs × square root (n), where n refers to the number of individuals in each group. In order to estimate medians, ranges, and 95% confidence intervals, the authors of the current study used Hozo et al.'s method (37). We used the Get Data Graph Digitizer software to extract the data (38) form the results in the form of graphs. Statistical evaluation of heterogeneity was performed using Cochran's *Q*-test with significance set at 0.1 and the I^2 test to calculate the percentage of heterogeneity (I^2 value ≥50% indicates significant heterogeneity). In order to assess how each trial impacted the overall effect size, we conducted a sensitivity analysis using the leave-one-out method (39). In order to determine the influence of factors including dose, duration, and design of CTs, sub-group analysis was performed. In the current study, the authors also used meta-regressions to assess the association between moderating variables, including dose and duration of the intervention, and effect sizes. Crippa et al. (40) suggestion was used to analyze the dose–response effect of ACV intakes on FBS among people with T2DM. We performed a dose–response analysis using the command "drmeta" in Stata, version 17 (StataCorp, Texas, USA).

To assess the publication bias, we used the funnel plot, in addition to Begg's rank correlation and Egger's weighted regression analysis. To adjust for publication bias, "trim and fill" and "fail-safe N" methods of Duval and Tweedie (41) were applied.

3 Results

3.1 Findings from the systematic search

According to the results of the initial search in the online databases, we found 517 articles. Among them, 121 papers were duplicates; therefore, they were excluded. Based on the titles and abstracts of the remaining articles, 381 were determined to be irrelevant. Thus, the full-text assessment consisted of 15 papers. Of the 15 articles, two were excluded for being non-CTs (42, 43). Additionally, two CTs did not measure the desired outcomes (18, 44). As an intervention, two CTs used a type of apple not considered in the analysis (45, 46). The study of Mousavi et al. (47) was excluded because of the short duration (<2 weeks intervention duration). The study of Heljić et al. (48) was also excluded due to the absence of a control group. Finally, seven studies were included in the current systematic review and meta-analysis with complete findings (24–30) (Figure 1).

3.2 Characteristics of included studies

In total, we randomly assigned 463 participants to 7 qualified studies (235 to the ACV group, and 228 to the control group) (Table 2). These trials had participants ranging from 38 (24) to 110 (28). The included studies were published between the years 2009 and 2023. The studies were done in Iran (five studies) (24, 25, 27, 29, 30), Tunisia (26) and Pakistan (28). The mean age of the participants ranged from 49.2 (30) to 54.6 (24) years old. All studies were conducted on both men and women except Halima et al. (26) study which did not report. Intervention duration ranged from 4 (26, 29) to 12 (28) weeks. All studies had parallel designs. Of the seven studies, one was single-blinded (28), two were double-blinded (26, 29), and four did not do blinding (24, 25, 27, 30). In all included studies, the ACV used was produced with the same procedure containing almost 5% acetic acid.

3.3 Data quality

Table 3 summarizes the results of Cochrane's risk of bias tool for the quality assessment of studies. Five trials were classified as low

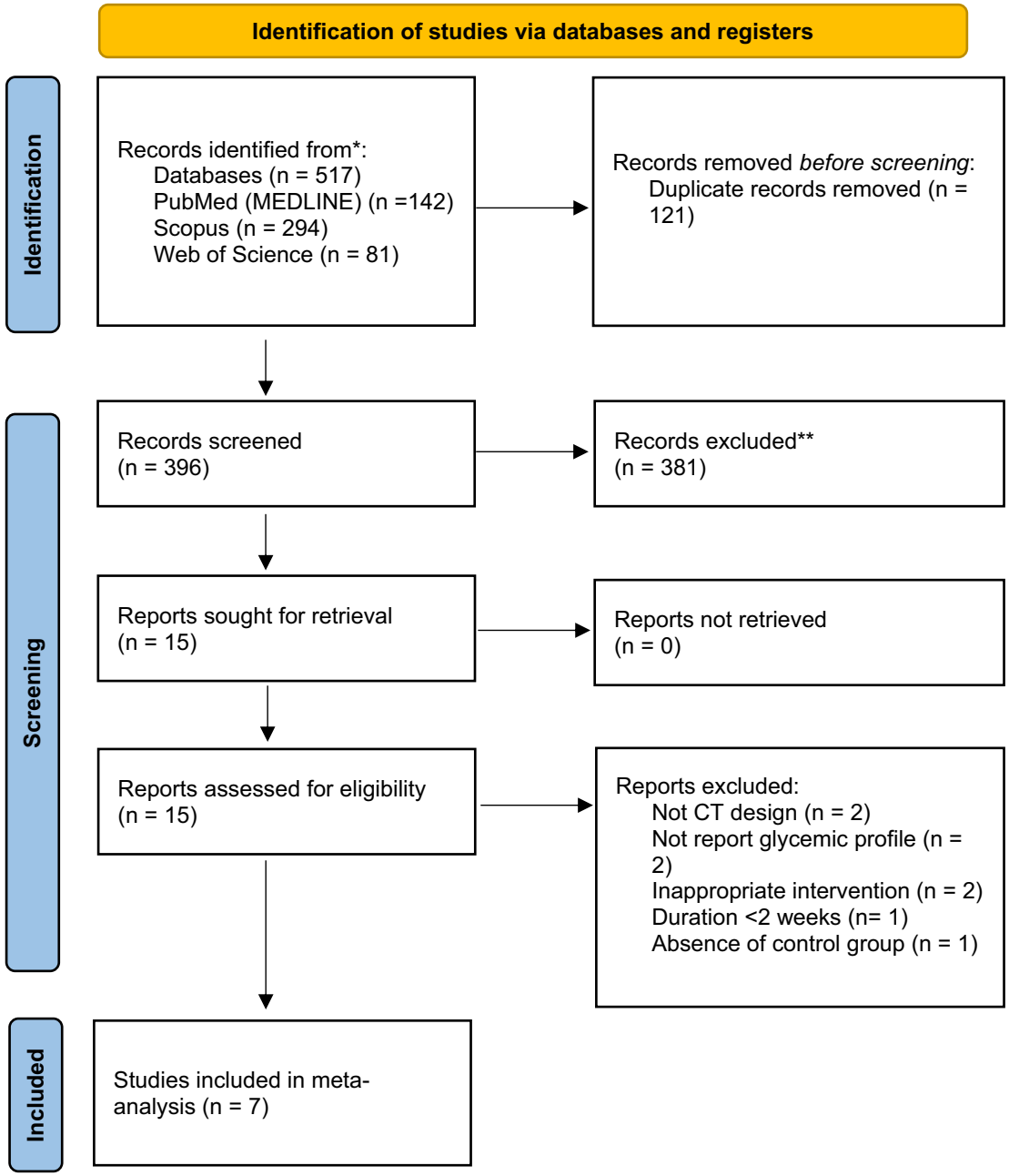

FIGURE 1
PRISMA 2020 flow diagram of databases searches, registers and other sources.

quality (high bias risk in >2 domains) (24, 25, 27, 28, 30), one trial was classified as moderate quality (high bias risk in 2 domains) (29) and one was classified as high quality (high bias risk in <2 domains) (26). Evidences for FBS and insulin were moderate GRADE while for HbA1c and HOMA-IR were low GRADE (Table 4).

3.4 Meta-analysis

The forest plots of FBS, HbA1c, HOMA-IR, and insulin levels from the meta-analysis are shown in Figures 2A–D. Just one study measured QUICKI; we could not perform a meta-analysis on this parameter. Because of the low number of studies, we have done subgroup analysis, meta-regression, and dose–response only for FBS.

3.4.1 Meta-analysis on ACV and FBS

We included seven studies involving 463 participants. ACV significantly reduced FBS based on the results of a random-effect model (WMD: −21.929 mg/dL, 95% CI: −29.19, −14.67, $p < 0.001$), with non-significant heterogeneity (I^2 = 20.11%, $p = 0.237$) (Figure 2A). We summarized the results of the subgroup analysis in Table 5. Considering the sub-group analysis based on the dose and duration, significant effects were observed in dosages>15 g/d, and durations ≥8 weeks. However, according to meta-regression, we found

TABLE 2 Demographic characteristics of the included studies.

Author (Year)	Design	Country	Patient status	Sample size (intervention/ control)	Age (years) (intervention/ control)	Gender	Duration (weeks)	Intervention/ control (type and dosage)	Registered	Funding
Ebrahimi-Mamaghani et al. (24)	Rn/Pa	Iran	Type 2 diabetes	19/19	54.6/53.8	Both	8	13.75 mL/d ACV/–	Yes	Investigator-initiated
Mahmoodi et al. (29)	Db/Pa	Iran	Type 2 diabetes	30/30	NR	Both	4	15 mL/d ACV/water	Yes	NR
Halima et al. (26)	Db/Rn/Pa	Tunisia	Type 2 diabetes	24/20	NR	NR	4	15 mL/d ACV/water	Yes	NR
Mohammadpourhodki et al. (30)	Rn/Pa	Iran	Type 2 diabetes	38/38	49.2/49.2	Both	8	20 mL/d ACV/–	Yes	NR
Gheflati et al. (25)	Rn/Pa	Iran	Type 2 diabetes	32/30	49.47/52.1	Both	8	20 mL/d ACV/P	Yes	Investigator-initiated
Kausar et al. (28)	Sb/Rn/Pa	Pakistan	Type 2 diabetes	55/55	51.1/50.4	Both	12	15 mL/d ACV/P	Yes	Investigator-initiated
Jafarirad et al. (27)	Rn/Pa	Iran	Type 2 diabetes	37/36	53.11/52.94	Both	8	30 mL/d ACV + dietary recommendation/ dietary recommendation	Yes	Investigator-initiated

Apple Cider Vinegar; NR, Not Reported; Db, Double-blinded; Sb, Single-blinded; Rn, Randomized; Pa, Parallel; P, Placebo.

10.3389/fnut.2025.1528383

10.3389/fnut.2025.1528383

TABLE 3 Results of risk of bias assessment for CTs included in the current meta-analysis on the effect of apple vinegar supplementation on glycemic control in patients with type 2.

Study	Sequence generation	Allocation concealment	Selective outcome reporting	Other sources of bias	Blinding of participants and personnel	Blinding of outcome assessment	Incomplete outcome data	Overall risk of bias
Ebrahimi-Mamaghani et al. (24)	U	U	H	L	H	H	L	H
Mahmoodi et al. (29)	H	U	H	L	L	U	L	M
Halima et al. (26)	U	U	H	L	L	U	L	L
Mohammadpourhodki et al. (30)	U	U	H	L	H	H	L	H
Gheflati et al. (25)	L	U	H	L	H	H	L	H
Kausar et al. (28)	L	U	H	L	H	H	L	H
Jafarirad et al. (27)	L	H	L	L	H	H	L	H

U, unclear risk of bias; L, low risk of bias; H, high risk of bias; M, moderate risk of bias.

no significant association between changes in FBS values with ACV dose ($p = 0.184$) and duration ($p = 0.928$) (Figures S2A,B). On the other hand, the dose–response meta-analysis of ACV intake and changes in FBS included 7 studies. The present study found a significant linear association between ACV consumption and changes in FBS so that each 1 mL/day increase in ACV consumption was associated with a-1.255 mg/dL reduction in FBS ($p < 0.001$). Moreover, the results showed a non-linear association, in which, a significant reduction in FBS was seen in dose >10 mL/d ($P_{dose-response} < 0.001$, $P_{non-linear} = 0.607$) (Figure 3).

Various results achieved from this part could cause uncertainty regarding the association between dose of ACV and FBS changes and needs further evaluations.

3.4.2 Meta-analysis on ACV and HbA1c

We included 4 studies and 319 participants in the HbA1c analysis. ACV significantly reduced HbA1c based on the results of a random-effect model (WMD: −1.53, 95% CI: −2.65, −0.41, $p = 0.008$), with significant heterogeneity ($I^2 = 83.31\%$, $p < 0.001$) (Figure 2B).

3.4.3 Meta-analysis on ACV and HOMA-IR

The present study included 3 studies and 173 participants in the HOMA-IR analysis. ACV did not influence HOMA-IR significantly (WMD: 0.631, 95% CI: −0.99, 2.25, $p = 0.446$), and the studies' heterogeneity was not significant ($I^2 = 56.2\%$, $p = 0.102$) (Figure 2C).

3.4.4 Meta-analysis on ACV and insulin

We included 3 studies and 173 participants in the serum insulin analysis. ACV increased insulin levels based on the results of a random-effect model (WMD: 2.059 μu/ml, 95% CI: 0.26, 3.86, $p = 0.025$), with non-significant heterogeneity ($I^2 = 0\%$, $p = 0.42$) (Figure 2D).

3.5 Sensitivity analysis

As shown in the leave-one-out sensitivity analysis, the effect sizes of ACV on FBS and HbA1c were robust, indicating that the removal of every trial had no significant impact on the meta-analysis results (Figures S1A,B). In spite of this, the effect of ACV on HOMA-IR, and insulin was sensitive to one (25) and two (24, 27) studies, respectively (Figures S1C,D).

3.6 Publication bias

According to the "trim and fill" method, for FBS, HbA1c, HOMA-IR and insulin there were 1, 0, 1 and 2 studies that were missing, respectively (Figure S3A,D). We summarized the corrected effect sizes and the results of Begg's rank correlation, Egger's linear regression, and "fail-safe N" tests in Table S2.

4 Discussion

This systematic review and meta-analysis reviewed the available literature and CTs assessing the effects of ACV on glycemic factors and insulin sensitivity in T2DM. ACV could significantly reduce FBS and

TABLE 4 GRADE.

Certainty assessment							No. of patients		Effect	Certainty	Importance
No. of studies	Study design	Risk of bias	Inconsistency	Indirectness	Imprecision	Other considerations	(ACV)	(placebo)	Absolute (95% CI)		
FBS											
7	Randomized trials	Serious[a]	Not serious	Not serious	Not serious	None	235	228	MD 21.929 mg/dL lower (29.19 lower to 14.67 lower)	⨁⨁⨁◯ Moderate	IMPORTANT
HbA1c											
4	Randomized trials	Serious[b]	Serious[c]	Not serious	Not serious	None	160	159	MD 1.53 mg/dL lower (2.65 lower to 0.41 lower)	⨁⨁◯◯ Low	IMPORTANT
HOMA-IR											
3	Randomized trials	Serious[d]	Not serious	Not serious	Serious[e]	None	88	85	MD 0.631 mg/dL higher (0.99 lower to 2.25 higher)	⨁⨁◯◯ Low	IMPORTANT
Insulin											
3	Randomized trials	Serious[f]	Not serious	Not serious	Not serious	None	88	85	MD 2.059 μu/ml higher (0.26 higher–3.86 higher)	⨁⨁⨁◯ Moderate	IMPORTANT

FBS, fasting blood sugar, HbA1c, glycated hemoglobin; HOMA-IR, homeostasis model assessment for insulin resistance; CI, confidence interval; MD, mean difference. [a]Serious risk of bias since 4 trials were at high risk of bias. Downgraded. [b]Serious risk of bias since 2 trials were at high risk of bias. Downgraded. [c]Serious inconsistency since $I^2 = 88.61\%$. Downgraded. [d]Serious risk of bias since all trials were at high risk of bias. Downgraded. [e]Serious imprecision since the result of the analysis is not meaningful. Downgraded. [f]Serious risk of bias since all trials were at high risk of bias. Downgraded.

10.3389/fnut.2025.1528383

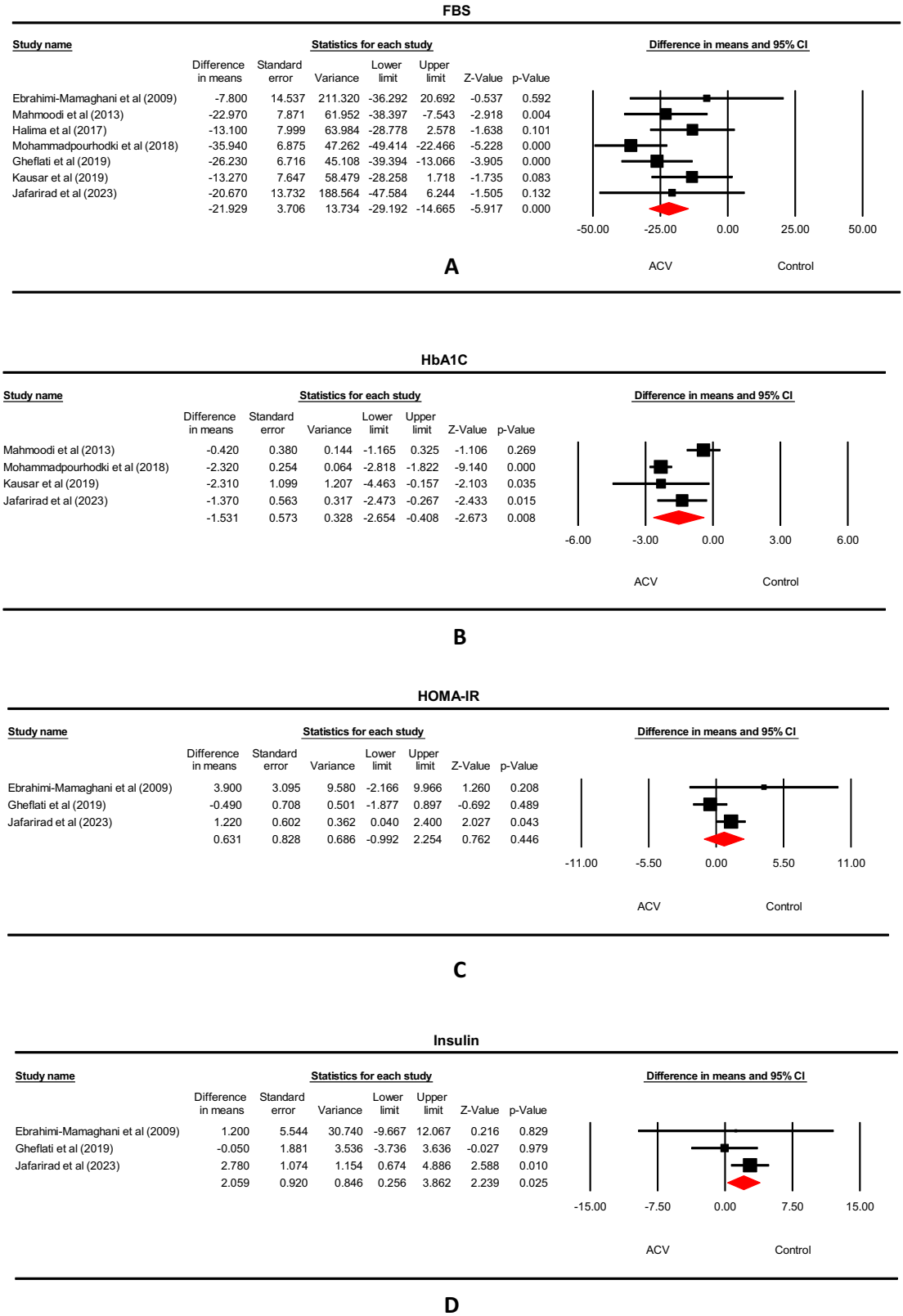

FIGURE 2
Forest plot for the effect of ACV on **(A)** FBS, **(B)** HbA1c, **(C)** HOMA-IR and **(D)** Insulin in T2DM patients, expressed as mean differences between intervention and control groups.

TABLE 5 Results of subgroup analysis of included randomized controlled trials in the meta-analysis of ACV and FBS in T2DM patients.

Variables	Dose (ml/d)		Duration (weeks)		Design	
FBS (mg/dl)	≤ 15	< 8	< 8	≥8	B	NB
Number of comparisons	4	2	2	5	3	4
WMD (95% CI)	−15.66 (−24.12, −7.19)	−18.12 (−29.11, −7.12)	−18.12 (−29.11, −7.12)	−24.34 (−31.73, −16.96)	−16.42 (−25.29, −7.55)	−27.89 (−36.38, −19.41)
p-value	< 0.001	0.001	0.001	< 0.001	< 0.001	< 0.001
P between	0.02		0.36		0.07	
I^2 (%)	0	0	0	37.38	0	17.1
P-heterogeneity	0.72	0.38	0.38	0.17	0.6	0.31

FBS, fasting blood sugar; B, blinded; NB, Not-blinded.

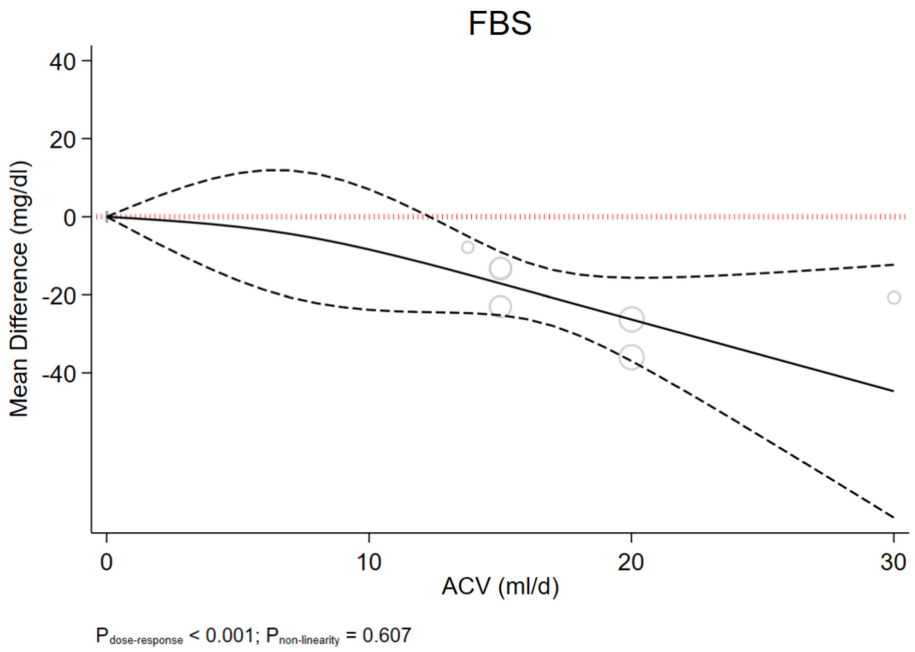

FIGURE 3
Non-linear dose–response effects of ACV dosages (ml/d) on FBS, in T2DM patients. The 95% CI is demonstrated in the dashed line.

HbA1c levels. However, ACV increased insulin levels. Based on the dose–response analysis, the present study found linear and non-linear associations between ACV doses and FBS levels. The present study showed significant reductions in doses >10 mL/dL.

Hence, the current study showed decreasing trends in FBS that were in line with that of a meta-analysis reporting the reducing effects of ACV on fasting plasma glucose (FPG) in individuals with diabetes, overweight, or obesity (31). However, they did not show any relationship between the dose and duration of the supplementation of ACV with the changes in FPG (31) which was different from the result of the present study focusing on the effects of ACV dose on the FBS changes. The main reason for this difference could be possibly due to the differences in the included population and their baseline FPG. The present study only included patients with T2DM, while in that study (31), they included non-diabetic patients as well. They also emphasized the glucose-lowering effects of ACV in patients with diabetes rather than the no-diabetic ones in their sub-group analysis. They emphasized that higher baseline FPG could cause better results following ACV supplementation (49). This could almost justify better results in higher doses of ACV in patients with diabetes as in the present study. On the other hand, in accordance with the present finding, in another meta-analysis, vinegar consumption could decrease FBS as an important cardio-metabolic factor (49).

It is important to note that, there are several mechanisms for justifying the effects of ACV on glycemic control and improving FBS concentrations. ACV could cause a delay in gastric emptying and could improve the utilization of glucose. On the other hand, ACV could decrease liver glucose production and enhance the secretion of insulin (50, 51). Acetic acid content of ACV could inhibit disaccharidase (52) and α-amylase (21). This way, it can consequently decrease blood glucose. This mechanism can also explain the glucose-lowering effects of ACV. Further, increases in hepatic and muscle uptake of glucose could happen following ACV consumption and this could also explain hypoglycemic effects of ACV. On the other hand, ACV could increase the activity of glycogen synthase and decrease glycolysis. It was observed that

acetic acid could increase glycogen repletion and this could also affect glucose uptake (53–55) and these could justify the possible role of ACV containing acetic acid in glycemic control. It was hypothesized that acetate metabolism through tricarboxylic acid cycle via acetyl-CoA (56) which can obtain acetate, could also affect glycogen synthase activation in the liver (57). All of these could help blood glucose control as well. However, these are mechanisms which have been explored, otherwise it remains a mere speculation. Moreover, one of the main polyphenols named chlorogenic acid present in ACV could cause glucose-6-phosphatase inhibition in rats. This can in turn decrease glucose release in the process of gluconeogenesis and glycogenolysis and decrease blood glucose consequently (58). It is clear that higher doses of ACV could exert more beneficial effects due to the higher active and effective components. All the aforementioned mechanisms could explain and justify the decreasing trend of FBS following ACV consumption. These effects can be more pronounced in the higher doses. However, further researches are warranted to better elucidate the exact dose of ACV with the maximum glucose-lowering effects.

In addition, as another finding, considering the results of ACV and HbA1C, we have seen a significant reduction in HbA1C following ACV consumption. However, the present study did not show any significant changes in the levels of insulin and HOMA-IR after ACV consumption. These results were in accordance with the results of the meta-analysis by Hadi et al. (31) that showed a decreasing trend in HbA1c after ACV consumption. However, they showed no changes in insulin or HOMA-IR. They also emphasized the beneficial effects of ACV on HbA1c in patients with diabetes with higher baseline FPG rather than non-diabetes ones (48). This was also seen in the current meta-analysis with the target population of patients with T2DM. This was also confirmed by two other meta-analyses which demonstrated that vinegar consumption could significantly decrease HbA1c (49, 59). HbA1c is considered a marker for glucose control in the past 2–3 months in patients with diabetes (52). Vinegar could ameliorate the insulin response to food glycemic index in patients with diabetes and could decrease HbA1c with this mechanism (60, 61). However, the current study showed increasing effects of ACV on insulin levels which seems unexpectable as is not in line with the results of other glycemic markers in the present meta-analysis. This finding was not in accordance with the finding of another meta-analysis by Shishehbor et al. (62) that mentioned the reducing trend in insulin levels following vinegar consumption. The main differences between that study and the present meta-analysis are related to the type of vinegar and the included studies containing insulin data (8 trials in their studies vs. three trials in the current study). On the other hand, in another meta-analysis by Hadi et al., no significant changes were seen in insulin concentration following ACV consumption in adults (31). Also, in a meta-analysis in 2022, vinegar consumption did not change serum insulin in healthy individuals and in those with cardio-metabolic diseases (49). Moreover, it is noteworthy to state that we included a small number of studies for assessing the effects of ACV on insulin and HOMA-IR (two for HOMA-IR and three for insulin). This cause uncertainty for drawing reliable conclusions in this regard. In addition, this issue was also mentioned in the study by Hadi et al. (31) as they included a few studies for these variables. Hence, the results considering the effects of ACV on insulin and HOMA-IR should be interpreted with caution. More investigations are warranted. However, a promising effect for HbA1c was observed.

Finally, regarding the sensitivity analysis, for all parameters, the removal of any study did not affect the results, except for HbA1c which was sensitive to two studies (28, 30) and insulin which was sensitive to one study that showed decreasing trends in insulin levels following ACV consumption in type 2 hyperlipidemic patients (25). Moreover, as we included only 3 studies for assessing the effects of ACV on insulin levels, the opposite effect of one study on the results could cause uncertainty regarding the increasing effects of ACV on insulin levels. On the other hand, the two studies affecting the results of HbA1c are those that showed promising effects of ACV on HbA1c. This could avoid reliable and definite conclusions to be drawn in this regard. Hence, the results of ACV on HbA1c and insulin should be interpreted with caution.

The present systematic review and meta-analysis pooled the available literature (CTs) assessing the effects of ACV on glycemic control and insulin sensitivity. This study had some limitations and strengths. As a limitation, we included the small number of studies for some variables such as insulin and HOMA-IR which could cause uncertainty regarding the final conclusions for those parameters. Also, we could not conduct sub-group analysis or meta-regression conduction for those variables. On the other hand, from seven included studies, five were conducted in Iran and totally 6 studies were in Asia (five in Iran and one in Pakistan) and this could affect the final interpretation of results and the results could not be possibly generalized to all populations in various geographical locations. Hence, interpretation of the final results should be done with caution. However, as a strength, meta-regression and sub-group analysis (based on dose, design, and duration of the studies) was done for FBS which could cause better definite results. Moreover, linear and non-linear dose–response relationships between the FBS parameter and ACV dosage were examined. Another strength is that we evaluated the ACV effects on a specific population (T2DM) in this meta-analysis. Also, as another strength, we observed non-significant heterogeneity among the included studies with most of the assessed parameters which could cause better uniformity among them. Hence, the final results could be possibly more reliable in this study from this point of view.

5 Conclusion

To sum up, the present systematic review and meta-analysis showed promising effects of ACV on FBS with a dose–response effect in patients with T2DM. The effects of ACV on decreasing HbA1c and increasing insulin were not definite due to the effects of omissions of two studies that could possibly change the results of HbA1c and one study that could affect insulin and the small number of studies included in insulin assessment. Moreover, we observed no changes in insulin resistance parameter including hemostatic model assessment for insulin resistance (HOMA-IR) following ACV consumption. This could be pertinent to the small number of studies that we included in this regard. Finally, it can be mentioned that further investigations are needed to better elucidate the exact effects of ACV on insulin, HOMA-IR, and HbA1c and to better definite the best effective dose of ACV with glucose-lowering effects, especially in various populations.

Data availability statement

The original contributions presented in the study are included in the article/Supplementary material, further inquiries can be directed to the corresponding author.

Author contributions

DA: Conceptualization, Data curation, Investigation, Supervision, Writing – original draft, Writing – review & editing. MB: Data curation, Formal analysis, Methodology, Software, Writing – original draft, Writing – review & editing. ZS: Supervision, Writing – original draft, Writing – review & editing. MM: Conceptualization, Investigation, Methodology, Writing – review & editing.

Funding

The author(s) declare that financial support was received for the research, authorship, and/or publication of this article. The research protocol was approved and supported by the student research committee, Shiraz University of Medical Sciences (registration code: 32102).

Conflict of interest

The authors declare that the research was conducted in the absence of any commercial or financial relationships that could be construed as a potential conflict of interest.

Generative AI statement

The author(s) declare that no Gen AI was used in the creation of this manuscript.

Publisher's note

All claims expressed in this article are solely those of the authors and do not necessarily represent those of their affiliated organizations, or those of the publisher, the editors and the reviewers. Any product that may be evaluated in this article, or claim that may be made by its manufacturer, is not guaranteed or endorsed by the publisher.

Supplementary material

The Supplementary material for this article can be found online at: https://www.frontiersin.org/articles/10.3389/fnut.2025.1528383/full#supplementary-material

References

1. Tsalamandris S, Antonopoulos AS, Oikonomou E, Papamikroulis G-A, Vogiatzi G, Papaioannou S, et al. The role of inflammation in diabetes: current concepts and future perspectives. *Eur Cardiol Rev*. (2019) 14:50–9. doi: 10.15420/ecr.2018.33.1

2. Association, AD. 2. Classification and diagnosis of diabetes: standards of medical care in diabetes—2021. *Diabetes Care*. (2021) 44:S15–33. doi: 10.2337/dc21-S002

3. Sun H, Saeedi P, Karuranga S, Pinkepank M, Ogurtsova K, Duncan BB, et al. Idf diabetes atlas: global, regional and country-level diabetes prevalence estimates for 2021 and projections for 2045. *Diabetes Res Clin Pract*. (2022) 183:109119. doi: 10.1016/j.diabres.2021.109119

4. Balakumar P, Maung-U K, Jagadeesh G. Prevalence and prevention of cardiovascular disease and diabetes mellitus. *Pharmacol Res*. (2016) 113:600–9. doi: 10.1016/j.phrs.2016.09.040

5. Chen R, Ovbiagele B, Feng W. Diabetes and stroke: epidemiology, pathophysiology, pharmaceuticals and outcomes. *Am J Med Sci*. (2016) 351:380–6. doi: 10.1016/j.amjms.2016.01.011

6. Lin KY, Hsih WH, Lin YB, Wen CY, Chang TJ. Update in the epidemiology, risk factors, screening, and treatment of diabetic retinopathy. *J Diab Inv*. (2021) 12:1322–5. doi: 10.1111/jdi.13480

7. Harding JL, Pavkov ME, Magliano DJ, Shaw JE, Gregg EW. Global trends in diabetes complications: a review of current evidence. *Diabetologia*. (2019) 62:3–16. doi: 10.1007/s00125-018-4711-2

8. Mcfarland LV. A review of the evidence of health claims for biotherapeutic agents. *Microb Ecol Health Dis*. (2000) 12:65–76. doi: 10.1080/089106000435446

9. Salminen S. Human studies on probiotics: aspects of scientific documentation. *Näringsforskning*. (2001) 45:8–12. doi: 10.3402/fnr.v45i0.1783

10. Ng SC, Xu Z, Mak JWY, Yang K, Liu Q, Zuo T, et al. Microbiota engraftment after faecal microbiota transplantation in obese subjects with type 2 diabetes: a 24-week, double-blind, randomised controlled trial. *Gut*. (2022) 71:716–23. doi: 10.1136/gutjnl-2020-323617

11. Umirah F, Neoh CF, Ramasamy K, Lim SM. Differential gut microbiota composition between type 2 diabetes mellitus patients and healthy controls: a systematic review. *Diabetes Res Clin Pract*. (2021) 173:108689. doi: 10.1016/j.diabres.2021.108689

12. Association, AD. Standards of medical care in diabetes—2022 abridged for primary care providers. *Clin Diabetes*. (2022) 40:10–38. doi: 10.2337/cd22-as01

13. Evert AB, Dennison M, Gardner CD, Garvey WT, Lau KHK, Macleod J, et al. Nutrition therapy for adults with diabetes or prediabetes: a consensus report. *Diabetes Care*. (2019) 42:731–54. doi: 10.2337/dci19-0014

14. Mohammadi-Sartang M, Sohrabi Z, Barati-Boldaji R, Raeisi-Dehkordi H, Mazloom Z. Flaxseed supplementation on glucose control and insulin sensitivity: a systematic review and meta-analysis of 25 randomized, placebo-controlled trials. *Nutr Rev*. (2018) 76:125–39. doi: 10.1093/nutrit/nux052

15. Saxena A, Vikram NK. Role of selected Indian plants in management of type 2 diabetes: a review. *J Altern Complement Med*. (2004) 10:369–78. doi: 10.1089/107555304323062365

16. Muhammad MA, Kawar NS. Behavior of parathion in tomatoes processed into juice and ketchup. *J Environ Sci Health Part B*. (1985) 20:499–510. doi: 10.1080/03601238509372491

17. Khezri SS, Saidpour A, Hosseinzadeh N, Amiri Z. Beneficial effects of apple cider vinegar on weight management, visceral adiposity index and lipid profile in overweight or obese subjects receiving restricted calorie diet: a randomized clinical trial. *J Funct Foods*. (2018) 43:95–102. doi: 10.1016/j.jff.2018.02.003

18. Dupont MS, Bennett RN, Mellon FA, Williamson G. Polyphenols from alcoholic apple cider are absorbed, metabolized and excreted by humans. *J Nutr*. (2002) 132:172–5. doi: 10.1093/jn/132.2.172

19. Natera R, Castro R, De Valme García-Moreno M, Hernández MJ, García-Barroso C. Chemometric studies of vinegars from different raw materials and processes of production. *J Agric Food Chem*. (2003) 51:3345–51. doi: 10.1021/jf021180u

20. Bounihi A, Bitam A, Bouazza A, Yargui L, Koceir EA. Fruit vinegars attenuate cardiac injury via anti-inflammatory and anti-adiposity actions in high-fat diet-induced obese rats. *Pharm Biol*. (2017) 55:43–52. doi: 10.1080/13880209.2016.1226369

21. Iman M, Moallem SA, Barahoyee A. Effect of apple cider vinegar on blood glucose level in diabetic mice. *Pharm Sci*. (2015) 20:163

22. Nazıroğlu M, Güler M, Özgül C, Saydam G, Küçükayaz M, Sözbir E. Apple cider vinegar modulates serum lipid profile, erythrocyte, kidney, and liver membrane oxidative stress in ovariectomized mice fed high cholesterol. *J Membr Biol*. (2014) 247:667–73. doi: 10.1007/s00232-014-9685-5

23. Shishehbor F, Mansoori A, Sarkaki A, Jalali M, Latifi S. Apple cider vinegar attenuates lipid profile in normal and diabetic rats. *PJBS*. (2008) 11:2634–8.

24. Ebrahimi-Mamaghani A, Golzarand A, Vahed-Jabbary. Long-term effects of processed *Berberis Vulgaris* on some metabolic syndrome components. *Iranian J Endocrinol Metab*. (2009) 11:41–7.

25. Gheflati A, Bashiri R, Ghadiri-Anari A, Reza JZ, Kord MT, Nadjarzadeh A. The effect of apple vinegar consumption on glycemic indices, blood pressure, oxidative stress, and homocysteine in patients with type 2 diabetes and dyslipidemia: a randomized controlled clinical trial. *Clin Nutr ESPEN*. (2019) 33:132–8. doi: 10.1016/j.clnesp.2019.06.006

26. Halima BH, Sarra K, Mohamed S, Louay T, Fethi BS, Houda BJ, et al. Apple cider vinegar ameliorates hyperglycemia and hyperlipidemia in Tunisian type 2 diabetic patients. *Int J Multidisciplinary Curr Res*. (2017) 5:1453–9.

27. Jafarirad S, Elahi M-R, Mansoori A, Khanzadeh A, Haghighizadeh M-H. The improvement effect of apple cider vinegar as a functional food on anthropometric indices, blood glucose and lipid profile in diabetic patients: a randomized controlled clinical trial. *Front Clin Diab Healthcare*. (2023) 4:1288786. doi: 10.3389/fcdhc.2023.1288786

28. Kausar S, Abbas MA, Ahmad H, Yousef N, Ahmed Z, Humayun N, et al. Effect of apple cider vinegar in type 2 diabetic patients with poor glycemic control: a randomized placebo controlled design®. *Int J Med Res Health Sci*. (2019) 8:149–59.

29. Mahmoodi M, Hosseini-Zijoud S-M, Hassanshahi G, Nabati S, Modarresi M, Mehrabian M, et al. The effect of white vinegar on some blood biochemical factors in type 2 diabetic patients. *J Diab Endocrinol*. (2013) 4:1–5. doi: 10.5897/JDE12.015

30. Mohammadpourhodki R, Sargolzaei M. The effects of apple vinegar on fasting blood sugar (Fbs) and glycosylated hemoglobin in patients with type 2 diabetes. *Prensa Medica Argentina*. (2018) 104:1–22.

31. Hadi A, Pourmasoumi M, Najafgholizadeh A, Clark CC, Esmaillzadeh A. The effect of apple cider vinegar on lipid profiles and glycemic parameters: a systematic review and meta-analysis of randomized clinical trials. *BMC Compl Med Ther*. (2021) 21:179. doi: 10.1186/s12906-021-03351-w

32. Page MJ, Moher D, Bossuyt PM, Boutron I, Hoffmann TC, Mulrow CD, et al. Prisma 2020 explanation and elaboration: updated guidance and exemplars for reporting systematic reviews. *BMJ*. (2021) 372:n160. doi: 10.1136/bmj.n160

33. Higgins JP, Altman DG, Gøtzsche PC, Jüni P, Moher D, Oxman AD, et al. The Cochrane Collaboration's tool for assessing risk of bias in randomised trials. *BMJ*. (2011) 343:d5928. doi: 10.1136/bmj.d5928

34. Guyatt GH, Oxman AD, Vist GE, Kunz R, Falck-Ytter Y, Alonso-Coello P, et al. Grade: an emerging consensus on rating quality of evidence and strength of recommendations. *BMJ*. (2008) 336:924–6. doi: 10.1136/bmj.39489.470347.AD

35. Borenstein M. Comprehensive meta-analysis software. *Syst Rev Health Res Meta-Anal Context*. (2022) 22:535–48. doi: 10.1002/9781119099369.ch27

36. Higgins J. (2011). *Cochrane handbook for systematic reviews of interventions. Version 5.1. 0 [updated March 2011]*. The Cochrane Collaboration. Available at: www.cochrane-handbook.org.

37. Hozo SP, Djulbegovic B, Hozo I. Estimating the mean and variance from the median, range, and the size of a sample. *BMC Med Res Methodol*. (2005) 5:1–10.

38. Digitizer, IP. (2020). How to extract data from graphs using plot digitizer or getdata graph digitizer.

39. Sahebkar A. Are curcuminoids effective C-reactive protein-lowering agents in clinical practice? Evidence from a meta-analysis. *Phytother Res*. (2014) 28:633–42. doi: 10.1002/ptr.5045

40. Crippa A, Discacciati A, Bottai M, Spiegelman D, Orsini N. One-stage dose–response meta-analysis for aggregated data. *Stat Methods Med Res*. (2019) 28:1579–96. doi: 10.1177/0962280218773122

41. Duval S, Tweedie R. Trim and fill: a simple funnel-plot–based method of testing and adjusting for publication bias in meta-analysis. *Biometrics*. (2000) 56:455–63. doi: 10.1111/j.0006-341X.2000.00455.x

42. Basharat S, Gilani SA, Qamar MM, Basharat A. Therapeutic effect of apple cider vinegar on diabetes mellitus. *Rawal Med J*. (2019) 44:884–4.

43. Siddiqui FJ, Assam PN, De Souza NN, Sultana R, Dalan R, Chan ES-Y. Diabetes control: is vinegar a promising candidate to help achieve targets? *J Evid Based Int Med*. (2018) 23:2156587217753004. doi: 10.1177/2156587217753004

44. Bashiri R, Ghadiri-Anari A, Hekmatimoghadam H, Dehghani A, Najarzadeh A. The effect of apple vinegar on lipid profiles and anthropometric indices in type 2 diabetes patients with dyslipidemia: a randomized clinical trial. *Ssu_J*. (2014) 22:1543–53.

45. Dange N, Deshpande K. Effect of apple on fasting blood sugar and plasma lipids levels in type ii diabetes. *Int J Pharm Bio Sci*. (2013) 4:B511–7.

46. Mayne P, Mcgill A, Gormley TR, Tomkin G, Julian T. The effect of apple fibre on diabetic control and plasma lipids. *Ir J Med Sci*. (1982) 151:36–41. doi: 10.1007/BF02940140

47. Mousavi E, Sajjadi P, Firoozjahi A, Moazezi Z. Effect of apple cider vinegar on postprandial blood glucose in type 2 diabetic patients treated with hypoglycemic agents. *J Babol Univ Med Sci*. (2013) 15:7–11. doi: 10.18869/acadpub.jbums.15.6.7

48. Heljić B, Velija-Ašimi Z, Bureković A, Karlović V, Avdagić A, Ćemalović M. The role of natural supplement of apple vinegar and syrup in the management of type 2 diabetes mellitus. *J Health Sci*. (2014) 4:176–80. doi: 10.17532/jhsci.2014.220

49. Sohouli MH, Kutbi E, Al Masri MK, Dadhkhah H, Fatahi S, Santos HO, et al. Effects of vinegar consumption on cardiometabolic risk factors: a systematic review and meta-analysis of randomized controlled trials. *Eur J Integr Med*. (2022a) 55:102176. doi: 10.1016/j.eujim.2022.102176

50. Kausar S, Humayun A, Ahmed Z, Abbas MA, Tahir A. Effect of apple cider vinegar on glycemic control, hyperlipidemia and control on body weight in type 2 diabetes patients. *Health Sci*. (2019) 8:59–74.

51. Petsiou EI, Mitrou PI, Raptis SA, Dimitriadis GD. Effect and mechanisms of action of vinegar on glucose metabolism, lipid profile, and body weight. *Nutr Rev*. (2014) 72:651–61. doi: 10.1111/nure.12125

52. Ogawa N, Satsu H, Watanabe H, Fukaya M, Tsukamoto Y, Miyamoto Y, et al. Acetic acid suppresses the increase in disaccharidase activity that occurs during culture of caco-2 cells. *J Nutr*. (2000) 130:507–13. doi: 10.1093/jn/130.3.507

53. Fushimi T, Sato Y. Effect of acetic acid feeding on the circadian changes in glycogen and metabolites of glucose and lipid in liver and skeletal muscle of rats. *Br J Nutr*. (2005) 94:714–9. doi: 10.1079/BJN20051545

54. Fushimi T, Tayama K, Fukaya M, Kitakoshi K, Nakai N, Tsukamoto Y, et al. Acetic acid feeding enhances glycogen repletion in liver and skeletal muscle of rats. *J Nutr*. (2001) 131:1973–7. doi: 10.1093/jn/131.7.1973

55. Fushimi T, Tayama K, Fukaya M, Kitakoshi K, Nakai N, Tsukamoto Y, et al. The efficacy of acetic acid for glycogen repletion in rat skeletal muscle after exercise. *Int J Sports Med*. (2002) 23:218–22. doi: 10.1055/s-2002-23172

56. Ballard F. Supply and utilization of acetate in mammals. *Am J Clin Nutr*. (1972) 25:773–9. doi: 10.1093/ajcn/25.8.773

57. Des Rosiers C, David F, Garneau M, Brunengraber H. Nonhomogeneous labeling of liver mitochondrial acetyl-CoA. *J Biol Chem*. (1991) 266:1574–8. doi: 10.1016/S0021-9258(18)52332-2

58. Hemmerle H, Burger H-J, Below P, Schubert G, Rippel R, Schindler PW, et al. Chlorogenic acid and synthetic chlorogenic acid derivatives: novel inhibitors of hepatic glucose-6-phosphate translocase. *J Med Chem*. (1997) 40:137–45. doi: 10.1021/jm9607360

59. Cheng LJ, Jiang Y, Wu VX, Wang W. A systematic review and meta-analysis: vinegar consumption on glycaemic control in adults with type 2 diabetes mellitus. *J Adv Nurs*. (2020) 76:459–74. doi: 10.1111/jan.14255

60. Nakajima A, Ebihara K. Effect of prolonged vinegar feeding on postprandial blood glucose response in rats. 日本栄養・食糧学会誌. (1988) 41:487–9.

61. Saint C, Gaulejac N, Provoab C. Polyphenol profile of French cider apple varieties. *Agric Food Chem*. (1999) 7:425

62. Shishehbor F, Mansoori A, Shirani F. Vinegar consumption can attenuate postprandial glucose and insulin responses; a systematic review and meta-analysis of clinical trials. *Diabetes Res Clin Pract*. (2017) 127:1–9. doi: 10.1016/j.diabres.2017.01.021

frontiers | Frontiers in Nutrition

TYPE Original Research
PUBLISHED 18 February 2025
DOI 10.3389/fnut.2025.1498004

Check for updates

OPEN ACCESS

EDITED BY
Bwalya Angel Witika,
Sefako Makgatho Health Sciences University, South Africa

REVIEWED BY
Pugazhendhi Srinivasan,
University of Kansas Medical Center, United States
Aristote Buya,
University of Kinshasa, Democratic Republic of Congo

*CORRESPONDENCE
Yali Huang
✉ avonlii@163.com
Wei Wang
✉ wangwei16400@163.com

†These authors have contributed equally to this work

RECEIVED 18 September 2024
ACCEPTED 05 February 2025
PUBLISHED 18 February 2025

CITATION
Wei Y, Chen S, Ling Y, Wang W and Huang Y (2025) Multi-omics revealed that the postbiotic of hawthorn-probiotic alleviated constipation caused by loperamide in elderly mice.
Front. Nutr. 12:1498004.
doi: 10.3389/fnut.2025.1498004

COPYRIGHT
© 2025 Wei, Chen, Ling, Wang and Huang. This is an open-access article distributed under the terms of the Creative Commons Attribution License (CC BY). The use, distribution or reproduction in other forums is permitted, provided the original author(s) and the copyright owner(s) are credited and that the original publication in this journal is cited, in accordance with accepted academic practice. No use, distribution or reproduction is permitted which does not comply with these terms.

Multi-omics revealed that the postbiotic of hawthorn-probiotic alleviated constipation caused by loperamide in elderly mice

Yu Wei[1,2,3†], Shuai Chen[4†], Ying Ling[1†], Wei Wang[1,3*] and Yali Huang[1,2*]

[1]Guangzhou University of Chinese Medicine, Guangzhou, China, [2]Basic Medical Science College, Guangzhou University of Chinese Medicine, Guangzhou, China, [3]The First Clinical Medical School, Guangzhou University of Chinese Medicine, Guangzhou, China, [4]Yunnan University of Chinese Medicine, Kunming, China

Background: Constipation is a prevalent and recurrent gastrointestinal disorder causing significant discomfort. However, current treatments often prove ineffective. Previous research indicates that the postbiotic derived from a combination of hawthorn and probiotics can alleviate constipation. This study aimed to investigate its mechanisms using loperamide-induced constipation in aged KM mice.

Methods: Constipated mice were divided into groups receiving 10% lactulose (Y), hawthorn extract (S), probiotics (F), and the postbiotic of hawthorn-probiotic (FS). UPLC–MS metabolomics identified constituents of F, S, and FS. Network pharmacological analysis identified targets affected by FS. RT-qPCR assessed target expression in mouse colons, along with IL-6 and IL-17A levels. Molecular docking with AutoDock Tools1.5.6 evaluated interactions between FS components and targets. ex vivo colonic organ culture and RT-qPCR assessed target changes. Molecular dynamics analysis further scrutinized interactions. Targeted metabolomics measured short-chain fatty acid levels in mouse stool.

Results: UPLC–MS metabolomics revealed distinct profiles for F, S, and FS, with FS showing decreased toxic substances and increased beneficial ones compared to S. Network pharmacology identified 20 cross-targets of FS in constipation. RT-qPCR showed decreased NR1I2 and SULT1A1 and increased GLP-2r in FS-treated mice. Inflammatory cytokines IL-6 and IL-17A were also reduced. ex vivo colonic organ culture and molecular docking identified effective combinations such as TNF-Baicalin and AQP3-Quinacridone. RMSD, RMSF, and RG analyses indicated favorable interactions between small molecules and targets. Targeted metabolomics revealed differing short-chain fatty acid contents in feces among groups.

Conclusion: The postbiotic of hawthorn-probiotic alleviates constipation by regulating intestinal water and sodium metabolism, maintaining the intestinal barrier and gut flora, promoting epithelial cell proliferation, reducing inflammatory responses, and improving short-chain fatty acid metabolism.

KEYWORDS

postbiotic, hawthorn, probiotic, constipation, inflammation, intestinal microenvironment

1 Introduction

Chronic senile constipation is one of the common digestive system problems in the elderly (>65-70 years) (1, 2), and its incidence increases with the increase of age (3). This type of constipation can be caused by a variety of factors, including lifestyle factors, dietary habits, side effects of medications, neuromuscular dysfunction, and digestive disorders (4, 5). In addition to traditional drug treatment and dietary changes, some new treatment methods are gradually attracting attention, such as probiotics, prebiotics and post-biologics, which can relieve constipation by regulating intestinal flora and improving intestinal function (6–12).

Our previous research efforts have identified the potential of hawthorn-probiotic post-biotics in alleviating constipation (13). We found that postbiotic of hawthorn-probiotic exerts remarkable effects on constipation by regulating water and sodium metabolism, repairing intestinal barrier, relieving inflammation, and restoring microflora structure (13). Recently we make some progress on the postbiotic of hawthorn-probiotic metabolites and targets for constipation. We think these might offer a promising therapy for constipation.

2 Materials and methods

2.1 Materials

2.1.1 Metabolite

Pubchem CID	Metabolite name	Source	CAS number	Purity
13976	Quinacridone	Chengdu Must Bio-Technology Co., Ltd.	1047-16-1	98%
5282151	vitexin-2″-o-rhamnoside		64820-99-1	HPLC≥98%
9830628	L-Isoleucine		73-32-5	99%
64982	Baicalin		21967-41-9	HPLC≥98%
60198	Exemestane		107868-30-4	98%
5281643	Hyperoside		482-36-0	HPLC≥98%
5280343	Quercetin		117-39-5	HPLC≥98%
5280443	Apigenin		520-36-5	HPLC≥98%
8679	N-Phenyl-2-naphthylamine		135-88-6	98%
5280961	Genistein		446-72-0	97%
5281708	Daidzein		486-66-8	HPLC≥98%

2.1.2 Short chain fatty acids standard

Name	CAS number	Molecular formula	Molecular weight
Acetic acid	64-19-7	$C_2H_4O_2$	60.05
Propionic acid	79-09-4	$C_3H_6O_2$	74.08
Isobutyric acid	79-31-2	$C_4H_8O_2$	88.11
Butyric Acid	107-92-6	$C_4H_8O_2$	88.11
Valeric acid	109-52-4	$C_5H_{10}O_2$	102.13
Isovaleric acid	503-74-2	$C_5H_{10}O_2$	102.13
Hexanoic acid	142-62-1	$C_6H_{12}O_2$	116.16

2.1.3 Chemicals

Name	Source	Cat. number
Methanol, LC–MS Grade	CNW	CAEQ-4-000306-4000
Acetonitrile, LC–MS Grade	CNW	CAEQ-4-000308-4000
Acetice Acid, LC–MS Grade	CNW	CAEQ-4-000319-0050
Ammonium Acetate, LC–MS Grade	CNW	CAEQ-4-000314-0050
Krebs-Ringer Buffer	Solarbio	G0430-500 ml

2.1.4 Critical commercial assays

Name	Source	Cat. number
RNAiso Plus	Vazyme	R401
SweScript RT I First Strand cDNA Synthesis Kit	Servicebio	G3330
2X Universal Blue SYBR Green qPCR Master Mix	Servicebio	G3326

2.1.5 Software and Algorithms

R version3.6.3	The R Foundation	N/A
SIMCA	Umetrics AB	N/A

2.2 Preparation and metabolic constituents of hawthorn-probiotic

2.2.1 Preparation of hawthorn aqueous extract and postbiotic

According to the preparation process of the previous study (13), the sequence of *Lactobacillus paracasei* is shown in Supplementary Table S1. We prepared three groups of fermentation liquid required for the experiment [hawthorn group (S), probiotic group (F) and postbiotic of hawthorn-probiotic group (FS)].

2.2.2 Metabolite extraction

The collected samples were thawed on ice, and metabolite were extracted with 80% methanol Buffer. Briefly, 100 μl of sample was extracted with 400 μl of precooled methanol. The extraction mixture was then stored in 30 min at −20°C. After centrifugation at 20,000*g* for 15 min, the supernatants were transferred into new tube to and vacuum dried. The samples were redissolved with 100 μl 80% methanol and stored at −80°C prior to the LC-MS analysis. In addition, pooled QC samples were also prepared by combining 10 μl of each extraction mixture (14).

2.2.3 High performance liquid chromatography

All samples were acquired by the LC–MS system followed machine orders. Firstly, all chromatographic separations were performed using a Vanquish Flex UPLC system (Thermo Fisher Scientific, Bremen, Germany). An ACQUITY UPLC T3 column (100 mm*2.1 mm, 1.8 μm, Waters, Milford, USA) was used for the reversed phase separation. The column oven was maintained at 40°C. The flow rate was 0.3 mL/min and the mobile phase consisted of solvent A (water, 5 mM ammonium acetate and 5 mM acetic acid) and solvent B (Acetonitrile). Gradient elution conditions were set as follows: 0 ~ 0.8 min, 2% B; 0.8 ~ 2.8 min, 2 to 70% B; 2.8 ~ 5.3 min, 70 to 90% B; 5.3 ~ 5.9 min, 90 to 100% B; 5.9 ~ 7.5 min, 100% B; 7.5 ~ 7.6 min, 100 to 2% B; 7.6 ~ 10 min, 2%B.

2.2.4 High resolution mass spectrometry

A high-resolution tandem mass spectrometer Q-Exactive (Thermo Scientific) was used to detect metabolites eluted from the column. The Q-Exactive was operated in both positive and negative ion modes. Precursor spectra (70–1,050 m/z) were collected at 70,000 resolution to hit an AGC target of 3e6. The maximum inject time was set to 100 ms. A top 3 configuration to acquire data was set in DDA mode. Fragment spectra were collected at 17,500 resolution to hit an AGC target of 1e5 with a maximum inject time of 50 ms. In order to evaluate the stability of the LC–MS during the whole acquisition, a quality control sample (Pool of all samples) was acquired after every 10 samples.

2.3 The analysis of the online pharmacology of post-biologics

2.3.1 The collection and arrangement of the action target of the postbiotic of hawthorn-probiotic and constipation

TCMID, Batman and Herb databases were used to search for the corresponding target of the active ingredients of the postbiotic of hawthorn-probiotic.

No corresponding target ingredients were found for the time being, and Swisstargetprediction platform was used to predict the target. The results of these database searches would overlap. Excel software was used to remove duplicate targets and integrate, and the target name was imported into the Uniport database, and the type was set as "*Homo sapiens*" to obtain the corresponding gene name.

Disease targets by using "Constipation" as key word were searched and extracted by TTD, Herb and Omim databases.

2.3.2 Analysis of Venn diagram and construction of target network of "TCM active ingredients-intersection target-disease"

Venny2.10 platform was used to analyze the target of drug action and the target of intestinal adhesion disease, and statistical intersection was formed and Wayne diagram was formed. The collected data were compiled and imported into Cytoscape3.91 software to construct the target network diagram of "TCM active ingredients—intersection targets—diseases."

2.3.3 PPI protein interaction network construction

The intersection targets were imported into the String platform and the type was defined as "*Homo sapiens*" to analyze and construct the PPI protein interaction network.

2.3.4 Molecular docking

Acquisition and preprocessing of receptor proteins and compounds: The three-dimensional (3D) structures of the receptor proteins were obtained by jointly utilizing the UniProt[1] and PDB[2] databases. The protein structures were then processed using PyMOL version 2.3.0 to remove crystallographic water, irrelevant protein chains, and the original ligands. The 3D structures of the compounds were retrieved from the PubChem database,[3] and the molecular structures were optimized using the MMFF94 force field with Open Babel3.1.1, resulting in the lowest energy conformation of the molecule. Detailed information about the compounds is provided in Table 1 at the end of the manuscript.

Molecular Docking: Hydrogen atoms were added to both the receptor proteins and the compounds using AutoDock Tools1.5.6. The rotatable bonds of the compounds were identified, and the structures were saved in pdbqt format. The docking grid parameters were set using the Grid module. Receptor protein details and docking range parameters provided in Table 2. The docking protocol was set to semi-flexible docking, employing the Lamarckian genetic algorithm for docking with an exhaustiveness value of 25. Molecular docking was performed using AutoDock Vina 1.2.0 to obtain the binding free energy and docking result files.

2.3.5 Molecular dynamics simulation

The Gromacs2020 software was used to simulate the molecular dynamics of the protein-compound complexes obtained by molecular docking. Amber14sb was selected as the protein force field, Gaff2 as the coordination force field, TIP3P water model was selected to add solvent to the protein ligand system and establish a water box with periodic boundary of 1.2 nm. Charges in the equilibrium system of sodium and chloride ions were added to restore the real experimental environment as far as possible. Prior to the formal kinetic simulation, the complex was minimized for 50,000 steps using a conjugate gradient algorithm, followed by a further equilibrium system of 100 ps using an isothermal (310 K) system (NVT) and an isobaric (1 standard atmosphere) system (NPT), and finally a molecular dynamics simulation of 100 Ns at normal temperature and pressure.

Analysis of molecular dynamics simulation results:

At present, the semi-flexible docking used for molecular docking cannot take into account the flexibility of protein structure. In order to further prove the degree and stability of binding between compounds and proteins, molecular dynamics simulations of 100 ns were performed for each group of docking results. We analyze the root mean square deviation (RMSD), root mean square fluctuation (RMSF), radius of rotation (Rg) and Gibbs free energy landscape in the molecular dynamics simulation trajectory of the complex.

2.4 Animals and groups

240-day-old, male KM mice obtained from the Guangzhou Regal Biotechnology Co., Ltd., SCXK [Yue] 2018–0182, SYXK [Yue] 2021–0059) were pair-housed in plastic cages in a temperature-controlled (25 ± 2°C) colony room under a 12/12-h light/dark cycle, with free access

1 https://www.uniprot.org/
2 https://www1.rcsb.org/
3 https://pubchem.ncbi.nlm.nih.gov/

TABLE 1 The primers' sequences of genes in this study.

Genes	Sequence of primers
ABCB1B	5′-AGTGTTAAAGGGGCGATGGG-3′
	5′-GACTCCTGTCCCGAGGTTTG-3′
NR1L2	5′-AGACCTGAGGAGAGCTGGAG-3′
	5′-TTGGCCTTGTCCCCACATAC-3′
NR1L3	5′-GTCCATGGGTTCCAGTACGAG-3′
	5′-TAACTCCGGGTCTGTCAGGG-3′
SULT1A1 (ST1A1)	5′-AGGTGATCTACGTTGCCCGAAATG-3′
	5′-GTACCACGACCCATAGGACACTTTC-3′
IL-6	5′-GGCGGATCGGATGTTGTGAT-3′
	5′-GGACCCCAGACAATCGGTTG-3′
IL-17A	5′-TGATGCTGTTGCTGCTGCTGAG-3′
	5′-CACATTCTGGAGGAAGTCCTTGGC-3′
GLP-2r	5′-TTCTGCCTCCTGCCGCTCTG-3′
	5′-AGTCCTTCAACCAGCAACCACAAG-3′
AQP-3	5′-CGCTGGTGTCTTCGTGTACC-3′
	5′-TGTGGGCCAGCTTCACATTC-3′
ENAC-γ (SCNN1G)	5′-TGAGTGACCTCCTGACTGACTTGG-3′
	5′-GAAATCTGGGTGGTGTGCCTTCC-3′
TNF-α	5′-GGAACACGTCGTGGGATAATG-3′
	5′-GGCAGACTTTGGATGCTTCTT-3′
β-actin	5′-CGTTGACATCCGTAAAGACC-3′
	5′-AACAGTCCGCCTAGAAGCAC-3′

to food and water. The aged KM male mice were administrated with distilled water throughout the whole course and 6 mice were grouped as the normal controls without any other intervention(N). The rest mice were treated with 5 mg/kg loperamide (imodium, SOURCE: Xian Janssen Pharmaceutical Ltd. IDENTIFIER: LGJ0549.) for 1 week and randomly divided into model group (M), positive drug group (Y), hawthorn group (S), probiotic group (F) and postbiotic of hawthorn-probiotic group (FS). Mice in Y group were intragastrically treated with 10% lactulose (0.2 ml/day/per mouse), S group with 1 g/ml pure hawthorn solution (0.2 ml/day/per mouse), F group with *Lactobacillus paracasei* supernatant (0.2 ml/day/per mouse) and FS group with postbiotic of hawthorn-probiotic (0.2 ml/day/per mouse) for another week.

The inclusion criteria were normal development, appropriate age, and weight. The exclusion criteria were abnormal development, inappropriate age, or weight. Any single criterion not met resulted in exclusion. Grouping was conducted randomly according to cage order, and blind method was employed to select one individual for gavage. The experimenter assigned a number to the gavage material, and the individual performing the gavage administered it based on the assigned number. During the observation period, the condition of all KM mice was closely monitored. If any adverse reactions were detected, the gavage was immediately discontinued. However, throughout the entire experiment, the mice remained in good health and no abnormalities were observed.

These KM mice were sacrificed after anesthesia with pentobarbital sodium. The structure of colon, and fecal metabolite of mice were determined. All experimental protocols were approved by the Animal Center, Guangzhou University of Chinese Medicine.

2.5 RNA isolation and quantitative analysis

RNA was extracted from colon tissue using RNAiso Plus according to the instructions. Then, cDNA was obtained using the ImProm-II™ Reverse Transcription System (Promega) and RT-qPCR was carried out with custom designed oligonucleotides using the SweScript RT I First Strand cDNA Synthesis Kit and 2X Universal Blue SYBR Green qPCR Master Mix in a total volume of 20 μl: 95°C for 1 min and 40 cycles of denaturation (95°C for 15 s) and extension (60°C for 1 min). Experiments were performed in triplicates. Following amplification, dissociation curve analyses were performed to confirm the amplicon specificity for each PCR run. The relative level of gene expression in mouse colon tissue was normalized against mouse β-actin, respectively. Analysis of relative expression was performed using the $2(-\Delta\Delta CT)$ method.

2.6 KM mouse ex vivo colonic organ culture

KM mouse (M group; with 5 mg/kg loperamide for 1 week; Constipation was diagnosed by insufficient fecal water content, long defecation time, small fecal volume and light weight) sacrificed after anesthesia with pentobarbital sodium. The colon were collected. The feces were removed with sterile syringes in a continuously ventilated (5% CO_2 + 95% O_2) Krebs-Ringer Buffer, and then cut colon into small segments 1 cm long. These colonal segments were then cut into sheets and placed in 24-well plates, respectively. Each well contained Krebs-Ringer Buffer continuously ventilated at 37°C and corresponding drug with a final concentration of 10 M and a volume of 1 ml. The culture was kept at 37°C, 5%CO_2 + 95%O_2, PH 7.4 for 5 h, and the tissue status was examined under the microscope every 15 min. Further experiments were carried out 5 h later.

2.7 Targeting metabolomics

The collected samples were thawed on ice, and metabolite were extracted with 80% methanol Buffer. Briefly, 50 mg of sample was extracted with 0.5 ml of precooled 80% methanol. The extraction mixture was then stored in 30 min at −20°C. After centrifugation at 20,000 g for 15 min, the supernatants were transferred into new tube to and vacuum dried. The samples were redissolved with 100 μl 80% methanol and stored at −80°C prior to the LC–MS analysis. In addition, pooled QC samples were also prepared by combining 10 μl of each extraction mixture.

Chromatographic mass spectrometry condition parameters are as follows: Chromatographic column: Waters ACQUITY UPLC BEH C18 (3.0 × 100 mm, 1.7 μm). Column temperature: 40°C. Sample size: 2 μl. Mobile phase: A: primary aqueous solution; B: Methanol: acetonitrile (volume ratio 1:1). The mass spectrum condition parameters are as follows: Sampling mode: MRM mode. See Materials section for standards. The standard curve is shown in Supplementary Table S2.

10.3389/fnut.2025.1498004

TABLE 2 The top 10 metabolites of each protein by binding energy.

Protein name	Pubchem CID	Metabolite name	Binding energy
AQP3	13976	Quinacridone	−9.3
AQP3	5282151	Vitexin-2-O-rhamnoside	−9.3
AQP3	9830628	L-Isoleucine	−9.2
AQP3	64982	Baicalin	−9.1
AQP3	6198	EXEMESTANE	−8.5
AQP3	441793	Eurycomalactone	−8.4
AQP3	5281643	Hyperoside	−8.4
AQP3	76005853	6-[4-(3-Chlorophenyl)-1-Piperazinyl]-3-Cyclohexyl-2	−8.4
AQP3	6030	Uridine 5′-Monophosphate	−8.3
AQP3	13653606	Furanylfentanyl	−8.2
IL17A	64,982	Baicalin	−8.4
IL17A	13976	Quinacridone	−7.9
IL17A	441793	Eurycomalactone	−7.9
IL17A	60198	EXEMESTANE	−7.9
IL17A	76005853	6-[4-(3-Chlorophenyl)-1-Piperazinyl]-3-Cyclohexyl-2	−7.6
IL17A	9830628	L-Isoleucine	−7.5
IL17A	5280343	Quercetin	−7.3
IL17A	5282151	Vitexin-2-O-rhamnoside	−7.3
IL17A	13653606	Furanylfentanyl	−7
IL17A	5280443	Apigenin	−7
SCNN1G	13976	Quinacridone	−8.7
SCNN1G	5282151	Vitexin-2-O-rhamnoside	−8.3
SCNN1G	64982	Baicalin	−8.2
SCNN1G	13653606	Furanylfentanyl	−8.1
SCNN1G	5280448	Calycosin	−8
SCNN1G	9830628	L-Isoleucine	−8
SCNN1G	60198	EXEMESTANE	−7.9
SCNN1G	441793	Eurycomalactone	−7.7
SCNN1G	5281643	Hyperoside	−7.7
SCNN1G	76005853	6-[4-(3-Chlorophenyl)-1-Piperazinyl]-3-Cyclohexyl-2	−7.7
SULT1A1	8679	N-Phenyl-2-naphthylamine	−11.2
SULT1A1	5280443	Apigenin	−11.1
SULT1A1	5280343	Quercetin	−10.7
SULT1A1	15394713	(2S,4R)-4-(9H-Pyrido[3,4-b]indol-1-yl)-1,2,4-butanetriol	−10.4
SULT1A1	5280961	Genistein	−10.1
SULT1A1	6030	Uridine 5′-Monophosphate	−10
SULT1A1	10107340	N-Acetyl Retigabine	−9.9
SULT1A1	9830628	L-Isoleucine	−9.9
SULT1A1	5281708	Daidzein	−9.8
SULT1A1	575067	5-Hydroxy-4-methoxy-6-(2-phenylethyl)-5,6-dihydro-2H-pyran-2-one	−9.8
TNF	64982	Baicalin	−10.2
TNF	13653606	Furanylfentanyl	−9.7
TNF	6351946	L-prolyl-L-phenylalanine	−9.7
TNF	263426	(1xi,3S)-1,2,3,4-Tetrahydro-1-methyl-beta-carboline-1,3-dicarboxylic acid	−9.4

(Continued)

TABLE 2 (Continued)

Protein name	Pubchem CID	Metabolite name	Binding energy
TNF	5280448	Calycosin	−9.4
TNF	78651	2-Amino-4-methylbenzophenone	−9.4
TNF	8679	N-Phenyl-2-naphthylamine	−9.4
TNF	5281708	Daidzein	−9.3
TNF	5280443	Apigenin	−9.2
TNF	73530	Tetrahydroharman-3-carboxylic acid	−9.2
GLP-2r	9830628	L-Isoleucine	−8.8
GLP-2r	5282151	Vitexin-2-O-rhamnoside	−8.7
GLP-2r	64982	Baicalin	−8.7
GLP-2r	441793	Eurycomalactone	−8.4
GLP-2r	13976	Quinacridone	−8.2
GLP-2r	263426	(1xi,3S)-1,2,3,4-Tetrahydro-1-methyl-beta-carboline-1,3-dicarboxylic acid	−8.2
GLP-2r	5281643	Hyperoside	−8.1
GLP-2r	60198	EXEMESTANE	−8
GLP-2r	580443	Apigeni	−7.9
GLP-2r	76005853	6-[4-(3-Chlorophenyl)-1-Piperazinyl]-3-Cyclohexyl-2	−7.9

3 Results

3.1 The postbiotic of hawthorn-probiotic metabolites are quite different from the postbiotic of hawthorn and the postbiotic of hawthorn

The TIC (Total Ion Chromotogram) of the metabolites of Lactobacillus (F), postbiotic of hawthorn-probiotic(FS), hawthorn (S) is shown in Figure 1A. We found that after fermentation, the FS group was significantly different from the F and S groups in both anion and cationic tests. According to the Mz-rt figrure (Figure 1B), it can be found that the main detection period of metabolic ions in this test is 0–5 min, and the main detection m/z is 100–500. In this test, there were a total of 12,009 anion peaks and 20,611 cation peaks. The types of metabolic ion peaks are mainly lipids and lipid-like molecules, Organoheterocyclic compounds, Organic acids and derivatives, Benzenoids, Phenylpropanoids and polyketides, and Organic oxygen compounds.

After further analysis of primary metabolites (Figure 2A), we found that group FS integrated some components of group F and group S, and the part with effective increase in content was in the lower right corner of the way. As can be seen from Figures 2B–D, the differences within the test group were small, while the differences between the groups were large, and the biological repeatability was relatively good.

3.2 The postbiotic of hawthorn-probiotic is more abundant than the postbiotic of hawthorn and the postbiotic of hawthorn

We analyzed the secondary metabolites (Figure 3A) and found that the three groups were still very different. FS/S mainly increased, while FS/F mainly decreased (Figure 3B). However, in general, the metabolite content of FS was higher than that of F and S (Figure 3C). As can be seen from Figure 4A, the difference within the test group is small, while the difference between groups is large, which is close to the real data.

With VIP > 1 and Pvalue <0.05, differential secondary metabolites were screened, and Figure 4B was obtained. Then, K-mean cluster analysis was performed on these differential secondary metabolites (Figure 4C), and it was found that Organic acids and derivatives, Organoheterocyclic compounds, lipids and lipid-like molecules, Benzenoids, Phenylpropanoids and polyketides are the main rising components of FS, but many components are unknown.

3.3 Network pharmacology and preliminary experiments have found common targets of constipation and postbiotic of hawthorn-probiotic

Then we went on target hunting. Through network pharmacology, we found 20 common targets for metabolic mixtures and constipation (Figure 5A). The PPI network between them is plotted (Figure 5B). In the previous study (Figure 5C), we also found and verified several other targets, including TNF-α, Mucin2, Enac-γ, and AQP3. Among them, TNF-α has attracted our attention, and after reviewing the literature, we also included IL-6 and IL-17A in the experiment. By conducting RT-qPCR on the colons of mice in normal group (N), model group (M), and postbiotic of hawthorn-probiotic group (FS), the primers are listed in Table 1. We found that the postbiotic of hawthorn-probiotic was capable of decreasing the expression of NR1I2 and ST1A1 (SULT1A1), and increased the expression of GLP-2r, a receptor for GCG. However, the expression of ABCB1B, NR1I3, IL-6, and IL-17A showed a decreased trend, with no statistical significance (Figure 5D).

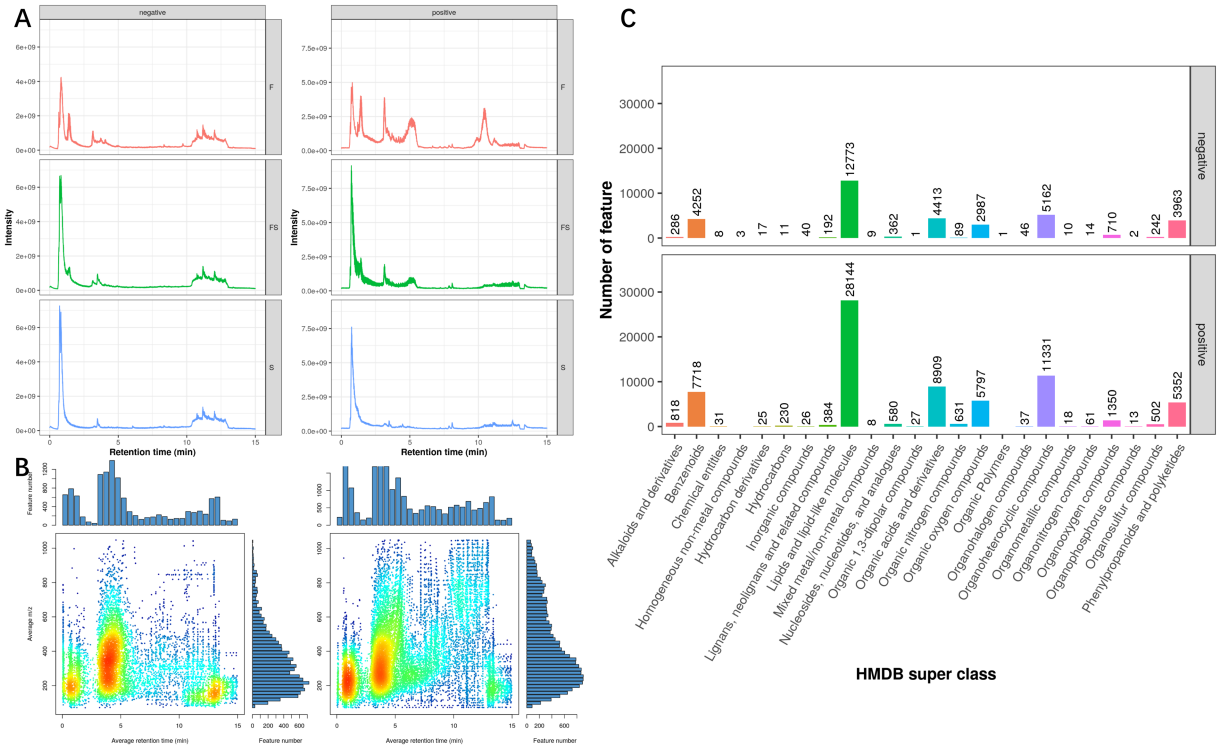

FIGURE 1
(A) TIC (Total Ion Chromotogram), a superposition of all metabolite strengths of each sample, with the retention time of the liquid chromatography as the horizontal coordinate and the ion strength as the vertical coordinate, reflecting the overall situation of the metabolite peak in the sample. **(B)** Mass-Charge Ratio and Retention time (mz-rt, mass-charge Ratio and Retention time). Each point is a metabolite peak, with the retention time of metabolites as the horizontal coordinate and the mass-charge ratio as the vertical coordinate, reflecting the overall hydrophilicity and molecular weight of all the metabolites in this project. The color of the dots represents the density of the region (the chromatographies are spectral series, red is dense, and blue is sparse). **(C)** Statistical map of metabolite species for first-order molecular weight identification. The figure extracts the classification information of the substance in which the substance is located and performs the number statistics. The horizontal coordinate is the classification and the vertical coordinate is the number of metabolic peaks.

3.4 Molecular docking and molecular dynamics analysis proved that the postbiotic of hawthorn-probiotic target metabolite was stable in binding to the target

We found 131 significantly elevated secondary metabolites (see Supplementary material), and then searched for the postbiotic of hawthorn-probiotic that was significantly higher (VIP > 1.2, FC > 2or < 0.5, $p < 0.01$). We then used 112 metabolites for which we found a clear chemical structure to intermingle with previously screened targets (AQP3, Enac-γ, SULT1A1, TNF) and those we are still interested in (IL17A, IL6R). NR1I2 was found in the nucleus, and we did not focus on this target because we had no evidence that our metabolites could enter the nucleus. Subsequently, we found (Figure 6A) that these metabolites are generally combined with SULT1A1 and TNF. They bind well to parts of AQP3, GLP-2R, Enac-γ (SCNIG), and IL17A. But they do not combine well with IL6R. We used the index of binding energy to sort from large to small, and selected the top 10 compounds in each target for presentation (Table 2). Then, we combined the best groups and visualized them (Figures 6B–G). These are TNF-Baicalin, AQP3-Quinacridone, Enacγ-Quinacridone, IL17A-Baicalin, SULT1A1-N-Phenyl-2 naphthylamine, GLP2R-L-Isoleucine. We also performed molecular dynamics analysis on them (Figure 7). The results of RMSD, RMSF, and RG of the above small molecules and targets were all good.

3.5 Ex vivo colonic organ culture demonstrated that the target metabolite can be effective by loperamide to model the corresponding target of mouse colon

We tried our best to purchase the 11 compounds that were virtually screened (Quinacridone, vitexin-2 "-o-rhamnoside, L-Isoleucine, Baicalin, Exemestane, Hyperoside, Quercetin, Apigenin, N-Phenyl-2-naphthylamine, Genistein, Daidzein. See the Materials section for specific information), and the colons of loperamide modeled mice were removed for experiments. Finally, we found (Figure 8) that in general, the compound regulated the intestinal targets of the model mice in a favorable direction, especially Enac-γ. However, some compounds resulted in increased expression of the target, and there is a worsening trend. Daidzein, for example, increased TNF expression.

3.6 Targeted metabolomics found that postbiotic of hawthorn-probiotic regulated short chain fatty acids metabolism in the gut of loperamide modelled mice

So we found that the postbiotic of hawthorn-probiotic regulated the gut microbiome structure of loperamide in mice and their ability

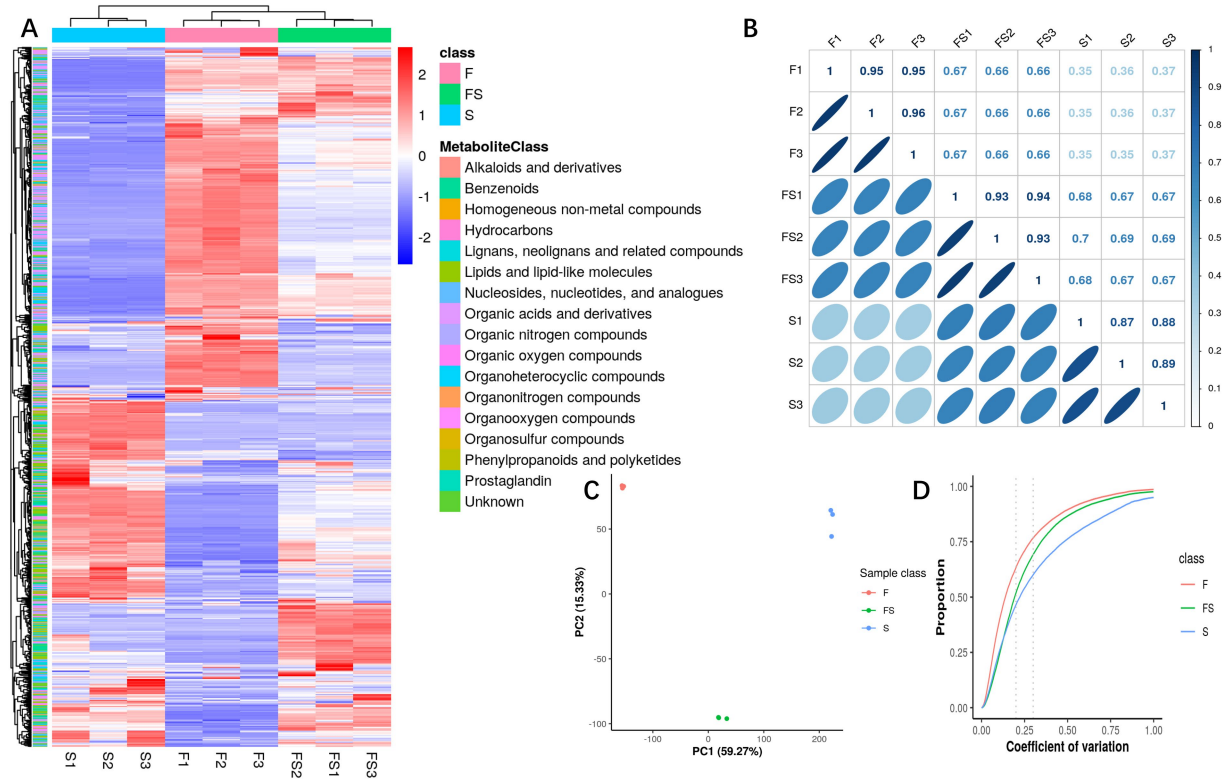

FIGURE 2
(A) Heatmap of metabolite intensity. Each column has a sample, each behavior has a displacement peak, and the color represents the intensity information (Log10 value). **(B)** Pairwise correlation heat map of samples. Pairwise sample correlation analysis was performed using all metabolic intensity of each sample. The upper right part of the figure shows the correlation coefficient, and the lower left part of the figure shows the degree of correlation fitting with an ellipse. **(C)** Principal component score chart. For PCA analysis of detected substances and identified metabolites, PCA score plot mainly represents the distribution trend of data points, each point in the graph represents a sample, and the similarities and differences between all samples are reflected in the separation trend or aggregation degree of samples in the score plot. The aggregation of points indicates that the observed variables have a high degree of similarity, and the dispersion of points indicates that the observed variables have obvious differences. **(D)** Biorepeat CV cumulative map. The difference coefficients of all replicates under each phenotype were calculated, and the cumulative statistics of each difference coefficient were carried out to show the repeated differences of different phenotypes. The horizontal coordinate of the CV cumulative curve represents the number of CV, and the vertical coordinate represents the proportion of metabolites smaller than the CV in the total number of metabolites.

to produce biofilms (13). So we conducted targeted metabolomic analysis on feces, and we found (Figure 9A) that the short chain fatty acids profiling of normal group (N), model group (M), postbiotic of hawthorn-probiotic (FS) was completely different. The three groups had good differentiation and intra-group repeatability (Figure 9B). By analyzing short chain fatty acids separately (Figures 9C–I), Butyric acid and Propionic acid contents rise significantly in the intestine of constipated mice, while Isovaleric acid and Hexanoic acid contents decline. The postbiotic of hawthorn-probiotic can reduce Butyric acid content to normal level, and it can also increase Valeric acid and Isobutyric acid content. However, Acetic acid and Propionic acid did not change significantly.

4 Discussion

With the exacerbation of population aging, constipation, a common gastrointestinal disease, is receiving increasing attention. As a novel approach, post-biotics are being studied in many diseases, including constipation. In our preliminary research (13), aged KM mice were modeled with loperamide, and we found that the postbiotic combination of hawthorn-probiotic was safe and effective. It alleviated intestinal water-sodium metabolism and chronic inflammation, promoted cell proliferation, and reduced apoptosis. By inhibiting harmful bacterial colonization, increasing the abundance of probiotics, and maintaining intestinal microbiota, it improved the gut microbiome. In this study, we observed an increase in the content of some secondary metabolites compared to hawthorn or probiotic alone. Through network pharmacology and mouse colonic tissue analysis, we identified new targets, particularly SULT1A1 and GLP-2r. Subsequently, molecular docking, molecular dynamics analysis, and *in vitro* experiments using colonic tissue from KM mice revealed stable binding between targets and secondary metabolites, especially TNF-Baicalin, AQP3-Quinacridone, Enacγ-Quinacridone, IL17A-Baicalin, SULT1A1-N-Phenyl-2 naphthylamine, and GLP2R-L-Isoleucine. Furthermore, short chain fatty acids metabolism analysis of feces from KM mice in this experiment indicated that the hawthorn-probiotic postbiotic improved short chain fatty acid profiling.

SULT1A1 is a sulfotransferase enzyme that participates in the metabolism and detoxification (15, 16) processes of various endogenous and exogenous compounds within the body (17). Its primary function involves conjugating electrophilic compounds with

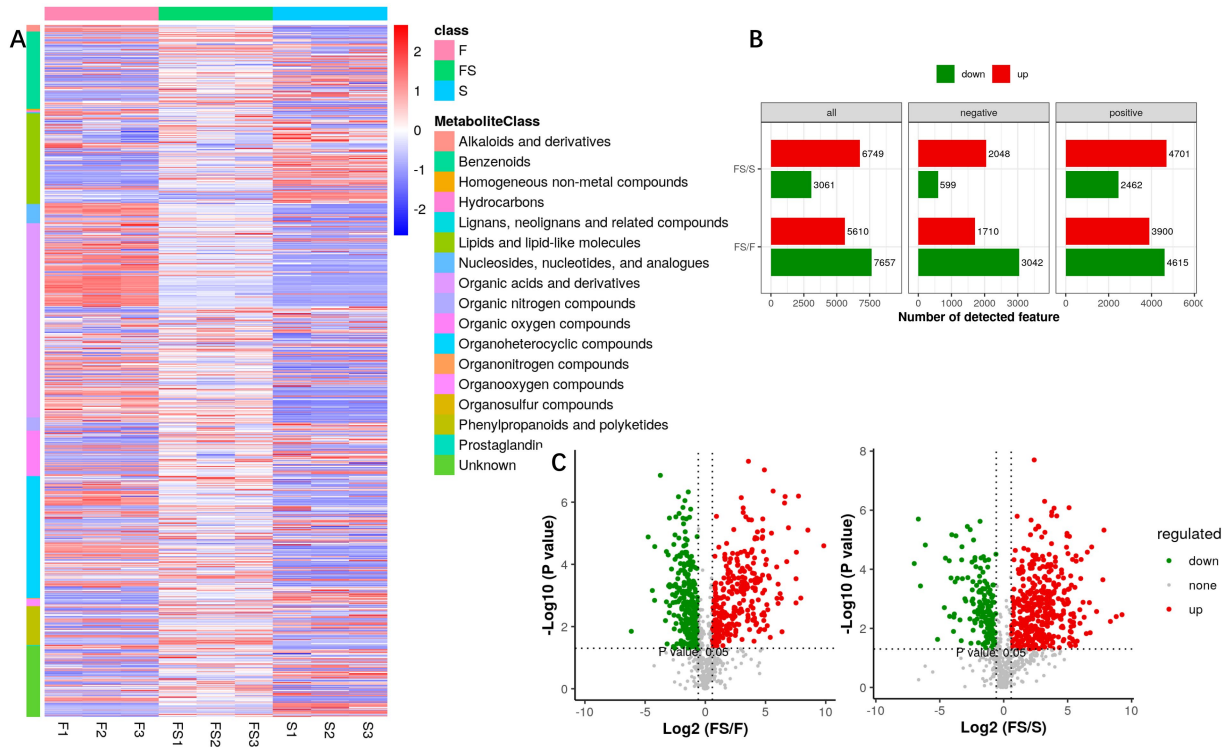

FIGURE 3
(A) Heatmap of the intensity of metabolites for secondary identification. Quantitative information was extracted from the secondary identified metabolites with high confidence, each of which was classified as a sample, each of which had a metabolic peak, and the color represented the intensity information (Log10 value). **(B)** Univariate analysis of fold-change and *p*-value obtained by T statistical test were used in this project to screen differentially expressed metabolites. Differential ions simultaneously satisfy: ratio > 1.5 or ratio < 1/1.5; *p* value < 0.05. **(C)** VolcanoPlot displays univariate statistical tests using volcanic maps. The horizontal coordinate is the ratio of the mean values of the two phenotypic strengths, and the vertical coordinate is the significance p-value (or corrected *p*-value) of the statistical test, and −log10 is taken. The greater the value, the more significant the difference.

water-soluble sulfate substrates, thereby increasing their water solubility and facilitating their excretion from the body. In terms of research progress, SULT1A1 has been extensively studied and demonstrated significant roles in numerous fields (18, 19). For instance, in cancer research, the expression levels of SULT1A1 are closely associated with the occurrence and progression of tumors (20, 21), including colorectal cancer, by influencing tumor growth and metastasis through the regulation of endogenous hormone and carcinogen metabolism (17). Additionally, in drug metabolism and toxicology studies, SULT1A1 is also considered as one of the crucial enzymes involved in drug metabolism and detoxification, exerting significant effects on the metabolic pathways of many drugs and the formation of toxic metabolites (15). We found that the expression level of SULT1A1 in postbiotic of hawthorn-probiotic (FS) was lower than that in constipation model (M). This showed that the intestines of mice in FS group recovered and almost no toxins needed to be excreted.

GLP-2r, the receptor for the intestinal hormone glucagon-like peptide-2 (GLP-2), is widely expressed in intestinal tissues (22). GLP-2 is a gastrointestinal hormone secreted by enteroendocrine cells in the intestine (23), and its primary function is to promote proliferation and repair of intestinal mucosal cells, increase mucosal cell survival, while reducing intestinal motility and secretion (22, 24). These effects contribute to maintaining the integrity of the intestinal mucosa and promoting intestinal health. In terms of research progress, GLP-2r has been extensively studied and has shown potential roles in the treatment of various intestinal-related diseases. For example, GLP-2r agonists have been used in the treatment of inflammatory bowel diseases (such as Crohn's disease and ulcerative colitis) (25) because they can promote intestinal mucosal repair and regeneration, improving patients' symptoms and quality of life. Additionally, GLP-2r agonists are also being investigated for the treatment of other intestinal disorders such as intestinal fistulas and short bowel syndrome (22, 24). We found that the postbiotic of hawthorn-probiotic mice had elevated GLP-2r expression in colon. In previous studies, we observed by CCK8 and flow cytometry that postbiotic of hawthorn-probiotic promoted intestinal epithelial cell proliferation and reduced apoptosis. These suggest that the postbiotic of hawthorn-probiotic secondary metabolites bind to GLP-2r, promoting intestinal cell proliferation, reducing intestinal cell apoptosis, and restoring intestinal barrier function.

IL-17A is a cytokine belonging to the IL-17 family, primarily produced by T cells and other immune cells such as NK cells and lymphocytes (26), serving as a crucial inflammatory mediator (27, 28). It plays key roles in immune regulation, inflammatory responses (29) (particularly against bacterial and fungal infections (30)), and tissue repair (31). Inhibitors of IL-17A and its receptor have emerged as important targets for the treatment of autoimmune diseases (such as rheumatoid arthritis, psoriasis, etc.) and inflammatory bowel diseases (26). Relevant drugs have been developed and entered clinical trial phases. We found that the postbiotic of hawthorn-probiotic (FS) group had reduced IL-17A

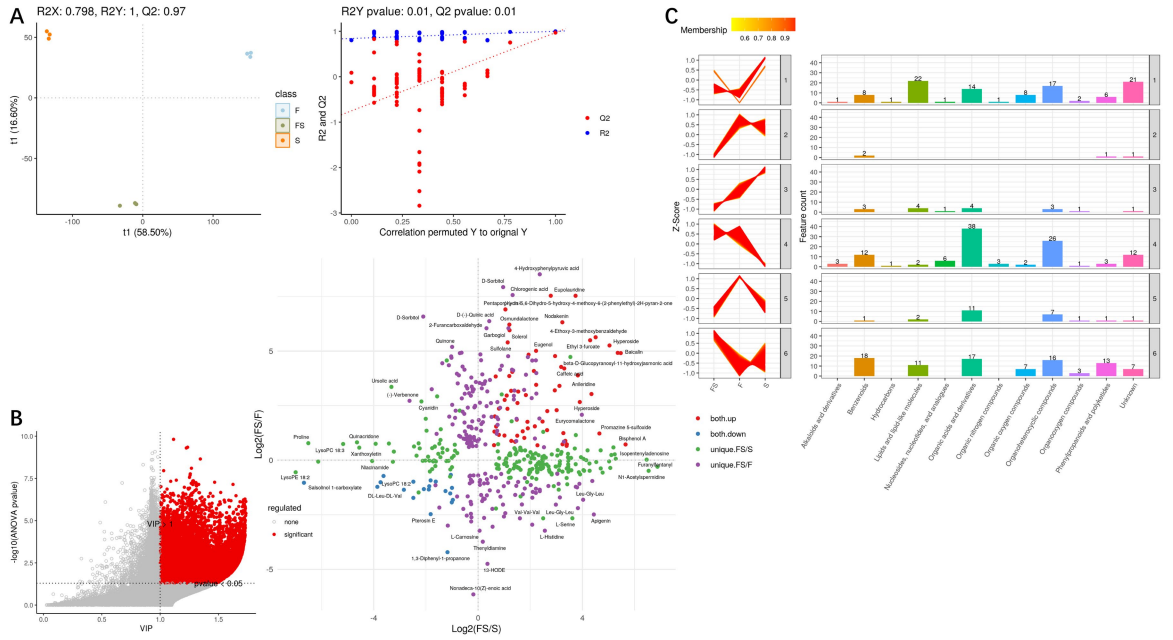

FIGURE 4
(A) PLS-DA score plots (left) are used to evaluate the relationships between samples, with the abscissa representing the first principal component and the ordinate representing the second principal component. Each dot represents a sample, and each color represents a phenotype; PLS-DA model check (right). The Permutation test tested whether the PLS-DA model was overfitted with a number of 100. The x-coordinate is the correlation of the Q2 and R2 calculated by the permutation to the original Q2 and R2 values, and the y-coordinate is the R2 and Q2 calculated by each permutation. Pvalue shows the significance of the replacement test, Q2's pvalue< 0.05 indicates that the model is not overfitted. **(B)** For metabolites of global correlation in multiple comparison groups, metabolites with differential and secondary identification are extracted, each point of the correlation plot is a metabolite, and the horizontal and vertical coordinates are the ratio (logarithm) of each comparison group. **(C)** Multi-group secondary K clustering. The HMDB classification information was extracted from the metabolites identified by differential ions, and the metabolites were classified and counted for each expression category.

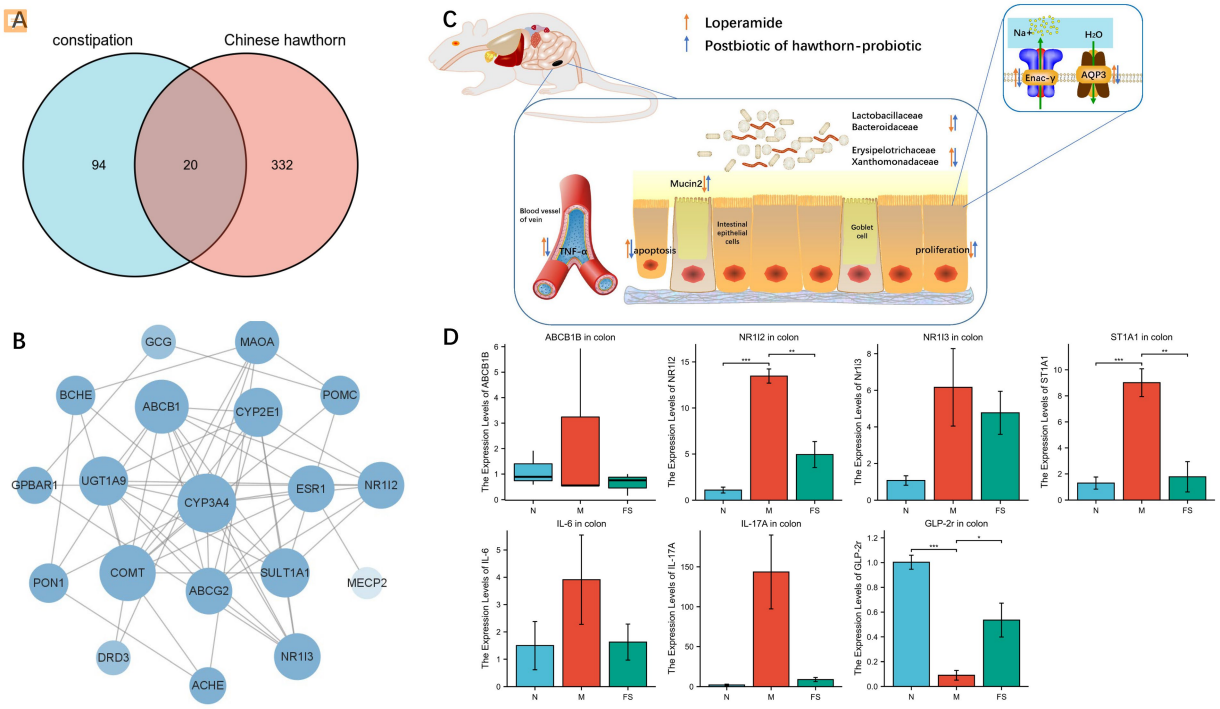

FIGURE 5
(A) Venn diagram, common target of constipation and fermentation fluid. **(B)** PPI maps of common targets. **(C)** Flow chart of the preliminary work. **(D)** Changes in target gene expression levels verified by colon RT-qPCR. NS; *$p < 0.05$; **$p < 0.01$; ***$p < 0.001$.

10.3389/fnut.2025.1498004

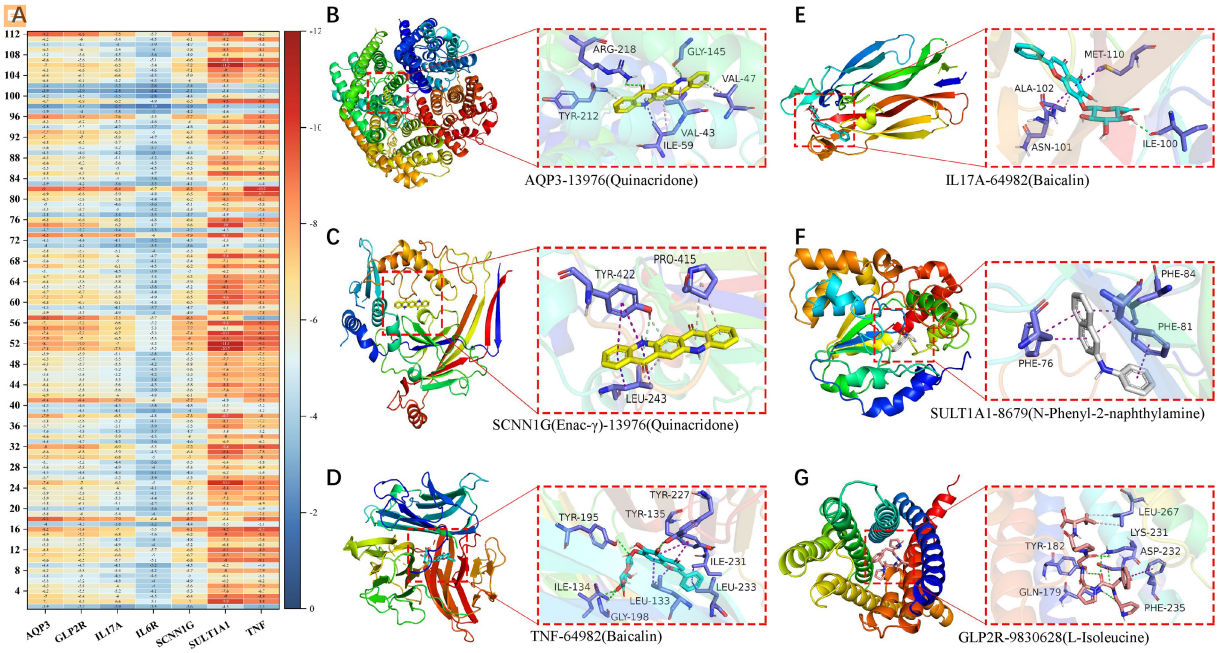

FIGURE 6
(A) Heat maps of binding energies of 112 secondary metabolites to 7 targets. Visualization of the combination with the highest binding energy of the **(B–G)** secondary metabolite and target protein.

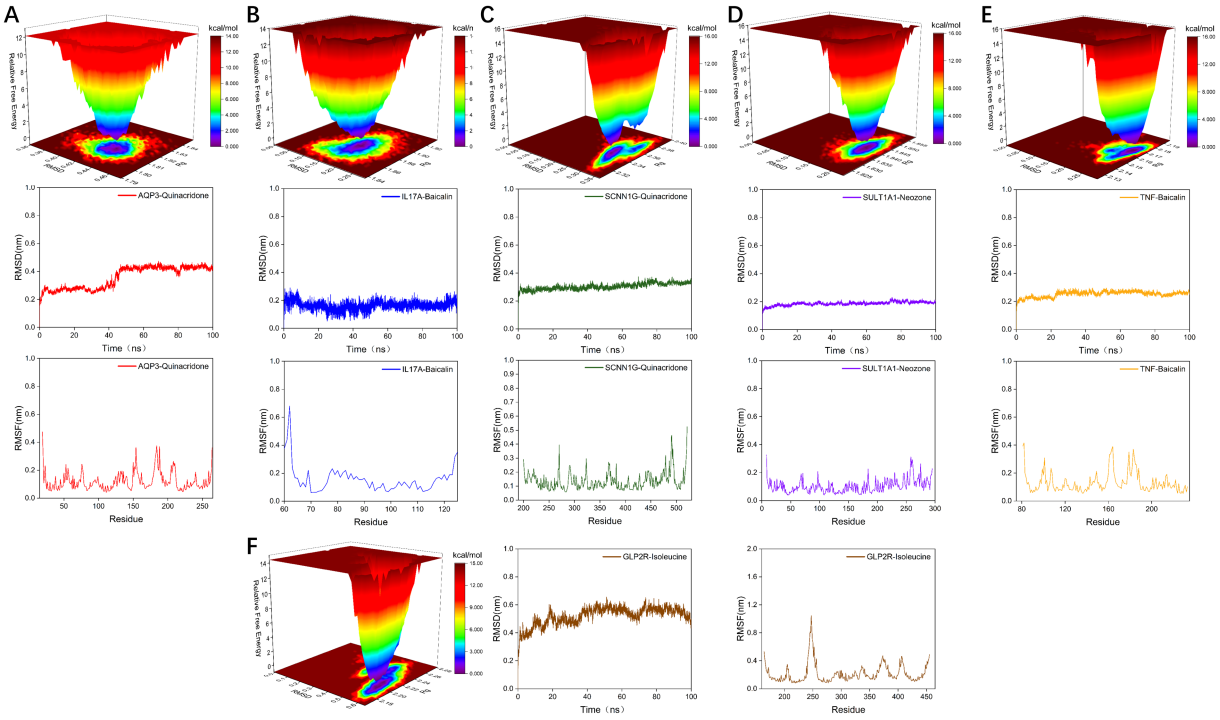

FIGURE 7
(A–F) Visualization of molecular dynamics analysis results of the combination with the highest binding energy of secondary metabolites and target proteins.

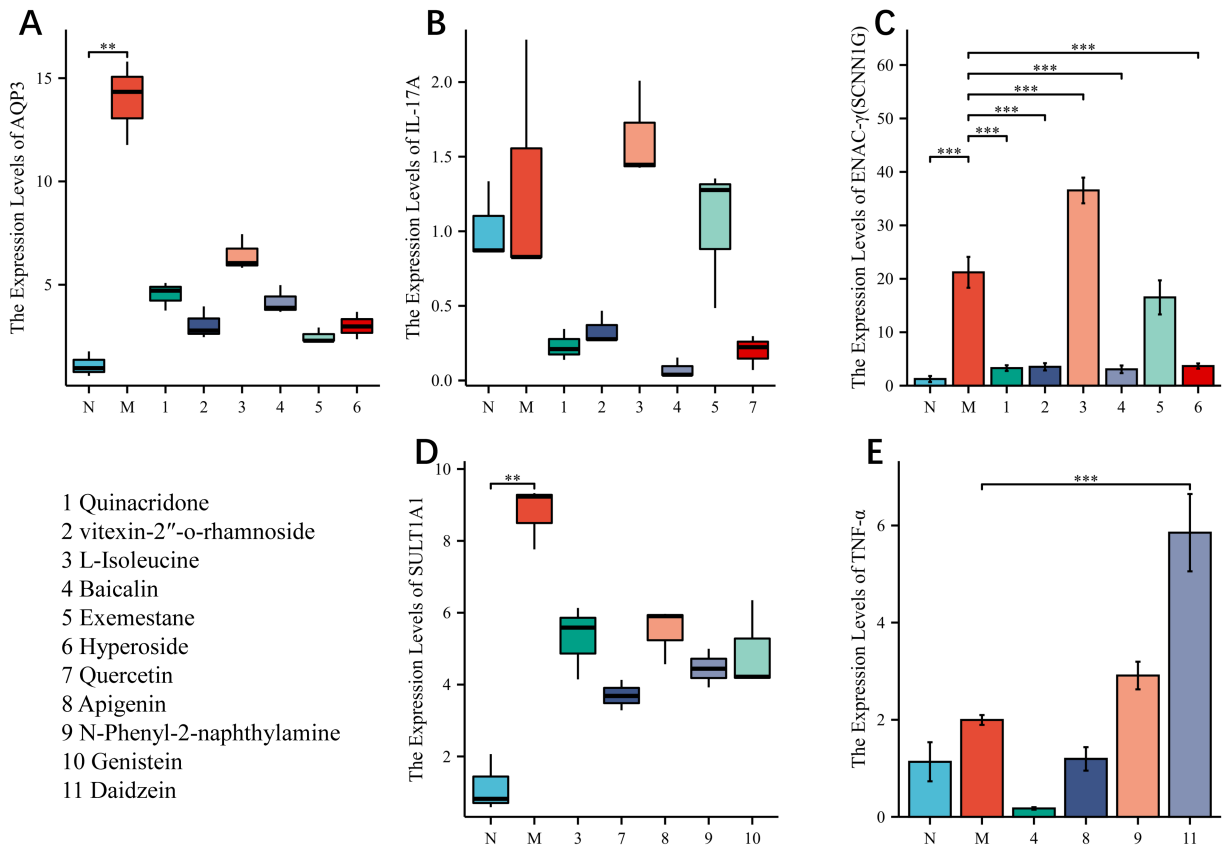

FIGURE 8
(A–E) *In vitro* experiments to verify the gene expression levels of the compound—target protein combinations with higher binding energy. NS; *$p < 0.05$; **$p < 0.01$; ***$p < 0.001$.

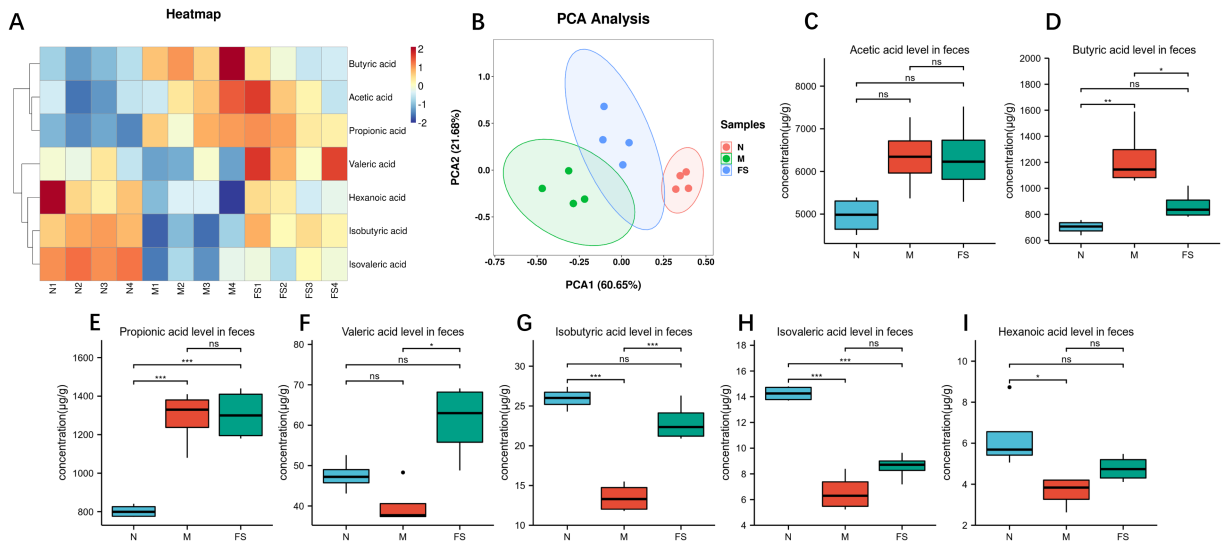

FIGURE 9
(A) Heat maps of various short chain fatty acids contents in feces of KM mice in groups N, M and FS. **(B)** PCA plots of the three groups. **(C–I)** Bar chart for the comparison of various short chain fatty acids contents in the three groups. NS; *$p < 0.05$; **$p < 0.01$; ***$p < 0.001$.

expression in colon tissue. So this suggests that the postbiotic of hawthorn-probiotic secondary metabolites are capable of reducing inflammation in the gut. Our previous studies found that postbiotic of hawthorn-probiotic could improve intestinal flora structure and short chain fatty acids metabolism in elderly constipated mice. IL-17A plays an important role in this.

In conclusion, our study once again proves that postbiotic of hawthorn-probiotic is beneficial to senile constipation, and the key secondary metabolites and targets are found and preliminarily verified. Our findings can be used as a reference for the treatment of constipation and other intestinal disorders.

Data availability statement

The original contributions presented in the study are included in the article/Supplementary material, further inquiries can be directed to the corresponding authors.

Ethics statement

The animal study was approved by 240 days old, male KM mice obtained from the Guangzhou Regal Biotechnology Co., Ltd., (SCXK [Yue] 20180182, SYXK [Yue] 2021-0059) were pair-housed in plastic cages in a temperature-controlled (25 ± 2°C) colony room under a 12/12-h light/dark cycle, with free access to food and water. All experimental protocols were approved by the Animal Center, Guangzhou University of Chinese Medicine. The study was conducted in accordance with the local legislation and institutional requirements.

Author contributions

YW: Conceptualization, Data curation, Methodology, Project administration, Writing – original draft, Writing – review & editing. SC: Formal analysis, Methodology, Software, Writing – original draft. YL: Formal analysis, Validation, Writing – original draft. WW: Project administration, Resources, Supervision, Writing – review & editing. YH: Funding acquisition, Methodology, Project administration, Resources, Supervision, Writing – review & editing.

Funding

The author(s) declare that financial support was received for the research, authorship, and/or publication of this article. This research was funded by grants from the Chinese National Natural Science Foundation (Grant no.: 31700288) and the University - Hospital Joint Fund Project of Guangzhou University of Chinese Medicine (GZYSE2024U05).

Acknowledgments

I would like to thank the School of Basic Medicine of Guangzhou University of Chinese Medicine for providing the experimental platform. Thank you to Chen Yongjie from servicebio for his fast delivery of experimental reagents.

Conflict of interest

The authors declare that the research was conducted in the absence of any commercial or financial relationships that could be construed as a potential conflict of interest.

Publisher's note

All claims expressed in this article are solely those of the authors and do not necessarily represent those of their affiliated organizations, or those of the publisher, the editors and the reviewers. Any product that may be evaluated in this article, or claim that may be made by its manufacturer, is not guaranteed or endorsed by the publisher.

Supplementary material

The Supplementary material for this article can be found online at: https://www.frontiersin.org/articles/10.3389/fnut.2025.1498004/full#supplementary-material

References

1. Gallagher P, O'Mahony D. Constipation in old age. *Best Pract Res Clin Gastroenterol*. (2009) 23:875–87. doi: 10.1016/j.bpg.2009.09.001

2. Barbara G, Barbaro MR, Marasco G, Cremon C. Chronic constipation: from pathophysiology to management. *Minerva Gastroenterol (Torino)*. (2023) 69:277–90. doi: 10.23736/S2724-5985.22.03335-6

3. Broad J, Kung V, Palmer A, Elahi S, Karami A, Darreh-Shori T, et al. Changes in neuromuscular structure and functions of human colon during ageing are region-dependent. *Gut*. (2019) 68:1210–23. doi: 10.1136/gutjnl-2018-316279

4. Camilleri M, Lee JS, Viramontes B, Bharucha AE, Tangalos EG. Insights into the pathophysiology and mechanisms of constipation, irritable bowel syndrome, and diverticulosis in older people. *J Am Geriatr Soc*. (2000) 48:1142–50. doi: 10.1111/j.1532-5415.2000.tb04793.x

5. O'Mahony D, O'Leary P, Quigley EM. Aging and intestinal motility: a review of factors that affect intestinal motility in the aged. *Drugs Aging*. (2002) 19:515–27. doi: 10.2165/00002512-200219070-00005

6. Zhang J, Chai X, Zhao F, Hou G, Meng Q. Food applications and potential health benefits of hawthorn. *Food Secur*. (2022) 11:11. doi: 10.3390/foods11182861

7. Ford AC, Quigley EMM, Lacy BE, Lembo AJ, Saito YA, Schiller LR, et al. Efficacy of prebiotics, probiotics, and synbiotics in irritable bowel syndrome and chronic idiopathic constipation: systematic review and meta-analysis. *Am J Gastroenterol*. (2014) 109:1547–61. doi: 10.1038/ajg.2014.202

8. Bazzocchi G, Giovannini T, Giussani C, Brigidi P, Turroni S. Effect of a new synbiotic supplement on symptoms, stool consistency, intestinal transit time and gut microbiota in patients with severe functional constipation: a pilot randomized double-blind, controlled trial. *Tech Coloproctol*. (2014) 18:945–53. doi: 10.1007/s10151-014-1201-5

9. Dan LW, Luciana CL, Amanda FB, Raquel ST, Glaucia MS, Natalia PP, et al. Effect of synbiotic in constipated adult women – a randomized, double-blind, placebo-controlled study of clinical response. *Clin Nutr*. (2013) 32:27–33. doi: 10.1016/j.clnu.2012.08.010

10. Ying JL, Rosita J, Abu SH, Jin YC. Effects of Synbiotics among constipated adults in Serdang, Selangor, Malaysia—a randomised, double-blind, placebo-controlled trial. *Nutrients*. (2018) 10:10. doi: 10.3390/nu10070824

11. Linetzky WD, Alves PCC, Logullo L, Manzoni JT, Almeida D, Teixeira DSML, et al. Microbiota benefits after inulin and partially hydrolized guar gum supplementation: a randomized clinical trial in constipated women. *Nutr Hosp*. (2012) 27:123–9. doi: 10.1590/S0212-16112012000100014

12. Ahmad K, Mozhgan S. Role of Synbiotics in the treatment of childhood constipation: a double-blind randomized placebo controlled trial. *Iran J Pediatr*. (2010) 20:387–92.

13. Wei Y, Huang N, Ye X, Liu M, Wei M, Huang Y. The postbiotic of hawthorn-probiotic ameliorating constipation caused by loperamide in elderly mice by regulating intestinal microecology. *Front Nutr*. (2023) 10:1103463. doi: 10.3389/fnut.2023.1103463

14. Dunn WB, Broadhurst D, Begley P, Zelena E, Francis-McIntyre S, Anderson N, et al. Procedures for large-scale metabolic profiling of serum and plasma using gas chromatography and liquid chromatography coupled to mass spectrometry. *Nat Protoc*. (2011) 6:1060–83. doi: 10.1038/nprot.2011.335

15. Cook I, Wang T, Leyh TS. Isoform-specific therapeutic control of sulfonation in humans. *Biochem Pharmacol*. (2019) 159:25–31. doi: 10.1016/j.bcp.2018.11.010

16. Tyapochkin E, Kumar VP, Cook PF, Chen G. Reaction product affinity regulates activation of human sulfotransferase 1A1 PAP sulfation. *Arch Biochem Biophys*. (2011) 506:137–41. doi: 10.1016/j.abb.2010.11.018

17. Suzuki H, Morris JS, Li Y, Doll MA, Hein DW, Liu J, et al. Interaction of the cytochrome P4501A2, SULT1A1 and NAT gene polymorphisms with smoking and dietary mutagen intake in modification of the risk of pancreatic cancer. *Carcinogenesis*. (2008) 29:1184–91. doi: 10.1093/carcin/bgn085

18. Pietrauszka K, Bergler-Czop B. Sulfotransferase SULT1A1 activity in hair follicle, a prognostic marker of response to the minoxidil treatment in patients with androgenetic alopecia: a review. *Postepy Dermatol Alergol*. (2022) 39:472–8. doi: 10.5114/ada.2020.99947

19. Paul S, Gangwar A, Patir H, Bhargava K, Ahmad Y. Reverse translating SULT1A1, a potential biomarker in roentgenographically tested rat model of rapid HAPE induction. *Life Sci*. (2019) 229:132–8. doi: 10.1016/j.lfs.2019.05.035

20. Shi L, Shen W, Davis MI, Kong K, Vu P, Saha SK, et al. SULT1A1-dependent sulfonation of alkylators is a lineage-dependent vulnerability of liver cancers. *Nat Can*. (2023) 4:365–81. doi: 10.1038/s43018-023-00523-0

21. Santos SS, Koifman RJ, Ferreira RM, Diniz LF, Brennan P, Boffetta P, et al. SULT1A1 genetic polymorphisms and the association between smoking and oral cancer in a case-control study in Brazil. *Front Oncol*. (2012) 2:183. doi: 10.3389/fonc.2012.00183

22. Cheng W, Wang K, Zhao Z, Mao Q, Wang G, Li Q, et al. Exosomes-mediated transfer of miR-125a/b in cell-to-cell communication: a novel mechanism of genetic exchange in the intestinal microenvironment. *Theranostics*. (2020) 10:7561–80. doi: 10.7150/thno.41802

23. Lee SJ, Lee J, Li KK, Holland D, Maughan H, Guttman DS, et al. Disruption of the murine Glp2r impairs Paneth cell function and increases susceptibility to small bowel enteritis. *Endocrinology*. (2012) 153:1141–51. doi: 10.1210/en.2011-1954

24. Austin K, Imam NA, Pintar JE, Brubaker PL. IGF binding protein-4 is required for the growth effects of glucagon-like peptide-2 in murine intestine. *Endocrinology*. (2015) 156:429–36. doi: 10.1210/en.2014-1829

25. Shinzaki S, Sato T, Fukui H. Antidiabetic drugs for IBD: a long but promising road ahead for drug repositioning to target intestinal inflammation. *J Gastroenterol*. (2023) 58:598–9. doi: 10.1007/s00535-023-01983-y

26. Akitsu A, Iwakura Y. Interleukin-17-producing gammadelta T (gammadelta17) cells in inflammatory diseases. *Immunology*. (2018) 155:418–26. doi: 10.1111/imm.12993

27. Chung SH, Ye XQ, Iwakura Y. Interleukin-17 family members in health and disease. *Int Immunol*. (2021) 33:723–9. doi: 10.1093/intimm/dxab075

28. McGeachy MJ, Cua DJ, Gaffen SL. The IL-17 family of cytokines in health and disease. *Immunity*. (2019) 50:892–906. doi: 10.1016/j.immuni.2019.03.021

29. Grizotte-Lake M, Zhong G, Duncan K, Kirkwood J, Iyer N, Smolenski I, et al. Commensals suppress intestinal epithelial cell retinoic acid synthesis to regulate Interleukin-22 activity and prevent microbial Dysbiosis. *Immunity*. (2018) 49:1103–1115.e6. doi: 10.1016/j.immuni.2018.11.018

30. Conti HR, Bruno VM, Childs EE, Daugherty S, Hunter JP, Mengesha BG, et al. IL-17 receptor signaling in Oral epithelial cells is critical for protection against oropharyngeal candidiasis. *Cell Host Microbe*. (2016) 20:606–17. doi: 10.1016/j.chom.2016.10.001

31. Göbel K, Pankratz S, Asaridou CM, Herrmann AM, Bittner S, Merker M, et al. Blood coagulation factor XII drives adaptive immunity during neuroinflammation via CD87-mediated modulation of dendritic cells. *Nat Commun*. (2016) 7:11626. doi: 10.1038/ncomms11626

frontiers | Frontiers in Nutrition

TYPE Systematic Review
PUBLISHED 26 February 2025
DOI 10.3389/fnut.2025.1502720

Check for updates

OPEN ACCESS

EDITED BY
Ntethelelo Sibiya,
Rhodes University, South Africa

REVIEWED BY
Andrea Quartieri,
University of Modena and Reggio Emilia, Italy
Shoeshoe Mokhele,
Sefako Makgatho Health Sciences University, South Africa

*CORRESPONDENCE
Amrullah Shidiki
✉ amarullahsidhiqie24@gmail.com
Gaurav Kumar
✉ gaurav.19454@gmail.com;
✉ gauravkr01@gmail.com

RECEIVED 27 September 2024
ACCEPTED 03 February 2025
PUBLISHED 26 February 2025

CITATION
Jangid H, Shidiki A and Kumar G (2025) Cranberry-derived bioactives for the prevention and treatment of urinary tract infections: antimicrobial mechanisms and global research trends in nutraceutical applications.
Front. Nutr. 12:1502720.
doi: 10.3389/fnut.2025.1502720

COPYRIGHT
© 2025 Jangid, Shidiki and Kumar. This is an open-access article distributed under the terms of the Creative Commons Attribution License (CC BY). The use, distribution or reproduction in other forums is permitted, provided the original author(s) and the copyright owner(s) are credited and that the original publication in this journal is cited, in accordance with accepted academic practice. No use, distribution or reproduction is permitted which does not comply with these terms.

Cranberry-derived bioactives for the prevention and treatment of urinary tract infections: antimicrobial mechanisms and global research trends in nutraceutical applications

Himanshu Jangid[1], Amrullah Shidiki[2]* and Gaurav Kumar[1,3]*

[1]Department of Microbiology, School of Bioengineering and Biosciences, Lovely Professional University, Phagwara, Punjab, India, [2]Department of Microbiology, National Medical College and Teaching Hospital, Birgunj, Nepal, [3]Amity Institute of Microbial Technology (AIMT), Jaipur, Rajasthan, India

Introduction: Urinary tract infections (UTIs) are a global health concern, increasingly complicated by antibiotic resistance. Cranberry-derived bioactive compounds, particularly proanthocyanidins (PACs), have emerged as a promising non-antibiotic strategy for UTI prevention. This review examines their efficacy, mechanisms of action, and the evolving research landscape through bibliometric analysis.

Methods: A comprehensive literature review was conducted to assess the role of cranberry metabolites in UTI prevention, focusing on anti-adhesive and antimicrobial mechanisms. Additionally, a bibliometric analysis of publications from 1962 to 2024 was performed to evaluate research trends, collaboration networks, and thematic developments.

Results: Cranberry metabolites, particularly A-type PACs, flavonoids, and phenolic acids, inhibit *Escherichia coli* adhesion to urothelial cells, reducing UTI recurrence. Gut microbiota-driven transformation of PACs into bioactive metabolites enhances their efficacy, while cranberry oligosaccharides disrupt biofilm formation in high-risk populations. Bibliometric analysis reveals a surge in research interest post-2000, with increasing global collaborations and a focus on clinical applications.

Discussion and conclusion: Cranberry bioactives demonstrate significant potential in UTI management, yet variations in formulation, dosage, and metabolic bioavailability present challenges. The growing research interest underscores the need for standardized clinical studies to optimize therapeutic efficacy and establish evidence-based guidelines for their use.

KEYWORDS

nutraceuticals, functional foods, cranberry, metabolites, urinary tract infections, proanthocyanidins, bibliometric analysis, bioactive compounds

1 Introduction

Urinary Tract Infections (UTIs) pose a significant global health concern affecting people of all ages. Each year, UTIs contribute to around 400 million cases, placing substantial strains on healthcare systems and individuals alike (1). Aside from causing immediate discomfort, UTIs lead to substantial economic costs due to medical expenses, reduced productivity, and increased demand for healthcare services. The widespread impact of UTIs highlights the urgent need for new and effective approaches to their prevention and treatment (2). UTIs

disproportionately affect women, primarily due to anatomical differences, with nearly half of all women experiencing at least one UTI during their lives. This gender gap results in billions of dollars in healthcare expenditures annually, including direct costs of treatment and indirect costs such as lost workdays (3, 4).

Given the significant impact of UTIs in women, targeted interventions are crucial to address this healthcare challenge. The urgency to tackle UTIs is compounded by the escalating problem of antibiotic resistance. Misuse and overuse of antibiotics have reduced the effectiveness of traditional treatments, increasing infection rates, recurrence, and mortality (5). This crisis highlights the necessity for alternative preventive and therapeutic methods. Cranberries, including their derivatives like juice and extracts, have attracted significant interest due to their historical use in indigenous communities for treating urinary ailments. Initial investigations into their potential for preventing UTIs focus on proanthocyanins, which inhibit *Escherichia coli*—the primary bacterium causing UTIs—from adhering to the urinary tract lining (6). This mechanism presents a promising non-antibiotic approach to managing UTIs. However, scientific opinion on the effectiveness of cranberries in UTI prevention is divided, with some studies highlighting their benefits while others expressing doubts (7–10). To navigate the complexities of UTI management and the role of cranberries, this review utilizes bibliometric and patent analyses as key tools. These methods allow for an examination of publication and citation trends, innovation patterns, and the commercial landscape, providing insights into research dynamics, leading contributors, and potential gaps in knowledge. By systematically exploring literature and patents, this study aims to offer a comprehensive view of current UTI research, identify promising avenues for future investigation, and assess the economic motivations behind cranberry-related interventions. In summary, the global health challenge posed by UTIs, especially amid rising antibiotic resistance, necessitates a reassessment of current treatment approaches. Cranberries represent a potential non-antibiotic strategy for managing UTIs, yet their effectiveness remains contentious. Through an integrated review and analytical assessment, this study aims to advance our understanding of UTI interventions and inspire innovative solutions to improve healthcare outcomes to combat the growing issue of resistance.

2 Literature review

2.1 Prevalence of urinary tract infection

The incidence of urinary tract infections (UTIs) is a substantial public health concern, exhibiting variability in occurrence rates among distinct age cohorts and genders. It is worth noting that there is a significant disparity in the prevalence rates among those aged 20–29, with a remarkable rate of 32.6% (11, 12). On the other hand, there is a notable disparity in the occurrence of this phenomenon among adolescents, namely within the age range of 10–19, where the prevalence is far lower, amounting to a measly 1.2%. The notable disparity highlights the increased vulnerability to urinary tract infections (UTIs) throughout the transition from youth to early adulthood. The prevalence of urinary tract infections (UTIs) is influenced by gender variations, wherein females demonstrate a higher incidence rate of 37.5% as a result of anatomical and physiological variables, while males exhibit a comparatively lower rate of 22.0%. The presence of a gender-related disparity underscores the distinct susceptibilities linked to urinary tract infections (UTIs) (12).

In order to formulate efficacious therapy approaches, it is vital to possess a thorough comprehension of the causative agents behind urinary tract infections (UTIs). According to the findings of Odoki (12), *E. coli* has been identified as the predominant bacterial pathogen, accounting for 41.9% of urinary tract infection (UTI) cases. Moreover, *Staphylococcus aureus* plays a substantial role, representing 31.4% of the total infection cases. Additional causal pathogens that can be identified include *Klebsiella pneumoniae*, accounting for 11.6% of cases, *Klebsiella oxytoca,* accounting for 7.0% of cases, *Proteus mirabilis,* accounting for 3.5% of cases, *Enterococcus faecalis*, accounting for 3.5% of cases, and *Proteus vulgaris*, accounting for 1.2% of cases. The presence of several strains of bacteria in urinary tract infections (UTIs) underscores the intricate nature of this condition, with *E. coli* routinely identified as the primary causative agent (12). Urinary tract infections (UTIs) have emerged as a substantial public health issue on a global scale, as evidenced by the findings of Wagenlehner (13), statistics are concerning, as there is an approximate global incidence of 404.61 million documented urinary tract infections (UTI) cases, resulting in 236,790 deaths and a significant burden of 520,200 disability-adjusted life years (DALYs) (13). Of particular worry is the notable 2.4-fold rise in mortality associated with urinary tract infections (UTIs) recorded between 1990 and 2019, highlighting the pressing necessity to address this worldwide menace. In terms of demographic characteristics, urinary tract infections (UTIs) exhibit a global prevalence rate of 33.54%. There is a notable gender imbalance, as evidenced by females accounting for 66.78% of cases, which is nearly double the rate observed in males at 33.22%. The observed gender disparity can be expressed as a ratio of 2:1. Upon further examination, it becomes evident that there are distinct age-related trends, with the overall incidence reaching its highest point among those aged 45 years and above. In the female population, the age group that has the highest incidence of urinary tract infections (UTIs) is between 31 and 45 years (13). Conversely, UTIs primarily manifest in males beyond the age of 45. In a recent study conducted by Tegegne (14), it was found that *E. coli* remains the most prevalent pathogen causing urinary tract infections (UTIs), accounting for 53.77% of cases (14). Following *E. coli, Klebsiella pneumoniae* was identified as the second most common pathogen, responsible for 27.40% of UTIs. This study highlights the significant importance of antibiotic selection in determining treatment results (14). Tegegne (14) emphasizes the urgent need for careful consideration of antimicrobial choices in the treatment of urinary tract infections (UTIs), as widespread resistance has been observed in commonly prescribed medications such as fluoroquinolones, amoxicillin, and third-generation cephalosporins (14). While drugs like meropenem, gentamicin, nitrofurantoin, and cotrimoxazole have demonstrated effectiveness, the prevalence of resistance underscores the importance of selecting appropriate antimicrobial agents for UTI treatment.

2.2 Prevalence of multi-drug resistant urinary tract infections

Urinary tract infections (UTIs), once viewed as manageable health issues, have undergone a significant transformation in recent times due to the alarming rise in multi-drug resistance (MDR). This troubling trend, where pathogens develop resistance to multiple

antibiotics, now presents a major challenge to the fundamental approaches for UTI treatment. Table 1 below lists multi-drug resistance UTI pathogens.

In a groundbreaking study conducted by Dasgupta and colleagues in 2020, an exploration of this changing scenario revealed a concerning reality. The prevalence of MDR UTIs showed significant variation, with some regions reporting rates as low as 3.7%, while others faced alarmingly high rates, reaching up to 88.1%. These findings have profound implications, especially considering that previously effective antibiotics like ciprofloxacin, cephalosporin, azithromycin, aztreonam, cotrimoxazole, and nalidixic acid now encounter resistance rates ranging from 28.6 to 92.9% (15).

Building on this foundational research, a subsequent investigation led by Umemura and their team in 2022 revealed even more concerning insights. Their data analysis highlighted the prevalence of *Klebsiella* spp. among MDR pathogens, accounting for 29% of cases. *E. coli* closely followed, contributing to 24% of MDR UTIs. These MDR strains were notably detected in a substantial 50% of the analyzed samples, emphasizing the pervasive and deeply rooted nature of this resistance problem (16). Adding to the worries, the study also uncovered that a significant 26% of UTI isolates were producing extended-spectrum beta-lactamases (ESBL), enzymes that provide resistance against a wide range of beta-lactam antibiotics. However, amidst this grim scenario, there is a glimmer of hope: carbapenem resistance, often seen as the last line of defense against antibiotic resistance, remains rare, identified in only 0.1% of cases. Although this finding is relatively small, it offers a ray of hope within the otherwise bleak landscape of MDR UTIs (17).

2.3 Medicinal plants with uroprotective activity

The utilization of medicinal plants in traditional healing practices has played a vital role in human health for countless centuries (18). These plants, rich in a wide array of bioactive compounds, have served as the basis for many contemporary pharmaceuticals. Among the numerous therapeutic properties associated with medicinal plants, their ability to safeguard the urinary system, particularly the kidneys, from harm, has gained significant attention recently (19).

The term "uroprotective activity" denotes the capacity of certain substances to protect the urinary system, especially the kidneys, from potential damage. This becomes especially critical in situations where the kidneys may be exposed to harmful agents, such as chemotherapy or extended use of specific medications. Damage to the urinary system can result in various complications, ranging from urinary tract

TABLE 1 Overview of multi-drug resistance in uropathogens across different geographic regions.

Pathogen	Resistant antibiotics	Mechanism of resistance	Geographic region	Reference
Escherichia coli	Ampicillin, Amoxicillin, TMP/SMX, Cefuroxime, Ciprofloxacin	Beta-lactamase production, Efflux pump activation	Asia (India, Nepal, Bangladesh), Africa (Nigeria, South Africa), Middle East (Iran, Saudi Arabia), Europe (Romania), North America (United States), South America (Brazil, Argentina), Australia	(15)
Enterococcus spp.	Most antibiotics except Linezolid and Tigecycline	Altered target sites	Europe (Romania, Spain), Asia (India, Japan), North America (United States), South America (Argentina), Middle East (Iran), Australia	(70)
Klebsiella spp.	Ampicillin, Amoxicillin, TMP/SMX, Cefuroxime, Ciprofloxacin	Beta-lactamase production, Efflux pump activation	Asia (India, Nepal, Bangladesh), Europe (Romania, Italy), North America (United States, Canada), South America (Brazil), Middle East (Saudi Arabia, Turkey), Africa (Nigeria, Egypt)	(71)
Staphylococcus saprophyticus	Multiple antibiotics (specifics not mentioned)	Novobiocin-resistant GyrB protein	Asia (India, Nepal, Bangladesh), Europe (Romania, Italy), North America (United States, Canada), South America (Brazil), Middle East (Saudi Arabia, Turkey), Africa (Nigeria, Egypt)	(72)
Escherichia coli (ESBL-producing)	Ampicillin, Amoxicillin, Amikacin, Cefotaxime, Ceftazidime, Chloramphenicol, Ciprofloxacin, Nitrofurantoin, Norfloxacin, Tetracycline, Amoxicillin/Clavulanic acid	ESBL production	United States, Asia (Nepal, Bangladesh), Africa (Nigeria), Middle East (Iran)	(73)
Proteus spp.	Tetracycline, Cefuroxime, Penicillin, Ceftriaxone	Altered target sites, Efflux pump activation	Asia (India, Bangladesh), Europe (Romania, Germany), North America (United States, Canada), South America (Brazil), Africa (Nigeria)	(74)
Escherichia coli	Sulfonamide, Tetracycline	Efflux pump activation	Middle East	(75)
Stenotrophomonas maltophilia	Trimethoprim, TMP/SMX	Efflux pump activation	Asia (China, India), Africa (Egypt), North America (United States), South America (Brazil), Australia	(76)

infections to chronic kidney diseases (20). A multitude of medicinal herbs have been recognized for their substantial uroprotective properties. The botanical specimens frequently possess antioxidants, anti-inflammatory agents, and additional bioactive constituents that have the potential to mitigate oxidative stress, reduce inflammation, and promote general renal wellbeing (21). The utilization of these plants offers a natural and comprehensive method for uroprotection, which has the potential to decrease reliance on synthetic medications and their accompanying adverse effects (22). Medicinal plants exhibit uroprotective activity through several key mechanisms. Firstly, they combat oxidative stress by neutralizing reactive oxygen species (ROS) with their high antioxidant content, as seen in plants like *Camellia sinensis* (green tea) and *Punica granatum* (pomegranate) (23). Secondly, their anti-inflammatory properties reduce inflammation in the urinary tract by downregulating pro-inflammatory markers such as TNF-α and IL-6. For example, apigenin from *Chamomilla recutita* inhibits inflammatory pathways, restoring normal bladder tissue function (24). Thirdly, bioactive compounds in plants like *Hemidesmus indicus* and *Tinospora cordifolia* enhance diuresis and mitigate bacterial colonization through anti-adhesive and antimicrobial actions, disrupting biofilm formation by pathogens such as *Escherichia coli* and *Klebsiella pneumoniae* (25). Lastly, these plants can modulate immune responses and maintain the oxidative/antioxidative balance in the urinary system, contributing to their protective effects against various toxic insults, such as those induced by chemotherapeutic agents (26). The subsequent Table 2 presents accumulated data regarding diverse medicinal plants that are well-known for their uroprotective properties. The primary objective of this compilation is to emphasize the potential of these plants in the context of contemporary medicine, while also promoting further investigation into their mechanisms of action and prospective clinical uses.

2.4 Cranberry: composition and properties

Cranberry (*Vaccinium macrocarpon*) has been highly regarded for its culinary and medicinal qualities, especially for its effectiveness in managing and preventing urinary tract infections (UTIs). This small, evergreen shrub, native to North America, yields tart, red berries containing a diverse array of bioactive compounds. The interaction of these compounds gives cranberry its unique pharmacological characteristics, leading to sustained scientific curiosity and research (27).

2.4.1 Phytochemical profile

At the core of the cranberry's pharmacological capabilities are its proanthocyanidins (PACs), a group of polyphenolic compounds that have gained significant attention for their ability to prevent urinary tract infections (UTIs). Cranberry PACs are notable for their unique A-type chemical structure, which differs from the B-type linkages found in the PACs of other fruits. This structural distinction is believed to be crucial for the cranberry's capacity to hinder bacterial adhesion to the bladder wall, a critical step in UTI development (10). However, the cranberry's phytochemical profile extends beyond PACs. The fruit is also abundant in other flavonoids, such as anthocyanins responsible for its deep red color, and flavonols like quercetin and myricetin, which act as potent antioxidants, neutralizing free radicals and reducing oxidative stress in the body. Additionally, cranberries contain various phenolic acids like benzoic acid and hydroxycinnamic acid, which have been studied for their antimicrobial and anti-inflammatory properties (28, 29). Triterpenoids and small amounts of alkaloids found in cranberries further diversify its phytochemical composition, potentially contributing to its health benefits. The combined effects of these diverse compounds are believed to underpin the cranberry's overall health-promoting qualities, extending beyond UTI prevention to encompass cardiovascular health, cancer prevention, and other areas of wellness (30).

2.4.2 Mechanisms of action: contribution of cranberry components to UTI management

The effectiveness of cranberry in managing urinary tract infections (UTIs) stems from its varied phytochemical makeup, which operates through several mechanisms to provide a comprehensive approach to UTI development. These mechanisms, largely based on the bioactive components of cranberry such as proanthocyanidins (PACs), flavonoids, and phenolic acids, provide a detailed understanding of how cranberry constituents contribute to UTI management (6, 31).

2.4.2.1 Anti-adhesion activity

The key feature of cranberry's effectiveness against UTIs is its anti-adhesion properties, mainly due to the presence of unique A-type proanthocyanidins (PACs). These compounds disrupt the ability of P-fimbriated *Escherichia coli*, the most common bacteria causing urinary tract infections, to adhere to the epithelial cells lining the urinary tract. A-type PACs are believed to bind specifically to the P-fimbriae on the surface of *E. coli,* altering the bacterial cell surface and preventing attachment to uroepithelial cells. This mechanism helps reduce the likelihood of bacterial colonization and subsequent infection development (32, 33). Research conducted by Howell provided initial evidence for this anti-adhesion mechanism, demonstrating that cranberry PACs significantly decrease the adhesion of P-fimbriated *E. coli* to uroepithelial cells in laboratory settings. Subsequent studies have confirmed these findings, emphasizing cranberry's targeted action against P-fimbriated strains of *E. coli*, which are responsible for a substantial number of UTI cases (34, 35).

2.4.2.2 Antimicrobial properties

In addition to preventing bacterial adhesion, cranberry components demonstrate direct antimicrobial effects against a range of uropathogens. The flavonoids and phenolic acids found in cranberries have been investigated for their ability to inhibit bacterial growth and kill bacteria (36). These compounds can disrupt bacterial cell walls, interfere with quorum sensing (bacterial communication), and inhibit the activity of essential bacterial enzymes. For example, research conducted by Côté (37) showed that cranberry extracts possess antimicrobial properties against antibiotic-resistant strains of *E. coli,* suggesting a potential role for cranberry in addressing the escalating issue of antibiotic resistance in UTI treatment (37, 38).

2.4.2.3 Antioxidant and anti-inflammatory effects

The oxidative stress and inflammation linked to the development of UTIs can worsen the condition and extend recovery time. Cranberries are rich in flavonoids and other antioxidants, which play a critical role in reducing oxidative

10.3389/fnut.2025.1502720

TABLE 2 Medicinal plants exhibiting uroprotective properties.

Plant scientific name	Plant part used	Activity	Population group/study model	Specific pathogens	Specific phytochemicals	Reference
Ocimum gratissimum L. (African Basil)	Essential oils	Antimicrobial activity, particularly effective against *Klebsiella pneumoniae* and *Escherichia coli*.	In vitro studies	*Klebsiella pneumoniae*, *Escherichia coli*	Eugenol, linalool	(77)
Salvia officinalis L. (Common Sage)	Essential oils	Diuretic, antipyretic, anti-inflammatory activity against uropathogens.	In vitro studies	*Escherichia coli*, *Proteus mirabilis*	Thujone, camphor	(78)
Mangifera indica L. (Mango Tree)	Seed kernel, Leaves, Bark	Anti-biofilm and antimicrobial activity against uropathogenic *E. coli*.	In vitro studies, clinical settings	Uropathogenic *E. coli* (UPEC)	Mangiferin	(79)
Carica papaya L. (Papaya Plant)	Seeds	Antimicrobial activity against multiple uropathogens.	In vitro studies	*Escherichia coli*, *Pseudomonas aeruginosa*, *Enterococcus faecalis*, *Klebsiella* spp.	Papain, carpaine	(80)
Allium sativum L. (Garlic)	Extract in ethanol/ methanol	Broad-spectrum antimicrobial properties against uropathogens.	Clinical trials, in vitro studies	*Escherichia coli*, *Klebsiella pneumoniae*, *Proteus mirabilis*	Allicin	(81)
Adiantum lunulatum Burm. f. (Green Maidenhair Fern)	Roots	Diuretic and anti-urolithiatic properties; treatment for hematuria.	Traditional medicine	–	–	(82)
Zingiber officinale Roscoe (Ginger)	Extract	Antimicrobial activity and relief from urinary infections.	In vitro studies	*Escherichia coli*, *Staphylococcus aureus*	Gingerol, shogaol	(83)
Coccinia grandis L. (Ivy Gourd)	Leaves and stems	Antimicrobial activity against uropathogens.	In vitro studies	*Escherichia coli*, *Klebsiella pneumoniae*	–	(84)
Coleus aromaticus Lour. (Indian Borage)	Extract	Antimicrobial activity, potential against UTIs.	In vitro studies	*Escherichia coli*	Carvacrol, thymol	(85)
Ocimum sanctum L. (Holy Basil)	Essential oils, leaves	Antimicrobial agent against various uropathogens.	Traditional medicine, in vitro studies	*Escherichia coli*, *Klebsiella pneumoniae*	Eugenol	(86)
Arctostaphylos uva-ursi (Uva Ursi)	Leaves	Diuretic and antiseptic properties for UTIs.	Clinical studies, traditional medicine	*Escherichia coli*, *Proteus mirabilis*	Arbutin	(87)
Taraxacum officinale (Dandelion)	Extracts, Roots, Leaves	Diuretic and antimicrobial activity against uropathogens.	In vitro studies	*Escherichia coli*, *Proteus mirabilis*	Taraxasterol	(88)
Equisetum arvense (Horsetail)	Aerial parts, extracts	Astringent, diuretic, and tissue-healing properties.	Traditional medicine	–	Silica, equisetonin	(89)
Vaccinium macrocarpon (Cranberry)	Fruits	Prevents UTIs by inhibiting bacterial adhesion; antimicrobial properties.	Clinical trials with recurrent UTI patients	*Escherichia coli* (*P-fimbriae blockade*)	Proanthocyanidins, quercetin	(31)
Juniperus communis (Juniper)	Berries, essential oils	Diuretic, antiseptic, and anti-biofilm properties for UTIs.	Traditional medicine, in vitro studies	*Escherichia coli*, *Proteus mirabilis*	Alpha-pinene, sabinene	(90)
Solidago virgaurea (Goldenrod)	Aerial parts	Diuretic, anti-inflammatory, and antimicrobial properties.	Traditional medicine	*Escherichia coli*, *Klebsiella pneumoniae*	Quercetin, rutin	(91)
Althaea officinalis (Marshmallow)	Root	Soothes urinary tract tissues; inhibits bacterial growth.	Traditional medicine	*Escherichia coli*, *Proteus mirabilis*	Mucilage compounds	(92)

(Continued)

TABLE 2 (Continued)

Plant scientific name	Plant part used	Activity	Population group/study model	Specific pathogens	Specific phytochemicals	Reference
Agathosma betulina (Buchu)	Leaves, extract, essential oils	Diuretic and antiseptic properties for UTIs.	Traditional medicine	*Escherichia coli*, *Klebsiella pneumoniae*	Diosmin, hesperidin	(93)
Zea mays (Corn Silk)	Stigmas from female flowers	Diuretic properties; soothes urinary tract.	Traditional medicine	–	Polyphenols, tannins	(94)
Serenoa repens (Saw Palmetto)	Berries	Supports prostate health; diuretic properties.	Clinical trials, traditional medicine	–	Beta-sitosterol	(95)

damage and regulating inflammatory responses. These compounds scavenge reactive oxygen species (ROS) and influence signaling pathways involved in inflammation, potentially lessening the severity of UTIs and aiding in recovery (39). Vostalova (40) emphasized the anti-inflammatory potential of cranberry, demonstrating that its consumption could alter biomarkers of inflammation in UTI contexts. This suggests that cranberry's antioxidant and anti-inflammatory properties work synergistically in managing UTIs, complementing its antimicrobial and anti-adhesion effects (40, 41).

The various ways in which cranberry components contribute to UTI management highlight its potential as a complementary strategy for preventing and treating these infections. The anti-adhesion and antimicrobial properties specifically target the initial stages of infection, while antioxidant and anti-inflammatory effects may help alleviate symptoms and decrease recurrence. These discoveries support the traditional use of cranberry in preventing UTIs, though additional research is needed to fully grasp the best practices and clinical effectiveness of cranberry in different populations and UTI scenarios (42).

2.5 Pharmacokinetics

The pharmacokinetics of cranberry, which involves the processes of absorption, distribution, metabolism, and excretion (ADME) of its active constituents, is crucial for understanding its effectiveness in managing urinary tract infections (UTIs) and its interactions with pharmaceuticals. Cranberry's bioactive compounds, including proanthocyanidins (PACs), flavonoids, and phenolic acids, possess unique pharmacokinetic properties that impact their therapeutic efficacy and safety profile (43).

Absorption: The absorption of cranberry's bioactive compounds depends on their chemical characteristics and the formulation of the cranberry product consumed (e.g., juice, extract, capsule). Studies indicate that PACs, due to their large molecular size and complexity, have limited oral bioavailability. However, small amounts that are absorbed through the gastrointestinal tract can still exert systemic effects. Flavonoids and phenolic acids are absorbed more readily, and their bioavailability can be influenced by modifications from gut microbiota. Once absorbed, these compounds can influence various biochemical pathways, including those involved in inhibiting bacterial adhesion and enhancing antioxidant defense (32, 36, 43).

Distribution: Following absorption, cranberry's bioactive components are distributed throughout the body, with specific affinity for certain tissues influenced by their lipophilicity and molecular size. The distribution is critical for the compounds' ability to reach the urinary tract, where they can exert local antimicrobial and anti-adhesion effects. Studies have shown the presence of metabolites derived from cranberry compounds in urine, indicating successful distribution to the urinary system (43, 44).

Metabolism: The metabolism of cranberry components primarily occurs in the liver and gut, where they undergo extensive biotransformation. This process involves conjugation reactions that enhance their water solubility, facilitating their excretion. The gut microbiota also plays a vital role in metabolizing cranberry compounds, converting them into various metabolites with potential health benefits. These metabolites, including those from PACs and flavonoids, have been identified in plasma and urine, indicating systemic exposure and biological activity (45, 46).

Excretion: The excretion of cranberry-derived compounds, including proanthocyanidins, hippuric acid, benzoic acid derivatives, and urinary phenolic acids, ensures their activity within the urinary tract. These metabolites inhibit bacterial adhesion, acidify the urine, and create an antimicrobial environment that supports cranberry's UTI-preventive effects. Additionally, some components are excreted through bile into feces, completing their elimination from the body (43, 47, 48).

2.6 Interactions

Interactions between cranberry and pharmaceuticals are a subject of significant interest and concern, particularly with medications that have narrow therapeutic windows, such as warfarin. The concern stems from cranberry's potential to affect the pharmacokinetics of co-administered drugs, either by altering their metabolism or by influencing their distribution and excretion. There have been reports of increased bleeding risk and elevated international normalized ratio (INR) levels in patients consuming cranberry products concurrently with warfarin. This interaction is believed to occur due to cranberry's impact on the cytochrome P450 enzyme system and/or platelet function, potentially inhibiting the metabolism of warfarin and intensifying its anticoagulant effect (49, 50). Given the intricate pharmacokinetics of cranberry and its capacity to interact with medications, healthcare providers must be mindful of these interactions. Patients taking medications with narrow therapeutic indices should receive counseling regarding the potential risks associated with concurrent cranberry consumption and should be monitored for any adverse effects. Further research is essential to uncover the underlying mechanisms of these interactions and to establish guidelines for the safe co-administration of cranberry products with other medications.

2.7 Cranberry metabolites in UTI management

Cranberry metabolites have gained substantial attention due to their potential role in preventing urinary tract infections (UTIs) through a variety of mechanisms. Among the major metabolites studied in this respect, more importantly, are proanthocyanidins (PACs); among them, A-type PACs have a specific molecular structure and are responsible for anti-adhesion of bacteria (48). This anti-adhesion activity is primarily directed at *Escherichia coli,* the most common pathogen causing UTIs. PACs prevent the adhesion of the bacteria to the uroepithelial lining, thus limiting the initial steps of infection. However, studies on their bioavailability have shown that, as such in their natural form, PACs are not readily bioavailable. It would seem that much of the biological activity realized is a result of metabolites—valeric acid derivatives—generated during the metabolism of PACs (51). A randomized controlled trial that demonstrated that, in women undergoing surgery, cranberry capsules significantly reduced recurrence of UTI by 50%, supporting clinical relevance of the metabolites of PACs (3). Besides PAC, flavonoids and phenolic acids are bioactive compounds in cranberry, which contribute to the prevention of UTIs because of their antioxidant and anti-inflammatory activities. Among these metabolites, quercetin and its derivatives have previously been shown for being able to modulate oxidative stress, which is known to frequently lead to an inflammatory response during infections. Some clinical trials with a placebo control have reported that UTI incidence can be reduced by 26% in women identified with recurrent UTIs, thus further justifying the potential ability to reduce oxidative damage and enhance anti-inflammatory pathways of the cranberry-containing products (9). This multi-factorial representation highlights defense mechanisms against bacterial invasion beyond the antiadhesive action of PACs. Recent studies have shown that cranberry-derived oligosaccharides, although free of phenolic compounds, exhibit potential to inhibit biofilm formation. Biofilms protect bacteria like *E. coli* from immune response, and treatment with antimicrobials makes them resilient within the urinary tract. Since the biofilm is disrupted, cranberry oligosaccharides can help reduce chronic and recurrent infections, particularly in patients with conditions that predispose them to persistent bacterial colonization, such as neurogenic bladder. One randomized clinical study illustrated that cranberry supplementation drastically reduced biofilm formation, which contributed to a reduction in the incidence of UTI among populations at risk (8). Last but not least, the special metabolic processing of the cranberry constituents underlines the relevance of understanding the pharmacokinetics of those compounds. Whereas complex absorption and metabolism with glucuronidation and sulfation have been demonstrated for PACs and flavonoids, it is most probably the catabolism products such as valerolactones and their conjugates that might substantially contribute to the antimicrobial activity expressed in the urinary tract. In one study where cranberry was compared with conventional antibiotic treatments, PAC metabolites showed anti-adhesive activity in urine, and consumption of cranberry did not promote antibiotic resistance, unlike conventional treatments (52). This thus would imply that the subsequent studies should be oriented toward the metabolites per se rather than the parent compounds only, and that would perfectly help in realizing the optimum therapeutic potential of cranberry in UTIs prevention. Further Table 3 includes major bioactive metabolites from cranberries, their chemical classes, modes of action against UTIs, and their bioavailability profiles, while supporting clinical evidence of their activities, accompanied by key metabolites reported from biological studies, is also presented. This assures that the active principles of cranberry have multifaceted pharmacological potential against bacterial adhesion, inflammation, and biofilm development (Figure 1).

2.8 Role of gut microbiota in metabolite production of cranberry compounds

Recent research highlights the vital role of gut microbiota in transforming cranberry PACs into bioactive metabolites, which are essential for understanding the efficacy of cranberry in UTI prevention. Cranberry PACs, particularly those with A-type linkages, are poorly absorbed in their intact form. Instead, they are metabolized by gut microbiota into low molecular weight metabolites, such as valerolactones and phenolic acids, which exhibit anti-adhesion bioactivity in urine and contribute to their effectiveness against urinary tract infections. A more recent, comprehensive study by Gregorio et al. (51) found urinary excretion of low molecular weight metabolites following consumption of cranberry and spotted major metabolite 5-(3′,4′-dihydroxyphenyl)-γ-valerolactone responsible for the inhibition of *E. coli* adhesion to bladder epithelial cells. The conversion of PACs into valerolactones is believed to be very important, as naturally occurring PACs per se show low bioavailability and are negligibly excreted in the urine. Urinary excretion of those gut microbiota-derived metabolites peaked at 6–8 h and coincided with maximal antiadhesive activity against uropathogenic *E. coli* strains in the *in vitro* assay. The present study contributes further to the growing evidence that microbial metabolism is a necessary step in mediating the UTI-preventing effects of cranberry PACs (51).

Besides that, interindividual variability in the microbe composition has great influence on the effectiveness of cranberry, with respect to UTI. The composition lacks a specific active binding component, typically found in monoaromatic and monoaliphatic acids. A high molecular weight structure is often required for effective interaction with uropathogenic bacteria along the urinary tract (53). Interestingly, in one *in vitro* study, metabolites were found from cranberry, particularly valeric acid derivatives, which turned out to be more potent in bacterial inhibition than intact cranberry PACs. The primary contributors to anti-adhesion properties were microbial degradation products of PACs, rather than the PACs themselves. This does indicate an unexploited therapeutic potential for cranberry PACs if this is not converted by gut microbial activity. These microbial metabolites were active with durability for a longer period, which indicated the involvement of gut microbiota in such durability (54). The outcome reveals differences in the production of metabolites related to specific strains of gut bacteria: indeed, under particularly tightly controlled conditions, it was found that the individuals with high levels of members from two bacterial families—*Ruminococcaceae* and *Lachnospiraceae*—already known for being active polyphenol metabolizers—showed enhanced excretion of valerolactone metabolites. The microbial profile was strongly correlated with higher anti-adhesion activity in urine samples, confirming variability in PAC metabolism among individuals. The latter is an important factor to explain the inconsistent clinical results so far obtained in

TABLE 3 Bioactive cranberry metabolites and their role in urinary tract infection prevention.

Cranberry metabolite	Mechanism of action	Bioavailability	Clinical evidence (study)	Notable metabolites	Reference
Proanthocyanidins (PACs)	Inhibits *E. coli* adhesion to uroepithelial cells	Poor bioavailability, PAC metabolites like valeric acid and valerolactone detected in urine	PACs found to reduce UTI incidence by 26% in women with a history of UTI	Valeric acid, Valerolactone derivatives	(51)
Flavonoids (Quercetin, Myricetin)	Antioxidant, anti-inflammatory	Moderate bioavailability; metabolites such as quercetin-3-galactoside detected in urine	Significant urinary excretion of quercetin metabolites linked to anti-inflammatory effects in UTIs	Quercetin-3-galactoside, Myricetin-3-arabinoside	(96)
Phenolic Acids (Benzoic, Cinnamic Acids)	Antimicrobial, anti-inflammatory	Moderate bioavailability, detected in urine after cranberry intake	Reduced bacterial adhesion and UTI incidence in clinical trials	Benzoic acid, Vanillic acid, Cinnamic acid	(48)
Triterpenoids (ursolic acid)	Anti-inflammatory, antimicrobial	Limited bioavailability data	Inhibits biofilm formation in *E. coli* and *Staphylococcus* spp., linked to lower UTI recurrence rates	None reported	(97)
Anthocyanins (peonidin-3-galactoside and cyanidin-3-galactoside)	Antioxidant, reduces oxidative stress	Low bioavailability, metabolites detectable in plasma	Shown to reduce oxidative stress in UTI-related inflammation	Anthocyanidin derivatives	(34)
Cranberry oligosaccharides (fructo-oligosaccharides)	Inhibits biofilm formation, primarily in *E. coli*	Limited bioavailability information, microbial transformation involved	Reduces biofilm production and adhesion of pathogens	Xyloglucan, Arabinan residues	(97)
Proanthocyanidins (PACs)	Inhibits *E. coli* adhesion to uroepithelial cells	Dose-dependent, urine detection up to 24 h post-ingestion	Dosage of 72 mg PAC reduced UTI recurrence in clinical trials	PAC-A2 metabolites	(10)

supplementation studies with cranberry products for UTI prevention (55). A multi-centric randomized trial was targeted to determine the dose–response relationship of cranberry and its metabolite production. Results from this trial have depicted that higher the dose of cranberry PAC, the higher the microbial-derived valerolactones concentrations, although anti-adhesion activity increased proportionally. The dose of cranberry, combined with the gut microbiota's capacity to metabolize PACs, is a key determinant of the effectiveness of cranberry-based interventions for UTI prevention (34). This is a gut microbiota job and draws attention to their contribution to the biotransformation of cranberry PACs into active metabolites (as depicted in Figure 2). Real-world evidence highlights significant variability in microbiota composition and the production of valerolactones and phenolic acids, which greatly influence the effectiveness of cranberry supplementation. Knowledge and considerations about such microbial dynamics provide an important rationale for personalized approaches to the maximum use of cranberry in UTI prevention.

2.9 Clinical trials related to cranberry's effects on UTIs

The efficacy of cranberry in preventing urinary tract infections (UTIs) is widely recognized, primarily attributed to its rich content of bioactive compounds, especially proanthocyanidins (PACs), which are believed to interfere with the attachment of uropathogenic bacteria to the cells lining the urinary tract (31). Several clinical trials have been conducted to investigate the impact of cranberry consumption on UTI occurrence, particularly among high-risk populations, such as women with recurrent UTIs or elderly individuals in long-term care facilities (56). These studies have significantly enhanced our understanding of cranberry's potential as a non-pharmacological approach to preventing UTIs. This segment focuses on key clinical trials investigating the impact of cranberry and cranberry-derived products on UTIs. These trials have provided crucial information on cranberry's efficacy, suitable dosages, and mechanisms for reducing UTI recurrences. By thoroughly analyzing the results of these trials, the aim is to clarify the current understanding of cranberry's role in preventing UTIs, while recognizing the existing debates and the necessity for further research in this area (9) Commencing with the elderly demographic, a carefully designed randomized, double-blind, placebo-controlled trial involved 153 elderly women. These individuals were divided into two groups: one group consumed 300 mL of cranberry juice daily, while the other received a placebo. Interestingly, the cranberry group displayed a lower UTI incidence at 15%, compared to 28.1% in the placebo group (57). However, it's important to note that this encouraging trend did not reach statistical significance. This suggests that while there may be potential advantages to cranberry, it cannot be definitively regarded as a preventive measure for UTIs in this age group.

Shifting to a different patient demographic, a randomized, single-blind crossover study focused on 21 patients with neuropathic bladders. These individuals were either given 15 mL of cranberry juice per kilogram of body weight or administered a water placebo. The findings here were mixed: 18 patients (nine from each group)

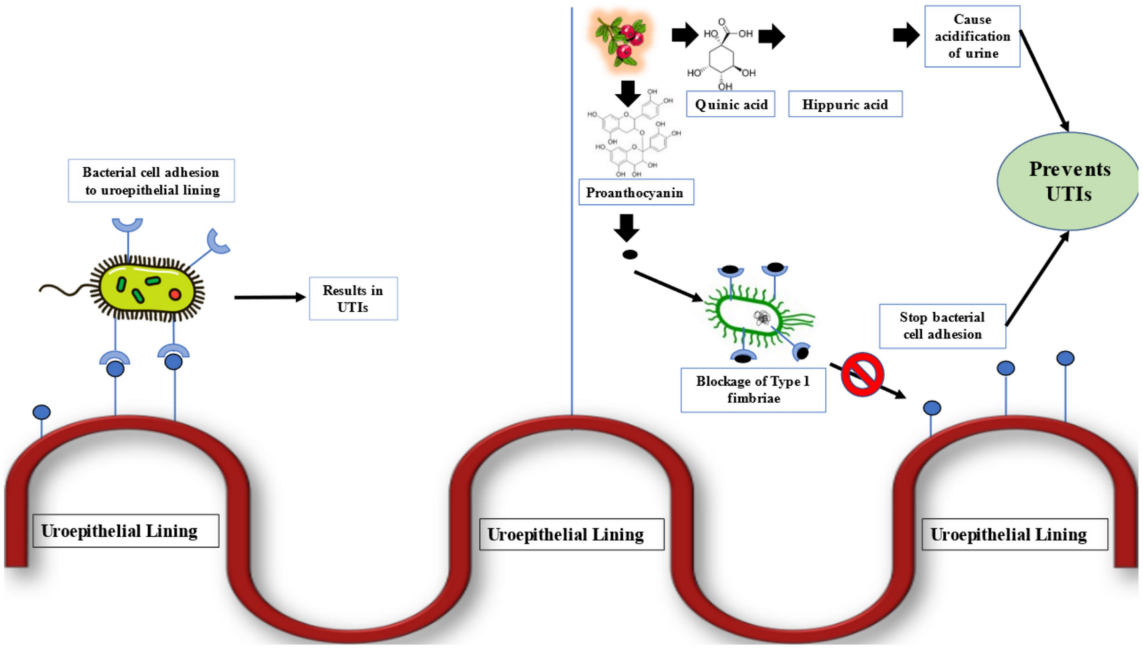

FIGURE 1
Cranberry bioactive compounds against urinary tract infection pathogens (28, 69).

exhibited a reduced infection rate, while the remaining three did not show any marked difference. This variation underscores the inconsistent efficacy of cranberry and emphasizes the significant role played by individual physiological factors (6). Another noteworthy trial, targeting women with recurrent UTIs, employed a randomized, double-blind, crossover design. This study involved 19 female participants, who were administered 400 mg cranberry capsules. While the cranberry group reported a UTI incidence of 2.4 cases per subject per year—significantly lower than the 6.0 figure in the placebo group—a substantial withdrawal rate of 47.4% raised concerns. This high dropout rate suggests potential challenges, either related to the study's methodology or the participants' experience with the capsules, necessitating a more thorough examination of the results (58). Finally, children undergoing intermittent catheterization became the focus of a double-blind, placebo-controlled trial with a crossover design. In this study, 15 children were provided with either 60 mL of cranberry juice daily or a placebo. Contrary to some expectations, the outcomes did not reveal significant differences between the groups in terms of bacteriuria or UTI incidence. This study serves as a cautionary example, highlighting the potential risks of generalizing the benefits of cranberry across diverse age groups (59). Further Table 4 listed clinical studies to test cranberry efficacy in treating urinary tract infections.

2.10 Studies on cranberry consumption: safety, health benefits, and adverse effects

Scientific research has extensively explored the safety and health advantages of consuming cranberries among different populations and for various health conditions. While cranberry's positive effects, particularly in preventing and managing urinary tract infections (UTIs), are widely recognized, there is a limited amount of direct research on its potential toxicity. This comprehensive Table 5 below consolidates findings from multiple studies to clarify the broader impact of cranberry consumption on health, its interaction with medications, and its safety profile (60).

3 Methodology

In this review, a systematic approach was employed to thoroughly investigate the effectiveness of cranberry in managing Urinary Tract Infections (UTIs) resistant to multiple drugs. Additionally, a bibliometric analysis was conducted to evaluate the current state of research in this field (61).

3.1 Literature search strategy

A thorough exploration of the literature was performed utilizing Scopus databases, specifically concentrating on the use of cranberry as an alternative remedy for urinary tract infections. Relevant articles were identified using a combination of specific keywords ("Cranberry" and "Urinary tract infection") and Boolean operators. The objective of this search strategy was to encompass a wide range of research related to cranberry and UTIs, ensuring the inclusion of recent studies up until the knowledge cutoff date in September 2024.

3.2 Inclusion and exclusion criteria

The retrieved articles were meticulously processed based on well-defined inclusion and exclusion criteria to refine the selection process:

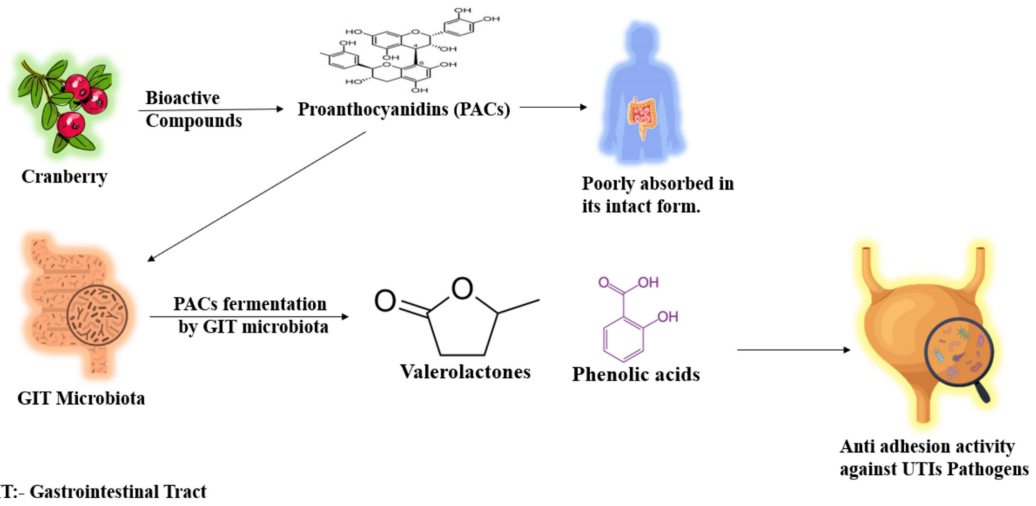

FIGURE 2
Role of gut microbiota in metabolite production of cranberry compounds.

3.2.1 Inclusion criteria

- Articles published in peer-reviewed journals.
- Articles written exclusively in the English language.
- Articles investigating the efficacy of cranberry in the context of both UTIs and multi-drug resistant UTIs.
- Studies conducted on humans as well as *in vitro*/ex vivo experiments.
- Articles focusing on topics such as antibiotic resistance, cranberry's mechanisms of action, or clinical outcomes.
- Articles published up to September 2024.

3.2.2 Exclusion criteria

- Non-English articles were excluded from the analysis.
- Articles not directly addressing the role of cranberry in UTIs were excluded.
- Conference abstracts, posters, and presentations were not considered in the review process.

By adhering to these rigorous criteria, the review ensured a comprehensive and focused analysis of the relevant literature, contributing to a thorough understanding of cranberry's potential in managing multi-drug resistant UTIs.

3.3 Bibliometric analysis

This section presents a comprehensive bibliometric analysis undertaken in conjunction with a systematic review to elucidate the complex association between cranberries and urinary tract infections (UTIs). This investigation sought to uncover trends, significant researchers, and key research issues through the use of data-driven approaches. The scientific publications were subjected to thorough examination, wherein many aspects such as publication years, journal sources, author affiliations, keywords, and citation counts were analyzed (62). Through the utilization of temporal data tracking and exploration of academic publications, the investigation uncovered the progression of research activities and the emergence of specialized platforms dedicated to the dissemination of research findings (63). Thorough investigations into the affiliations of authors have brought attention to significant contributors and collaboration networks, while the study of keywords has revealed repeating themes and new issues. These findings provide valuable insights into specific research fields that are of academic interest (64).

The thorough bibliometric analysis, in conjunction with the qualitative insights derived from the systematic review, yielded a comprehensive portrayal of the body of research pertaining to urinary tract infections (UTIs) and cranberries. The text provided offers a comprehensive perspective on the historical development, prominent individuals involved, and significant research areas related to cranberries, so providing a comprehensive comprehension of their potential in managing urinary tract infections (UTIs). The aforementioned integrated strategy has effectively emphasized the accomplishments, obstacles, and prospective areas of investigation within this pivotal realm of research (65).

4 Results and discussion

In September 2024, data extracted from the Scopus database in BibTeX format revealed a total of 1,005 publications related to Cranberry as an alternative treatment for urinary tract infections within the period from 1962 to 2024. We focused on English-language publications, narrowing the selection down to 981 publications. To ensure the study's precision, we excluded 316 reviews, 68 Notes, 42 letters, 41 Short surveys, 20 book chapters, 19 editorials, and 17 conference papers, as they did not align with our specific target article types, as indicated in PRISMA diagram (as depicted in Figure 3). Consequently, 556 original articles remained for our quantitative analysis.

The data collected is summarized comprehensively in Figure 4, presented using R-Studio (66). This bibliometric overview offers a detailed analysis of publication data sourced from the Scopus database covering the period from 1962 to 2024. During these 61 years, a total of

TABLE 4 Clinical trials related to cranberry's effects on UTIs.

Study design	Population	Preparation	Findings	Efficacy	Reference
Randomized, double-blind, placebo-controlled	Kidney transplant recipients	Cranberry capsules	Cranberry capsules showed potential in preventing UTIs.	Effective and Safe	(98)
Observational Study	Females with recurrent UTIs	Cranberry extract	Cranberry extract was effective in preventing recurrent UTIs in 81.3% of cases.	Highly Effective	(99)
Experimental Study	General Population	Cranberry juice	Cranberry juice significantly reduced UTI risk by inhibiting bacterial adherence.	Effective	(100)
Systematic Review and Meta-Analysis	Individuals with recurrent UTIs	Cranberry products	Cranberry ingestion significantly reduced UTI incidence, especially in recurrent cases.	Highly Effective	(101)
Comparative Study	Children with recurrent UTIs	Cranberry syrup	Cranberry syrup was effective in treating recurrent UTIs in children.	Effective	(102)
Double-blind Randomized Controlled Trial	Healthy women	High-dose cranberry extract	High-dose cranberry extract was not significantly more effective than low-dose in preventing UTIs.	Moderately Effective	(58)
Observational Study	Women with a recent history of UTIs	Cranberry beverage	Daily cranberry beverage consumption significantly reduced clinical UTIs.	Highly Effective	(103)
Clinical Experience and Research Review	General Population	Cranberry juice	Cranberry juice may help prevent UTIs due to its anti-adhesion mechanism.	Potentially Effective	(104)
Randomized Placebo-Controlled Trial	Healthy college women	Cranberry juice	Drinking cranberry juice did not significantly decrease the incidence of recurrent UTIs.	Not Effective	(105)
Clinical Study	Infants and Children with recurrent UTIs	Cranberry products	Cranberry was found to be a safe and effective prophylactic treatment for recurrent UTIs in children.	Effective	(106)

379 sources contributed to the publication of 556 documents, indicating an annual growth rate of 5.64% in the body of work. The authorship involved is extensive, involving 2,070 individual authors. Notably, there were 87 documents authored by single individuals, showcasing the significant role of individual contributions in research. Collaboration remains vital, with international co-authorship accounting for 10.79% of the total, demonstrating the journal's commitment to global scholarly exchange. The documents have an average age of 10.7 years, suggesting continued relevance to current research discussions. The average number of citations per document stands at 28.91, indicating the substantial impact and influence of these works in the academic community. Keywords are essential for indexing and discoverability within databases like Scopus. The 936 unique author's keywords listed reflect the breadth and specificity of covered topics, contributing to the journal's extensive reference network of 16,308 citations, enriching the research ecosystem, and providing a valuable resource for academia. The data also reveals an average of 4.53 co-authors per document, underscoring the collaborative nature of modern research endeavors, which enriches research with diverse perspectives and expertise. In essence, this bibliometric analysis from the Scopus database underscores the journal's robust growth, international collaboration, and significant scholarly impact over the last six decades, highlighting its prestige and importance within the academic community.

4.1 Trends in cranberry-UTI research publications

The analysis of published literature shows a significant increase in research on the use of cranberries for managing UTIs from 1960 to the present (as depicted in Figure 5). Initially, interest in this topic was limited, with few publications until the late 1990s. However, there has been a noticeable surge in research activity starting from the early 2000s, reaching a peak in publication frequency over the last decade. This peak reflects heightened scientific interest, possibly in response to the growing global burden of UTIs and concerns about antibiotic resistance. Fluctuations in publication numbers in recent years could be due to various factors, such as changes in research funding, evolving public health priorities, or the natural variability in scientific exploration. Nevertheless, the overall trend indicates sustained attention within the research community toward exploring the role of cranberries in managing UTIs.

The rise in publications likely reflects a growing consensus on the potential of cranberries as an alternative or adjunctive treatment for UTIs, aligning with the urgent need for new therapeutic approaches in the face of antibiotic resistance (as shown in Figure 4). The heightened interest observed in the early 2000s coincides with pivotal clinical trials and systematic reviews exploring the efficacy of cranberry products in preventing recurrent UTIs (7). These influential studies likely stimulated further investigation into the mechanisms of cranberry phytochemicals, optimal dosages, and formulations for maximum effectiveness. Despite the surge in research output, the fluctuation in publication numbers suggests that there are lingering questions or emerging challenges requiring deeper exploration. For example, the specific bioactive components of cranberries responsible for anti-adhesion properties, the most efficacious forms and doses, and the patient groups that may benefit most from these interventions remain fertile areas for investigation. The recent decline in publications may signal a saturation point in fundamental research, indicating a need for more applied studies and clinical trials to bridge

TABLE 5 Overview of studies on cranberry consumption.

Study focus	Study population	Findings	Adverse effects/safety remarks	Sample size	Reference
Health Impact & Nutrient Intake	US adults	Healthier body composition and macronutrient intake in cranberry consumers	None reported, indicating safety in dietary amounts	10,891	(107)
Impact on C-reactive Protein Levels	US adults	Lower levels of C-reactive protein in cranberry juice consumers	None mentioned, suggesting anti-inflammatory effects without adverse effects	10,334	(108)
Supplement Use for UTIs	Women with recurrent UTIs	Significant decrease in UTIs with cranberry supplement use	No significant adverse effects reported	23	(109)
Use During Pregnancy	Pregnant women	No increased risk of malformations or negative pregnancy outcomes	None were reported, suggesting safety of cranberry consumption during pregnancy	68,522	(110)
Diabetes Management	Type II diabetic patients	Improvement in glycemic control with cranberry addition	No specific toxicity reported; beneficial effect on blood glucose levels	60	(111)
Pediatric Use	Pediatric nephrology patients	Common use of cranberry for UTI prevention; perceived as useful by parents	Only 1 parent reported a side effect (nausea)	117	(112)
UTI Prevention with SGLT2i Use	T2DM patients using SGLT2i	Significant reduction in the incidence of GUTI with cranberry extract use	No significant side effects reported	103	(113)
Warfarin Interaction	Healthy subjects	No significant pharmacokinetic interaction with warfarin observed	Cranberry considered safe with warfarin under study conditions, but monitoring recommended	Not specified	(114)
Urinary Tract Infection Prophylaxis	Renal transplant recipients	Reduced incidence of UTI with cranberry and L-methionine prophylaxis	No significant adverse effects reported, indicating safety and efficacy	82	(115)
Use for UTI in Pakistani Population	Outpatients aged 20–65 years	100% of UTI patients were cured with cranberry and elderberry extracts	Compliance and tolerability were considerable obstacles, though no specific adverse effects mentioned	55	(116)
Major Intraoperative Bleeding	74-year-old woman	Severe bleeding during surgery due to aspirin-like effect from cranberry	Cranberry may increase the risk of bleeding due to its aspirin-like effect on platelets	Case report	(117)
Fatal Hemopericardium & Gastrointestinal Hemorrhage	Elderly man	Fatal internal hemorrhage linked to cranberry juice and warfarin interaction	Suggests cranberry juice may potentiate the effects of warfarin, increasing bleeding risk	Case report	(118)
Warfarin-Cranberry Juice Interaction	Patient on warfarin	Elevation of INR on two separate occasions linked to cranberry juice	Cranberry juice cocktail may interact with warfarin, necessitating monitoring	Case report	(49)
Interaction with Tacrolimus Serum Levels	Renal transplant patient	Decrease in serum levels of tacrolimus possibly due to cranberry extract interaction	Unreported decrease in tacrolimus serum levels due to interaction with cranberry extract	Case report	(119)

the gap between laboratory discoveries and practical healthcare solutions. It also underscores the importance of comprehensive reviews and meta-analyses to synthesize existing evidence and offer clear, evidence-based guidelines for using cranberries in UTI management. Research on cranberries and UTIs holds significant implications for public health, particularly in women's health and the management of antibiotic-resistant infections. Given that UTIs contribute significantly to morbidity, especially among women, identifying effective non-antibiotic prophylactic measures is imperative. The research trajectory revealed by our bibliometric analysis highlights the critical need for continued exploration into cranberry-derived interventions, not only for their potential therapeutic advantages but also for their role in combating antibiotic overuse. The bibliometric analysis unveils a dynamic research field marked by a substantial increase in publications concerning cranberries and UTIs over the past six decades. The data suggest that while the scientific community has shown considerable interest in the therapeutic potential of cranberries, there remains a need for more

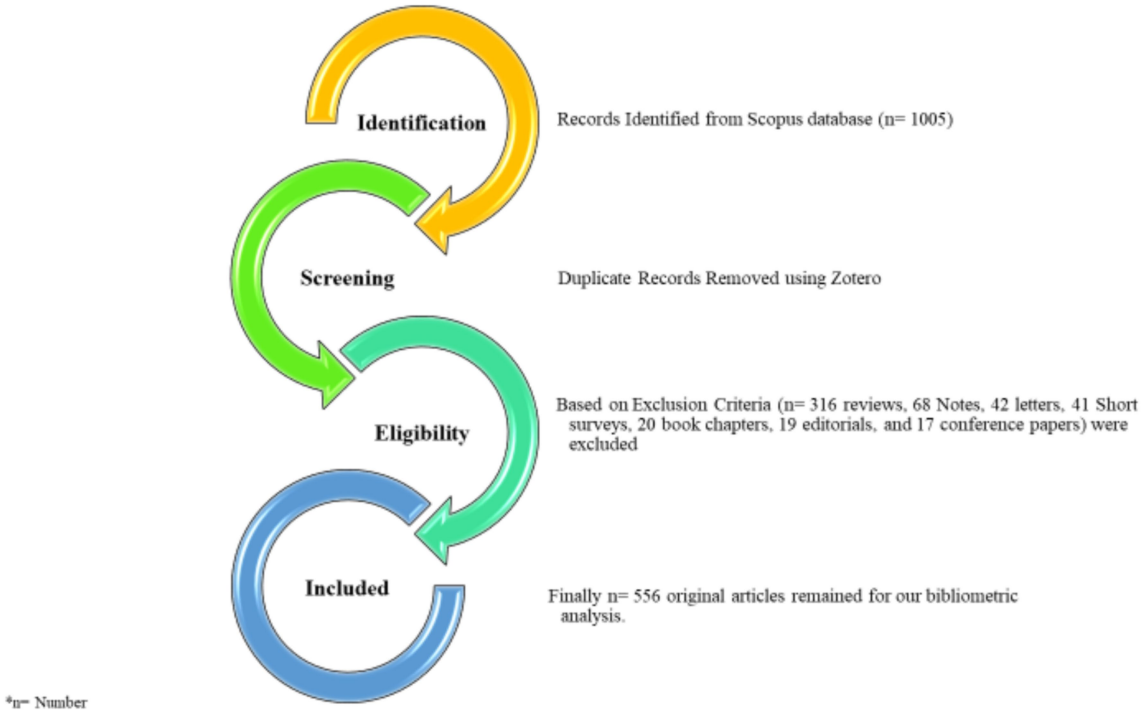

FIGURE 3
PRISMA flow diagram of the systematic literature review on cranberry in treatment of urinary tract infections (UTIs) 1962–2024.

FIGURE 4
Visual representation of data collected using R-studio (66).

targeted research to elucidate their role in UTI management and address the challenges posed by antibiotic resistance. Future research endeavors should aim to consolidate fragmented knowledge, identify evidence-based applications, and ultimately inform clinical practice and public health policies.

4.2 Publication based on geographic distribution

A comprehensive analysis was conducted, spanning publications from 1962 to 2024, to examine the worldwide geographic distribution of research contributions focusing on the use of cranberry in managing urinary tract infections (UTIs) (as shown in Figure 6). This research entailed classifying nations according to their publication outputs, offering insights into the extent of their engagement in urinary tract infection (UTI) research related to the use of cranberries. The key contributors to this field, identified by the frequency of their publications, can be summarized as follows: The United States [705], Italy [277], the United Kingdom [158], Canada [139], and France [110].

For a visual representation of the global distribution of scientific publications concerning cranberry use in UTI management, please refer to Figure 5. This map illustrates the concentration of research articles from various countries, highlighting the extensive engagement of nations in exploring cranberry applications for UTIs. This

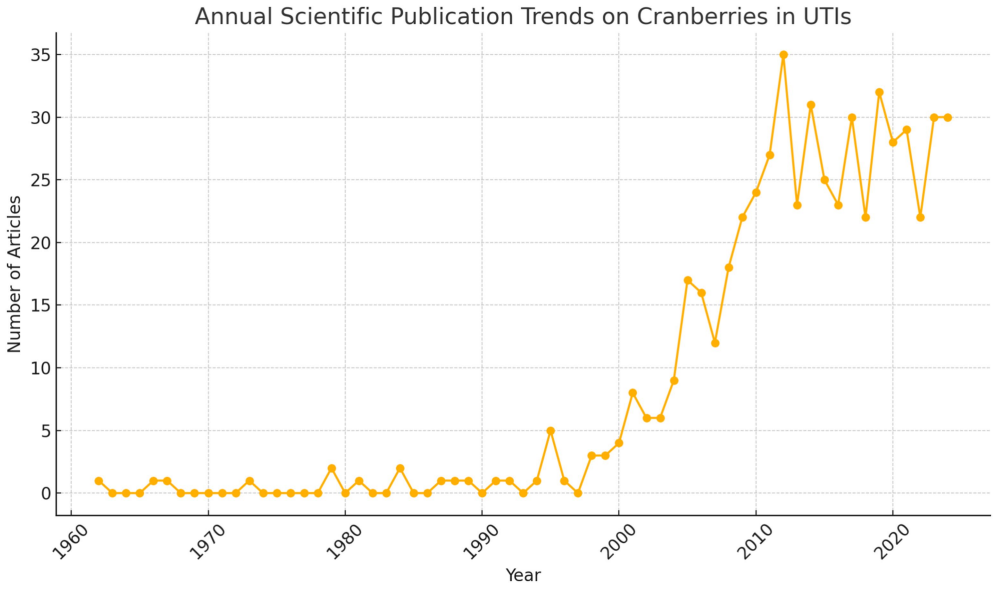

FIGURE 5
Trends in scientific research on cranberry use for UTI management (1960–2024).

geographical overview underscores the widespread international involvement in addressing the critical healthcare challenge of UTI management. It emphasizes the collaborative and collective nature of global efforts in this field.

4.3 Co-authorship analysis

This section presents a bibliometric study that specifically examines co-authorship within the field of cranberry research for the management of urinary tract infections (UTIs). This analysis provides significant insights into prominent authors and institutional contributions within this crucial field of research.

After doing an analysis of co-authorship networks, it has been determined that there are five notable authors that stand out in this regard. These authors are Khoo C, Howell AB, Reed JD, Krueger CG, and Lavigne J-P. These individuals have continuously engaged in collaborations with other researchers, demonstrating their commitment to the advancement of knowledge in the field of urinary tract infection care using cranberry-based interventions as mentioned in Table 6. The combined endeavors of these individuals constitute a crucial framework for doing research on the therapy of urinary tract infections through the use of cranberry therapies. Figure 7 illustrates the author's productivity over the years, represented by the number of publications.

Furthermore, our approach provides insight into the institutional framework. The University of Wisconsin-Madison has emerged as a notable contributor to the subject, as seen by the substantial number of 39 publications produced by researchers linked with this university as shown in Figure 8. This statement emphasizes the university's dedication to leading the way in managing urinary tract infections (UTIs) with cranberry-based methods. It also emphasizes the importance of institutional support and joint research activities in this endeavor to deepen the understanding of co-authorship networks, Vosviewer, a powerful visualization tool, was employed. Vosviewer enables researchers to explore and visually represent co-authorship networks based on linkage strength. This tool facilitates interactive visualizations, aiding in identifying research clusters and key connections among scholars in the field (as shown in Figure 9). Utilizing Vosviewer enriches research by providing a comprehensive and visually engaging perspective on the collaborative dynamics in cranberry research for UTI management.

4.4 Citation analysis

Utilizing bibliometric analysis to assess citations represents a crucial methodological approach in academic and scientific research. It serves as a potent tool for uncovering valuable insights into the influence, significance, and dissemination patterns of knowledge within scholarly and scientific communities (67). In our examination of data, we have undertaken the task of ranking the top 10 most frequently referenced documents in the field of cranberry research, particularly in the context of treating urinary tract infections. These rankings are meticulously detailed in Table 7. At the forefront of this ranking is the research conducted by Kontiokari in 2001, titled "Randomised trial of cranberry-lingonberry juice and *Lactobacillus* GG drink for the prevention of urinary tract infections in women." This document proudly holds the distinction of being the most cited work within this research domain (68).

In the realm of citations, the United States (USA) stands out as the primary contributor, with a significant total of 4,936 citations and an impressive average citation rate per article, calculated at 42.90, as detailed in Table 8. In a closely competitive position in this citation analysis is Italy, holding the second-highest citation count at 980, along with an associated average article citation rate of 25.10.

Concerning scholarly journals, the Journal of Agricultural and Food Chemistry commands significant attention. Publishing a total of 14

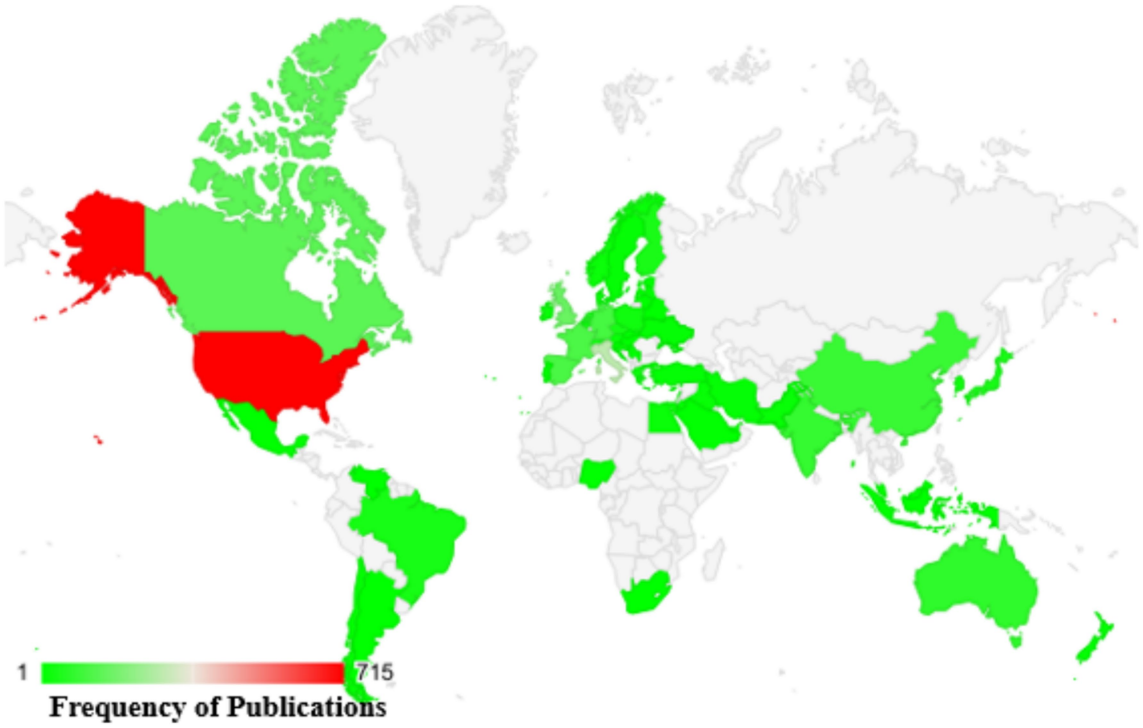

FIGURE 6
Worldwide distribution of scientific studies on cranberries in UTI management based on Scopus data from 1960 to 2024.

articles, it garners the highest number of citations, amassing a total count of 687 citations. Conversely, the Journal of Urology, with its substantial publication output of 8 articles, secures the second-highest position in terms of citations within the domain of Cranberry research, accumulating a commendable 1,030 citations, as vividly portrayed in Table 9.

Collectively, these findings underscore the profound impact and collaborative synergy prevalent within the research community dedicated to addressing the multifaceted challenges posed by Cranberry research in the context of urinary tract infection management. The visualization of the author's network, facilitated by Vosviewer and based on citations, includes 100 researchers, with a focus on highlighting the largest set of interconnected authors (Figure 10).

4.5 Keyword analysis

The analysis of keywords in bibliometric research proves to be a powerful method for discovering and understanding the essential themes, trends, and intellectual framework within a particular research domain. In our dataset, obtained from the Scopus database, we conducted a thorough exploration of keyword co-occurrence. Out of the 4,426 identified keywords, we classified those that recurred more than 5 times as high-frequency keywords, which were subsequently incorporated into our analysis. As a result, among the initial 4,426 keywords, 522 met this established criterion and were included in our research. The most frequently occurring keyword was "Urinary Tract Infections," appearing an impressive 332 times and exhibiting a substantial total linkage strength of 5,260. In close pursuit was the keyword "Cranberry," which made 275 appearances and displayed a total linkage strength of 4,270 (please refer to Table 10). To visually depict the co-occurrence patterns of the specified keywords, we employed VOSviewer, as illustrated in Figure 11. Furthermore, Figure 12 showcases a word cloud created with R Studio, emphasizing the keywords that emerged most frequently in our analysis.

4.6 Thematic mapping and trends topic analysis

Analyzing this bibliometric data reveals critical research themes and their evolution over two decades from 2002 to 2024. The increasing prominence of terms like "d-mannose," "antioxidant," and "bacteriuria" suggests a shifting focus toward a deeper mechanistic understanding of cranberry's action and its broader health implications. Essential research terms such as "urinary tract infection" and "cranberry" continue to hold central positions in the research landscape, emphasizing their enduring relevance. The emerging interest in terms like "bacterial adhesion" and "proanthocyanidins" indicates a refined inquiry into the specific bioactive constituents of cranberries and their anti-adhesion properties.

4.6.1 Niche developments

Certain terms such as "proanthocyanidin," "*vaccinium macrocarpon*," and "antibacterial activity" exhibit lower developmental density but high centrality, suggesting their foundational importance in cranberry-related UTI research. Themes like "pregnancy" and "probiotics" are categorized as niche areas, reflecting targeted research into specific applications of cranberries in UTI management that contribute valuable insights. The identification of niche themes

TABLE 6 Top 10 most productive authors in the field of cranberry research for UTI management.

Author	H-Index	G-Index	M-Index	Total citation	Number of publications	Article fractionalized
Khoo C	10	13	0.833	370	13	1.99
Howell AB	9	13	0.360	1,651	13	3.66
Krueger CG	8	11	0.400	625	11	2.04
Lavigne J-P	8	9	0.444	417	9	1.64
Reed JD2	8	12	0.400	631	12	2.20
Sotto A	7	7	0.389	404	7	1.29
Howell A	6	6	0.333	670	6	0.94
Liu H	6	8	1.000	169	8	1.45
Bartolome B	5	6	0.385	241	6	0.97
Botto H	5	5	0.263	464	5	0.87

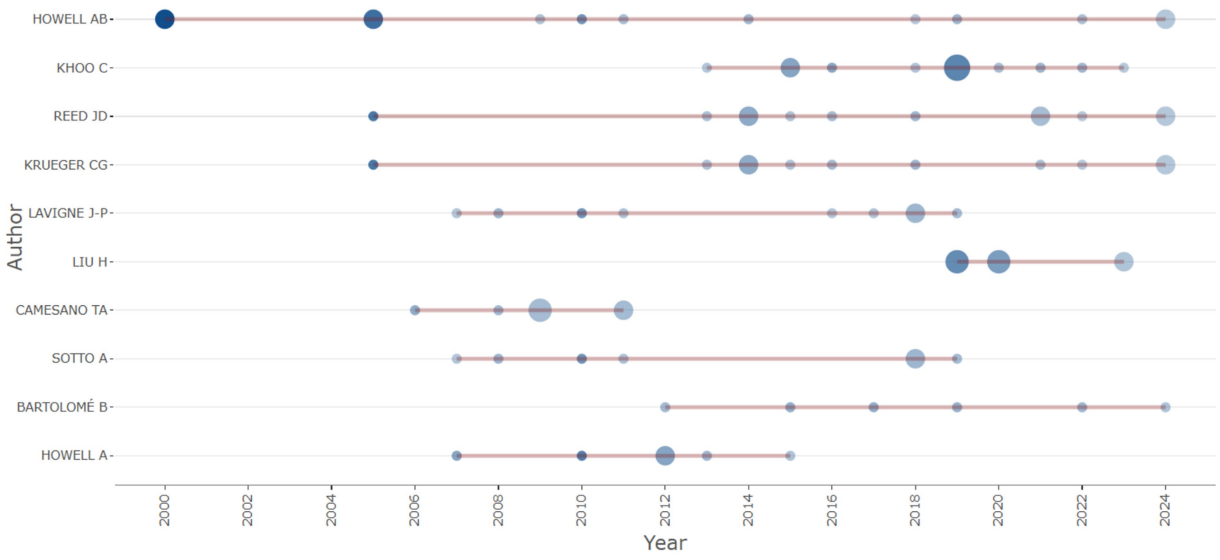

FIGURE 7
Timeline of key author contributions to cranberry UTI research from 2000 to 2024.

suggests growing interest in areas such as the impact of cranberries during "pregnancy" and their interaction with "probiotics." These areas offer promising avenues for future research, potentially leading to novel preventive and therapeutic approaches for UTIs.

4.6.2 Discussion emerging trends and their implications

The analysis indicates a shift in research focus from general investigations of cranberry's efficacy toward a more detailed exploration of its bioactive components, particularly their preventive role against UTI pathogens. The increasing body of evidence on "d-mannose" and "proanthocyanidins" reflects a growing interest in non-antibiotic preventive strategies and their mechanisms of action, which is crucial given the rising antibiotic resistance.

4.6.3 The persistence of central themes

Despite emerging trends, "cranberry" and "urinary tract infection" remain central in research, highlighting continued interest in cranberry's role in UTI prevention and treatment. The sustained centrality of these terms underscores their established presence in the literature and their importance as foundational concepts.

Thematic mapping (as shown in Figure 13) and trend analysis (as shown in Figure 14) illuminate the evolving research landscape on cranberries in UTI management. With a heightened focus on understanding the mechanistic action of cranberries and their bioactive compounds, the research community is moving toward optimizing cranberries' utility in combating UTIs beyond mere efficacy. These insights reinforce the significance of ongoing research and development in addressing antibiotic resistance challenges and advancing women's health through evidence-based non-antibiotic therapies.

5 Patents on cranberry in treatment of urinary tract infections

The introduction of Cranberry's utilization in addressing urinary tract infections (UTIs) represents a pivotal moment in

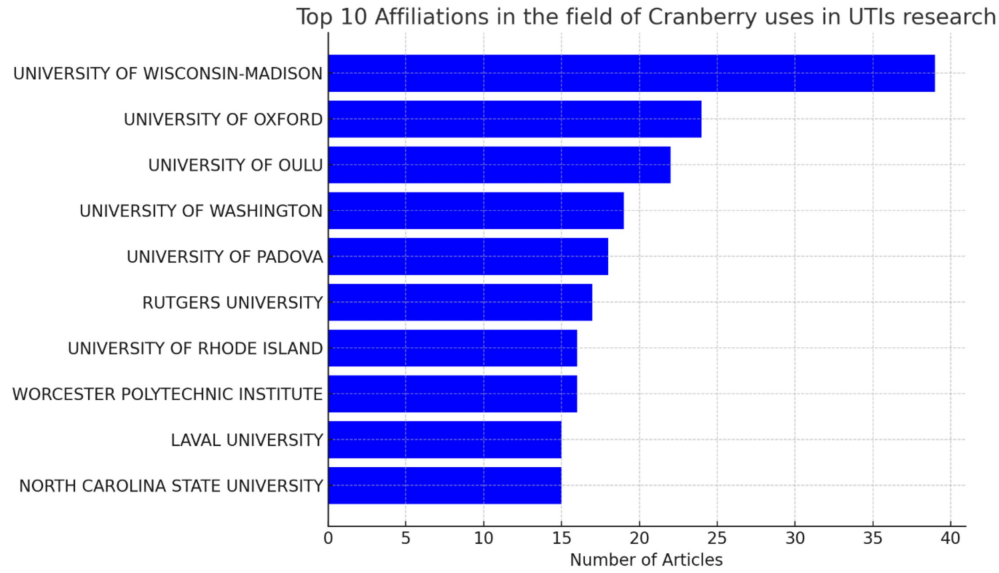

FIGURE 8
Top 10 institutions having the highest number of publications in the field of cranberry research in managing urinary tract infections.

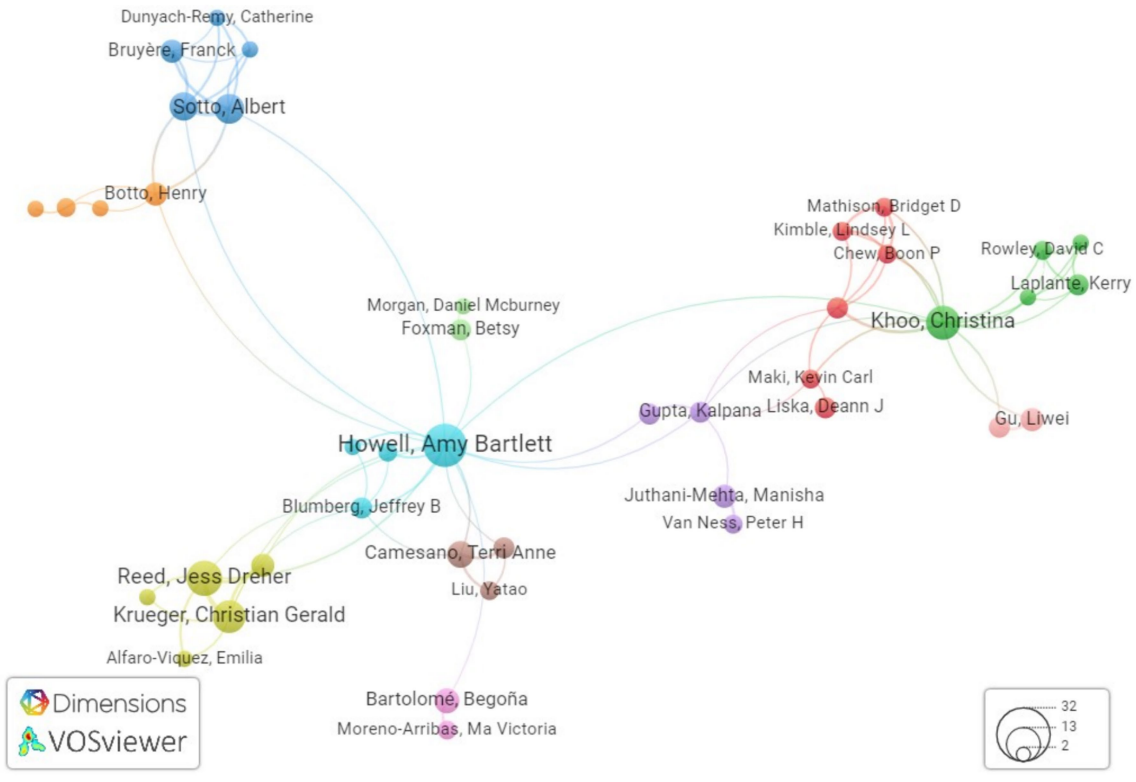

FIGURE 9
Network visualization showing the connections between researchers in the field of cranberry uses in UTI research using Vosviewer.

the realm of patent innovations. This groundbreaking advancement materialized in 1992 through the patent titled "Manufacture of Cranberry Juice," attributed to inventors Shimazu Yoshimi, Hashimoto Hikotaka, and Nakajima Yasuhiko. This patent, bearing the identification JPH04316468 and credited to Kikkoman Corp, laid the groundwork for subsequent innovations in harnessing cranberry's therapeutic potential against UTIs. Over time, the field has witnessed a gradual uptick

TABLE 7 Top 10 cited documents in the field of cranberry research in the treatment of urinary tract infections.

Paper title	Journal	Total citation (TC)	Total citations per year	Year of publication	Reference
"Randomised trial of cranberry-lingonberry juice and Lactobacillus GG drink for the prevention of urinary tract infections in women"	The BMJ	781	17.5217391	2001	(68)
"A-type cranberry proanthocyanidins and uropathogenic bacterial anti-adhesion activity"	Phytochemistry	650	21.5263158	2005	(120)
"A-Type Proanthocyanidin Trimers from Cranberry that Inhibit Adherence of Uropathogenic P-Fimbriated *Escherichia coli*"	Journal of Natural Products	592	16.875	2002	(121)
"The structure of cranberry proanthocyanidins which inhibit adherence of uropathogenic P-fimbriated *Escherichia coli* in vitro"	Phytochemistry	599	16.0416667	2002	(122)
"Inhibitory activity of cranberry juice on adherence of type 1 and type P fimbriated *Escherichia coli* to eucaryotic cells"	Antimicrobial Agents and Chemotherapy	558	8.97142857	1989	(123)
"Inhibition of bacterial adherence by cranberry juice: potential use for the treatment of urinary tract infections"	Journal of Urology	509	6.35	1984	(124)
"A randomized trial to evaluate the effectiveness and cost-effectiveness of naturopathic cranberry products as prophylaxis against urinary tract infection in women"	Canadian Journal of Urology	507	11.3636364	2002	(125)
"Multi-laboratory validation of a standard method for quantifying proanthocyanidins in cranberry powders"	Journal of the Science of Food and Agriculture	348	19	2010	(126)
"Phytochemicals of cranberries and cranberry products: characterization, potential health effects, and processing stability"	Critical review of food science nutrition	338	15.2	2009	(69)
"Recurrent Uncomplicated Urinary Tract Infections in Women: AUA/CUA/SUFU Guideline"	Journal of Urology	335	40	2019	(127)

in the number of patents related to cranberry-based approaches for UTI management. This journey of cranberry's emergence as a valuable resource in combating urinary tract infections commenced with the pioneering patent "Production of Cranberry Juice" in 1992. The subsequent surge in patent activity, alongside the global recognition signified by patent distribution among diverse patent offices, underscores the enduring influence of cranberry research in the domain of UTI management. The top 20 patents offer a comprehensive glimpse into the innovative advancements made in this field, reflecting the collective commitment to advancing cranberry-based solutions for urinary tract health (as shown in Table 11).

6 Challenges and future directions in cranberry research for UTI management

The exploration of cranberry's potential in managing urinary tract infections (UTIs) represents an exciting yet complex frontier in clinical research. As we endeavor to translate traditional remedies into evidence-based practices, several key challenges emerge, necessitating a strategic and multidisciplinary approach to guide future research directions.

6.1 Challenges in standardizing cranberry products for clinical research

A primary hurdle in studying cranberry's efficacy against UTIs is the lack of standardization in cranberry products. Variability in form (juice, extract, capsules), dosage, and concentration of active components like proanthocyanidins (PACs) significantly complicate the comparison of study outcomes. This variability arises from differences in cranberry cultivars, harvesting methods, processing techniques, and commercial product formulations, all of which can influence the bioactivity of the final product. To address this challenge, it is crucial to develop standardized guidelines for producing and characterizing cranberry products used in clinical trials. Establishing benchmarks for PAC content and other bioactive compounds, along with standardized dosing regimens, will enable more consistent and comparable research outcomes. Collaborative efforts involving researchers, industry stakeholders, and regulatory agencies will be essential in advancing these standardization initiatives.

6.2 The need for further research to clarify inconsistent findings

Inconsistent findings across clinical trials underscore the necessity for further research to elucidate the mechanisms and conditions under which cranberry is most effective. These inconsistencies may stem from the aforementioned lack of standardization, as well as differences in study populations, methodologies, and outcome measures. While meta-analyses and systematic reviews have provided some clarity, the heterogeneity of data often limits the conclusiveness of these analyses. Future studies should strive for methodological rigor, including larger sample sizes, well-defined control groups, and longer follow-up periods. Additionally, investigating genetic and metabolic factors that may influence individual responses to cranberry consumption could provide insights into its varying efficacy. Precision nutrition approaches, considering individual variability in gut microbiota composition and metabolism, may also enhance our understanding of cranberry's health benefits.

6.3 Emerging research areas and potential novel applications

Beyond UTI prevention, emerging research areas are exploring the broader therapeutic potential of cranberry. Its role in modulating the gut microbiome, combating antibiotic-resistant pathogens, and synergizing with other natural products opens new avenues for investigation. For instance, cranberry's potential to disrupt biofilm formation by uropathogens offers a promising strategy for combating chronic and recurrent infections.

6.4 Cranberry in addressing antibiotic resistance

The global challenge of antibiotic resistance amplifies the importance of alternative strategies for UTI management. Cranberry's unique mechanism of action, distinct from antibiotics, positions it as a valuable adjunct in the fight against resistant pathogens. Investigating cranberry's efficacy against multi-drug-resistant strains and its impact on antibiotic susceptibility patterns could provide critical insights into its role in mitigating antibiotic resistance.

6.5 Potential for cranberry in combination therapies

The integration of cranberry into combination therapies for UTI management represents a frontier with significant therapeutic promise. Combining cranberry with probiotics, other natural products, or low-dose antibiotics could enhance therapeutic outcomes while minimizing the risk of resistance development. Such combination therapies could leverage synergistic effects to optimize efficacy, reduce dosages of conventional antimicrobials, and broaden the spectrum of action against diverse uropathogens. The journey of cranberry from a traditional remedy to a scientifically validated agent for UTI management is filled with challenges yet ripe with potential. Overcoming hurdles related to standardization and inconsistent findings will pave the way for more definitive conclusions about its efficacy. Simultaneously, embracing emerging research areas and innovative applications of cranberry could significantly advance our

TABLE 8 Top 10 most cited countries in the field of cranberry research in managing urinary tract infections.

Country	TC	Average article citations
USA	4,936	42.9
ITALY	980	25.1
NEW ZEALAND	847	282.3
CANADA	721	40.1
UNITED KINGDOM	671	26.8
FRANCE	633	31.6
GERMANY	457	18.3
NETHERLANDS	359	39.9
AUSTRALIA	353	29.4
NORWAY	286	57.2

TABLE 9 Top 10 most cited journal in the field of cranberry research in managing urinary tract infections.

Element	H-Index	G-Index	M-Index	TC	NP	PY_start
JOURNAL OF AGRICULTURAL AND FOOD CHEMISTRY	13	14	0.65	687	14	2005
JOURNAL OF UROLOGY	7	8	0.171	1,030	8	1984
JOURNAL OF NATURAL PRODUCTS	5	5	0.2	499	5	2000
UROLOGY	5	7	0.096	177	7	1973
WORLD JOURNAL OF UROLOGY	5	6	0.192	226	6	1999
COCHRANE DATABASE OF SYSTEMATIC REVIEWS	4	4	0.333	85	4	2013
JOURNAL OF FUNCTIONAL FOODS	4	4	0.4	152	4	2015
JOURNAL OF OBSTETRICS AND GYNAECOLOGY CANADA	4	5	0.19	234	5	2004
PHYTOTHERAPY RESEARCH	4	4	0.308	144	4	2012
ANTIBIOTICS	3	5	0.273	51	5	2014

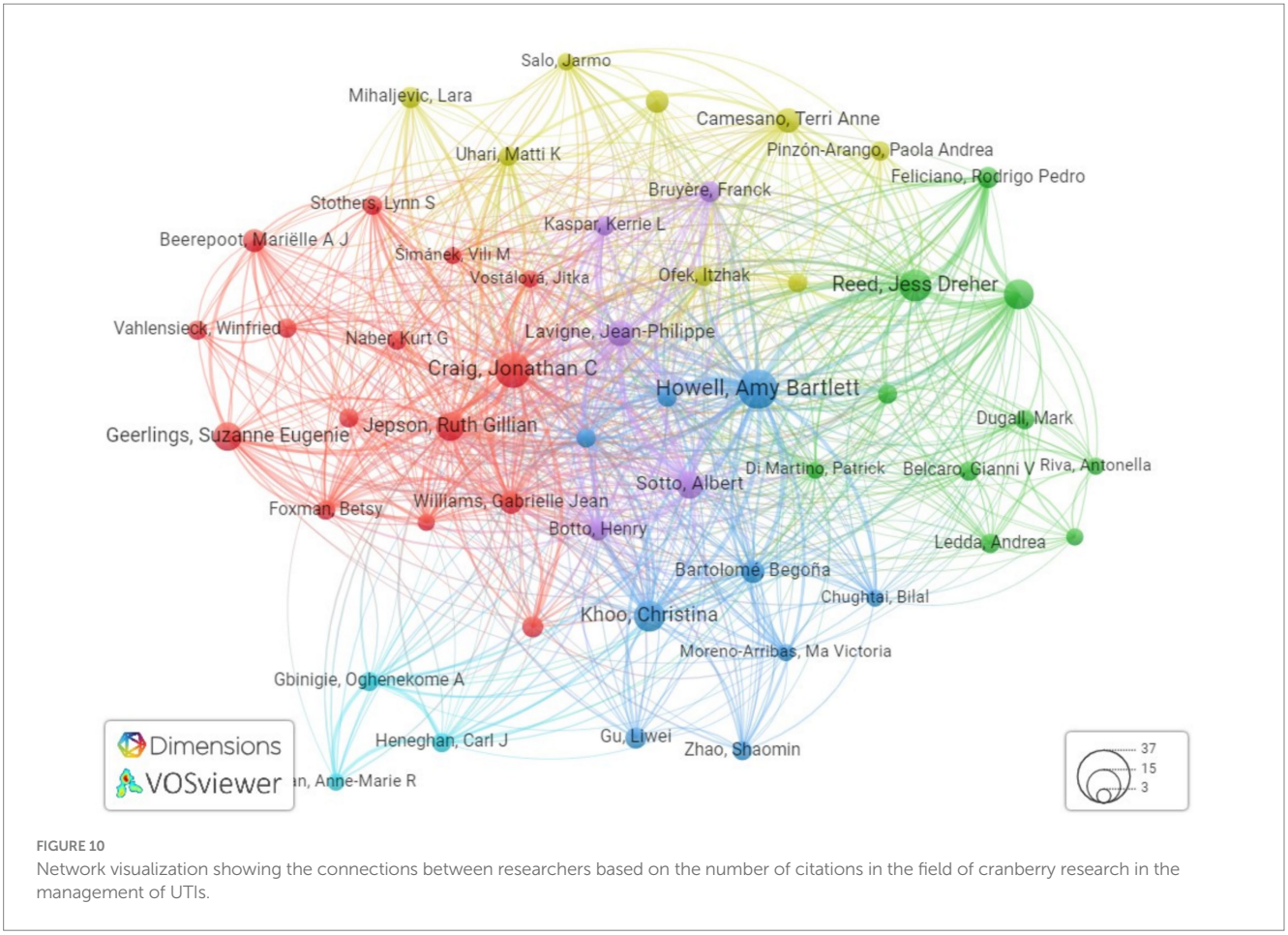

FIGURE 10
Network visualization showing the connections between researchers based on the number of citations in the field of cranberry research in the management of UTIs.

TABLE 10 **Bibliometric analysis of key topics in cranberry research for urinary tract infection management based on occurrences and linkage strengths.**

S. no.	Keyword	Occurrence	Total linkage strength
1	Urinary Tract Infections	332	5,260
2	Cranberry	275	4,270
3	*Vaccinium macrocarpon*	218	3,571
4	*Escherichia coli*	138	2,185
5	Cranberry Juice	107	1,861
6	Randomized controlled trial	72	1,646
7	Anti-infective agents	75	1,450
8	Recurrent infections	63	1,285
9	Proanthocyanidins	65	1,113
10	Infection Prevention	56	1,061

arsenal against UTIs, particularly in the era of antibiotic resistance. Future directions in cranberry research hold promise not only for enhanced UTI management but also for a broader understanding of its role in human health and disease prevention.

7 Limitations

7.1 Language exclusivity concerns

Although our emphasis on English language articles enhances accessibility and linguistic clarity, it introduces a language bias. Research conveyed in languages other than English may present unique viewpoints and insights that could escape our scrutiny. However, this linguistic bias has no potential to yield an incomplete portrayal of the global research landscape.

7.2 Reliance on a single database

Our exclusive reliance on the Scopus database raises the possibility of overlooking research available in other reputable databases. While Scopus boasts extensive coverage, pertinent studies might be situated in databases with specialized subject domains or regional emphases.

7.3 Publication-centric bias

Bibliometric analysis predominantly hinges on published works, which could inadvertently exclude unpublished or ongoing research endeavors. This inclination toward published data may inadvertently

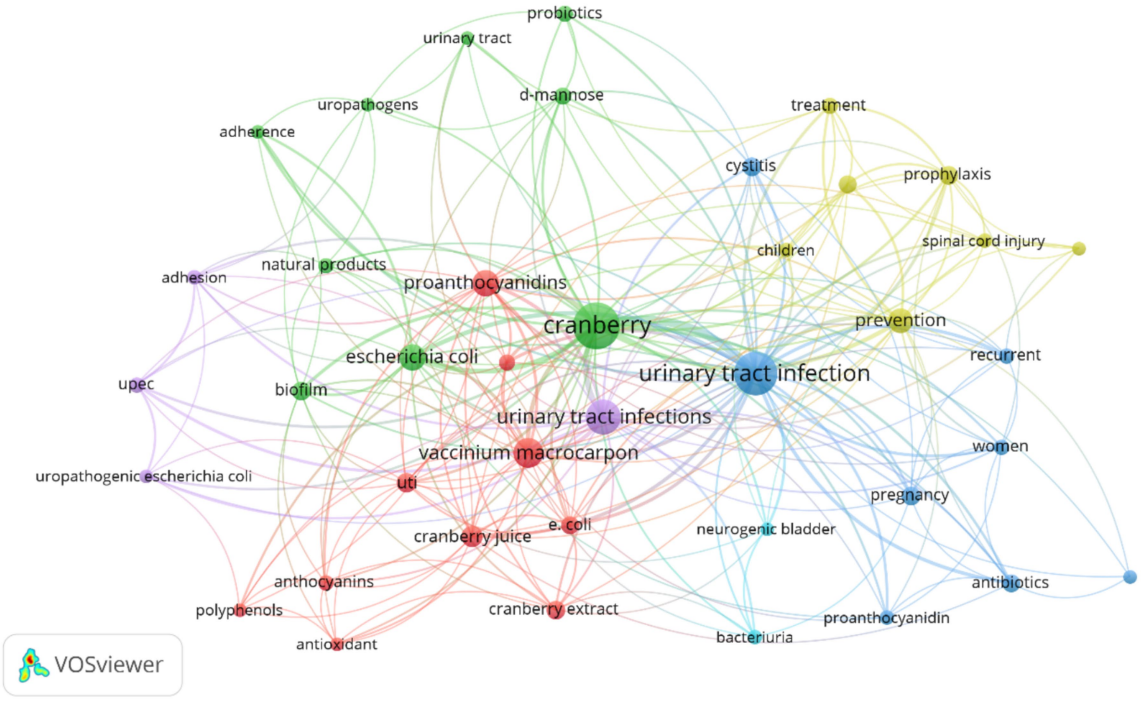

FIGURE 11
Network analysis of research keywords in cranberry studies for urinary tract infection prevention and management.

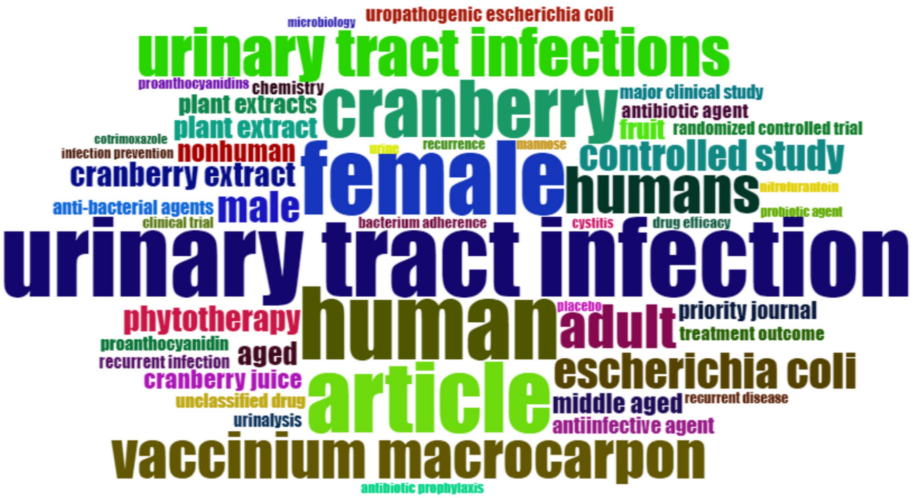

FIGURE 12
Word cloud prepared using R-Studio Bibliometrix package. Size of keyword denoted number of occurrence.

disregard emerging or less-recognized contributions that have yet to be incorporated into the scholarly canon.

8 Conclusion

This comprehensive evaluation extensively explores the changing role of cranberries in the treatment of urinary tract infections (UTIs), with a particular emphasis on their viability as a non-antibiotic alternative in the face of escalating antibiotic resistance. Through a thorough bibliometric analysis that underscores substantial global research contributions, notably from the United States, it is evident that there is a growing academic and clinical interest in utilizing cranberries for UTI management. This recognition reflects a broader acknowledgment of their potential advantages in both preventing and treating these infections. The key findings from our assessment highlight the distinctive attributes of cranberries, particularly the presence of proanthocyanidins. These compounds have demonstrated promising outcomes by impeding the adhesion of uropathogenic bacteria, primarily *E. coli*, to the urinary tract. This mechanism presents

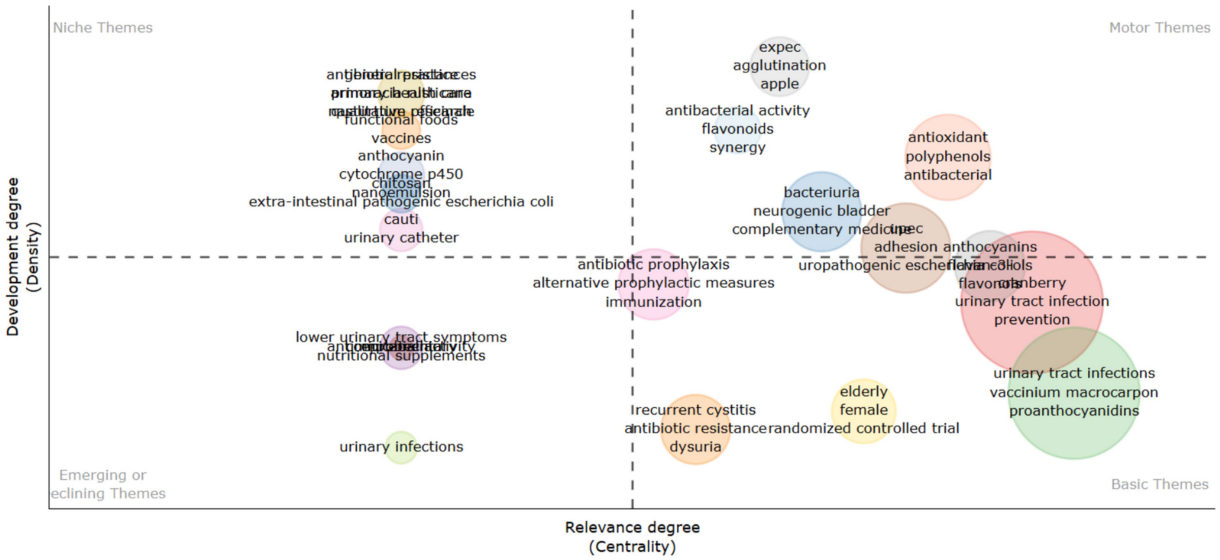

FIGURE 13
Thematic mapping based on the most occurred keyword on cranberry research in the treatment of urinary tract infections.

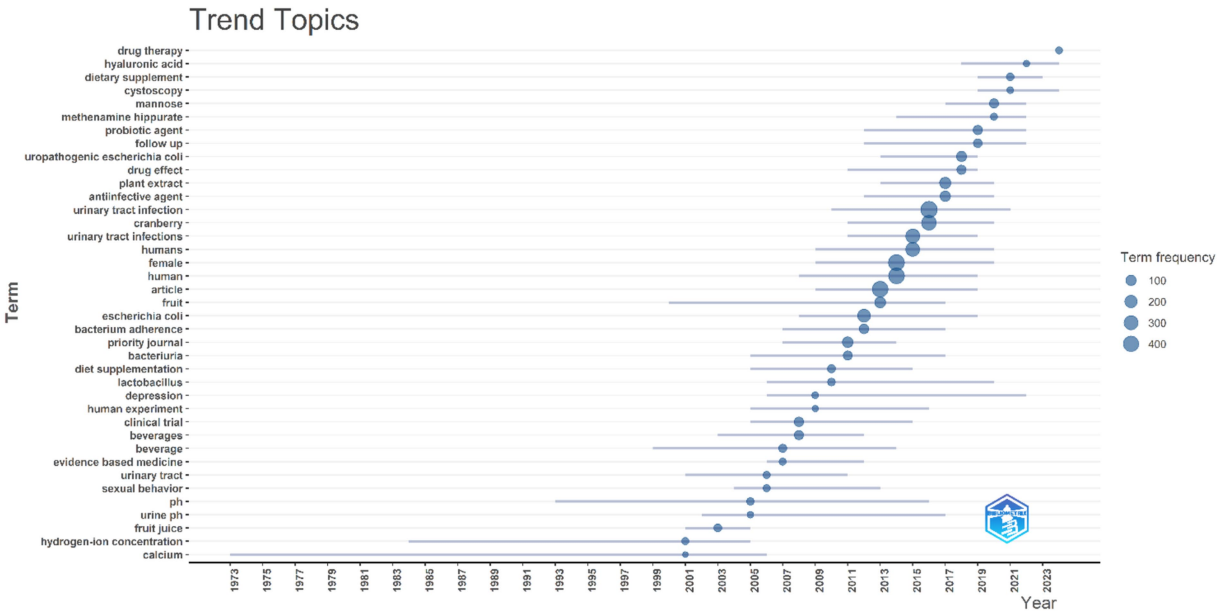

FIGURE 14
Trend topics analysis based on keyword occurrence over year. Blue circle size denoted the number of occurrences of the keyword.

an intriguing avenue for preventing and treating UTIs, especially given the challenges posed by antibiotic resistance. Our scrutiny of clinical trials reveals inconsistent results regarding the effectiveness of cranberries in UTI management, emphasizing the imperative for further well-designed studies to establish conclusive evidence. The variability in outcomes underscores the intricate task of translating the bioactive properties of cranberries into clinically effective applications. Significantly, our review underscores the necessity for standardization in cranberry products and advocates for additional exploration into optimal dosage, efficacy, and safety profiles. This standardization is crucial for providing precise guidelines for the use of cranberries in UTI management and their seamless integration into clinical practice. While cranberries demonstrate promising potential in UTI management, there exists a substantial gap in our comprehension that demands attention through rigorous scientific research. Future investigations should prioritize the standardization of cranberry-based interventions, elucidate their therapeutic roles, and comprehend their interactions with conventional treatments. This review establishes the foundation for forthcoming explorations, contributing to the formulation of innovative and efficient strategies for UTI management.

10.3389/fnut.2025.1502720

TABLE 11 Top 20 most relevant patents in the field of cranberry research in managing urinary tract infection.

S. no.	Patent title	Patent description	Patent ID	Year of publication	Reference
1	"Therapeutic compositions containing trimethoprim and cranberry extract and methods for treating and preventing urinary tract infections"	A blend of trimethoprim and cranberry extract, along with a pharmaceutical carrier to treat UTIs.	US20070166409	2007-07-19	(128)
2	"Composition for prevention or treatment of urinary tract infection"	A formulation consisting of the following components in suitable quantities: cranberry concentrate, D-mannose, ascorbic acid, bromelain, and inulin for the treatment of UTIs.	US20090175843	2009-07-09	(129)
3	"Cranberry extract useful in the treatment and prevention of urinary infections"	A highly concentrated extract derived from cranberry (*Vaccinium macrocarpon*), characterized by a complex composition that enhances its antibacterial properties	US10092539	2018-10-09	(130)
4	"Formulation and method for preventing urinary tract infections"	A combination of vitamin C, D-mannose, cranberry extract, and pineapple extract in the management of urinary tract infections (UTIs).	US20200060324	2020-02-27	(131)
5	"Cranberry extract for preventing and treating uncomplicated lower urinary tract infections"	A cranberry extract containing a total Proanthocyanidin degree of polymerization (%m/m) falling within the range of 12.5–15%, and with a ratio (weight of all proanthocyanidins polymers)/(total weight of proanthocyanidins) exceeding 60%. It serves as a standalone active ingredient preventing and treating uncomplicated lower UTIs.	EP3895761	2021-10-20	(132)
6	"Composition for the treatment or prevention of urinary tract infections and dosage form"	The composition includes an anti-adhesive substance made up of herbal extract(s) known for their ability to counteract bacterial adhesion in the urinary tract, combined with a diuretic component.	EP2662086	2013-11-13	(133)
7	"Method of preventing, controlling and ameliorating urinary tract infections using a synergistic cranberry derivative and d-mannose composition"	A formulation consisting of a cranberry derivative or a concentrated source of proanthocyanidins, along with D-mannose, presented in an orally consumable format for the purpose of UTI prevention.	US20090226548	2009-09-10	(134)
8	"Effervescent composition including cranberry extract"	An effervescent formulation, comprising both an effervescent agent and cranberry extract, ideally in an adequate quantity to reduce the detectable bacterial content in the urine of individuals afflicted with urinary tract infections.	US20050158381	2010-08-31	(135)
9	1. "Compositions comprising an American cranberry extract and phospholipids"	Combination of American cranberry extract with phospholipids, employed in the prevention and treatment of UTIs. Furthermore, it covers the procedures for crafting these mixtures and the oral administration formulations incorporating them.	US20210244782	2021-08-12	(136)
10	2. "Anti-inflammatory cranberry flavanol extract preparations"	Utilizing these extracts, including those containing the cranberry flavanol compound quercetin-3-α-arabinofuranoside, for addressing inflammatory disorders.	US20110195138	2011-08-11	(137)

(Continued)

TABLE 11 (Continued)

S. no.	Patent title	Patent description	Patent ID	Year of publication	Reference
11	"Plant proanthocyanidins extract effective at inhibiting adherence of bacteria with P-type fimbriae to surfaces"	The process of isolating and characterizing plant Proanthocyanidin extracts and specific Proanthocyanidin compounds to prevent and treat urinary tract infections caused by P-type *Escherichia coli*.	US6608102	2003-08-19	(138)
12	"Compositions and methods for treating and/or preventing a urinary tract infection"	This composition, which includes D-Mannose, Phellodendron Extract, and Cranberry, is revealed. It is effective for both treating and preventing microbial infections and the agglutination of red blood cells caused by such infections.	US20190000908	2019-01-03	(139)
13	"Cranberry-based dietary supplement and dental hygiene product"	Cranberry origins are blended with extracts derived from Lou Han Kuo fruit, and/or extracts obtained from *Stevia rebaudiana* leaves, and/or extracts derived from Chinese Blackberry leaves. The end product is an enjoyable dietary supplement with a pleasing taste.	US20030108627	2003-06-12	(140)
14	"Extracts of Cranberry and Methods of Using Thereof"	Merged extracts of cranberry and cinnamon are utilized. In specific variations, these combined extracts have been fine-tuned to manage urinary tract infections induced by *E. coli, S. aureus*, and *C. albicans*.	US20100028469	2010-02-04	(141)
15	"Cranberry Xyloglucan Oligosaccharide Composition"	A formulation derived from cranberry hulls that have undergone enzymatic treatment, aiming to diminish or prevent the attachment of microorganisms to cells possessing α-Gal-(1–4)-Gal terminal oligosaccharide receptors for adhesion.	US20130316025	2016-04-19	(142)
16	"Compositions Comprising Cranberry Extract and Methods of Use Thereof"	Presented here are formulations containing cranberry extract that are both potent and calorie-friendly. Additionally, methods for preventing or treating infections through the administration of these described formulations are included.	US20110280851	2011-11-17	(143)
17	"American cranberry extract and its use"	The current innovation pertains to an extract obtained from Vaccinium plants and the method for its extraction. This extract, rich in proanthocyanidins, can serve as a dietary or nutraceutical product.	US20090258940	2009-10-15	(144)
18	"Cranberry-derived compositions for potentiating antibiotic efficacy against bacterial persistence"	Formulations originating from cranberries, incorporate xyloglucan and pectic oligosaccharides, along with iridoid terpene glycosides. Employed alongside antibiotics to collectively eradicate bacterial persister cells and impede bacterial dormant states, thereby enhancing treatment effectiveness in recurrent and other infections.	US20200179434	2022-06-28	(145)
19	"Use of cranberries with herbal components for preventing urinary tract infections."	The utilization of polymeric proanthocyanidins (PACS) in amounts ranging from 36 mg to 120 mg for combatting urinary tract infections (UTIs).	EP3142678	2020-03-11	(146)
20	"Adjuvant comprising *vaccinium macrocarpon*"	Incorporating the bioactive compounds found in cranberry extract as a supplementary component in the treatment of urinary tract infections.	EP2227252	2012-07-25	(147)

Year of Publication format: YY-MM-DD.

Data availability statement

The original contributions presented in the study are included in the article/Supplementary material, further inquiries can be directed to the corresponding authors.

Author contributions

HJ: Conceptualization, Investigation, Methodology, Writing – original draft. AS: Supervision, Validation, Writing – review & editing. GK: Conceptualization, Supervision, Validation, Writing – review & editing.

Funding

The author(s) declare that no financial support was received for the research, authorship, and/or publication of this article.

Acknowledgments

I express sincere gratitude to Lovely Professional University and National Medical College & Teaching Hospital for creating an academic atmosphere and offering resources that greatly supported the successful culmination of this in-depth review paper.

Conflict of interest

The authors declare that the research was conducted in the absence of any commercial or financial relationships that could be construed as a potential conflict of interest.

Generative AI statement

The authors declare that no Gen AI was used in the creation of this manuscript.

Publisher's note

All claims expressed in this article are solely those of the authors and do not necessarily represent those of their affiliated organizations, or those of the publisher, the editors and the reviewers. Any product that may be evaluated in this article, or claim that may be made by its manufacturer, is not guaranteed or endorsed by the publisher.

Supplementary material

The Supplementary material for this article can be found online at: https://www.frontiersin.org/articles/10.3389/fnut.2025.1502720/full#supplementary-material

References

1. Yang X, Chen H, Zheng Y, Qu S, Wang H, Yi F. Disease burden and long-term trends of urinary tract infections: a worldwide report. *Front Public Health*. (2022) 10:888205. doi: 10.3389/fpubh.2022.888205

2. McCann E, Sung AH, Ye G, Vankeepuram L, Tabak YP. Contributing factors to the clinical and economic burden of patients with laboratory-confirmed Carbapenem-nonsusceptible gram-negative urinary tract infections. *Clinicoecon Outcomes Res*. (2020) 12:191–200. doi: 10.2147/CEOR.S234840

3. Foxman B. Epidemiology of urinary tract infections: incidence, morbidity, and economic costs. *Am J Med*. (2002) 113:5–13. doi: 10.1016/S0002-9343(02)01054-9

4. Griebling TL. Urologic diseases in America project: trends in resource use for urinary tract infections in women. *J Urol*. (2005) 173:1281–7. doi: 10.1097/01.ju.0000155596.98780.82

5. Chinemerem Nwobodo D, Ugwu MC, Oliseloke Anie C, Al-Ouqaili MTS, Chinedu Ikem J, Victor Chigozie U, et al. Antibiotic resistance: the challenges and some emerging strategies for tackling a global menace. *J Clin Lab Anal*. (2022) 36:e24655. doi: 10.1002/jcla.24655

6. Hisano M, Bruschini H, Nicodemo AC, Srougi M. Cranberries and lower urinary tract infection prevention. *Clinics (Sao Paulo)*. (2012) 67:661–7. doi: 10.6061/clinics/2012(06)18

7. Jepson RG, Williams G, Craig JC. Cranberries for preventing urinary tract infections. *Cochrane Database Syst Rev*. (2012) 2012:CD001321. doi: 10.1002/14651858.CD003265.pub3

8. Wang CH, Fang CC, Chen NC, Liu SSH, Yu PH, Wu TY, et al. Cranberry-containing products for prevention of urinary tract infections in susceptible populations: a systematic review and meta-analysis of randomized controlled trials. *Arch Intern Med*. (2012) 172:988–96. doi: 10.1001/archinternmed.2012.3004

9. Fu Z, Liska D, Talan D, Chung M. Cranberry reduces the risk of urinary tract infection recurrence in otherwise healthy women: a systematic review and meta-analysis. *J Nutr*. (2017) 147:2282–8. doi: 10.3945/jn.117.254961

10. Williams G, Hahn D, Stephens JH, Craig JC, Hodson EM. Cranberries for preventing urinary tract infections. *Cochrane Database Syst Rev*. (2023) 4:CD001321. doi: 10.1002/14651858.CD001321.pub6

11. Zeng Z, Zhan J, Zhang K, Chen H, Cheng S. Global, regional, and national burden of urinary tract infections from 1990-2019: an analysis of the global burden of disease study 2019. *World J Urol*. (2022) 40:755–63. doi: 10.1007/s00345-021-03913-0

12. Odoki M, Almustapha Aliero A, Tibyangye J, Nyabayo Maniga J, Wampande E, Drago Kato C, et al. Prevalence of bacterial urinary tract infections and associated factors among patients attending hospitals in Bushenyi District, Uganda. *Int J Microbiol*. (2019) 2019:1–8. doi: 10.1155/2019/4246780

13. Wagenlehner F, Nicolle L, Bartoletti R, Gales AC, Grigoryan L, Huang H, et al. A global perspective on improving patient care in uncomplicated urinary tract infection: expert consensus and practical guidance. *J Glob Antimicrob Resist*. (2022) 28:18–29. doi: 10.1016/j.jgar.2021.11.008

14. Tegegne KD, Wagaw GB, Gebeyehu NA, Yirdaw LT, Shewangashaw NE, Kassaw MW. Prevalence of urinary tract infections and risk factors among diabetic patients in Ethiopia, a systematic review and meta-analysis. *PLoS One*. (2023) 18:e0278028. doi: 10.1371/journal.pone.0278028

15. Dasgupta C, Rafi MA, Salam MA. High prevalence of multidrug resistant uropathogens: a recent audit of antimicrobial susceptibility testing from a tertiary care hospital in Bangladesh. Pak. *J Med Sci*. (2020) 36:1297–302. doi: 10.12669/pjms.36.6.2943

16. Umemura T, Kato H, Hagihara M, Hirai J, Yamagishi Y, Mikamo H. Efficacy of combination therapies for the treatment of multi-drug resistant gram-negative bacterial infections based on meta-analyses. *Antibiotics (Basel)*. (2022) 11:524. doi: 10.3390/antibiotics11040524

17. Bajpai T, Pandey M, Varma M, Bhatambare GS. Prevalence of extended spectrum beta-lactamase producing uropathogens and their antibiotic resistance profile in patients visiting a tertiary care hospital in Central India: implications on empiric therapy. *Indian J Pathol Microbiol*. (2014) 57:407–12. doi: 10.4103/0377-4929.138733

18. Das S. Natural therapeutics for urinary tract infections—a review. *Future J Pharm Sci*. (2020) 6:64. doi: 10.1186/s43094-020-00086-2

19. Muzammil M, Adnan M, Sikandar SM, Waheed MU, Javed N, Ur Rehman MF. Study of culture and sensitivity patterns of urinary tract infections in patients presenting with urinary symptoms in a tertiary care hospital. *Cureus*. (2020) 12:e7013. doi: 10.7759/cureus.7013

20. Zagaglia C, Ammendolia MG, Maurizi L, Nicoletti M, Longhi C. Urinary tract infections caused by Uropathogenic *Escherichia coli* strains—new strategies for an old pathogen. *Microorganisms*. (2022) 10:1425. doi: 10.3390/microorganisms10071425

21. Hasandka A, Singh AR, Prabhu A, Singhal HR, Nandagopal MSG, Mani NK. Paper and thread as media for the frugal detection of urinary tract infections (UTIs). *Anal Bioanal Chem*. (2022) 414:847–65. doi: 10.1007/s00216-021-03671-3

22. Abou Heidar NF, Degheili JA, Yacoubian AA, Khauli RB. Management of urinary tract infection in women: a practical approach for everyday practice. *Urol Ann*. (2019) 11:339–46. doi: 10.4103/UA.UA_104_19

23. Sherif I. Uroprotective mechanisms of natural products against cyclophosphamide-induced urinary bladder toxicity: a comprehensive review. *Acta Sci Pol Technol Aliment*. (2020) 19:333–46. doi: 10.17306/J.AFS.0832

24. Saima S, Anjum I, Mobashar A, Jahan S, Najm S, Nafidi HA, et al. Spasmolytic and uroprotective effects of Apigenin by downregulation of TGF-β and iNOS pathways and upregulation of antioxidant mechanisms: in vitro and in silico analysis. *Pharmaceuticals*. (2023) 16:811. doi: 10.3390/ph16060811

25. Das S, Naik P, Panda P. Effect of Hemidesmus indicus R.Br. root extract on urinary tract infection causing bacteria. *Int J Herbal Med*. (2017) 5:160–8.

26. Murali VP, Kuttan G. *Curculigo orchioides* Gaertn effectively ameliorates the Uro- and nephrotoxicities induced by cyclophosphamide administration in experimental animals. *Integr Cancer Ther*. (2016) 15:205–15. doi: 10.1177/1534735415607319

27. Chettaoui R, Mayot G, De Almeida L, Di Martino P. Cranberry (*Vaccinium macrocarpon*) dietary supplementation and fecal microbiota of Wistar rats. *AIMS Microbiol*. (2021) 7:257–70. doi: 10.3934/microbiol.2021016

28. Jurikova T, Skrovankova S, Mlcek J, Balla S, Snopek L. Bioactive compounds, antioxidant activity, and biological effects of European cranberry (*Vaccinium oxycoccos*). *Molecules*. (2019) 24:24. doi: 10.3390/molecules24010024

29. Nemzer BV, Al-Taher F, Yashin A, Revelsky I, Yashin Y. Cranberry: chemical composition, antioxidant activity and impact on human health: overview. *Molecules*. (2022) 27:1503. doi: 10.3390/molecules27051503

30. Šedbarė R, Sprainaitytė S, Baublys G, Viskelis J, Janulis V. Phytochemical composition of cranberry (*Vaccinium oxycoccos* L.) fruits growing in protected areas of Lithuania. *Plants (Basel)*. (2023) 12:1974. doi: 10.3390/plants12101974

31. González de Llano D, Moreno-Arribas MV, Bartolomé B. Cranberry polyphenols and prevention against urinary tract infections: relevant considerations. *Molecules*. (2020) 25:3523. doi: 10.3390/molecules25153523

32. Blumberg JB, Camesano TA, Cassidy A, Kris-Etherton P, Howell A, Manach C, et al. Cranberries and their bioactive constituents in human health. *Adv Nutr*. (2013) 4:618–32. doi: 10.3945/an.113.004473

33. Urena-Saborio H, Udayan APM, Alfaro-Viquez E, Madrigal-Carballo S, Reed JD, Gunasekaran S. Cranberry proanthocyanidins-PANI nanocomposite for the detection of bacteria associated with urinary tract infections. *Biosensors (Basel)*. (2021) 11:199. doi: 10.3390/bios11060199

34. Howell AB, Botto H, Combescure C, Blanc-Potard AB, Gausa L, Matsumoto T, et al. Dosage effect on uropathogenic *Escherichia coli* anti-adhesion activity in urine following consumption of cranberry powder standardized for proanthocyanidin content: a multicentric randomized double blind study. *BMC Infect Dis*. (2010) 10:94. doi: 10.1186/1471-2334-10-94

35. Howell AB, Dreyfus JF, Chughtai B. Differences in urinary bacterial anti-adhesion activity after intake of cranberry dietary supplements with soluble versus insoluble Proanthocyanidins. *J Diet Suppl*. (2022) 19:621–39. doi: 10.1080/19390211.2021.1908480

36. Colletti A, Sangiorgio L, Martelli A, Testai L, Cicero AFG, Cravotto G. Highly active Cranberry's polyphenolic fraction: new advances in processing and clinical applications. *Nutrients*. (2021) 13:2546. doi: 10.3390/nu13082546

37. Côté J, Caillet S, Doyon G, Dussault D, Sylvain JF, Lacroix M. Antimicrobial effect of cranberry juice and extracts. *Food Control*. (2011) 22:1413–8. doi: 10.1016/j.foodcont.2011.02.024

38. Samarasinghe S, Reid R, AL-Bayati M. The anti-virulence effect of cranberry active compound proanthocyanins (PACs) on expression of genes in the third-generation cephalosporin-resistant *Escherichia coli* CTX-M-15 associated with urinary tract infection. *Antimicrob Resist Infect Control*. (2019) 8:181. doi: 10.1186/s13756-019-0637-9

39. Allameh Z, Salamzadeh J. Use of antioxidants in urinary tract infection. *J Res Pharm Pract*. (2016) 5:79–85. doi: 10.4103/2279-042X.179567

40. Vostalova J, Vidlar A, Simanek V, Galandakova A, Kosina P, Vacek J, et al. Are high proanthocyanidins key to cranberry efficacy in the prevention of recurrent urinary tract infection? *Phytother Res*. (2015) 29:1559–67. doi: 10.1002/ptr.5427

41. Mantzorou M, Giaginis C. Cranberry consumption against urinary tract infections: clinical state of-the-art and future perspectives. *Curr Pharm Biotechnol*. (2018) 19:1049–63. doi: 10.2174/1389201020666181206104129

42. Cimolai N, Cimolai T. The cranberry and the urinary tract. *Eur J Clin Microbiol Infect Dis*. (2007) 26:767–76. doi: 10.1007/s10096-007-0379-0

43. Feliciano RP, Mills CE, Istas G, Heiss C, Rodriguez-Mateos A. Absorption, metabolism and excretion of cranberry (poly) phenols in humans: a dose response study and assessment of inter-individual variability. *Nutrients*. (2017) 9:268. doi: 10.3390/nu9030268

44. Barani M, Sangiovanni E, Angarano M, Rajizadeh MA, Mehrabani M, Piazza S, et al. Phytosomes as innovative delivery systems for phytochemicals: a comprehensive review of literature. *Int J Nanomedicine*. (2021) 16:6983–7022. doi: 10.2147/IJN.S318416

45. Luo B, Wen Y, Ye F, Wu Y, Li N, Farid MS, et al. Bioactive phytochemicals and their potential roles in modulating gut microbiota. *J Agric Food Res*. (2023) 12:100583. doi: 10.1016/j.jafr.2023.100583

46. Sallam IE, Abdelwareth A, Attia H, Aziz RK, Homsi MN, von Bergen M, et al. Effect of gut microbiota biotransformation on dietary tannins and human health implications. *Microorganisms*. (2021) 9:965. doi: 10.3390/microorganisms9050965

47. Baron G, Altomare A, Regazzoni L, Fumagalli L, Artasensi A, Borghi E, et al. Profiling *Vaccinium macrocarpon* components and metabolites in human urine and the urine ex-vivo effect on *Candida albicans* adhesion and biofilm-formation. *Biochem Pharmacol*. (2020) 173:113726. doi: 10.1016/j.bcp.2019.113726

48. González de Llano D, Esteban-Fernández A, Sánchez-Patán F, Martínlvarez PJ, Moreno-Arribas MV, Bartolomé B. Anti-adhesive activity of cranberry phenolic compounds and their microbial-derived metabolites against uropathogenic *Escherichia coli* in bladder epithelial cell cultures. *Int J Mol Sci*. (2015) 16:12119–30. doi: 10.3390/ijms160612119

49. Hamann GL, Campbell JD, George CM. Warfarin-cranberry juice interaction. *Ann Pharmacother*. (2011) 45:420–0. doi: 10.1345/aph.1P451

50. Paeng CH, Sprague M, Jackevicius CA. Interaction between warfarin and cranberry juice. *Clin Ther*. (2007) 29:1730–5. doi: 10.1016/j.clinthera.2007.08.018

51. Peron G, Pellizzaro A, Brun P, Schievano E, Mammi S, Sut S, et al. Antiadhesive activity and metabolomics analysis of rat urine after cranberry (*Vaccinium macrocarpon* Aiton) administration. *J Agric Food Chem*. (2017) 65:5657–67. doi: 10.1021/acs.jafc.7b01856

52. Beerepoot MAJ. Cranberries vs antibiotics to prevent urinary tract infections: a randomized double-blind noninferiority trial in premenopausal women. *Arch Intern Med*. (2011) 171:1270–8. doi: 10.1001/archinternmed.2011.306

53. Jensen HD, Struve C, Christensen SB, Krogfelt KA. Cranberry juice and combinations of its organic acids are effective against experimental urinary tract infection. *Front Microbiol*. (2017) 8:8. doi: 10.3389/fmicb.2017.00542

54. Liu H, Howell AB, Zhang DJ, Khoo C. A randomized, double-blind, placebo-controlled pilot study to assess bacterial anti-adhesive activity in human urine following consumption of a cranberry supplement. *Food Funct*. (2019) 10:7645–52. doi: 10.1039/C9FO01198F

55. Duncan SH, Conti E, Ricci L, Walker AW. Links between diet, intestinal anaerobes, microbial metabolites and health. *Biomedicines*. (2023) 11:1338. doi: 10.3390/biomedicines11051338

56. Xia JY, Yang C, Xu DF, Xia H, Yang LG, Sun GJ. Consumption of cranberry as adjuvant therapy for urinary tract infections in susceptible populations: a systematic review and meta-analysis with trial sequential analysis. *PLoS One*. (2021) 16:e0256992. doi: 10.1371/journal.pone.0256992

57. Juthani-Mehta M, Van Ness PH, Bianco L, Rink A, Rubeck S, Ginter S, et al. Effect of cranberry capsules on bacteriuria plus pyuria among older women in nursing homes: a randomized clinical trial. *JAMA*. (2016) 316:1879–87. doi: 10.1001/jama.2016.16141

58. Babar A, Moore L, Leblanc V, Dudonné S, Desjardins Y, Lemieux S, et al. High dose versus low dose standardized cranberry proanthocyanidin extract for the prevention of recurrent urinary tract infection in healthy women: a double-blind randomized controlled trial. *BMC Urol*. (2021) 21:44. doi: 10.1186/s12894-021-00811-w

59. Schlager TA, Anderson S, Trudell J, Hendley JO. Effect of cranberry juice on bacteriuria in children with neurogenic bladder receiving intermittent catheterization. *J Pediatr*. (1999) 135:698–702. doi: 10.1016/S0022-3476(99)70087-9

60. Zhao S, Liu H, Gu L. American cranberries and health benefits – an evolving story of 25 years. *J Sci Food Agric*. (2020) 100:5111–6. doi: 10.1002/jsfa.8882

61. Ardito L, Scuotto V, Del Giudice M, Petruzzelli AM. A bibliometric analysis of research on big data analytics for business and management. *Manag Decis*. (2018) 57:1993–2009. doi: 10.1108/MD-07-2018-0754

62. Sweileh WM. Bibliometric analysis of peer-reviewed literature on climate change and human health with an emphasis on infectious diseases. *Glob Health*. (2020) 16:44. doi: 10.1186/s12992-020-00576-1

63. Abdullah, Naved Khan M. Determining mobile payment adoption: a systematic literature search and bibliometric analysis. *Cogent Bus Manage*. (2021) 8:1893245. doi: 10.1080/23311975.2021.1893245

64. Fan J, Gao Y, Zhao N, Dai R, Zhang H, Feng X, et al. Bibliometric analysis on COVID-19: a comparison of research between English and Chinese studies. *Front Public Health*. (2020) 8:477. doi: 10.3389/fpubh.2020.00477

65. Sidhu AK, Singh H, Virdi SS, Kumar R. A bibliometric analysis on job stress using visualizing network. *JCCC*. (2020) 12:21–9. doi: 10.31620/JCCC.12.20/04

66. Aria M, Cuccurullo C. Bibliometrix: an R-tool for comprehensive science mapping analysis. *J Informet*. (2017) 11:959–75. doi: 10.1016/j.joi.2017.08.007

67. Piotrowski C. Bibliometrics and citation analysis for the psychologist-manager: a review and select readings. *Psychol Manager J*. (2013) 16:53–71. doi: 10.1037/h0094735

68. Kontiokari T, Sundqvist K, Nuutinen M, Pokka T, Koskela M, Uhari M. Randomised trial of cranberry-lingonberry juice and Lactobacillus GG drink for the prevention of urinary tract infections in women. *BMJ*. (2001) 322:1571. doi: 10.1136/bmj.322.7302.1571

69. Pappas E, Schaich KM. Phytochemicals of cranberries and cranberry products: characterization, potential health effects, and processing stability. *Crit Rev Food Sci Nutr*. (2009) 49:741–81. doi: 10.1080/10408390802145377

70. Bhargava K, Nath G, Bhargava A, Kumari R, Aseri GK, Jain N. Bacterial profile and antibiotic susceptibility pattern of uropathogens causing urinary tract infection in

the eastern part of northern India. *Front Microbiol*. (2022) 13:965053. doi: 10.3389/fmicb.2022.965053

71. Duicu C, Cozea I, Delean D, Aldea AA, Aldea C. Antibiotic resistance patterns of urinary tract pathogens in children from Central Romania. *Exp Ther Med*. (2021) 22:748. doi: 10.3892/etm.2021.10180

72. Madrazo M, Esparcia A, López-Cruz I, Alberola J, Piles L, Viana A, et al. Clinical impact of multidrug-resistant bacteria in older hospitalized patients with community-acquired urinary tract infection. *BMC Infect Dis*. (2021) 21:1232. doi: 10.1186/s12879-021-06939-2

73. Jalil MB, Al Atbee MYN. The prevalence of multiple drug resistance *Escherichia coli* and *Klebsiella pneumoniae* isolated from patients with urinary tract infections. *J Clin Lab Anal*. (2022) 36:e24619. doi: 10.1002/jcla.24619

74. Khan MI, Xu S, Ali MM, Ali R, Kazmi A, Akhtar N, et al. Assessment of multidrug resistance in bacterial isolates from urinary tract-infected patients. *J Radiat Res Appl Sci*. (2020) 13:267–75. doi: 10.1080/16878507.2020.1730579

75. Mazzariol A, Bazaj A, Cornaglia G. Multi-drug-resistant gram-negative bacteria causing urinary tract infections: a review. *J Chemother*. (2017) 29:2–9. doi: 10.1080/1120009X.2017.1380395

76. Umar Z, Ashfaq S, Parikh A, Ilyas U, Foster A, Bhangal R, et al. Stenotrophomonas Maltophilia and urinary tract infections: a systematic review. *Cureus*. 14:E26184.

77. Pandey S. Antibacterial and antifungal activities of *Ocimum gratissimum* L. *Int J Pharm Pharm Sci*. (2017) 9:26–31. doi: 10.22159/ijpps.2017v9i12.22678

78. Peng MM, Fang Y, Hu W, Huang Q. The pharmacological activities of compound Salvia Plebeia granules on treating urinary tract infection. *J Ethnopharmacol*. (2010) 129:59–63. doi: 10.1016/j.jep.2010.02.029

79. Prabhu K, Prasathkumar M, Sivaraman J, Sadhasivam S, Gajdács M, Gasimov EK, et al. Phytochemical characterization, antibacterial, and anti-biofilm efficacy of *Mangifera indica* seed kernel: a preliminary study using in vitro and in silico approaches. *J King Saud Univ Sci*. (2023) 35:102688. doi: 10.1016/j.jksus.2023.102688

80. Liya SJ, Siddique R. Determination of antimicrobial activity of some commercial fruit (apple, papaya, lemon and strawberry) against bacteria causing urinary tract infection. *Eur J Microbiol Immunol (Bp)*. (2018) 8:95–9. doi: 10.1556/1886.2018.00014

81. Lionel OO, Adegboyega IP, Ezekiel AO, Olufunke BC. Antimicrobial activity of garlic (*Allium sativum*) on selected uropathogens from cases of urinary tract infection. *Ann Trop Pathol*. (2020) 11:133. doi: 10.4103/atp.atp_9_20

82. Dehdari S, Hajimehdipoor H. Medicinal properties of *Adiantum capillus-veneris* Linn. in traditional medicine and modern phytotherapy: a review article. *Iran J Public Health*. (2018) 47:188–97.

83. Mohammed SS, Bashir A, David AA, Abdul-Rahman AA, Ninyio NN. Phytochemical constituents and antibacterial activity of ginger (Zingiber 1 officianale) extract on selected clinical isolates associated with urinary 2 tract infections (UTIS). *Fusion Engineering and Design*. (2019) 3:74–85.

84. Pekamwar SS, Kalyankar TM, Kokate SS. Pharmacological activities of *Coccinia grandis*: review. *J Appl Pharm Sci*. (2013) 3:114–9. doi: 10.7324/JAPS.2013.3522

85. Wadikar DD, Patki PE. Coleus aromaticus: a therapeutic herb with multiple potentials. *J Food Sci Technol*. (2016) 53:2895–901. doi: 10.1007/s13197-016-2292-y

86. Yamani HA, Pang EC, Mantri N, Deighton MA. Antimicrobial activity of Tulsi (*Ocimum tenuiflorum*) essential oil and their major constituents against three species of Bacteria. *Front Microbiol*. (2016) 7:681. doi: 10.3389/fmicb.2016.00681

87. Trill J, Simpson C, Webley F, Radford M, Stanton L, Maishman T, et al. Uva-ursi extract and ibuprofen as alternative treatments of adult female urinary tract infection (ATAFUTI): study protocol for a randomised controlled trial. *Trials*. (2017) 18:421. doi: 10.1186/s13063-017-2145-7

88. Díaz K, Espinoza L, Madrid A, Pizarro L, Chamy R. Isolation and identification of compounds from bioactive extracts of *Taraxacum officinale* Weber ex F. H. Wigg. (dandelion) as a potential source of antibacterial agents. *Evid Based Complement Alternat Med*. (2018) 2018:2706417. doi: 10.1155/2018/2706417

89. Fazly Bazzaz BS, Darvishi Fork S, Ahmadi R, Khameneh B. Deep insights into urinary tract infections and effective natural remedies. *Afr J Urol*. (2021) 27:6. doi: 10.1186/s12301-020-00111-z

90. Lagha R, Ben Abdallah F, AL-Sarhan BO, Al-Sodany Y. Antibacterial and biofilm inhibitory activity of medicinal plant essential oils against *Escherichia coli* isolated from UTI patients. *Molecules*. (2019) 24:1161. doi: 10.3390/molecules24061161

91. Fursenco C, Calalb T, Uncu L, Dinu M, Ancuceanu R. Solidago virgaurea L.: a review of its ethnomedicinal uses, phytochemistry, and pharmacological activities. *Biomol Ther*. (2020) 10:1619. doi: 10.3390/biom10121619

92. Ahmed J, Abdu A, Mitiku H, Ataro Z. In vitro antibacterial activities of selected medicinal plants used by traditional healers for treating urinary tract infection in Haramaya District, Eastern Ethiopia. *Infect Drug Resist*. (2023) 16:1327–38. doi: 10.2147/IDR.S398204

93. Brendler T, Abdel-Tawab M. Buchu (Agathosma betulina and *A. crenulata*): rightfully forgotten or underutilized? *Front Pharmacol*. (2022) 13:813142. doi: 10.3389/fphar.2022.813142

94. Sahib A, Mohammed H, Hamdan S. Use of aqueous extract of corn silk in the treatment of urinary tract infection. *J Intercult Ethnopharmacol*. (2012) 1:1. doi: 10.5455/jice.20120525123150

95. Trivisonno LF, Sgarbossa N, Alvez GA, Fieiras C, Escobar Liquitay CM, Jung JH, et al. *Serenoa repens* for the treatment of lower urinary tract symptoms due to benign prostatic enlargement: a systematic review and meta-analysis. *Investig Clin Urol*. (2021) 62:520–34. doi: 10.4111/icu.20210254

96. Wang Y, Singh AP, Nelson HN, Kaiser AJ, Reker NC, Hooks TL, et al. Urinary clearance of cranberry Flavonol glycosides in humans. *J Agric Food Chem*. (2016) 64:7931–9. doi: 10.1021/acs.jafc.6b03611

97. Sun J, Marais JPJ, Khoo C, LaPlante K, Vejborg RM, Givskov M, et al. Cranberry (*Vaccinium macrocarpon*) oligosaccharides decrease biofilm formation by uropathogenic *Escherichia coli*. *J Funct Foods*. (2015) 17:235–42. doi: 10.1016/j.jff.2015.05.016

98. Pereira TA, Fernandes AR, Mendes A, Oliveira R, Casqueiro A, Birne R, et al. Are cranberry capsules effective and safe in preventing urinary tract infections in kidney transplantation? A randomized pilot clinical trial. *Port J Nephrol Hypert*. (2017) 31:18–24.

99. Aziz U, Khan SK, Altaf U, Zainab A, Kanwal A, Naz F. Efficacy of cranberry juice in the prevention of recurrent urinary tract infection. *Pak J Med Health Sci*. (2022) 16:204–6. doi: 10.53350/pjmhs22162204

100. Tong H, Heong S, Chang S. Effect of ingesting cranberry juice on bacterial growth in urine. *Am J Health Syst Pharm*. (2006) 63:1417–9. doi: 10.2146/ajhp050499

101. Luís Â, Domingues F, Pereira L. Can cranberries contribute to reduce the incidence of urinary tract infections? A systematic review with meta-analysis and trial sequential analysis of clinical trials. *J Urol*. (2017) 198:614–21. doi: 10.1016/j.juro.2017.03.078

102. Uberos J, Rodríguez-Belmonte R, Rodríguez-Pérez C, Molina-Oya M, Blanca-Jover E, Narbona-Lopez E, et al. Phenolic acid content and antiadherence activity in the urine of patients treated with cranberry syrup (*Vaccinium macrocarpon*) vs. trimethoprim for recurrent urinary tract infection. *J Funct Foods*. (2015) 18:608–16. doi: 10.1016/j.jff.2015.08.009

103. Maki KC, Kaspar KL, Khoo C, Derrig LH, Schild AL, Gupta K. Consumption of a cranberry juice beverage lowered the number of clinical urinary tract infection episodes in women with a recent history of urinary tract infection 1. *Am J Clin Nutr*. (2016) 103:1434–42. doi: 10.3945/ajcn.116.130542

104. Nowack R, Schmitt W. Cranberry juice for prophylaxis of urinary tract infections – conclusions from clinical experience and research. *Phytomedicine*. (2008) 15:653–67. doi: 10.1016/j.phymed.2008.07.009

105. Barbosa LN, Rall VLM, Fernandes AAH, Ushimaru PI, da Silva PI, Fernandes A. Essential oils against foodborne pathogens and spoilage bacteria in minced meat. *Foodborne Pathog Dis*. (2009) 6:725–8. doi: 10.1089/fpd.2009.0282

106. Fernández-Puentes V, Uberos J, Rodríguez-Belmonte R, Nogueras-Ocaña M, Blanca-Jover E, Narbona-López E. Efficacy and safety profile of cranberry in infants and children with recurrent urinary tract infection. *An Pediatr (Barc)*. (2015) 82:397–403. doi: 10.1016/j.anpedi.2014.08.012

107. Duffey K, Sutherland L. Adult cranberry beverage consumers have healthier macronutrient intakes and measures of body composition compared to non-consumers: national health and nutrition examination survey (NHANES) 2005–2008. *Nutrients*. (2013) 5:4938–49. doi: 10.3390/nu5124938

108. Duffey KJ, Sutherland LA. Adult consumers of cranberry juice cocktail have lower C-reactive protein levels compared with nonconsumers. *Nutr Res*. (2015) 35:118–26. doi: 10.1016/j.nutres.2014.11.005

109. Jeitler M, Michalsen A, Schwiertz A, Kessler CS, Koppold-Liebscher D, Grasme J, et al. Effects of a supplement containing a cranberry extract on recurrent urinary tract infections and intestinal microbiota: a prospective, uncontrolled exploratory study. *J Integr Complement Med*. (2022) 28:399–406. doi: 10.1089/jicm.2021.0300

110. Heitmann K, Nordeng H, Holst L. Pregnancy outcome after use of cranberry in pregnancy – the Norwegian mother and child cohort study. *BMC Complement Altern Med*. (2013) 13:345. doi: 10.1186/1472-6882-13-345

111. Al-Juhaishi A, Al-Khafaji T, Mustafa R, Alshehristani R. Effect of cranberry in enhancing oral hypoglycemic agents in uncontrolled type-II diabetic patients. *J Glob Pharma Technol*. (2019) 10:319–24.

112. Super EA, Kemper KJ, Woods C, Nagaraj S. Cranberry use among pediatric nephrology patients. *Ambul Pediatr*. (2005) 5:249–52. doi: 10.1367/A04-185R1.1

113. Gautam A, Agrawal PK, Pursnani N, Maheshwari PK, Rani R. 764-P: preventive effect of cranberry extract for SGLT2i-associated urinary tract infection: a case control study. *Diabetes*. (2021) 70:764-P. doi: 10.2337/db21-764-P

114. Mohammed Abdul MI, Jiang X, Williams KM, Day RO, Roufogalis BD, Liauw WS, et al. Pharmacodynamic interaction of warfarin with cranberry but not with garlic in healthy subjects. *Br J Pharmacol*. (2008) 154:1691–700. doi: 10.1038/bjp.2008.210

115. Pagonas N, Hörstrup J, Schmidt D, Benz P, Schindler R, Reinke P, et al. Prophylaxis of recurrent urinary tract infection after renal transplantation by cranberry juice and L-methionine. *Transplant Proc*. (2012) 44:3017–21. doi: 10.1016/j.transproceed.2012.06.071

116. Mehmood Y, Umar H, Riaz H, Farooq U, Yousaf H. A clinical trial of cranberry and elderberry extracts (Berdi® sachet) for urinary tract infection in Pakistani population. *J Pharm Res Int*. (2019) 31:1–6. doi: 10.9734/jpri/2019/v31i630347

117. Moroi MK, Loloi J, Songdej N. Cranberry supplementation as a cause of major intraoperative bleeding during vascular surgery due to aspirin-like platelet inhibition. *Blood Coagul Fibrinolysis*. (2020) 31:402–4. doi: 10.1097/MBC.0000000000000912

118. Griffiths AP, Beddall A, Pegler S. Fatal haemopericardium and gastrointestinal haemorrhage due to possible interaction of cranberry juice with warfarin. *J R Soc Promot Health*. (2008) 128:324–6. doi: 10.1177/1466424008096615

119. Dave AA, Samuel J. Suspected interaction of cranberry juice extracts and tacrolimus serum levels: a case report. *Cureus*. (2016). doi: 10.7759/cureus.610

120. Howell AB, Reed JD, Krueger CG, Winterbottom R, Cunningham DG, Leahy M. A-type cranberry proanthocyanidins and uropathogenic bacterial anti-adhesion activity. *Phytochemistry*. (2005) 66:2281–91. doi: 10.1016/j.phytochem.2005.05.022

121. Foo LY, Lu Y, Howell AB, Vorsa N. A-type Proanthocyanidin trimers from cranberry that inhibit adherence of Uropathogenic P-Fimbriated *Escherichia coli*. *J Nat Prod*. (2000) 63:1225–8. doi: 10.1021/np000128u

122. Foo LY, Lu Y, Howell AB, Vorsa N. The structure of cranberry proanthocyanidins which inhibit adherence of uropathogenic P-fimbriated *Escherichia coli* in vitro. *Phytochemistry*. (2000) 54:173–81. doi: 10.1016/S0031-9422(99)00573-7

123. Zafriri D, Ofek I, Adar R, Pocino M, Sharon N. Inhibitory activity of cranberry juice on adherence of type 1 and type P fimbriated *Escherichia coli* to eucaryotic cells. *Antimicrob Agents Chemother*. (1989) 33:92–8. doi: 10.1128/AAC.33.1.92

124. Sobota AE. Inhibition of bacterial adherence by cranberry juice: potential use for the treatment of urinary tract infections. *J Urol*. (1984) 131:1013–6. doi: 10.1016/S0022-5347(17)50751-X

125. Stothers L. A randomized trial to evaluate effectiveness and cost effectiveness of naturopathic cranberry products as prophylaxis against urinary tract infection in women. *Can J Urol*. (2002) 9:1558–62.

126. Prior RL, Fan E, Ji H, Howell A, Nio C, Payne MJ, et al. Multi-laboratory validation of a standard method for quantifying proanthocyanidins in cranberry powders. *J Sci Food Agric*. (2010) 90:1473–8. doi: 10.1002/jsfa.3966

127. Anger J, Lee U, Ackerman AL, Chou R, Chughtai B, Clemens JQ, et al. Recurrent uncomplicated urinary tract infections in women: AUA/CUA/SUFU guideline. *J Urol*. (2019) 202:282–9. doi: 10.1097/JU.0000000000000296

128. Royds R. Therapeutic compositions containing trimethoprim and cranberry extract and methods for treating and preventing urinary tract infections. US20070166409A1. (2007). Available at: https://patents.google.com/patent/US20070166409A1/en?oq=US20070166409 (Accessed November 14, 2023).

129. Gans AM. Composition for prevention or treatment of urinary tract infection. US20090175843A1. (2009). Available at: https://patents.google.com/patent/US20090175843A1/en?oq=US20090175843 (Accessed November 14, 2023).

130. Sanoner P, Bochard V, Charissou L, Lastique B, Jacob M, Thomas P. Cranberry extract useful in the treatment and prevention of urinary infections. US10092539B2. (2018). Available at: https://patents.google.com/patent/US10092539B2/en?oq=US10092539 (Accessed November 14, 2023).

131. Truong JT. Formulation and method for preventing urinary tract infections. Us20200060324a1. (2020). Available at: https://patents.google.com/patent/US20200060324A1/en?oq=US20200060324 (Accessed September 18, 2023).

132. Baratto G. Cranberry extract for preventing and treating uncomplicated lower urinary tract infections. EP3895761A1. (2021). Available at: https://patents.google.com/patent/EP3895761A1/en?oq=EP3895761 (Accessed September 18, 2023).

133. Hendriks M, Bouter P, den Ende MV. Composition for the treatment or prevention of urinary tract infections and dosage form. EP2662086A1. (2013). Available at: https://patents.google.com/patent/EP2662086A1/en?oq=EP2662086 (Accessed September 18, 2023).

134. Minatelli JA, Hill WS. Method of preventing, controlling and ameliorating urinary tract infections using a synergistic cranberry derivative and d-mannose composition. US20090226548A1. (2009). Available at: https://patents.google.com/patent/US20090226548A1/en?oq=US20090226548 (Accessed September 18, 2023).

135. Aldritt M, Lee R, Wehling F. Effervescent composition including cranberry extract. US20050158381A1. (2005). Available at: https://patents.google.com/patent/US20050158381A1/en?oq=US20050158381 (Accessed September 18, 2023).

136. Arpini S, Mombelli G, Morazzoni P, Peterlongo F, Riva A, Ronchi M. Compositions comprising an American cranberry extract and phospholipids. US20210244782A1. (2021). Available at: https://patents.google.com/patent/US20210244782A1/en?oq=US20210244782 (Accessed September 18, 2023).

137. Vorsa N, Vvedenskaya IO, Huang MT, Rosen RT, Rosen SL. Anti-inflammatory cranberry flavonol extract preparations. US20110195138A1. (2011). Available at: https://patents.google.com/patent/US20110195138A1/en?oq=US20110195138 (Accessed September 18, 2023).

138. Howell AB, Vorsa N. Plant proanthocyanidin extract effective at inhibiting adherence of bacteria with P-type fimbriae to surfaces. US6608102B1. (2003). Available at: https://patents.google.com/patent/US6608102B1/en?oq=US6608102 (Accessed September 18, 2023).

139. Amir M. Compositions and methods for treating and/or preventing a urinary tract infection. US20190000908A1. (2019). Available at: https://patents.google.com/patent/US20190000908A1/en?oq=US20190000908 (Accessed September 18, 2023).

140. Selzer J, John FS. Cranberry based dietary supplement and dental hygiene product. US20030108627A1. (2003). Available at: https://patents.google.com/patent/US20030108627A1/en?oq=US20030108627 (Accessed September 18, 2023).

141. Alberte RS, Roschek WP Jr, Li D. Extracts of cranberry and methods of using thereof. US20100028469A1. (2010). Available at: https://patents.google.com/patent/US20100028469A1/en?oq=US20100028469 (Accessed September 18, 2023).

142. Hotchkiss AT, Nunez A, Khoo C, Strahan GD. Cranberry xyloglucan oligosaccharide composition. US20130316025A1. (2013). Available at: https://patents.google.com/patent/US20130316025A1/en?oq=US20130316025 (Accessed September 18, 2023).

143. Herzlinger AS, Wu TSP. Compositions comprising cranberry extract and methods of use thereof. US20110280851A1. (2011). Available at: https://patents.google.com/patent/US20110280851A1/en?oq=US20110280851 (Accessed September 18, 2023).

144. Besnard M, Inisan C, Rousseau I. American cranberry extract and its use. US20090258940A1. (2009). Available at: https://patents.google.com/patent/US20090258940A1/en?oq=US20090258940 (Accessed September 18, 2023).

145. Rowley D, Sun J, Deering R, Seeram N, Cohen P. Cranberry-derived compositions for potentiating antibiotic efficacy against bacterial persistence. US20200179434A1. (2020). Available at: https://patents.google.com/patent/US20200179434A1/en?oq=US20200179434 (Accessed September 18, 2023).

146. Scialpi A. Use of cranberries with herbal components for preventing urinary tract infections. EP3142678A1. (2017). Available at: https://patents.google.com/patent/EP3142678A1/en?oq=EP3142678 (Accessed September 18, 2023).

147. Hochman N, Hochman J, Weiss E, Ofek I. New adjuvant. EP2227252A2. (2010). Available at: https://patents.google.com/patent/EP2227252A2/en?oq=EP2227252 (Accessed September 18, 2023).

frontiers | Frontiers in Nutrition

TYPE Original Research
PUBLISHED 02 May 2025
DOI 10.3389/fnut.2025.1509734

Check for updates

OPEN ACCESS

EDITED BY
Ntethelelo Sibiya,
Rhodes University, South Africa

REVIEWED BY
Gloria O. Izu,
Central University of Technology, South Africa
Mapula Razwinani,
Durban University of Technology, South Africa

*CORRESPONDENCE
Ji Shi
✉ lnshiji@163.com
Guoshun Shan
✉ shanguoshun@126.com

RECEIVED 11 October 2024
ACCEPTED 16 April 2025
PUBLISHED 02 May 2025

CITATION
Lian J, Zhang Y, Dong K, Shi J, Zhang F, Shan G, Liu P, Wang N and Jia T (2025) Enhanced oral bioavailability of two Cistanche polysaccharides in acteoside: an in-depth analysis of intestinal flora, short-chain fatty acids, and pharmacokinetic regulation. *Front. Nutr.* 12:1509734. doi: 10.3389/fnut.2025.1509734

COPYRIGHT
© 2025 Lian, Zhang, Dong, Shi, Zhang, Shan, Liu, Wang and Jia. This is an open-access article distributed under the terms of the Creative Commons Attribution License (CC BY). The use, distribution or reproduction in other forums is permitted, provided the original author(s) and the copyright owner(s) are credited and that the original publication in this journal is cited, in accordance with accepted academic practice. No use, distribution or reproduction is permitted which does not comply with these terms.

Enhanced oral bioavailability of two Cistanche polysaccharides in acteoside: an in-depth analysis of intestinal flora, short-chain fatty acids, and pharmacokinetic regulation

Jing Lian[1], Yuan Zhang[1], Kexu Dong[1], Ji Shi[1,2,3]*, Fan Zhang[1,2,3], Guoshun Shan[1,2,3]*, Pengpeng Liu[1,2,3], Nan Wang[1] and Tianzhu Jia[1,2,3]

[1]Liaoning University of Traditional Chinese Medicine, Dalian, China, [2]Key Research Laboratory of Traditional Chinese Medicine Processing Process Principles of the State Administration of Traditional Chinese Medicine, Dalian, China, [3]Liaoning Provincial Traditional Chinese Medicine Processing Professional Technology Innovation Center, Dalian, China

Introduction: For centuries, *Cistanche deserticola* Y. C. Ma has been considered to have the effect of "tonifying the kidney and strengthening the yang," and is used for the prevention and treatment of diseases such as impotence, female infertility, lumbago and senile constipation. Polysaccharides and small molecules of acteoside are the main chemical compounds co-existing in *Cistanche deserticola* Y. C. Ma with health benefits, but the interaction of these two compounds *in vivo* is not yet known.

Methods: Here, we investigated the effects of unprocessed Cistanche polysaccharides and wine-processed Cistanche polysaccharides on the metabolism of acteoside *in vivo* through gut microbiota. Male Sprague–Dawley rats were randomly divided into Control group, unprocessed Cistanche polysaccharide group (UCP group) and wine-processed Cistanche polysaccharide group (WCP group). After 21 days of intervention with unprocessed Cistanche polysaccharides and wine-processed Cistanche polysaccharides, rats were given 100 mg/kg of acteoside on day 22. Acteoside and its associated metabolites pharmacokinetically studied were analysed using UPLC-QqQ-MS, and the composition of short-chain fatty acids (SCFAs) in excrement was measured using the technique of GC–MS. The microbiological composition of the intestines was discovered using 16S rRNA gene amplicon sequencing.

Results: The results showed that the Cistanche polysaccharides used in this experiment, including unprocessed Cistanche polysaccharides and wine-processed Cistanche polysaccharides, could regulate the diversity of gut microbiota and increase the number of beneficial bacteria, especially wine-processed Cistanche polysaccharides were able to promote the growth of *Ligilactobacillus* and *Duncaniella* genus, and improve the production of SCFAs and the absorption of acteoside.

Discussion: By exploring the synergistic effects of large molecules Cistanche polysaccharides and small molecule acteoside, this paper provides a new explanation for the scientific use of plant-derived polysaccharides to improve the bioavailability of oral drugs.

KEYWORDS

***Cistanche deserticola*, acteoside, polysaccharides, pharmacokinetics study, gut microbiota**

1 Introduction

Cistanche deserticola Y.C. Ma (CD), a perennial psammophytic species endemic to arid regions of China, Mongolia, Japan, and other East Asian territories, holds a distinguished position in traditional medicine systems spanning over two millennia. Revered as the principal constituent of the renowned *Wubishuyu* Pill in the classical medical compendium <*Beiji Qianjin Yaofang*>, CD demonstrates particular prominence in reproductive health formulations such as the *Suoyang Gujing Pill* - a testament to its historical application in replenishing kidney yang, enhancing essence-blood nourishment, and modulating immune resilience. Modern pharmacological investigations substantiate these traditional claims through evidence of multifaceted bioactivities including neuroprotection, immunomodulation, endocrine regulation, anti-fatigue effects, hepatoprotection, antioxidant capacity, antimicrobial/antiviral properties, and antineoplastic potential (1). Phytochemical analyses reveal acetoside, a phenylethanoid glycoside demonstrating remarkable biological versatility through its demonstrated antioxidant, anticonvulsant, neuroprotective, anti-inflammatory, antifungal, antihypertensive, and immunoenhancing properties. Cistanche polysaccharides have a variety of pharmacological activities, including immunomodulation, antioxidant, anti-aging, hepatoprotective, anti-inflammatory and intestinal microbiota regulation (2, 3). As this species' predominant bioactive component alongside polysaccharide macromolecules.

Current pharmacopoeial standards record raw *Cistanche deserticola* and its wine-steamed product. Pharmacodynamic studies demonstrate that steam by rice wine induces significant phytochemical transformations, notably a marked reduction in acteoside content coupled with a substantial increase in isoacteoside levels (4). This compositional shift correlates with enhanced therapeutic efficacy in kidney yang-tonifying applications, suggesting potential synergistic enhancement through processing. Furthermore, structural modification of polysaccharide components during wine steaming has been demonstrated to substantially improve antioxidant capacity (5), though the molecular mechanisms underlying this phenomenon remain incompletely elucidated. Notably, the potential synergistic interaction between bioactive polysaccharides and phenylethanoid glycosides, particularly isoacteoside, represents a critically understudied area requiring systematic investigation.

Emerging evidence suggests that acteoside's therapeutic efficacy is constrained by its limited bioavailability and rapid hepatic metabolism following oral administration, prompting investigations into complementary bioactive components capable of enhancing systemic delivery. Non-digestible polysaccharides from Traditional Chinese Medicine (TCM) have emerged as particularly promising candidates due to their unique structural characteristics that enable gastrointestinal resistance while modulating gut microbiota composition and metabolic activity (6, 7), thereby functioning as prebiotic agents that facilitate herbal compound absorption through microbial biotransformation (8). This symbiotic relationship is exemplified by multiple TCM systems where polysaccharides demonstrate synergistic interactions with bioactive small molecules: Ginseng polysaccharides enhance ginsenoside Rb1 bioavailability through microbiota-mediated metabolism, ameliorating dextran sulfate sodium (DSS)-induced colitis in rodent models (9); soybean-derived polysaccharides improve genistein bioavailability while attenuating high-fat diet-induced adiposity and metabolic dysfunction in murine studies (7); lotus root polysaccharides (LRPs) demonstrate antioxidant synergism with phenolic compounds through microbial fermentation (10); and Astragalus polysaccharides (APS) enhance flavonoid bioavailability via gastrointestinal stabilization and permeation enhancement (11). Building upon this foundational knowledge, our study specifically investigates two critical aspects of *Cistanche deserticola* Y.C. Ma (CD) polysaccharide functionality, the differential effects of raw versus wine-processed CD polysaccharides on gut microbiota profiles, and processing-induced alterations in acteoside's metabolic pathways and bioactive transformations that may influence its pharmacokinetic behavior and therapeutic potential.

This study systematically investigates the synergistic mechanisms between polysaccharides and acteoside in *Cistanche deserticola* through integrated multi-omics analysis. The experimental design scheme is shown in Figure 1. We developed a UPLC-QqQ-MS method for simultaneous quantification of acteoside metabolites (caffeic acid and hydroxytyrosol) in biological samples, coupled with 16S rRNA sequencing and SCFA metabolomics to profile gut microbiota modulation. Comparative evaluation of rice wine-processed versus raw polysaccharides revealed enhanced bioavailability enhancement correlated with structural characteristics of processed polysaccharides. Our findings establish a mechanistic framework for optimizing polysaccharide-phenylethanoid glycoside synergy through controlled processing, demonstrating enhanced therapeutic index potential for Cistanche-derived nutraceuticals.

2 Materials and methods

2.1 Materials

Cistanche deserticola Y.C. Ma was collected from Alashan mengrongshantang cistanche Co. Ltd. The samples were identified by Prof. Yanjun Zhai (Liaoning university of Traditional Chinese Medicine). The plant specimens (The herbarium voucher number of 20,210,508-111) were deposited in the herbarium of the Technical Innovation Center of Traditional Chinese Medicine Processing, Liaoning University of Traditional Chinese Medicine. China Chengdu Herb Substance Co. Ltd. was the source of the standard substances, including acteoside (NO: 220115), caffeic acid (NO: 220412), hydroxytyrosol (NO: 220214), and the internal standard genistein (NO: 220402). Fisher Scientific (Pittsburgh, PA) supplied chromatography-grade acetonitrile and methanol. Anaqua Chemical Supply Inc. (Wilmington, USA) provided the formic acid. Cellulase (batch number: C8260), Amylase (batch number: G8290), Papain (batch number: G8430) were purchased from Beijing Solebold Technology Co., Ltd. Pure water (ddH_2O, Milli-Q® IQ Element), Methyl tert-butyl ether (Lot number: 1634-04-4, HPLC grade, Shanghai Anpel Experimental Technology Co., LTD), Sulfuric acid (Lot number: 7664-93-9, Purity≥95(AR), Sinopharm Chemical Reagent Co., Ltd.) 2-Methylvaleric acid (Lot number: 97-61-0, Purity≥99.5), Acetic acid (Lot number:64-19-7, Lot number: Purity≥99.5), Propionic acid (Lot number: 79-09-4, Purity≥99.5), Isobutyric acid (Lot number: 79-31-2, Purity≥99.5), Butyric acid (Lot number: 107-92-6, Purity≥99.5), Isovaleric acid (Lot number: 503-74-2, Purity≥99.5), Valeric acid (Lot number:109-52-4, Purity≥99.5), Hexanoic acid (Lot number:142-62-1, Purity≥99.5),

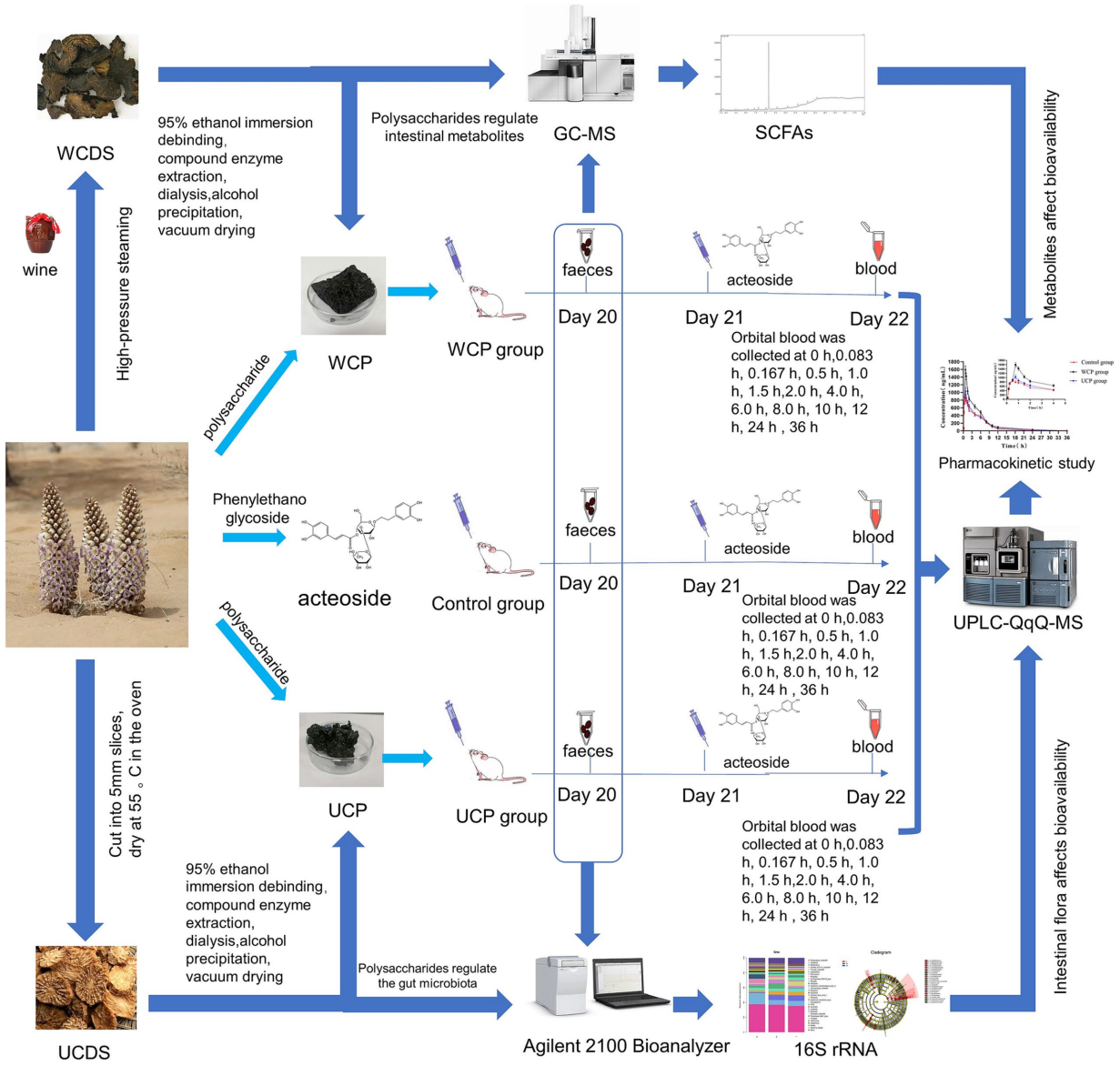

FIGURE 1
Experimental scheme. Cistanche polysaccharides regulate gut microbiota to increase acteoside bioavailability: an in-depth analysis of intestinal flora, short-chain fatty acids, and pharmacokinetic regulation.

Heptanoicacid (Lot number: 111-14-8, Purity≥99.5),Octanoic acid (Lot number: 124-07-2, Purity≥99.5), Nonanoic acid (Lot number: 112-05-0, Purity≥99.5), Decanoic acid (Lot number: 334-48-5, Purity≥99.5) all purchased from Dr. Ehrenstorfer GmbH. Analytical grade chemical reagents comprised the remaining ones.

2.2 The preparation and preliminary identification of Cistanche polysaccharides

2.2.1 The preparation of Cistanche polysaccharides

Unprocessed *Cistanche deserticola* slices (UCDS) and wine-processed *Cistanche deserticola* slices (WCDS) were processed according to *Chinese Pharmacopoeia* (2020 edition) (12). UCDS:Remove impurities, wash clean, moisten thoroughly, cut into 5 mm thick slices, and dry. WCDS: Take the cistanche slices and steam them according to the wine steaming method (General rule 0213) until the wine is exhausted and removed after being steamed for 4 h at 1.25 atmospheric pressure, then dried at 55°C in an oven for drying. A total of 2.0 kg of UCDS or WCDS was ground into a rough powder. Two additional times, at 60°C for 2 h each, dry coarse powder was extracted using an aqueous solution containing 95% ethanol (v/v). The proportions of solid to liquid were 1:12 and 1:10, respectively to remove fat and wax, filtered, and dried in a cool ventilated place.

The powder was immersed in purified water (material-liquid ratio 1:10) and extracted with composite enzymes (cellulase 30 g, amylase 10 g and papain 5 g) at 55°C for 1 h at reflux, and then boiling rapidly to render the enzyme inactive. A dialysis membrane (MWCO 3500 Da) was used to dialyze the permeate for 2 days after the water

solution was mixed and filtered. Then concentrated under reduced pressure and then precipitated in 80% ethanol, stood under 4°C for 24 h. The precipitate was isolated through centrifugation at 4,000 rpm for 5 min. After that, the water solution was concentrated under low pressure, five times as much anhydrous ethanol was added to make the ethanol v/v fraction 80%, stood under 4°C for 24 h. Centrifugation was used to separate the precipitate for 10 min at 4,000 rpm. To obtain the unprocessed Cistanche polysaccharide (UCP), the precipitate was dried within a vacuum drier at 50°C after 3 cycles of cleaning with acetone and anhydrous ethanol. The same method is used to obtain wine-processed Cistanche polysaccharide (WCP).

2.2.2 Preliminary identification of Cistanche polysaccharides

The sulfuric acid phenol method was used to determine the polysaccharide content, with glucose serving as a standard. Using the BCA method, the total protein content was calculated.

$$\text{Polysaccharide yield}(\%) = \frac{m1}{m0} \times 100\%$$

In the formula, m0 is the mass of cistanche slices before degreasing; m1 is the mass of dried crude polysaccharide.

The average molecular weight was measured by gel permeation chromatography (GPC) in combination with multiangle laser light scattering (DAWN HELEOS-II laser photometer Wyatt Technology Co., USA) and a differential refractive index detector Optilab T-rEX(RID) (Wyatt Technology Co., USA).The system was equipped with an Ohpak SB-803 + Ohpak SB-804 + Ohpak SB-805 (300 × 8 mm, 10 μm, Shodex, Japan) column. During analysis, ultrapure water was applied as the mobile phase with a flow rate of 0.3 mL/min (45°C). Data collection and analysis were performed by Wyatt Technology ARTRAV software.

The polysaccharide sample (5 mg) was dissolved in 2 M trifluoroacetic acid (TFA) and hydrolyzed in a sealed glass tube at 121°C for 2 h. The hydrolysate was dried with nitrogen, then followed by the addition of 10 mL deionized water and filtered through 0.22 μm microporous filtering film for measurement. The supernatant was injected into a ICS5000 system (Thermo Fisher, USA) with a Dionex™ CarboPac™ PA20(150*3.0 mm, 10 μm)columnn (mobile phase: A, ddH2O; B, 0.1 M NaOH; C, 0.1 M NaOH & 0.2 M NaAC; flow rate: 0.5 mL/min; column temperature:30°C) 0.13 kinds of monosaccharide standards including fucose, rhamnose, arabinose, galactose, glucose, xylose, mannose, fructose, ribose, galacturonic acid, glucuronic acid, mannuronic acid, guluronic acid were determined as references.

2.3 Experimental animals and sample collection

2.3.1 Animals

Liaoning Changsheng Biotechnology Co. Ltd. (Laboratory Animal Resource Center of Liaoning Province), license number: SCXK 2020–0001 (Benxi, Liaoning, China) supplied male Sprague–Dawley rats (SPF grade) weighing 250 ± 20 g. Each one was raised at an animal facility with SPF housing and breeding practices. In this study, all animal experiments were conducted in accordance with ARRIVE guidelines and in accordance with the National Research Council's Guidelines for the Care and Use of laboratory animals. The Research Ethics Committee of Liaoning University of Traditional Chinese Medicine has granted the ethical approval of animal participation in this study. (Approval No. 2020067). This study focused on the therapeutic effects of Cistanche polysaccharides and WCP on male kidney deficiency-related diseases, so male rats were selected as experimental subjects. *Cistanche deserticola* is mainly used in clinical treatment of male kidney deficiency impotence, infertility and other symptoms (13). The physiological and behavioral characteristics of male rats are relatively stable. On the one hand, female rats interfere with estrogen due to estrus cycles, the accuracy of experimental data (14); on the other hand, gender differences are the first factor affecting the intestinal barrier. The intestinal permeability of females is usually lower than that of males (15). In order to ensure the consistency and reliability of experimental results, male rats were selected in this experiment to be closer to clinical applications.

2.3.2 Cistanche polysaccharide intervention and sample collection

After a week of acclimatization, rats were split into three groups at random: the wine-processed Cistanche polysaccharide group (WCP group), the unprocessed Cistanche polysaccharide group (UCP group), and the blank control group (Control group). Six rats each group were raised in the same cage for breeding. Prior to the experiment, provide water and regular laboratory meals to the rats at will and fast for one night before the experiment.

In order to ensure the continuous intake of Cistanche polysaccharides, it was calculated according to the requirements of the *Chinese Pharmacopoeia* (16) based on the daily dosage of Cistanche for adults, the polysaccharide yield of Cistanche polysaccharides and the equivalent conversion formula of the drug administration between humans and rats (17). An appropriate amount of raw Cistanche polysaccharide and Cistanche wine polysaccharide were weighed, dissolved in pure water, and prepared with 15.06 $g \cdot kg^{-1}$ administration solution for continuous administration for 21 days. After fasting overnight, on day 22, two fresh fecal samples were collected from each rat, put straight into a sterile tube from the anus, avoiding contact with skin or urine, and stored in a −80°C freezer immediately after freezing with liquid nitrogen for subsequent analysis. For the pharmacokinetics, in a 1.5 mL heparinized centrifuge tube, 0.3 mL of continuous blood collected from the orbital vein was taken from 0 min, 5 min, 10 min, 30 min, 1.0 h, 1.5 h, 2.0 h, 4.0 h, 6.0 h, 8.0 h, 10 h, 12 h, 24 h, and 36 h following oral administration of acteoside (100 mg/kg) in the three groups. Using a cryo-centrifuge, plasma samples were produced by centrifuging at 800 g for ten minutes at 4°C. After that, plasma samples were gathered and kept for later examination at −80°C.

2.4 Pharmacokinetic study

2.4.1 Calibration standards and quality control (QC) sample preparation

Accurately weighed acteoside, caffeic acid, and hydroxytyrosol (1.0 mg) were put to a 1.5 mL brown centrifuge container along with 1.0 mL cold 50% methanol to dissolve and thoroughly mix. A 4°C freezer was then used to make and store the stock solution (1 mg/mL). Moreover, 50% methanol was used to dilute 1 μg/mL of the IS working solution. Acteoside, caffeic acid, and hydroxytyrosol mother

liquor were successively diluted with 50% methanol to produce a mixed control series of working solutions at concentrations of 50, 250, 500, 1,000, 2,000, 5,000, 10,000 and 20,000 ng/mL. The brown centrifuge tube was filled with 5 μL of the preceding working solutions, 45 μL of blank plasma, vortexed, and combined for a minute to make standard curve samples containing acteoside, caffeic acid, and hydroxytyrosol at 5, 25, 50, 100, 200, 500, 1,000, and 2,000 ng/mL. As low, medium, and high dosage quality control samples, plasma samples with concentrations of 25, 200, and 1,000 ng/mL were employed. Before being analyzed, the entire set of QC samples were kept at −80°C.

2.4.2 Preparation of plasma samples

A centrifuge was used to get 100 μL of plasma specimens for 15 min at 4°C. Following this,20 μL of genistein (1 μg/mL IS) solution and 600 μL of cold acetonitrile were then included and centrifuged for 5 min, the mutant proteins were separated by vortexing for 5 min, and then they were spun down for 15 min at 4°C at 14,000 rpm. The supernatant was gathered and dried at 40°C with a light nitrogen stream. The dried remnant was then immersed in 100 μL of 25% aqueous acetonitrile fluid, and centrifugation was performed again for 10 min at 4°C at 14,000 rpm. Ultimately, the LC–MS/MS system was injected with 2 μL of the liquid for analysis.

2.4.3 UPLC-QqQ-MS analysis

A 1.7 μm and 2.1 × 100 mm I.D. ACQUITY UPLC BEH C18 column was used to separate the samples. 0.1 percent formic acid in water (solvent A) and acetonitrile (solvent B) formed the mobile phase, which had the following gradient: 0 to 4 min, 90–35% A; 4 to 5 min, 35–10% A; 5 to 6 min, 10–0% A; 6.1 to 10 min, 10% A. With a column temperature of 30°C, the flow rate was fixed at 0.3 mL/min.

In the mass spectrometry analysis, negative ionization mode was performed with the following optimized parameters: capillary voltage, 3.0 kV; desolvation temperature, 400°C. Nitrogen was used as desolvation and cone gas, at a flow rate of 800 and 30 L/h, respectively. The mass spectrometry research employed negative ionization mode, with optimum values of 400°C for the desolvation temperature and 3.0 kV for the capillary voltage. Nitrogen served as the cone gas and for desolvation, with flow rates of 30 and 800 L/h, respectively. Thus, multiple reaction monitoring (MRM) of the acteoside transitions at 623.37 → 161.02 *m/z*, caffeic acid transitions at 179.01 → 135.03 *m/z*, hydroxytyrosol transitions at 153.03 → 122.95 *m/z*,genistein transitions at 269.08 → 132.57 *m/z* was used for quantification. The cone voltage for acteoside, caffeic acid, hydroxytyrosol and genistein were 64 V, 32 V, 32 V and 56 V; 38 V, 14 V, 14 V, and 34 V were the collision energies. The mass spectra of acteoside, caffeic acid, hydroxytyrosol and genistein were shown in Figure 2. Data were processed using Masslynx workstation data acquisition and qualitative analysis software (4.1, Waters, USA).

2.4.4 Validation of methods

In compliance with the International Conference on Harmonization Harmonized Guideline Bioanalytical Method Validation M10 and the U.S. Bioanalytical Method Validation Guidance for Industry, method validation was carried out to evaluate selectivity, lower limit of quantification (LLOQ), linearity, accuracy, precision, matrix effects, extraction recovery, and stability of pharmacokinetic studies.

To investigate the possible interference of endogenous chemicals with four compounds in animal plasma, the method's selectivity was assessed. In order to accomplish this, different chromatograms were reviewed, including plasma specimens from six blank animals, blank animal plasma samples that had been mixed with an internal standard solution and control solution, and plasma samples that were taken 1.0 h after the rats had been given acteoside orally.

A concentration range of 5.00 ~ 2000.00 ng/mL was used to determine linearity. The level of the analytical substance was determined as the abscissa (X) by injecting three samples of each concentration of the standard solution. The ratio of the analytical substance's peak area to the IS in the sample served as the ordinate (Y) to establish the standard curve. The weighted least squares linear regression method was then used to obtain the regression equation (weighted factor = $1/x^2$) By gradually diluting QC samples at low concentration levels with a signal-to-noise ratio of 3:10, the limits of detection (LOD) and quantitation (LOQ) were ascertained. A minimum limit of quantification (LLOQ) is the lowest concentration on the standard curve and the lowest amount of analyte that can be quantified with a precision (relative standard deviation, RSD) of no more than 15% and an acceptable accuracy (relative error, RE) of 85% ~ 115%.

By producing six samples in parallel at each concentration and analyzing them over the course of 1 day or three consecutive days, respectively, QC samples at low, medium, and high concentrations were used to calculate the intra-day and inter-day precision and accuracy. Precision, defined as RSD, which is, should be below 15 %, and accuracy is measured by comparing the average analyte concentration with the nominal concentration. Within 15% of the nominal value is the acceptable range for the proportion of the deviation (RE) from the average from the nominal value.

The peak areas obtained for the QC samples at low, medium, and high concentrations that were subjected to the extraction procedure were compared with those obtained from blank plasma extracts that had been spiked post-extraction at the corresponding concentrations to estimate the extraction recovery in sets of six replicates of QC samples.

An examination of stability using QC samples at low, medium, and high doses. Short-term stability was measured by injecting samples after staying 4 h at room temperature (25°C). After preparation, the sample was kept at 4°C for 24 h, and the dosage was injected to ascertain the sample's stability. To determine long-term stability, samples were frozen at −80°C for 15 days before being injected. By thawing the samples three times in a row at room temperature and a freezer at −20°C, the freeze–thaw stability was ascertained.

2.4.5 Statistical and pharmacokinetic evaluation

Using the DAS program (Chinese Pharmacological Society, Beijing, China), pharmacokinetic parameters were estimated. Every data point is displayed as mean ±SD. With SPSS 16.0, a one-way ANOVA was carried out. p values less than 0.05 were deemed to indicate an important variation in the data.

Statistical analysis Using the DAS program (Chinese Pharmacological Society, Beijing, China), pharmacokinetic parameters were estimated. Every data point is displayed as mean ±SD. With SPSS 16.0, a one-way ANOVA was carried out. p values less than 0.05 were deemed to indicate an important variation in the data.

10.3389/fnut.2025.1509734

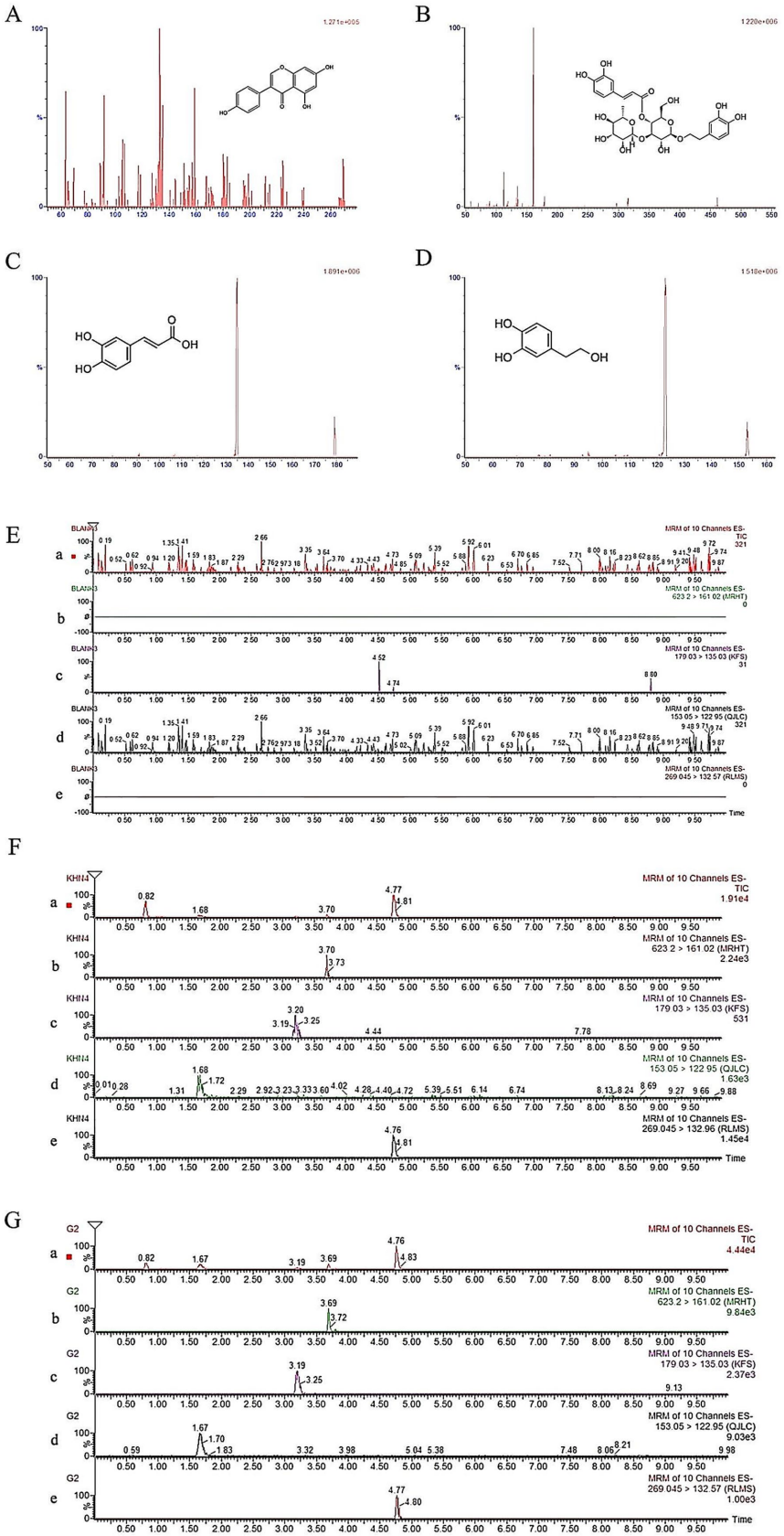

FIGURE 2
UPLC-QqQ-MS spectrums of genistein **(A)**, acteoside **(B)**, caffeic acid **(C)** and hydroxytyrosol **(D)** and instance chromatograms from blank plasma **(E)**, plasma spiking with analyte along with IS **(F)**, and plasma sample 1.0 h after acteoside oral administration **(G)** a: total ion current chromatogram; b: acteoside extract ion flow chromatogram; c: caffeic acid extract ion flow chromatogram; d: hydroxytyrosol extract ion flow chromatogram; e: genistein extract ion flow chromatogram.

Using the DAS program (Chinese Pharmacological Society, Beijing, China), pharmacokinetic parameters were estimated. Every data point is displayed as mean ±SD. With SPSS 16.0, a one-way ANOVA was carried out. p values less than 0.05 were deemed to indicate an important variation in the data.

2.5 Gut microbiota structural profiling

The CTAB technique was applied to extract the DNA. After being dissolved within 50 μL of elution buffer, the whole DNA remains freezing at −80°C. Universal primers were used for sequencing and individual barcods were added to the 5′ ends of the primers for each sample. A total of 25 μL of response mixture—which included 2.5 μL of each primer, 12.5 μL of PCR Premix, and 25 ng of target DNA—was used for the PCR amplification process. The first cycle of denaturation at 98°C for 30 s, the 32 cycles of denaturation at 98°C for 10 s, cooling at 54°C for 30 s, and extension at 72°C for 45 s, and the final elongation at 72°C for 10 min were the PCR settings used for amplified the microbiological 16S sequences.2% agarose gel electrophoresis was used to validate the PCR results. To eliminate the potential for false-positive PCR results as a negative control, ultrapure water was utilized during the DNA extraction procedure in place of an experiment solution. Qubit (Invitrogen, USA) was used to quantify the PCR products after they had been purified using AMPure XT beads (Beckman Coulter Genomics, Danvers, MA, USA). Prior to sequencing, the amplicon libraries were created, and the Agilent 2,100 Bioanalyzer (Agilent, USA) and the Library Quantification Kit for Illumina (Kapa Biosciences, Woburn, MA, USA) were used to measure the amplicon library's size and quantity. 250 bp paired-end reads were produced when the library was sequenced (Table 1) on the NovaSeq 6,000 platform.

TABLE 1 PCR primer sequences.

Region	Primers
V3-V4	341F(5′-CCTACGGGNGGCWGCAG-3′) 805R(5′-GACTACHVGGGTATCTAATCC-3′)
Archae	F(5′-GYGCASCAGKCGMGAAW-3′) R(5′-GGACTACHVGGGTWTCTAAT-3′)
V4	515F(5′-GTGYCAGCMGCCGCGGTAA-3′) 806R (5′-GGACTACHVGGGTWTCTAAT-3′)
V4-V5	F(5′-GTGCCAGCMGCCGCGG-3′) R(5′-CCGTCAATTCMTTTRAGTTT-3′)

2.6 Research on short-chain fatty acids (SCFAs)

Oral administration of WCP and UCP was conducted for 3 weeks in male Sprague–Dawley rats, respectively. On the twenty-second day of the trial, feces samples were gathered and promptly frozen at −80°C. Using gas chromatography (GC), the following SCFAs can be determined: acetic acid, butyric acid, decanoic acid, hexanoic acid, heptanoic acid, isovaleric acid, isobutyric acid, nonanoic acid, octanoic acid, propionic acid and valeric acid. The standardized parameters for SCFA measurements are shown in Supplementary Table S4, S5.

Enter 200 mg of feces into two milliliter EP tubes, extract with one milliliter of Milli-Q H_2O, and vortex combine for 10 sec. Pulverized in an iron ball crusher at 40 Hz for 4 min, followed by 3 repetitions of an ultrasonic treatment for 5 min while soaking in ice. At 5000 rpm and 4°C, centrifuge for 20 min. Add 0.1 mL of 50% H_2SO_4 and 0.8 mL of the extraction liquid (25 mg/L stock in methyl tert-butyl ether) as an internal standard. Swirl blend for 10 s, oscillate for 10 min, and then ultrasonic treat for 10 min (incubated in cold water). Deposit the 0.8 mL of supernatant into new 2 mL EP tubes. At 4°C and 10,000 rpm, centrifuge for 15 min. Retain approximately 30 min at −20°C. For GC–MS analysis, put the supernatant into a brand-new 2 mL container. Using the SHIMADZU-GC2030-QP2020-NX GC–MS, the HP-FFAP capillary column was linked. In (5:1) fractional mode, 1 μL was the injection volume. Helium serves as the carrier gas, and its front inlet purge flow rates are 3 3 mL·min^{-1} and 1 mL·min^{-1}, respectively. The predetermined heating mode was 80°C for 1 min, followed by a five-minute ramp to 200°C at 10°C/min and a one-minute ramp to 240°C at 40°C/min. The temperature of the ion source was 200°C, while the injection temperature was 240°C. Measurements from mass spectrometry were obtained in Scan/SIM mode with an electron's impact energies of −70 eV, covering the m/z range of 30–150 Da.

2.7 Bioinformatics analysis

Using the Illumina NovaSeq system, specimens were sequenced in accordance with the manufacturer's instructions. Sequence installation, data filtration, and barcodes and priming sequence cleavage in accordance with QIIME2 (18). After denoising using techniques like "DE-replication," which is comparable to clumping with 100% similarities, DADA2 (Divisive Amplicon Denoising Algorithm) technology was employed to create an OTU (Operational Taxonomic Units) database using the idea of ASVs (Amplicon Sequence Variants). After obtaining the final ASV characteristic tables and ASV characteristic sequence, the α-diversity index of the intestine microbe abundance (Observed_species and Chao1 indices) and community diversity (Shannon and Simpson indicators) were calculated and evaluated using the QIIME2. Bray-Curtis lengths are employed in β-diversity analysis to examine modifications to structure in communities of bacteria. The Linear Discriminant Analysis Effect Size technique is intended for the identification of biomarkers and for the evaluation of sequencing data. By comparing the species abundances of various groups, the groups with notable variations were identified. The Kruskal-Wallis rank-sum test was utilized to identify all characteristic species. To determine if all subspecies of the substantially different species found in the previous phase descended to the same biological level, the Wilcoxon rank-sum test was employed. The effect size of each differential gut microbiota and the traits linked to each group of rats were determined by linear discriminant analysis (LDA), and the R package ggcorrplot was used to accomplish the ultimate differential species. Using SPSS 22.0 carried out principal coordinate analysis (PCoA) correlation analysis. An ANOVA was used to examine the SCFA data. GraphPad Prism (GraphPad Prism version 5.1) was utilized for statistical examination and graphical representation of the data. To avoid false positive results, a Kruskal-Wallis test with Bonferroni correction was employed.

3 Results

3.1 Preparation and analysis of Cistanche polysaccharides

In this study, two *Cistanche deserticola* polysaccharides were obtained by complex enzyme extraction, dialysis, alcohol precipitation, washing and drying. Table 2 displays the composition of two polysaccharides. Using a glucose standard curve, the total sugar content of the specimen was ascertained. The results showed that after being steaming by rice-wine, the yield of polysaccharides increased, the total sugar content was higher, and the molecular weight decreased significantly. *Cistanche deserticola* polysaccharides are mainly composed of arabinose, galactose, glucose, and xylose. The proportion of xylose in UCP is higher than that in WCP, while the proportion of glucose and arabinose in WCP increases.

3.2 Effect of Cistanche polysaccharides on the pharmacokinetics of oral acteoside in rats

3.2.1 Method validation

The representative chromatograms of blank plasma, plasma samples spiked with the analytical substance and IS, and a plasma sample taken from a rat after acteoside was administered orally in Figure 2 demonstrated the method's selectivity by showing that there were no endogenous compound interference peaks in the chromatographic results and a good baseline resolution of the analyte acteoside, caffeic acid, hydroxytyrosol, and genistein (IS) at retention times of about 3.70 min, 3.19 min, 1.67 min, and 4.77 min, respectively.

Table 3 displayed the regression equations, linear ranges, correlation coefficients (R2), and LLOQs. Accuracy, precision, matrix effects, and extraction recoveries were shown in Table 4. In Table 3 excellent linearity across the concentration range was indicated by the R2 values for each regression equation above 0.994. The established technique for the measurement of analytes in rat plasma was found to be sensitive, as evidenced by the accuracy (RE, %) and precision (RSD, %) of the LLOQ for each analyte meeting the required standards. The analyte QC samples in Table 4 showed less than 15% intraday and interday accuracy and precision, demonstrating that the analytical approach is reliable and accurate for the pharmacokinetic investigations of analytes following oral acteoside administration. Caffeic acid, hydroxytyrosol, and acteoside extraction recoveries of QC samples ranged from 85.30 to 90.94% on average. There was no discernible matrix impact during the sample analysis, as indicated by the average matrix effect, which varied from 85.76 to 91.58%.

Table 5 displays the stability data, which comprise short-term, post-preparation, long-term, and freeze–thaw stability. Results reveal that the analytes in plasma samples show good stability in various circumstances.

3.2.2 Pharmacokinetic behaviors of acteoside

Acteoside's limited oral absorption, quick metabolism, and quick bodily excretion all lead to its incredibly low bioavailability. Acteoside's limited oral bioavailability makes it challenging for the drug to reach an exact concentration in the blood at the point of behavior, which restricts its biological activities. The majority of glycosides are digested in the gastrointestinal system by enzymes or microbes prior to being absorbed by the body (19). In order to clarify the gavage dose of acteoside and to explore its pharmacokinetic studies, the levels of acteoside and its two metabolite compounds in rat plasma were determined rapidly and reliably by UPLC-MS. In order to achieve acceptable resolution and symmetrical peak morphologies in a comparatively short analysis time, the chromatographic conditions were first optimized by column, mobile phase, and gradient elution methods. Following multiple optimization trials, the trio of compounds achieved a precise MS identification in under 10 min of well-separation on an ACQUITY UPLC BEH C18 (2.1 × 100 mm, 1.7 μm) column using a 0.1% formic acid-acetonitrile mobile phase. Scanners operating in MRM mode with an ESI-source were used to precisely and sensitively identify the chemical structures of the acteoside and its metabolites. To achieve the highest relative abundance of parent and product ions for various analytes, the MS/MS settings and collision energies (CE) were optimized.

Rats were given acteoside orally at a dose of 100 mg/kg, and the pharmacokinetic analysis of this dosage was effectively conducted using the approved methodology. Figure 3 displayed the acteoside mean plasma concentration-time curve. The DAS system (Chinese Pharmacological Society, Beijing, China) was utilized for pharmacokinetic analysis, which involved calculating the maximum plasma concentration after administration (C_{max}), drug half-life ($t_{1/2}$), drug peak time (T_{max}), and area under the plasma concentration-time curve (AUC). A two-compartment open model (weight = 1/cc) provided the best match to the primary pharmacokinetic parameters

TABLE 2 The compositions of cistanche polysaccharides.

Samples	Yield (%)	Total sugar (%)	Protein (%)	Molecular weight (kDa)	Monosaccharide constitutions (%)			
					Ara	Gal	Glc	Xyl
UCP	22.82	58.10	3.95	22.868	2.15	8.62	15.86	2.98
WCP	25.02	63.60	3.71	3.315	3.55	7.56	18.13	0.46

TABLE 3 Analytes in rat plasma: linearity and LLOQs.

Compounds	Calibration curve regression equation	R^2	Linear range (ng/ mL)	LLOQ (ng/ mL)
Acteoside	Y1 = 0.217351X1−2.9291	0.9983	5.00~2000.00	5
Caffeic acid	Y2 = 0.425741X2+3.72924	0.9971	5.00~2000.00	5
Hydroxytyrosol	Y3 = 0.401161X3+0.176857	0.9943	5.00~2000.00	5

TABLE 4 Measurements in rat plasma: exactness, consistency, matrix influence, and extraction recovery.

Compounds	Concentration (ng/mL)	Intra-day			Inter-da			Extraction recoveries (%)	Matrix effect (%)
		Mean ± SD (ng/mL)	Precision RSD (%)	Accuracy RE (%)	Mean ± SD (ng/mL)	Precision RSD (%)	Accuracy RE (%)		
Acteoside	25	27.61 ± 1.01	3.66	10.51	28.29 ± 1.12	3.96	10.71	88.79 ± 2.55	86.98 ± 7.13
	200	203.53 ± 0.96	0.47	5.09	205.44 ± 3.59	1.75	4.15	89.33 ± 3.62	88.18 ± 8.07
	1,000	1001.24 ± 0.94	0.094	0.12	1002.31 ± 4.21	0.42	0.11	88.79 ± 2.55	85.76 ± 10.23
Caffeic acid	25	23.13 ± 1.17	5.07	10.59	22.09 ± 1.18	5.33	10.44	85.30 ± 4.32	87.42 ± 4.71
	200	198.24 ± 0.63	0.32	5.11	197.67 ± 3.85	1.95	5.35	87.65 ± 5.04	86.09 ± 6.59
	1,000	999.35 ± 1.59	0.16	0. 40	997.55 ± 4.29	0.43	0.12	87.99 ± 3.14	85.78 ± 9.13
Hydroxytyrosol	25	22.25 ± 0.85	3.84	10.77	23.17 ± 1.07	4.63	10.04	89.79 ± 6.05	89.98 ± 2.36
	200	202.54 ± 3.22	1.59	5.21	201.33 ± 4.29	2.13	6.51	90.94 ± 4.35	91.34 ± 7.03
	1,000	1001.71 ± 2.8	0.28	0.31	1002.9 ± 2.11	0.21	0.23	89.45 ± 6.55	91.58 ± 5.37

TABLE 5 Stability of analytes under different storage conditions (n = 6).

Compounds	Concentration (ng/mL)	Short-term stability (RSD,%)	Post-preparation stability (RSD,%)	Long-term stability (RSD,%)	Freeze–thaw stability (RSD,%)
Acteoside	25	6.91	7.03	8.28	7.93
	200	3.15	3.46	6.67	4.56
	1,000	2.79	3.68	4.99	4.45
Caffeic acid	25	7.78	8.33	9.75	9.14
	200	7.34	7.87	8.56	8.23
	1,000	4.91	6.87	8.43	7.08
Hydroxytyrosol	25	5.34	6.32	7.78	7.04
	200	3.26	4.89	5.86	5.78
	1,000	2.44	3.21	4.63	4.24

10.3389/fnut.2025.1509734

given in Table 6 based on the Akaike Information Criterion (AIC) and R^2 values. The values of acteoside AUC (0-t), AUC (0-∞), T_{max} and C_{max} in the plasma of rats administered with Cistanche polysaccharides were significantly higher than those of contral group. The mean C_{max} of acteoside in WCP, UCP and Control groups was 1592.34 μg/L, 1031.34 μg/L and 863.45 μg/L, respectively, which was 1.84 times higher in WCP group and 1.19 times higher in UCP than control group. In addition, both T_{max} and $t_{1/2}$ of acteoside were prolonged in the WCP and UCP groups compared to the control group. The $t_{1/2}$ of the WCP group was 1.18 times higher than that of the UCP group.

3.2.3 Pharmacokinetic behaviors of metabolites from acteoside

A total of 11 metabolites, including hydroxytyrosol, hydroxytyrosol sulfate conjugation, caffeic acid, etc., have been found as a result of numerous investigations that have demonstrated the stability of acteoside in modeled gastric and intestinal liquids and its metabolism in human intestinal flora. These metabolites can be produced by eight different metabolic processes, such as deglycosylation, rhamnose removal, and hydroxytyrosol removal (20). Figure 4 displays the average plasma concentration-time curves of hydroxytyrosol and caffeic acid in the plasma of the three groups of rats following oral acteoside delivery. Figure 4A shows that, within 4 h, the WCP group's caffeic acid content was higher than that of the UCP group and the control group. This suggests that a greater amount of acteoside in the WCP group was hydrolyzed and converted to caffeic acid through metabolism. Furthermore, as Figure 4B illustrates, within a 2-h period, the WCP and UCP groups showed higher levels of hydroxytyrosol presence than the control group. The hydroxytyrosol mean plasma concentration-time curve revealed that the pharmacokinetic curve displayed a double-peak phenomena with a brief peak time interval. The quick metabolism of acteoside in the liver following absorption-acteoside is transformed into the secondary metabolite hydroxytyrosol and subsequently released into plasma-may account for the second peak (21). Table 7 demonstrates that the UCP group's $t_{1/2}$ for caffeic acid was longer than that of the control group, and that the WCP and UCP groups' AUC (0-∞) and C_{max} values for both caffeic acid and hydroxytyrosol were considerably greater than those of the control group. Compared to the UCP group, the WCP group's C_{max} for caffeic acid was 1.26 times higher, and the C_{max} of hydroxytyrosol was 1.61 times that of the UCP group.

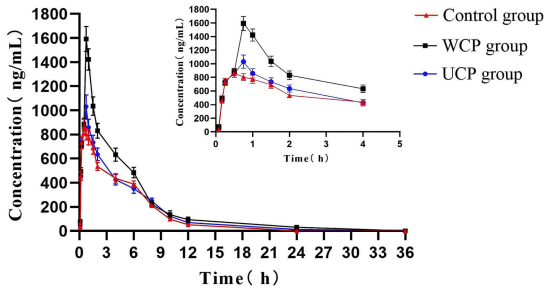

FIGURE 3
Acteoside's mean plasma concentration-time profiles in rats following oral administration.

3.3 Effect of Cistanche polysaccharides on the composition and diversity of gut microbiota

Using 16S rRNA gene sequencing research to assess the impact of WCP and UCP on the microbiota in the gut. After splicing, an overall of 1.333.424 valid tags were produced; 453,507 tags in the control group, 435,105 tags in the UCP group, and 444,812 tags in the WCP group were subjected to assurance of quality and chimeric screening (Supplementary Table S1). After denoising by the DADA2 method (22), 3,148 amplicon sequence variant (ASV) numbers of ASVs in the three groups sequences were generated. The Venn diagram (Figure 5A) illustrates the different. Of all ASVs in this work, 953 ASVs were shared by three groups. In addition, 2,743 ASVs were detected in WCP group, while no was detected in control group, and 2,247 ASVs were detected in UCP group. However, different groups had their own separate sets of ASVs: the UCP group was 1930, the WCP group was 2,426, and the control group was 1,677. Simultaneously, there were 3,314, 3,512 and 4,068 ASVs each in control group, UCP group and WCP group. This implies that the species richness of the rat gut microbiota was enhanced by Cistanche polysaccharides.

3.3.1 Examining the variations in the gut microbiome structure

When examining the microbial community's composition in intestinal fecal samples, *α*-and *β*-diversity are frequently employed to assess the microbial community's variation, complexity, and population makeup. When examining the microbial community's composition in intestinal fecal samples, α- and β-diversity are frequently employed to assess the microbial community's variation, complexity, and population makeup. With the use of the indices of Chao1, Observed species, Goods_coverage, Shannon, Simpson, and pielou-e, α-diversity primarily represents the richness and

TABLE 6 Acteoside's mean pharmacokinetic characteristics following oral treatment (100 mg/kg) in rats (n = 6).

Parameters	Unit	Control	UCP	WCP
AUC(0-t)	ug/L*h	4202.886 ± 153.241	4978.446 ± 230.543	6656.577 ± 542.814
AUC(0-∞)	ug/L*h	4356.133 ± 129.766	5051.794 ± 266.616	6689.322 ± 632.723
MRT(0-t)	h	3.942 ± 0.165	4.938 ± 0.165	4.996 ± 0.032
MRT(0-∞)	h	4.337 ± 0.512	5.294 ± 0.629	5.598 ± 0.837
$t_{1/2}$	h	2.062 ± 1.296	3. 237 ± 1.431	3. 804 ± 1.763
T_{max}	h	0.50	0.75	0.75
C_{max}	ug/L	863.45 ± 63.43	1031.34 ± 98.32	1592.34 ± 103.21

homogeneity. Chao1 and Observed_species provide an estimate of the number of species present in a community, which is known as abundance. Microbial coverage is expressed in Goods_coverage, which requires the coverage index to be equal to 1, that is, most of each base in the genome of the sample to be tested can be sequenced. The Pielou-e index represents evenness, while the Shannon and Simpson indices suggest diversity. Figures 5B-G shows that all five indices in the WCP group were considerably higher than those in the control group ($p < 0.05$), indicating that the administration of WCP improved community homogeneity and richness. The gut microbiota's diversity was found to be improved by UCP, as evidenced by the greater Shannon and Simpson indices of the UCP group compared to the control group ($p < 0.05$). Conversely, when comparing the UCP group to the control group, there were no appreciable changes in any of the three indexes of Chao1, Observed species, and Pielou-e. This suggested that the UCP intervention had no discernible impact on the diversity of the gut microbiome. β-diversity is a measure of the variations in species between environmental communities. To perform β-diversity analysis, the distance matrix between any two samples in the environment must be calculated. Principal coordinate analysis (PCoA) (23) and cluster analysis (UPGMA) (24) are then used to identify sample differences. Figure 5H displays the findings of the PCoA analysis using the feature sequence, which is able to differentiate characteristics between various groups. The samples from the control group and the WCP group were separated by a considerable amount, suggesting that the two groups' microbial structures and compositions were very different from one another. There was little variation in the microorganism structure and makeup of the UCP group and the control group, as evidenced by the close spacing between the samples in the two groups. The clustered tree grouping in the UPGMA diagram is represented by branches of different colors. The shorter the branch length, the more similar the two samples are, and the higher the similarity of the samples. Figures 5H,I illustrates how distinct the WCP group and the control group are from each other, and this visualization of the data could be used to graphically represent how the microbial evolution of the two groups is unique, suggesting that the WCP has the ability to regulate the intestinal flora of normal rats.

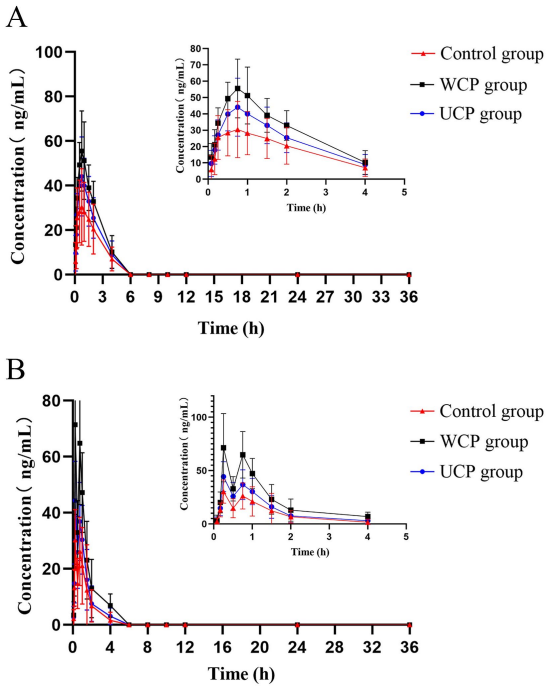

FIGURE 4
After oral delivery, mean plasma concentration-time profiles containing hydroxytyrosol **(B)** and caffeic acid **(A)** in rats.

3.3.2 Evaluating the gut microbiota's composition

In the three groups, totals of 23 different phyla of gut microbiota were identified., and the phylum data with significant differences are shown in Supplementary Table S2. Among them *Firmicutes*, *Bacteroidota*, *Actinobacteriota*, *Campylobacterota*, *Desulfobacterota*, *Proteobacteria*, *Patescibacteria*, *Cyanobacteria*, *Verrucomicrobiota* are

TABLE 7 Average pharmacokinetic characteristics of metabolites following oral acteoside delivery (100 mg/kg) in rats (n = 6).

Analytes	Parameters	Unit	Control	UCP	WCP
Caffeic acid	AUC(0-t)	ug/L*h	76.094 ± 13.35	99.992 ± 17.68	124.683 ± 25.89
	AUC(0-∞)	ug/L*h	109.781 ± 15.36	117.183 ± 13.35	143.676 ± 26.67
	MRT(0-t)	h	1.564 ± 0.172	1.539 ± 0.166	1.525 ± 0.161
	MRT(0-∞)	h	2.508 ± 0.273	2.182 ± 0.267	2.098 ± 0.256
	t1/2	h	2.166 ± 0.693	1.329 ± 0.824	1.289 ± 0.914
	T_{max}	h	0.75	0.75	0.75
	C_{max}	ug/L	30.43 ± 14.22	44.09 ± 15.75	55.54 ± 16.89
Hydroxytyrosol	AUC(0-t)	ug/L*h	40.596 ± 3.243	56.452 ± 5.413	90.562 ± 6.728
	AUC(0-∞)	ug/L*h	42.519 ± 4.243	60.485 ± 5.722	91.323 ± 6.925
	MRT(0-t)	h	1.203 ± 0.132	1.186 ± 0.124	1.266 ± 0.139
	MRT(0-∞)	h	1.383 ± 0.145	1.461 ± 0.153	1.536 ± 0.168
	t1/2	h	0.813 ± 0.129	0.908 ± 0.106	0.537 ± 0.116
	T_{max}	h	0.25	0.25	0.25
	C_{max}	ug/L	30.32 ± 10.92	44.36 ± 14.02	71.43 ± 32.02

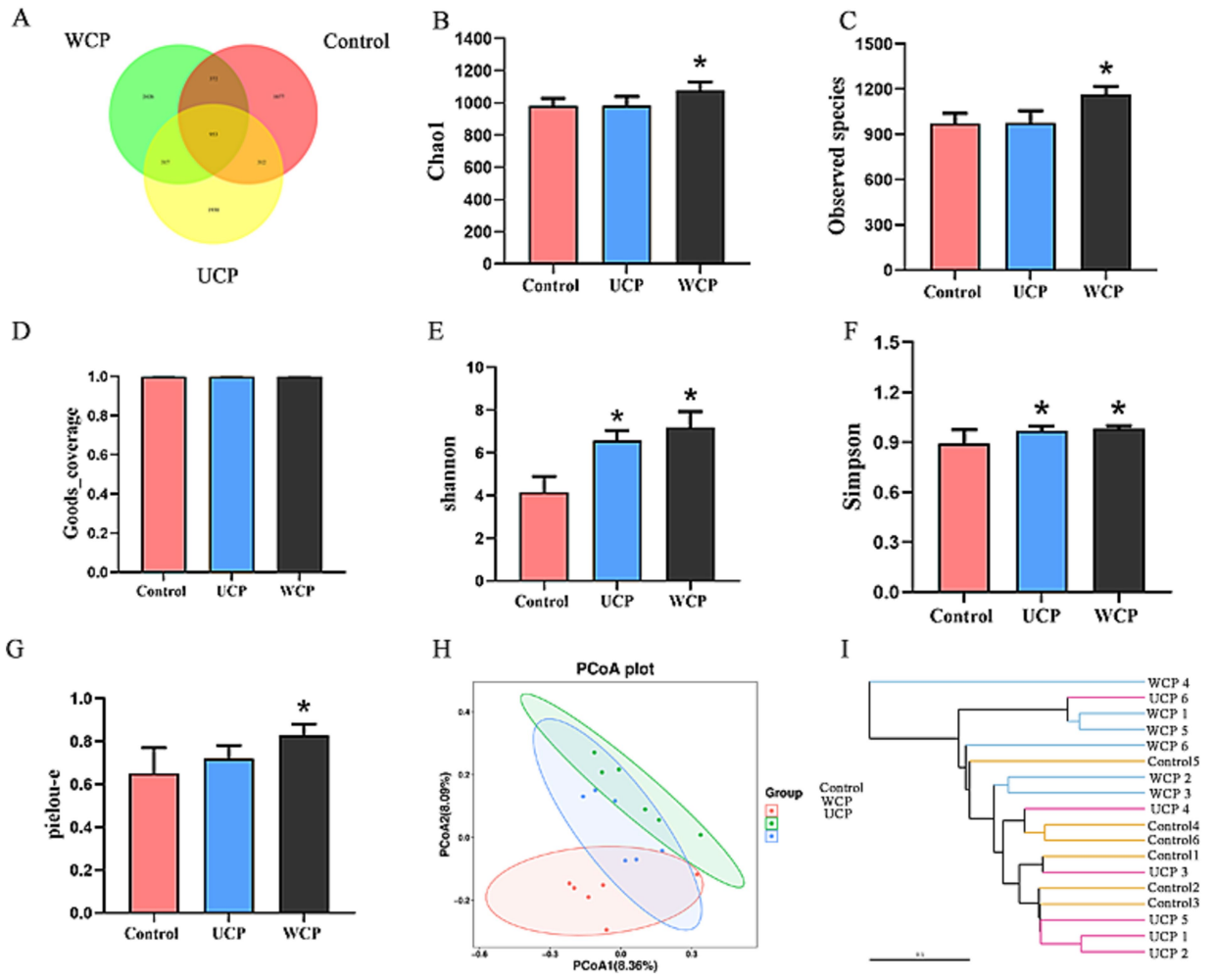

FIGURE 5
Venn diagram showing the composition of the intestinal microbiota in the WCP, UCP, and Control groups **(A)**; Effect of Cistanche polysaccharides on gut microbiota α-diversity: Chao1 index **(B)**, observed species index **(C)**, Goods_coverage index **(D)**, shannon index **(E)**, Simpson index **(F)** and pielou-e index **(G)**.The data is shown as mean ± SD (n = 6). Using SPSS (version 33.0) software, one-way ANOVA and the independent-samples Kruskal-Wallis test were used to identify significant differences. *$p < 0.05$ vs. Control group; Impact of Cistanche polysaccharides on the β-diversity of the gut microbiota: PCoA analysis adopting the unweighted UniFrac distances **(H)** and UPGMA applying the weighted UniFrac distance-based methods **(I)**. Six samples were represented by each plot.

the main phylum. As Figures 6A,B illustrates, the distribution of these phylums is different among the three groups. Furthermore, the WCP group had a higher number of species detected at the phylum level than control group and the *Elusimicrobiota* phylum was newly added to the WCP. The abundance of *Firmicutes*, *Actinobacteriota*, *Patescibacteria*, *Cyanobacteria*, and *Verrucomicrobiota* increase during the same period. At the genus level, 31 genera of gut microbiota have been discovered, and the data with significant differences are shown in Supplementary Table S3. The groups WCP and UCP can increase *Bifidobacterium*, *Romboutsia* and decrease the *Lachnospiraceae_NK4A136_group* to varying degrees. *Ligilactobacillus* and *Duncaniella* were observed to be considerably higher in the WCP group according to the control group (Figures 6C–F).

3.3.3 PICRUSt2 predicting function prediction

Microbiota and function were "mapped" with PICRUSt2 (25). The PICRUSt2 program was utilized to estimate the function based on the species annotation and OTU abundance data from the database. The samples were functionally annotated with KEGG COG, EC, KO, PFAM, TIGRFAM pathways, and STAMP was employed to do the comparison analysis. Figure 6G displays the prediction results with $p < 0.05$. With respect to abundance, the Cistanche polysaccharide-administered WCP and UCP groups were found to be more abundant than the Control group in the following pathways: TCA cycle I (prokaryotic), L-alanine biosynthesis superpathway, UDP-N-acetylglucosamine-derived O-antigen building blocks biosynthesis superpathway and peptidoglycan biosynthesis II (staphylococci).These pathways directly affect the metabolism of acteoside or lead to the production of metabolites into the bloodstream and exert pharmacological effects.

3.4 Effect of Cistanche polysaccharides on short-chain fatty acids (SCFAs) of rats

Figure 7A illustrates that following 21 days of Cistanche polysaccharide administration, the levels of acetic acid, propionic acid,

10.3389/fnut.2025.1509734

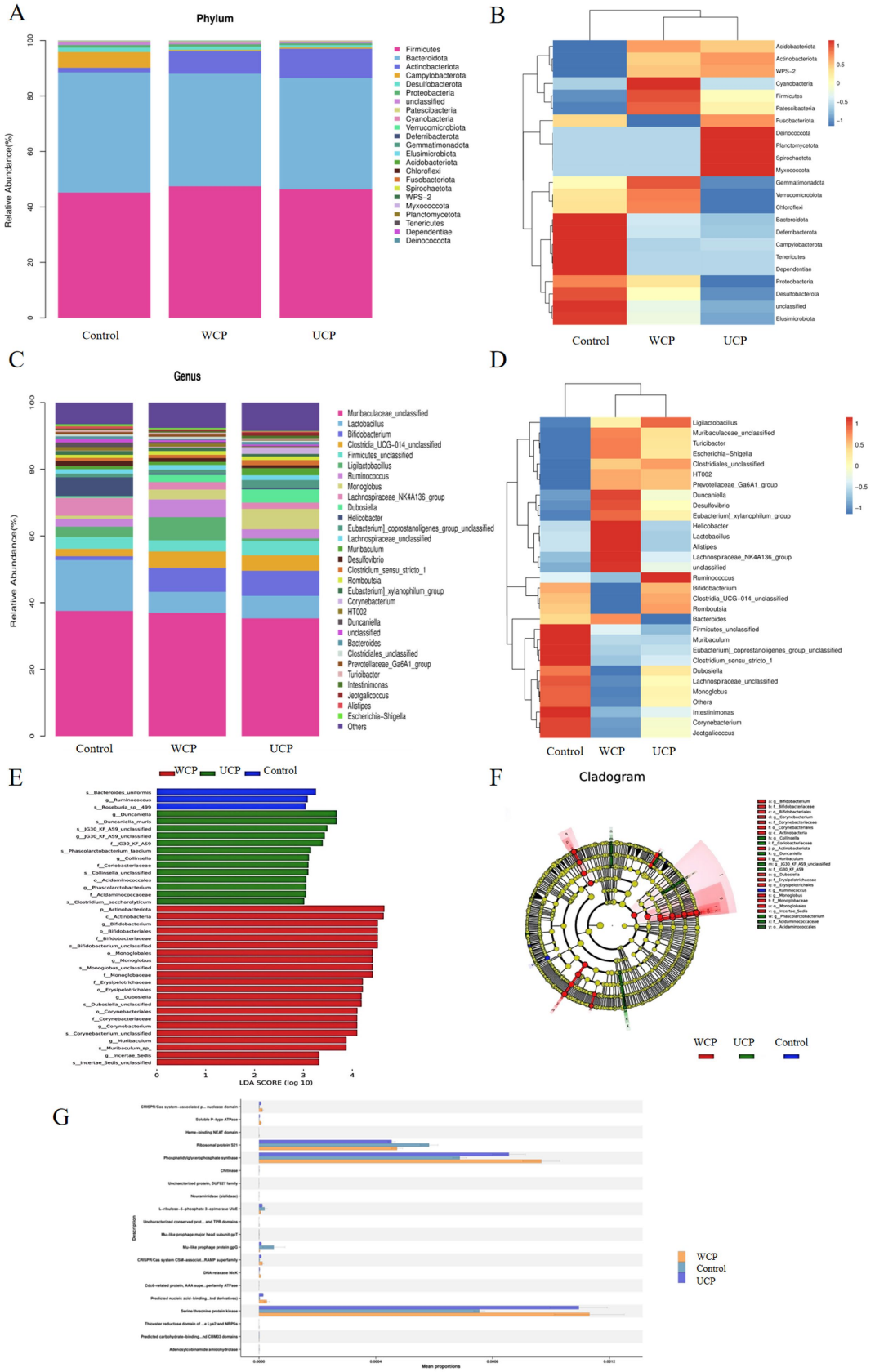

FIGURE 6
Relative abundance of the phylum-level microbial makeup **(A)**. A heatmap displaying the corresponding abundances of a given phylum, highlighting notable variations within each group **(B)**. The microbial composition's proportions divided based on genus **(C)**. A heatmap showing the corresponding

(Continued)

FIGURE 6 (Continued)
abundances of specific specified genera, with notable variations between each group **(D)**. Linear discriminant analysis (LDA) effect sizes were used to examine variations in microbial taxa among the three groups **(E)**. The taxa that belong in each group with the greatest differential abundance are indicated by LEfSe plots. **(F)**; PICRUSt2 functional annotation of pathway **(G)**. *n* = 6.

isobutyric acid, butyric acid, isovaleric acid, valeric acid, and octanoic acid were significantly elevated ($p < 0.05$) in the WCP group compared to the control group; the levels of acetic acid, propionic acid, isobutyric acid, butyric acid, isovaleric acid, valeric acid, and octanoic acid ($p < 0.05$) in the UCP group increased significantly than those in the control group (Figures 7B–L) but lower than those in the WCP group. The findings demonstrated that the intake of WCP and UCP both enhanced the quantity of SCFAs in the rat intestinal tract and could have improved the low bioavailability of oral acteoside in the gut. The effect of WCP is better than that of UCP.

In addition, the relationship between SCFA and gut microbiota was assessed. Figure 7M illustrates this relationship. SCFAs had a positive correlation ($p < 0.05$) with *Corynebacterium*, *Lactobacillus*, and *Muribaculum*, however a negative correlation ($p < 0.05$) with the gut microbes *Bacteroides*, *Ruminococcus*, *Turicibacter* and *Subdolilegum*.

4 Discussion

Cistanche deserticola is used as both food and medicine in China. Chemical analysis showed phenylethanoid glycoside and polysaccharides were the main active constituents. Acteoside, the main phenylethanoid in *Cistanche deserticola*, has anti-oxidation, sex hormones regulation (26), neuroprotective (27) and anti-inflammatory (28) biological activities, However, its druggability is limited due to the poor bioavailability, fast and extensive metabolism *in vivo*. Non-digested polysaccharides can serve as carriers or excipients in drug delivery systems, inhibiting the degradation of glycoside drugs in the intestine, improving drug absorption, increasing drug solubility, and enhancing drug bioavailability in vivo, achieving synergistic efficacy enhancement of drug (29). Cistanche polysaccharides induce core changes in the composition and diversity of intestinal microbiota and promote the absorption of echinacoside *in vivo* (30). Ginseng polysaccharides enhance ginsenoside Rb1 intestinal absorption by enhancing gut microbial metabolism and exposure to microbial metabolites (9). Soybean soluble polysaccharides modulate gut microbes and enhance the absorption of genistein in soybean in mice (31). These studies show that polysaccharides can promote the absorption of small molecule *in vivo* by regulating the diversity of the gut microbiota.

Chemical analysis of Cistanche polysaccharides showed that there was no significant change in the protein content of polysaccharides after rice-wine process. The total sugar content increased from 58.1 to 63.6%, and sugar yield increased from 22.82 to 25.02%. The increase of polysaccharide yield after being processed may be related to the hydrolysis of polysaccharides during the rice-wine steaming process (32, 33). The molecular weight for UCP and WCP was 22.868 kDa and 3.315 kDa separately. Results showed a significant change in the proportion of monosaccharide composition, with an increase in Glc and Ara content and a decrease in Gal and Xyl ratio in the WCP group.

Pharmacokinetic studies have shown that C_{max} of acteoside increased by 1.19 times and 1.84 times, AUC(0-∞) increased by 1.16 times and 1.54 times after oral administration of UCP and WCP, respectively. According to literature reports, acteoside may generate caffeic acid, hydroxytyrosol, and 3-HPP through ester and glycosidic bond cleavage *in vivo* (34–37) (Figure 8) The C_{max} of caffeic acid in plasma increased by 1.45 times and 1.83 times, and the AUC(0-∞) increment rate can reach 142 and 214% times for hydroxytyrosol. Administration of WCP significantly increased the level of absorption of acteoside and its metabolites *in vivo*.

Cistanche polysaccharides induced core changes in abundance and diversity of gut microbiota. After 21 days of administration of WCP and UCP, there were differences in the composition and structure of the gut microbiota in rats. The abundance of *Firmicutes*, *Actinobacteriota*, *Patescibacteria* in WCP and UCP group was significantly increased, while the *Elusimicrobiota* phylum was newly added to the WCP. Gut *Firmicutes* has an important role in health, it is one of the main phylum in the human intestine (38), *Firmicutes* establishes a symbiotic relationship with the host through innate tolerance and resistance to control systemic immunity and avoid widespread inflammatory damage (39). The *Elusimicrobiota* phylum has been found to promote fatty acid and amino acid synthesis, and ultimately improve the growth (40). *Firmicutes* may have great potential in the treatment of metabolic and inflammatory diseases (41), suggesting that Cistanche polysaccharide administration promotes intestinal *Firmicutes* supplementation and thus exerts anti-inflammatory effects. Level of *Genus Bifidobacterium* and *Romboutsia* in WCP and UCP groups increased. *Bifidobacterium* as a type of intestinal degrading bacteria, maintains the balance of the intestinal environment and protects the host (42). *Romboutsia* can reduce the occurrence of inflammatory reactions (43). Reduced abundance of *Lachnospiraceae_NK4A136_group* in the WCP and UCP groups compared to the control group. High level of *Lachnospiraceae_NK4A136_group* can be observed in intestinal barrier damage rats induced by high-fat diet (HFD). Low levels of *Lachnospiraceae_NK4A136_group* can reduce the risk of intestinal pathogen colonization and inflammation (44). *Ligilactobacillus*, which is significantly increased in the WCP group, is a beneficial bacterium with anti-inflammatory effects both *in vivo* and *in vitro* (45). The WCP group significantly increased the abundance of *Duncaniella*. *Duncaniella* has been shown to protect the host from DSS-induced inflammatory colonic injury (46). These results show that the wine-processed *Cistanche deserticola* polysaccharides may regulate intestinal microorganisms and enhance anti-inflammatory ability.

The products of polysaccharides decomposition and metabolism by gut microbiota play an important role in various metabolic processes of the body. Intestinal flora decomposes polysaccharides by secreting enzymes (glycoside hydrolase, lyase, and esterase), produces short-chain fatty acids (SCFAs) including formic acid, acetic acid, propionic acid, and butyric acid (47). Cistanche polysaccharides improve intestinal microbiota disorders by influencing the structure and function of intestinal microbiota, inducing beneficial bacteria to produce a variety of metabolites such as short-chain fatty acids (SCFAs). Our experimental results showed that the content of acetic acid, butyric acid, propionic acid and isobutyric acid significantly increased in the WCP group.

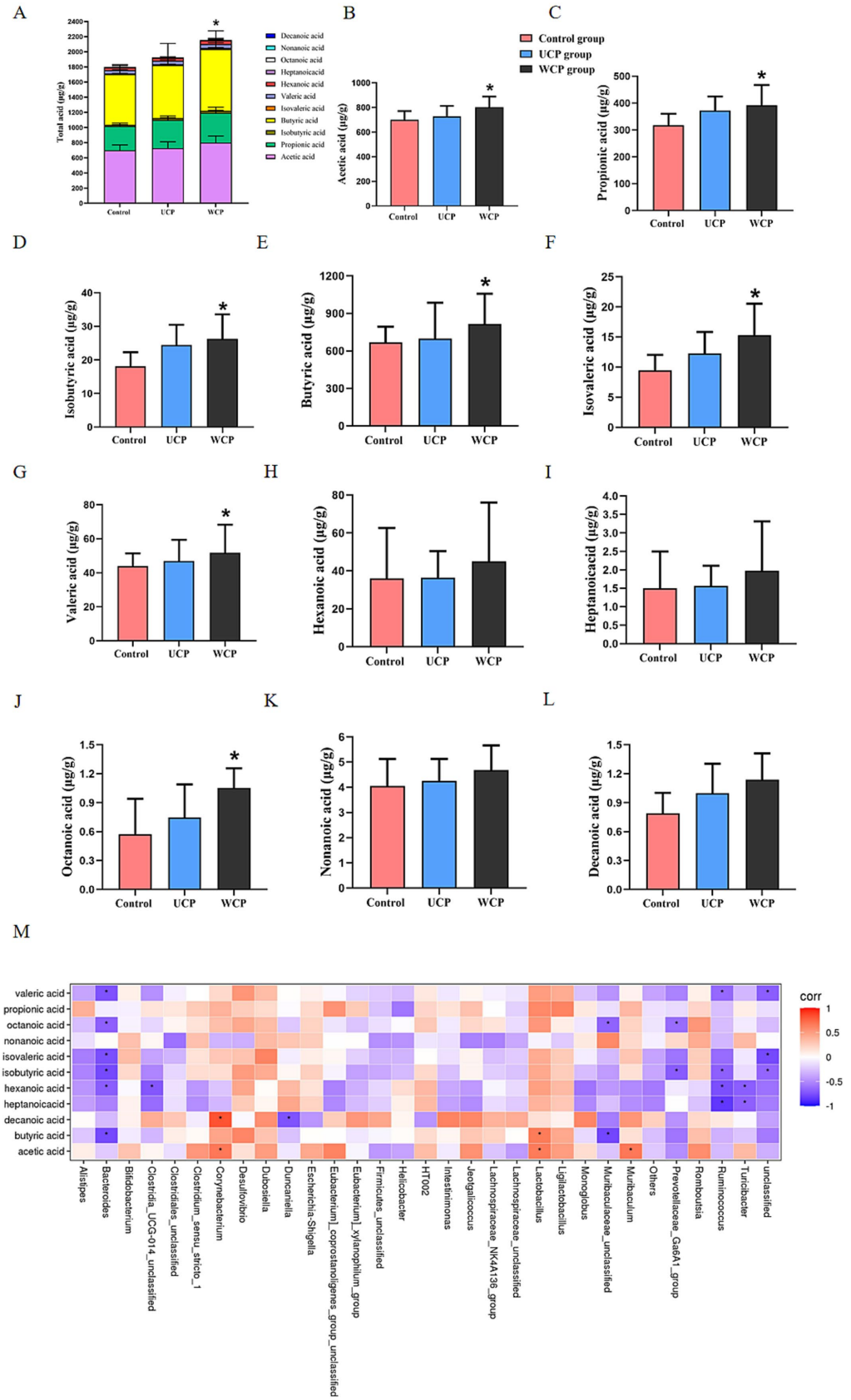

FIGURE 7
Cistanche polysaccharides administration increased the production of microbial SCFA metabolites. Measured by GC–MS in the stool of the Control, UPS, and WPS groups, **(A)** Total acid, **(B)** Acetic acid, **(C)** Propionic acid, **(D)** Isobutyric acid, **(E)** Butyric acid, **(F)** Isovaleric acid, **(G)** Valeric acid,

(Continued)

FIGURE 7 (Continued)
(H) Hexanoic acid, **(I)** Heptanoicacid, **(J)** Octanoic acid, **(K)** Nonanoic acid, **(L)** Decanoic acid, and **(M)** Correlation heat map between fecal microbiota and fecal SCFAs content after Cistanche polysaccharides administration. ANOVA was used to establish significance, and values were reported as mean ± SD. *$p < 0.05$ in comparison to the control group.

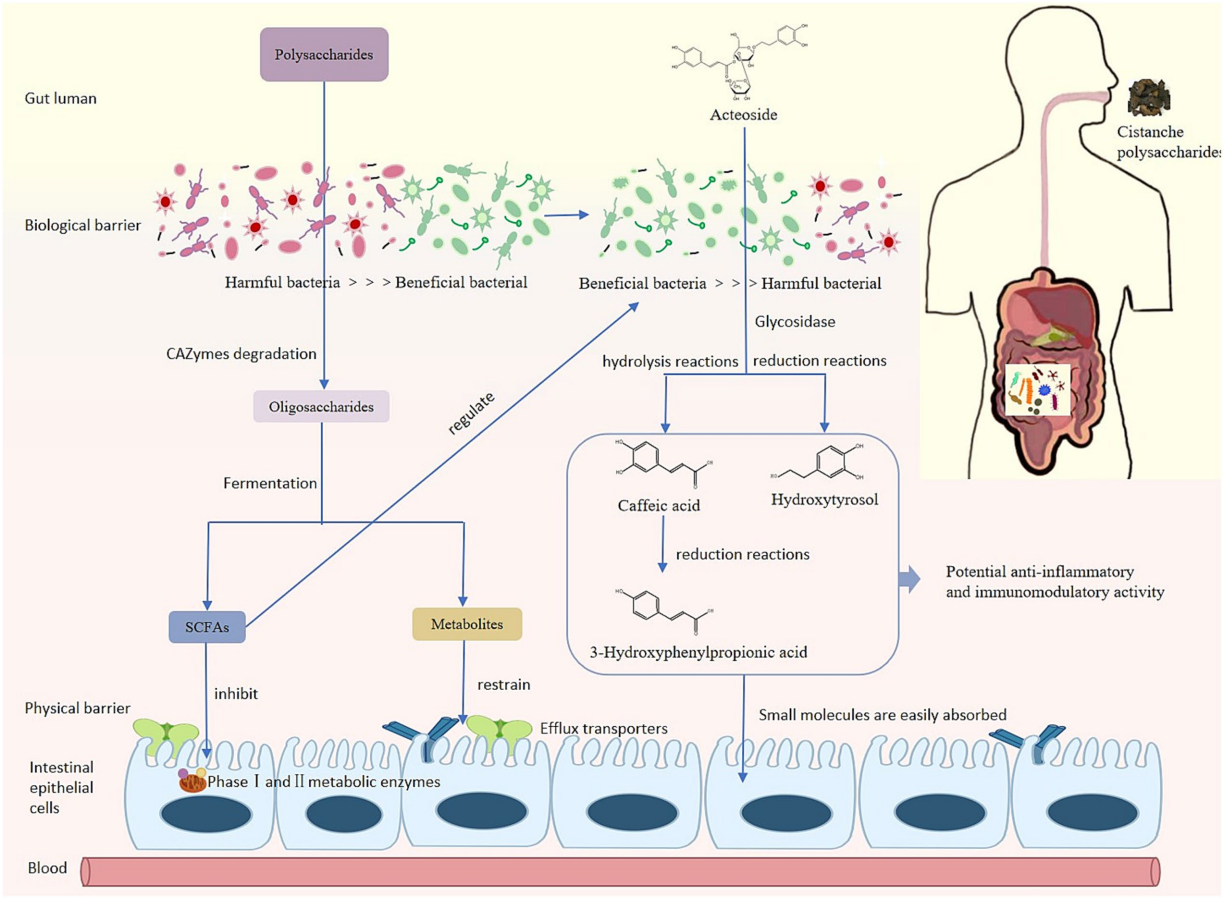

FIGURE 8
Metabolism process of phenylethanoid glycosides *in vivo*.

Many factors affect the level of SCFAs in the feces, including the composition and the amount of gut microbiota, the dietary source (48). Accumulating studies shows that polysaccharides structure, including composition of monosaccharide residues, degree of polymerization, both can affect fermentation properties and SCFAs production (49). From our results, we illustrated that Cistanche polysaccharides modulate SCFAs production and polysaccharides of different processed products have different effect.

The correlation analysis showed that *Corynebacterium*, *Lactobacillus*, and *Muribaculum* were positively correlated with SCFAs, while *Bacteroides*, *Ruminococcus*, *Turicibacter* and *Subdolilegum* were negatively correlated. Butyric acid and propionic acid are produced by glycolysis of carbohydrates in the intestine through the action of *Firmicutes*; *Bacteroides* contribute to the formation of acetic acid and propionic acid in the intestine. Butyrate can regulate the intestinal immunity and inflammatory response of epithelial cells through inhibition of histone deacetylases (HDACs) and induction of anti-inflammatory cytokine expression (50), propionate exerts an immunomodulatory mechanism in acute myeloid leukemia by inducing ferroptosis (51). In this experiment, the content of butyrate and propionate was significantly increased in the WCP group. Cistanche polysaccharides, particularly wine-processed products, demonstrate prebiotic-like activity through SCFA-mediated immunomodulatory pathways that enhance acteoside bioavailability, optimize gut barrier integrity, and facilitate small molecule absorption via microbiota-mediated metabolic activation.

5 Conclusion

In this work, we developed a quick and easy-to-use UPLC-QqQ-MS technique and effectively used it to investigate the acteoside pharmacokinetics in rat plasma following oral administration of Cistanche polysaccharides. This study indicated that 21 days

continuous administration of Cistanche polysaccharides can improve the composition and structure of intestinal microbiota, especially increased the level of *Ligilactobacillus* and *Duncaniella*, then promote the absorption of acteoside and its metabolites caffeic acid and hydroxytyrosol. The effect of WCP is superior to that of UCP. Comparative analysis revealed that both WCP and UCP exert comparable prebiotic-like effects on intestinal microbiota modulation, with WCP demonstrating superior capacity for short-chain fatty acid production and immune-enhancing bioactivities. They also promote higher C_{max} of acteoside and their metabolites, which is an effective way to enhance small molecule absorption and metabolism. In the further research, to clarify the mechanism by which polysaccharides from *Cistanche deserticola* increase the metabolism and absorption of small compounds *in vivo*, we will concentrate on the regulatory effects of the second phase metabolic enzymes and transporters of efflux in the inrastinal tract. In addition, we will examine gender bias and extended intervention time to assess the long-term effects of Cistanche polysaccharides on the microbiota and sustained improvement in bioavailability.

Data availability statement

The original contributions presented in the study are included in the article/Supplementary material, further inquiries can be directed to the corresponding authors.

Ethics statement

The animal study was approved by The Research Ethics Committee of Liaoning University of Traditional Chinese Medicine has granted the ethical approval of animal participation in this study. (Approval No. 2020067). The study was conducted in accordance with the local legislation and institutional requirements.

Author contributions

JL: Writing – original draft, Writing – review & editing. YZ: Conceptualization, Writing – review & editing. KD: Data curation, Writing – review & editing. JS: Funding acquisition, Investigation, Supervision, Writing – review & editing. FZ: Formal analysis, Writing – review & editing. GS: Project administration, Writing – review & editing. PL: Supervision, Writing – review & editing. NW: Methodology, Writing – review & editing. TJ: Validation, Writing – review & editing.

Funding

The author(s) declare that financial support was received for the research and/or publication of this article. This work was supported by the National Natural Science Foundation of China (81874345) and the Natural Science Foundation of Liaoning Province (2020-MS-223).

Conflict of interest

The authors declare that the research was conducted in the absence of any commercial or financial relationships that could be construed as a potential conflict of interest.

Generative AI statement

The authors declare that no Gen AI was used in the creation of this manuscript.

Publisher's note

All claims expressed in this article are solely those of the authors and do not necessarily represent those of their affiliated organizations, or those of the publisher, the editors and the reviewers. Any product that may be evaluated in this article, or claim that may be made by its manufacturer, is not guaranteed or endorsed by the publisher.

Supplementary material

The Supplementary material for this article can be found online at: https://www.frontiersin.org/articles/10.3389/fnut.2025.1509734/full#supplementary-material

References

1. Lei H, Wang X, Zhang Y, Cheng T, Mi R, Xu X, et al. Herba Cistanche (Rou Cong Rong): a review of its Phytochemistry and pharmacology. *Chem Pharm Bull*. (2020) 68:694–712. doi: 10.1248/cpb.c20-00057

2. Yang B, Wu X, Zeng J, Song J, Qi T, Yang Y, et al. A multi-component Nano-co-delivery system utilizing Astragalus polysaccharides as carriers for improving biopharmaceutical properties of Astragalus flavonoids. *Int J Nanomedicine*. (2023) 18:6705–24. doi: 10.2147/ijn.S434196

3. Xue T, Zheng D, Wen L, Hou Q, He S, Zhang H, et al. Advance in *Cistanche deserticola* Y. C. Ma. Polysaccharides: isolation, structural characterization, bioactivities and application: a review. *Int J Biol Macromol*. (2024) 278:134786. doi: 10.1016/j.ijbiomac.2024.134786

4. Ai Z, Zhang Y, Li X, Sun W, Liu Y. Widely targeted metabolomics analysis to reveal transformation mechanism of *Cistanche deserticola* active compounds during steaming and drying processes. *Front Nutr*. (2021) 8:742511. doi: 10.3389/fnut.2021.742511

5. Hou S, Tan M, Chang S, Zhu Y, Rong G, Wei G, et al. Effects of different processing (Paozhi) on structural characterization and antioxidant activities of polysaccharides from *Cistanche deserticola*. *Int J Biol Macromol*. (2023) 245:125507. doi: 10.1016/j.ijbiomac.2023.125507

6. Holscher HD. Dietary Fiber and prebiotics and the gastrointestinal microbiota. *Gut Microbes*. (2017) 8:172–84. doi: 10.1080/19490976.2017.1290756

7. Lu Y, Zhao A, Wu Y, Zhao Y, Yang X. Soybean soluble polysaccharides enhance bioavailability of Genistein and its prevention against obesity and metabolic syndrome of mice with chronic high fat consumption. *Food Funct*. (2019) 10:4153–65. doi: 10.1039/c8fo02379d

8. Zhang J, Zhang J, Wang R. Gut microbiota modulates drug pharmacokinetics. *Drug Metab Rev*. (2018) 50:357–68. doi: 10.1080/03602532.2018.1497647

9. Shen H, Gao XJ, Li T, Jing WH, Han BL, Jia YM, et al. Ginseng polysaccharides enhanced Ginsenoside Rb1 and microbial metabolites exposure through enhancing intestinal absorption and affecting gut microbial metabolism. *J Ethnopharmacol*. (2018) 216:47–56. doi: 10.1016/j.jep.2018.01.021

10. Peng K, Li Y, Sun Y, Xu W, Wang H, Zhang R, et al. Lotus root polysaccharide-phenol complexes: interaction, structure, antioxidant, and anti-inflammatory activities. *Food Secur*. (2023) 12:577. doi: 10.3390/foods12030577

11. Zhang Y, Lin Y, Wu K, Jiang M, Li L, Liu Y. Pleurotus Abieticola polysaccharide alleviates hyperlipidemia symptoms via inhibition of nuclear factor-Kb/signal transducer and activator of transcription 3-mediated inflammatory responses. *Nutrients*. (2023) 15:904. doi: 10.3390/nu15234904

12. Li Z, Ryenchindorj L, Liu B, Shi J, Zhang C, Hua Y, et al. Chemical profiles and metabolite study of raw and processed *Cistanche deserticola* in rats by Uplc-Q-Tof-Ms(E). *Chin Med*. (2021) 16:95. doi: 10.1186/s13020-021-00508-0

13. Zhang X-y, Jiang Q-w, Yang S-h, Li P, Chang Z-y, Li F. The Chemometrics analysis and integrated pharmacology approach to decipher the effect and mechanism between raw and processed Cistanche Tubulosa. *J Ethnopharmacol*. (2024) 328:118097. doi: 10.1016/j.jep.2024.118097

14. Montoya G, van Ravenzwaay B, Seefelder W, Haake V, Kamp H. Unanticipated differences in the rat plasma metabolome of Genistein and Daidzein. *Arch Toxicol*. (2025) 99:1387–1406. doi: 10.1007/s00204-025-03967-8

15. Liu S, Zhou W, Deng X, Jiang W, Wang Y, Zhan J, et al. Inonotus obliquus polysaccharide are linear molecules that Alter the abundance and composition of intestinal microbiota in Sprague Dawley rats. *Front Nutr*. (2023) 10:1231485. doi: 10.3389/fnut.2023.1231485

16. NMPA. Pharmacopeia of the People's republic of China. Beijing: Pharmacopeia of The People's Republic of China (2020). 140 p.

17. Janhavi P, Divyashree S, Sanjailal KP, Muthukumar SP. Dosecal: a virtual calculator for dosage conversion between human and different animal species. *Arch Physiol Biochem*. (2022) 128:426–30. doi: 10.1080/13813455.2019.1687523

18. Bolyen E, Rideout JR, Dillon MR, Bokulich NA, Abnet CC, Al-Ghalith GA, et al. Author correction: reproducible, interactive, scalable and extensible microbiome data science using Qiime 2. *Nat Biotechnol*. (2019) 37:1091. doi: 10.1038/s41587-019-0252-6

19. Zhou W, Tan X, Shan J, Liu T, Cai B, Di L. Effect of Chito-oligosaccharide on the intestinal absorptions of Phenylethanoid glycosides in Fructus Forsythiae extract. *Phytomedicine*. (2014) 21:1549–58. doi: 10.1016/j.phymed.2014.06.016

20. Huang J, Zhao D, Cui C, Hao J, Zhang Z, Guo L. Research Progress and trends of Phenylethanoid glycoside delivery systems. *Food Secur*. (2022) 11:769. doi: 10.3390/foods11050769

21. Ma YM, Sun RY. Second peak of plasma diazepam concentration and Enterogastric circulation. *Zhongguo Yao Li Xue Bao*. (1993) 14:218–21.

22. Callahan BJ, Wong J, Heiner C, Oh S, Theriot CM, Gulati AS, et al. High-throughput amplicon sequencing of the full-length 16s Rrna gene with single-nucleotide resolution. *Nucleic Acids Res*. (2019) 47:e103. doi: 10.1093/nar/gkz569

23. Rognes T, Flouri T, Nichols B, Quince C, Mahé F. Vsearch: a versatile open source tool for metagenomics. *PeerJ*. (2016) 4:e2584. doi: 10.7717/peerj.2584

24. Caporaso JG, Kuczynski J, Stombaugh J, Bittinger K, Bushman FD, Costello EK, et al. Qiime allows analysis of high-throughput community sequencing data. *Nat Methods*. (2010) 7:335–6. doi: 10.1038/nmeth.f.303

25. Langille MG, Zaneveld J, Caporaso JG, McDonald D, Knights D, Reyes JA, et al. Predictive functional profiling of microbial communities using 16s Rrna marker gene sequences. *Nat Biotechnol*. (2013) 31:814–21. doi: 10.1038/nbt.2676

26. Li Z, Li J, Li Y, Guo L, Xu P, Du H, et al. The role of Cistanches Herba and its ingredients in improving reproductive outcomes: a comprehensive review. *Phytomedicine*. (2024) 129:155681. doi: 10.1016/j.phymed.2024.155681

27. Liao Y, Hu J-p, Guo C, Wen A, Wen L-m, Hou Q, et al. Acteoside alleviates blood-brain barrier damage induced by ischemic stroke through inhibiting microglia Hmgb1/Tlr4/Nlrp3 signaling. *Biochem Pharmacol*. (2023) 220:115968. doi: 10.1016/j.bcp.2023.115968

28. Zhu K, Meng Z-q, Tian Y, Gu R, Xu Z-k, Fang H, et al. Hypoglycemic and Hypolipidemic effects of Total glycosides of Cistanche Tubulosa in diet/Streptozotocin-induced diabetic rats. *J Ethnopharmacol*. (2021) 276:113991. doi: 10.1016/j.jep.2021.113991

29. Feng M, Dai X, Yang C, Zhang Y, Tian Y, Qu Q, et al. Unification of medicines and excipients: the roles of natural excipients for promoting drug delivery. *Expert Opin Drug Deliv*. (2023) 20:597–620. doi: 10.1080/17425247.2023.2210835

30. Fu Z, Han L, Peng Z, Mao H, Zhang H, Wang Y, et al. Cistanche polysaccharides enhance Echinacoside absorption in vivo and affect the gut microbiota. *Int J Biol Macromol*. (2020) 149:732–40. doi: 10.1016/j.ijbiomac.2020.01.216

31. Lu Y, Li W, Yang X. Soybean soluble polysaccharide enhances absorption of soybean Genistein in mice. *Food Res Int*. (2018) 103:273–9. doi: 10.1016/j.foodres.2017.10.054

32. Zhao X, Xing J-j, An N-n, Li D, Wang L, Wang Y. Succeeded high-temperature acid hydrolysis of granular maize starch by introducing heat-moisture pre-treatment. *Int J Biol Macromol*. (2022) 222:2868–77. doi: 10.1016/j.ijbiomac.2022.10.065

33. Zhenli L, Zhimao C, Yuanyan L, Zhiqian S, Aiping L. Maillard reaction involved in the steaming process of the root of *Polygonum multiflorum*. *Planta Med*. (2008) 75:84–8. doi: 10.1055/s-0028-1088349

34. Qi M, Xiong A, Li P, Yang Q, Yang L, Wang Z. Identification of Acteoside and its major metabolites in rat urine by ultra-performance liquid chromatography combined with electrospray ionization quadrupole time-of-flight tandem mass spectrometry. *J Chromatogr B Anal Technol Biomed Life Sci*. (2013) 940:77–85. doi: 10.1016/j.jchromb.2013.09.023

35. Cui Q, Pan Y, Xu X, Zhang W, Wu X, Qu S, et al. The metabolic profile of Acteoside produced by human or rat intestinal Bacteria or intestinal enzyme in vitro employed Uplc-Q-Tof-Ms. *Fitoterapia*. (2016) 109:67–74. doi: 10.1016/j.fitote.2015.12.011

36. Guo Y, Cui Q, Ren S, Hao D, Morikawa T, Wang D, et al. The Hepatoprotective efficacy and biological mechanisms of three Phenylethanoid glycosides from Cistanches Herba and their metabolites based on intestinal Bacteria and network pharmacology. *J Nat Med*. (2021) 75:784–97. doi: 10.1007/s11418-021-01508-y

37. Cui Q, Pan Y, Bai X, Zhang W, Chen L, Liu X. Systematic characterization of the metabolites of Echinacoside and Acteoside from Cistanche Tubulosa in rat plasma, bile, urine and feces based on Uplc-Esi-Q-Tof-Ms. *Biomed Chromatogr*. (2016) 30:1406–15. doi: 10.1002/bmc.3698

38. Payling L, Fraser K, Loveday S, Sims I, Roy N, McNabb W. The effects of carbohydrate structure on the composition and functionality of the human gut microbiota. *Trends Food Sci Technol*. (2020) 97:233–48. doi: 10.1016/j.tifs.2020.01.009

39. Jordan CK, Brown RL, Larkinson MLY, Sequeira RP, Edwards AM, Clarke TB. Symbiotic Firmicutes establish mutualism with the host via innate tolerance and resistance to control systemic immunity. *Cell Host Microbe*. (2023) 31:1433–1449.e9. doi: 10.1016/j.chom.2023.07.008

40. Liu T, Wang Q, Gao C, Long S, He T, Wu Z, et al. Drinking warm water promotes performance by regulating ruminal microbial composition and serum metabolites in yak calves. *Microorganisms*. (2023) 11:2092. doi: 10.3390/microorganisms11082092

41. Sun Y, Zhang S, Nie Q, He H, Tan H, Geng F, et al. Gut Firmicutes: relationship with dietary Fiber and role in host homeostasis. *Crit Rev Food Sci Nutr*. (2023) 63:12073–88. doi: 10.1080/10408398.2022.2098249

42. Martin AJM, Serebrinsky-Duek K, Riquelme E, Saa PA, Garrido D. Microbial interactions and the homeostasis of the gut microbiome: the role of Bifidobacterium. *Microbiome Res Rep*. (2023) 2:17. doi: 10.20517/mrr.2023.10

43. Gao M, Wang J, Liu P, Tu H, Zhang R, Zhang Y, et al. Gut microbiota composition in depressive disorder: a systematic review, Meta-analysis, and Meta-regression. *Transl Psychiatry*. (2023) 13:379. doi: 10.1038/s41398-023-02670-5

44. Zhu X, Cai J, Wang Y, Liu X, Chen X, Wang H, et al. A high-fat diet increases the characteristics of gut microbial composition and the intestinal damage associated with non-alcoholic fatty liver disease. *Int J Mol Sci*. (2023) 24:24. doi: 10.3390/ijms242316733

45. Carbonne C, Chadi S, Kropp C, Molimard L, Chain F, Langella P, et al. Ligilactobacillus Salivarius Cncm I-4866, a potential probiotic candidate, shows anti-inflammatory properties in vitro and in vivo. *Front Microbiol*. (2023) 14:14. doi: 10.3389/fmicb.2023.1270974

46. Chang C-S, Liao Y-C, Huang C-T, Lin C-M, Cheung CHY, Ruan J-W, et al. Identification of a gut microbiota member that ameliorates Dss-induced colitis in intestinal barrier enhanced Dusp6-deficient mice. *Cell Rep*. (2021) 37:110016. doi: 10.1016/j.celrep.2021.110016

47. Xue H, Liang B, Wang Y, Gao H, Fang S, Xie K, et al. The regulatory effect of polysaccharides on the gut microbiota and their effect on human health: a review. *Int J Biol Macromol*. (2024) 270:132170. doi: 10.1016/j.ijbiomac.2024.132170

48. Kasubuchi M, Hasegawa S, Hiramatsu T, Ichimura A, Kimura I. Dietary gut microbial metabolites, short-Chain fatty acids, and host metabolic regulation. *Nutrients*. (2015) 7:2839–49. doi: 10.3390/nu7042839

49. Gao Y, Wang J, Xiao Y, Yu L, Tang Q, Wang Y, et al. Structure characterization of an Agavin-type Fructan isolated from Polygonatum Cyrtonema and its effect on the modulation of the gut microbiota in vitro. *Carbohydr Polym*. (2024) 330:121829. doi: 10.1016/j.carbpol.2024.121829

50. Parada Venegas D, De la Fuente MK, Landskron G, González MJ, Quera R, Dijkstra G, et al. Short Chain fatty acids (Scfas)-mediated gut epithelial and immune regulation and its relevance for inflammatory bowel diseases. *Front Immunol*. (2019) 10:277. doi: 10.3389/fimmu.2019.00277

51. Wei Y, Liu W, Wang R, Chen Y, Liu J, Guo X, et al. Propionate promotes Ferroptosis and apoptosis through Mitophagy and Acsl4-mediated Ferroptosis elicits anti-leukemia immunity. *Free Radic Biol Med*. (2024) 213:36–51. doi: 10.1016/j.freeradbiomed.2024.01.005

frontiers | Frontiers in Nutrition

TYPE Original Research
PUBLISHED 13 May 2025
DOI 10.3389/fnut.2025.1549120

Check for updates

OPEN ACCESS

EDITED BY
Ntethelelo Sibiya,
Rhodes University, South Africa

REVIEWED BY
Veronica I. Dodero,
Bielefeld University, Germany
Bing Li,
Zhoukou Normal University, China

*CORRESPONDENCE
Maria Vittoria Barone
✉ mv.barone@unina.it

RECEIVED 20 December 2024
ACCEPTED 09 April 2025
PUBLISHED 13 May 2025

CITATION
Bellomo C, Mauriello F, Nigro F, Passannanti F, Colucci Cante R, Nigro R, Barone MV and Nanayakkara M (2025) Sustainable milk-based postbiotics beverages fermented by *Lactobacillus plantarum*: allies in celiac disease inflammation.
Front. Nutr. 12:1549120.
doi: 10.3389/fnut.2025.1549120

COPYRIGHT
© 2025 Bellomo, Mauriello, Nigro, Passannanti, Colucci Cante, Nigro, Barone and Nanayakkara. This is an open-access article distributed under the terms of the Creative Commons Attribution License (CC BY). The use, distribution or reproduction in other forums is permitted, provided the original author(s) and the copyright owner(s) are credited and that the original publication in this journal is cited, in accordance with accepted academic practice. No use, distribution or reproduction is permitted which does not comply with these terms.

Sustainable milk-based postbiotics beverages fermented by *Lactobacillus plantarum*: allies in celiac disease inflammation

Claudia Bellomo[1,2], Francesca Mauriello[3], Federica Nigro[4], Francesca Passannanti[3,4], Rosa Colucci Cante[3,5], Roberto Nigro[3], Maria Vittoria Barone[1,2]* and Merlin Nanayakkara[2,6]

[1]Department of Translational Medical Science, Section of Pediatrics, University Federico II, Naples, Italy, [2]ELFID (European Laboratory for the Investigation of Food Induced Diseases), University Federico II, Naples, Italy, [3]Department of Chemical Engineering, Materials, and Industrial Production, University of Naples Federico II, Naples, Italy, [4]I.T.P. Innovation and Technology Provider S.r.l., Naples, Italy, [5]Department of Business Engineering Mario Lucertini, University of Tor Vergata, Rome, Italy, [6]Federico II University Hospital, Naples, Italy

Background: Celiac disease (CeD) is an autoimmune disorder characterized by damage to the small intestine that occurs in genetically predisposed individuals after gluten consumption. Dietary exclusion is the only treatment. Gliadin is one of the main protein component of wheat gluten, and is poorly digested. Undigested peptide, p31-43, triggers several different processes, including inflammation. Intestinal organoids from CeD biopsies are good models for studying CeD inflammation. Postbiotics have been shown to modulate the effects of p31-43 in Caco-2 cells and inflammation in CeD organoids. The aims of this study was to study the anti-inflammatory activity of milk-based postbiotics from of *L. plantarum*.

Methods: Postbiotics from *L. plantarum* CECT 749-fermented milk enriched with LA (linoleic acid), SCGs (Spent Coffee Grounds) and SCG oil were produced. Gliadin peptide p31-43 was used to induce inflammation on Caco2 cells. Organoids were derived from intestinal biopsies of 3 controls (CTRs) and 3 GCD (gluten containing diet)-CeD patients. NF-kB activation, a marker of inflammation, was evaluated by Western Blot analysis.

Results: The results showed that pretreatment with all milk-based postbiotics of *L. plantarum*, except for SCG oil, inhibited the activation of NF-kB in the presence of the gliadin peptide in Caco-2 cells. The most efficient postbiotics, namely, milk-based postbiotics of *L. plantarum* with or without SCGs, could also reduce inflammation in intestinal organoids from CeD patients.

Conclusion: Milk-based postbiotics of *L. plantarum*, with or without SCGs, prevents the proinflammatory effects of gliadin on Caco-2 cells and constitutive inflammation in CeD intestinal organoids, independent of the CLA (Conjugated linoleic acid) concentration.

KEYWORDS

celiac disease, postbiotic, CLA, Caco-2 cells, intestinal organoids, inflammation

1 Introduction

Celiac disease (CeD) is an immune-mediated enteropathy that primarily affects the small intestine in response to the ingestion of gluten, a protein present in wheat, barley, and rye. A gluten-free diet is the only therapy for these patients, who must eliminate gluten-containing cereals from their diet for life. CeD results from interactions between genetic factors, which

are characterized mainly by HLAs, Human Leukocyte Antigen, class I and II genes, and environmental factors, which contribute to the generation of inflammation in the intestine (1–3). Among the environmental factors that induce inflammation, nutrients, including gluten, play a central role. Nutrients may have two effects, proinflammatory or anti-inflammatory effects, and the microbiota may mediate their destiny (4). However, how, when, and where inflammation is generated in CeD is still being determined (5).

Gliadin, the main protein in wheat-gluten, is a protein that is difficult to digest by intestinal endopeptidases. Undigested gliadin peptides may have biological activity (6). Some of them can activate the adaptive immune response, as they are well presented to T cells. Other peptides, such as the p31–43 peptide, play key roles in the inflammatory/innate immune response to gliadin (6). Specifically, this peptide has pleiotropic activity, including the induction of proliferation and inflammation with the activation of the nuclear transcription factor-B (NF-kB) pathway (7–9). The nuclear factor kappa B (NF-κB) family of transcription factors is a key regulator of immune development, immune responses, inflammation, and cancer. However, it is activated after phosphorylation mechanisms (pNF-kB). The activation of this pathway is associated with several stimuli, and upon ligand-receptor engagement, distinct cellular outcomes, appropriate to the specific signal received, are set into motion (10).

NF-kB is also a key protein in the regulation of inflammation in the intestine (11). Moreover, the NF-kB pathway has been found to be altered in intestinal biopsy samples from CeD patients, both at GCD (Gluten Containing Diet) and GFD (Gluten Free Diet) (12, 13), and in intestinal organoids (13). Interestingly, after gluten treatment, there was an increase in NF-kB expression in CeD biopsy samples at both GCD and GFD (1, 12).

Interestingly, in CeD biopsy samples and organoids, constitutive inflammation, characterized by an increase in IL6 and IL1B, which are also part of the NF-kB pathway, has been described even before the occurrence of the intestinal lesion (13, 14). The constitutive inflammation of intestinal organoids from CeD patients is reduced in the presence of probiotics from *Lactobacillus paracasei* and *Lactobacillus rhamnosus* GG (15–17).

Pro- and postbiotics and conjugated linoleic acids (CLAs) are helpful in treating inflammatory-related diseases (18–20). CLAs are polyunsaturated acids and are a mixture of positional and geometric isomers of linoleic acid, a polyunsaturated omega-6 fatty acid also known as cis, cis-9,12-octadecadienoic acid. Linoleic acid and CLA are essential fats that must be part of the diet. The concentration of CLAs can be increased naturally by the selection of *ad hoc* microorganisms and fermentation conditions. Linoleic acid is a precursor in the synthesis of CLA; it is often added to the matrix to be fermented in its pure form (21, 22) or by adding vegetable oils, such as safflower oil (23) and sunflower oil (24). Interestingly, the line guide written by Vitale and Giacco in 2020 defined roasted coffee waste, such as spent coffee grounds (SCGs), as foods which contains a high concentration of linoleic acid (25).

SCGs are the most abundant coffee byproduct (26), and in 2017, its worldwide production reached 9.6 million tons as described in International Coffee Organization (ICO). SCGs have been widely studied as a material for biodiesel production (27). However, in recent years, it has also been used for food applications (26).

The aims of the present work was both the sustainable production of a functional milk-based beverage fermented by *L. plantarum* CECT 749 that was enriched in CLAs after the addition of LA, SCGs and SCG oil, and the study of the potential anti-inflammatory effects of these compounds in the presence of p31-43 in Caco-2 cells and CeD intestinal organoids.

2 Materials and methods

2.1 Fermentation experimental apparatus

The system consisted of a Pyrex batch reactor (20 cm, ID of 10 cm, 1.5 L) equipped with an external jacket to circulate a service fluid from a thermostatically controlled water bath. The mixing system consisted of a stainless-steel impeller equipped with three Rushton turbines. It was connected to a motor that adjusted the stirring speed. The head plate was equipped with an input for the insertion of an In Pro 3,100 probe (Mettler Toledo, Milan, Italy) that was connected to an M300 transmitter (Mettler Toledo, Milan, Italy), which is helpful for inline temperature/pH measurements, and an input connected to a tank containing a 4 M NaOH solution that was fed by a peristaltic pump for pH control.

2.2 Strain

Lactobacillus plantarum CECT 749 (from the Spanish Type Culture Collection, CECT, Valencia Spain) is a gram-positive bacterium that has been studied for its antifungal activity (28) and ability to produce CLA (21, 23, 29). The strain was stored at −20°C in cryovials containing 1 mL of a solution of animal-free broth [AFB-Animal Free Broth; composition: 20 g/L Bacto Yeast Extract (BD Biosciences, Milan, Italy), 0.5 g/L $MgSO_4$ (Sigma–Aldrich, Milan, Italy), 50 g/L glucose (Sigma–Aldrich), 0.5 g/L citric acid (Sigma–Aldrich) and glycerol (20%, Sigma–Aldrich)]. Before each fermentation, after thawing, the strain was revitalized by adding 9 mL of AFB and then incubated for 24 h at 37°C. The revitalized strain had a bacterial concentration of 10^8 CFU/mL, and the inoculum contained 1% v/v fermentation substrate.

2.3 Fermentation substrates and experimental conditions

The fermentation substrate was 1 L of skim milk (Granarolo® - UHT), which was purchased from a local market and contained 20 g/L glucose (Sigma–Aldrich, Milan, Italy). To test the microbial capacity in the production of CLA, different compounds, as CLA precursors, were used, allowing the following experimental conditions (30) to be defined:

- Exp. Condition 1 (milk): Milk with only glucose as a negative control.
- Exp. Condition 2 (milk + LA): Milk with glucose and 0.5 mg/mL free linoleic acid (LA, 99% purity; Sigma Aldrich, St. Louis, MO, USA), since a previous study suggested this concentration as the best concentration for maximum CLA production (31).
- Exp. Condition 3 (milk + SCG oil): Milk with glucose and 1.3 g of the oil extracted from *Passalacqua*® spent coffee grounds (*Passalacqua*®, *Mexico* blend type, 100% Arabica) to guarantee

that the free LA (from now on LA) concentration was the same as that in Exp. Condition 2 (where the LA concentration in spent coffee grounds corresponds to 40% of the total fat in the spent coffee ground oil) (32). The extraction method used to obtain the coffee oil is described below. "Free LA" are the linoleic acids totally available for the conversion in a conjugated form.

- Exp. Condition 4 (milk + SCG): Milk with glucose and 20 g of *Passalacqua*® spent coffee grounds; this amount was chosen since the literature reported that, to obtain the optimal LA concentration (0.5 mg/mL), 10 grams of dry waste would be needed. Wet spent coffee grounds contain an average of 50–60% water; therefore, to release the abovementioned amount of LA, two times the weight (20 grams) of spent coffee grounds was added (32).

Glucose was added for each experimental condition to favor a more rapid fermentation process. The addition of linoleic acid, SCG oil, and raw SCGs to milk was followed by sonication to homogenize the matrix to be fermented and promote the dispersion and extraction of the fat phase in the dairy matrix.

For each condition tested, fermentation was carried out for 48 h at 37°C. Fermented samples were withdrawn aseptically from the reactor at specific times (after inoculation (t_0) and after 24 (t_{24}) and 48 (t_{48}) hours).

2.4 SCG oil extraction method

SCG oil extraction was performed using a hydrofluorocarbon (HFC) solvent, 1,1,1,2-tetrafluoromethane (Norflurane, R134a), under subcritical conditions with a laboratory-scale system via a patented process (51). Norflurane is a haloalkane refrigerant with a boiling point of 26.3°C at atmospheric pressure and a vapor pressure of 6.61 bar at 25°C (33). Liquid Norflurane was percolated through a dry SCG matrix bed and placed in an extraction chamber at 8–10 bar to enrich its coffee oil content. The mixture was subsequently passed through an expansion vessel, where Norflurane was gasified at lower pressure (approximately 4–5 bar), and the oily solute was released at the bottom. Afterwards, the clean gaseous Norflurane was recompressed and recycled in liquid form to the extraction chamber, where the extraction phase was repeated.

2.5 Analytical methods

2.5.1 Microbiological analysis

A spread plate method was used to determine the vital bacterial load of the inoculum, the microbial concentration during the entire process, and the presence of contaminants. After serial dilutions, the sample was spread on MRS agar (Oxoid, Basingstoke, UK) for the enumeration of lactobacilli; MacConkey agar (Oxoid, Basingstoke, UK) and Gelatin peptone agar (Biolife, Milan, Italy) were used for the detection of eventual contaminants. All the plates were incubated at 37°C for 48 h before being read. Anaerobic kits (Anaerogen Compact, Oxoid, Basingstoke, UK) were used for MRS plates to guarantee anaerobic growth conditions for *L. plantarum CECT 749* during incubation.

2.5.2 Lactic acid quantification

The concentration of lactic acid was determined by high-performance liquid chromatography (HPLC) on an Agilent Technologies 1,100 instrument equipped with an Agilent Synergi Hydro-RP C18 column (250 mm × 4.6 mm and a pore size of 4 µm) and a visible/UV detector. The mobile phase consisted of 0.27% KH_2PO_4 aqueous solution at a pH of 2 modified with H_3PO_4 (eluent A) and 100% methanol (eluent B), and a gradient consisting of 30% B in 2.6 min followed by 100% A in 2.9 min with a flow rate of 1 mL/min was used. The detection wavelength was set at 210 nm.

2.5.3 CLA analysis

Fat extraction was performed according to Stefanov et al. (33). A total of 10 g of milk fermented samples (collected at times t0, t24, t48 and postbiotics for each tested condition) was mixed with 16 mL of previously prepared dichloromethane–ethanol (DM–E) solution (2:1 ratio, v/v) in a 40 mL centrifuge-grade glass test tube, vortexed for 90 s and then centrifuged for 8 min (2,500 g at −4°C, MPW Med. Instruments, MPW-352R, Warszawa, Polonia). The supernatant was discharged, and 10 mL of the DM-E solution was added to the test tube. The mixture was vortexed and then centrifuged for 6 min (2,500 × g at −4°C). The upper organic phase containing the milk fat was filtered (597½, 240 mm diameter, Schleicher & Schuell, Dassel, Germany), dichloromethane was removed by a reduced pressure rotary evaporator (Bibby Sterilin RE-100, Bibby Scharlau Italia S.r.l., Riozzo di Cerro al Lambro (MI) Italia), and the samples were evaporated until dryness was achieved. After extraction, the fats were transesterified according to the method of Ichihara et al. (52). The lipid sample was dissolved in 0.20 mL of toluene, and then, 1.50 mL of methanol and 0.30 mL of the reagent mixture (consisting of 9.7 mL of HCI (35%, w/w) diluted with 41.5 mL of methanol) were added in this order. The tube was vortexed and then heated at 100°C for 1 h. After cooling, 1 mL of hexane and 1 mL of water were added to extract the methyl esters in the hexane phase. Finally, the samples were analyzed via GC (Varian CP 3800 Gascromatographer, Palo Alto, United States) equipped with an FID detector and a ZB WAX plus column (60 m 0.25 mm 0.2 µm, Phenomenex, Aschaffenburg, Germany), with helium used as the gas carrier (1.2 mL/min).

2.6 Caco-2 cells and treatment

Human colon adenocarcinoma-derived cells (Caco-2) obtained from the Interlab Cell Line Collection (Centro di Biotecnologie Avanzate, Genoa, Italy) were grown in DMEM supplemented with 10% fetal calf serum, 100 units of penicillin–streptomycin/mL, and 1 mmol/L glutamine (Gibco Invitrogen, Milan, Italy). The cells were maintained in a humidified atmosphere (95% air and 5% CO2) at 37°C. The postbiotic milk-based beverages were obtained by thermal treatment (85°C, 30 s). The milk-based postbiotic beverages were freeze-dried, resuspended in DMEM-free medium (2% w/v), centrifuged thrice at 1500 rpm for 5 min and after each centrifugation the supernatant was recovered, and after the last centrifugation, the supernatant was filtered using the 0.22 µm filter (ref SLGS033SS, Merk, Ireland). The sequence of P31-43, an LPS-free synthetic peptide, was LGQQQPFPPQQPY (Caslo > 95% purity, MALDITOF analysis; DK-2800 Kongens Lyngby, Denmark), and it was used at 100 µg/mL

(15, 16). Previous studies describe the optimal concentration of p31-43 on Caco-2 cells to be 100 μg/mL, in these studies this concentration was able to have several different effects (6, 34).

For the treatment, more than 2×10^6 cells were seeded in 60 mm culture dishes overnight for attachment. The next day, the cells were exposed in presence or not to milk-based probiotics and postbiotics supplemented with LA, SCG and SCG for 1 h, as based on previous published data. Caco-2 cells were pretreated with milk-based postbiotics at 2% w/v for 30 min and subsequently stimulated with P31–43 at 100 μg/mL (15, 16, 35).

2.6.1 Cell viability and optimal concentrations of milk-based postbiotic

For the cell viability experiment, more than 2×10^6 cells were seeded in 60 mm culture dishes overnight for attachment. The next day, the cells were exposed in presence or not to milk-based probiotics and postbiotics supplemented with LA for 24 and 48 h of fermentation at concentrations between 0.1 and 10% for 1 h at 37°C in DMEM-free medium. At the end of incubation, cell viability was assessed by a trypan blue dye exclusion assay based on the microscopic quantitation of live cells (unstained) and dead cells (blue cytoplasm). Cells were automatically counted using the Countess automated cell counter (Thermo Fisher Scientific, Milan, Italy). A high viability range was evident at concentrations of 0, 1, 1, and 2% (Supplementary Figures 1, 2). As the CLA concentration in the matrix studied was the same after 24 and 48 h of fermentation and considering that the viability did not change at 0.1% (1.3×10^7 CFU/g), 1, and 2%, we used the postbiotics after 24 h at concentrations of 1% (1.3×10^8 CFU/g) and 2% (2.6×10^8 CFU/g) weight/volume.

2.7 Intestinal organoids

One to two duodenal biopsies were taken with standard endoscopic EGD (esophageal gastroduodenoscopy) from three control subjects, for which the final diagnosis is attributed to functional disorders, and three patients with CeD. The CeD patients was diagnosed following the ESPGHAN 2020 guidelines they presented villus atrophy in the intestinal biopsy (MARSH T3c) and were positive for anti-tTg antibodies in the serum. These conditions satisfied the ESPGHAN 2020 guidelines that state HLA-testing is not required in patients with positive TGA-IgA, if they qualify for CD diagnosis with biopsies or if they have high serum TGA-IgA ≥ 10xULN and EMA-IgA positivity. The biopsy samples were placed in 10 mL of ice-cold PBS supplemented with 2 mM EDTA (cat. 15,575,020, Thermo Fisher, Milan, Italy) and 0.5 mM DDT (D0632, Sigma–Aldrich, Milan, Italy). After 60 min, Crypt units were isolated by using washing buffer (WB) containing penicillin (100 units/mL), streptomycin (0.1 mg/mL), l-glutamine (2 mM), and FBS (10%, v/v) in DMEM/F12 with HEPES on ice for 30 min. The digest was filtered through a 70 m strainer (Falcon, Milan, Italy). Crypts were collected by centrifugation at 2800 rpm for 5 min. The supernatant was discarded, and the crypts were carefully resuspended in 40 μL of ice-cold Matrigel matrix (Corning 356,231, Milan, Italy) to enable three-dimensional growth in 48-well plates; the plates were incubated in a cell culture incubator at 37°C and 5% carbon dioxide for 10 min to allow the Matrigel to solidify. Afterwards, 300 μL of cell culture medium enriched with supplements (CM-S) (13) was added to each well and replaced every second day. For 2D organoids, organoids were seeded in six wells pretreated with Matrigel diluted at 1:40 in phosphate-buffered saline (PBS) (13, 15, 16, 36) (Table 1).

2.8 Western blot

After treatment, the Caco-2 cells were washed twice with cold PBS and resuspended in lysis buffer (50 mM Tris–HCl (pH 7.4), 1 mM EDTA, 1 mM EGTA, 5 mM $MgCl_2$, 150 mMNaCl, 1% Triton, 1 mM PMSF, 1 mM VO4, 100 × Aprotinin, and 50 × LAP, all of which were purchased from Sigma, Milan, Italy, except for LAP, which was obtained from Roche, Milan, Italy). The cell lysates were analyzed using SDS-PAGE with a standard running buffer (25 mM Tris, 192 mM glycine, and 0.1% SDS) and transferred onto nitrocellulose membranes by a Trans-Blot Turbo transfer system (cat. 1704158; Bio-Rad, Milan, Italy) in a stain free gel at 10% (#cat 4,568,033; Bio-Rad, Milan, Italy). The membranes were washed, blocked with 5% non-fat dry milk, and probed with onto nitrocellulose membranes (Whatman Gmbh, Dassel, Germany). The membranes were blotted with rabbit anti-pNF-kB (Elabscience, Microtech, Naples, Italy) and mouse anti-GAPDH (Glyceraldehyde-3-phosphate dehydrogenase) (cat. G8795, Sigma-Aldrich). GAPDH or total protein intensity were used as loading controls. The bands were visualized using enhanced chemiluminescence (ECL) plus (Cat. 1705062 Bio-Rad Milan, Italy) with 2–10 min exposure times. The band intensity was evaluated by integrating all the pixels of a band after subtraction of the background to calculate the average of the pixels surrounding the band (13, 15, 16, 36).

2.9 ELISA

The levels of IL-8 were measured using commercial test kits (IL-8/CXCL8 cat.#D8000C, Bio-techne R&D System, Milan, Italy) on culture media of GCD-CeD intestinal organoids treated and not with milk-based *L. plantarum* of postbiotics with and without SCG respect to CTRs'.

TABLE 1 Organoids characteristics.

Patients	Age range (Years)	Sex	Biopsy (marsh classification*)	Serum antiTG2 (U/mL)	Anti-endomysial antibody (EMA)
CTR (n = 3)	4–15	M = 2 F = 1	3 = T0	Negative	Negative
GCD-CeD (n = 3)	3–17	M = 2 F = 1	3 = T3c	>100	Positive

*T3: Flat destructive lesion (c: total).
The sex classification: M represent the male group, F represent the female group.
The serum antibody antiTG2 is Anti-Transglutaminase-2.

2.10 Statistical analysis

Statistical analysis and graphics were obtained from Graph Pad Prism (San Diego, CA, USA). The means and standard deviations of the experimental data were calculated; their significance was evaluated by Student's *t* test and two way ANOVA multiple comparison, with only results that presented values of $p < 0.05$ considered significant.

3 Results

3.1 Spent coffee grounds (SCGs) improved bacterial growth and lactic acid production

We studied Plantarum CECT 749 bacterial growth under different conditions (Figure 1). In all cases, the initial concentration was approximately 10^6 CFU/mL, reaching $1.8\times10^8 \pm 2.6\times10^7$ CFU/mL after 24 h of fermentation in the case of the negative control (milk); $1.5\times10^7 \pm 7.1\times10^6$ CFU/mL when milk was supplemented with linoleic acid (milk +LA); $6.7\times10^7 \pm 2.3\times10^7$ CFU/mL when milk was supplemented with spent coffee ground oil (milk + SCGs oil); and $5.0\times10^8 \pm 7.1\times10^7$ CFU/mL when milk was supplemented with raw spent coffee grounds (milk + SCGs) (Figure 1A).

Milk supplemented with SCGs resulted in the best matrix for *L. plantarum* growth, reaching $6.6\times10^8 \pm$ CFU/mL at 48 h of fermentation, a value that was one log higher than that observed for milk fermented with LA ($5.8\times10^7 \pm 2.5\times10^7$ CFU/mL) and that observed for milk fermented with SCG oil ($6.2\times10^7 \pm 1.6\times10^7$ CFU/mL) (Figure 1A).

The amount of lactic acid produced in fermented milk (Figure 1B) in the presence of SCGs was 5.46 ± 0.05 g/L after 24 h ($p < 0.05$ respect to Milk, Milk with LA and Milk with SCG oil) and 12.66 ± 0.88 g/L after 48 h ($p < 0.05$ respect to Milk with LA) of fermentation. Milk fermented with only glucose (negative control) showed lactic acid production (lactic acid at 24 h: 1.46 ± 0.12 g/L; at 48 h: 3.94 ± 0.10 g/L) amounts that were similar to that measured in milk fermented with LA (lactic acid at 24 h: 0.98 ± 0.22 g/L; at 48 h: 2.05 ± 0.24 g/L) and with SCG oil (lactic acid at 24 h: 1.32 ± 0.13 g/L; at 48 h: 2.99 ± 0.15 g/L).

3.2 LA supplementation of milk promoted CLA production during fermentation with *Lactobacillus plantarum*

The concentration of total CLAs found during fermentation is shown in Figure 2. SCG oil and SCGs, which were used as sources of

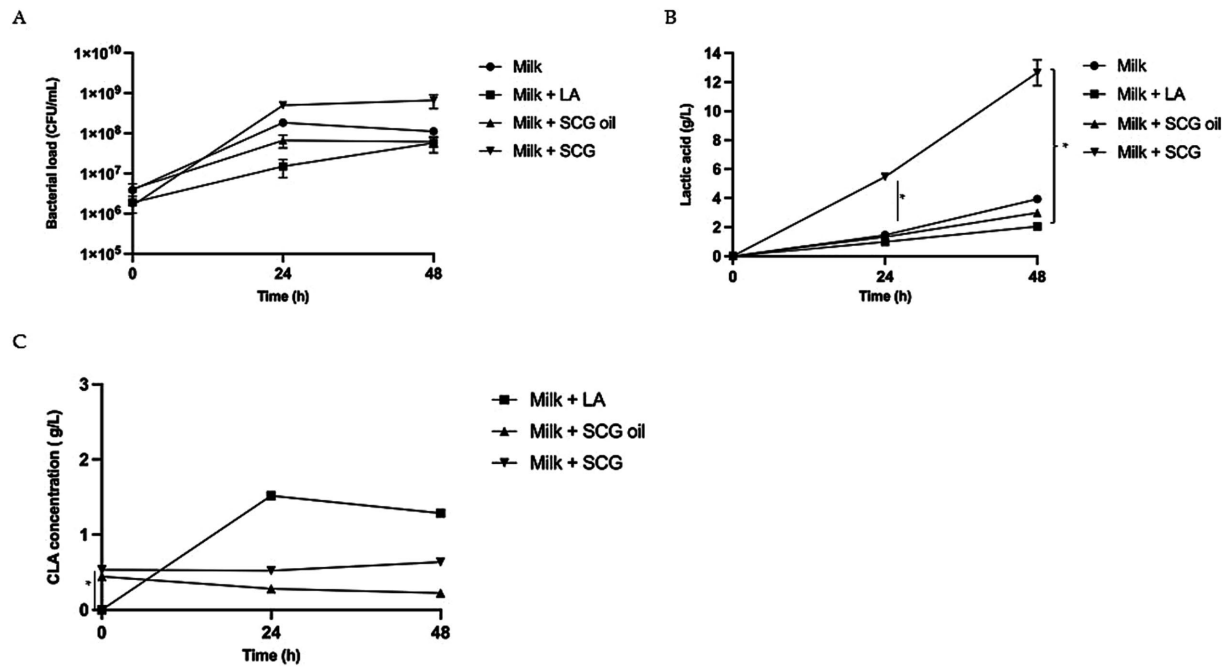

FIGURE 1
Bacterial growth, lactic acid production and CLAs concentration in milk-based postbiotics with linoleic acid (LA), Spent Coffee Grounds (SCGs) and SCG oil. **(A)** Bacterial growth (CFU/mL) observed after 0, 24 and 48 h of fermentation in milk alone (milk, circles), milk fermented with linoleic acid (milk + LA; squares), milk fermented with spent coffee ground oil (milk + SCG oil; triangles) and milk fermented with raw spent coffee grounds (milk + SCGs; inverted triangles). The bars represent the standard deviations of three independent experiments. Different letters indicate significant differences. ANOVA test: * = $p < 0.05$. **(B)** Lactic acid production observed after 0, 24 and 48 h of fermentation in milk alone (milk, circles), milk fermented with linoleic acid (milk + LA; squares), milk fermented with spent coffee ground oil (milk + SCG oil; triangles) and milk fermented with raw spent coffee grounds (milk + SCGs; inverted triangles). The bars represent the standard deviations of three independent experiments. Different letters indicate significant differences ANOVA test: * = $p < 0.05$. **(C)** Concentration of total CLAs (g/L) observed after 0, 24 and 48 h of fermentation in milk fermented with linoleic acid (Milk + LA; squares), milk fermented with spent coffee ground oil (milk + SCG oil; triangles) and milk fermented with raw spent coffee grounds (milk + SCGs; inverted triangles). The bars represent the standard deviations of three independent experiments. Different letters indicate significant differences ANOVA test: * = $p < 0.05$.

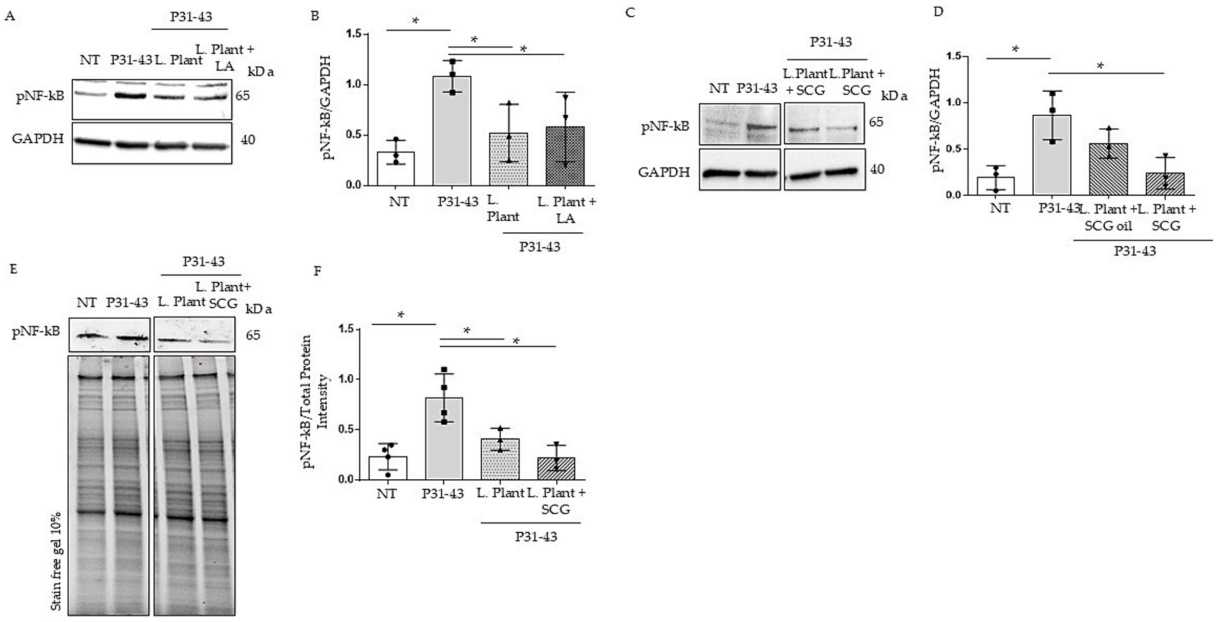

FIGURE 2
Effects of milk based postbiotics of *L. plantarum* CECT 749, with or without the addition of LA, SCG oil or SCGs at 2% concentration, after 24 h of fermentation on Caco-2 cells after treatment with P31-43. **(A)** Western blot analysis of protein lysates from untreated Caco-2 cells (NT), those treated with P31-43 for 1 h, and those pretreated with milk based postbiotic of *L. plantarum* CECT 749 after 24 h of fermentation with the addition of LA, blotted with antibodies against pNF-kB. GAPDH was used as a loading control. The immunoblotting analysis was representative of three independent experiments. **(B)** Densitometric analysis of bands from the WB shown in **A**. Columns represent the mean, and bars represent the standard deviation of the relative intensity of pNF-kB with respect to the total GAPDH protein. Student's *t* test: * = $p < 0.05$. **(C)** Western blot analysis of protein lysates from untreated Caco-2 cells (NT), those treated with P31-43 for 1 h, and those pretreated with milk-based postbiotic of *L. plantarum* CECT 749 after 24 h of fermentation with the addition of SCG oil and SCGs, were blotted with antibodies against pNF-kB. GAPDH was used as a loading control. The immunoblotting analysis was representative of three independent experiments. **(D)** Densitometric analysis of bands from the WB shown in **A**. Columns represent the mean, and bars represent the standard deviation of the relative intensity of pNF-kB with respect to the total GAPDH protein. Student's *t* test: * = $p < 0.05$. **(E)** Western blot analysis of protein lysates from untreated Caco-2 cells (NT), those treated with P31-43 for 1 h, and those pretreated with milk based postbiotic of *L. plantarum* CECT 749 after 24 h of fermentation, and alone and with the addition of SCGs, were blotted with antibodies against pNF-kB. Stain-free gel was used as a loading control. The immunoblotting analysis was representative of three independent experiments. **(F)** Densitometric analysis of the bands from the WB shown in **A**. Columns represent the mean, and bars represent the standard deviation of the relative intensity of pNF-kB with respect to the total protein intensity. Student's *t* test: * = $p < 0.05$.

linoleic acid, were tested for CLA production. CLAs were present at T0 in the samples containing SCG and SGC oil even before fermentation, with concentrations of approximately 0.5 g/L for both samples. The difference was statistically significant for both SCG and SGC oil respect to the sample milk added with LA ($p < 0.05$ for both matrix) (Figure 1C). Milk fermented alone is not represented in the graph because no CLAs were detected, as expected. Milk fermentation in the presence of LA was the only sample in which CLAs were produced, with concentrations of 1.52 ± 0.06 g/L ($p < 0.05$) and 1.29 ± 0.04 g/L ($p < 0.05$) after 24 h and 48 h, respectively. The CLA concentration in the different tested postbiotics remained approximately the same as that evaluated in the probiotic samples confirming that the mild heat treatment did not affect the CLA concentration.

3.3 Pretreatment of milk-based postbiotics with or without the addition of LA or SCGs prevented the P31-43-induced increase in pNF-kB

We tested the effects of milk-based postbiotics on Caco-2 at concentrations of 1 and 2%, because these were able to preserve the cell viability (Supplementary Figures 1, 2). Both 1% (Supplementary Figure 1) and 2% concentrations were used to prevent on NF-kB increase mediated by p31-43, but only the 2% w/v of the postbiotics (2.6×10^8 CFU/g) was able to prevent p31-43 effects on NF-kB activation (Figures 2A,B). Indicating that the concentration of the post biotic is an important factor for its activity. Caco-2 cells were treated with milk-based postbiotics with the addition of LAs to understand whether CLAs exert different biological effects on inflammation pathways. Caco-2 cells were pretreated with milk-based *L. plantarum* postbiotics at 2% w/v, with or without the addition of LA, for 30 min, and subsequently stimulated with p31-43. To assess inflammation, we evaluated the phosphorylation of NF-kB by WB. Our data revealed an increase in pNF-kβ levels after stimulation with P31-43. Both milk-based postbiotics (with and without the addition of an LA source) reduced the level of pNF-kβ induced by p31-43. These findings indicated that milk-based postbiotics with LA achieved the same pNF-kβ reduction effect as milk-based postbiotic with only *L. plantarum* (Figures 2A,B, $p < 0.05$ for both).

Additionally, we evaluated the effects of milk-based postbiotics added with SCGs and SCG oil in Caco-2 cells in the presence of the gliadin peptide. For this purpose, Caco-2 cells were pretreated with milk-based postbiotics at 2% w/v for 30 min and subsequently stimulated with P31-43, and the activation of pNF-kβ was evaluated via WB. Pretreatment with milk-based postbiotics combined with SCGs reduced in a statistically significant way the levels of pNF-kβ

induced by p31-43 (Figures 2C,D, $p < 0.05$). However, milk-based postbiotics with SCG oil did not significantly inhibit the increase in pNF-kβ levels induced by P31-43 (Figures 2C,D).

The milk-based postbiotic with SCGs was more efficient than the milk-based postbiotic in preventing P31-43-induced activation of NF-kB under the same conditions (Figures 2E,F). In fact, the mean phosphorylation of NF-kB in Caco-2 cells pretreated with the milk-based *L. plantarum* postbiotic with SCGs was half than that of NF-kB in Caco-2 cells pretreated with the milk-based *L. plantarum* postbiotic, although a significant difference was not detected between the two groups analyzed.

3.4 In CeD intestinal organoids milk based postbiotic of *Lactobacillus plantarum* with or without SCGs reduced inflammation

The milk-based postbiotic activity of *L. plantarum* was tested in intestinal organoids derived from CeD patients with villus atrophy and compared with that of intestinal organoids derived from control subjects. Intestinal organoids can be obtained from stem cells LGR5 + present in intestinal crypts. This kind of multipotent cells could differentiate toward a limited number of cell types in the presence of specific growth factors. The stem cells are grown in 3D and enclosed in a matrix, which serves as a basal membrane. By using appropriate stimuli, they differentiate into epithelial cells. They can be grown and amplified for several weeks as spheroids. However, to know the response to stimuli of a pro-inflammatory nature or to investigate the possible beneficial effect of pre-pro-postbiotics and nutraceuticals or drugs, it is necessary to create a 2D monolayer of intestinal epithelial cells. Two-dimensional monolayers of intestinal organoids allow direct contact of the apical, adsorptive pole of the cells with the culture medium; this cannot occur in 3D culture as the apical sides of the cells are enclosed in the spherical organoids. Due to the lack of an appropriate scaffold, they do not form villi, instead the crypts are nicely represented as budding from the main spheroid (Supplementary Figure 2). Morphologically they do not show great differences although we (13) and others (37) have noticed that GCD-CeD organoids appear more dense respect to controls.

To test postbiotic activity, intestinal organoids were opened in 2D on Matrigel pretreated plates and treated with milk-based postbiotics from *L. plantarum* with or without SCGs for 3 h. Compared with CTRs organoids, intestinal organoids from CeD patients were inflamed (Figures 3A,B, $p < 0.01$). In fact, CeD organoids presented increased NF-kB phosphorylation levels, as measured by WB[13]. Compared with that of the untreated CeD intestinal organoid, the pNF-kB of the milk-based *L. plantarum* postbiotic with or without the addition of SCGs was reduced by 4.63- and 5.42-fold, respectively (Figures 3A,B, $p < 0.05$ for both). Interestingly, the levels of pNF-kB in intestinal organoids from CeD patients after treatment with milk-based *L. plantarum* postbiotics with and without SCGs were similar to the levels found in intestinal organoids from controls.

IL-8 an inflammatory cytokine most abundant in the intestinal epithelium can induce NF-kB activation (38) and is increased in IBD and CeD intestinal biopsies (39). Culture media from CTR and GCD-CeD, treated and not with milk- based *L. plantarum* postbiotics

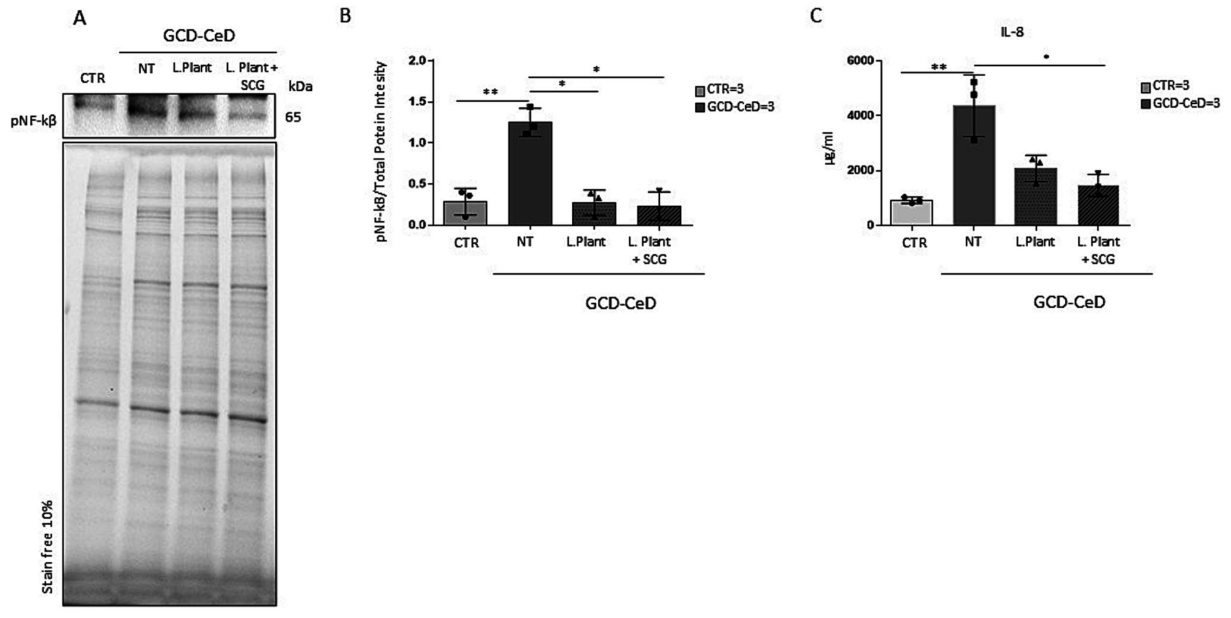

FIGURE 3
Effects of the milk-based postbiotic of *L. plantarum CECT 749* and milk-based postbiotic of *L. plantarum* alone or with the addition of SCGs in intestinal organoids of CeD patients. **(A)** Western blot analysis of protein lysates from organoids from CeD patients, untreated and treated with milk-based postbiotic of *L. plantarum* alone or with the addition of SCGs for 3 h, and control organoids were blotted with antibodies against pNF-kB. **(B)** Densitometric analysis of the bands from the WB shown in **A**. Columns represent the mean, and bars represent the standard deviation of the relative intensity of pNF-kB with respect to the total protein intensity. Number of organoids was indicated. Student's *t* test: * = $p < 0.05$. **(C)** ELISA showing IL-8 cytokine levels in the culture media of GCD-CeD intestinal organoids treated with and without milk-based postbiotics of *L. plantarum*, with and without SCG and CTR organoids. The numbers of organoids analyzed are indicated. The columns represent the media, and bars represent the standard deviation. Student's *t* test: * = $p < 0.05$, ** = $p < 0.05$.

with and without the addition of SCG were analyzed by ELISA assay to test IL-8 levels. The results shown in Figure 3C indicate that IL-8 increased in CeD respect to CTR in a statistically significant way. The treatment with both the postbiotics, with and without, SCG was able to decrease IL-8 levels, but only the postbiotic with SCG reduced this cytokine in a statistically significant way, indicating that the SCG on some read outs is more efficient than the postbiotic alone.

3.5 Discussion

We demonstrated that the presence of LA and SCG oil in the fermented milk negatively affected both bacterial growth and lactic acid production during 48 h of fermentation. On the other side the addition of SCG promoted microbial proliferation and lactic acid formation which were even higher than those observed in fermented milk without any additives. Indicating that the SCG probably is improving the bacterial growth and lactic acid formation. *L. plantarum* could convert LA to conjugated linoleic acids (CLAs). As a source of LA we used not only LA, but also the used food waste SCGs and SCG oil that are a natural source of LA (32). The maximum amount of CLAs was produced after 24 h of fermentation in milk supplemented with LA, with a higher CLA concentration being achieved than other concentrations reports in the literature where the same fermentation conditions (31) or the same microorganisms (21) were used. During fermentation in milk supplemented with SCGs or SCG oil, no CLA production was observed, probably because CLAs were already abundant in the matrix supplemented with the coffee byproducts.

The higher bacterial growth and lactic acid production observed when SCGs was added to milk could be due to the presence of some oligosaccharides (40), such as mannooligosaccharides (MOS) and galactomannans, for which previous works have already shown the prebiotic effect on lactic acid bacteria (41). SCGs has already been used as a substrate to be fermented by lactic acid bacteria to produce lactic acid (42, 43), after preliminary chemical and enzymatic pretreatments. In the present work, *L. plantarum* was able to metabolize SCGs and to use it as prebiotic without any pretreatment, to the best of our knowledge this has been unreported before.

SCGs are a rich source of polysaccharides (more than 50% by dry weight), such as cellulose and hemicellulose; among the sugars, mannose, galactose, and glucose are the most abundant. Lignin is also present in significant amounts (close to 25%), and the total fiber content is 60% (44). Approximately 20% of SCGs consist of proteins. SCGs have antioxidant potential (44) because of the presence of phenolic compounds (Supplementary Table 3) such as chlorogenic acid, caffeine, and flavonoids; considering its high fiber content, high concentration of linoleic acid and anti-inflammatory potential, it can be considered for the development of functional foods.

In the present study, we investigated the effects of milk-based postbiotics obtained from *L. plantarum* CECT 749 with and without free LA, SCGs or SCG oil on inflammation in Caco-2 cells after treatment with the gliadin peptide P31-43 and in intestinal organoids from CeD patients. Intestinal epithelial cells derived from intestinal carcinoma, Caco-2 cells, or staminal intestinal cells such as intestinal organoids were used to test the ability of milk-based postbiotics to prevent gliadin peptide P31-43-induced inflammation.

Caco-2 cells are widely used as an *in vitro* model to study the intestinal barrier and intestinal absorption in patients with celiac disease and gluten sensitivity (8, 34). After exposure to gluten peptides, Caco-2 cells exhibit increased intestinal permeability, and several other pathways, such as inflammation are altered (8). Conte et al. demonstrated that in the presence of both P31-43 and PTG, Caco-2 cells were inflamed and exhibited increased pNF-kB levels (15). In the same model, postbiotics from both *L. paracasei* and *L. rhamnosus* GG prevented the proinflammatory effects induced by gliadin peptides on Caco-2 cells (15, 16).

The effect was observed only with 2% fermented products, indicating that their activity is concentration dependent and that *L. plantarum* with added LA was able to prevent the effects of P31-43 on NF-kB activation. Although *L. plantarum* with SCGs was more efficient than *L. plantarum* alone in preventing P31-43 activity, the difference was not statistically significant. *L. plantarum* with SCG oil alone was not able to prevent the effects of P31-43 on CaCo2 cells. This is probably due to the fact that SCG oil does not benefit the bacteria's growth, activities and the production of active metabolites. The interference of the fatty matrix on bacterial activities has already been described in the literature (45, 46).

Considering that three different postbiotic samples characterized by a different CLA concentration (namely milk with LA: 1,5 g/L CLA; milk without any addition: no CLA detected; milk with SCG: 0,5 g/L CLA) all showed a similar anti-inflammatory capacity, it is very likely that the effects on P31–43-induced inflammation did not depend on CLA production. We do not know why *L. plantarum* lost its activity after treatment with SCG oil; very likely, the high-fat matrix was not ideal for the production of one or more metabolites needed for the anti-inflammatory effect.

Intestinal organoids, which mimic miniature of the intestine, are a cell model used to study pathogenic agents and mechanisms related to celiac disease, such as inflammation (37, 47–49). Organoids are good models for studying some pathogenetic mechanisms of CeD, such as proliferation and constitutive inflammation, because they reproduce these alterations found in CeD biopsy samples (13, 36). Moreover, other studies demonstrated that treatment with *L. paracasei* and *L. rhamnosus* GG was able to reduce constitutive inflammation in CeD intestinal organoids (15, 16). In this manuscript we have confirmed that GCD-CeD organoids were inflamed respect to the controls by using two different read outs, namely the activation of NF-kB and the levels of IL-8 in the culture media. Both were increased in GCD-CeD organoids and decreased by the milk-based postbiotic with and without the addition of SCG. To note is the result on IL-8 reduction that was statistically significant only after treatment with milk-based *L. plantarum* postbiotic added with SCG.

The mechanism by which milk-based postbiotics obtained by the fermentation of *L. plantarum*, with and without the addition of LA or SCGs, exert their biological effects after treatment with P31-43 in Caco-2 cells and CeD intestinal organoids still needs to be clarified. The possible ability of milk-based postbiotics of *L. plantarum* with SCGs to prevent P31-43-induced inflammation could be associated with the presence of molecules with antioxidant activity and anti-inflammatory effects in this waste product (50). Further studies will be necessary to investigate which metabolites exert anti-inflammatory effects. Interestingly, in presence of SCG the bacteria grow was better and produce more lactic acids, indicating a better fermentation activity, but the production of CLA that was basically absent. All this indicating that CLA are not responsible for the anti-inflammatory activity, probably mediated by other metabolites. However, this observation confirms the possibility of reusing food waste from coffee processing to produce functional foods with improved

beneficial properties. This enhanced effect of SCGs cannot be described on the constitutive inflammation of CeD organoids. This is probably because different inflammatory pathways are engaged in intestinal organoids.

In conclusion, milk-based postbiotics of *L. plantarum*, with or without SCGs, can prevent P31-43-induced inflammation in Caco-2 cells and reduce constitutive inflammation in CeD organoids.

These preclinical studies provide a good basis for initiating clinical trials in celiac patients to prevent the proinflammatory effects of gliadin peptides. It would be interesting to test the ability of postbiotics to prevent disease in potential patients who have anti-transglutaminase antibodies but have not yet developed the intestinal lesions typical of celiac disease. However, more studies are needed to investigate the related safety parameters and biological activity of postbiotics *in vivo*. Despite patients' best efforts, some subjects can experience continuous exposure due to cross-contamination or traces of gluten in food. These risks could, in some cases, compromise the health and quality of life of these patients. Therefore, it is generally useful to study compounds that can prevent the inflammatory effects of gliadin with the hope of reducing the burden of living with celiac disease and improving long-term health outcomes.

Data availability statement

The original contributions presented in the study are included in the article/Supplementary material, further inquiries can be directed to the corresponding author.

Ethics statement

The studies involving human samples were reviewed and approved by the Ethical Committee of the Federico II University of Naples Ethical approval: 115/09/ESPROT. Written informed consent to participate in this study was provided by the participants' legal guardian/next of kin. Written informed consent was obtained from the minor(s)' legal guardian/next of kin for the publication of any potentially identifiable images or data included in this article.

Author contributions

CB: Conceptualization, Data curation, Formal analysis, Methodology, Validation, Writing – original draft, Writing – review & editing. FM: Formal analysis, Methodology, Writing – original draft. FN: Data curation, Validation, Writing – original draft. FP: Data curation, Methodology, Writing – original draft. RC: Data curation, Formal analysis, Writing – original draft. RN: Conceptualization, Data curation, Validation, Writing – original draft. MB: Conceptualization, Data curation, Validation, Writing – original draft, Writing – review & editing. MN: Conceptualization, Data curation, Validation, Writing – review & editing.

Funding

The author(s) declare that no financial support was received for the research and/or publication of this article.

Conflict of interest

FN and FP were employed by company I.T.P. Innovation and Technology Provider S.r.l.

The remaining authors declare that the research was conducted in the absence of any commercial or financial relationships that could be construed as a potential conflict of interest.

Generative AI statement

The authors declare that no Gen AI was used in the creation of this manuscript.

Publisher's note

All claims expressed in this article are solely those of the authors and do not necessarily represent those of their affiliated organizations, or those of the publisher, the editors and the reviewers. Any product that may be evaluated in this article, or claim that may be made by its manufacturer, is not guaranteed or endorsed by the publisher.

Supplementary material

The Supplementary material for this article can be found online at: https://www.frontiersin.org/articles/10.3389/fnut.2025.1549120/full#supplementary-material

References

1. Barone MV, Auricchio R, Nanayakkara M, Greco L, Troncone R, Auricchio S. Pivotal role of inflammation in celiac disease. *Int J Mol Sci*. (2022) 23:7177. doi: 10.3390/ijms23137177

2. Barone MV, Salvatore A. Pro-inflammatory nutrient: focus on gliadin and celiac disease. *Int J Mol Sci*. (2022) 23:5577. doi: 10.3390/ijms23105577

3. Barone MV, Auricchio S. A cumulative effect of food and viruses to trigger celiac disease (CD): a commentary on the recent literature. *Int J Mol Sci*. (2021) 22:2027. doi: 10.3390/ijms22042027

4. Tilg H, Moschen AR. Food, immunity, and the microbiome. *Gastroenterology*. (2015) 148:1107–19. doi: 10.1053/j.gastro.2014.12.036

5. Bouziat R, Hinterleitner R, Brown JJ, Stencel-Baerenwald JE, Ikizler M, Mayassi T, et al. Reovirus infection triggers inflammatory responses to dietary antigens and development of celiac disease. *Science*. (2017) 356:44–50. doi: 10.1126/science.aah5298

6. Chirdo FG, Auricchio S, Troncone R, Barone MV. The gliadin p31-43 peptide: inducer of multiple proinflammatory effects. *Int Rev Cell Mol Biol*. (2021) 358:165–205. doi: 10.1016/bs.ircmb.2020.10.003

7. Barone MV, Troncone R, Auricchio S. Gliadin peptides as triggers of the proliferative and stress/innate immune response of the celiac small intestinal mucosa. *Int J Mol Sci*. (2014) 15:20518–37. doi: 10.3390/ijms151120518

8. Nanayakkara M, Lania G, Maglio M, Auricchio R, de Musis C, Discepolo V, et al. P31-43, an undigested gliadin peptide, mimics and enhances the innate immune response to viruses and interferes with endocytic trafficking: a role in celiac disease. *Sci Rep*. (2018) 8:10821. doi: 10.1038/s41598-018-28830-y

9. Maiuri MC, de Stefano D, Mele G, Fecarotta S, Greco L, Troncone R, et al. Nuclear factor kappa B is activated in small intestinal mucosa of celiac patients. *J Mol Med*. (2003) 81:373–9. doi: 10.1007/s00109-003-0440-0

10. Liu T, Zhang L, Joo D, Sun S-C. NF-κB signaling in inflammation. *Signal Transduct Target Ther*. (2017) 2:17023. doi: 10.1038/sigtrans.2017.23

11. Hayden MS, Ghosh S. NF-κB in immunobiology. *Cell Res*. (2011) 21:223–44. doi: 10.1038/cr.2011.13

12. Fernandez-Jimenez N, Castellanos-Rubio A, Plaza-Izurieta L, Irastorza I, Elcoroaristizabal X, Jauregi-Miguel A, et al. Coregulation and modulation of NFκB-related genes in celiac disease: uncovered aspects of gut mucosal inflammation. *Hum Mol Genet*. (2014) 23:1298–310. doi: 10.1093/hmg/ddt520

13. Porpora M, Conte M, Lania G, Bellomo C, Rapacciuolo L, Chirdo FG, et al. Inflammation is present, persistent and more sensitive to Proinflammatory triggers in celiac disease enterocytes. *Int J Mol Sci*. (2022) 23:1973. doi: 10.3390/ijms23041973

14. Andrews C, McLean MH, Durum SK. Cytokine tuning of intestinal epithelial function. *Front Immunol*. (2018) 9:1270. doi: 10.3389/fimmu.2018.01270

15. Conte M, Nigro F, Porpora M, Bellomo C, Furone F, Budelli AL, et al. Gliadin peptide P31-43 induces mTOR/NFkβ activation and reduces autophagy: the role of *Lactobacillus paracasei* CBA L74 Postbiotc. *Int J Mol Sci*. (2022) 23:3655. doi: 10.3390/ijms23073655

16. Furone F, Bellomo C, Carpinelli M, Nicoletti M, Hewa-Munasinghege FN, Mordaa M, et al. The protective role of *Lactobacillus rhamnosus* GG postbiotic on the alteration of autophagy and inflammation pathways induced by gliadin in intestinal models. *Front Med*. (2023) 10:1085578. doi: 10.3389/fmed.2023.1085578

17. Freire R, Ingano L, Serena G, Cetinbas M, Anselmo A, Sapone A, et al. Human gut derived-organoids provide model to study gluten response and effects of microbiota-derived molecules in celiac disease. *Sci Rep*. (2019) 9:7029. doi: 10.1038/s41598-019-43426-w

18. He M, Shi B. Gut microbiota as a potential target of metabolic syndrome: the role of probiotics and prebiotics. *Cell Biosci*. (2017) 7:54. doi: 10.1186/s13578-017-0183-1

19. Zheng HJ, Guo J, Jia Q, Huang YS, Huang WJ, Zhang W, et al. The effect of probiotic and synbiotic supplementation on biomarkers of inflammation and oxidative stress in diabetic patients: a systematic review and meta-analysis of randomized controlled trials. *Pharmacol Res*. (2019) 142:303–13. doi: 10.1016/j.phrs.2019.02.016

20. Putera HD, Doewes RI, Shalaby MN, Ramírez-Coronel AA, Clayton ZS, Abdelbasset WK, et al. The effect of conjugated linoleic acids on inflammation, oxidative stress, body composition and physical performance: a comprehensive review of putative molecular mechanisms. *Nutr Metab*. (2023) 20:35. doi: 10.1186/s12986-023-00758-9

21. Ares-Yebra A, Garabal JI, Carballo J, Centeno JA. Formation of conjugated linoleic acid by a *Lactobacillus plantarum* strain isolated from an artisanal cheese: evaluation in miniature cheeses. *Int Dairy J*. (2019) 90:98–103. doi: 10.1016/j.idairyj.2018.11.007

22. Sosa-Castañeda J, Hernández-Mendoza A, Astiazarán-García H, Garcia HS, Estrada-Montoya MC, González-Córdova AF, et al. Screening of Lactobacillus strains for their ability to produce conjugated linoleic acid in milk and to adhere to the intestinal tract. *J Dairy Sci*. (2015) 98:6651–9. doi: 10.3168/jds.2014-8515

23. Özer CO, Kılıç B. Utilization of optimized processing conditions for high yield synthesis of conjugated linoleic acid by *L. plantarum* AB20-961 and *L. plantarum* DSM2601 in semi-dry fermented sausage. *Meat Sci*. (2020) 169:108218. doi: 10.1016/j.meatsci.2020.108218

24. Özer CO, Kılıç B, Kılıç GB. In-vitro microbial production of conjugated linoleic acid by probiotic *L. plantarum* strains: utilization as a functional starter culture in sucuk fermentation. *Meat Sci*. (2016) 114:24–31. doi: 10.1016/j.meatsci.2015.12.005

25. Le PTK, Vu QTH, Nguyen QTV, Tran KA, Le KA. Extraction and evaluation the biological activities of oil from spent coffee grounds. *Chem Eng Trans*. (2017) 56:1729–34. doi: 10.3303/CET1756289

26. Martinez-Saez N, García AT, Pérez ID, Rebollo-Hernanz M, Mesías M, Morales FJ, et al. Use of spent coffee grounds as food ingredient in bakery products. *Food Chem*. (2017) 216:114–22. doi: 10.1016/j.foodchem.2016.07.173

27. McNutt J, He Q. Spent coffee grounds: a review on current utilization. *J Ind Eng Chem*. (2019) 71:78–88. doi: 10.1016/j.jiec.2018.11.054

28. Luz C, D'Opazo V, Mañes J, Meca G. Antifungal activity and shelf life extension of loaf bread produced with sourdough fermented by *Lactobacillus* strains. *J Food Process Preserv*. (2019) 43:126. doi: 10.1111/jfpp.14126

29. Ando A, Ogawa J, Kishino S, Shimizu S. Conjugated linoleic acid production from castor oil by *Lactobacillus plantarum* JCM 1551. *Enzym Microb Technol*. (2004) 35:40–5. doi: 10.1016/j.enzmictec.2004.03.013

30. Colucci Cante R, Recupero A, Prata T, Nigro F, Passannanti F, Gallo M, et al. Valorisation through lactic fermentation of industrial wastewaters from a bean blanching treatment. *Fermentation*. (2023) 9:350. doi: 10.3390/fermentation9040350

31. Dahiya DK, Puniya AK. Optimisation of fermentation variables for conjugated linoleic acid bioconversion by *Lactobacillus fermentum* DDHI 27 in modified skim milk. *Int J Dairy Technol*. (2018) 71:46–55. doi: 10.1111/1471-0307.12375

32. Colucci Cante R, Garella I, Gallo M, Nigro R. Effect of moisture content on the extraction rate of coffee oil from spent coffee grounds using Norflurane as solvent. *Chem Eng Res Des*. (2021) 165:172–9. doi: 10.1016/j.cherd.2020.11.002

33. Stefanov I, Vlaeminck B, Fievez V. A novel procedure for routine milk fat extraction based on dichloromethane. *J Food Compos Anal*. (2010) 23:852–5. doi: 10.1016/j.jfca.2010.03.016

34. Barone MV, Gimigliano A, Castoria G, Paolella G, Maurano F, Paparo F, et al. Growth factor-like activity of gliadin, an alimentary protein: implications for coeliac disease. *Gut*. (2007) 56:480–8. doi: 10.1136/gut.2005.086637

35. Sarno M, Lania G, Cuomo M, Nigro F, Passannanti F, Budelli A, et al. *Lactobacillus paracasei* CBA L74 interferes with gliadin peptides entrance in Caco-2 cells. *Int J Food Sci Nutr*. (2014) 65:953–9. doi: 10.3109/09637486.2014.940283

36. Nanayakkara M, Bellomo C, Furone F, Maglio M, Marano A, Lania G, et al. PTPRK, an EGFR phosphatase, is decreased in CeD biopsies and intestinal organoids. *Cells*. (2022) 12:115. doi: 10.3390/cells12010115

37. Dieterich W, Neurath MF, Zopf Y. Intestinal ex vivo organoid culture reveals altered programmed crypt stem cells in patients with celiac disease. *Sci Rep*. (2020) 10:3535. doi: 10.1038/s41598-020-60521-5

38. Lee BC, Kim SH, Choi SH, Kim TS. Induction of interleukin-8 production via nuclear factor-kappaB activation in human intestinal epithelial cells infected with *Vibrio vulnificus*. *Immunology*. (2005) 115:506–15. doi: 10.1111/j.1365-2567.2005.02185.x

39. Aghamohamad E, Asri N, Odak A, Rostami-Nejad M, Chaleshi V, Hajinabi Y, et al. Correction: gene expression analysis of intestinal IL-8, IL-17 a and IL-10 in patients with celiac and inflammatory bowel diseases. *Mol Biol Rep*. (2024) 51:569. doi: 10.1007/s11033-024-09440-6

40. Genovese A, de Vivo A, Aprea A, Cristina Tricarico M, Sacchi R, Sarghini F. Particle size and variety of coffee used as variables in mitigation of furan and 2-methylfuran content in espresso coffee. *Food Chem*. (2021) 361:130037. doi: 10.1016/j.foodchem.2021.130037

41. Gu J, Pei W, Tang S, Yan F, Peng Z, Huang C, et al. Procuring biologically active galactomannans from spent coffee ground (SCG) by autohydrolysis and enzymatic hydrolysis. *Int J Biol Macromol*. (2020) 149:572–80. doi: 10.1016/j.ijbiomac.2020.01.281

42. Hudeckova H, Neureiter M, Obruca S, Frühauf S, Marova I. Biotechnological conversion of spent coffee grounds into lactic acid. *Lett Appl Microbiol*. (2018) 66:306–12. doi: 10.1111/lam.12849

43. Lee XJ, Ong HC, Gao W, Ok YS, Chen WH, Goh BHH, et al. Solid biofuel production from spent coffee ground wastes: process optimisation, characterisation and kinetic studies. *Fuel*. (2021) 292:120309. doi: 10.1016/j.fuel.2021.120309

44. Ballesteros LF, Teixeira JA, Mussatto SI. Chemical, functional, and structural properties of spent coffee grounds and coffee Silverskin. *Food Bioprocess Technol*. (2014) 7:3493–503. doi: 10.1007/s11947-014-1349-z

45. Desbois AP, Smith VJ. Antibacterial free fatty acids: activities, mechanisms of action and biotechnological potential. *Appl Microbiol Biotechnol*. (2010) 85:1629–42. doi: 10.1007/s00253-009-2355-3

46. Kankaanpää PE, Salminen SJ, Isolauri E, Lee YK. The influence of polyunsaturated fatty acids on probiotic growth and adhesion. *FEMS Microbiol Lett*. (2001) 194:149–53. doi: 10.1111/j.1574-6968.2001.tb09460.x

47. Dotsenko V, Sioofy-Khojine A-B, Hyöty H, Viiri K. Human intestinal organoid models for celiac disease research. *Methods Cell Biol*. (2023) 179:173–93. doi: 10.1016/bs.mcb.2023.01.008

48. Simpson HL, Smits E, Moerkens R, Wijmenga C, Mooiweer J, Jonkers IH, et al. Human organoids and organ-on-chips in coeliac disease research. *Trends Mol Med*. (2024) 31:117–37. doi: 10.1016/j.molmed.2024.10.003

49. Zhang M, Liu Y, Chen Y-G. Generation of 3D human gastrointestinal organoids: principle and applications. *Cell Regen*. (2020) 9:6. doi: 10.1186/s13619-020-00040-w

50. Acevedo F, Rubilar M, Scheuermann E, Cancino B, Uquiche E, Garcés M, et al. Spent coffee grounds as a renewable source of bioactive compounds. *J Biobased Mater Bioenergy*. (2013) 7:420–8. doi: 10.1166/jbmb.2013.1369

51. Garella R, Baccari MC. Endocannabinoids modulate non-adrenergic, non-cholinergic inhibitory neurotransmission in strips from the mouse gastric fundus. *Acta Physiol (Oxf)* (2012) 206:80–7.

52. Ichihara K, Fukubayashi Y. Preparation of fatty acid methyl esters for gas-liquid chromatography. *J Lipid Res*. (2010) 51:635–40. doi: 10.1194/jlr.D001065

frontiers | Frontiers in Nutrition

TYPE Original Research
PUBLISHED 14 May 2025
DOI 10.3389/fnut.2025.1556527

Check for updates

OPEN ACCESS

EDITED BY
Alina Kurylowicz,
Polish Academy of Sciences, Poland

REVIEWED BY
Iftikhar Younis Mallhi,
Minhaj University Lahore, Pakistan
Zhengqi Liu,
Shenzhen University, China

*CORRESPONDENCE
She-Ching Wu
✉ scwu@mail.ncyu.edu.tw

†These authors share first authorship

RECEIVED 07 January 2025
ACCEPTED 14 April 2025
PUBLISHED 14 May 2025

CITATION
Liu C-Y, Liu W-Y, Shi Y-C and Wu S-C (2025) Unveiling the therapeutic benefits of black chokeberry (*Aronia melanocarpa*) in alleviating hyperuricemia in mice. *Front. Nutr.* 12:1556527. doi: 10.3389/fnut.2025.1556527

COPYRIGHT
© 2025 Liu, Liu, Shi and Wu. This is an open-access article distributed under the terms of the Creative Commons Attribution License (CC BY). The use, distribution or reproduction in other forums is permitted, provided the original author(s) and the copyright owner(s) are credited and that the original publication in this journal is cited, in accordance with accepted academic practice. No use, distribution or reproduction is permitted which does not comply with these terms.

Unveiling the therapeutic benefits of black chokeberry (*Aronia melanocarpa*) in alleviating hyperuricemia in mice

Chin-Yuan Liu[1†], Wen-Yu Liu[2†], Yeu-Ching Shi[1] and She-Ching Wu[1*]

[1]Department of Food Sciences, National Chiayi University, Chiayi, Taiwan, [2]Department of Food Safety/Hygiene and Risk Management, College of Medicine, National Cheng Kung University, Tainan, Taiwan

Background: Hyperuricemia not only increases the risk of cardiovascular diseases such as dyslipidemia, hypertension, coronary artery disease, obesity, metabolic syndrome, and type-2 diabetes, but also severely impacts kidney function, potentially leading to acute kidney injury and chronic kidney disease.

Methods: This study aims to investigate the health benefits of black chokeberry (*Aronia melanocarpa*) on hyperuricemic mice induced by oxonic acid.

Result: The experimental results showed that black chokeberry had no significant toxic or negative effects in mice. The measurement of uric acid (UA) indicated that black chokeberry suppressed the UA levels. Additionally, the xanthine oxidase activity in the high-dose group was significantly decreased, along with reductions in serum urea nitrogen and creatinine levels. Black chokeberry effectively increased the glutathione levels in hyperuricemic mice and reduced malondialdehyde levels, as well as significantly inhibiting adenosine deaminase activity.

Conclusion: Its efficacy is comparable to that of the marketed drug allopurinol, underscoring the potential of black chokeberry as a functional product for uric acid reduction.

KEYWORDS

adenosine deaminase, black chokeberry, hyperuricemia, uric acid, xanthine oxidase

1 Introduction

Hyperuricemia refers to an excessively high concentration of uric acid (UA) in the serum. Typically, hyperuricemia is diagnosed when serum UA levels exceed 7 mg/dL in men and 6 mg/mL in women. The global prevalence of hyperuricemia is approximately 19.37%, with higher incidences observed in men and postmenopausal women (1). As the condition progresses, it may develop into gouty arthritis, kidney stones, and cause renal damage (2).

UA is the final product of purine metabolism, with most serum UA originating from endogenous purines, and about one-third coming from dietary sources. Hyperuricemia is caused by excessive production of UA and insufficient renal excretion. Therefore, current medications for lowering UA primarily work by promoting UA excretion and inhibiting xanthine oxidase (XO) (3). However, these drugs are often associated with side effects such as allergies, diarrhea, hepatotoxicity, and nephrotoxicity (4, 5). Hence, there is a need for alternative safe and effective treatments for hyperuricemia.

Aronia melanocarpa, commonly known as black chokeberry, is a berry rich in polyphenolic compounds and flavonoids. Its main active components include chlorogenic acid, neochlorogenic acid, anthocyanins, proanthocyanidins, and quercetin derivatives. Numerous studies have confirmed its health benefits, including antioxidant, anti-inflammatory, antimicrobial, antihypertensive, lipid-lowering, antidiabetic, hepatoprotective, and neuroprotective effects (6). Previous studies have shown that black chokeberry can improve serum UA levels, reduce xanthine oxidase activity, and inhibit inflammation associated with acute gout in rat models (7). Additionally, black chokeberry has been shown to alleviate kidney damage by reducing the expression of pro-inflammatory factors, oxidative stress, lipid peroxidation, and apoptosis, thereby improving renal function (8).

This study used domestically sourced black chokeberry to evaluate serum UA, blood urea nitrogen (BUN), and creatinine (CRE) levels in mice, assessing kidney function. It also measured xanthine oxidase, glutathione (GSH), malondialdehyde (MDA), and adenosine deaminase (ADA) activity to assess liver function. The UA-lowering effects of black chokeberry were further explored in hyperuricemic mice induced by oxonic acid potassium salt (OA). Black chokeberry demonstrated potential in inhibiting UA production, reducing BUN, and lowering creatinine levels, while also inhibiting the activity of xanthine oxidase and adenosine deaminase. These results suggest that black chokeberry may improve both kidney and liver function in mice and holds promise as a functional product for lowering UA.

2 Methods

2.1 Sample preparation

After juicing for black chokeberries, the juice was filtered through a 40-mesh sieve and then vacuum filtered to remove the skin and pulp. The filtrate was then freeze-dried using a vacuum freeze dryer, and the resulting dried powder constituted the black chokeberry. This powder was stored at −20°C for subsequent experiments.

2.2 Animals

This study was approved by the Laboratory Animal Care and Use Committee of National Chiayi University (Approval No. 112021). Male ICR mice, 5 weeks old, were purchased from LASCO Biotechnology Co., Ltd. to establish an oxonic acid potassium salt (OA)-induced hyperuricemia model by ip. After acclimatizing the mice for 1 week, they were randomly divided into six groups, each with six mice: blank, OA (250 mg/kg bw/day) induction by intraperitoneal injections, OA + allopurinol (10 mg/kg bw/day), OA + low-dosage sample (450 mg/kg bw/day), OA + medium-dosage sample (900 mg/kg bw/day), and OA + high-dosage sample (1800 mg/kg bw/day). The experiment lasted for 1 week. After the experiment, blood was collected via cardiac puncture for biochemical analysis, and the liver and kidneys were dissected. The organs were rinsed with saline, weighed, wrapped in aluminum foil, and rapidly frozen in liquid nitrogen, then stored at-80°C for further analysis.

2.3 Serum preparation

Place the collected blood in a tube without anticoagulant and allow it to clot at room temperature for 1 h, and then centrifugation was carried out at 3,000 rpm for 10 min at 4°C to separate the serum and stored at −80°C.

2.4 Liver homogenate preparation

Liver (0.4 g) was homogenated with PBS, and the solution was centrifuged at 5,000 rpm for 10 min at 4°C, the supernatant was collected and stored at −80°C.

2.5 Measurement of blood urea nitrogen

Analyze using the Urea Enzymatic Kinetic Method commercial kit (RANDOX). Add 10 μL of serum and the standard solution to 1 mL of the reaction reagent containing α-oxoglutarate, ADP, urease, GLDH, NADH, and Tris buffer (pH 7.6) for incubation at 37°C for 30 s, then the absorbance at 340 nm was measured. Continue the reaction for another 60 s and measure the absorbance at 340 nm again.

The calculation formula: BUN = Standard concentration × $\Delta A_{sample,\ 340\ nm}/\Delta A_{standard,\ 340\ nm}$.

2.6 Measurement of serum creatinine content

Analyze using the Creatinine commercial kit (RANDOX). Add 100 μL of serum and the standard solution to 1 mL of the reaction reagent containing 35 μmol/L picric acid and 0.32 mol/L sodium hydroxide. Measure the absorbance at 492 nm after 30 s and again after 150 s.

The calculation formula: CRE = Standard concentration × $\Delta A_{sample,\ 492\ nm}/\Delta A_{standard,\ 492\ nm}$.

2.7 Measurement of serum uric acid content

Analyze using the Uric Acid commercial kit (RANDOX). Add 20 μL of serum and the uric acid standard solution to 1 mL of the reaction reagent containing HEPES buffer, 3,5-dichloro-2-hydroxybenzenesulfonic acid, 4-aminophenazone, uricase, and peroxidase. Mix thoroughly and incubate in a water bath at 37°C for 5 min. Measure the absorbance at 520 nm.

The calculation formula: UA = Standard concentration × ($A_{sample,\ 520\ nm}/A_{standard,\ 520\ nm}$).

2.8 Measurement of xanthine oxidase activity

The activity of xanthine oxidase in the liver is measured based on the conversion of xanthine to uric acid (9). Adding 100 μL of liver homogenate and the uric acid standard solution to 4.9 mL of the

reaction reagent containing 50 μM xanthine and 5 mM EDTA. Incubate at 37°C for 30 min, then add 500 μL of 0.58 M HCl to terminate the reaction. Measure the absorbance at a wavelength of 290 nm.

2.9 Measurement of glutathione content

Liver homogenate (100 μL) to 100 μL of 5% TCA solution and incubate on ice for 5 min. Centrifugating at 12,000 rpm for 15 min, and collect 150 μL of the supernatant. Add this to 750 μL of Tris/EDTA solution (pH 8.2) and mix thoroughly. Then, add 37.5 μL of 5,5′-DithioBis-(2-Nitrobenzoic Acid) (DTNB) solution, incubate for 5 min, and measure the absorbance at 412 nm (10).

2.10 Measurement of malondialdehyde content

Liver tissue homogenate (40 μL) and TEP standard to 120 μL of deionized water and 40 μL of 8.1% SDS solution. Mix thoroughly and incubate at room temperature for 5 min. Then, add 300 μL of 20% ethanolic acid (pH 3.5) and 300 μL of 0.8% TBA reagent, and incubate at 95°C for 1 h. After cooling, centrifuge at 4,000 rpm for 10 min and measure the absorbance of the supernatant at 532 nm (11).

2.11 Measurement of adenosine deaminase activity

Analyze using the Elabscience commercial kit (Metabolism Assay). Add 10 μL of liver homogenate and the standard solution to 180 μL of Reagent-1 and 90 μL of Reagent-2. Incubate at 37°C for 7 min, then measure the absorbance at 550 nm. After this, continue the reaction at 37°C for another 10 min and measure the absorbance again at 550 nm.

2.12 Statistical methods

The results of this experiment are expressed as mean ± standard deviation (S.D.). Data analysis was conducted using SPSS (Statistical Product and Service Solutions 22.0). One-way ANOVA was used to compare differences between groups, followed by Duncan's multiple range test for significance comparisons. A p-value of < 0.05 indicates a statistically significant difference in the data.

3 Results and discussion

3.1 Body weight, food intake, water intake, and organ weight

If toxic substances enter the experimental animals, they can affect their physiological condition or metabolic processes, leading to significant changes in body weight. To observe whether intraperitoneal injection or feeding of drugs and samples causes toxicity in animals, changes in body weight can be used as a preliminary indicator of potential poisoning (12).

Table 1 presents the body weight changes in hyperuricemia-induced mice. No significant differences in body weight were observed among the groups, except for the positive control group, where drug treatment likely improved physiological status, leading to better dietary intake and increased weight. Daily food and water intake were monitored, with an average consumption of 5.3 g and 9.1 g per mouse, respectively. In conclusion, black chokeberry supplementation did not cause toxicity or significantly affect body weight, food and water intake in hyperuricemic mice induced by intraperitoneal OA injection.

3.2 Serum BUN and CRE

BUN is a nitrogenous molecule produced in the liver and excreted by the kidneys, commonly used to assess kidney function (13). This experiment evaluates whether different doses of black chokeberry can reduce BUN levels in hyperuricemic mice (Table 2). The OA-induced group exhibited BUN level (13.51 mmol/L) compared to the control group (4.54 mmol/L). In the low-, medium-, and high-dosage groups, the levels of BUN were reduced to 10.21, 9.56, and 4.86 mmol/L, reflecting reductions of 24.43, 29.24, and 64.03%, respectively, compared to the OA-induced group. Notably, the high-dosage group showed a significant reduction, with levels falling below those of the allopurinol-treated group (6.81 mmol/L). Moreover, the high-dosage group outperformed the OA-induced mice treated with allopurinol, showing no significant difference compared to the control group. These findings suggested that high-dosage sample treatment in hyperuricemic mice lowered BUN.

TABLE 1 Changes in body weight, dietary intake, and water intake of OA-induced hyperuricemia mice.

Groups	Body weight (g)		Food intake (g)		Water intake (g)	
	Day-1	Day-7	Day-1	Day-7	Day-1	Day-7
Blank	27.78 ± 2.9[a]	29.98 ± 2.37[a]	6.8	6.27	7	12
OA	27.90 ± 1.64[a]	28.48 ± 2.06[a]	5.22	5.67	8	9
OA + allopurinol	28.53 ± 1.02[b]	30.62 ± 1.83[a]	5.66	5.96	10	11
OA + low dosage	27.78 ± 1.39[a]	27.7 ± 4.29[a]	5.61	4.74	8	12
OA + medium dosage	27.70 ± 0.95[a]	28.17 ± 1.33[a]	4.98	4.58	8	6
OA + high dosage	27.45 ± 1.24[a]	28.51 ± 3.10[a]	5.71	4.52	8	11

Each value is expressed as mean ± S.D. ($n = 6$). Value in row with the different superscripts are significantly different ($p < 0.05$).

TABLE 2 Effect of black chokeberry on blood urea nitrogen and creatinine levels in hyperuricemic mice.

Groups	BUN (mmol/L)	CRE (μmol/L)
Blank	4.54 ± 1.14^{c}	9.01 ± 0.98^{d}
OA	13.51 ± 3.57^{a}	38.87 ± 1.69^{a}
OA + allopurinol	6.81 ± 1.63bc	11.83 ± 2.93^{cd}
OA + low dosage	10.21 ± 2.26^{ab}	23.66 ± 4.78^{b}
OA + medium dosage	9.56 ± 1.79^{ab}	15.21 ± 1.69^{c}
OA + high dosage	4.86 ± 2.35^{c}	9.58 ± 0.98^{d}

Each value is expressed as mean ± S.D. (n = 6). Value in row with the different superscripts are significantly different ($p < 0.05$).

Table 2 presents the effects of black chokeberry on CRE levels in hyperuricemic mice. The negative control group exhibited CRE level (38.87 μmol/L), which approximately three times higher than that of the control group (9.01 μmol/L). In the low-, medium-, and high-dose groups (black chokeberry), the CRE levels were 23.66, 15.21, and 9.58 μmol/L, respectively, showing a dose-dependent reduction of 39.13, 60.87, and 75.35%. The CRE level in the high-dose group was comparable to that of the control group and not significantly different from the positive control group, suggesting that high-dose black chokeberry treatment achieved similar reductions in CRE as drug treatment and brought levels close to those of uninduced mice.

Hyperuricemia induced by OA can lead to nitric oxide-related endothelial dysfunction, affecting the kidney's ability to transport urate and other organic ions, thereby worsening renal dysfunction and damage (14). Cherry has known for its immunomodulatory properties, can enhance the immune system through various mechanisms (14, 15). These findings suggest that high-dose wild cherry effectively reduces CRE levels in hyperuricemic mice, highlighting potential of black chokeberry used as a natural kidney-protective agent.

3.3 Serum uric acid and xanthine oxidase activity

Uricase is an enzyme in mammals that converts uric acid to allantoin. In animal studies, oxonic acid, a commonly used uricase inhibitor, induces hyperuricemia by raising serum uric acid levels. It is cost-effective, fast-acting, and widely used in preliminary research to evaluate the uric acid-lowering effects of new treatments for hyperuricemia (16, 17). Clinically, hyperuricemia is treated with drugs that either promote uric acid excretion (such as probenecid, benzbromarone, and sulfinpyrazone) or inhibit uric acid production (such as allopurinol and febuxostat). However, these medications are associated with side effects, including renal toxicity, liver damage, and an increased risk of cardiovascular disease (18, 19). This has led to growing interest in natural products rich in phytochemicals as alternative treatments for hyperuricemia, offering potential uric acid-lowering effects with fewer side effects.

Figure 1A illustrates the effects of black chokeberry on serum uric acid level in hyperuricemic mice. One week after OA injection, the serum uric acid level in the OA-induced mice was rose to 5.40 mg/dL compared to the control group (3.35 mg/dL). In contrast, the OA-induced mice treated with allopurinol showed a reduction to 2.66 mg/dL, below the level of the control group. In the low-, medium-, and high-dosage groups, serum uric acid level was decreased in a dose-dependent manner, reaching 4.98, 3.61, and 2.87 mg/dL, respectively. The high-dosage group demonstrated the most pronounced effect, with results comparable to the allopurinol group.

Patients using allopurinol for hyperuricemia are at an increased risk of requiring dialysis (10). This study showed the effects of black chokeberry treating hyperuricemia in mice are comparable to those of the synthetic drug allopurinol. The results suggested that black chokeberry has notable uric acid-lowering efficacy, likely due to its phenolic acid components (19, 20), making it a promising candidate for development into health products targeting uric acid-related conditions.

Xanthine oxidase is the primary enzyme for purine metabolism in the liver (21, 22). It oxidizes hypoxanthine to xanthine and then xanthine to uric acid, generating superoxide anions (O_2^-) and peroxides, which increase cellular oxidative stress. Excess uric acid in the body can lead to hyperuricemia and gout, caused by the crystallization of uric acid in joints and surrounding tissues (23). Increased intake of high-purine foods can lead to overactivity of xanthine oxidase, raising the prevalence of hyperuricemia. Allopurinol and febuxostat are two xanthine oxidase inhibitors but can have significant side effects (24).

Developing natural compounds as xanthine oxidase inhibitors is essential. Figure 1B showed the effects of black chokeberry on xanthine oxidase activity in the livers of hyperuricemic mice. No significant differences were observed in xanthine oxidase activity among the low-, medium-, and high-dosage groups compared to the control group. However, both the high-dosage and allopurinol treatment showed significant reductions compared to the OA-induced group. These findings suggest that high-dosage sample effectively reduces xanthine oxidase activity, with similar efficacy to allopurinol, thereby lowering uric acid level.

3.4 GSH and MDA levels in hyperuricemic mice

Glutathione (GSH) is present in most mammals, synthesized from glutamate and cysteine, and plays a crucial role as a key antioxidant. It helps generate iron–sulfur proteins and neutralizes reactive oxygen species (ROS), controlling redox states (25). High concentrations of GSH protect the liver from oxidative stress (26). Research by Zhang et al. (27) shows that CCl_4-induced liver damage depletes GSH due to its conversion to oxidized glutathione during free radical scavenging.

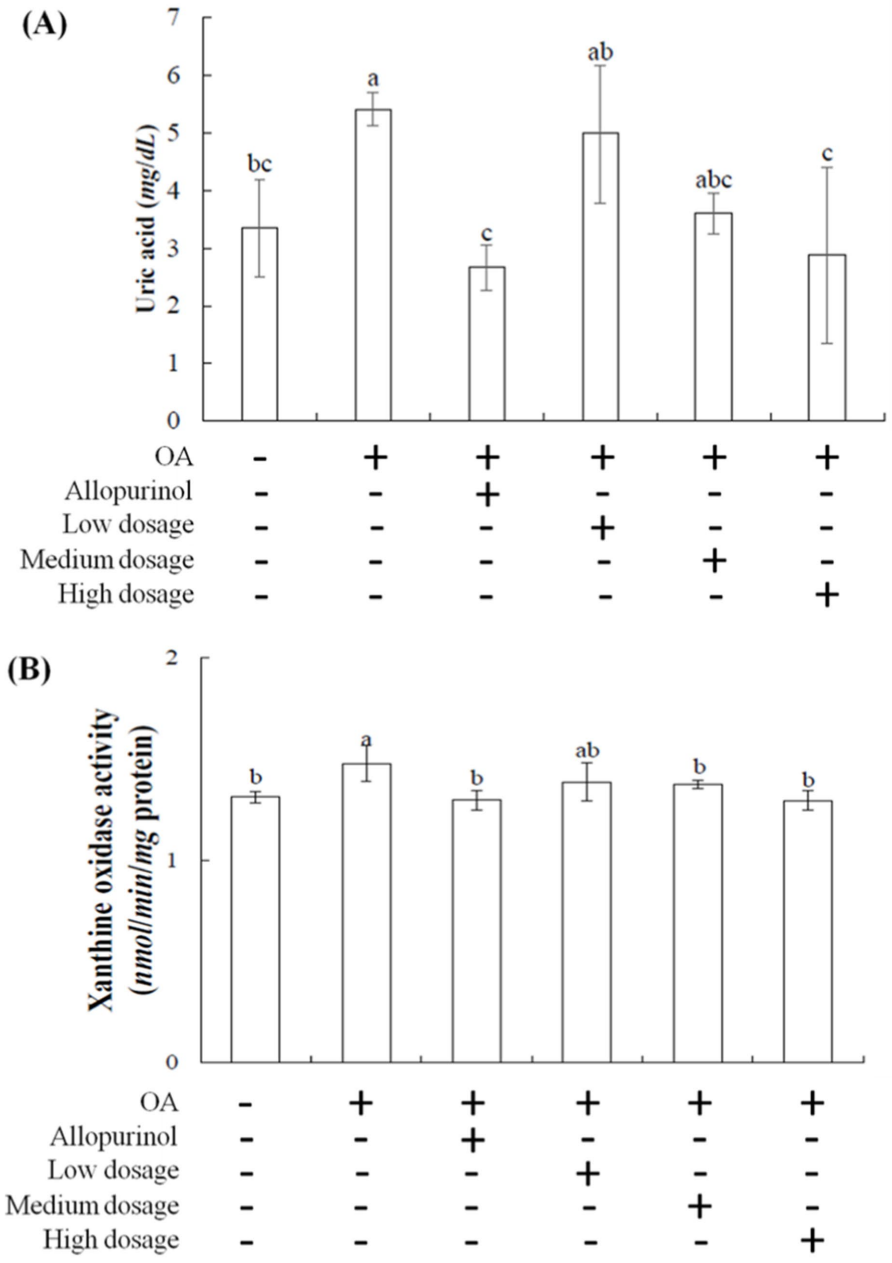

FIGURE 1
Effect of black chokeberry on serum **(A)** uric acid levels and **(B)** liver xanthine oxidase activity in hyperuricemicmice. Each value is expressed as mean ± S.D. (n = 6). Value in row with the different superscripts are significantly different ($p < 0.05$).

Notably, anthocyanins in wild cherries may help maintain liver GSH levels.

Table 3 showed the effects of black chokeberry on GSH content in the livers of hyperuricemic mice. The GSH levels in the control, OA induction, allopurinoll, low-dosage, medium-dosage, and high-dosage treated-groups were 2.82, 1.90, 3.18, 3.29, 3.47, and 3.88 μmol/mg protein, respectively. Black chokeberry treatment resulted in an upward trend in GSH content. These results suggested that high doses of black chokeberry may boost GSH levels, helping to prevent or mitigate liver damage caused by oxidative stress, thereby reducing hepatic oxidative stress injury.

Malondialdehyde (MDA) is widely used as an indicator of lipid peroxidation and reflects oxidative stress in cells, particularly from reactive oxygen species (ROS) (28). MDA can disrupt lipid membrane structures, leading to severe cellular damage (29). A study indicated that flavonoids in black chokeberry can reduce CCl_4-induced lipid peroxidation in the liver (30). Table 3 presents the protection of black chokeberry on MDA levels in the livers of OA-induced hyperuricemic mice. The MDA concentrations for the control, OA induction, allopurinol, low-dosage, medium-dosage, and high-dosage groups being 1.09, 1.31, 1.13, 1.14, 1.09, and 1.01 μmol/mg protein, respectively. Notably, there was a significant difference between the high-dose and positive control groups. Elseweidy et al. (31) showed

TABLE 3 The GSH and MDA contents in the liver of OA-induced hyperuricemic mice.

Groups	GSH (umol/mg protein)	MDA (umol/mg protein)
Blank	2.82 ± 0.34^{ab}	1.12 ± 0.09^{bc}
OA	1.9 ± 0.67^{c}	1.29 ± 0.09^{a}
OA + allopurinol	3.18 ± 1.16^{ab}	1.19 ± 0.1^{b}
OA + low dosage	3.29 ± 1.34^{ab}	1.18 ± 0.11^{b}
OA + medium dosage	3.47 ± 1.24^{b}	1.13 ± 0.13^{bc}
OA + high dosage	3.88 ± 1.32^{b}	1.07 ± 0.11^{c}

Each value is expressed as mean ± S.D. ($n = 6$). Value in row with the different superscripts are significantly different ($p < 0.05$).

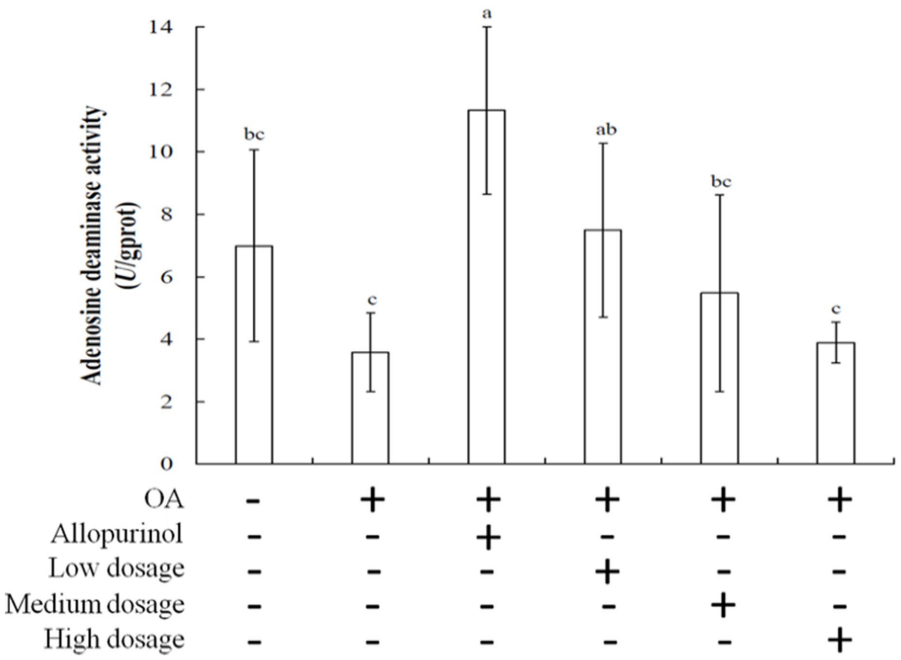

FIGURE 2
Effect of black chokeberry on liver adenosine deaminase activity in hyperuricemic mice. Each value is expressed as mean ± S.D. ($n = 6$). Value in row with the different superscripts are significantly different ($p < 0.05$).

that allopurinol treatment could modulate liver lipid metabolism and reduce MDA levels in fructose-induced non-alcoholic fatty liver models. These findings suggest that high-dosage black chokeberry can significantly lower liver MDA levels, thereby mitigating oxidative stress-related damage.

3.5 Adenosine deaminase activity in the OA-induced hyperuricemic mice

Adenosine deaminase (ADA) is a hydrolytic enzyme involved in purine metabolism, converting adenosine and 2′-deoxyadenosine into inosine and 2′-deoxyinosine, respectively (32). ADA is found in various organisms, including plants, bacteria, and animals (33). Inhibition of ADA can modulate inflammation by increasing adenosine levels in damaged tissues, thereby reducing inflammatory responses. Figure 2 illustrated the effects of wild cherry on ADA activity in the livers of hyperuricemic mice. The ADA activities for the control, OA induction, allopurinol, low-dosge, medium-dosage, and high-dosage groups were 6.99, 11.33, 3.58, 7.50, 5.47, and 3.89 μmol/mg protein, respectively. Notably, the high-dosage group showed lower ADA activity than the control group. Due to ADA activity increases with rising uric acid level; therefore, administering high-dosage of black chokeberry can lower uric acid levels and inhibit ADA activity, subsequently reducing inflammation.

Gout is an inflammatory disease caused by excessive uric acid levels in the blood, leading to the formation of insoluble monosodium urate (MSU) crystals. These crystals drive neutrophil activation and infiltration into joint tissues, resulting in severe pain in the affected areas. MSU crystals mediate oxidative stress through the nucleotide-binding oligomerization domain-like receptor pyrin domain-containing 3 (NLRP3) inflammasome, which subsequently triggers interleukin-1β production, exacerbating the inflammatory response (34–36).

Xanthine oxidase is a key enzyme in the purine metabolism pathway, and clinical and experimental studies have suggested that its activity may have pro-inflammatory effects (37). Currently, various anti-gout medications are available, including nonsteroidal anti-inflammatory drugs (NSAIDs) such as allopurinol, which are

commonly used as first-line treatments for acute gout. However, their use is limited by adverse effects, including gastrointestinal toxicity, renal toxicity, and gastrointestinal bleeding. Therefore, the development of more effective anti-gout arthritis drugs remains of great significance (38, 39). In recent years, we have identified the bioactive compounds and antioxidants in black chokeberry (40). These findings suggest that black chokeberry has the potential for gout prevention and management.

4 Conclusion

Hyperuricemia is a pathological condition characterized by an abnormal increase in serum uric acid levels due to excessive uric acid production or reduced excretion. The main pathogenic mechanisms include xanthine oxidase overactivation and phosphoribosyl pyrophosphate synthetase (PRPP synthetase) hyperactivity. For xanthine oxidase, which promotes the conversion of xanthine to uric acid, leading to excessive uric acid production, but PRPP synthetase is able to enhance purine synthesis, subsequently increasing uric acid production. Uric acid is the final product of purine metabolism, derived from both endogenous (cellular metabolism) and exogenous (dietary) purine breakdown. A high-purine diet (e.g., red meat, organ meats, and seafood), excessive fructose intake, alcohol consumption, and obesity are closely associated with the development of hyperuricemia. In this study, our results demonstrate that black chokeberry can reduce xanthine oxidase activity and uric acid production. In the future, it may serve as a potential functional ingredient for gout prevention.

Data availability statement

The raw data supporting the conclusions of this article will be made available by the authors, without undue reservation.

Ethics statement

The animal study was approved by the Laboratory Animal Care and Use Committee of National Chiayi University (Approval No. 112021). The study was conducted in accordance with the local legislation and institutional requirements.

Author contributions

C-YL: Data curation, Investigation, Methodology, Writing – original draft. W-YL: Writing – review & editing, Formal analysis, Methodology, Investigation, Software. Y-CS: Formal analysis, Funding acquisition, Resources, Writing – review & editing. S-CW: Investigation, Methodology, Project administration, Resources, Writing – original draft, Writing – review & editing.

Funding

The author(s) declare that no financial support was received for the research and/or publication of this article.

Conflict of interest

The authors declare that the research was conducted in the absence of any commercial or financial relationships that could be construed as a potential conflict of interest.

Generative AI statement

The authors declare that no Gen AI was used in the creation of this manuscript.

Publisher's note

All claims expressed in this article are solely those of the authors and do not necessarily represent those of their affiliated organizations, or those of the publisher, the editors and the reviewers. Any product that may be evaluated in this article, or claim that may be made by its manufacturer, is not guaranteed or endorsed by the publisher.

References

1. He H, Guo P, He J, Zhang J, Niu Y, Chen S, et al. Prevalence of hyperuricemia and the population attributable fraction of modifiable risk factors: evidence from a general population cohort in China. *Front Public Health*. (2022) 10:936717. doi: 10.3389/fpubh.2022.936717

2. Sapankaew T, Thadanipon K, Ruenroengbun N, Chaiyakittisopon K, Ingsathit A, Numthavaj P, et al. Efficacy and safety of urate-lowering agents in asymptomatic hyperuricemia: systematic review and network meta-analysis of randomized controlled trials. *BMC Nephrol*. (2022) 23:223. doi: 10.1186/s12882-022-02850-3

3. Shi Z, Ge X, Zheng S, Zeng P, Su Z, Li X, et al. Mangiferin reduces uric acid via regulation of amino acid and lipid metabolism. *J Funct Foods*. (2023) 108:105716. doi: 10.1016/j.jff.2023.105716

4. Lee SJ, Terkeltaub RA. New developments in clinically relevant mechanisms and treatment of hyperuricemia. *Curr Rheumatol Rep*. (2006) 8:224–30. doi: 10.1007/s11926-996-0029-z

5. Shahid H, Singh JA. Investigational drugs for hyperuricemia. *Expert Opin Investig Drugs*. (2015) 24:1013–30. doi: 10.1517/13543784.2015.1051617

6. Sidor A, Drożdżyńska A, Gramza-Michałowska A. Black chokeberry (*Aronia melanocarpa*) and its products as potential health-promoting factors—an overview. *Trends Food Sci Technol*. (2019) 89:45–60. doi: 10.1016/j.tifs.2019.05.006

7. Wang Z, Wang X, Yan H, Liu Y, Li L, Li S, et al. *Aronia melanocarpa* ameliorates gout and hyperuricemia in animal models. *Food Agric Immunol*. (2018) 30:47–59. doi: 10.1080/09540105.2018.1541967

8. Olechno E, Puścion-Jakubik A, Elżbieta ZM. Chokeberry (*A. melanocarpa* (Michx.) Elliott)—a natural product for metabolic disorders? *Nutrients*. (2022) 14:2688. doi: 10.3390/nu14132688

9. Shi YC, Lin KS, Jhai YF, Lee BH, Han Y, Cui Z, et al. Miracle fruit (*Synsepalum dulcificum*) exhibits as a novel anti-hyperuricaemia agent. *Molecules*. (2016) 21:140. doi: 10.3390/molecules21020140

10. Hsu WH, Lee BH, Pan TM. Protection of *Monascus*-fermented dioscorea against DMBA-induced oral injury in hamster by anti-inflammatory and antioxidative potential. *J Agric Food Chem*. (2010) 58:6715–20. doi: 10.1021/jf100889w

11. Lee BH, Wu SC, Shen TL, Hsu YY, Chen CH, Hsu WH. The applications of *Lactobacillus plantarum*-derived extracellular vesicles as a novel natural antibacterial agent for improving quality and safety in tuna fish. *Food Chem*. (2021) 340:128104. doi: 10.1016/j.foodchem.2020.128104

12. Rajesh MG, Latha MS. Preliminary evaluation of the antihepatotoxic activity of Kamilari, a polyherbal formulation. *J Ethnopharmacol*. (2004) l:99–104. doi: 10.1016/j.jep.2003.12.011

13. Hao J, Zhou F. Antihyperuricemic and nephroprotective effects of the total flavonoids from *Carya cathayensis*leaves (CCTF) in potassium oxonate/hypoxanthine-induced hyperuricemic mice. *Clin Complement Med Pharmacol*. (2023) 3:100104. doi: 10.1016/j.ccmp.2023.100104

14. Liu YL, Pan Y, Wang X, Fan CY, Zhu Q, Li JM, et al. Betaine reduces serum uric acid levels and improves kidney function in hyperuricemic mice. *Biol Pharmacol Act*. (2014) 80:39–47. doi: 10.1055/s-0033-1360127

15. Jurikova T, Mlcek J, Skrovankova S, Sumczynski D, Sochor J, Hlavacova I, et al. Fruits of black chokeberry *Aronia melanocarpa* in the prevention of chronic diseases. *Molecules*. (2017) 22:944. doi: 10.3390/molecules22060944

16. Araújo MCPM, Ferraz-Filha ZS, Ferrari FC, Saude-Guimaraes DA. *Campomanesia velutina*leaves extracts exert hypouricemic effects through inhibition of xanthine oxidase and ameliorate inflammatory response triggered by MSU crystals. *Rev Bras Epidemiol*. (2016) 26:720–7. doi: 10.1016/j.bjp.2016.05.016

17. Ishikawa T, Maeda T, Hashimoto T, Nakagawa T, Ichikawa K, Sato Y, et al. Long-term safety and effectiveness of the xanthine oxidoreductase inhibitor, topiroxostat in Japanese hyperuricemic patients with or without gout: a 54-week open-label, multicenter, post-marketing observational study. *Clin Drug Investig*. (2020) 40:847–59. doi: 10.1007/s40261-020-00941-3

18. Liu W, Peng J, Wu Y, Ye Z, Zong Z, Wu R, et al. Immune and inflammatory mechanisms and therapeutic targets of gout: an update. *Int Immunopharmacol*. (2023) 121:110466. doi: 10.1016/j.intimp.2023.110466

19. Liu G, Chen X, Lu X, Zhao J, Li X. Sunflower head enzymatic hydrolysate relives hyperuricemia by inhibiting crucial proteins (xanthine oxidase, adenosine deaminase, uric acid transporter1) and restoring gut microbiota in mice. *J Funct Foods*. (2020) 72:104055:104055. doi: 10.1016/j.jff.2020.104055

20. Chen PE, Liu CY, Chien WH, Chieh CW, Tung TH. Effectiveness of cherries in reducing uric acid and gout: a systematic review. *Evid Based Complement Alternat Med*. (2019) 2019:9896757. doi: 10.1155/2019/9896757

21. Peglow S, Toledo AH, Anaya-Prado R, Lopez-Neblina F, Toledo-Pereyra LH. Allopurinol and xanthine oxidase inhibition in liver ischemia reperfusion. *J Hepatobiliary Pancreat Sci*. (2011) 18:137–46. doi: 10.1007/s00534-010-0328-7

22. Era B, Delogu GL, Pintus F, Fais A, Gatto G, Uriarte E, et al. Looking for new xanthine oxidase inhibitors: 3-Phenylcoumarins versus 2-phenylbenzofurans. *Int J Biol Macromol*. (2020) 162:774–80. doi: 10.1016/j.ijbiomac.2020.06.152

23. Richette P, Doherty M, Pascual E, Barskova V, Castaneda-Sanabria J, Coyfish M, et al. 2016 updated EULAR evidence-based recommendations for the management of gout. *Ann Rheum Dis*. (2017) 76:29–42. doi: 10.1136/annrheumdis-2016-209707

24. Zhao Q, Meng Y, Liu J, Hu Z, Du Y, Sun J, et al. Separation, identification and docking analysis of xanthine oxidase inhibitory peptides from pacific cod bone-flesh mixture. *LWT*. (2022) 167:113862. doi: 10.1016/j.lwt.2022.113862

25. Meister A, Anderson M. Glutathione. *Annu Rev Biochem*. (1983) 52:711–60. doi: 10.1146/annurev.bi.52.070183.003431

26. Lei XG, Cheng WH. New roles for an old selenoenzyme: evidence from glutathione peroxidase-1 null and overexpressing mice. *J Nutr*. (2005) 135:2295–8. doi: 10.1093/jn/135.10.2295

27. Zhang G, Jiang Y, Liu X, Deng Y, Wei B, Shi L. Lingonberry anthocyanins inhibit hepatic stellate cell activation and liver fibrosis via TGFbeta/Smad/ERK signaling pathway. *J Agric Food Chem*. (2021) 69:13546–56. doi: 10.1021/acs.jafc.1c05384

28. Ayala A, Muñoz MF, Argüelles S. Lipid peroxidation: production, metabolism, and signaling mechanisms of malondialdehyde and 4-hydroxy-2-nonenal. *Oxid Med Cell Longev*. (2014) 2014:360438. doi: 10.1155/2014/360438

29. Chen JJ. Effects of two DLCs on hepatic MDA, SOD and GST in zebrafish. *Food Sci Biotechnol*. (2009) 28:210–3.

30. Valcheva-Kuzmanova S, Borisova P, Galunska B, Krasnaliev I, Belcheva A. Hepatoprotective effect of the natural fruit juice from *Aronia melanocarpa* on carbon tetrachloride-induced acute liver damage in rats. *Exp Toxicol Pathol*. (2004) 56:195–201. doi: 10.1016/j.etp.2004.04.012

31. Elseweidy MM, Elesawy AE, Sobh MS, Elnagar GM. Ellagic acid ameliorates high fructose-induced hyperuricemia and non-alcoholic fatty liver in Wistar rats: focusing on the role of C1q/tumor necrosis factor-related protein-3 and ATP citrate lyase. *Life Sci*. (2022) 305:120751. doi: 10.1016/j.lfs.2022.120751

32. Gao ZW, Wang X, Zhang HZ, Lin F, Liu C, Dong K. The roles of adenosine deaminase in autoimmune diseases. *Autoimmun Rev*. (2021) 20:102709. doi: 10.1016/j.autrev.2020.102709

33. Cristalli G, Costanzi S, Lambertucci C, Lupidi G, Volpini R, Camaioni E. Adenosine deaminase: functional implications and different classes of inhibitors. *Med Res Rev*. (2001) 21:105–28. doi: 10.1002/1098-1128(200103)21:2<105::AID-MED1002>3.0.CO;2-U

34. Martin WJ, Walton M, Harper J. Resident macrophages initiating and driving inflammation in a monosodium urate monohydrate crystal-induced murineperitoneal model of acute gout. *Arthritis Rheum*. (2009) 60:281–9. doi: 10.1002/art.24185

35. Zhou R, Tardivel A, Thorens B, Choi I, Tschopp J. Thioredoxin interacting protein links oxidative stress to inflammasome activation. *Nat Immunol*. (2010) 11:136–40. doi: 10.1038/ni.1831

36. Jhang JJ, Cheng YT, Ho CY, Yen GC. Monosodium urate crystals trigger Nrf2- and heme oxygenase-1-dependent inflammation in THP-1 cells. *Cell Mol Immunol*. (2014) 12:424–34. doi: 10.1038/cmi.2014.65

37. Wang Y, Zhu X, Kong LD, Yang C, Cheng H, Zhang X. Administration of procyanidins from grape seeds reduces serum uric acid levels and decreases hepatic xanthine dehydrogenase/oxidase activities in oxonate-treated mice. *Basic Clin Pharmacol Toxicol*. (2004) 94:232–7. doi: 10.1111/j.1742-7843.2004.pto940506.x

38. Martinon F. Signaling by ROS drives inflammasome activation. *Eur J Immunol*. (2010) 40:616–9. doi: 10.1002/eji.200940168

39. Zhou CX, Kong LD, Ye WC, Cheng CHK, Tan RX. Inhibition of xanthine and monoamine oxidases by stilbenoids from *Veratrum taliense*. *Planta Med*. (2001) 67:158–61. doi: 10.1055/s-2001-11500

40. Liu CY, Chang WF, Chen CT, Wang CH, Wu SC. Evaluation of health efficacy of domestic black chokeberry (*Aronia melanocarpa*) in antioxidation and inhibiting xanthine oxidase activity. *Taiwan J Agric Chem Food Sci*. (2024) 62:91–8.

41. Kong LD, Zhou J, Wen YL, Li J, Cheng CHK. Aesculin possesses potent hypouricemic action in rodents but is devoid of xanthine oxidase/dehydrogenase inhibitory activity. *Planta Med*. (2002) 68:175–8. doi: 10.1055/s-2002-20262

frontiers | Frontiers in Nutrition

TYPE Original Research
PUBLISHED 27 May 2025
DOI 10.3389/fnut.2025.1574151

Check for updates

OPEN ACCESS

EDITED BY
Ntethelelo Sibiya,
Rhodes University, South Africa

REVIEWED BY
Kristina Brooke Martinez-Guryn,
Midwestern University, United States
Angezwa Siboto,
Nelson Mandela University, South Africa

*CORRESPONDENCE
Keke Shao
✉ keke87890394@163.com
Liang Wu
✉ wlujs@ujs.edu.cn

†These authors have contributed equally to this work and share first authorship

RECEIVED 10 February 2025
ACCEPTED 29 April 2025
PUBLISHED 27 May 2025

CITATION
Tan J, Sun W, Dong X, He J, Ali A, Chen M, Zhang L, Wu L and Shao K (2025) D-Psicose mitigates NAFLD mice induced by a high-fat diet by reducing lipid accumulation, inflammation, and oxidative stress. *Front. Nutr.* 12:1574151. doi: 10.3389/fnut.2025.1574151

COPYRIGHT
© 2025 Tan, Sun, Dong, He, Ali, Chen, Zhang, Wu and Shao. This is an open-access article distributed under the terms of the Creative Commons Attribution License (CC BY). The use, distribution or reproduction in other forums is permitted, provided the original author(s) and the copyright owner(s) are credited and that the original publication in this journal is cited, in accordance with accepted academic practice. No use, distribution or reproduction is permitted which does not comply with these terms.

D-Psicose mitigates NAFLD mice induced by a high-fat diet by reducing lipid accumulation, inflammation, and oxidative stress

Jiajun Tan[1,2†], Wen Sun[3†], Xueyun Dong[1], Jiayuan He[4], Asmaa Ali[1,5], Min Chen[6], Leilei Zhang[1], Liang Wu[1,2*] and Keke Shao[2,7*]

[1]Department of Laboratory Medicine, School of Medicine, Jiangsu University, Zhenjiang, China, [2]Department of Laboratory Medicine, The Yancheng Clinical College of Xuzhou Medical University, The First People's Hospital of Yancheng, Yancheng, China, [3]Critical Care Medicine, Jurong Hospital Affiliated to Jiangsu University, Zhenjiang, China, [4]Health Testing Center, Zhenjiang Center for Disease Control and Prevention, Zhenjiang, China, [5]Department of Pulmonary Medicine, Abbassia Chest Hospital, EMOH, Cairo, Egypt, [6]Public Experiment and Service Center, Jiangsu University, Zhenjiang, China, [7]Molecular Medical Research Center, Yancheng Clinical Medical College of Jiangsu University, Yancheng, China

D-Psicose (DPS) serves as an optimal sucrose substitute, providing only 0.3% of sucrose's energy content, while exhibiting anti-inflammatory properties and inhibiting lipid synthesis. However, its efficacy in managing non-alcoholic fatty liver disease (NAFLD) remains unclear. This study employed network pharmacology and molecular docking to identify potential DPS targets for NAFLD treatment. A high-fat diet was used to induce a NAFLD mouse model, with DPS administered in drinking water at 5% (high dose DPS group, DPSH group) and 2.5% (low dose DPS group, DPSL group) concentrations. After 12 weeks, blood lipid levels, liver lipid deposition, and inflammation were evaluated to assess the therapeutic effects of DPS. To explore its underlying mechanisms, colon contents 16S rRNA sequencing and serum untargeted metabolomics were performed. Results indicated that DPS significantly reduced lipid accumulation and inflammatory damage in the livers of NAFLD mice, improving both blood lipid profiles and oxidative stress. Network pharmacology analysis revealed that DPS primarily targets pathways associated with inflammation and oxidative stress, while molecular docking suggested its potential to inhibit the NF-κB pathway activation and the expression of the receptor for advanced glycation end-products (RAGE), findings corroborated by Western blotting. Additionally, gut microbiota and serum metabolomics analyses demonstrated that DPS improved microbiota composition by increasing the abundance of beneficial bacteria, such as *Akkermansia*, and restored serum metabolomic balance, enhancing anti-inflammatory and antioxidant metabolites like Tretinoin and Pyridoxamine. The non-targeted metabolomics results suggest that DPS is mediated by glutathione metabolism, arginine and proline metabolism, unsaturated fatty acid biosynthesis, and linoleic acid metabolism interferes with NAFLD progression. In conclusion, DPS may alleviate oxidative stress and lipid accumulation in NAFLD mice through the AGEs/RAGE/NF-κB pathway, while also ameliorating gut microbiota dysbiosis and serum metabolomic disturbances, fostering the production of anti-inflammatory and antioxidant metabolites.

KEYWORDS

D-Psicose, non-alcoholic fatty liver disease, oxidative stress, gut microbiota, metabolomics

1 Introduction

D-Psicose (DPS), a ketohexose monosaccharide and epimer of D-fructose at the C-3 position, is found in trace amounts in wheat, itea plants, and processed cane and beet molasses, and can be bioengineered from fruit and vegetable waste (1, 2). With 70% of the sweetness of sucrose but only 0.3% of its caloric content, DPS presents an ideal sucrose alternative (3–5). It offers several health benefits, including anti-inflammatory, antioxidant, glucose and lipid metabolism regulation, and neuroprotective effects (6–8). Animal studies suggest DPS can inhibit liver fat-producing enzymes and intestinal α-glucosidase, potentially reducing body fat accumulation (9, 10). However, its therapeutic potential for non-alcoholic fatty liver disease (NAFLD) remains underexplored.

NAFLD affects approximately 25% of the global population and is a major contributor to cirrhosis and hepatocellular carcinoma (11, 12). The disease progresses from steatosis, with or without mild inflammation, to non-alcoholic steatohepatitis (NASH), leading to significant necroinflammation and accelerated fibrosis compared to simple fatty liver (13–15). NAFLD is closely associated with metabolic syndrome, with type 2 diabetes significantly increasing the risk of cirrhosis and its complications (16–18). Currently, no specific treatments for NAFLD have been approved (13, 19–21). The recent FDA approval of Resmetirom (Rezdiffra™) in March 2024 marked a milestone as the first drug specifically indicated for non-cirrhotic NASH with moderate-to-advanced fibrosis (22). However, its clinical adoption faces notable limitations including diarrhea, nausea, and transient elevations in LDL cholesterol, posing risks for long-term use in metabolically compromised populations (23). Existing strategies emphasize the importance of lifestyle modifications and weight loss for both prevention and management (24–26). Leveraging DPS's low-calorie and anti-inflammatory properties, network pharmacology, molecular docking, and an NAFLD mouse model were employed to investigate its therapeutic effects. Additionally, gut microbiota 16S rRNA sequencing and serum untargeted metabolomics were utilized to uncover the underlying mechanisms of DPS in NAFLD treatment, presenting a novel therapeutic approach.

2 Materials and methods

2.1 Network pharmacology and molecular docking analysis of DPS in the treatment of NAFLD

The DPS structure, obtained from the PubChem database, was imported into the SwissTarget Prediction and Superpred databases to predict potential targets. Searches were conducted in the OMIM[1] and GeneCards[2] databases using the keyword "Nonalcoholic fatty liver disease." A Venn diagram was generated using the VennDiagram package in R Studio[3] to display the overlapping potential targets of DPS for NAFLD treatment. The identified targets were imported into the STRING database, with "*Homo sapiens*" specified as the species. The results were saved and imported into Cytoscape 3.10.0 for visualization, where the CytoHubba plugin was employed to rank the top 10 key targets by "Degree."

The potential targets were uploaded to the DAVID database[4] for GO functional enrichment and KEGG pathway analyses, applying a significance threshold of $p < 0.05$ to identify relevant signaling pathways associated with DPS treatment of NAFLD. The ggplot2 package in R Studio was used to generate bar charts for the top 10 signaling pathways in the biological process (BP), cellular component (CC), and molecular function (MF) GO enrichment categories. Additionally, the top 15 KEGG pathway results were visualized as a bubble chart.

The 3D structures of DPS active components were retrieved from the PubChem database as small molecule ligands. Core target proteins with high degree values in the PPI network were selected as receptor proteins, and their 3D structures were obtained from the PDB database.[5] PyMOL software was utilized to prepare receptor proteins by adding hydrogen atoms, removing water molecules, and eliminating small molecule ligands. AutoDockTools was used to validate the molecular docking of key active components with core target proteins, and PyMOL was used for visualizing the results with enhanced activity.

2.2 Experimental animals and grouping

Eight-week-old male institute of cancer research (ICR) mice, purchased from Wukong Biotechnology (Nanjing, China), were housed at Jiangsu University's Experimental Animal Center. The mice were maintained under controlled conditions (25°C, 50% relative humidity, 12 h light/dark cycle). They were randomly assigned to four groups: normal control (NC, $n = 6$), non-alcoholic fatty liver disease (NAFLD, $n = 6$), low-dose DPS (DPSL, $n = 6$), and high-dose DPS (DPSH, $n = 6$). The NC group received a standard diet, while the NAFLD, DPSL, and DPSH groups were fed a high-fat diet to induce NAFLD, following the method outlined by Sun et al. (27). The DPSL and DPSH groups received DPS in drinking water at concentrations of 2.5 and 5%, respectively, for 12 weeks. At the end of the treatment period, the mice were euthanized with an intraperitoneal injection of urethane (700 mg/kg; Sigma-Aldrich, St. Louis, MO, United States), and serum, liver, and colonic content were collected.

2.3 Analysis of serum biochemical markers

According to He et al. (28), kits from Nanjing Jiancheng Bioengineering Institute (Nanjing, China) were used to measure the concentrations and activities of alanine aminotransferase (ALT, C009-2-1), aspartate aminotransferase (AST, C010-2-1), triglycerides (TG, A110-1-1), total cholesterol (TC, A111-1-1), low-density lipoprotein cholesterol (LDL-C, A113-1-1), high-density lipoprotein cholesterol (HDL-C, A112-1-1), malondialdehyde (MDA, A003-1-2), and

1 http://omim.org/
2 https://www.genecards.org/
3 https://www.rstudio.com/
4 https://david.ncifcrf.gov/
5 http://www.resb.org/

superoxide dismutase (SOD, A001-3-2) in mouse serum. Testing procedures followed the kit manuals' instructions.

2.4 Analysis of hepatic inflammatory factor expression

The expression levels of inflammatory factors in mouse liver, including TNF-α, IL-1β, IL-10, NLRP3, and Caspase-1 mRNA, were measured using the qRT-PCR assay, as outlined by He et al. (28). Reagents for the qRT-PCR assay were provided by Vazyme Biotech Co., Ltd. (Nanjing, China). Primer sequences are listed in Supplementary Table S1.

2.5 Western blotting assay

The expression of the inflammation-related factor RAGE and the phosphorylation level of NF-κB p65 in the mouse liver were determined *via* Western blotting, with experimental procedures detailed in Supplement S2.

2.6 Histological analysis of mouse liver tissue using HE and Oil Red O staining

Liver damage was assessed using H&E staining, while lipid deposition in the liver was evaluated with Oil Red O staining. The staining procedures are described in Supplement S3.

2.7 Analysis of gut microbiota 16S rRNA sequencing

The procedure for microbial 16S rRNA analysis of mouse colon contents can be found in Supplement S4. Genomic DNA was extracted from mouse colon microbiota using a genomic DNA extraction kit (TIANGEN, Beijing, China) for subsequent gut microbiota analysis, conducted by Wekemo Tech Group Co., Ltd. (Shenzhen, China). Bioinformatics analysis facilitated sequencing and species identification. The α-diversity (shannon) and β-diversity (unweighted unifrac and bray curtis) of the gut microbiota in mice were applied to evaluate microbial composition similarity or dissimilarity between groups. A clustering heatmap was used to investigate the impact of DPS on the gut microbiota.

2.8 Analysis of untargeted serum metabolomics

The untargeted metabolomics analysis of mouse serum was performed as follows: 120 μL of precooled 50% methanol was mixed with 20 μL of serum, incubated at room temperature for 10 min, and stored overnight at −20°C. After centrifugation at 4000 × g for 20 min, the supernatant was collected for untargeted metabolomics analysis. This analysis was conducted by Wekemo Tech Group Co., Ltd. (Shenzhen, China). PCA was used to illustrate the differences in serum metabolites across groups, while OPLS-DA provided the variable importance in projection (VIP) and significance values (p-value) for metabolite differences between groups. Metabolites were considered significant if VIP > 1.0 and $p < 0.05$ and were uploaded to the MetaboAnalyst 6.0 platform for pathway analysis.

2.9 Statistical analysis

Data analysis was performed using SPSS 20.0 (SPSS, Chicago, IL, United States), with results presented as mean ± SD. One-way ANOVA and Tukey's *post hoc* method was used to assess significant differences across groups, with $p < 0.05$ considered statistically significant. Graphs were generated using GraphPad Prism, the Bioincloud platform[6], and R Studio.

3 Results

3.1 Network pharmacology analysis results of DPS in the treatment of NAFLD

The SwissTargetPrediction and Targets SUPPERD databases were utilized to identify 212 potential targets related to DPS, while 1929 NAFLD-related targets were obtained from the GeneCards and OMIM databases (Figure 1A). Forty-one overlapping targets between DPS and NAFLD were identified as candidate genes for DPS treatment of NAFLD. These target genes were subsequently input into the STRING database to generate the protein–protein interaction (PPI) network (Figure 1B). A PPI network comprising 40 nodes (representing functional proteins) and 146 edges (depicting protein–protein interactions) was constructed using Cytoscape software. The top 10 hub genes, ranked by degree, were HSP90AA1, HSP90AB1, STAT3, CASP3, and NFKB1 (Figure 1C). These hub genes are likely key targets for DPS in the treatment of NAFLD. GO enrichment analysis was performed using the DAVID database, revealing 145 statistically significant GO terms. The analysis indicated that the DPS treatment targets were predominantly enriched in biological processes such as the inflammatory response, RNA polymerase II-mediated transcription regulation, gene expression enhancement, and lipopolysaccharide response. CCs were primarily enriched in the cytoplasm, nucleoplasm, cell surface, and plasma membrane. MFs of DPS targets were enriched in processes like identical protein binding, cannabinoid receptor activity, protein binding, and ubiquitin protein ligase binding (Figure 1D).

To further explore the mechanisms underlying DPS's effects on NAFLD, KEGG pathway analysis of the DPS targets was performed using the DAVID database, identifying 56 statistically significant pathways. The top five pathways were Th17 cell differentiation, NOD-like receptor signaling, chemical carcinogenesis *via* receptor activation, lipid metabolism and atherosclerosis, and alcoholic liver disease (Figure 1E). These results suggest that DPS may exert its therapeutic effects by inhibiting inflammation and alleviating NAFLD symptoms through multiple pathways.

6 https://bioincloud.tech/

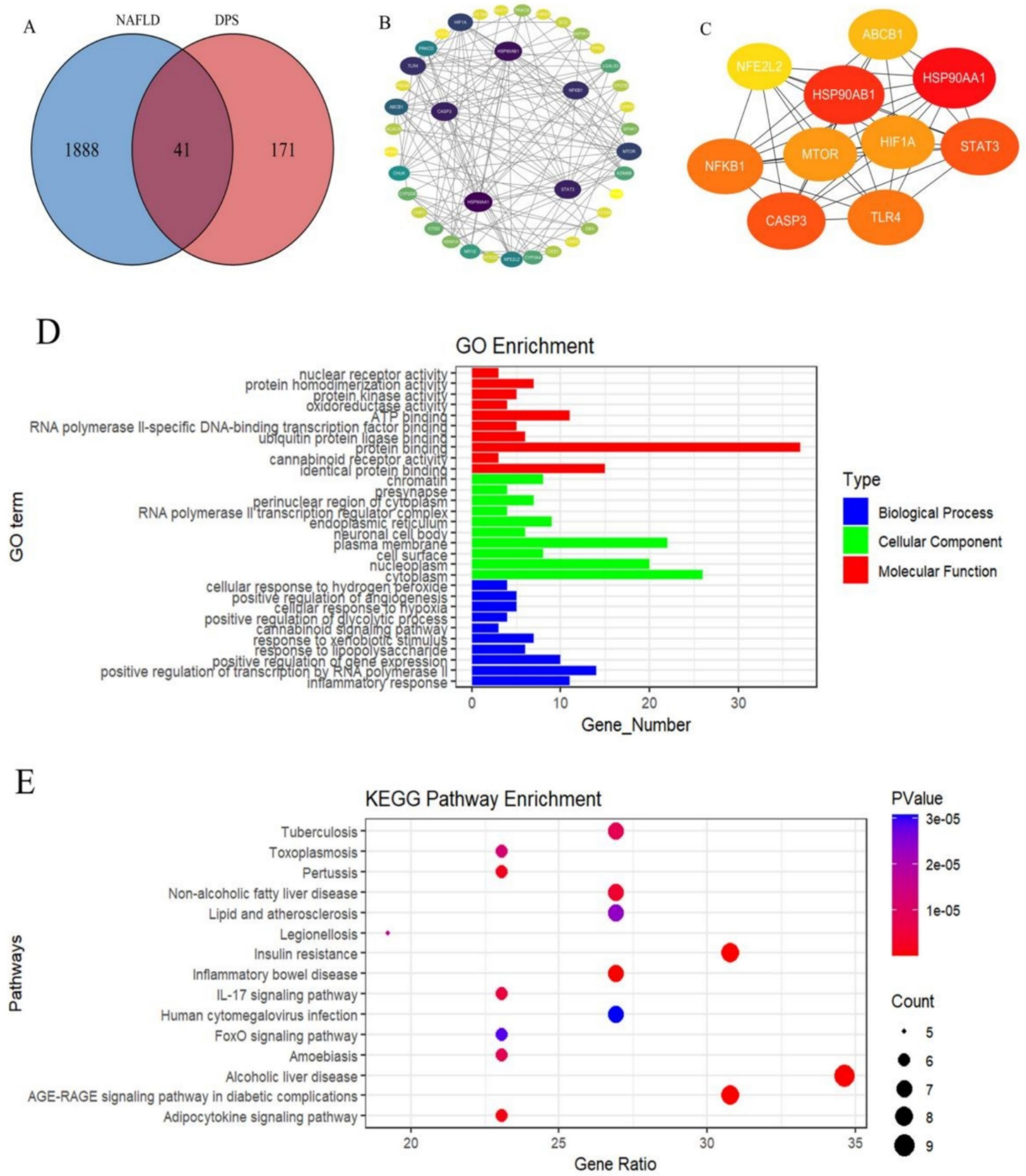

FIGURE 1
Using network pharmacology analysis to identify the targets of DPS in treating NAFLD. There were 41 target genes for DPS in treating NAFLD **(A)**. These 41 targets were input into the STRING database to obtain the PPI network **(B)**. A PPI network consisting of 40 nodes (representing functional proteins) and 146 edges (representing interactions between proteins) was constructed using Cytoscape software, and the top 10 hub genes in the PPI network were identified based on "Degree" **(C)**. Further, GO enrichment analysis of DPS treatment targets was performed using the DAVID database **(D)**, and the KEGG signaling pathways of DPS treatment targets for NAFLD were predicted **(E)**.

3.2 The molecular docking results of DPS with key therapeutic targets for NAFLD

RAGE was selected as the receptor for molecular docking, based on its role as a hub target gene in the NF-κB pathway and its involvement in the AGE-RAGE signaling pathway, which is critical in diabetic complications. DPS was used as the ligand for molecular docking, with binding stability assessed by binding energy. A binding energy below −20.0 kJ/mol indicates strong molecular affinity with the protein. Molecular docking results showed that DPS forms three hydrogen bonds

with RAGE (GLY-48, VAL-58, and ARG-57) and the lowest binding energy of −20.50 kJ/mol (Figure 2A). Additionally, DPS and NF-κB formed five hydrogen bonds (ARG-174, THR-164, VAL-163, ARG-95, and GLN-162), with a binding energy of −23.01 kJ/mol (Figure 2B). These results suggest that DPS exhibits strong binding affinity with both NF-κB and RAGE.

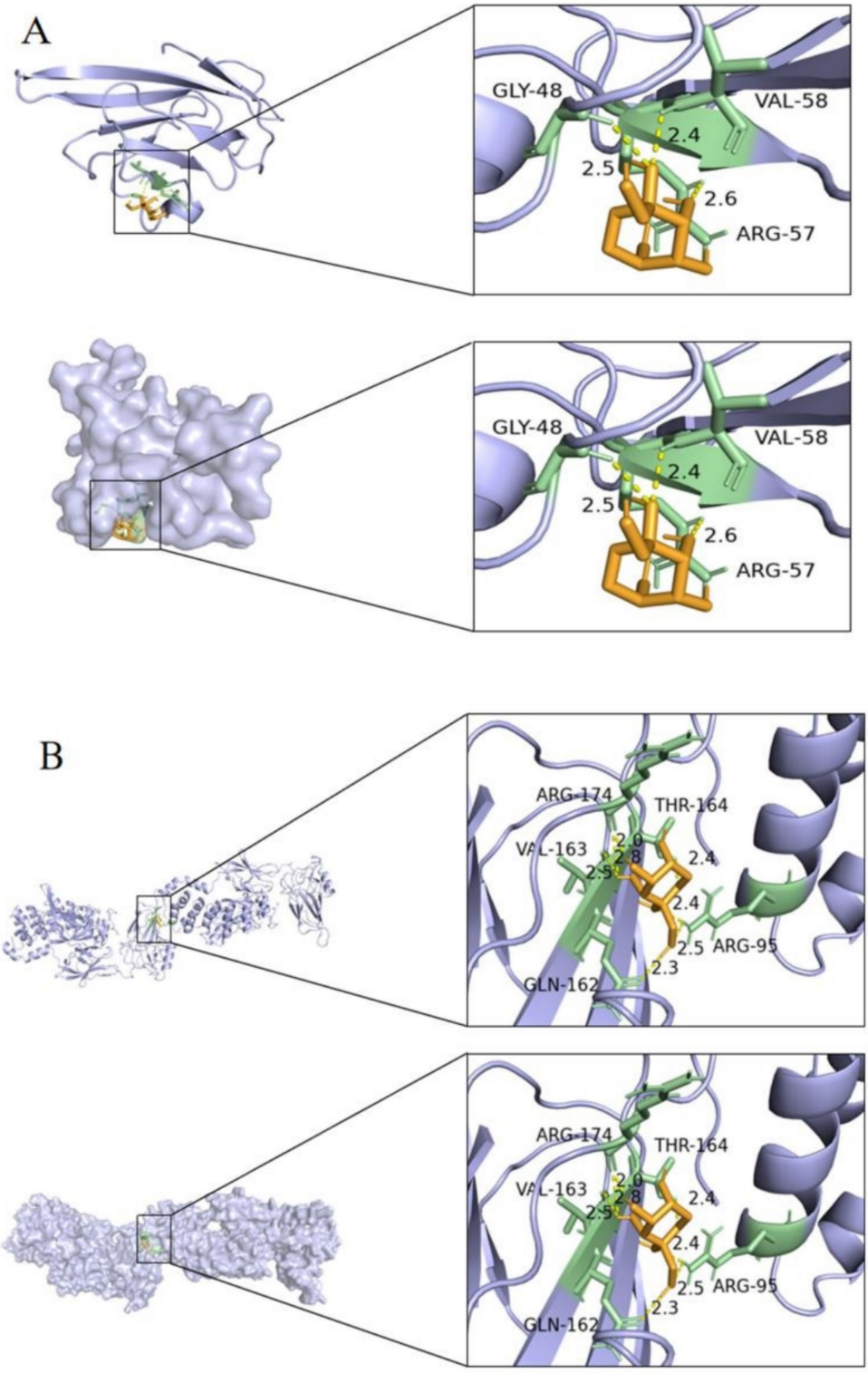

FIGURE 2
Diagram of the docking model between DPS and key targets. The minimum binding energy between DPS and RAGE was less than −20.50 kJ/mol **(A)**, and the minimum binding energy between DPS and NF-κB was less than −23.01 kJ/mol **(B)**. These results indicate that DPS has a good binding ability with both NF-κB and RAGE.

3.3 DPS reduced liver lipid accumulation and liver lesions in NAFLD mice

From week 6 onwards, the NAFLD group exhibited a significant increase in body weight compared to the NC group. No significant differences in body weight were observed between the NAFLD, DPSL, and DPSH groups during the experiment ($p > 0.05$) (Figure 3A). HE staining revealed a marked reduction in hepatocyte ballooning degeneration and necrosis in the DPSL and DPSH groups relative to the NAFLD group (Figures 3B–E). Oil Red O staining showed a significant reduction in hepatocyte fat deposition in the DPSL and DPSH groups (Figures 3F–I).

Compared to the NAFLD group, the DPSL and DPSH groups exhibited significantly lower serum levels of TC, TG, and LDL-C, while the DPSH group demonstrated a significant increase in HDL-C levels ($p < 0.05$) (Figures 4A–D). Oxidative stress in serum was notably diminished, as indicated by a significant increase in SOD activity and a marked decrease in MDA levels ($p < 0.05$) (Figures 4E,F).

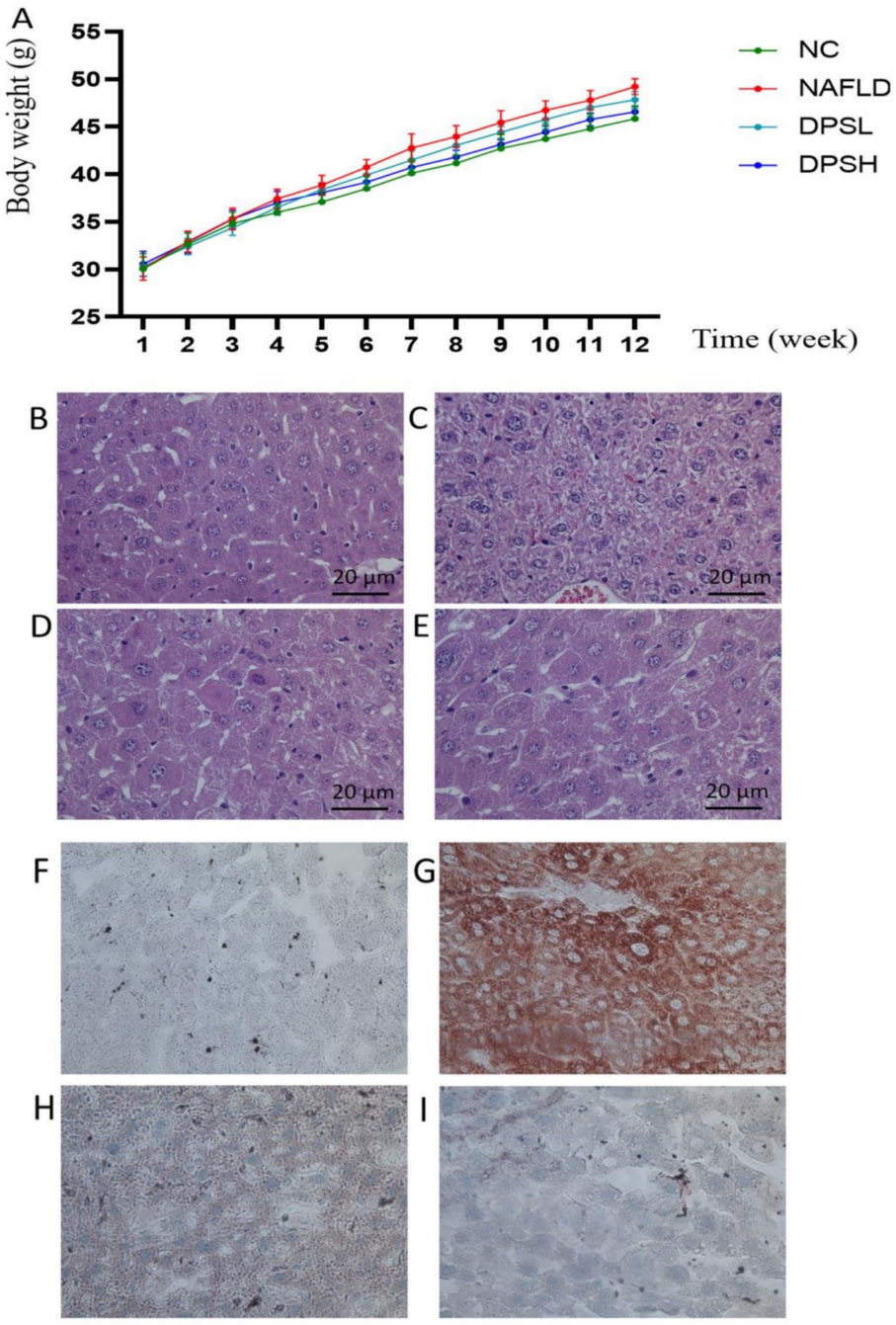

FIGURE 3
Body weight of mice in the experiment **(A)**. Liver damage in mice was observed using HE staining **(B–E)**, and lipid deposition in the liver was assessed using Oil Red O staining **(F–I)**. **(B,F)** The NC group; **(C,G)** The NAFLD group; **(D,H)** The DPSL group; **(E,I)** The DPSH group.

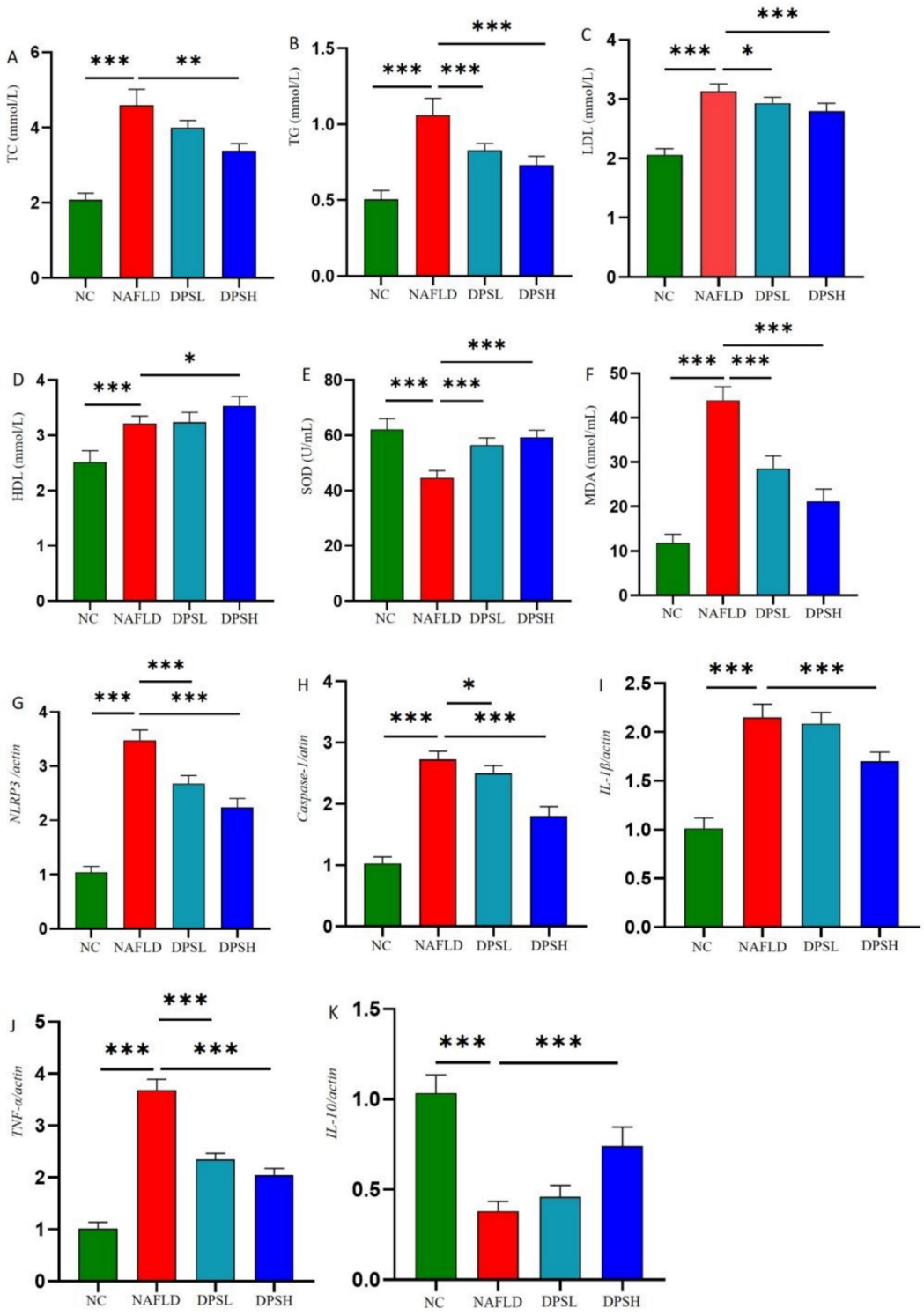

FIGURE 4
Levels of lipid-related indicators in mouse serum: TC **(A)**, TC **(B)**, LDL **(C)**, and HDL **(D)**; levels of oxidative stress-related indicators in serum: SOD **(E)** and MDA **(F)**; inflammatory factors in mouse liver: NLRP3 **(G)**, Caspase-1 **(H)**, IL-1β **(I)**, TNF-α **(J)**, and IL-10 **(K)**. $n = 6$. *: $p < 0.05$; **: $p < 0.01$; ***: $p < 0.001$.

qPCR analysis of liver tissue showed that DPS significantly reduced hepatic expression of inflammatory factors. The DPSL and DPSH groups exhibited lower mRNA levels of *NLRP3*, *Caspase-1*, and *TNF-α* compared to the NAFLD group, with *IL-1β* also significantly reduced in the DPSH group ($p < 0.05$). Furthermore, the DPSH group demonstrated a significant increase in hepatic IL-10 mRNA expression ($p < 0.05$) (Figures 4G–K).

3.4 DPS reduced RAGE expression and NF-κB p65 protein phosphorylation in the liver

RAGE, a receptor for advanced glycation end products (AGEs) and a novel pattern recognition receptor, plays a pivotal role in the pathogenesis of diseases such as diabetes, Alzheimer's, and cancer. Western blotting results showed that the high-dose DPS (DPSH group) significantly reduced RAGE expression and NF-κB p65 protein phosphorylation in the liver of NAFLD mice ($p < 0.05$) (Figure 5).

3.5 DPS improves gut microbiota dysbiosis in NAFLD mice

A high dose of DPS significantly inhibited liver inflammation and oxidative stress in NAFLD mice. This study further investigates the underlying mechanism of high-dose DPS treatment for NAFLD using gut microbiota analysis (*via* 16S rRNA sequencing) and serum non-targeted metabolomics. α-diversity analysis (Shannon index) showed no significant differences in microbial diversity among the three groups of mice (Figure 6A). β-diversity analysis (PCoA scatter plot) revealed distinct separation and clustering of the three groups, with DPS samples more closely resembling the NC group than the NAFLD group, suggesting that DPS ameliorates gut microbiota dysbiosis in NAFLD mice (Figure 6B).

Further analysis at the phylum and genus levels assessed the effects of oral DPS on the gut microbiota in NAFLD mice. At the phylum level, the NAFLD group exhibited a significant increase in the abundance of Patescibacteria, Firmicutes, and Actinobacteria, coupled with a notable decrease in Bacteroidetes, Verrucomicrobia, and Deferribacteres compared to the NC group ($p < 0.05$). Following DPS treatment, the DPS group showed a marked reduction in Patescibacteria, Deferribacteres, Firmicutes, and Actinobacteria, alongside a significant increase in Bacteroidetes, Verrucomicrobia, and Proteobacteria, relative to the NAFLD group ($p < 0.05$) (Figure 6C).

At the genus level, the NAFLD group exhibited a significant increase in the abundance of *Odoribacter* and *Mailhella*, while *Ligilactobacillus*, *Akkermansia*, and *Alistipes* were significantly reduced compared to the NC group ($p < 0.05$). After DPS intervention, the DPS group showed a significant decrease in *Odoribacter* and *Mailhella*, with a significant increase in the abundance of *Ligilactobacillus*, *Duncaniella*, and *Akkermansia* compared to the NAFLD group ($p < 0.05$) (Figure 6D).

3.6 DPS significantly improved serum metabolomics disorders in NAFLD mice

The PCA plot revealed distinct differences in serum metabolomics among the three groups of mice. In both ESI + and ESI- modes, the NAFLD group samples formed distinct clusters, significantly separated from those of the NC and DPS groups. The DPS group samples closely resembled those of the NC group, indicating a significant restorative effect of DPS on serum metabolomic alterations in NAFLD mice (Figures 7A,B).

To identify differential metabolites, the OPLS-DA model was applied with criteria of VIP > 1 and $p < 0.05$ (Figures 7C,D). In the ESI + mode, 301 differential metabolites were identified between the NAFLD and DPS groups. Of these, 174 were highly expressed, and 127 were downregulated in the DPS group compared to the NAFLD group. In the ESI- mode, 255 differential metabolites were identified, with 93 highly expressed and 162 downregulated

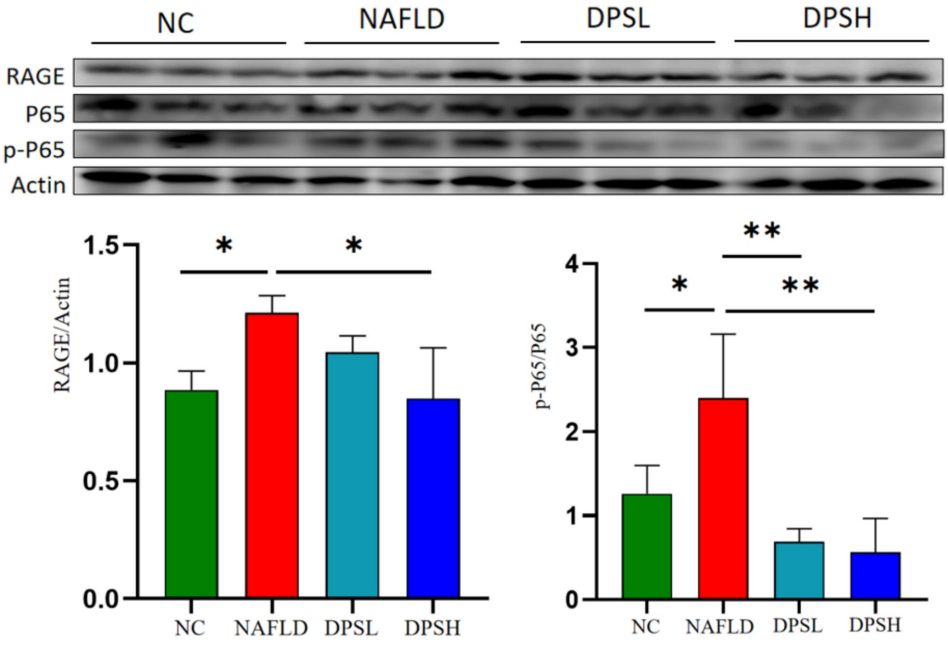

FIGURE 5
The expression of receptor for advanced glycation end products (RAGE) and the phosphorylation level of NF-κB P65 protein in mouse liver were detected using the Western blotting assay. $n = 3$. *: $p < 0.05$; **: $p < 0.01$.

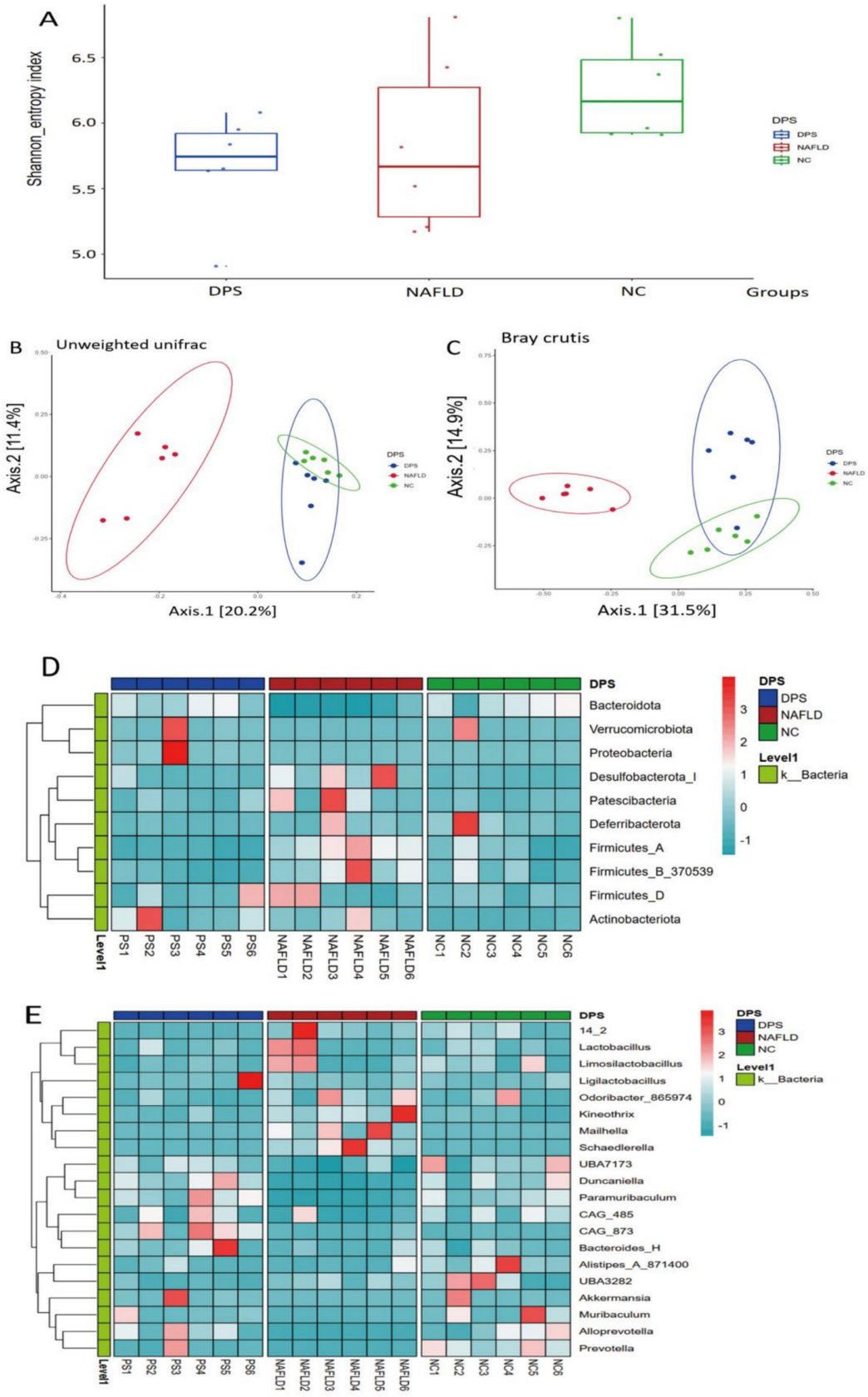

FIGURE 6
The gut microbiota of mice was analyzed using 16S rRNA amplicon sequencing. The α-diversity of shannon index **(A)**, β-diversity with unweighted unifrac **(B)** and bray curtis **(C)** of the gut microbiota in mice are shown, respectively. **(D,E)** Displayed the differences in the gut microbiota at the species level and genus level among the three groups of mice using heat maps. *n* = 6.

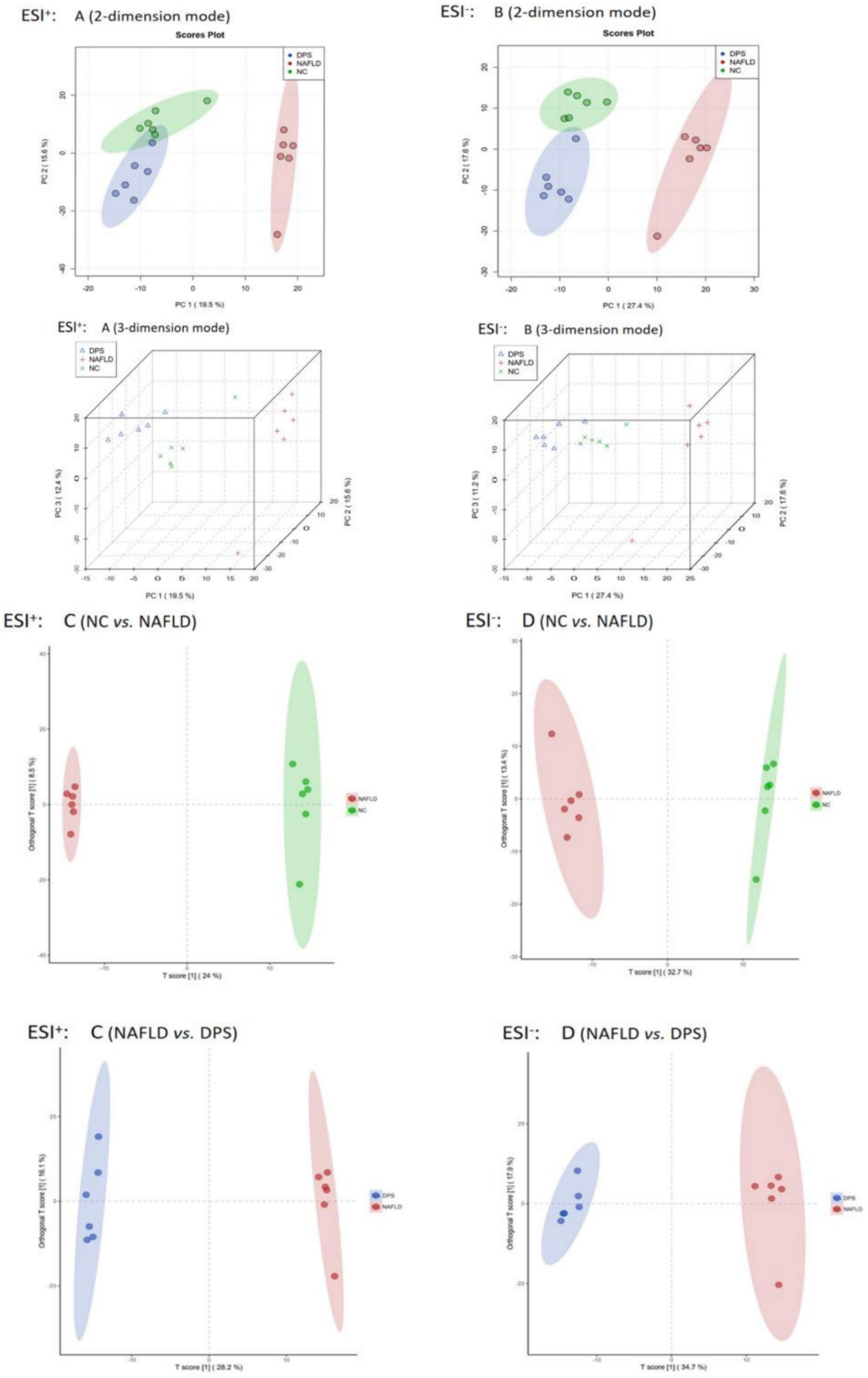

FIGURE 7 (CONTINUED)

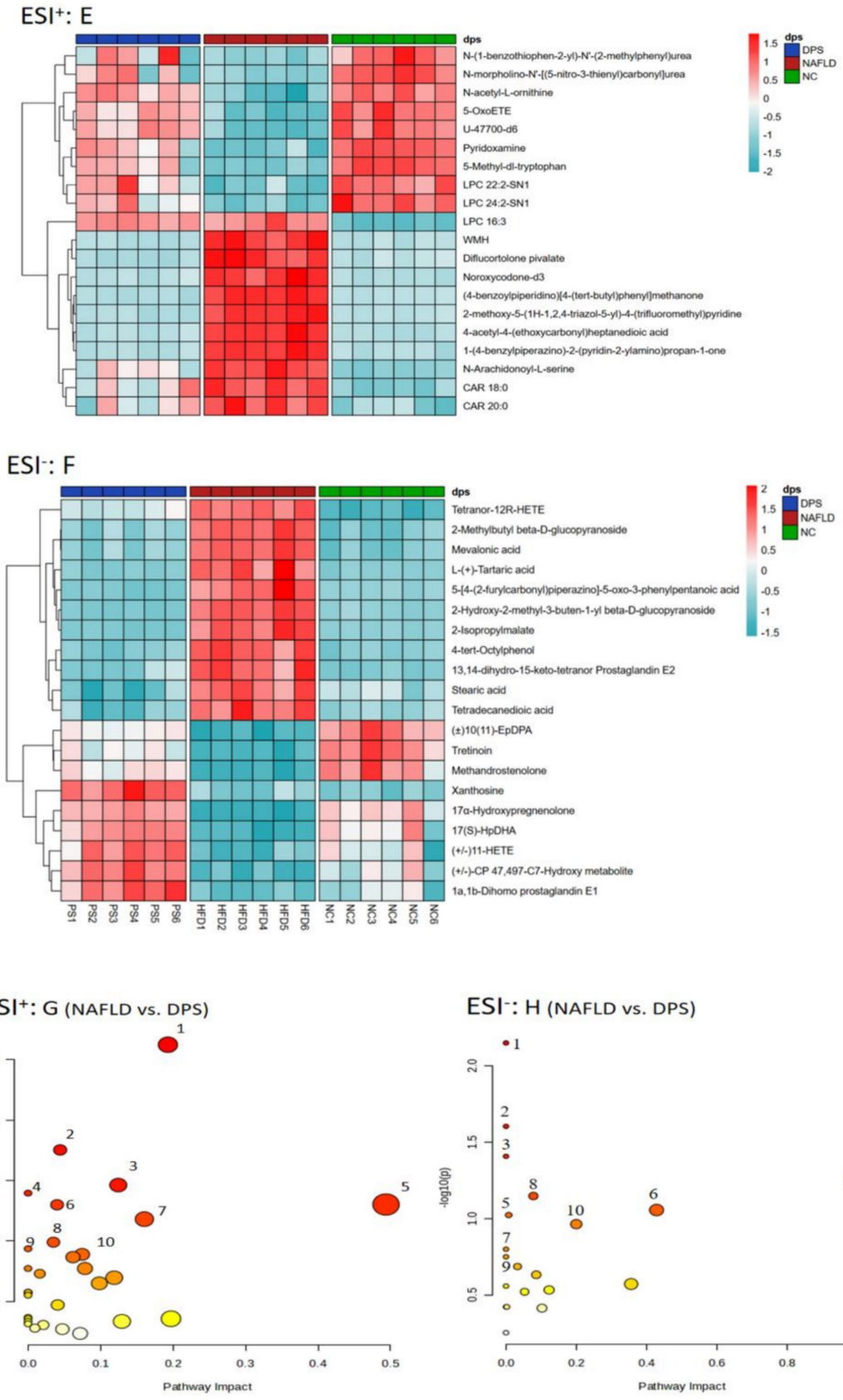

FIGURE 7
Untargeted metabolomics analysis of mouse serum. The PCA plot showed that samples from each group were significantly separated and clustered individually **(A,B)**. Through OPLS-DA model analysis **(C,D)**, differential metabolites were identified based on the screening criteria of VIP > 1 & $p < 0.05$ **(E,F)**. These metabolites were then input into the MetaboAnalyst 6.0 platform for enrichment analysis to obtain metabolic pathways **(G,H)**. $n = 6$.

(Figures 7E,F). Metabolic pathway enrichment analysis, performed using the MetaboAnalyst 6.0 platform, revealed involvement in pathways such as arginine biosynthesis, glutathione metabolism, arginine and proline metabolism, unsaturated fatty acid biosynthesis, propionate metabolism, alanine, aspartate and glutamate metabolism, and linoleic acid metabolism (Figures 7G,H).

3.7 Relationship between gut microbiota and serum metabolites

Pearson correlation analysis was conducted to explore the relationship between gut microbiota and serum metabolites in mice following DPS treatment, to further investigate the underlying mechanism of DPS in NAFLD. The results showed that serum levels of unsaturated fatty acids, specifically linoleic acid and eicosapentaenoic acid, were positively correlated with gut microbiota species such as *UBA3263*, *Prevotella*, *Rikenella*, and *COE1* while showing a negative correlation with *Schaedlerella* and *Acetatifactor*. Additionally, serum uridine levels were positively associated with gut microbiota *CAG_873* and *Paramuribaculum* but negatively correlated with *Merdisoma*, *Enterenecus*, *Dysosmobacter*, and *Lawsonibacter* (Figure 8).

4 Discussion

NAFLD, a metabolic disorder characterized by excessive hepatic fat accumulation, is a major contributor to liver fibrosis and cancer (29–31). The accumulation of lipids in the liver plays a pivotal role in disease progression through oxidative stress and inflammation (32–34). Furthermore, chronic inflammation resulting from endotoxins released into the bloodstream, due to the excessive proliferation of Gram-negative bacteria in the intestines, is a key factor in NAFLD progression (35, 36). Endotoxin levels in the blood can also serve as an indicator of NAFLD severity (37–39). The supplementation of anti-inflammatory and antioxidant agents, including α-lipoic acid, vitamin E, and various plant-derived antioxidants, represents an effective therapeutic approach for treating NAFLD (40–42).

Network pharmacology analysis identified the novel pattern recognition receptor RAGE and the inflammation-related NF-κB signaling pathway as key players in NAFLD pathogenesis. Initially, RAGE was regarded primarily as a receptor for AGEs (43, 44), which are formed through the non-enzymatic glycation of free sugars such as glucose and galactose (45, 46). Elevated blood glucose in diabetic patients leads to a marked increase in AGEs, which are pivotal in the development of diabetic complications (44, 47, 48). Recent studies have expanded the role of RAGE as a novel pattern recognition receptor, capable of binding not only with AGEs but also with ligands such as HMGB1, S100, and Aβ (49–52). RAGE's functions are implicated in diseases related to homeostasis, development, and inflammation, including diabetes, atherosclerosis, and Alzheimer's disease (49, 53, 54). Moreover, RAGE signaling in tumor and immune cells can drive tumor progression, migration, and immune evasion, promoting cancer development (55–58).

DPS is a rare sugar found in fruits such as figs and raisins, and it has been approved as a safe food additive by the U.S. FDA and the European Union (59). Acute/subchronic toxicity tests show that even with high doses (4 g/kg body weight/day) consumed over a long period (90 days), no significant organ damage or blood biochemical abnormalities were observed (60). Additionally, only about 30% of DPS is absorbed in the intestines, with the rest being fermented by intestinal flora (61). Its low-calorie characteristic (0.4 kcal/g) helps prevent exacerbation of NAFLD due to excess calorie intake (62). Compared to other sugar alcohols like erythritol, DPS has better gastrointestinal tolerance, and even daily intake of high doses of DPS ($\leq$30 g/day) does not cause noticeable bloating or diarrhea, making it an ideal sugar substitute for individuals with obesity and diabetes (7).

Our study reveals that DPS significantly improves serum lipid profiles in HFD-induced NAFLD mice. These findings suggest that DPS exerts systemic metabolic benefits beyond its direct hepatic effects, potentially through multi-target modulation of cholesterol homeostasis. The AGEs/RAGE/NF-κB axis inhibition by DPS may restore hepatic LDL receptor (LDLR) functionality. However, the mechanism of DPS regulation of blood lipid metabolism still needs to be further studied.

In NAFLD, excessive lipid peroxides in the liver not only induce inflammation but also foster the formation of AGEs (63). Upon binding to RAGE, AGEs initiate intracellular signaling that generates reactive oxygen species, which can damage hepatocytes (44, 64–66). Recent studies suggest that activation of the AGEs/RAGE/NF-κB pathway plays a significant role in the complications of type 2 diabetes (50, 67–69). Inhibiting the RAGE and NF-κB signaling pathways may provide therapeutic benefits in preventing and treating diabetes complications (67, 70, 71).

Molecular docking analysis demonstrated that DPS effectively binds to both NF-κB p65 and RAGE proteins, significantly inhibiting the activation of both the NF-κB and AGEs/RAGE pathways. Western blot assays confirmed that DPS significantly reduces RAGE expression and NF-κB p65 protein phosphorylation in the livers of NAFLD mice. These findings suggest that DPS may alleviate inflammation and liver damage in NAFLD by modulating the AGEs/RAGE/NF-κB pathway.

Notably, our data reveal that DPS administration significantly attenuated hepatic MDA accumulation while enhancing SOD activity, suggesting its potent capacity to counteract the redox imbalance characteristic of NAFLD progression. Mounting evidence implicates AGEs as critical mediators in NAFLD pathogenesis, where their interaction with RAGE not only perpetuates inflammatory cascades *via* NF-κB activation but also directly amplifies oxidative damage through NADPH oxidase-driven ROS generation (72, 73). Our findings align with these mechanisms, as DPS treatment effectively suppressed RAGE overexpression and downstream NF-κB phosphorylation. This dual modulation likely disrupts the self-reinforcing cycle between AGEs accumulation and oxidative stress – a phenomenon particularly relevant in lipid-laden hepatocytes where β-oxidation overload exacerbates mitochondrial ROS production.

Furthermore, the antioxidant effects of DPS may synergize with its anti-inflammatory actions. NF-κB activation stimulates pro-oxidant enzymes while suppressing antioxidant genes, creating a pathogenic feedback loop. DPS-mediated NF-κB inhibition could therefore break this cycle. Such coordinated modulation of oxidative-inflammatory crosstalk positions DPS as a promising multi-target agent for NAFLD management.

Han et al. (74) demonstrated that DPS modulates gut microbiota and promotes the production of beneficial metabolites, such as short-chain fatty acids (SCFAs), while also alleviating diabetes and

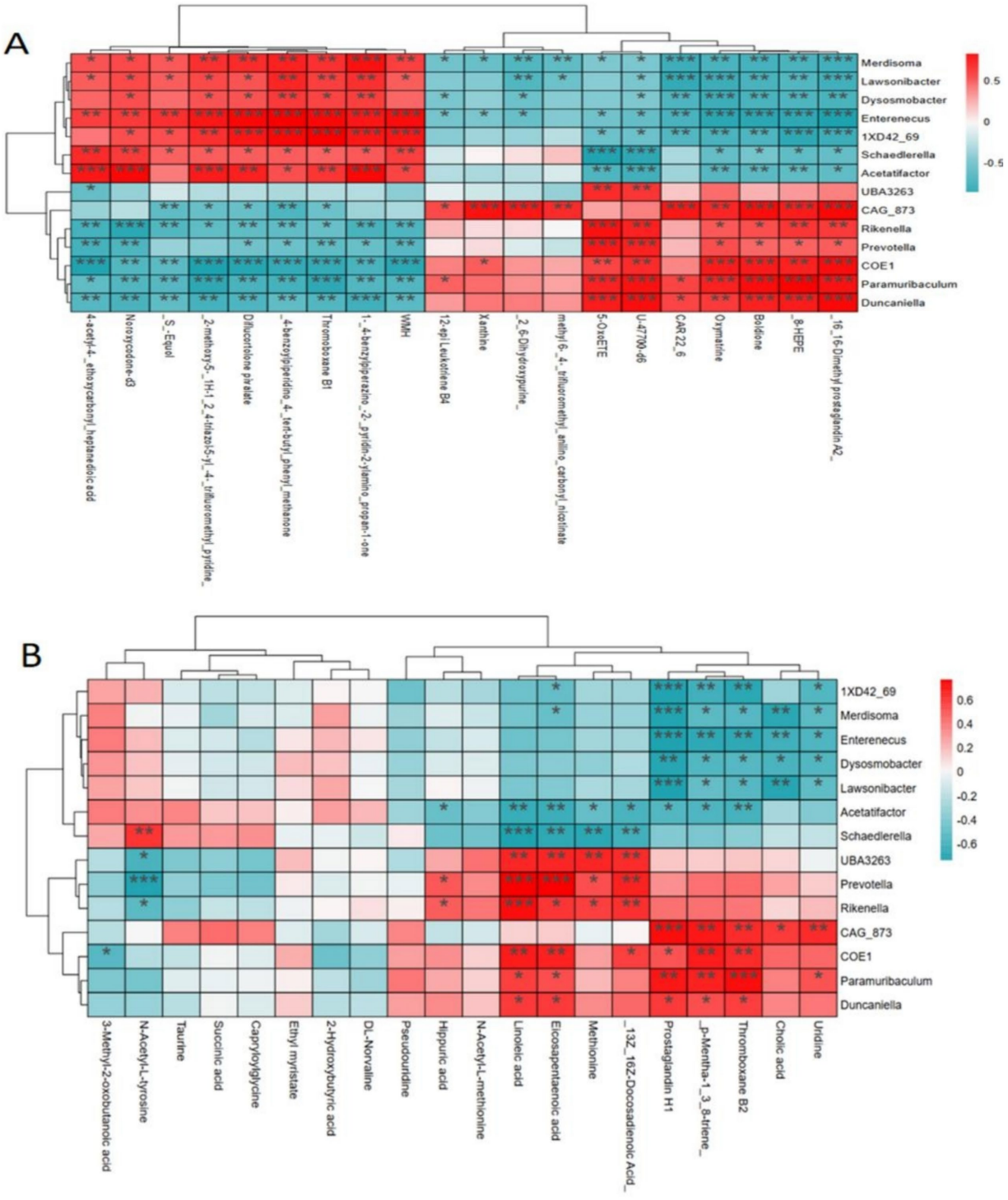

FIGURE 8
Pearson correlation analysis of the relationship between gut microbiota and serum metabolites. **(A)** ESI$^+$ mode; **(B)** ESI$^-$ mode. $n = 6$.

obesity in experimental animals (75). Through 16S rRNA sequencing, oral DPS administration was found to notably increase the abundance of beneficial gut bacteria, including *Akkermansia* and *Duncaniella*, in NAFLD mice, which are associated with SCFA production (76, 77). Furthermore, DPS enhanced the abundance of *Ligilactobacillus*, which plays a role in inhibiting liver fat accumulation and hyperlipidemia (78, 79). Significant improvements were also observed in oxidative stress and blood lipid levels in NAFLD mice. These findings suggest that DPS exerts therapeutic effects on NAFLD by reshaping gut microbiota and elevating beneficial metabolites like SCFAs.

Addressing gut dysbiosis represents an innovative approach to NAFLD management (80, 81). Both *Akkermansia* and *Duncaniella* contribute to NAFLD modulation by influencing gut and liver functions. *Akkermansia* reduces TLR2 expression and macrophage activation (82), while *Duncaniella* regulates the production of

3,7-dihydroxy-12-oxocholanoic acid, inhibiting hepatic gluconeogenesis and lipid metabolism (83).

Untargeted metabolomics analysis further revealed that DPS significantly alters the serum metabolome in NAFLD mice, boosting the levels of anti-inflammatory and antioxidant metabolites. Notably, tretinoin, a bioactive metabolite of vitamin A, is found at markedly lower concentrations in the serum of patients with NAFLD compared to healthy controls (84). Tretinoin promotes the reduction of fat deposition and ameliorates NAFLD symptoms by enhancing fatty acid β-oxidation in the liver (85). Additionally, it may enhance liver antioxidant capacity *via* the Sirt1 pathway, thereby mitigating high-fat diet-induced liver steatosis (86). These findings suggest that DPS treatment elevates serum tretinoin levels in NAFLD mice, providing a potential mechanism for its therapeutic action in NAFLD. Pyridoxamine, a derivative of vitamin B6, is critical for preventing multiple diseases when deficient, although its role in metabolic syndrome remains underexplored. Patients with NAFLD exhibit significantly lower serum pyridoxamine levels than healthy individuals (87). Pyridoxamine prevents AGE formation (88), improves lipid metabolism in NAFLD rats (89), and reduces hepatic lipid peroxidation and inflammation (90). Our data indicate that oral DPS administration significantly increases serum pyridoxamine concentrations in NAFLD mice, suggesting that this elevation may suppress AGEs-RAGE pathway activation, thereby mitigating inflammation and oxidative stress in NAFLD.

Statins regulate blood lipids and exert anti-inflammatory effects by inhibiting mevalonic acid synthesis in the liver and activating hepatic stellate cells, thereby preventing the progression of liver fibrosis (91–93). In this study, DPS also significantly reduced serum mevalonic acid levels in NAFLD mice, suggesting that DPS may regulate blood lipids and mitigate inflammatory liver damage *via* the mevalonic acid synthesis pathway.

The study further identified increased levels of eicosapentaenoic acid (EPA) and linoleic acid in DPS-treated mice, with a significant positive correlation between these unsaturated fatty acids and the relative abundance of *Duncaniella*. Clinical studies have shown that elevated EPA concentrations in the serum of patients with cirrhosis are associated with a reduced risk of progression to liver cancer (94). EPA exhibits potent anti-inflammatory and antioxidant properties, which can significantly prevent liver cell degeneration and fibrosis in patients with NAFLD (95). Linoleic acid, a gut microbial metabolite, inhibits the activation of the TGF-β signaling pathway in hepatic stellate cells, thus preventing liver fibrosis progression (18). These findings suggest that DPS significantly increases serum linoleic acid levels in NAFLD mice, pointing to a potential mechanism underlying DPS's therapeutic effects on NAFLD.

5 Conclusion

Our results indicate that oral DPS administration effectively regulates blood lipids in NAFLD mice and ameliorates inflammation and oxidative stress in the liver. The therapeutic action of DPS in NAFLD likely involves the modulation of gut microbiota and the enhancement of anti-inflammatory and antioxidant metabolites in the serum.

However, we believe that the biggest obstacle for DPS from the laboratory to the market is its high production cost, which is more than 2–3 times the cost of alternative sweeteners such as erythritol and steviol glycosides. We think that DPS therapy might be more suitable for prioritization in high-risk populations for NAFLD (such as pre-diabetic patients) rather than the general healthy population, in order to reduce medical costs. This is because the cost of using DPS therapy to prevent the progression of NAFLD is lower compared to the treatment expenses after NAFLD progresses to NASH.

Data availability statement

The original contributions presented in the study are publicly available. This data can be found here: https://ngdc.cncb.ac.cn/search/all?&q=PRJCA039581.

Ethics statement

The animal studies were approved by the Ethics Committee of the Jiangsu University. The studies were conducted in accordance with the local legislation and institutional requirements. Written informed consent was obtained from the owners for the participation of their animals in this study.

Author contributions

JT: Conceptualization, Data curation, Investigation, Methodology, Resources, Validation, Visualization, Writing – original draft. WS: Conceptualization, Formal analysis, Funding acquisition, Investigation, Methodology, Project administration, Resources, Validation, Writing – original draft. XD: Conceptualization, Formal analysis, Investigation, Methodology, Validation, Writing – original draft. JH: Data curation, Formal analysis, Funding acquisition, Methodology, Project administration, Resources, Visualization, Writing – original draft. AA: Conceptualization, Data curation, Methodology, Project administration, Resources, Supervision, Validation, Visualization, Writing – original draft, Writing – review & editing. MC: Data curation, Investigation, Methodology, Writing – original draft. LZ: Investigation, Methodology, Software, Writing – original draft. LW: Conceptualization, Formal analysis, Funding acquisition, Investigation, Supervision, Writing – original draft, Writing – review & editing. KS: Investigation, Methodology, Resources, Software, Supervision, Validation, Writing – original draft, Writing – review & editing.

Funding

The author(s) declare that financial support was received for the research and/or publication of this article. This work was supported by Zhenjiang Key R&D Program – Social Development Project (SH2023073) and Jiangsu Province Traditional Chinese Medicine Science and Technology Development Project (MS2022126).

Conflict of interest

The authors declare that the research was conducted in the absence of any commercial or financial relationships that could be construed as a potential conflict of interest.

Generative AI statement

The authors declare that no Gen AI was used in the creation of this manuscript.

Publisher's note

All claims expressed in this article are solely those of the authors and do not necessarily represent those of their affiliated organizations, or those of the publisher, the editors and the reviewers. Any product that may be evaluated in this article, or claim that may be made by its manufacturer, is not guaranteed or endorsed by the publisher.

Supplementary material

The Supplementary material for this article can be found online at: https://www.frontiersin.org/articles/10.3389/fnut.2025.1574151/full#supplementary-material

References

1. Jung YS, Kim HG, Cho CH, Lee SH, Lee N, Yang J, et al. Trapping mechanism by di-d-psicose anhydride with methylglyoxal for prevention of diabetic nephropathy. *Carbohydr Res*. (2024) 540:109125. doi: 10.1016/j.carres.2024.109125

2. Song Y, Maskey S, Lee YG, Lee DS, Nguyen DT, Bae HJ. Optimizing bioconversion processes of rice husk into value-added products: D-psicose, bioethanol, and lactic acid. *Bioresour Technol*. (2024) 395:130363. doi: 10.1016/j.biortech.2024.130363

3. Natsume Y, Yamada T, Iida T, Ozaki N, Gou Y, Oshida Y, et al. Investigation of d-allulose effects on high-sucrose diet-induced insulin resistance via hyperinsulinemic-euglycemic clamps in rats. *Heliyon*. (2021) 7:e08013. doi: 10.1016/j.heliyon.2021.e08013

4. Teysseire F, Bordier V, Budzinska A, Weltens N, Rehfeld JF, Holst JJ, et al. The role of D-allulose and erythritol on the activity of the gut sweet taste receptor and gastrointestinal satiation hormone release in humans: a randomized, controlled trial. *J Nutr*. (2022) 152:1228–38. doi: 10.1093/jn/nxac026

5. Watthanasakphuban N, Srila P, Pinmanee P, Punvittayagul C, Petchyam N, Ninchan B. Production, purification, characterization, and safety evaluation of constructed recombinant D-psicose 3-epimerase. *Microb Cell Factories*. (2024) 23:216. doi: 10.1186/s12934-024-02487-x

6. Van Laar A, Grootaert C, Van Camp J. Rare mono- and disaccharides as healthy alternative for traditional sugars and sweeteners. *Crit Rev Food Sci Nutr*. (2021) 61:713–41. doi: 10.1080/10408398.2020.1743966

7. Lei P, Chen H, Ma J, Fang Y, Qu L, Yang Q, et al. Research progress on extraction technology and biomedical function of natural sugar substitutes. *Front Nutr*. (2022) 9:952147. doi: 10.3389/fnut.2022.952147

8. Li J, Li H, Liu H, Luo Y. Recent advances in the biosynthesis of natural sugar substitutes in yeast. *J Fungi (Basel)*. (2023) 9:907. doi: 10.3390/jof9090907

9. Kanasaki A, Niibo M, Iida T. Effect of D-allulose feeding on the hepatic metabolomics profile in male Wistar rats. *Food Funct*. (2021) 12:3931–8. doi: 10.1039/d0fo03024d

10. Xie X, Li C, Ban X, Yang H, Li Z. D-allulose 3-epimerase for low-calorie D-allulose synthesis: microbial production, characterization, and applications. *Crit Rev Biotechnol*. (2024) 45:1–20. doi: 10.1080/07388551.2024.2368517

11. Mantovani A, Csermely A, Petracca G, Beatrice G, Corey KE, Simon TG, et al. Non-alcoholic fatty liver disease and risk of fatal and non-fatal cardiovascular events: an updated systematic review and meta-analysis. *Lancet Gastroenterol Hepatol*. (2021) 6:903–13. doi: 10.1016/S2468-1253(21)00308-3

12. Quek J, Chan KE, Wong ZY, Tan C, Tan B, Lim WH, et al. Global prevalence of non-alcoholic fatty liver disease and non-alcoholic steatohepatitis in the overweight and obese population: a systematic review and meta-analysis. *Lancet Gastroenterol Hepatol*. (2023) 8:20–30. doi: 10.1016/S2468-1253(22)00317-X

13. Tacke F, Weiskirchen R. Non-alcoholic fatty liver disease (NAFLD)/non-alcoholic steatohepatitis (NASH)-related liver fibrosis: mechanisms, treatment and prevention. *Ann Transl Med*. (2021) 9:729. doi: 10.21037/atm-20-4354

14. Ramai D, Facciorusso A, Vigandt E, Schaf B, Saadedeen W, Chauhan A, et al. Progressive liver fibrosis in non-alcoholic fatty liver disease. *Cells*. (2021) 10:3401. doi: 10.3390/cells10123401

15. Gallage S, Avila J, Ramadori P, Focaccia E, Rahbari M, Ali A, et al. A researcher's guide to preclinical mouse NASH models. *Nat Metab*. (2022) 4:1632–49. doi: 10.1038/s42255-022-00700-y

16. Muzurović E, Mikhailidis DP, Mantzoros C. Non-alcoholic fatty liver disease, insulin resistance, metabolic syndrome and their association with vascular risk. *Metabolism*. (2021) 119:154770. doi: 10.1016/j.metabol.2021.154770

17. Ziolkowska S, Binienda A, Jabłkowski M, Szemraj J, Czarny P. The interplay between insulin resistance, inflammation, oxidative stress, base excision repair and metabolic syndrome in nonalcoholic fatty liver disease. *Int J Mol Sci*. (2021) 22:11128. doi: 10.3390/ijms222011128

18. Kasahara N, Imi Y, Amano R, Shinohara M, Okada K, Hosokawa Y, et al. A gut microbial metabolite of linoleic acid ameliorates liver fibrosis by inhibiting TGF-β signaling in hepatic stellate cells. *Sci Rep*. (2023) 13:18983. doi: 10.1038/s41598-023-46404-5

19. Attia SL, Softic S, Mouzaki M. Evolving role for pharmacotherapy in NAFLD/NASH. *Clin Transl Sci*. (2021) 14:11–9. doi: 10.1111/cts.12839

20. Pafili K, Roden M. Nonalcoholic fatty liver disease (NAFLD) from pathogenesis to treatment concepts in humans. *Mol Metab*. (2021) 50:101122. doi: 10.1016/j.molmet.2020.101122

21. Lee YA, Friedman SL. Inflammatory and fibrotic mechanisms in NAFLD-implications for new treatment strategies. *J Intern Med*. (2022) 291:11–31. doi: 10.1111/joim.13380

22. Kokkorakis M, Boutari C, Hill MA, Kotsis V, Loomba R, Sanyal AJ, et al. Resmetirom, the first approved drug for the management of metabolic dysfunction-associated steatohepatitis: trials, opportunities, and challenges. *Metabolism*. (2024) 154:155835. doi: 10.1016/j.metabol.2024.155835

23. Chen VL, Morgan TR, Rotman Y, Patton HM, Cusi K, Kanwal F, et al. Resmetirom therapy for metabolic dysfunction-associated steatotic liver disease: October 2024 updates to AASLD practice guidance. *Hepatology*. (2025) 81:312–20. doi: 10.1097/HEP.0000000000001112

24. Raza S, Rajak S, Upadhyay A, Tewari A, Anthony SR. Current treatment paradigms and emerging therapies for NAFLD/NASH. *Front Biosci (Landmark Ed)*. (2021) 26:206–37. doi: 10.2741/4892

25. Kobayashi T, Iwaki M, Nakajima A, Nogami A, Yoneda M. Current research on the pathogenesis of NAFLD/NASH and the gut-liver axis: gut microbiota, dysbiosis, and leaky-gut syndrome. *Int J Mol Sci*. (2022) 23:11689. doi: 10.3390/ijms231911689

26. Vetrano E, Rinaldi L, Mormone A, Giorgione C, Galiero R, Caturano A, et al. Non-alcoholic fatty liver disease (NAFLD), type 2 diabetes, and non-viral hepatocarcinoma: pathophysiological mechanisms and new therapeutic strategies. *Biomedicines*. (2023) 11:468. doi: 10.3390/biomedicines11020468

27. Sun C, Qiu C, Zhang Y, Yan M, Tan J, He J, et al. Lactiplantibacillus plantarum NKK20 alleviates high-fat-diet-induced nonalcoholic fatty liver disease in mice through regulating bile acid anabolism. *Molecules*. (2023) 28:4042. doi: 10.3390/molecules28104042

28. He J, Li X, Yan M, Chen X, Sun C, Tan J, et al. Inulin reduces kidney damage in type 2 diabetic mice by decreasing inflammation and serum metabolomics. *J Diabetes Res*. (2024) 2024:1222395. doi: 10.1155/2024/1222395

29. Geng Y, Faber KN, de Meijer VE, Blokzijl H, Moshage H. How does hepatic lipid accumulation lead to lipotoxicity in non-alcoholic fatty liver disease. *Hepatol Int*. (2021) 15:21–35. doi: 10.1007/s12072-020-10121-2

30. Fujiwara N, Kubota N, Crouchet E, Koneru B, Marquez CA, Jajoriya AK, et al. Molecular signatures of long-term hepatocellular carcinoma risk in nonalcoholic fatty liver disease. *Sci Transl Med*. (2022) 14:eabo4474. doi: 10.1126/scitranslmed.abo4474

31. Guo W, Ge X, Lu J, Xu X, Gao J, Wang Q, et al. Diet and risk of non-alcoholic fatty liver disease, cirrhosis, and liver cancer: a large prospective cohort study in UK biobank. *Nutrients*. (2022) 14:5335. doi: 10.3390/nu14245335

32. Madduma Hewage S, Prashar S, Karmin O, Siow YL. Lingonberry improves non-alcoholic fatty liver disease by reducing hepatic lipid accumulation, oxidative stress and inflammatory response. *Antioxidants (Basel)*. (2021) 10:565. doi: 10.3390/antiox10040565

33. Martín-Fernández M, Arroyo V, Carnicero C, Sigüenza R, Busta R, Mora N, et al. Role of oxidative stress and lipid peroxidation in the pathophysiology of NAFLD. *Antioxidants (Basel)*. (2022) 11:2217. doi: 10.3390/antiox11112217

34. Li L, Wang YM, Zeng XY, Hu Y, Zhang J, Wang B, et al. Bioactive proteins and antioxidant peptides from *Litsea cubeba* fruit meal: preparation, characterization and ameliorating function on high-fat diet-induced NAFLD through regulating lipid metabolism, oxidative stress and inflammatory response. *Int J Biol Macromol*. (2024) 280:136186. doi: 10.1016/j.ijbiomac.2024.136186

35. Kessoku T, Kobayashi T, Imajo K, Tanaka K, Yamamoto A, Takahashi K, et al. Endotoxins and non-alcoholic fatty liver disease. *Front Endocrinol (Lausanne)*. (2021) 12:770986. doi: 10.3389/fendo.2021.770986

36. Bergheim I, Moreno-Navarrete JM. The relevance of intestinal barrier dysfunction, antimicrobial proteins and bacterial endotoxin in metabolic dysfunction-associated steatotic liver disease. *Eur J Clin Investig*. (2024) 54:e14224. doi: 10.1111/eci.14224

37. Barchetta I, Cimini FA, Sentinelli F, Chiappetta C, Di Cristofano C, Silecchia G, et al. Reduced lipopolysaccharide-binding protein (LBP) levels are associated with non-alcoholic fatty liver disease (NAFLD) and adipose inflammation in human obesity. *Int J Mol Sci*. (2023) 24:17174. doi: 10.3390/ijms242417174

38. Soppert J, Brandt EF, Heussen NM, Barzakova E, Blank LM, Kuepfer L, et al. Blood endotoxin levels as biomarker of nonalcoholic fatty liver disease: a systematic review and meta-analysis. *Clin Gastroenterol Hepatol*. (2023) 21:2746–58. doi: 10.1016/j.cgh.2022.11.030

39. Yuan H, Wu X, Wang X, Zhou JY, Park S. Microbial dysbiosis linked to metabolic dysfunction-associated fatty liver disease in Asians: *Prevotella copri* promotes lipopolysaccharide biosynthesis and network instability in the prevotella enterotype. *Int J Mol Sci*. (2024) 25:2183. doi: 10.3390/ijms25042183

40. Mosca A, Crudele A, Smeriglio A, Braghini MR, Panera N, Comparcola D, et al. Antioxidant activity of hydroxytyrosol and vitamin E reduces systemic inflammation in children with paediatric NAFLD. *Dig Liver Dis*. (2021) 53:1154–8. doi: 10.1016/j.dld.2020.09.021

41. Tutunchi H, Zolrahim F, Nikbaf-Shandiz M, Naeini F, Ostadrahimi A, Naghshi S, et al. Effects of oleoylethanolamide supplementation on inflammatory biomarkers, oxidative stress and antioxidant parameters of obese patients with NAFLD on a calorie-restricted diet: a randomized controlled trial. *Front Pharmacol*. (2023) 14:1144550. doi: 10.3389/fphar.2023.1144550

42. Mohammadian K, Fakhar F, Keramat S, Stanek A. The role of antioxidants in the treatment of metabolic dysfunction-associated fatty liver disease: a systematic review. *Antioxidants (Basel)*. (2024) 13:797. doi: 10.3390/antiox13070797

43. Twarda-Clapa A, Olczak A, Białkowska AM, Koziołkiewicz M. Advanced glycation end-products (AGEs): formation, chemistry, classification, receptors, and diseases related to AGEs. *Cells*. (2022) 11:1312. doi: 10.3390/cells11081312

44. Wu XQ, Zhang DD, Wang YN, Tan YQ, Yu XY, Zhao YY. AGE/RAGE in diabetic kidney disease and ageing kidney. *Free Radic Biol Med*. (2021) 171:260–71. doi: 10.1016/j.freeradbiomed.2021.05.025

45. Wu Q, Liang Y, Kong Y, Zhang F, Feng Y, Ouyang Y, et al. Role of glycated proteins in vivo: enzymatic glycated proteins and non-enzymatic glycated proteins. *Food Res Int*. (2022) 155:111099. doi: 10.1016/j.foodres.2022.111099

46. Shen CY, Lu CH, Cheng CF, Li KJ, Kuo YM, Wu CH, et al. Advanced glycation end-products acting as immunomodulators for chronic inflammation, inflammaging and carcinogenesis in patients with diabetes and immune-related diseases. *Biomedicines*. (2024) 12:1699. doi: 10.3390/biomedicines12081699

47. Deng L, Du C, Song P, Chen T, Rui S, Armstrong DG, et al. The role of oxidative stress and antioxidants in diabetic wound healing. *Oxidative Med Cell Longev*. (2021) 2021:8852759. doi: 10.1155/2021/8852759

48. Samsu N. Diabetic nephropathy: challenges in pathogenesis, diagnosis, and treatment. *Biomed Res Int*. (2021) 2021:1497449. doi: 10.1155/2021/1497449

49. Dong H, Zhang Y, Huang Y, Deng H. Pathophysiology of RAGE in inflammatory diseases. *Front Immunol*. (2022) 13:931473. doi: 10.3389/fimmu.2022.931473

50. Liu S, Zhang Y, Yang F, Gu J, Zhang R, Kuang Y, et al. Modified Cangfu Daotan decoction ameliorates polycystic ovary syndrome with insulin resistance via NF-κB/LCN-2 signaling pathway in inflammatory microenvironment. *Front Endocrinol (Lausanne)*. (2022) 13:975724. doi: 10.3389/fendo.2022.975724

51. Maheshwari S. AGEs RAGE pathways: Alzheimer's disease. *Drug Res (Stuttg)*. (2023) 73:251–4. doi: 10.1055/a-2008-7948

52. Sarkar S. Pathological role of RAGE underlying progression of various diseases: its potential as biomarker and therapeutic target. *Naunyn Schmiedeberg's Arch Pharmacol*. (2024) 398:3467–87. doi: 10.1007/s00210-024-03595-6

53. Juranek J, Mukherjee K, Kordas B, Załęcki M, Korytko A, Zglejc-Waszak K, et al. Role of RAGE in the pathogenesis of neurological disorders. *Neurosci Bull*. (2022) 38:1248–62. doi: 10.1007/s12264-022-00878-x

54. Zhou M, Zhang Y, Shi L, Li L, Zhang D, Gong Z, et al. Activation and modulation of the AGEs-RAGE axis: implications for inflammatory pathologies and therapeutic interventions – a review. *Pharmacol Res*. (2024) 206:107282. doi: 10.1016/j.phrs.2024.107282

55. Taneja S, Vetter SW, Leclerc E. Hypoxia and the receptor for advanced glycation end products (RAGE) signaling in cancer. *Int J Mol Sci*. (2021) 22:8153. doi: 10.3390/ijms22158153

56. Waghela BN, Vaidya FU, Ranjan K, Chhipa AS, Tiwari BS, Pathak C. AGE-RAGE synergy influences programmed cell death signaling to promote cancer. *Mol Cell Biochem*. (2021) 476:585–98. doi: 10.1007/s11010-020-03928-y

57. Amornsupak K, Thongchot S, Thinyakul C, Box C, Hedayat S, Thuwajit P, et al. HMGB1 mediates invasion and PD-L1 expression through RAGE-PI3K/AKT signaling pathway in MDA-MB-231 breast cancer cells. *BMC Cancer*. (2022) 22:578. doi: 10.1186/s12885-022-09675-1

58. Park WY, Gray JM, Holewinski RJ, Andresson T, So JY, Carmona-Rivera C, et al. Apoptosis-induced nuclear expulsion in tumor cells drives S100a4-mediated metastatic outgrowth through the RAGE pathway. *Nat Cancer*. (2023) 4:419–35. doi: 10.1038/s43018-023-00524-z

59. Chen J, Chen D, Ke M, Ye S, Wang X, Zhang W, et al. Characterization of a recombinant D-Allulose 3-epimerase from Thermoclostridium caenicola with potential application in D-Allulose production. *Mol Biotechnol*. (2021) 63:534–43. doi: 10.1007/s12033-021-00320-z

60. Matsuo T, Ishii R, Shirai Y. The 90-day oral toxicity of d-psicose in male Wistar rats. *J Clin Biochem Nutr*. (2012) 50:158–61. doi: 10.3164/jcbn.11-66

61. Li J, Dai Q, Zhu Y, Xu W, Zhang W, Chen Y, et al. Low-calorie bulk sweeteners: recent advances in physical benefits, applications, and bioproduction. *Crit Rev Food Sci Nutr*. (2024) 64:6581–95. doi: 10.1080/10408398.2023.2171362

62. Iida T, Hayashi N, Yamada T, Yoshikawa Y, Miyazato S, Kishimoto Y, et al. Failure of d-psicose absorbed in the small intestine to metabolize into energy and its low large intestinal fermentability in humans. *Metabolism*. (2010) 59:206–14. doi: 10.1016/j.metabol.2009.07.018

63. Pang Q, Sun Z, Shao C, Cai H, Bao Z, Wang L, et al. CML/RAGE signal bridges a common pathogenesis between atherosclerosis and non-alcoholic fatty liver. *Front Med (Lausanne)*. (2020) 7:583943. doi: 10.3389/fmed.2020.583943

64. Jahan H, Choudhary MI. Gliclazide alters macrophages polarization state in diabetic atherosclerosis in vitro via blocking AGE-RAGE/TLR4-reactive oxygen species-activated NF-kβ nexus. *Eur J Pharmacol*. (2021) 894:173874. doi: 10.1016/j.ejphar.2021.173874

65. Abouelezz HM, Shehatou G, Shebl AM, Salem HA. A standardized pomegranate fruit extract ameliorates thioacetamide-induced liver fibrosis in rats via AGE-RAGE-ROS signaling. *Heliyon*. (2023) 9:e14256. doi: 10.1016/j.heliyon.2023.e14256

66. Sakasai-Sakai A, Takeda K, Takeuchi M. Involvement of intracellular TAGE and the TAGE-RAGE-ROS axis in the onset and progression of NAFLD/NASH. *Antioxidants (Basel)*. (2023) 12:748. doi: 10.3390/antiox12030748

67. Mazumder K, Biswas B, Al Mamun A, Billah H, Abid A, Sarkar KK, et al. Investigations of AGEs' inhibitory and nephroprotective potential of ursolic acid towards reduction of diabetic complications. *J Nat Med*. (2022) 76:490–503. doi: 10.1007/s11418-021-01602-1

68. Horvat A, Vlašić I, Štefulj J, Oršolić N, Jazvinšćak JM. Flavonols as a potential pharmacological intervention for alleviating cognitive decline in diabetes: evidence from preclinical studies. *Life (Basel)*. (2023) 13:2291. doi: 10.3390/life13122291

69. Apte MM, Khattar E, Tupe RS. Mechanistic role of *Syzygium cumini* (L.) Skeels in glycation induced diabetic nephropathy via RAGE-NF-κB pathway and extracellular proteins modifications: a molecular approach. *J Ethnopharmacol*. (2024) 322:117573. doi: 10.1016/j.jep.2023.117573

70. Nguyen HN, Ullevig SL, Short JD, Wang L, Ahn YJ, Asmis R. Ursolic acid and related analogues: triterpenoids with broad health benefits. *Antioxidants (Basel)*. (2021) 10:1161. doi: 10.3390/antiox10081161

71. Zhuang LG, Zhang R, Jin GX, Pei XY, Wang Q, Ge XX. Asiaticoside improves diabetic nephropathy by reducing inflammation, oxidative stress, and fibrosis: an in vitro and in vivo study. *World J Diabetes*. (2024) 15:2111–22. doi: 10.4239/wjd.v15.i10.2111

72. Milione S, Di Caterino M, Monaco L, Rinaldi L. Mediation of inflammation, obesity and fatty liver disease by advanced glycation endoproducts. *Eur Rev Med Pharmacol Sci*. (2018) 22:578–9. doi: 10.26355/eurrev_201802_14267

73. Fernando DH, Forbes JM, Angus PW, Herath CB. Development and progression of non-alcoholic fatty liver disease: the role of advanced glycation end products. *Int J Mol Sci*. (2019) 20:5037. doi: 10.3390/ijms20205037

74. Han Y, Park H, Choi BR, Ji Y, Kwon EY, Choi MS. Alteration of microbiome profile by D-allulose in amelioration of high-fat-diet-induced obesity in mice. *Nutrients*. (2020) 12:352. doi: 10.3390/nu12020352

75. Baek SH, Park SJ, Lee HG. D-psicose, a sweet monosaccharide, ameliorate hyperglycemia, and dyslipidemia in C57BL/6J db/db mice. *J Food Sci*. (2010) 75:H49–53. doi: 10.1111/j.1750-3841.2009.01434.x

76. Feng P, Li Q, Liu L, Wang S, Wu Z, Tao Y, et al. Crocetin prolongs recovery period of DSS-induced colitis via altering intestinal microbiome and increasing intestinal permeability. *Int J Mol Sci*. (2022) 23:3832. doi: 10.3390/ijms23073832

77. Zhu Y, Chen B, Zhang X, Akbar MT, Wu T, Zhang Y, et al. Exploration of the Muribaculaceae family in the gut microbiota: diversity, metabolism, and function. *Nutrients*. (2024) 16:2660. doi: 10.3390/nu16162660

78. Liang C, Zhou XH, Jiao YH, Guo MJ, Meng L, Gong PM, et al. Ligilactobacillus Salivarius LCK11 prevents obesity by promoting PYY secretion to inhibit appetite and regulating gut microbiota in C57BL/6J mice. *Mol Nutr Food Res*. (2021) 65:e2100136. doi: 10.1002/mnfr.202100136

79. Wei B, Peng Z, Xiao M, Huang T, Yang S, Liu K, et al. Modulation of the microbiome-fat-liver axis by lactic acid bacteria: a potential alleviated role in high-fat-diet-induced obese mice. *J Agric Food Chem*. (2023) 71:10361–74. doi: 10.1021/acs.jafc.3c03149

80. Leung H, Long X, Ni Y, Qian L, Nychas E, Siliceo SL, et al. Risk assessment with gut microbiome and metabolite markers in NAFLD development. *Sci Transl Med*. (2022) 14:eabk0855. doi: 10.1126/scitranslmed.abk0855

81. Kuang J, Wang J, Li Y, Li M, Zhao M, Ge K, et al. Hyodeoxycholic acid alleviates non-alcoholic fatty liver disease through modulating the gut-liver axis. *Cell Metab*. (2023) 35:1752–66.e8. doi: 10.1016/j.cmet.2023.07.011

82. Han Y, Ling Q, Wu L, Wang X, Wang Z, Chen J, et al. *Akkermansia muciniphila* inhibits nonalcoholic steatohepatitis by orchestrating TLR2-activated γδT17 cell and macrophage polarization. *Gut Microbes*. (2023) 15:2221485. doi: 10.1080/19490976.2023.2221485

83. Lin J, Zhang R, Liu H, Zhu Y, Dong N, Qu Q, et al. Multi-omics analysis of the biological mechanism of the pathogenesis of non-alcoholic fatty liver disease. *Front Microbiol*. (2024) 15:1379064. doi: 10.3389/fmicb.2024.1379064

84. Liu Y, Chen H, Wang J, Zhou W, Sun R, Xia M. Association of serum retinoic acid with hepatic steatosis and liver injury in nonalcoholic fatty liver disease. *Am J Clin Nutr*. (2015) 102:130–7. doi: 10.3945/ajcn.114.105155

85. Zhu S, Zhang J, Zhu D, Jiang X, Wei L, Wang W, et al. Adipose tissue plays a major role in retinoic acid-mediated metabolic homoeostasis. *Adipocytes*. (2022) 11:47–55. doi: 10.1080/21623945.2021.2015864

86. Geng C, Xu H, Zhang Y, Gao Y, Li M, Liu X, et al. Retinoic acid ameliorates high-fat diet-induced liver steatosis through sirt1. *Sci China Life Sci*. (2017) 60:1234–41. doi: 10.1007/s11427-016-9027-6

87. Liu Z, Li P, Zhao ZH, Zhang Y, Ma ZM, Wang SX. Vitamin B6 prevents endothelial dysfunction, insulin resistance, and hepatic lipid accumulation in apoe (−/−) mice fed with high-fat diet. *J Diabetes Res*. (2016) 2016:1748065. doi: 10.1155/2016/1748065

88. Reeve EH, Kronquist EK, Wolf JR, Lee B, Khurana A, Pham H, et al. Pyridoxamine treatment ameliorates large artery stiffening and cerebral artery endothelial dysfunction in old mice. *J Cereb Blood Flow Metab*. (2023) 43:281–95. doi: 10.1177/0271678X221130124

89. Pereira E, Silvares RR, Rodrigues KL, Flores E, Daliry A. Pyridoxamine and caloric restriction improve metabolic and microcirculatory abnormalities in rats with non-alcoholic fatty liver disease. *J Vasc Res*. (2021) 58:1–10. doi: 10.1159/000512832

90. Pereira E, Silvares RR, Flores E, Rodrigues KL, Daliry A. Pyridoxamine improves metabolic and microcirculatory complications associated with nonalcoholic fatty liver disease. *Microcirculation*. (2020) 27:e12603. doi: 10.1111/micc.12603

91. Quist-Paulsen P. Statins and inflammation: an update. *Curr Opin Cardiol*. (2010) 25:399–405. doi: 10.1097/HCO.0b013e3283398e53

92. Satny M, Hubacek JA, Vrablik M. Statins and inflammation. *Curr Atheroscler Rep*. (2021) 23:80. doi: 10.1007/s11883-021-00977-6

93. Kitsugi K, Noritake H, Matsumoto M, Hanaoka T, Umemura M, Yamashita M, et al. Simvastatin inhibits hepatic stellate cells activation by regulating the ferroptosis signaling pathway. *Biochim Biophys Acta Mol basis Dis*. (2023) 1869:166750. doi: 10.1016/j.bbadis.2023.166750

94. Khan IM, Gjuka D, Jiao J, Song X, Wang Y, Wang J, et al. A novel biomarker panel for the early detection and risk assessment of hepatocellular carcinoma in patients with cirrhosis. *Cancer Prev Res (Phila)*. (2021) 14:667–74. doi: 10.1158/1940-6207.CAPR-20-0600

95. Tanaka N, Sano K, Horiuchi A, Tanaka E, Kiyosawa K, Aoyama T. Highly purified eicosapentaenoic acid treatment improves nonalcoholic steatohepatitis. *J Clin Gastroenterol*. (2008) 42:413–8. doi: 10.1097/MCG.0b013e31815591aa

frontiers | Frontiers in Nutrition

TYPE Original Research
PUBLISHED 02 June 2025
DOI 10.3389/fnut.2025.1580684

Check for updates

OPEN ACCESS

EDITED BY
Pedzisai Makoni,
Sefako Makgatho Health Sciences University, South Africa

REVIEWED BY
Kah Hui Yap,
Thomson Hospital, Malaysia
Anqi Chen,
Jiangnan University, China
Shun-ichi Wada,
Institute of Microbial Chemistry (IMC), Japan
Tianlin Wang,
Henan Agricultural University, China

*CORRESPONDENCE
Babak Razani
✉ brazani@pitt.edu

RECEIVED 20 February 2025
ACCEPTED 15 May 2025
PUBLISHED 02 June 2025

CITATION
Yeh Y-S, Evans TD, Jeong S-J, Liu Z, Ajam A, Cosme C Jr, Huang J, Peroumal D, Zhang X, Javaheri A, Cho J, Lodhi IJ and Razani B (2025) Assessing the efficacy of the natural disaccharide trehalose in ameliorating diet-induced obesity and metabolic dysfunction.
Front. Nutr. 12:1580684.
doi: 10.3389/fnut.2025.1580684

COPYRIGHT
© 2025 Yeh, Evans, Jeong, Liu, Ajam, Cosme, Huang, Peroumal, Zhang, Javaheri, Cho, Lodhi and Razani. This is an open-access article distributed under the terms of the Creative Commons Attribution License (CC BY). The use, distribution or reproduction in other forums is permitted, provided the original author(s) and the copyright owner(s) are credited and that the original publication in this journal is cited, in accordance with accepted academic practice. No use, distribution or reproduction is permitted which does not comply with these terms.

Assessing the efficacy of the natural disaccharide trehalose in ameliorating diet-induced obesity and metabolic dysfunction

Yu-Sheng Yeh[1,2], Trent D. Evans[3], Se-Jin Jeong[3], Ziyang Liu[1,2], Ali Ajam[1,2], Carlos Cosme Jr.[1], Jun Huang[1], Doureradjou Peroumal[1,2], Xiangyu Zhang[1,2], Ali Javaheri[3], Jaehyung Cho[4], Irfan J. Lodhi[5] and Babak Razani[1,2]*

[1]Department of Medicine, Vascular Medicine Institute, University of Pittsburgh School of Medicine and UPMC, Pittsburgh, PA, United States, [2]Pittsburgh VA Medical Center, Pittsburgh, PA, United States, [3]Cardiovascular Division, Department of Medicine, Washington University School of Medicine, St. Louis, MO, United States, [4]Division of Hematology, Department of Medicine, Washington University School of Medicine, St. Louis, MO, United States, [5]Division of Endocrinology, Metabolism, and Lipid Research, Department of Medicine, Washington University School of Medicine, St. Louis, MO, United States

Trehalose is a naturally occurring disaccharide with versatile commercial applications and health benefits, including promise as a therapeutic for obesity and diabetes. Although numerous previous reports purport the therapeutic uses of orally ingested trehalose, the abundance of glycosidases in the gastrointestinal tract suggest the potential for significant limitations of oral trehalose that have not been addressed. We first fed mice a high-fat diet (HFD) while providing trehalose by both oral and intraperitoneal routes. This combined strategy was broadly efficacious in reversing HFD-induced weight gain, fat mass, insulin resistance, and the development of hepatosteatosis. In contrast, oral-only trehalose failed to improve HFD-induced obesity and insulin resistance. This was due to trehalase (Treh)-mediated metabolism as blood trehalose levels remained low despite a significant rise in glucose. We next developed systemically deficient Trehalase (Treh-KO) mice to enhance the efficacy of trehalose. Surprisingly, oral trehalose therapy could not be facilitated resulting in neither an increase in serum trehalose levels nor metabolic benefits. Parenteral trehalose resulted in higher trehalose levels with lower serum glucose in Treh-KO mice, yet no additive metabolic benefits were observed. Overall, our findings still support a therapeutic role for trehalose in obesity and metabolic disease but with practical limitations in its delivery by oral route.

KEYWORDS

trehalose, obesity, insulin resistance, hepatosteatosis, trehalase, oral vs. parenteral

Introduction

Western diets and increasingly sedentary lifestyles have contributed significantly to the growing rate of obesity over the last several decades (1). Obesity is simply defined as the over-accumulation of fat in white adipose tissue (WAT) due to an increase in the ratio of energy intake to energy expenditure (2). However, accumulating evidence has shown that adipose tissue is not a simple, dormant site of energy storage but a dynamic metabolic organ that secretes a large number of factors, such as lipids and cytokines (i.e., adipokines), with hormonal, autocrine, and paracrine properties (3, 4). Adipose tissue is therefore thought to actively participate in the modulation of systemic metabolic homeostasis, and adipose tissue

dysfunction is believed to be a major culprit for obesity-related metabolic diseases, such as insulin resistance and fatty liver disease (3).

Dietary and lifestyle changes such as consuming balanced diet low in saturated fats and high in complex carbohydrates are considered the most effective means of reducing obesity, yet obesity remains a major health epidemic, especially when considering its burgeoning comorbidities in conjunction. There are various anti-obesity medications available including the popular GLP-1 receptor agonists which are appetite suppressants leading to reduced caloric intake, but these are accompanied by adverse side effects which can curtail their long-term use (5–7). Natural anti-obesity agents are always an attractive alternative which raise the prospect of trehalose with several proposed benefits in obesity and the metabolic syndrome.

Trehalose is a disaccharide produced naturally by a wide variety of plants, insects, and microorganisms such as bacteria, yeast, and fungi, and synthesized commercially as a sweetener and preservative (8). Trehalose is composed of two glucose molecules linked by a unique α,α-1,1-glycosidic bond which provides it exceptional stability under a wide range of conditions, including high temperatures, low pH, and freezing temperatures. It is notable that in nature trehalose acts as a protective agent against stress, allowing microorganisms to survive in adverse conditions, such as desiccation, heat, or cold. Although trehalose is not able to be synthesized in vertebrates (9), accumulating data indicate that it acts as a functional molecular compound to modulate metabolic and cellular processes in mammals, including humans. The abundance of trehalase in the GI tract allows its enzymatic hydrolysis into glucose as an obvious source of carbon. However, in an intact form, its structural properties might contribute to the ability of trehalose to alter the gut microbiome (10) and alter glucose homeostasis (11).

Much of the excitement for the therapeutic impact of trehalose in various chronic diseases lies in its ability to induce autophagy and in turn reduce the burden of cytotoxic protein aggregates. Trehalose has been proposed as a therapy for neurodegenerative diseases (12) with a significant burden of protein aggregation such as Parkinson's Disease (13), Alzheimer's Disease (14), and Huntington Disease (15), as well as cardiovascular disease, including atherosclerosis (16, 17), and hypertension (18). Although the mechanisms remain unclear including whether autophagy is primarily involved, several studies have shown that trehalose also improves metabolic health including dyslipidemia, obesity, diabetes, and fatty liver disease. For example, oral trehalose treatment reverses plasma insulin levels and homeostasis model assessment-insulin resistance (HOMA-IR) in mice fed a high-fat diet (HFD) (19), whereas intraperitoneal injection (i.p.) ameliorates insulin resistance in ob/ob mice (20). Similar results were obtained using a mouse model of established obesity (21). Reduced adipocyte size with enhanced thermogenic brown fat markers in WAT have also been reported (19, 21, 22). Trehalose treatment also improves hepatic steatosis including reduced accumulation of lipid droplets in hepatocytes (23). Similarly, db/db mice treated with trehalose exhibited decreased lipid inclusions in the liver accompanied by an increase in glycogen content (24). Trehalose supplementation has been shown to reduce hepatic endoplasmic reticulum stress and inflammatory signaling in aged mice (25). Collectively, these studies strongly support trehalose as a therapeutic candidate for the prevention and possible reversal of obesity-associated metabolic disorders.

An outstanding issue in the practical therapeutic use of trehalose in metabolic disease is the lack of consensus regarding trehalose dosage, administration route, or treatment time course. The presence of trehalase in the GI tract would suggest that absorption of trehalose should be compromised, albeit many studies report positive findings with oral-only trehalose formulations without taking into account confounding effects on microbiota or osmotic effects in the GI tract. In the current study, we aimed to definitively study the efficacy of trehalose in obesity and metabolic disease while taking into account both the route of administration and the oft neglected role for trehalase. We develop and characterize Trehalase-deficient mice (Treh-KO) both at baseline and in the context of trehalose under HFD condition. Our findings that an oral route of trehalose administration as well as inhibition of trehalase are ineffective in mitigating diet-induced obesity and metabolic disease should provide clarity for the field.

Results

Trehalose treatment reduces high fat diet-induced obesity

We previously demonstrated that the combination of oral and intraperitoneal (i.p.) administration of trehalose is atheroprotective in mice fed a western diet (40% high-fat diet, HFD) (26). To investigate the effects of trehalose on obesity and other metabolic parameters, 8-week-old C57BL/6 J mice fed a HFD received i.p. administration (3 g/Kg body weight) of trehalose 3 times per week, along with drinking water supplemented with 3% trehalose. Control mice received the equivalent co-administered doses of either saline or sucrose, a similarly structured non-reducing disaccharide composed of glucose and fructose (Figure 1A). HFD-induced body weight gain was significantly suppressed after 12–16 weeks of trehalose administration, in contrast to the sucrose-treated group, which was indistinguishable from the saline control (Figure 1B). Additionally, the trehalose group showed an overall significantly lower fat mass compared to controls without a reduction in lean mass (Figure 1C). Inguinal WAT (iWAT) weight was similarly reduced only in trehalose treated mice (Figure 1D). There were no changes in body weight, fat mass, and adipose tissue weight with saline or sucrose treatments for the same time course (Figures 1B–D).

To examine functional duration and efficacy of treatment, mice were fed a HFD for 4 months (4 M) and co-administrated trehalose by i.p. (3 g/Kg body weight) and in drinking water (3%) 3 times per week for a total treatment time of 3 M, 2 M, or 1 M after HFD feeding as compared with an un-treated HFD group denoted as 0 M (Figure 1E). The trehalose 3 M-treated group, but not 1 M and 2 M groups, exhibited a dramatic decrease in HFD-induced body weight gain (Figure 1F). Although no significance was noticed in the iWAT weight, the epididymal WAT (eWAT) weight was significantly reduced in the 3 M group, compared to that in the 0 M control group (Figure 1G), indicating an effective intervention period requires sustained exposure to trehalose.

Trehalose ameliorates high fat diet-induced insulin resistance and hepatic lipid accumulation

To investigate whether trehalose modulates HFD-associated metabolic parameters, we measured the levels of serum glucose, triglyceride, free fatty acid, and cholesterol after co-administration of

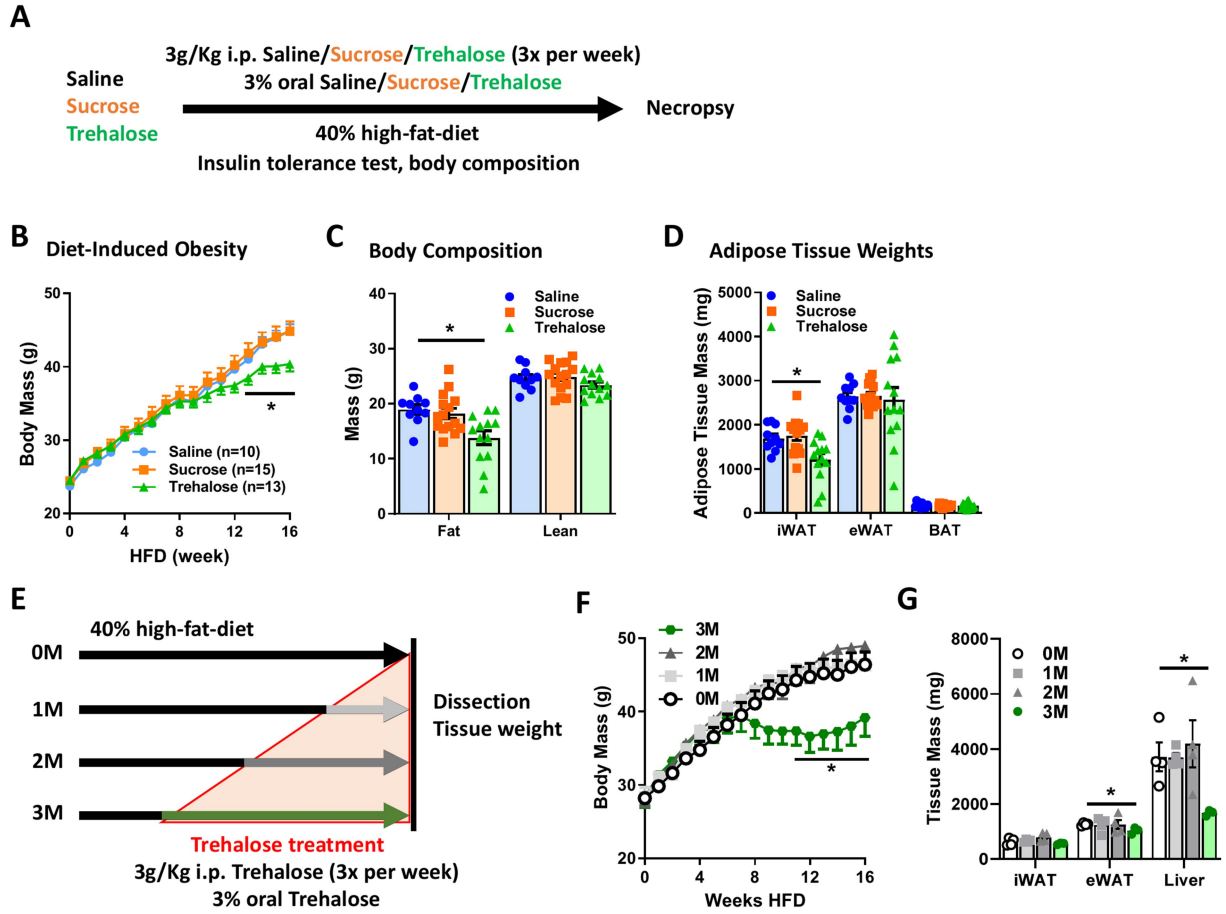

FIGURE 1
Combination of oral and intraperitoneal trehalose treatment abrogates high-fat diet-induced obesity. **(A)** Schematic process of trehalose or sucrose intervention experiment. The mice were treated with saline, sucrose, or trehalose by injecting intraperitoneally (3 times per week) and as a supplement to drinking water. **(B)** Body weight gain, **(C)** body composition, and **(D)** iWAT, eWAT, and BAT weights of mice treated with saline (n = 10), sucrose (n = 15), or trehalose (n = 13) under HFD condition were measured after 16 weeks of HFD feeding. **(E)** Schematic illustration of trehalose treatment time course experiment. The mice were fed HFD for 16 weeks, during which time mice also received trehalose for 0, 1, 2, or 3 months (0 M, 1 M, 2 M or 3 M) both orally and intraperitoneally. **(F)** Body weight variation, and **(G)** Tissue mass of iWAT, eWAT, and liver in the mice after 16 weeks of HFD treatment, along with trehalose added to drinking water for 0 M, 1 M, 2 M, and 3 M (n = 4). All mice were male and fed HFD. Values are presented as mean ± SE. Significant differences were determined by Student's t-test, with comparison to Saline or 0 M group: $^*p < 0.05$.

trehalose for 4 M. Although trehalose reduced HFD-induced weight gain (Figures 1B–D), no significant changes were found in the evaluated serum metabolites (Figure 2A). However, insulin tolerance testing (ITT) revealed significantly decreased blood glucose levels at 30 and 60 min after insulin administration in the trehalose group, compared with saline and sucrose control groups (Figure 2B), suggesting enhanced insulin sensitivity with trehalose treatment concomitant with the observed reductions in body weight and adiposity.

We also noticed a significant decrease in the liver weight in the trehalose group (Figure 2C). Given obesity and adipose tissue dysfunction lead to ectopic lipid accumulation in lean organs such as liver (27), we suspected the effect of trehalose on the liver might be due to lower hepatic lipid accumulation. To confirm this, the degree of hepatic lipid accumulation was quantified biochemically and by histological analysis. As shown in Figure 2D, trehalose treatment reduced hepatic lipid content by ~40%, compared with saline or sucrose treatments. Similarly, there were marked reductions in lipid droplet accumulation in hematoxylin and eosin (H&E)-stained liver sections from trehalose-treated mice (Figure 2E), indicating the ability of trehalose to reduce overall hepatic lipid burden instigated by HFD feeding. It should be noted that trehalose treatment did not result in significant changes in the expression of genes related to either adipose tissue browning, mitochondrial lipid metabolism, or the autophagy-lysosomal system (Supplementary Figure S1). Although transcriptional effects were not noted to be relevant to trehalose function, this does not preclude direct effects on autophagy and the lysosomal system as has been previously reported (16, 28).

Oral trehalose is therapeutically ineffective in ameliorating obesity and insulin resistance

Although oral-only and i.p.-only trehalose treatments have been independently reported to have metabolic benefits (20, 21), relative contributions of each to its metabolic efficacy remain unknown. We thus examined each trehalose treatment route individually, beginning with oral-only administration in drinking water (3% w/v) with HFD for

10.3389/fnut.2025.1580684

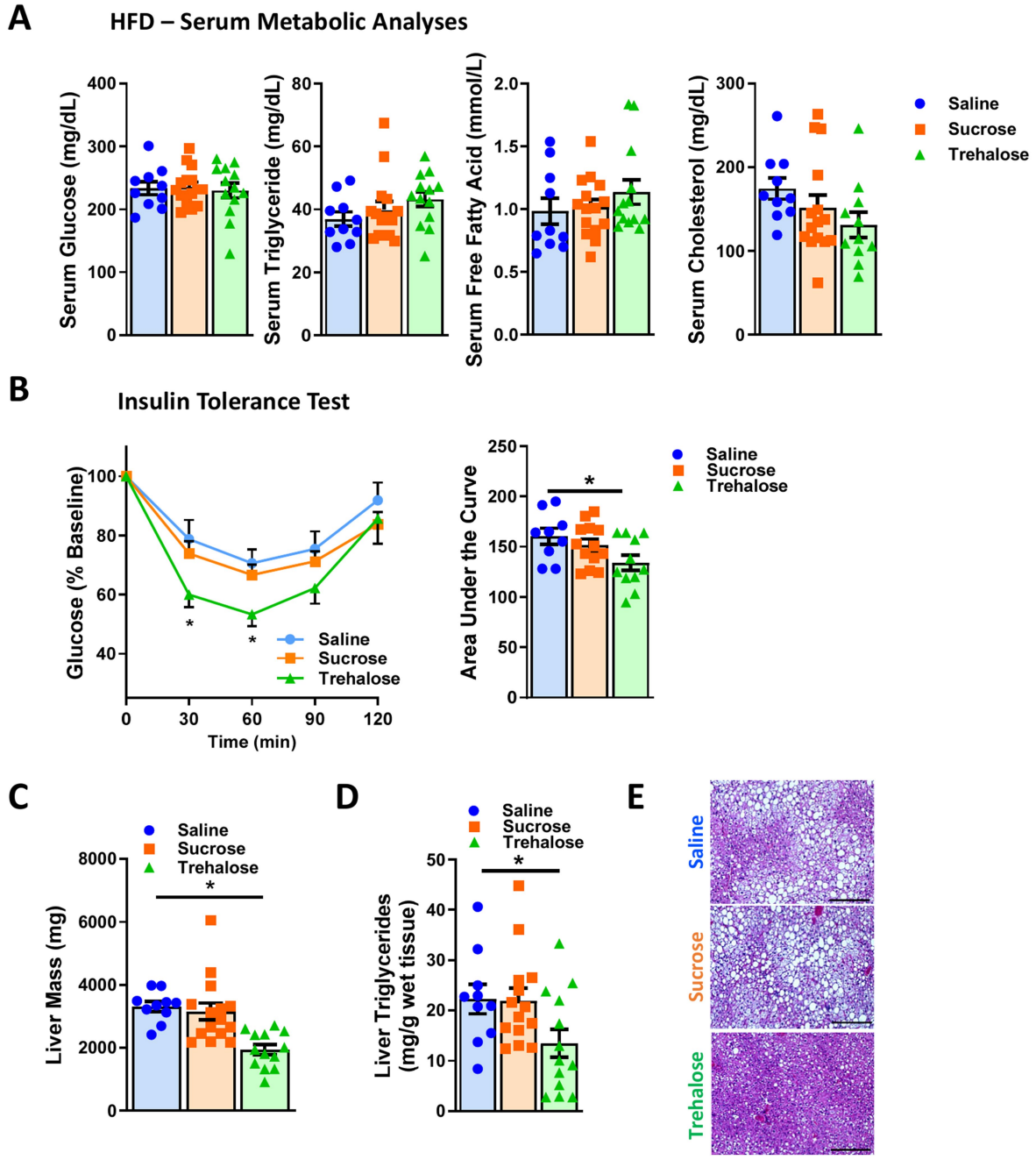

FIGURE 2
Combination of oral and intraperitoneal trehalose treatment improved high-fat diet-induced insulin resistance and fatty liver. **(A)** Serum glucose, triglyceride, free fatty acid, and cholesterol levels of mice receiving saline (n = 10), sucrose (n = 15), or trehalose (n = 13) were measured at 16 weeks of HFD feeding. **(B)** Insulin tolerance test was performed at 15 weeks of HFD-fed mice treated with saline (n = 10), sucrose (n = 15), or trehalose (n = 13). Results were shown as a time-dependent graph (left panel) or as the area (%*min) under the curve (right panel). **(C)** Liver mass, **(D)** triglyceride content, and **(E)** histological analysis with H&E staining were performed. Liver samples from 16 weeks HFD-fed mice treated with saline (n = 10), sucrose (n = 15), or trehalose (n = 13). Scale bars, 200 μm. All mice were male and fed HFD. Values are presented as mean ± SE. Significant differences were determined by Student's t-test, as compared with Saline group: *$p < 0.05$.

16 weeks (Figure 3A). Body weight gain was slightly lower in oral trehalose-treated mice, but this difference was insignificant compared with control animals (Figure 3B). Likewise, there was no change in body composition (Figure 3C), nor in tissue mass including iWAT, eWAT, or liver between controls and the oral trehalose-treated group (Figure 3D). Oral trehalose treatment also had no effect on insulin sensitivity as gaged by similar glucose levels after an ITT assay (Figure 3E).

Oral trehalose treatment has negligible effects on circulating trehalose levels

To ascertain whether the lack of effectiveness for oral trehalose against obesity and metabolic dysfunction is due to low absorption or high catabolic rate, we performed a trehalose tolerance test to compare blood trehalose levels between oral and i.p. trehalose administration.

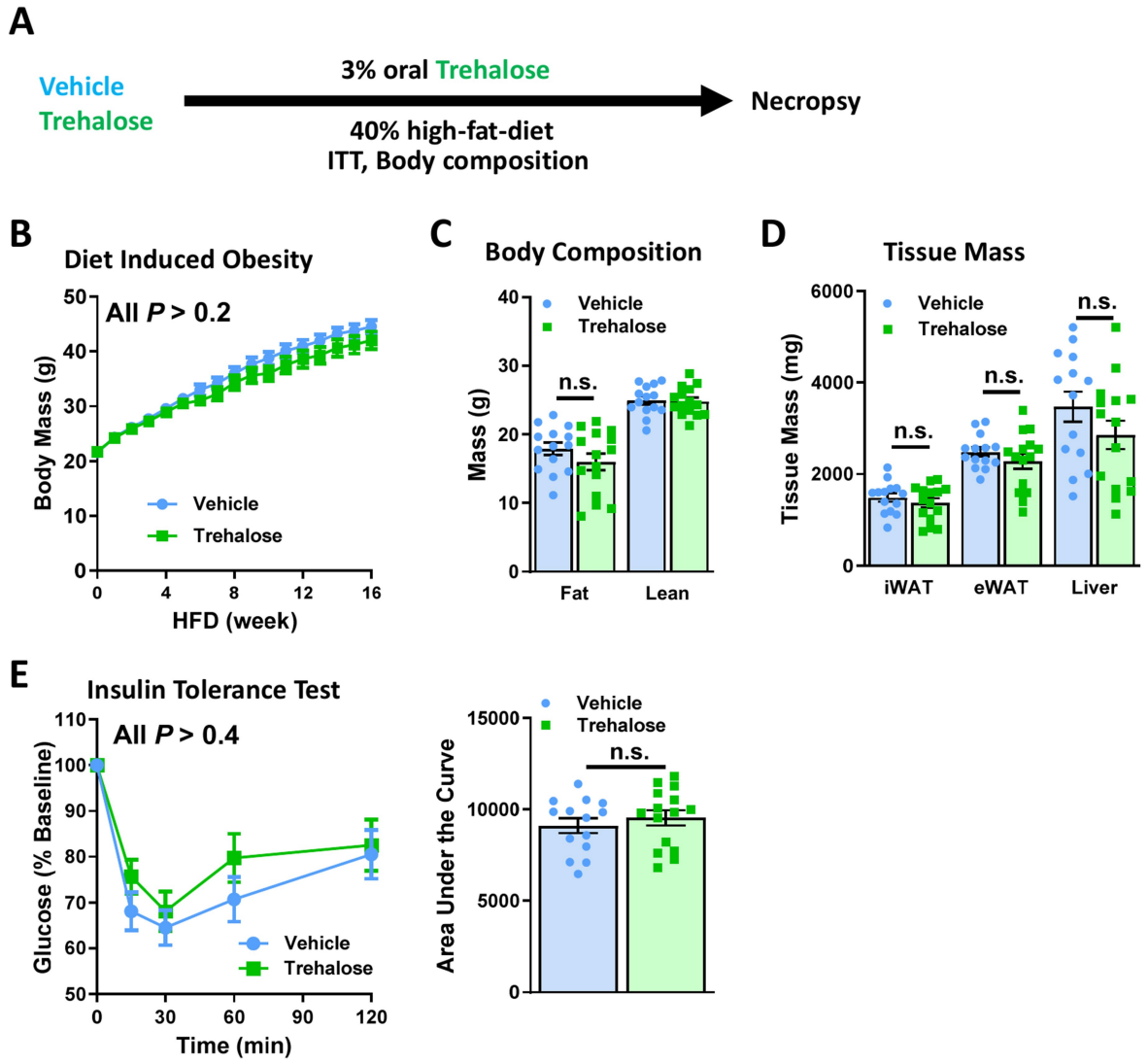

FIGURE 3
Oral trehalose is therapeutically ineffective. **(A)** Schematic representation of trehalose or vehicle intervention experiment. Treatments were provided as supplementation to drinking water. **(B)** Body weights were measured in mice provided drinking water with or without 3% w/v trehalose (n = 15). **(C)** Body composition, and **(D)** tissue weights of iWAT, eWAT, and liver were measured after 16 weeks of HFD feeding with or without 3% w/v trehalose as a supplement in drinking water (n = 15). **(E)** Insulin tolerance test was performed at 15 weeks HFD-fed mice treated with or without 3% w/v trehalose, provided as a supplement in drinking water (n = 15). Results were shown as a time-dependent graph (left panel) or as the area (%*min) under the curve (right panel). All mice were male and fed HFD. Values are presented as mean ± SE.

Interestingly, serum trehalose was enhanced to ~400 mg/dL at 30 min after i.p. trehalose administration and decreased gradually in a time-dependent manner (Figure 4A). However, oral trehalose failed to elevate serum trehalose levels (Figure 4A), suggesting that trehalose does not enter the bloodstream, possibly because it is hydrolyzed by trehalase (Treh) into its two component glucose molecules in the gastrointestinal tract (Figure 4B). This was corroborated by portal vein sampling in conjunction with assessment of serum glucose and trehalose levels upon oral trehalose administration. Whereas serum glucose rises significantly after 30 min of trehalose ingestion, a minimal rise in portal vein levels of trehalose is observed indicating near complete trehalose hydrolysis in the intestine (Figure 4C).

To determine the plausibility of these two possibilities, we next measured expression and activity levels of Treh in several tissues, including the duodenum (the absorptive portion of the intestine). We found that Treh was highly expressed in the duodenum and kidney, but was not detectable in colon, liver, or quadriceps (Figure 4D). The duodenum also had the highest Treh enzymatic activity among the evaluated tissues (Figure 4E), consistent with the possibility that higher catabolism of trehalose in the intestine accounts for lower observed blood levels of trehalose. To determine whether trehalose might indeed be degraded in orally treated mice, blood glucose levels were monitored during the trehalose tolerance test. In contrast to mice administered trehalose by i.p., which had only 1.7-fold increase in blood glucose levels relative to baseline, glucose increased 3.6-fold in mice treated orally with trehalose (Figure 4F), indicating more than twice as much enzymatic digestion prior to absorption.

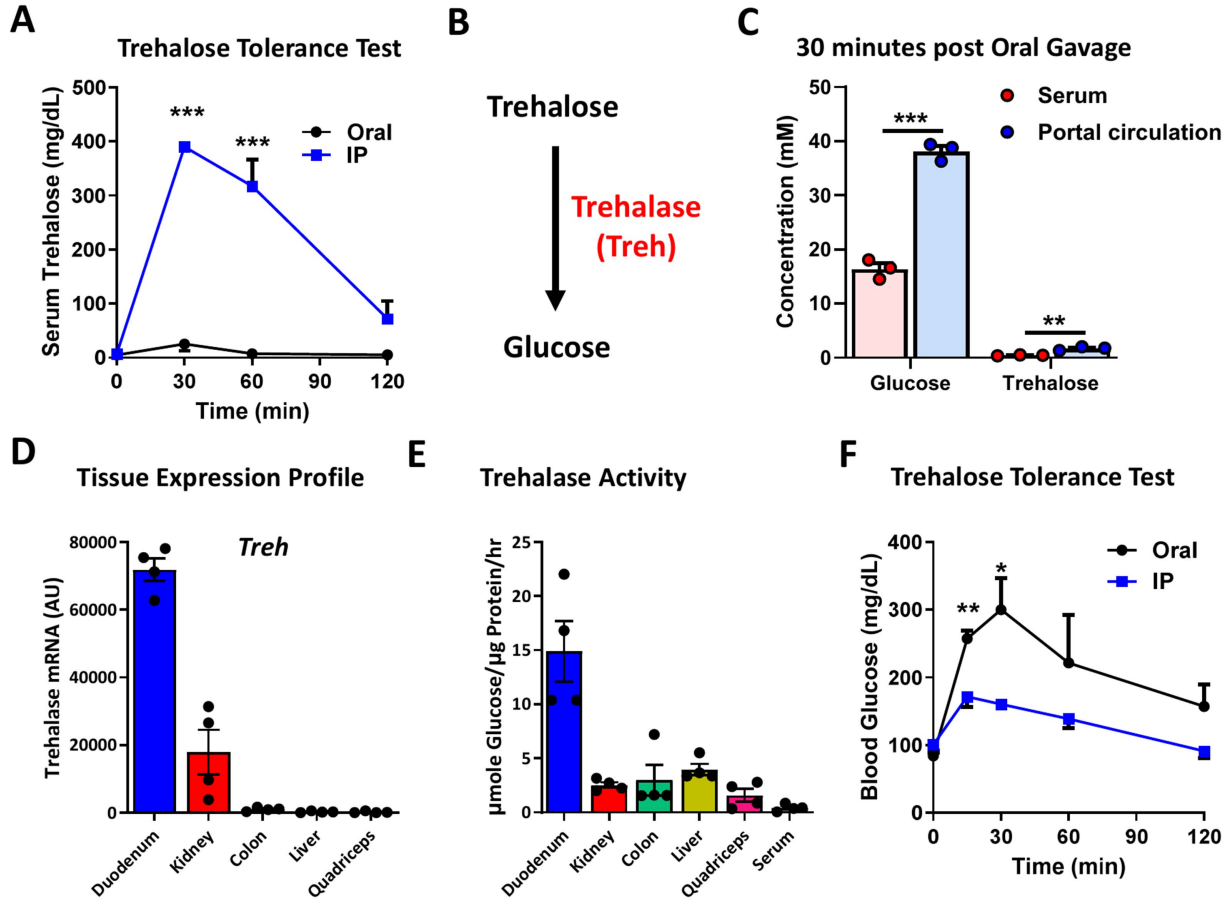

FIGURE 4
Oral trehalose treatment enhanced blood glucose level but only show a minor effect on serum trehalose. **(A)** Trehalose tolerance test was performed based on oral (Oral) and intraperitoneal (IP) treatment (3 g/Kg body weight) and the serum trehalose level was measured at indicated time points (n = 4). **(B)** Schematic image of the metabolism of trehalose through trehalose (Treh) to glucose. **(C)** Glucose and trehalose levels were measured in serum and portal circulation 30 min after oral trehalose treatment (n = 3). **(D)** Tissue mRNA expression and **(E)** activity of Treh were measured in the duodenum, kidney, colon, liver, and quadriceps of 8-week-old male C57BL/6 J mice (n = 4). **(F)** Trehalose tolerance test was performed based on oral (Oral) and intraperitoneal (IP) treatment (3 g/Kg body weight) and the serum glucose level was measured at indicated time points (n = 4). All mice were male and fed a normal chow diet. Values are presented as mean ± SE. Significant differences were determined by Student's t-test compared with IP group: $^{*}p < 0.05$, $^{**}p < 0.01$, $^{***}p < 0.001$.

Mice with systemic trehalase deficiency have not metabolic defects at baseline

To determine whether suppression of trehalose catabolism could be a useful approach of maintaining elevated trehalose levels, a trehalose tolerance test was performed after pretreatment with Validamycin, a known Treh inhibitor (29). Enhancement of blood glucose levels in response to oral trehalose treatment was partially suppressed in the presence of Validamycin in a dose-dependent manner (Figure 5A), suggesting the utility of sustained Treh inhibition in achieving enhanced uptake and efficacy of trehalose *in vivo*.

We therefore engineered a mouse model with Treh deficiency via CRISPR/Cas9 (Figure 5B) by removal of a 13 bp region within exon 8 of the Treh gene (Figure 5B). To confirm whether Treh expression was successfully disrupted in homozygous Treh knockout (KO) mice, transcriptional and protein expression of Treh in kidney and duodenum were measured by qPCR and Western blotting, respectively. As shown in Figure 5C, mRNA levels of *Treh* were suppressed ~90% in Treh KO kidney and duodenum tissues, compared with those from the wildtype (WT) group. Protein levels of Treh in the KO group were likewise nearly undetectable in both tissues (Figure 5D), suggesting that a systemic Treh-disrupted mouse model was successfully established. In 8-week-old adult mice, no body weight differences were noted (Figure 5E). Serum glucose, triglyceride, free fatty acid, and cholesterol levels were also similar between WT and Treh KO groups (Figure 5F).

Systemic trehalase deficiency does not improve the negligible rise of circulating trehalose in mice treated by oral administration

To determine the effect of trehalase deficiency on the kinetics of serum trehalose and glucose, Treh KO mice and WT controls were administered trehalose either by i.p. (3 g/kg) or oral routes (3 g/kg) and trehalose tolerance tests performed (Figure 6A). Similar to the results shown in Figure 4F, i.p. trehalose treatment increased serum glucose levels 1.8-fold in the WT group but only

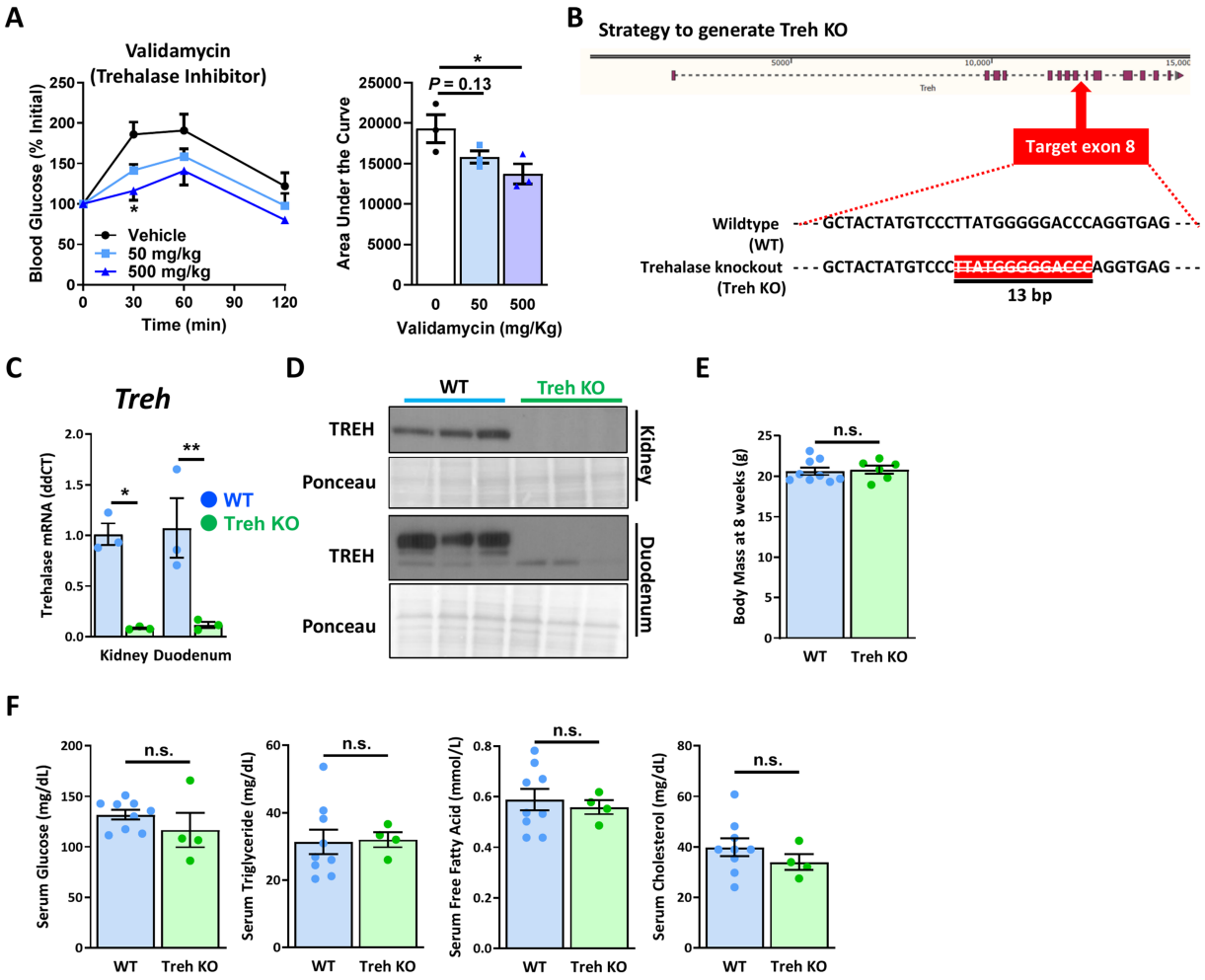

FIGURE 5
Systemic trehalase-deficient mice showed no metabolic changes at baseline. **(A)** Indicated dose of validamycin (Trehehalase inhibitor) was used for mice treated with trehalose (3 g/Kg body weight), after 6 h fasting. Blood glucose levels were measured at indicated time points (left panel), and area under the curve (%*min) was calculated (right panel) (n = 3). **(B)** Illustration of strategy used to establish a systemic trehalase (Treh) knockout (Treh KO) mouse model. Treh DNA genotyping was performed on mouse tail clippings from heterozygous (Het), wildtype (WT) and Treh KO mice (Embedded panel). **(C)** mRNA and **(D)** protein expression levels of Treh in the kidney and duodenum of 8-week-old WT and Treh KO male mice (n = 3). **(E)** Body weight, and **(F)** serum glucose, triglyceride, free fatty acid, and cholesterol levels were measured in 8-week-old female WT (n = 9) and Treh KO (n = 6) mice. All mice were fed a normal chow diet. Values are presented as mean ± SE. Significant differences were determined by Student's t-test in comparison with vehicle or WT group: $^*p < 0.05$, $^{**}p < 0.01$.

1.25-fold in Treh KO mice (Figure 6B). In orally treated WT mice, serum glucose levels were enhanced more than 3-fold, while only a minor rise was observed in the Treh KO group (Figure 6C). With regard to serum trehalose levels, the contrasts between the oral and parenteral routes were highly revealing. Serum trehalose levels were substantially increased in WT mice administered trehalose by i.p., and this effect was increased even further in Treh KO animals (Figure 6D). Serum trehalose WT group reached peak levels at 15 min and returned nearly to baseline by 120 min, whereas levels in the Treh KO group reached a peak at 30 min followed by a gradual decrease (Figure 6D), suggesting that Treh deficiency was efficacious in reducing trehalose clearance. In contrast to the efficacy seen with i.p. trehalose, serum levels of trehalose in mice treated orally were only negligibly altered for both WT and Treh KO groups, suggesting trehalose hydrolysis is not responsible for poor oral absorption (Figure 6B).

Systemic trehalase deficiency does not augment the metabolic benefits of parenteral trehalose in high fat diet-fed mice

Given the blunted serum trehalose clearance observed in Treh KO mice administered trehalose by i.p., we wondered whether increased trehalose levels in the setting of Treh deficiency might lead to enhanced metabolic benefits. WT and Treh KO mice were fed HFD while injected with trehalose (3 g/Kg body weight i.p., 3x/week) or vehicle control (Figure 7A). After 16 weeks of diet with and without concomitant trehalose, there were no notable differences in body weight, fat mass, or tissue mass, including iWAT, eWAT, and liver, between WT and Treh KO groups (Figures 7B–D). However, the previously demonstrated trehalose-mediated reduction in HFD-induced body weight gain (Figure 1B) was replicated (Figure 7B). The HFD-induced increases in fat mass in WT mice were also significantly reduced in the Trehalose i.p.

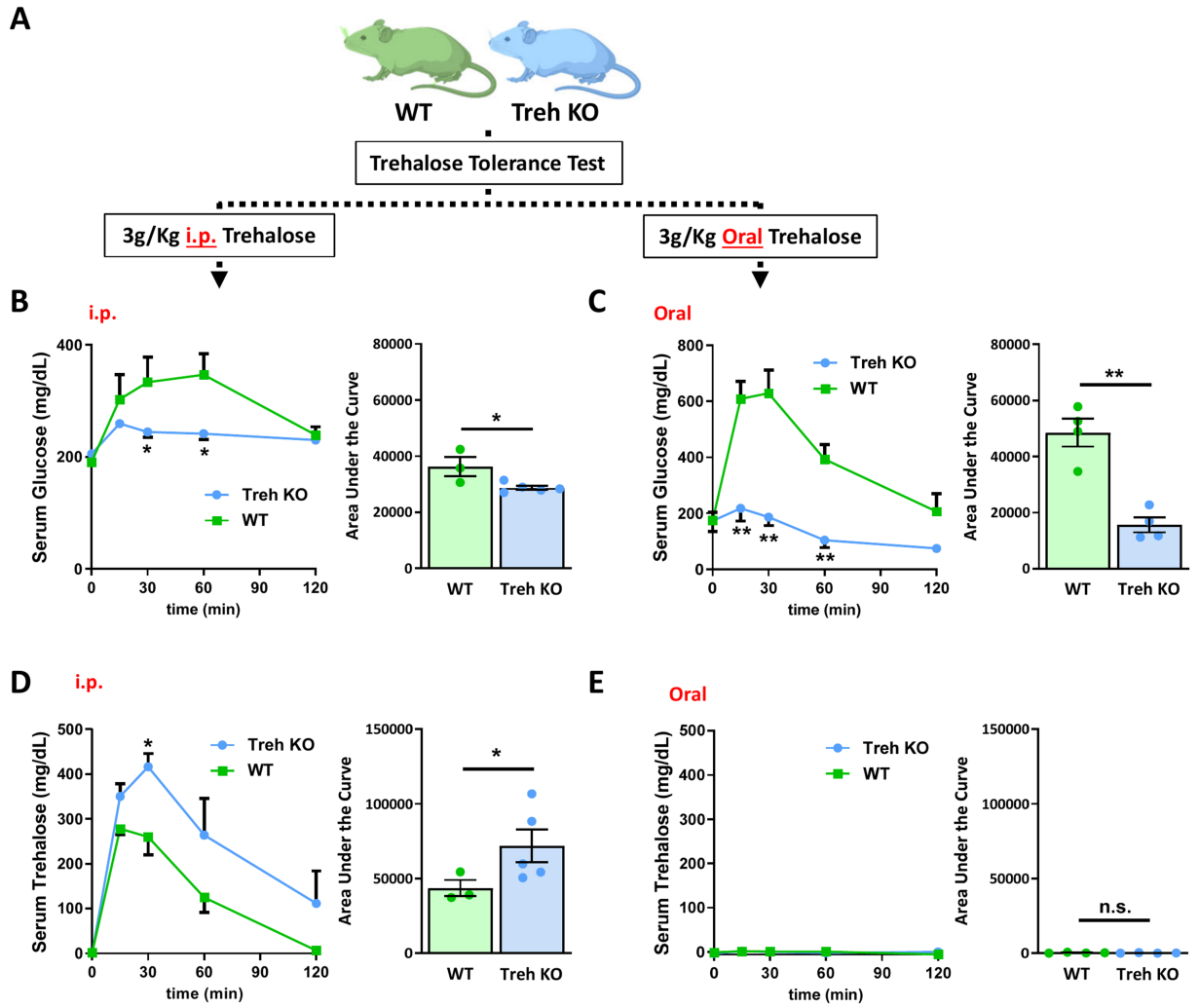

FIGURE 6
Systemic trehalase deficiency delayed serum trehalose clearance but did not improve trehalose oral absorption. **(A)** Schematic illustration of the experimental process employed. WT and Treh KO mice were tested for trehalose tolerance test after oral or i.p. trehalose administration. Serum glucose levels were quantified at indicated time points (left panel) after **(B)** i.p. (WT and Treh KO, n = 3 and 5) or **(C)** oral (n = 4) trehalose treatment (3 g/Kg body weight) and area under the curve calculated (mg/dL*min, right panel). Serum trehalose levels were quantified at indicated time points (left panel) after **(D)** i.p. (WT and Treh KO, n = 3 and 5) or **(E)** oral (n = 4) trehalose treatment (3 g/Kg body weight), and area under the curve calculated (mg/dL*min, right panel). All mice were male and fed a normal chow diet. Values are presented as mean ± SE. Significant differences were determined by Student's t-test, as compared with WT group: $*p < 0.05$, $**p < 0.01$.

group, compared with the Vehicle control group (Figures 7C,D). Although i.p. administration of trehalose elicited a similar anti-obesity effect in Treh KO mice, there was no significant difference between WT and Treh KO mice based on treatment (Figures 7B–D). Likewise, similar effects on blood glucose were observed for both WT and Treh KO mice, as demonstrated by equivalent percent glucose decline relative to baseline after insulin tolerance testing (Figure 7E). Overall, these data suggest that parenteral treatment of trehalose is effective against HFD-induced obesity although no additive metabolic benefits are realized in the setting of elevated trehalose levels from Treh inhibition.

Discussion

In the present study, we demonstrated that the putative anti-obesity disaccharide trehalose reduces body weight, fat mass, hepatic lipid accumulation, and insulin insensitivity in HFD-fed mice. Trehalose improved hepatic lipid accumulation with a decrease in liver weight, which is in line with previous studies showing positive effects of trehalose on hepatic lipid accumulation and stress (23–25). This evidence implies a possibility that the liver is the primary organ affected by trehalose, either directly or indirectly, which requires further study. We previously observed protection from atherosclerosis in mice via dual oral and i.p. trehalose treatment and found i.p. administration of trehalose leads to far greater elevations in serum trehalose relative to oral dosing without observable changes on either atherosclerosis or serum cholesterol (26). Sahebkar et al. similarly showed that i.p. trehalose treatment attenuates atherosclerosis in rabbits (17). Our data also confirmed that i.p. trehalose treatment is therapeutically effective against weight gain and insulin insensitivity, but strikingly that oral-only administration failed to rescue HFD-induced obesity and insulin resistance.

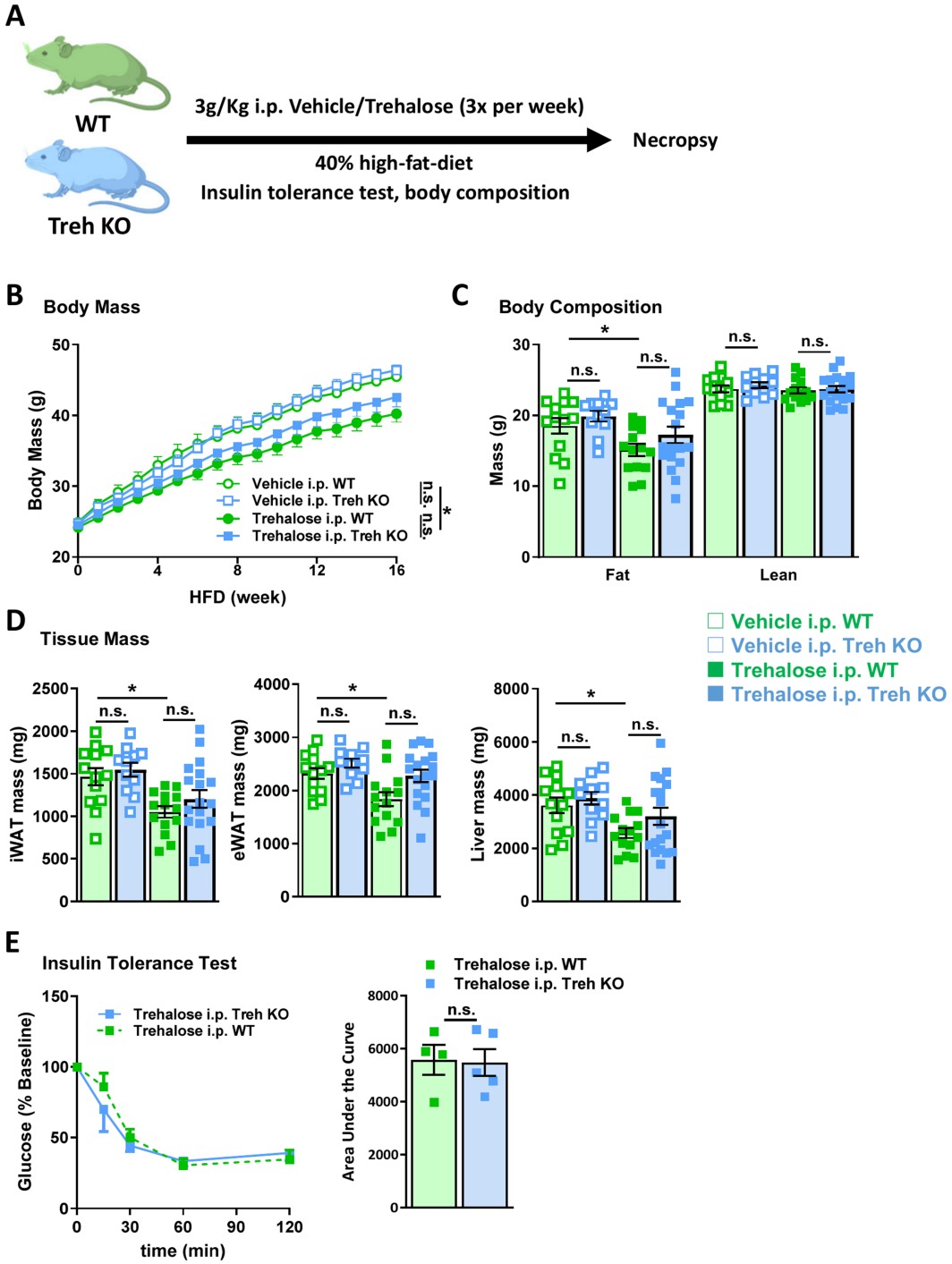

FIGURE 7
I.P. trehalose alone effectively reduced obesity and trehalase deficiency did not improve efficacy. **(A)** Schematic representation of trehalose or vehicle intervention experiment. WT and Treh KO mice were treated with vehicle or trehalose by i.p. injection. **(B)** Body weight, **(C)** body composition, and **(D)** tissue mass of iWAT (left panel), eWAT (middle panel), and liver (right panel) were measured in WT and Treh KO mice fed a HFD and treated by i.p. injection of trehalose or vehicle (3 g/Kg body weight, 3 times per week) for 16 weeks (Vehicle i.p. WT, Trehalose i.p. WT, Vehicle i.p. Treh KO, and Trehalose i.p. Treh KO, n = 13, 14, 11, and 18). **(E)** Insulin tolerance test was performed in WT (n = 4) and Treh KO (n = 5) mice i.p. injected with trehalose (3 g/Kg body weight, 3 times per week) for 15 weeks. Blood glucose level were measured at indicated time points (left panel), and area under the curve was calculated (mg/dL*min, right panel). All mice were male and fed HFD. Values are presented as mean ± SE. Significant differences were determined by Student's t-test compared with indicated groups: *$p < 0.05$.

Our results are surprising, because orally administered trehalose has been shown to exert significant biological effects in numerous mouse models of adiposity (19, 21, 22), hepatic steatosis/fat accumulation (23, 24), Alzheimer's and Parkinson's diseases (13, 30), and even kidney injury (31). We have compiled a large list of published references detailing the various diseases trehalose has

been proposed as a therapeutic strategy and the route of administration for these studies (Table 1). For instance, Arai et al. reported that oral trehalose administration functionally mitigates insulin resistance without affecting body weight (21), but we did not find a similar reduction in insulin resistance, suggesting that oral-only trehalose treatment does not provide a therapeutic benefit under high fat feeding conditions. One possible explanation for this discrepancy is variable experimental conditions, such as diet (e.g., 40% versus 56.7% HFD) or model (e.g., C57BL/6 J mouse versus db/db or ob/ob mouse, or rabbit). However, given that our current and previous data show an almost complete enterohepatic clearance for oral trehalose (26), its bioavailability via parenteral means is likely required to exert clinically important metabolic effects. Moreover, Yasugi et al. suggested that the use of trehalose as a nutrient by organisms was gained via adaption, secondary to trehalose's ability to contribute to glucose homeostasis by buffering circulating glucose levels, thereby imparting improved metabolism (32). Although this hypothesis is largely based on work done using *Drosophila*, which might not translate to mammals, it would be interesting to know alterations in circulating levels of trehalose in prior studies reporting the metabolic benefits observed with oral trehalose treatment. In all these studies, secondary effects from trehalose on the gastrointestinal tract including effects on gut microbiota may be operative.

Trehalose is a known nutrient for bacteria and in the could have functional consequences on microbiota which in turn would exert physiological and pathophysiological effects on organisms ingesting

TABLE 1 XXX.

Articles	Route	Model
Kaplon et al. (45)	PO	Human
Yoshizane et al. (46)	PO	Human
Yoshizane et al. (47)	PO	Human
Jamialahmadi et al. (48)	IV	Human
Hashemian et al. (49)	PO	Human
Rodríguez-Navarro et al. (50)	PO	Mouse
Castillo et al. (51)	IP	Mouse
Arai et al. (19)	PO	Mouse
Sarkar et al. (52)	PO	Mouse
Kim et al. (53)	IP	Mouse
Ferguson et al. (54)	PO	Mouse
Tanji et al. (55)	PO or IP	Mouse
Sergin et al. (26)	PO + IP	Mouse
Liu et al. (56)	PO	Mouse
Miyake et al. (57)	IP	Mouse
Liu et al. (58)	IP	Mouse
Zhu et al. (31)	IP	Mouse
Gong et al. (59)	PO	Mouse
Pradeloux et al. (60)	PO	Mouse
Yang et al. (61)	PO or PO + IP	Mouse
Lee et al. (62)	PO	Mouse
Forouzanfar et al. (63)	IP	Rat
Wang et al. (64)	PO	Rat

trehalose either as part of the diet or as an oral therapeutic. In this regard, contrary to what has been previously reported by others, our data show that metabolic benefits were only observed when trehalose was delivered by parenteral means (i.p. injection) and not by oral administration. Clearly more mechanistic studies are required to determine the underlying basis for trehalose's modulatory effects on metabolism in mammals, whether previously reported efficacy is dependent on increased blood trehalose levels, and most importantly whether trehalose directly or indirectly influences HFD-induced pathophysiology. Accumulative evidence indicates that trehalose can affect gut microbiota (10, 33, 34), which has been proposed to influence hepatic gene expression (34). This raises the possibility that some of the metabolic benefits attributable to trehalose might therefore be indirect.

It is notable that low serum trehalose levels coupled with high expression of Treh in the intestine would at least theoretically limit the effectiveness of oral treatment versus i.p. administration. One possibility for lack of effect when orally provided is that trehalose is enzymatically cleaved by trehalase in the intestine, where it is highly expressed (35), before entering the bloodstream. This theory is supported by our results showing higher blood glucose levels in mice treated orally with trehalose, compared to those receiving trehalose via i.p. injection (Figure 3). Ishihara and colleagues established a complete cDNA clone of human Treh and showed that Treh mRNA is highly expressed in the kidney, liver and small intestine in humans (36). Similarly, our current findings revealed that Treh is highly expressed in the kidney and duodenum of mice (Figure 4C), results that are identical to what was previously shown by Northern blot (35). Yu et al. reported an association between Treh genetic variance and serum trehalase levels in African Americans and that serum trehalose levels were significantly associated with glucose levels and increased risk of incident diabetes (37). Furthermore, it was recently reported that genetic variants in or near the TREH locus in Pima Indians are strongly associated with trehalase activity, and one of these variants is also reproducibly associated with type 2 diabetes (38).

Kamiya et al. suggested that Treh-deficient mice should be used to observe any physiologically relevant functions of trehalose based on the fact Treh KO abolishes oral trehalose treatment-induced blood glucose without affecting glucose tolerance (39). Our findings indicating that Treh KO boosted the serum trehalose levels via i.p. but not oral treatment (Figure 6) support this idea. However, we failed to find any advanced metabolic benefits due to i.p. trehalose treatment in Treh KO mice (Figure 7), which is similar to what was reported by the Arai group showing that Treh KO failed to boost the anti-obese effect brought by trehalose treatment (40). This evidence implies that systemic Treh is not a clinically appropriate target for treating obesity and related complications, but this does not exclude the possibility of potential metabolic benefits related to tissue-specific suppression of Treh, which should be further studied.

Several unanswered questions remain, particularly the mechanism of action of trehalose in the context of HFD-induced obesity. We previously demonstrate that trehalose triggers autophagy-lysosome biogenesis in macrophages (26) in response to low-grade lysosomal stress, via activation of transcription factor EB (TFEB) (41). This would stimulate a key cellular degradation system including lipid metabolism (via the autophagy of lipid droplets known as lipophagy and lipid hydrolysis in lysosomes). Zhu et al. similarly showed trehalose-mediated induction of TFEB transcriptional activity in a mouse model of acute kidney injury (31). In addition to TFEB activation, trehalose enhances adipocyte lysosomal activity and antioxidative responses via

the Sequestosome 1 (SQSTM1/p62)-activated nuclear factor erythroid-derived 2-like 2 (NRF2) (42). Similar findings were described in hepatoma cells, in which trehalose protected against oxidative stress via autophagy, which was regulated by the SQSTM1/p62- Kelch-like ECH-associated protein 1 (KEAP1)-NRF2 pathway (43). Moreover, trehalose can influence autophagy by inhibiting SLC2A family members, such as SLC2A2 and SLC2A8, through AMPK-mammalian target of rapamycin (mTOR) complex 1 (mTORC1) signaling pathway in hepatocytes (23). Although these accumulated reports emphasize an autophagy-dependent role of trehalose in several models, autophagy-independent mechanisms should also be investigated. For example, Pagliassottia et al. showed that trehalose reduces hepatic endoplasmic reticulum stress and inflammatory signaling via restoration of proteasome activity in aged mice (25). Additional mechanistic studies such as these would undoubtedly provide much needed insights into the perceived effects of trehalose on physiologically relevant metabolic homeostasis under basal versus pathological conditions.

Overall, our study shows that trehalose, a natural disaccharide, is a potential candidate for the treatment of HFD-induced obesity, including prevention of insulin resistance and fatty liver, but only when delivered parenterally. In fact, oral trehalose treatment was therapeutically ineffective, and absorption of trehalose could not be improved even in the absence of Treh. Although Treh KO suppressed serum trehalose clearance, it provided no additional anti-obesity benefits or insulin tolerance conferred by i.p. trehalose treatment. Our data provide valuable insight regarding the potential metabolic benefits of trehalose and its effective treatment route, which are especially applicable to its eventual usage clinically, as well as its current use as a supplement for a variety of commercial products.

Materials and methods

Animals

Animal protocols were approved by the University of Pittsburgh and Washington University Animal Studies Committees (IACUC 23032631 and 21–0163, respectively). Five-week-old C57BL/6 J male mice were purchased from the Jackson Laboratory (Bar Harbor, ME, United States). Unless otherwise stated, mice were housed at 23 ± 1°C and maintained on a 12-h light/dark cycle. For all experiments, mice were fed a commercial chow diet (Purina 5,053) until 8 weeks of age and then randomly divided into groups for the experiments.

Strategy and generation of trehalase KO mice

Trehalase (Treh) whole-body knockout mice were established by Genome Engineering &.

Stem Cell Center (McDonnell Genome Institute, Washington University School of Medicine, St. Louis, MO). Briefly, the CRISPR/Cas9 technique was used to target Treh exon 8, and a 13 bp sequence was successfully removed (Figure 5B). Heterozygous Treh knockout ($Treh^{+/-}$) mice were crossed to generate homozygous Treh knockout ($Treh^{-/-}$, Treh KO) mice. Mice without disrupted Treh ($Treh^{+/+}$) were considered as the wildtype (WT) control group. Primer sequences for genotyping were as follows: Forward 5′-AGG ACT GTC TCT GTA GTC TCA GGA GG-3′; Reverse 5′-GAT GCT CAT GTC AGA GTG AGC TGA TGG-3′. Genomic DNA was extracted from mouse tails and amplified using EmeraldAmp PCR Master Mix, followed by visualization by 3% agarose gel electrophoresis (44).

Mouse phenotype assessment

For examining the influence of trehalose on the metabolic state, mice were fed a chow diet until the indicated age. A diet containing 40% kcal fat (TD 88137, Harlan, United States) was used for all experiments involving high fat diet (HFD) treatment. During HFD feeding, mice were treated with saline, sucrose, or trehalose, by intraperitoneal injection [3 g/Kg body weight (0.3 g trehalose/mL and 10 uL/g body weight), three times per week] and/or by oral route in the drinking water (3% w/v). For trehalose tolerance tests, mice were fasted for 6 h, and a blood sample was taken from the mouse tail vein (0 min point). Subsequently, mice were intraperitoneally treated with a solution of trehalose [3 g/Kg body weight (0.3 g trehalose/mL and 10 uL/g body weight)], and blood samples were collected at indicated time points. For insulin tolerance tests, 15-week HFD-fed mice were fasted for 6 h, blood samples were collected from the mouse tail vein (0 min point) and the mice were then intraperitoneally injected with insulin [1 U/Kg body weight (0.1 U of insulin/ml of sterile PBS, 10 µL/g body weight)]. Mice were pretreated with indicated doses of Validamycin (Cayman Chemicals, Ann Arbor, MI, United States) intraperitoneally, followed by trehalose (3 g/Kg body weight), 3 h before assessment of blood glucose levels. Blood samples were obtained at indicated time points. Body composition was determined by EchoMRI-100H (EchoMRI LLC) and presented as fat and lean mass, in accordance with the manufacturer's instructions. For tissue *Treh* expression profiles and for tissue Treh activity assays, tissues were harvested from 8-week-old male C57BL/6 J mice.

Histological analysis and tissue weights

BAT, iWAT, eWAT, and liver were weighed upon mouse dissection. Liver tissue samples were fixed in 4% paraformaldehyde overnight and then transferred to 70% ethanol. The fixed samples were embedded in paraffin for staining with hematoxylin and eosin Y.

Analysis of plasma parameters

Glucose, cholesterol, TGs, and FFA concentrations were determined using commercially available kits: Autokit Glucose (NC9927772, Wako Chemicals, Richmond, VA, United States), Infinity Cholesterol Liquid Stable Reagent (TR13421, Thermo Fisher), Infinity Triglyceride Reagent (TR22421, Thermo Fisher), and NEFA HR[2; Reagent 1 (434–91,795) and Reagent 2 (436–91,995), Wako Chemicals], respectively. All kits were used in accordance with the manufacturer's instructions.

Analysis of trehalose and trehalase activity

Trehalose concentration and trehalase activity were measured using Trehalose Assay Kit (Megazyme, Bray, Ireland) according to manufacturer

protocol. Briefly, tissue homogenate (equal protein concentrations between samples) or plasma was treated with an equal volume of 5 g/L trehalose and then incubated at 37°C for 30 min. After that, the plate was read at 340 nm every 5 min or until values stop changing.

Gene expression quantification

RNA was isolated with Ambion PureLink RNA Kit (Life Technologies, Foster City, CA) and then reverse-transcribed using SuperScript VILO (Life Technologies). For quantification of mRNA expression, real-time PCR was performed with a LightCycler system (QuantStudio; Thermo Fisher, Waltham, MA) using SYBR Green fluorescence signals (SYBR Select Master Mix, 4,472,908, Thermo Fisher). The protocol for amplification was as follows: denaturation, 95°C for 1 min; annealing, 60°C for 10 s; extension, 72°C for 40 s. Gene expression levels were normalized to the levels of ribosomal protein lateral stalk subunit P0 (Rplp0) Forward 5′- ATC CCT GAC GCA CCG CCG TGA-3′; Reverse 5′- TGC ATC TGC TTG GAG CCC ACG TT-3′. Primer sequences used for *Treh*: Forward 5'-TCA TCT TGG TAG AGC TGG GC-3′; Reverse 5′- ATG ACC TGG GAG CTG CAC-3′.

Western blotting

Cells or tissues were lysed in a standard RIPA lysis buffer. Standard techniques were used for protein quantification, separation, transfer, and blotting. The following primary antibody was used: Treh (1:1000, sc-390034, Santa Cruz, Heidelberg, Germany). Ponceau-S total protein staining was used as a loading control.

Quantification and statistical analysis

All results are presented as mean ± SEM. Bars in graphs represent standard errors, and significance was assessed by two-tailed Student's *t* tests.

Data availability statement

The datasets presented in this article are not readily available because no dataset used in the current manuscript. Requests to access the datasets should be directed to brazani@pitt.edu.

Ethics statement

The animal study was approved by University of Pittsburgh and Washington University Animal Studies Committees. The study was conducted in accordance with the local legislation and institutional requirements.

Author contributions

Y-SY: Conceptualization, Data curation, Formal analysis, Funding acquisition, Investigation, Methodology, Project administration, Resources, Software, Supervision, Validation, Visualization, Writing – original draft, Writing – review & editing. TE: Conceptualization, Data curation, Formal analysis, Investigation, Methodology, Software, Visualization, Writing – original draft, Writing – review & editing. S-JJ: Conceptualization, Investigation, Methodology, Writing – review & editing. ZL: Writing – review & editing. AA: Writing – review & editing. CC: Writing – review & editing. JH: Writing – review & editing. DP: Writing – review & editing. XZ: Conceptualization, Formal analysis, Investigation, Methodology, Software, Writing – review & editing. AJ: Writing – review & editing. JC: Writing – review & editing. IL: Conceptualization, Writing – review & editing. BR: Conceptualization, Data curation, Formal analysis, Funding acquisition, Investigation, Methodology, Project administration, Resources, Software, Supervision, Validation, Visualization, Writing – original draft, Writing – review & editing.

Funding

The author(s) declare that financial support was received for the research and/or publication of this article. This work was supported by R01 HL125838, R01 HL159461, R01 DK131188, and VA MERIT I01 BX003415 (to BR), American Heart Association Postdoctoral Fellowship 897628 and 24POST1198554 (to Y-SY).

Acknowledgments

The authors thank Karyn Holloway for technical support.

Conflict of interest

The authors declare that the research was conducted in the absence of any commercial or financial relationships that could be construed as a potential conflict of interest.

Generative AI statement

The author(s) declare that no Gen AI was used in the creation of this manuscript.

Publisher's note

All claims expressed in this article are solely those of the authors and do not necessarily represent those of their affiliated organizations, or those of the publisher, the editors and the reviewers. Any product that may be evaluated in this article, or claim that may be made by its manufacturer, is not guaranteed or endorsed by the publisher.

Supplementary material

The Supplementary material for this article can be found online at: https://www.frontiersin.org/articles/10.3389/fnut.2025.1580684/full#supplementary-material

References

1. Rakhra V. Obesity and the Western diet: how we got Here. *Mo Med*. (2020) 117:536–8.

2. Gonzalez-Muniesa P. Obesity. *Nat Rev Dis Primers*. (2017) 3:17034. doi: 10.1038/nrdp.2017.34

3. Kahn CR, Wang G, Lee KY. Altered adipose tissue and adipocyte function in the pathogenesis of metabolic syndrome. *J Clin Invest*. (2019) 129:3990–4000. doi: 10.1172/JCI129187

4. Ahima RS, Lazar MA. Adipokines and the peripheral and neural control of energy balance. *Mol Endocrinol*. (2008) 22:1023–31. doi: 10.1210/me.2007-0529

5. Srivastava G, Apovian CM. Current pharmacotherapy for obesity. *Nat Rev Endocrinol*. (2018) 14:12–24. doi: 10.1038/nrendo.2017.122

6. Do D. GLP-1 receptor agonist discontinuation among patients with obesity and/or type 2 diabetes. *JAMA Netw Open*. (2024) 7:e2413172. doi: 10.1001/jamanetworkopen.2024.13172

7. Sodhi M, Rezaeianzadeh R, Kezouh A, Etminan M. Risk of gastrointestinal adverse events associated with glucagon-like Peptide-1 receptor agonists for weight loss. *JAMA*. (2023) 330:1795–7. doi: 10.1001/jama.2023.19574

8. Elbein AD, Pan YT, Pastuszak I, Carroll D. New insights on trehalose: a multifunctional molecule. *Glycobiology*. (2003) 13:17R–127R. doi: 10.1093/glycob/cwg047

9. Elbein AD. The metabolism of α,α-Trehalose. *Adv Carbohydr Chem Biochem*. (1974) 30:227–56.

10. Di Rienzi SC, Britton RA. Adaptation of the gut microbiota to modern dietary sugars and sweeteners. *Adv Nutr*. (2020) 11:616–29. doi: 10.1093/advances/nmz118

11. Yaribeygi H, Yaribeygi A, Sathyapalan T, Sahebkar A. Molecular mechanisms of trehalose in modulating glucose homeostasis in diabetes. *Diabetes Metab Syndr*. (2019) 13:2214–8. doi: 10.1016/j.dsx.2019.05.023

12. Yap KH, Azmin S, Makpol S, Damanhuri HA, Mustapha M, Hamzah JC, et al. Profiling neuroprotective potential of trehalose in animal models of neurodegenerative diseases: a systematic review. *Neural Regen Res*. (2023) 18:1179–85. doi: 10.4103/1673-5374.360164

13. Khalifeh M, Barreto GE, Sahebkar A. Trehalose as a promising therapeutic candidate for the treatment of Parkinson's disease. *Br J Pharmacol*. (2019) 176:1173–89. doi: 10.1111/bph.14623

14. Khalifeh M, Read MI, Barreto GE, Sahebkar A. Trehalose against Alzheimer's disease: insights into a potential therapy. *BioEssays*. (2020) 42:e1900195. doi: 10.1002/bies.201900195

15. Eskelinen EL, Schmidt CK, Neu S, Willenborg M, Fuertes G, Salvador N, et al. Disturbed cholesterol traffic but normal proteolytic function in LAMP-1/LAMP-2 double-deficient fibroblasts. *Mol Biol Cell*. (2004) 15:3132–45. doi: 10.1091/mbc.e04-02-0103

16. Evans TD, Sergin I, Zhang X, Razani B. Target acquired: selective autophagy in cardiometabolic disease. *Sci Signal*. (2017) 10:eaag2298. doi: 10.1126/scisignal.aag2298

17. Sahebkar A, Hatamipour M, Tabatabaei SA. Trehalose administration attenuates atherosclerosis in rabbits fed a high-fat diet. *J Cell Biochem*. (2019) 120:9455–9. doi: 10.1002/jcb.28221

18. Forte M, Marchitti S, Cotugno M, di Nonno F, Stanzione R, Bianchi F, et al. Trehalose, a natural disaccharide, reduces stroke occurrence in the stroke-prone spontaneously hypertensive rat. *Pharmacol Res*. (2021) 173:105875. doi: 10.1016/j.phrs.2021.105875

19. Arai C, Arai N, Mizote A, Kohno K, Iwaki K, Hanaya T, et al. Trehalose prevents adipocyte hypertrophy and mitigates insulin resistance. *Nutr Res*. (2010) 30:840–8. doi: 10.1016/j.nutres.2010.10.009

20. Lim YM, Lim H, Hur KY, Quan W, Lee HY, Cheon H, et al. Systemic autophagy insufficiency compromises adaptation to metabolic stress and facilitates progression from obesity to diabetes. *Nat Commun*. (2014) 5:4934. doi: 10.1038/ncomms5934

21. Arai C. Trehalose prevents adipocyte hypertrophy and mitigates insulin resistance in mice with established obesity. *J Nutr Sci Vitaminol (Tokyo)*. (2013) 59:393–401. doi: 10.3177/jnsv.59.393

22. Arai C, Arai N, Arai S, Yoshizane C, Miyata S, Mizote A, et al. Continuous intake of Trehalose induces white adipose tissue Browning and Enhances energy metabolism. *Nutr Metab (Lond)*. (2019) 16:45. doi: 10.1186/s12986-019-0373-4

23. DeBosch BJ, Heitmeier MR, Mayer AL, Higgins CB, Crowley JR, Kraft TE, et al. Trehalose inhibits solute carrier 2A (SLC2A) proteins to induce autophagy and prevent hepatic steatosis. *Sci Signal*. (2016) 9:ra21. doi: 10.1126/scisignal.aac5472

24. Korolenko TA, Ovsyukova MV, Bgatova NP, Ivanov ID, Makarova SI, Vavilin VA, et al. Trehalose activates hepatic and myocardial autophagy and has anti-inflammatory effects in db/db diabetic mice. *Life (Basel)*. (2022) 12:442. doi: 10.3390/life12030442

25. Pagliassotti MJ, Estrada AL, Hudson WM, Wei Y, Wang D, Seals DR, et al. Trehalose supplementation reduces hepatic endoplasmic reticulum stress and inflammatory signaling in old mice. *J Nutr Biochem*. (2017) 45:15–23. doi: 10.1016/j.jnutbio.2017.02.022

26. Sergin I, Evans TD, Zhang X, Bhattacharya S, Stokes CJ, Song E, et al. Exploiting macrophage autophagy-lysosomal biogenesis as a therapy for atherosclerosis. *Nat Commun*. (2017) 8:15750. doi: 10.1038/ncomms15750

27. Despres JP. BMI versus obesity subtypes in the era of precision medicine. *Lancet Diabetes Endocrinol*. (2023) 11:382–4. doi: 10.1016/S2213-8587(23)00088-8

28. Yeh YS, Evans TD, Iwase M, Jeong SJ, Zhang X, Liu Z, et al. Identification of lysosomal lipolysis as an essential noncanonical mediator of adipocyte fasting and cold-induced lipolysis. *J Clin Invest*. (2025) 135:e185340. doi: 10.1172/JCI185340

29. Asano N. Glycosidase inhibitors: update and perspectives on practical use. *Glycobiology*. (2003) 13:93R–104R. doi: 10.1093/glycob/cwg090

30. Wu F, Xu HD, Guan JJ, Hou YS, Gu JH, Zhen XC, et al. Rotenone impairs autophagic flux and lysosomal functions in Parkinson's disease. *Neuroscience*. (2015) 284:900–11. doi: 10.1016/j.neuroscience.2014.11.004

31. Zhu L, Yuan Y, Yuan L, Li L, Liu F, Liu J, et al. Activation of TFEB-mediated autophagy by trehalose attenuates mitochondrial dysfunction in cisplatin-induced acute kidney injury. *Theranostics*. (2020) 10:5829–44. doi: 10.7150/thno.44051

32. Yasugi T, Yamada T, Nishimura T. Adaptation to dietary conditions by trehalose metabolism in Drosophila. *Sci Rep*. (2017) 7:1619. doi: 10.1038/s41598-017-01754-9

33. Buckley AM, Moura IB, Arai N, Spittal W, Clark E, Nishida Y, et al. Trehalose-induced Remodelling of the human microbiota affects Clostridioides difficile infection outcome in an in vitro colonic model: a pilot study. *Front Cell Infect Microbiol*. (2021) 11:670935. doi: 10.3389/fcimb.2021.670935

34. Zhang Y, DeBosch BJ. Microbial and metabolic impacts of trehalose and trehalose analogues. *Gut Microbes*. (2020) 11:1475–82. doi: 10.1080/19490976.2020.1750273

35. Oesterreicher TJ, Markesich DC, Henning SJ. Cloning, characterization and mapping of the mouse trehalase (Treh) gene. *Gene*. (2001) 270:211–20. doi: 10.1016/S0378-1119(01)00474-7

36. Ishihara R, Taketani S, Sasai-Takedatsu M, Kino M, Tokunaga R, Kobayashi Y. Molecular cloning, sequencing and expression of cDNA encoding human trehalase. *Gene*. (1997) 202:69–74.

37. Yu B, Zheng Y, Alexander D, Morrison AC, Coresh J, Boerwinkle E. Genetic determinants influencing human serum metabolome among African Americans. *PLoS Genet*. (2014) 10:e1004212. doi: 10.1371/journal.pgen.1004212

38. Muller YL, Hanson RL, Knowler WC, Fleming J, Goswami J, Huang K, et al. Identification of genetic variation that determines human trehalase activity and its association with type 2 diabetes. *Hum Genet*. (2013) 132:697–707. doi: 10.1007/s00439-013-1278-3

39. Kamiya T, Hirata K, Matsumoto S, Arai C, Yoshizane C, Kyono F, et al. Targeted disruption of the trehalase gene: determination of the digestion and absorption of trehalose in trehalase-deficient mice. *Nutr Res*. (2004) 24:185–96. doi: 10.1016/j.nutres.2004.01.001

40. Arai C, Suyama A, Arai S, Arai N, Yoshizane C, Koya-Miyata S, et al. Trehalose itself plays a critical role on lipid metabolism: Trehalose increases jejunum cytoplasmic lipid droplets which negatively correlated with mesenteric adipocyte size in both HFD-fed trehalase KO and WT mice. *Nutrition & Metabolism*. (2020) 17:22. doi: 10.1186/s12986-020-00443-1

41. Jeong SJ, Stitham J, Evans TD, Zhang X, Rodriguez-Velez A, Yeh YS, et al. Trehalose causes low-grade lysosomal stress to activate TFEB and the autophagy-lysosome biogenesis response. *Autophagy*. (2021) 17:3740–52. doi: 10.1080/15548627.2021.1896906

42. Kobayashi M, Yasukawa H, Arikawa T, Deguchi Y, Mizushima N, Sakurai M, et al. Trehalose induces SQSTM1/p62 expression and enhances lysosomal activity and antioxidative capacity in adipocytes. *FEBS Open Bio*. (2021) 11:185–94. doi: 10.1002/2211-5463.13055

43. Mizunoe Y, Kobayashi M, Sudo Y, Watanabe S, Yasukawa H, Natori D, et al. Trehalose protects against oxidative stress by regulating the Keap1-Nrf2 and autophagy pathways. *Redox Biol*. (2018) 15:115–24. doi: 10.1016/j.redox.2017.09.007

44. Yeh YS, Jheng HF, Iwase M, Kim M, Mohri S, Kwon J, et al. The mevalonate pathway is indispensable for adipocyte survival. *iScience*. (2018) 9:175–91. doi: 10.1016/j.isci.2018.10.019

45. Kaplon RE, Hill SD, Bispham NZ, Santos-Parker JR, Nowlan MJ, Snyder LL, et al. Oral trehalose supplementation improves resistance artery endothelial function in healthy middle-aged and older adults. *Aging (Albany NY)*. (2016) 8:1167–83. doi: 10.18632/aging.100962

46. Yoshizane C, Mizote A, Yamada M, Arai N, Arai S, Maruta K, et al. Glycemic, insulinemic and incretin responses after oral trehalose ingestion in healthy subjects. *Nutr J*. (2017) 16:9. doi: 10.1186/s12937-017-0233-x

47. Yoshizane C, Mizote A, Arai C, Arai N, Ogawa R, Endo S, et al. Daily consumption of one teaspoon of trehalose can help maintain glucose homeostasis: a double-blind, randomized controlled trial conducted in healthy volunteers. *Nutr J*. (2020) 19:68. doi: 10.1186/s12937-020-00586-0

48. Jamialahmadi T, Emami F, Bagheri RK, Alimi H, Bioletto F, Bo S, et al. The effect of trehalose administration on vascular inflammation in patients with coronary artery disease. *Biomed Pharmacother*. (2022) 147:112632. doi: 10.1016/j.biopha.2022.112632

49. Hashemian S, Shojaei M, Radbakhsh S, Ashari S, Matbou Riahi M, Shateri Amiri Z, et al. The effects of oral trehalose on glycaemia, inflammation, and quality of life in patients with type 2 diabetes: a pilot randomized controlled trial. *Arch Med Sci*. (2023) 19:1693–700. doi: 10.5114/aoms/159048

50. Rodriguez-Navarro JA. Trehalose ameliorates dopaminergic and tau pathology in parkin deleted/tau overexpressing mice through autophagy activation. *Neurobiol Dis*. (2010) 39:423–38. doi: 10.1016/j.nbd.2010.05.014

51. Castillo K, Nassif M, Valenzuela V, Rojas F, Matus S, Mercado G, et al. Trehalose delays the progression of amyotrophic lateral sclerosis by enhancing autophagy in motoneurons. *Autophagy*. (2013) 9:1308–20. doi: 10.4161/auto.25188

52. Sarkar S, Chigurupati S, Raymick J, Mann D, Bowyer JF, Schmitt T, et al. Neuroprotective effect of the chemical chaperone, trehalose in a chronic MPTP-induced Parkinson's disease mouse model. *Neurotoxicology*. (2014) 44:250–62. doi: 10.1016/j.neuro.2014.07.006

53. Kim J, Cheon H, Jeong YT, Quan W, Kim KH, Cho JM, et al. Amyloidogenic peptide oligomer accumulation in autophagy-deficient beta cells induces diabetes. *J Clin Invest*. (2014) 124:3311–24. doi: 10.1172/JCI69625

54. Ferguson SA, Law CD, Sarkar S. Chronic MPTP treatment produces hyperactivity in male mice which is not alleviated by concurrent trehalose treatment. *Behav Brain Res*. (2015) 292:68–78. doi: 10.1016/j.bbr.2015.05.057

55. Tanji K, Miki Y, Maruyama A, Mimura J, Matsumiya T, Mori F, et al. Trehalose intake induces chaperone molecules along with autophagy in a mouse model of Lewy body disease. *Biochem Biophys Res Commun*. (2015) 465:746–52. doi: 10.1016/j.bbrc.2015.08.076

56. Liu K, Jing MJ, Liu C, Yan DY, Ma Z, Wang C, et al. Effect of trehalose on manganese-induced mitochondrial dysfunction and neuronal cell damage in mice. *Basic Clin Pharmacol Toxicol*. (2019) 125:536–47. doi: 10.1111/bcpt.13316

57. Miyake T, Sakai N, Tamai A, Sato K, Kamikawa Y, Miyagawa T, et al. Trehalose ameliorates peritoneal fibrosis by promoting snail degradation and inhibiting mesothelial-to-mesenchymal transition in mesothelial cells. *Sci Rep*. (2020) 10:14292. doi: 10.1038/s41598-020-71230-4

58. Liu S, Yang Y, Gao H, Zhou N, Wang P, Zhang Y, et al. Trehalose attenuates renal ischemia-reperfusion injury by enhancing autophagy and inhibiting oxidative stress and inflammation. *Am J Physiol Ren Physiol*. (2020) 318:F994–F1005. doi: 10.1152/ajprenal.00568.2019

59. Gong F, Ge T, Liu J, Xiao J, Wu X, Wang H, et al. Trehalose inhibits ferroptosis via NRF2/HO-1 pathway and promotes functional recovery in mice with spinal cord injury. *Aging (Albany NY)*. (2022) 14:3216–32. doi: 10.18632/aging.204009

60. Pradeloux S, Coulombe K, Ouamba AJK, Isenbrandt A, Calon F, Roy D, et al. Oral Trehalose intake modulates the microbiota-gut-brain Axis and is neuroprotective in a Synucleinopathy mouse model. *Nutrients*. (2024) 16:3309. doi: 10.3390/nu16193309

61. Yang J, Yuan L, Li L, Liu F, Liu J, Chen Y, et al. Trehalose activates autophagy to alleviate cisplatin-induced chronic kidney injury by targeting the mTOR-dependent TFEB signaling pathway. *Theranostics*. (2025) 15:2544–63. doi: 10.7150/thno.102559

62. Lee H, Han JH, Jeong RG, Kang YJ, Choi BH, Kim SR, et al. Oral trehalose improves histological and behavior symptoms of mucopolysaccharidosis type II in iduronate 2-sulfatase deficient mice. *Sci Rep*. (2025) 15:4882. doi: 10.1038/s41598-025-88362-0

63. Forouzanfar F, Hoseini A, Sahebkar A. Neuroprotective effects of trehalose following middle cerebral artery occlusion in rats. *Interdis Neurosurg*. (2023) 34:101827. doi: 10.1016/j.inat.2023.101827

64. Wang Y, Li X, Gao H, Lu Q. Trehalose delays postmenopausal osteoporosis by enhancing AKT/TFEB pathway-dependent autophagy flow in rats. *Exp Ther Med*. (2023) 26:538. doi: 10.3892/etm.2023.12237

frontiers | Frontiers in Nutrition

TYPE Original Research
PUBLISHED 04 August 2025
DOI 10.3389/fnut.2025.1601867

Check for updates

OPEN ACCESS

EDITED BY
Pedzisai Makoni,
Sefako Makgatho Health Sciences University, South Africa

REVIEWED BY
Yongjie Xu,
Xinyang Normal University, China
Heloisa Balan Assalin,
State University of Campinas, Brazil

*CORRESPONDENCE
Jingxuan Ke
✉ jingxKe@163.com

†These authors have contributed equally to this work

RECEIVED 28 March 2025
ACCEPTED 21 July 2025
PUBLISHED 04 August 2025

CITATION
Ma Y, Ke J, Wang Y, Zhou Y, Gao X, Wang X and Shen Q (2025) The improvement effect of insoluble dietary fiber of *Polygonatum sibiricum* on hyperlipidemia in high-fat diet mice via gut microbiota and metabolites.
Front. Nutr. 12:1601867.
doi: 10.3389/fnut.2025.1601867

COPYRIGHT
© 2025 Ma, Ke, Wang, Zhou, Gao, Wang and Shen. This is an open-access article distributed under the terms of the Creative Commons Attribution License (CC BY). The use, distribution or reproduction in other forums is permitted, provided the original author(s) and the copyright owner(s) are credited and that the original publication in this journal is cited, in accordance with accepted academic practice. No use, distribution or reproduction is permitted which does not comply with these terms.

The improvement effect of insoluble dietary fiber of *Polygonatum sibiricum* on hyperlipidemia in high-fat diet mice via gut microbiota and metabolites

Yanli Ma[1†], Jingxuan Ke[1*†], Yuan Wang[1], Yuhui Zhou[1], Xinyu Gao[1], Xin Wang[2] and Qingshan Shen[1]

[1]Zhang Zhongjing School of Chinese Medicine, Nanyang Institute of Technology, Nanyang, China, [2]College of Food Science and Technology, Hebei Agricultural University, Baoding, China

Objective: *Polygonatum sibiricum* is rich in insoluble dietary fiber (IDF), but its antihyperlipidemic effect remains unclear. This study investigated the antihyperlipidemic effect of *Polygonatum sibiricum*'s IDF (PIDF) in high-fat diet mice.

Methods: Male C57BL/6 J mice were fed with a high-fat diet continuously for 8 weeks. At the same time, the low-dose and high-dose groups were supplemented with 0.5 g/kg·BW and 1.0 g/kg·BW of PIDF, respectively. The weight and food intake of the mice were measured during the experiment. After 8 weeks of feeding, the organ weight, serum indexes, and liver function were investigated. Furthermore, the mechanism of antihyperlipidemic was explained by analyzing the gut microbiota and metabolites.

Results: The results of the LIDF and HIDF showed that the PIDF treatment significantly alleviated the liver and kidney weight and body fat index. PIDF administration remarkably increased the high-density lipoprotein cholesterol level and enhanced hepatic superoxide dismutase activity in high-fat diet-fed mice. The levels of total cholesterol, triglycerides, low-density lipoprotein cholesterol, glucose, and aspartate transaminase in the HIDF were significantly lower than in the high-fat diet group. In addition, PIDF supplements also decreased the ratio of *Bacillota* to *Bacteroidota*, increasing the relative abundance of *Alistipes* and *Akkermansia*. Furthermore, metabolites suggest that dietary increases in PIDF can promote lipid and amino acid metabolism. Hence, PIDF improves lipid metabolism by regulating the gut microbiome and influencing host metabolism.

Conclusion: It can be concluded that PIDF may alleviate hyperlipidemia by regulating cholesterol metabolism, increasing the abundance of beneficial microorganisms, and controlling its metabolites. The results of this study accelerated the application of PIDF in the health food industry.

KEYWORDS

insoluble dietary fiber, *Polygonatum sibiricum*, antihyperlipidemic effect, gut microbiome, metabolite profile

1 Introduction

With high-fat diets becoming the eating habit or hobby of most people, hyperlipidemia has become a global problem of chronic diseases that threaten human health. Animal experiments and pharmacological studies have shown that hyperlipidemia and obesity are closely related to gut microbiota (1, 2). The interaction between non-starch polysaccharides, especially plant dietary fiber and intestinal microorganisms, has become a new research focus (3, 4). Dietary fiber can improve gut microbes, clean the intestinal tract, and prevent intestinal diseases (5). According to its water solubility, dietary fiber can be divided into two categories: water-insoluble dietary fiber (IDF) and water-soluble dietary fiber (SDF). Among these, IDF can also increase satiety and exhibit other beneficial effects (6). Moreover, IDF cannot be digested by the body's digestive enzymes and passes directly to the large intestine, where it is metabolized by microorganisms in the gut (7). Therefore, IDF also has significant efficacy in improving intestinal microbes (8). The balanced dietary guidelines for residents suggest that a plant-based diet can lead to higher dietary fiber intake, thereby improving human health (6). Natural plant dietary fiber possesses the characteristics of green health, is a vast source, and has a low cost, which makes it a considerable application prospect in developing functional foods for antihyperlipidemic purposes.

The hypolipidemic effect of dietary fiber from natural plants has been widely studied. Still, the mechanism is different, and it is typically the result of the combined action of several mechanisms. Reports from animal experiments indicated that plant dietary fiber can play a role in the hypolipidemic effect by regulating oxidative stress and lipid metabolism. The mechanism by which plant dietary fiber improves hyperlipidemia is as follows: (1) regulating triglyceride and fatty acid metabolism. The study of Wang et al. (9) demonstrated that soybean IDF can inhibit the expression of SREBP1c and SCD1 mRNA in hyperlipidemia liver, thereby reducing TC and TG levels, and play a beneficial role in improving HFD-induced dyslipidemia and liver steatosis in mice. (2) Regulate cholesterol metabolism. Liu et al. (10) found that dietary fibers from bergamot could inhibit the increase of LDL-C in the blood, promote the transport and consumption of oil in the liver, and subsequently reduce the levels of cholesterol and lipids in the body, demonstrating a noticeable hypolipidemic effect. (3) Regulate gut microbes. Zhang et al. (11) reported that after 8 weeks of intervention with a high-fat diet in mice, those fed an IDF diet extracted from brown seaweed *Laminaria japonica* showed a significant improvement in intestinal microbial composition, primarily by substantially increasing the relative abundance of *Akkermansia*. Additionally, biochemical results showed that serum cholesterol concentration and glucose level were significantly reduced. Another study also showed that insoluble dietary fibers and total dietary fiber obtained from *Caulerpa lentillifera* exhibited increased levels of acetic acid and propionic acid in metabolites in the supplemental dietary fiber groups compared to the high-fat diet group (12). It has been reported that under the fermentation of gut microbiota, dietary fiber produces more short-chain fatty acids, which have a noticeable effect on improving metabolic syndrome, especially hyperlipidemia (3).

Polygonatum sibiricum is one of the homologous resources of traditional medicine and food, which has essential edibility and therapeutic value. Except for polysaccharides and saponins, *Polygonatum sibiricum* is rich in IDF, with a content of up to 88% (13). Currently, research on *Polygonatum sibiricum* primarily focuses on identifying functional ingredients, including polysaccharides and saponins (5). A large amount of residue is generated after the extraction of active ingredients and is not fully utilized. The *Polygonatum sibiricum* residue contains a large amount of dietary fiber, which has potential applications in the food industry (13).

In our previously published report, PIDF was the high purity (76.7%) (14). Additionally, *in vitro* studies have demonstrated that PIDF is more effective in adsorbing cholesterol (35.95 mg/g) and glucose (24.63 μmoL/g) (15). However, there is no report on the actual hypolipidemic effect of PIDF *in vivo* experiments, and its mechanism remains largely unrecognized. Furthermore, this study highlighted its anti-hyperlipidemic effect and modulation of gut microbiota in high-fat-fed mice. Therefore, this study investigated the mechanism by which gut microbiome regulates anti-hyperlipidemia. In addition, we also investigated the regulatory effect of PIDF on caecum metabolites to further elucidate the mechanism of its hypolipidemic action. This study will provide valuable theoretical evidence for applying PIDF as a food for alleviating hyperlipidemia.

2 Materials and methods

2.1 *Polygonatum sibiricum* insoluble dietary fiber

Simply, *Polygonatum sibiricum* residue powder was enzymatic hydrolysis by α-amylase (0.25%) at pH 6, 60°C for 1 h. Next, the mixture was enzymatically hydrolyzed by papain (0.125%) at pH 5, 50°C for 1 h. After enzymolysis, the mixture was subjected to ultrasonic treatment (Ningbo Xinzhi Biotechnology Co., Ltd., Ningbo, China) at 50°C for 20 min (ultrasonic 2 s and intermittent 2 s). Then, collect the residue after centrifuging (2,683 g for 10 min) the mixture. Finally, the residue was washed twice with water and once with 70% ethanol; the residue was ball-milled (CJM-SY-B, Qinhuangdao Bomao New Material Technology Co., Ltd., Qinhuangdao, China) at 380 rpm for 8 h to obtain a consistent particle size distribution, and the processed powders were designated as PIDF. The PIDF has a consistent purity (76.7%) and consists mainly of cellulose (24.4%), hemicellulose (31.5%), lignin (20.8%), protein (7.5%), starch (4.1%), and ash (0.97%) (14). According to our report (15), PIDF exhibited better functional properties: water-holding capacity (4.36 g/g), oil-holding capacity (2.62 g/g), water-swelling capacity (2.40 mL/g), ion exchange capacity (0.27 mmol/g), and cholesterol (35.95 mg/g) and glucose (24.63 μmoL/g) adsorption capacity. The particle size distribution and zeta-potential of PIDF were 9.96 μm and −25.95 mV, respectively (15).

2.2 Animal experiment

The ethics committee for experimental animals of Nanyang Institute of Technology reviewed all the animal experiments (Animal Experiment Ethics Review No. [2024]001). Here, seven-week-old male C57BL/6 J mice (SPF grade, 18 ± 2 g) were purchased from Beijing Vital River Laboratory Animal Technology Co., Ltd. (Beijing, China). During the adaptation feeding period (7 days), all mice were

fed with a standard diet. All mice had free access to water and food. The feeding temperature was maintained at 22 ± 2°C, with a relative humidity of 55 ± 10%, and a 12 h light–dark cycle. The obesity model was established according to Wang et al. (9) and Zhang et al. (11). After adaptive feeding, the mice (eight-week-old male) were randomly divided into 4 groups, with 8 animals in each group and 4 animals in each cage. If the data of 1–2 animals were outliers, the data of that mouse were excluded. The normal control group (NC) was fed a standard diet. The high-fat diet control group (HC) was fed a high-fat diet (60% kcal fat: protein 26%, carbohydrate 26%, fat 35%). According to the report (9), the low-dose group (LIDF) was fed with a high-fat diet supplemented with gavage administration of 0.5 g per kg·BW of PIDF per mouse per day, and the high-dose group (HIDF) was fed a high-fat diet supplemented with gavage administration of 1.0 g per kg·BW of PIDF per mouse per day. The mice were fed a PIDF-supplemented diet for 8 weeks.

2.3 Body weight and tissues collected

The weight of each mouse in each group was recorded weekly. The food intake of each cage was recorded every day. The total amount of food divided by the number of mice in the cage gives the daily food intake for each mouse. At the end of the 8-week experiment, the abdomen of the mouse was gently pressed to stimulate defecation. After the mouse defecated, the fresh fecal samples were quickly collected into a sterile test tube. Mice were anesthetized with isoflurane after a 12 h fast (Jiangsu Hengfengqiang Biotechnology Co., LTD., Jiangsu, China). Blood was collected through the orbital venous plexus, centrifuged at 4°C, and serum was obtained by spinning at 3500 rpm for 15 min. The serum was stored at −80°C for biochemical analysis.

After euthanasia, the kidneys, spleen, liver, and adipose tissue of the mice (perirenal and epididymis) were dissected and weighed. At the same time, cecal contents were collected. The organ index was measured by calculating the ratio of organ weight to body weight. Divide the liver into two parts, wrap one in tin foil, and freeze at −80°C. The other part of the liver, perirenal fat, and epididymal fat were soaked with 4% paraformaldehyde at room temperature.

2.4 Serum biochemical analysis

Serum lipid parameters, including total cholesterol (TC), triglycerides (TG), glucose (GLU), aspartate transaminase (AST), alanine aminotransferase (ALT), high-density lipoprotein cholesterol (HDL-C), and low-density lipoprotein cholesterol (LDL-C) were measured using commercial kits (Shandong Biobase Industry Co., LTD, Jinan, China) per the manufacturer's instructions.

2.5 Histological analysis

Liver and epididymal fats fixed in 4% paraformaldehyde were embedded and sectioned into 4 μm sections. The slices were stained with hematoxylin–eosin (H&E) (12). Then, it was viewed under a light microscope (Olympus, Japan) and photographed. Additionally, the Nonalcoholic Fatty Liver Disease (NAFLD) activity score of liver slices was evaluated. The detailed scoring criteria refer to the guidelines of the National Institute of Health's NASH Clinical Research Pathology Working Group of the United States (16).

2.6 Biochemical indexes of liver tissue

The activities of glutathione peroxidase (GSH-PX) and superoxide dismutase (SOD), malondialdehyde (MDA) content, and total antioxidant capacity (T-AOC) of liver tissue were determined according to the instructions of special kits (Nanjing Jiancheng Biotechnology Company, Nanjing, China).

2.7 Gut microbiota analysis

Mouse feces were collected to isolate total DNA, and the V3–V4 region of the 16S rRNA gene was amplified using PCR with forward primer 341F (CCTAYGGGRBGCASCAG) and reverse primer 806R (GGACTACNNGGGTATCTAAT). Overlapping paired-end reads were merged using fast-join and processed with QIIME. Illumina readings with an average score more excellent than 20 were selected for further analysis (8). The 16S rRNA gene sequence was used to classify the operational taxon units (OTUs) of the detected bacteria. Alpha diversity analysis was performed for the classified microorganisms, and Chao, Pielou's, Shannon, and Simpson indices were used to characterize microbial diversity and richness. The Beta diversity of the classified microorganisms was analyzed, and a Venn diagram represented the intersection size of OTUs between different groups. Meanwhile, the similarity of microorganisms between various groups was illustrated using principal component analysis (PCA) (17).

2.8 Non-targeted metabolite analysis

Metabolomics analysis was performed using ultra-high-performance liquid chromatography (LC) tandem mass spectrometry (MS/MS). Briefly, the cecum was frozen with liquid nitrogen. Take a 100 mg tissue sample into an EP test tube, then add 500 μL of an 80% methanol solution. Next, the mixture was swirled over an ice bath for 5 min until well mixed. The mixture is then centrifuged at 15000 g, 4°C for 20 min. Collect the supernatant and add mass spectrometry water to adjust the methanol concentration of the supernatant to 53%. Then, the mixture was centrifuged at 15000 g, 4°C for 20 min. Finally, the supernatant was analyzed by LC–MS/MS.

LC was performed using the Vanquish UHPLC System (Thermo Fisher Scientific, Germany) and a Hypersil Gold column (100 × 2.1 mm, 1.9 μm) (Thermo Fisher Scientific, United States); the column temperature was maintained at 40°C. The flow rate was set at 0.2 mL/min. The mobile phases consisted of 0.1% formic acid (v/v) (A) and methanol (B). The gradient elution program was as follows: 0–1.5 min, 98% A; 1.5–3 min, 98–15% A; 3–10 min, 15–0% A, 10–10.1 min, 0–98% A, 10.1–12 min, 98% A. ESI (+) and ESI (−) were analyzed by Q Exactive™ HF/Q

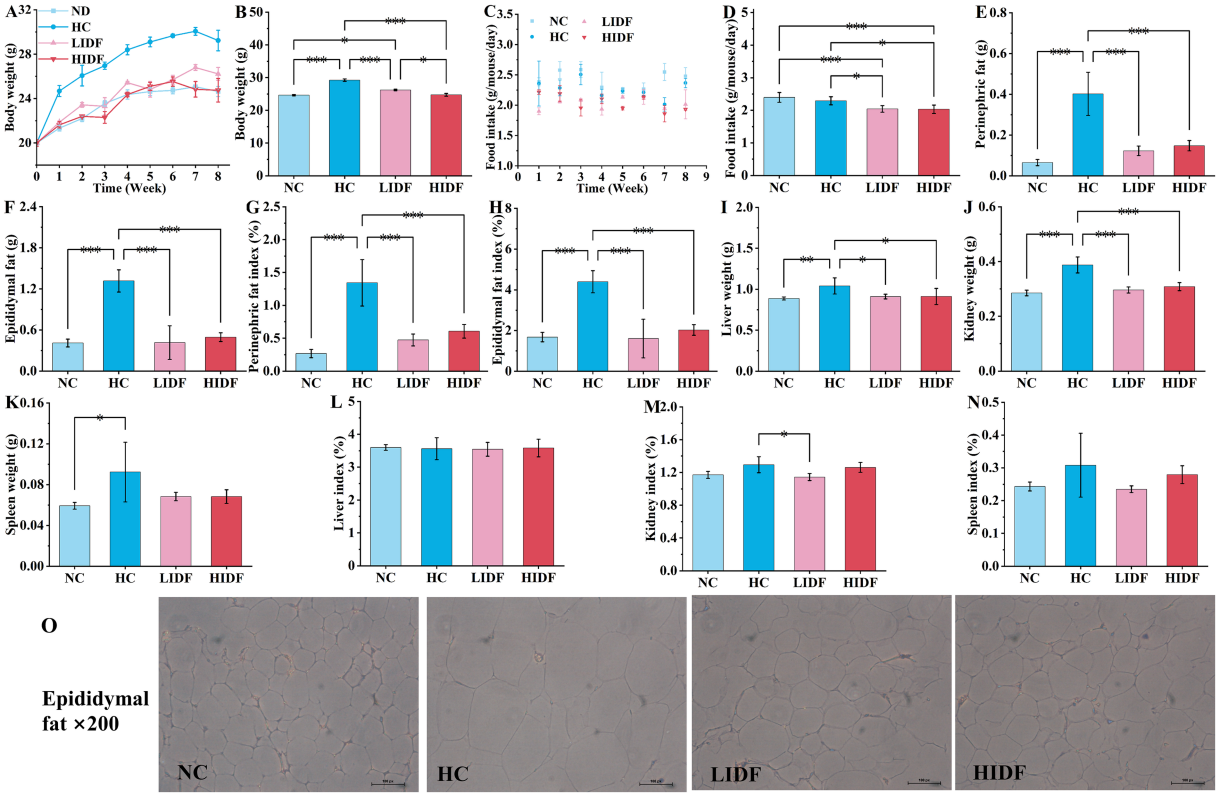

FIGURE 1
Effects of PIDF on high-fat diet mice. **(A)** Body weight of every week; **(B)** Body weight at the end of the experiment; **(C)** Food intake during 8 weeks; **(D)** The average food intake of each mouse; **(E)** Perinephric fat; **(F)** Epididymal fat; **(G)** Perinephric fat indexes; **(H)** Epididymal fat indexes; **(I)** Liver weight; **(J)** Kidney weight; **(K)** Spleen weight; **(L)** Liver indexes; **(M)** Kidney indexes; **(N)** Spleen indexes; **(O)** H&E staining of epididymal fat. Data presented as mean SEM, $n = 6$, * $p < 0.05$, ** $p < 0.01$, *** $p < 0.001$.

Exactive™ HF-X MS/MS (Thermo Fisher Scientific, Germany) with an ESI ion source, respectively. The parameters were set as follows: Spray Voltage: 3.5 kV, sheath gas pressure: 35 psi; aux gas flow:10 mL/min; capillary Temp: 320°C, S-lens RF level: 60, Aux gas heater temp:350°C, MS/MS scans: data-dependent scans, MS1 range: m/z 100–1,500 (18). All multivariate data analyses and modeling were performed using the NovoMagic Platform.[1] After scaling the data, the models were constructed using principal component analysis (PCA) and partial least squares discriminant analysis (PLS-DA).

2.9 Statistical analysis

Statistical analysis was performed with SPSS 27.0 software (IBM Corporation, NY, United States) and Origin 2024 software (OriginLab, UAS). Results were presented as means ± standard deviation. Differences in experimental data were analyzed by one-way analysis of variance (ANOVA) with Duncan's test. The statistically significant results were considered as $p < 0.05$, $n = 6$.

1 www.novogene.cn

3 Results

3.1 PIDF alleviates body weight

Figure 1A illustrates the weekly weight change curve for the four groups of mice over 8 weeks. The weight of mice is a direct indicator of their health, especially whether they are overweight or obese (19). During the experimental feeding period, the weight of each group of mice increased with age. Compared with the NC group, the weight gain trend in the HC group was significantly accelerated after the second week ($p < 0.05$). It is worth mentioning that at the end of the experiment, the weight of the mice in the HC group (29.23 g ± 0.92 g) exceeded that of the NC group (24.63 g ± 0.45 g) by more than 15%, indicating that the obese mice had been successfully modeled. As depicted in Figure 1A, the weight gain rate of mice in the LIDF and HIDF groups was significantly reduced after PIDF supplementation, and this trend became more pronounced as the mice aged.

Figure 1B shows the weight of the four groups of mice at the end of the experiment. As expected, the body weight of mice in the LIDF (26.22 g ± 0.57 g) and HIDH (24.75 g ± 0.45 g) groups was significantly lower than that in the HC group ($p < 0.001$) (Figure 1B). The body weight of mice in the HIDF group was the same as that in the NC group, with no significant difference ($p > 0.05$) (Figure 1B). In addition, compared with the LIDF group, high doses of PIDF supplementation (the HIDF group) resulted in more significant

weight loss in mice ($p < 0.05$) (Figure 1B). The results showed that the dietary addition of PIDF could conspicuously slow the weight gain of mice on a high-fat diet (20).

3.2 Effect of PIDF on food intake in high-fat diet mice

Figure 1C illustrates the trends in the average food intake of each mouse over the 8-week experiment period. Figure 1D compares the average food intake of each mouse in different groups throughout the experiment. The results showed that, without the PIDF dietary supplement, the food intake of the HC group (2.29 g/mouse/day) mice was significantly higher than that in the LIDF (2.04 g/mouse/day) and HIDF (2.03 g/mouse/day) groups ($p < 0.05$). Furthermore, the food intake of the LIDF and HIDF groups was considerably lower than that of the NC group (2.39 g/mouse/day) ($p < 0.001$), possibly due to the satiety induced by PIDF intake in the LIDF and HIDF groups.

3.3 The effect on the body fat index of mice

The effects of dietary supplementation of IDF on epididymal fat and perinephric fat accumulation in mice are described in Figures 1E,F. It was observed that at the end of the experiment, after 8 weeks of high-fat diet feeding, the fat accumulation in the HC group was excessive. Compared with the NC group (0.065 g ± 0.02 g, 0.41 g ± 0.06 g, respectively), the perinephric fat accumulation in the HC group increased by 83.8% ($p < 0.001$), and epididymal fat accumulation increased by 68.9% ($p < 0.001$). While PIDF significantly inhibited fat accumulation in the LIDF and HIDF groups ($p < 0.001$, Figures 1E,F) compared to the HC group, which ranged from 62.3 to 69.5%. Similarly, as shown in Figures 1G,H, the perinephric and epididymal fat indexes in the LIDF (0.47% ± 0.09, 1.61% ± 0.94%, respectively, $p < 0.001$) and HIDF (0.61% ± 0.10, 2.02% ± 0.26%, respectively, $p < 0.001$) groups were remarkably lower than in the HC group. No significant difference was observed in the effect of PIDF on fat accumulation in mice between the LIDF and HIDF groups, indicating that PIDF has a beneficial impact in inhibiting body fat accumulation. Meanwhile, as shown in Figure 1O, the adipocytes in the HC group were the largest, while those in the LIDF and HIDF groups were significantly reduced, indicating that PIDF decreased the lipid content of adipocytes (21). Overall, these results showed that PIDF treatment significantly alleviated the weight of perinephric and epididymal fat induced by a high-fat diet.

3.4 The effect on organ indices of mice

The effects of PIDF on organ weight and organ index in mice were observed in Figures 1I–N. After 8 weeks of high-fat diet feeding, the weight of the liver (1.0403 g ± 0.00986 g, $p < 0.01$), kidney (0.3875 g ± 0.0293 g, $p < 0.001$), and spleen (0.0925 g ± 0.0216 g, $p < 0.05$) in the HC group was the heaviest, which was significantly higher than that in the NC group (0.88763 g ± 0.0179 g, 0.2853 g ± 0.0104 g, 0.0525 g ± 0.0033 g, respectively). After the addition of PIDF, the organ weight of high-fat diet mice in the LIDF and HIDF groups was significantly reduced, especially the weight of the liver (0.9108 g ± 0.0285 g, 0.9120 g ± 0.098 g, respectively, $p < 0.05$, Figure 1I) and kidney (0.2960 g ± 0.111 g, 0.3082 g ± 0.0147 g, respectively, $p < 0.001$, Figure 1J) was markedly lower than that in the HC group. In addition, spleen weight was also lower in the PIDF dietary intervention groups compared to the HC group, although the difference was not significant ($p > 0.05$) (Figure 2K). The more fat it contains, the more its function is affected. As shown in Figures 1L–N, the kidney index in the LIDF group (1.1437% ± 0.0432%) was significantly decreased compared with the HC group (1.2942% ± 0.0976%, $p < 0.05$). However, there were no significant differences in liver and spleen indexes between the LIDF group and the HIDF group ($p > 0.05$).

3.5 The effect on the blood lipid level of mice

To investigate the alleviating effect of PIDF on hyperlipidemia in mice, the serum lipid indexes of mice were measured, and the results are shown in Figures 2A–G. It could be seen from the second column set, the level of TC (4.88 mmol/L ± 0.30 mmol/L, Figure 2A) and TG (1.35 mmol/L ± 0.22 mmol/L, Figure 2B), LDL-C (0.92 mmol/L ± 0.14 mmol/L, Figure 2D), AST (129.24 U/L ± 34.93 U/L, Figure 2F), and GLU-YA (10.07 mmol/L ± 1.30 mmol/L, Figure 2G) in the HC group mice significantly increased by 41.78% ($p < 0.001$), 25.44% ($p < 0.05$), 32.18% ($p < 0.05$), 44.54% ($p < 0.05$), and 43.49% ($p < 0.05$), respectively, and HDL-C decreased by 8.78% (3.59 mmol/L ± 0.49 mmol/L, Figure 2C) compared with the NC group, which indicated that the long-term feeding of high-fat diet resulted in dyslipidemia in mice (10, 22). Compared with the HC group, the contents of TC (4.05 mmol/L ± 0.46 mmol/L and 4.02 mmol/L ± 0.52 mmol/L, respectively, Figure 2A) and AST (92.61 U/L ± 22.3 U/L, 91.01 U/L ± 13.18 U/L, respectively, Figure 2F) in the mice's serum of the LIDF and HIDF groups were significantly ameliorated ($p < 0.01$), and the content levels were similar to those in the NC group ($p > 0.05$). At the same time, there was no significant difference in the ALT content in the blood of mice in the NC, HC, LIDF, and HIDF groups ($p > 0.05$).

However, when high doses of PIDF were given (HIDF group), the TG, LDL-C, and GUL-YA levels in the serum of the mice were significantly lower than those in the HC group, with content of (1.08 ± 0.13) mmol/L, (0.68 ± 0.22) mmol/L, and (6.87 ± 1.80) mmol/L, respectively ($p < 0.05$). The findings of this study are consistent with those reported in previous research by Isken et al. (23) and Fang et al. (24). In addition, when supplementing a low dose of PIDF, there was no significant effect on these three serum biochemical indexes between the LIDF group and the HC mice ($p > 0.05$). It is worth mentioning that compared with the HC group, PIDF supplementation significantly increased the serum HDL-C content in the LIDF and HIDF groups by 35.08% ($p < 0.01$) and 21.30% ($p < 0.05$), respectively (Figure 2C). HDL-C is considered the "good" cholesterol because of its ability to transport cholesterol from peripheral tissues back to the liver for metabolism, helping to reduce the risk of cardiovascular disease (25, 26). These results indicated that a specific dose of PIDF can significantly reduce the serum TC, TG, and LDL-C levels and increase HDL-C level in hyperlipidemia animal models, which improves blood lipid health.

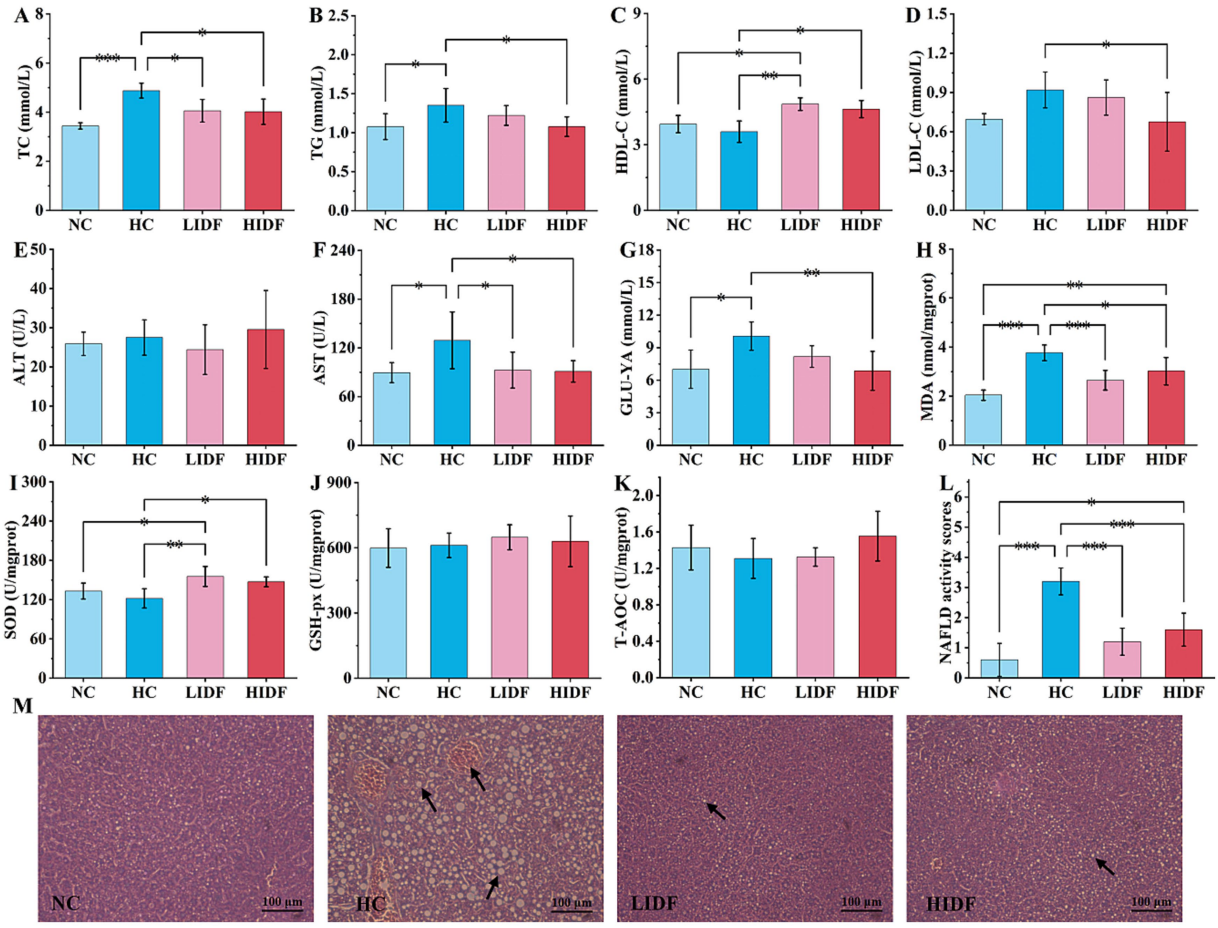

FIGURE 2
Effects of PIDF on blood lipid levels and activity of antioxidant enzymes in high-fat diet mice. **(A)** TC; **(B)** TG; **(C)** HDL-C; **(D)** LDL-C; **(E)** ALT; **(F)** AST; **(G)** GLU-YA; **(H)** MDA; **(I)** SOD; **(J)** GSH-Px; **(K)** T-AOC; **(L)** NAFLD activity score of the livers. **(M)** H&E staining of the liver (The arrows in images indicate hepatocyte fatty degeneration). Data presented as mean SEM, $n = 6$, * $p < 0.05$, ** $p < 0.01$, *** $p < 0.001$.

3.6 Activity of antioxidant enzymes in the liver of mice

The detected indicators of oxidative stress are described in Figures 2H–K. The content of MDA in the NC group was the lowest (2.03 nmol/mgprot ± 0.20 nmol/mgprot, $p < 0.001$), indicating that a regular diet would not cause abnormal liver metabolism (Figure 2H) (27). As shown in Figure 2H, MDA content in the HC group mice (3.76 nmol/mgprot ± 0.32 nmol/mgprot) was significantly higher than in the other three groups, indicating that a high-fat diet caused certain liver damage. After the PIDF diet intervention, MDA levels decreased in both the high-dose group (2.68 nmol/mgprot ± 0.40 nmol/mgprot, $p < 0.01$) and the low-dose group (3.02 nmol/mgprot ± 0.56 nmol/mgprot, $p < 0.001$), with proportions of 19.80 and 29.68%, respectively. The results showed that PIDF had a protective effect on the liver, preventing liver damage caused by a high-fat diet. As expected, the high-fat diet reduced SOD activity (121.83 U/mgprot ± 14.72 U/mgprot) in the mice's liver compared to the NC group (133.06 U/mgprot ± 12.07 U/mgprot), resulting in oxidative stress. The SOD activity in LIDF and HIDF groups was increased by 27.51% (155.35 U/mgprot ± 15.25 U/mgprot, $p < 0.01$) and 20.81% (147.18 U/mgprot ± 7.51 U/mgprot, $p < 0.05$), respectively (Figure 2I). The results showed that the PIDF dietary intervention could effectively improve the oxidative stress caused by a high-fat diet. Simultaneously, there was no detectable increase in GSH-Px and T-AOC activity in the LIDF and HIDF groups (Figures 2J,K, $p > 0.05$). The results suggest that PIDF intervention may help alleviate liver disease caused by a high-fat diet.

The liver is a vital organ in the human body, and a prolonged high-fat diet can lead to excessive fat accumulation in the liver, ultimately causing liver damage. Therefore, to demonstrate that the PIDF diet can improve this phenomenon, the livers of four groups of mice were sliced and stained with H&E to observe the accumulation of fat in the liver more clearly (Figure 2M). The results showed that the liver cells of mice on a standard diet had normal morphology, clear boundaries, and a neat arrangement, with no fat accumulation observed (17). However, hepatocytes in the HC group were severely damaged, mainly due to the accumulation of a large number of fat particles within hepatocytes, which crowded out the nucleus to the edge, with the possibility of lipopathy (28). This indicated that a high-fat diet can seriously damage the liver, resulting in a considerable accumulation of fat in the liver and affecting liver function. On the contrary, the form of liver cells in the PIDF supplementation mice was as expected. Additionally, the fat accumulation in the livers of mice in the LIDF and HIDF groups was reduced, which slowed the damage to

liver cells caused by a high-fat diet (29). Furthermore, the NAFLD activity score of the livers in the four groups was assessed (Figure 2L). The results indicated that the NAFLD activity score of the liver in the HC group was 3.2 ± 0.45, and extremely significantly higher than that of the other three groups ($p < 0.001$). Hence, the livers of mice in the HC group were identified as NAFLD. At the same time, the NAFLD activity scores of the livers of mice in the NC, LIDF, and HIDF groups were less than 2, which could exclude the possibility of NAFLD (30). In conclusion, these findings demonstrated that PIDF supplementation successfully ameliorated lipid metabolic disorders in mouse livers caused by long-term high-calorie diets.

3.7 The effects on the gut microbiota of mice

In this study, the regulatory effect of PIDF on intestinal microbes was investigated. Firstly, the Alpha diversity index of mouse gut microbiota was analyzed, and the results are shown in Table 1. The results showed that the Chao1, Shannon, and Simpson indices of the HIDF and LIDF groups were increased with dietary fiber intake. These results suggested that IDF could increase the richness and diversity of gut microbiota. On this basis, a Venn diagram based on operational taxon (OTUs) was used to analyze the similarity of gut microbiota among different groups. According to the Venn diagram of the four groups of mice (Figure 3A), 348, 686, 666, and 693 OTUs were detected in the NC, HC, LIDF, and HIDF groups, respectively. The four unique sections were 167, 158, 112, and 130 OTUs, respectively. The OTUs shared by the HC, LIDF, and HIDF groups with the NC group were 152, 146, and 146, respectively. The OTUs shared by the LIDF and HIDF groups with the HC group were 378 and 469, respectively. These results suggest that PIDF may play a role in regulating the intestinal microbial structure of mice on a high-fat diet (17). The dilution curve and species accumulation curve for each group of samples are shown in Figure 3B. At the initial sequencing stage, the curve exhibited a rapidly rising trend, and as the sequencing quantity increased, the curve for each group gradually leveled off. After further increasing the sequencing volume, only a few new OTUs were produced, indicating that the sequencing has reached saturation. These results suggest that the amount of sequencing data has fully covered the microbial diversity in the samples.

Additionally, β diversity analysis revealed the differences between the gut microbial communities of various mouse groups (31). Then, principal coordinate analysis (PCoA) was used to investigate the overall differences in the composition of intestinal bacteria in the four groups. Figure 3C showed that the four groups of microbial communities were distributed in different regions, and each group formed relatively close clusters. In particular, the clusters of the LIDF and HIDF groups with PIDF intervention were significantly different from those of the HC group. The results showed that a dietary increase in PIDF altered the intestinal microbial composition of mice fed a high-fat diet. The results were consistent with the report by Liu et al. (32).

Further, we determined the composition of gut microbes in four groups of mice at the phylum, family, and genus levels to explore the effects of PIDF on microbial species and their relative abundance. The differences in gut microbiome composition at the phylum level among the four groups of mice are illustrated in Figure 3D. For the NC group, the dominant phyla are *p_Pseudomonadota*, *p_Bacillota*, *p_Bacteroidota*, and *p_Verrucomicrobiota*. At the same time, *Bacillota* and *Bacteroidota* are the dominant phyla in the other three groups. Figures 4A–D illustrates the changes in the relative abundance of specific bacteria. Compared with the NC group, the relative abundances of *p_Bacillota* ($p < 0.001$) and *p_Bacteroidota* ($p < 0.01$) in the HC group were significantly increased, resulting in a significant increase in the ratio of *Bacillota* to *Bacteroidota* (1.89 ± 0.11). In addition, the relative abundance of *p_Verrucomicrobiota* was significantly decreased in the HC group ($p < 0.001$). Multiple studies have shown that metabolic syndrome is associated with an increased ratio of *Bacillota* to *Bacteroidota* (31). This also suggested that the mice in the HC group had abnormal lipid metabolism. As can be seen in Figure 4A, PIDF intervention resulted in a considerable reduction in the abundance of *p_Bacillota*, from 58.65% ± 1.31% (HC group) to 46.59% ± 3.07% in the LIDF group ($p < 0.05$) and 43.27% ± 3.81% in the HIDF group ($p < 0.01$). On the contrary, compared to the HC group (30.93 ± 1.17%), the abundance of *p_Bacteroidota* exhibited a significant increase in the LIDF (41.83 ± 3.26%, $p < 0.01$) and HIDF (46.92 ± 2.75%, $p < 0.001$) groups. As a result (Figure 4C), the *Bacillota* to *Bacteroidota* ratio of the LIDF (1.12 ± 0.15) and HIDF (0.92 ± 0.11) groups was significantly decreased, which is similar to levels in NC mice (0.67 ± 0.53) ($p > 0.05$). These results suggest that PIDF can regulate gut microbiome and metabolic function and improve hyperlipidemia induced by a high-fat diet in mice. The study results of Yang et al. (33) showed that flaxseed polysaccharide also regulates the composition of intestinal microbes in high-fat diet mice by reducing the *Bacillota* to *Bacteroidota* ratio, thereby exerting an effect on decreasing serum lipids. In addition, as shown in Figure 4D, PIDF supplementation successfully increased the relative abundance of *p_Verrucomicrobiota* from 0.03% in the HC group to 6.05% ± 1.94% in the LIDF group and 6.18% ± 3.53% in the HIDF group.

At the family level (Figure 3E), compared with the NC group, high-fat diet feeding increased the relative abundance of these two types of harmful bacteria (*f_Erysipelotrichaceae* and *f_Desulfovibrionaceae*) in the HC group ($p < 0.001$, Figures 4E,F). In contrast, this trend was significantly suppressed after the daily addition of the PIDF diet, especially in the high-dose group ($p < 0.001$, Figures 4E,F). As shown in Figure 4G, the relative abundance of

TABLE 1 Alpha diversity analysis.

Groups	Chao1	Pielou's	Shannon	Simpson
NC	175.2 ± 26.80***	0.50 ± 0.01***	3.65 ± 0.20***	0.83 ± 0.02***
HC	427.46 ± 25.09	0.75 ± 0.09	5.71 ± 1.40	0.91 ± 0.08
LIDF	493.29 ± 11.58*	0.80 ± 0.01	7.14 ± 0.06***	0.99 ± 0.00**
HIDF	501.59 ± 19.44**	0.80 ± 0.01	7.17 ± 0.12***	0.98 ± 0.00**

* Significant difference compared to the HC group. * $p < 0.05$; ** $p < 0.01$; and *** $p < 0.001$.

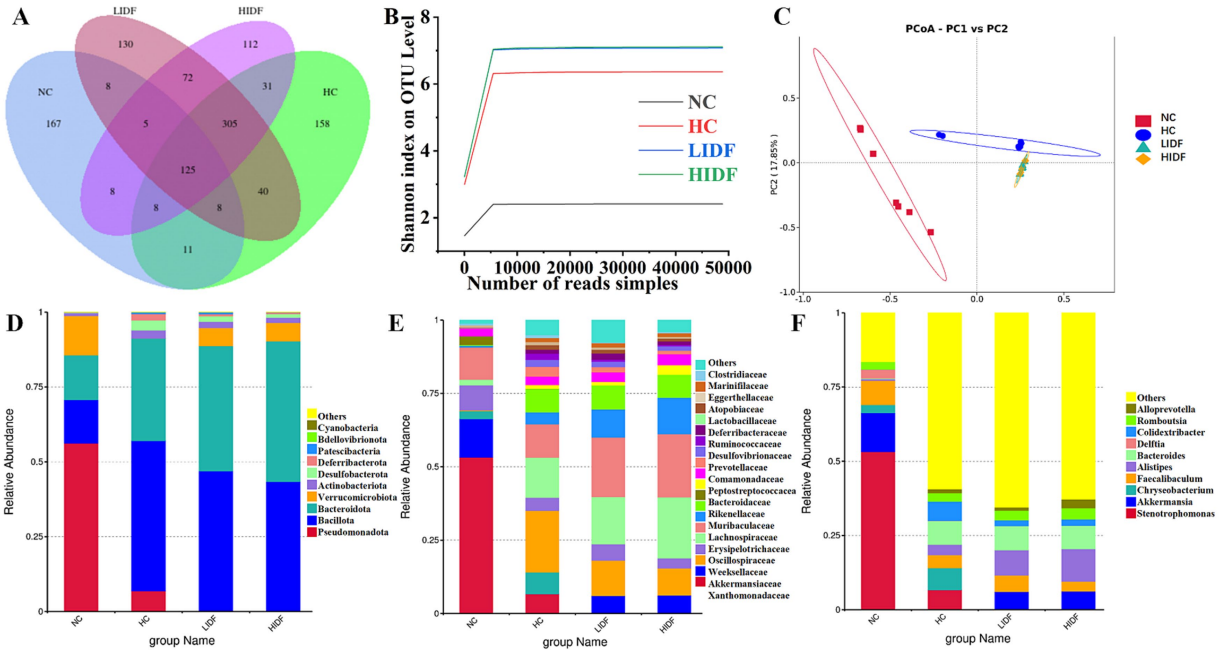

FIGURE 3
Effects of PIDF on gut microbiota in high-fat diet mice. **(A)** Venn diagram; **(B)** Dilution curve and species accumulation curve of each group; **(C)** PCoA; **(D)** Gut microbial composition at the phylum levels; **(E)** Gut microbial composition at the family levels; **(F)** Gut microbial composition at the genus levels.

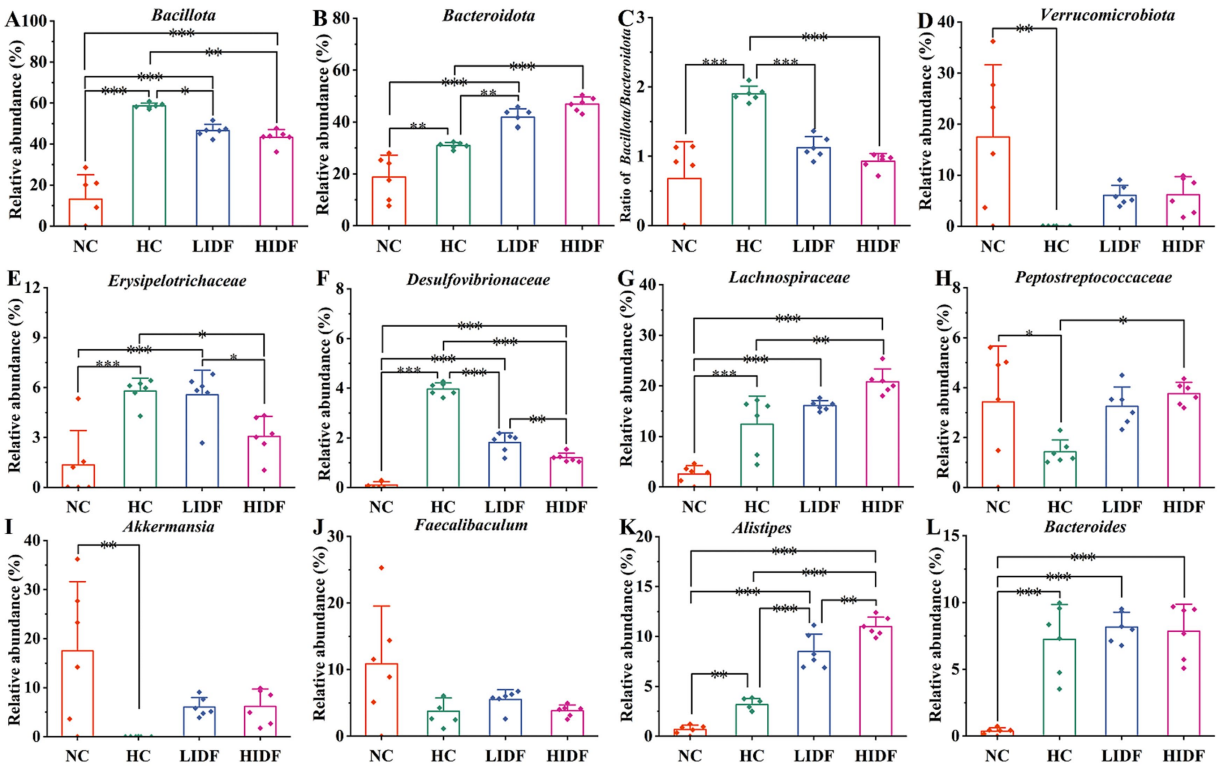

FIGURE 4
Relative abundances of **(A)** *Bacillota* and **(B)** *Bacteroidota*; **(C)** *Bacillota*/*Bacteroidota* ratio; **(D)** Relative abundances of *Verrucomicrobiota*; **(E)** *Erysipelotrichaceae*; **(F)** *Desulfovibrionaceae*; **(G)** *Lachnospiraceae*; **(H)** *Peptostreptococcaceae*; **(I)** *Akkermansia*; **(J)** *Faecalibaculum*; **(K)** *Alistipes*; **(L)** *Bacteroides*. Data presented as mean SEM, $n = 6$, * $p < 0.05$, ** $p < 0.01$, *** $p < 0.001$.

f_Lachnospiraceae in the HIDF and LIDF groups was higher than in the HC group. Studies have shown that low fermentable polysaccharides can increase the relative abundance of *f_Lachnospiraceae* in the gut (34). The growth of *f_Peptostreptococcaceae* in the intestines of high-fat diet mice was significantly inhibited, and the PIDF diet significantly increased the relative abundance of this bacteria, the level of which was similar to that of the NC group ($p > 0.05$, Figure 4H). This result agreed with the report by Yue et al. (35).

At the genus level (Figure 3F), compared with the NC group, the relative abundance of *g_Akkermansia* ($p < 0.01$) and *g_Faecalibaculum* in the HC group was decreased, and the relative abundances of *g_Bacteroides* ($p < 0.001$) and *g_Alistipes* ($p < 0.01$) were significantly increased (Figures 4I–L). After PIDF supplementation, the relative abundance of *g_Akkermansia* and *g_Faecalibaculum* was improved in both the LIDF and the HIDF groups, although this was insignificant. Meanwhile, the relative abundance of *g_Alistipes* in LIDF and HIDF groups significantly increased by 2.68 times and 3.46 times, respectively (Figure 4K). At the same time, feeding a high-fat diet increased the relative abundance of *g_Bacteroides* (Figure 4L).

Furthermore, linear discriminant analysis effect size (LEfSe) was used to analyze the typical bacterial groups with rich differences in the four groups of mice and to explore the influence of PIDF supplementation on the characteristic strains, and the results are shown in Figures 5A,B. The results showed that 52 bacterial taxa, whose abundance was significantly affected by the high-fat diet and PIDF intervention, were selected as OTUs. In the NC group, the dominant bacterial taxa are *c_Gammaproteobacteria*, *p_Pseudomonadota*, *f_Xanthomonadaceae*, *o_Xanthomonadales*, and *g_Stenotrophomonas*. The HC group was distinguished by *c_Clostridia*, *p_Bacillota*, *o_Oscillospirales*, and *f_Oscillospiraceae*. However, the LIDF group had a high abundance of *g_Bacteroides*, *f_Bacteroidaceae*, *g_Blautia*, and *s_Lachnospiraceae*. The similarity is that *o_Bacteroidales*, *c_Bacteroidia*, *p_Bacteroidota*, *o_Lachnospirales*, and *f_Lachnospiraceae* were more enriched in the HIDF group. This result was consistent with the findings of Zhao et al. (19), which reported that flaxseed cake dietary fiber ameliorates the harm of a high-fat diet mainly by restoring the gut microbiota composition.

Next, to explore the characteristics of the intestinal microbiome composition of mice in each group, correlation analysis was conducted between the top 10 bacterial taxa at the genus level and environmental factors. The results were visualized in the heat map (Figure 5C). The data showed that the relative abundance of *g_Colidextribacter*, *g_Chryseobacterium*, *g_Romboutsia*, and *g_Bacteroides* in the HC group increased due to a high-fat diet. In addition, the bacterial taxa of the LIDF and HIDF groups decreased to different degrees due to the treatment of PIDF. The functional prediction (PICRUSt) of the dominant gut microbiome was determined, and the functional composition of the intestinal microbiota at level 2 was shown in Figure 6. Compared with the HC group, the intervention of high-dose PIDF significantly changed 13 pathways, including 9 up-regulated

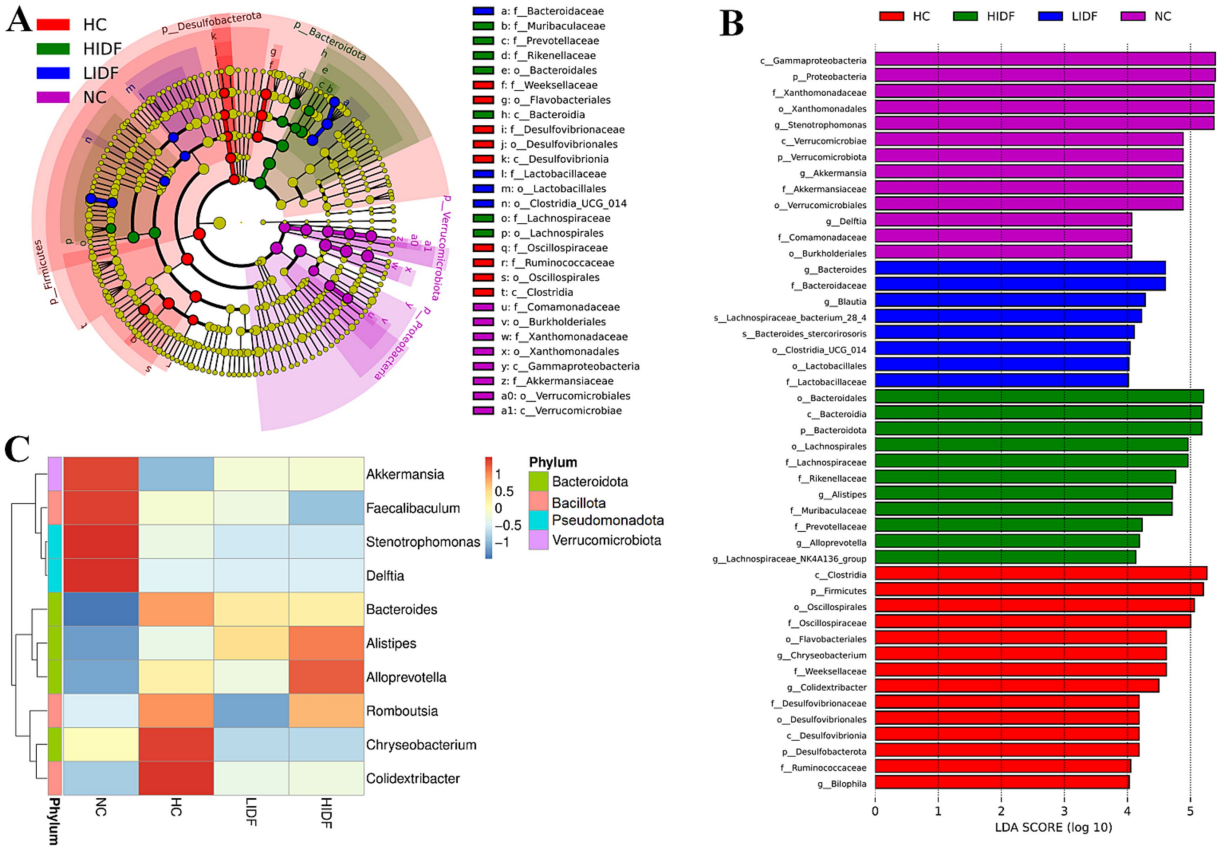

FIGURE 5
Regulation of PIDF on gut microbiota of high-fat diet mice. **(A)** LEfSe; **(B)** Linear discriminative analysis effect size analyses of statistically significant taxa; **(C)** Heat maps between the top 10 genera and physiological indexes.

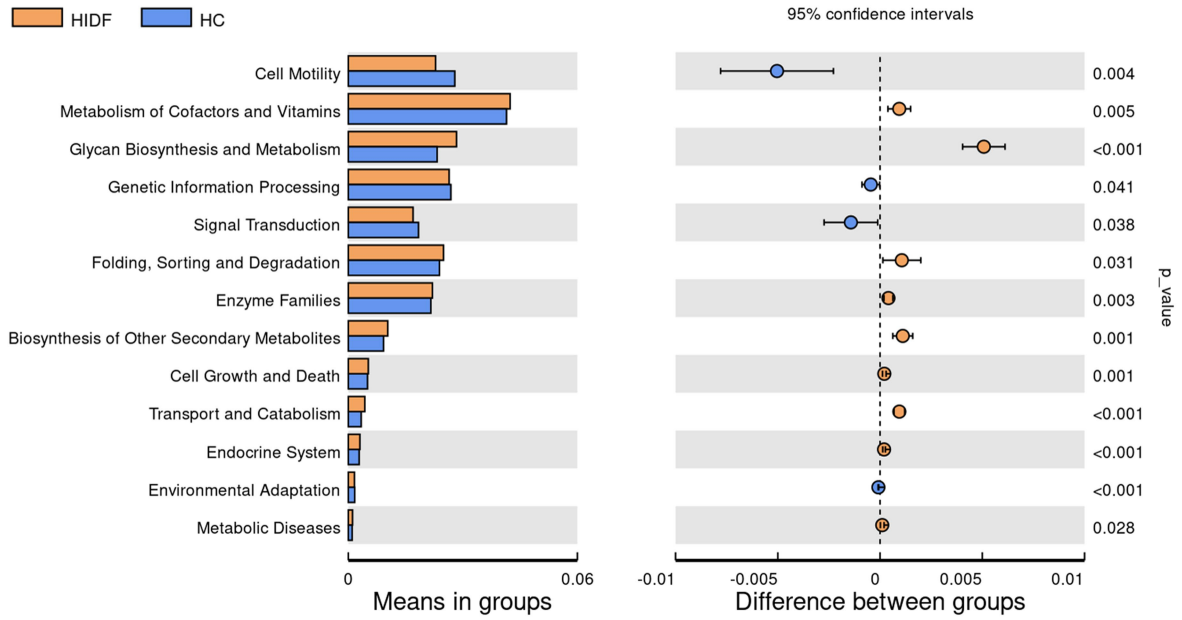

FIGURE 6
The functional prediction (PICRUSt) of the dominant gut microbiome.

pathways and 4 down-regulated pathways. The result indicated that high-dose PIDF supplementation significantly increased the abundance of Metabolism of Cofactors and Vitamins, Folding, Sorting and Degradation, Enzyme Families, Biosynthesis of Other Secondary Metabolites, Transport and Catabolism than that of the HC group, which is beneficial to lipid metabolism.

3.8 The effects on mouse caecum contents metabolic profiles

The cecum contents of mice were analyzed using non-targeted metabolomics by LC–MS/MS. The substances detected in the positive and negative ion scans were used for further analysis. PCA analysis was performed for the three groups (NC, HC, and HIDF), and the three groups were clustered separately, as depicted in Figure 7A. In the PLS-DA results, the HC and NC groups (Figure 7B) and the HIDF and HC groups (Figure 7C) were clearly separated, confirming the PCA findings. This showed that PIDF significantly altered the metabolites of high-fat-fed mice.

A total of 1,662 metabolites (including those detected by positive and negative ion scanning) were identified based on VIP values greater than 1.0 and *p*-values less than 0.05. The results of the volcano plot showed that 333 metabolites were up-regulated, and 204 metabolites were down-regulated by the high-fat diet (Figure 7D). In the meantime, after the PIDF diet intervention, compared with the HC group, 126 metabolites were up-regulated, and 142 metabolites were down-regulated (Figure 7E). Based on the differential expression of metabolites in the HIDF and HC groups, we performed pathway analysis using the Kyoto Encyclopedia of Genes and Genomes (KEGG) topology. As seen from Figure 8A, lipid acid (spiculisporic acid, FAHFA 16:0/18:2, and palmitic acid), and amino acid (L-aspartic acid,) metabolism are the most significantly affected pathways. Further, MetaboAnalyst revealed that the PIDF diet led to the enrichment of pyrimidine metabolism, purine metabolism, glycine, serine, and threonine metabolism, as well as glycerophospholipid metabolism, as highly enriched metabolic pathways (Figure 8B). Therefore, these pathways may be key sites for PIDF to demonstrate its efficacy in reducing blood lipids.

3.9 Correlation between gut microbiota and metabolites and hyperlipidemia

To verify the effect of IDF on regulating intestinal microorganisms, Spearman analysis was used to study the correlation between key bacterial genera in feces and differential metabolites in cecum contents, and the results are shown in Figure 8C. Figure 8C showed that *p_Bacteroidota* and *p_Verrucomicrobiota* showed a significant correlation with 5 altered metabolites (spiculisporic acid, L-ascorbate, FAHFA 16:0/18:2, L-aspartic acid, and palmitic acid). Fatty acids play an essential role in regulating energy metabolism. Especially, *g_Bacteroidota* showed a significant correlation with hyperlipidemia indexes (TC, TG, MDA, and AST). In addition, the relative abundances of *g_Desulfobacterota*, *g_Deferribacterota*, *g_Patescibacteria*, and *g_Cyanobacteria* were correlated with some metabolites and hyperlipidemia indexes. The results showed that PIDF dietary supplements could regulate the gut microbiota and may influence its metabolites. This might be the reason why PIDF can alleviate hyperlipidemia caused by a high-fat diet.

4 Discussion

Hyperlipidemia is a disease with too much lipid in the blood, which can be induced by a high-energy diet (36, 37). *Polygonatum*

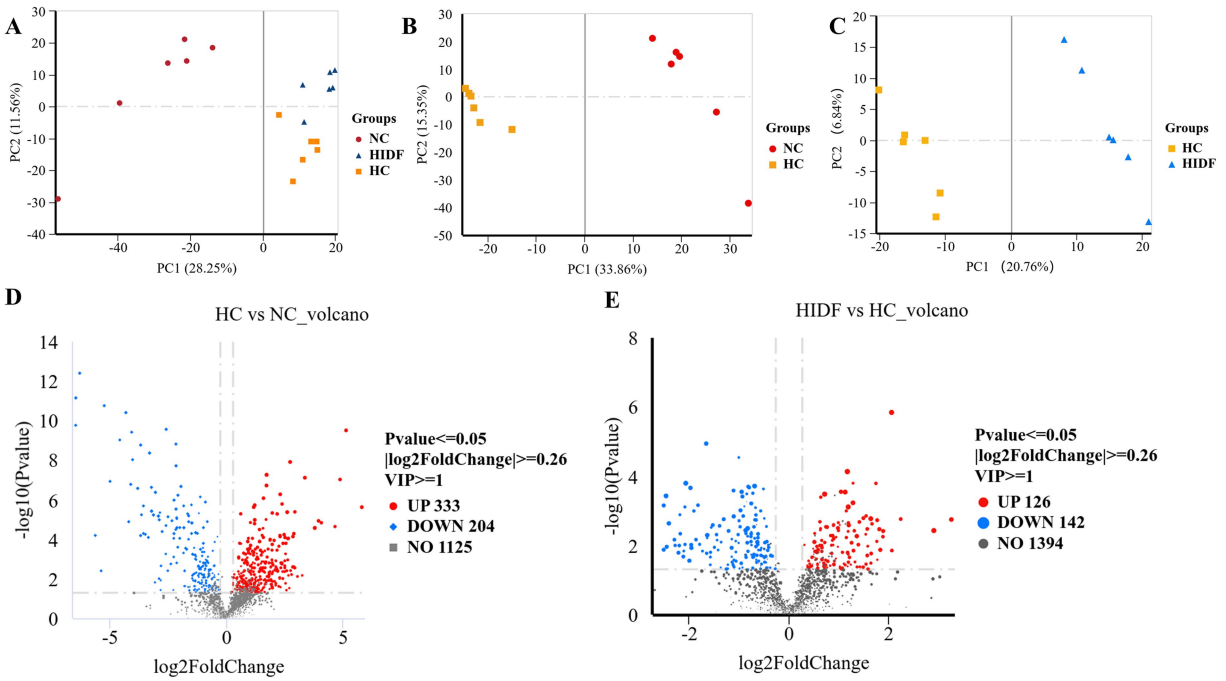

FIGURE 7
Effects of PIDF on metabolite profiles in high-fat diet mice. **(A)** PCA; **(B)** PLS-DA between HC and NC; **(C)** PLS-DA between HIDF and HC; **(D)** Volcano plot between HC and NC; **(E)** Volcano plot between HIDF and HC.

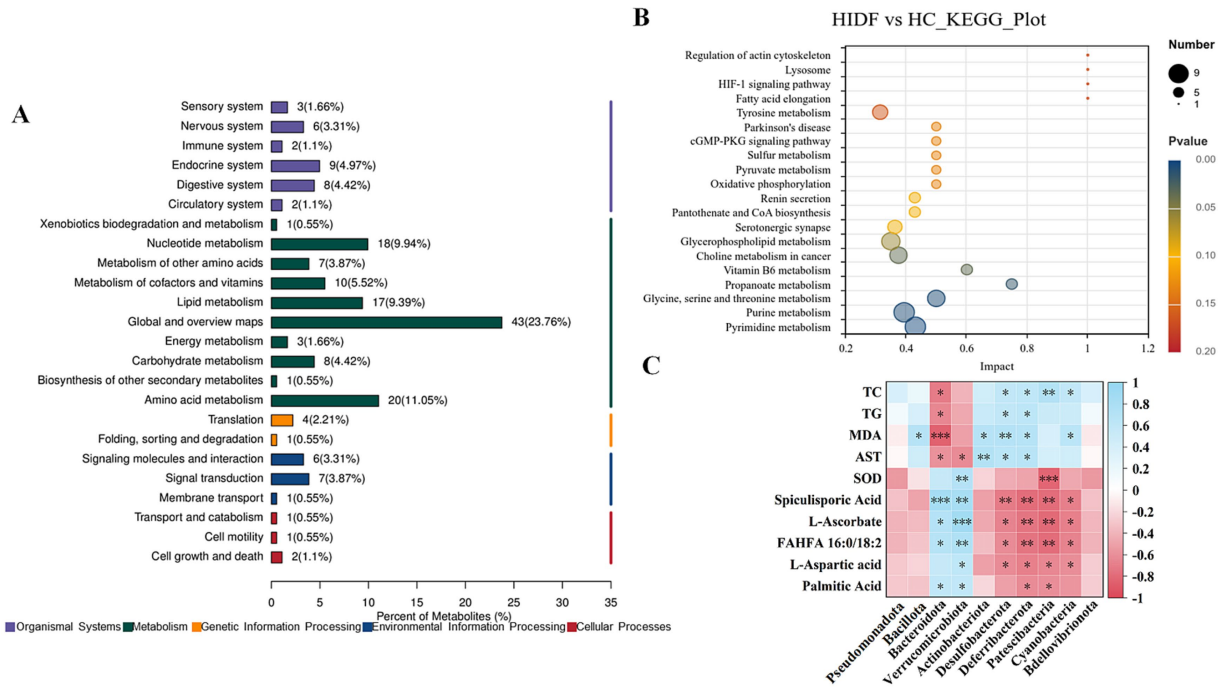

FIGURE 8
(A) KEGG topology; **(B)** KEGG pathway enrichment analysis; **(C)** Correlation between gut microbiota and its metabolites and hyperlipidemia.

sibiricum has excellent health benefits, such as hypoglycemic, hypolipidemic, regulating immunity, and so on (5). The activity study of the PIDF of *Polygonatum sibiricum* is not as extensive as those on polysaccharides and saponins. Hence, the high-fat diet-induced hyperlipidemia mouse model was used to research the anti-hyperlipidemic effect of PIDF (37). After 8 weeks of continuous PIDF supplementation, the dietary intake of mice in the low-dose and high-dose groups was significantly reduced. In our previous reports

(15), it was indicated that PIDF exhibits strong oil-holding and water-holding properties, which increase the volume of food in the stomach and enhance satiety. Therefore, the body weights of mice in the LIDF and HIDF groups were significantly lower than those in the HC group. These results suggest that weight gain may be partially attributable to reduced energy intake. The result agreed with the report of Wang et al. (9), which revealed that okara's IDF has an improving effect on hyperlipidemia in C57BL/6 J mice caused by a high-fat diet. In addition, the results of Chang et al. (38) showed that dietary supplementation with pear residue IDF slowed the weight gain caused by a high-fat diet, which agrees with this finding. In conclusion, the PIDF can alleviate excessive weight gain caused by sustained high energy intake.

As expected, PIDF supplementation significantly inhibited epididymal and perinephric fat weight in mice in the LIDF and HIDF. Consistent with the results of this study, Zhang et al. (39) reported that the IDF of soybean residue also showed a similar effect in alleviating fat accumulation in high-fat diet-fed mice. The same results reported by Chang et al. (38) indicated that in the high-fat diet group, adipocyte size decreased significantly after adding pear pomace's IDF. In the meantime, the organ weights of mice in the LIDF and HIDF groups were significantly lower than those in the HC group. In the research by Fang et al. (24), *Auricularia polytricha* noodles supplemented in high-fat diet mice diets could significantly reduce liver weight accumulation and mitigate the development of fatty liver caused by a high-fat diet. In conclusion, the dietary intervention of PIDF can reduce fat accumulation and thereby alleviate metabolic diseases caused by excessive fat.

Hyperlipidemia often manifests as abnormal cholesterol metabolism and high lipid levels (40). Therefore, this study investigated the effects of PIDF on biochemical indices in high-fat diet mice. The results show that the TC and AST levels of the mice in the LIDF and HIDF groups were significantly lower than those of the HC group. In particular, the level of AST in the LIDF and HIDF was nearly identical to that of the NC group. AST was a standard detection indicator that evaluated liver function and detected liver lesions or damage in time (41). Meanwhile, TG, LDL-C, and GLU-YA levels in the HIDF were lower than those in the HC. In addition, the TG level of HIDF (1.08 mmol/L) was lower than that of pear pomace IDF (1.31 mmol/L) (38). The TC (4.01 mmol/L) and LDL-C (0.68 mmol/L) levels of HIDF were lower than those of soybean IDF (5.11 and 1.30 mmol/L, respectively) (9). These can be illustrated that PIDF has certain advantages in improving hyperlipidemia. While HDL-C is considered the good cholesterol in the human body, its increase benefits the body; conversely, a reduction in HDL-C content also falls under the category of dyslipidemia (42). The PIDF intervention significantly increased HDL-C in mice. These results suggest that PIDF can regulate cholesterol metabolism by binding to cholesterol and lowering cholesterol absorption. Those results were consistent with the previous reports. The study of Wang et al. (9) indicated that soybean insoluble dietary fiber plays a role in antihyperlipidemic effect by reducing TG, TC, and LDL-C levels and improving HDL-C levels in high-fat diet animals. Similarly, Liu et al. (32) demonstrated that dietary fiber from Ougan residue improved obesity caused by HFD, which was associated with a reduction in TC and TG levels and an increase in HDL-C levels in mice. In conclusion, dietary intake of PIDF can effectively alleviate symptoms of hyperlipidemia.

Oxidative stress is an adverse effect of free radicals in the body and is an essential factor in aging and disease (43). In the LIDF and HIDF, PIDF protects the liver from damage by reducing MDA levels, increasing SOD activity, and inhibiting fat accumulation in the liver. Consistent with previous reports, the mechanism by which polysaccharides from *Pleurotus eryngii* lower blood lipids also reflects a reduction in fatty liver and oxidative stress in high-fat diet mice (27). Meanwhile, the research conducted by Zhang et al. (11) emphasizes that IDF from brown seaweed *Laminaria japonica* can improve the morphology of liver cells in high-fat diet mice and play a significant protective role in liver injury. The current research results show that both low-dose (0.5 g/kg·BW) and high-dose (1.0 g/kg·BW) intake of PIDF has a good effect on improving hyperlipidemia. The World Health Organization suggests that adults should consume at least 25 g of dietary fiber every day. Additionally, the American Heart Association recommends that women consume approximately 25 g and men about 38 g of dietary fiber daily. Hence, the research dosage has certain potential implications for human nutrition.

The IDF can proceed directly to the cecum for fermentation without undergoing digestion. It is generally recognized that the community structure of gut microbial colonies plays a crucial role in regulating lipids (24, 33, 35). The impact of PIDF on the gut microbiome significantly reduces the *Bacillota* to *Bacteroidota* ratio. *Bacillota and Bacteroidota* played an essential role in regulating the metabolism of carbohydrates, bile acids, and lipids in the host (44). *p_Bacillota* can absorb energy, intensify fat accumulation, and increase the risk of metabolic diseases such as obesity. *p_Bacteroidota* reduces cholesterol synthesis and is a kind of probiotic (45). It is reported that a high *Bacillota* to *Bacteroidota* ratio will promote high energy intake and cause metabolic diseases (10). It is worth noting that this finding is consistent with the study results showing lower food intake in the LIDF and HIDF groups of mice. Besides, the reduction in the *Bacillota* to *Bacteroidota* ratio in the PIDF-supplement groups may be closely related to the up-regulation of fatty acids, which are indispensable to the human body (18). Furthermore, the functional prediction results suggested that the microbial abundance related to Transport and Catabolism metabolism increased in the HIDF group. This might explain the reason why the TG, TC, GLU-A, and LDL-C levels were lower in the HIDF group.

In addition, the PIDF supplement significantly improves the abundance of beneficial bacteria in the gut, such as *p_Bacteroidota*, *f_Muribaculaceae*, *f_Lachnospiraceae*, *f_Peptostreptococcaceae*, *g_Akkermansia*, and *g_Alistipes*. *p_Bacteroidota* can ferment carbohydrates and biotransform bile acids and other steroids, producing nutrients and energy needed by the body, which mainly lowers blood lipids and maintains health. It is reported that the reason why *f_Lachnospiraceae* is considered a beneficial bacterium is mainly related to its participation in the production of fatty acids (20). The metabolic products of the cecum of mice contain a considerable amount of fatty acid substances (FAHFA 16:0/18:2 and palmitic acid), which might be related to the increase in the richness of the relative abundance of beneficial microbial colonies.

Moreover, *f_Peptostreptococcaceae* is another category of bacteria that helps curb obesity. The report confirms that the increased quantity of *g_Akkermansia* can improve intestinal barrier integrity and alleviate obesity symptoms (33). Additionally, according to the report by Zhang et al. (11), *g_Akkermansia* was the dominant strain in the high-dose brown seaweed *Laminaria japonica* IDF treatment group. Moreover, Tian et al. (46) studied the mechanism by which

barley leaf IDF improves intestinal inflammation in mice. They found that barley leaf IDF supplementation regulated the gut microbiome of mice by increasing the relative abundance of *g_Alistipes* by 5.2-fold, which was consistent with the results of this study. Moreover, short-chain fatty acids can regulate the immune response and inflammatory response of the body (47). On the one hand, *p_Bacteroidota* reduce cholesterol synthesis; *f_Lachnospiraceae*, *f_Peptostreptococcaceae*, and *g_Alistipes* could help reduce low-grade chronic inflammation in the body. On the other hand, *g_Akkermansia* could improve the integrity of the intestinal barrier. In conclusion, the beneficial bacteria play a synergistic role in the process of improving hyperlipidemia.

Meanwhile, the PIDF supplement significantly reduced the relative abundance of *f_Erysipelotrichaceae* and *f_Desulfovibrionaceae*, two types of bacteria closely associated with obesity and considered harmful (48, 49). Research indicates that *f_Desulfovibrionaceae* can increase the level of gut-derived lipopolysaccharides, which could cause damage to the integrity of the intestinal barrier, resulting in chronic inflammation and associated metabolic disorders (50). The results of Zhao et al. (19) showed that flaxseed dietary fiber also reduced the growth of these two types of harmful bacteria in the gut of mice on a high-fat diet. Hence, the intervention of PIDF can maintain the integrity of the intestinal barrier.

Furthermore, the results of functional prediction of the dominant gut microbiome indicated that relative abundance related to Metabolism of Cofactors and Vitamins was significantly increased ($p < 0.01$). Meanwhile, L-Ascorbate level in the metabolites of mice in the HIDF group was relatively higher and was proportional to the *p_Bacteroidota* and *p_Verrucomicrobiota*. In addition, in the HIDF group, Glycan Biosynthesis and Metabolism were extremely significantly up-regulated pathways ($p < 0.001$). Glycan metabolism may produce fatty acids, which may explain the increase in fatty acid substances (spiculisporic acid, FAHFA 16:0/18:2, and palmitic acid) in metabolites. In conclusion, the PIDF intervention treatment can regulate the microbial community structure of hyperlipidemic mice, improve intestinal barrier integrity caused by a high-fat diet, and thereby alleviate the symptoms of hyperlipidemia.

The results of the caecum contents metabolic profiles revealed that PIDF supplements improved the metabolism of lipids, amino acids, and glycerophospholipids, which alleviated the abnormal blood lipid metabolism caused by a high-fat diet. It has been reported that lipid metabolism is related to the PI3K/Akt signaling pathway. Once this signaling pathway is activated, it can promote the synthesis of fatty acids and the storage of triglycerides while inhibiting fat breakdown (51). In addition, Cho et al. (52) mentioned that enhanced glycerophospholipid metabolism can improve lipase activity and inhibit lipid metabolism abnormalities. Amino acid metabolism is closely related to glycolipid metabolism, which can affect the synthesis and decomposition of triglycerides by regulating the activity of enzymes (ACC and FAS) related to lipid metabolism and signaling pathways (such as mTORC1) (53, 54). Obesity and other metabolic diseases are affected by the amino acid metabolism, which will produce various metabolic products, such as SCFAs, branched-chain fatty acids, and other substances. Furthermore, amino acid metabolism can accelerate the tricarboxylic acid cycle, increasing energy consumption (55). In conclusion, the correlation analysis between gut microbiota and metabolites and hyperlipidemia indicated that PIDF supplementation increased the relative abundance of beneficial microorganisms and promoted the metabolism of lipids, amino acids, and glycerophospholipids.

5 Conclusion

The results of this study suggested that the improvement of lipid metabolism in mice induced by a high-fat diet with PIDF is associated with the regulation of the gut microbiota. The levels of TC, TG, and LDL-C in PIDF-supplemented mice were significantly reduced, while the levels of HDL-C were increased. Additionally, oxidative damage in the liver was alleviated, the *Bacillota* to *Bacteroidota* ratio of intestinal bacteria was decreased, and the abundance of beneficial bacteria was increased. In addition, the results of the correlation analysis showed that PIDF supplementation stimulated gut microbes, which may be the mechanism of action of PIDF in reducing blood lipids. However, the interaction between PIDF and gut microbes requires further study. In addition, the absence of dietary fiber from other sources is a limitation of this study. The results suggest that PIDF, as a low-fermentation dietary fiber, alleviates hyperlipidemia induced by a high-fat diet by reshaping the gut microbiota and regulating its metabolites. Therefore, these findings can provide a basis for applying PIDF in developing functional foods.

Data availability statement

The raw data supporting the conclusions of this article will be made available by the authors, without undue reservation.

Ethics statement

The animal study was approved by the ethics committee for experimental animals of Nanyang Institute of Technology reviewed all the animal experiments (Animal Experiment Ethics Review No. [2024]001). The study was conducted in accordance with the local legislation and institutional requirements.

Author contributions

YM: Resources, Data curation, Formal analysis, Funding acquisition, Writing – original draft. JK: Funding acquisition, Writing – review & editing, Formal analysis, Writing – original draft, Methodology, Data curation. YW: Writing – review & editing, Investigation. YZ: Conceptualization, Writing – review & editing. XG: Writing – review & editing, Conceptualization. XW: Writing – review & editing, Supervision. QS: Supervision, Writing – review & editing.

Funding

The author(s) declare that financial support was received for the research and/or publication of this article. This work was supported by the Henan Province Science and Technology research project (252102111046), the Natural Science Foundation Project of Henan Province (252300420708), the Young Backbone Teacher Training Program Project of Higher Learning of Henan Province (2020GGJS226), the Collaborative Innovation Major Project of Nanyang City (21XTCX12005), Interdisciplinary Sciences Project of Nanyang Institute of Technology (23NGJY011), and the Doctoral

Research Foundation Project of the Nanyang Institute of Technology (NGBJ-2022-04).

Conflict of interest

The authors declare that the research was conducted in the absence of any commercial or financial relationships that could be construed as a potential conflict of interest.

Generative AI statement

The authors declare that no Gen AI was used in the creation of this manuscript.

Publisher's note

All claims expressed in this article are solely those of the authors and do not necessarily represent those of their affiliated organizations, or those of the publisher, the editors and the reviewers. Any product that may be evaluated in this article, or claim that may be made by its manufacturer, is not guaranteed or endorsed by the publisher.

Supplementary material

The Supplementary material for this article can be found online at: https://www.frontiersin.org/articles/10.3389/fnut.2025.1601867/full#supplementary-material

References

1. Liu B-N, Liu X-T, Liang ZH, Wang JH. Gut microbiota in obesity. *World J Gastroenterol*. (2021) 27:3837–50. doi: 10.3748/wjg.v27.i25.3837

2. Wu H, Chen QY, Wang WZ, Chu S, Liu XX, Liu YJ, et al. Compound sophorae decoction enhances intestinal barrier function of dextran sodium sulfate induced colitis via regulating notch signaling pathway in mice. *Biomed Pharmacother*. (2021) 133:110937. doi: 10.1016/j.biopha.2020.110937

3. Huang R, Zhang J, Xu X, Sun M, Xu L, Kuang H, et al. The multiple benefits of bioactive polysaccharides: from the gut to overall health. *Trends Food Sci Tech*. (2024) 152:104677. doi: 10.1016/j.tifs.2024.104677

4. Chen T, Xie L, Shen M, Yu Q, Chen Y, Xie J. Recent advances in Astragalus polysaccharides: structural characterization, bioactivities and gut microbiota modulation effects. *Trends Food Sci Tech*. (2024) 153:104707. doi: 10.1016/j.tifs.2024.104707

5. Li XL, Ma RH, Zhang F, Ni ZJ, Thakur K, Wang S, et al. Nutrition. Evolu-tionary research trend of *Polygonatum* species: a comprehensive account of their transformation from traditional medicines to functional foods. *Crit Rev Food Sci*. (2021) 63:3803–20. doi: 10.1080/10408398.2021.1993783

6. Baky MH, Salah M, Ezzelarab N, Shao P, Elshahed MS, Farag MA. Insoluble dietary fibers: structure, metabolism, interactions with human microbiome, and role in gut homeostasis. *Crit Rev Food Sci*. (2022) 64:1954–68. doi: 10.1080/10408398.2022.2119931

7. Lamothe LM, Cantu-Jungles TM, Chen T, Green S, Naqib A, Srichuwong S, et al. Boosting the value of insoluble dietary fiber to increase gut fermentability through food processing. *Food Funct*. (2021) 12:10658–66. doi: 10.1039/D1FO02146J

8. Sun SS, Wang K, Ma K, Bao L, Liu HW. An insoluble polysaccharide from the sclerotium of *Poria cocos* improves hyperglycemia, hyperlipidemia and hepatic steatosis in Ob/Ob mice via modulation of gut microbiota. *Chin J Nat Med*. (2019) 17:3–0014. doi: 10.1016/S1875-5364(19)30003-2

9. Wang S, Sun W, Swallah MS, Amin K, Lyu B, Fan H, et al. Preparation and characterization of soybean insoluble dietary fiber and its prebiotic effect on dyslipidemia and hepatic steatosis in high fat-fed C57BL/6J mice. *Food Funct*. (2021) 12:8760–73. doi: 10.1039/d1fo01050f

10. Liu J, Hua J, Chen S, Zhao L, Wang Q, Zhou A. The potential mechanisms of bergamot-derived dietary fiber alleviating high-fat diet-induced hyperlipidemia and obesity in rats. *Food Funct*. (2022) 13:8228–42. doi: 10.1039/d2fo00747a

11. Zhang Y, Zhao N, Yang L, Hong Z, Cai B, Le Q, et al. Insoluble dietary fiber derived from brown seaweed *Laminaria japonica* ameliorate obesity-related features via modulating gut microbiota dysbiosis in high-fat diet–fed mice. *Food Funct*. (2021) 12:587–601. doi: 10.1039/d0fo02380a

12. You Y, Song H, Yan C, Ai C, Tong Y, Zhu B, et al. Dietary fibers obtained from *Caulerpa lentillifera* prevent high-fat diet-induced obesity in mice by regulating the gut microbiota and metabolite profiles. *Food Funct*. (2022) 13:11262–72. doi: 10.1039/d2fo01632j

13. Lan G, Chen H, Chen S, Tian J. Chemical composition and physicochemical properties of dietary fiber from Polygonatum odoratum as affected by different processing methods. *Food Res Int*. (2012) 49:406–10. doi: 10.1016/j.foodres.2012.07.047

14. Wang X, Ke J, Wang Y, Sun J, Liu H, Wan P, et al. Effects of extraction methods on structural and functional properties of water-insoluble dietary Fiber from *Polygonatum Sibiricum* residue. *Sci Tech Food Ind*. (2024) 45:187–95. doi: 10.13386/j.issn1002-0306.2024010181

15. Ke J, Wang X, Gao X, Zhou Y, Wei D, Ma Y, et al. Ball milling improves physicochemical, functionality, and emulsification characteristics of insoluble dietary Fiber from *Polygonatum sibiricum*. *Foods*. (2024) 13:2323. doi: 10.3390/foods13152323

16. Brunt EM, Kleiner DE, Wilson LA, Belt P, Neuschwander-Tetri BA, Network FC. Nonalcoholic fatty liver disease (NAFLD) activity score and the histopathologic diagnosis in NAFLD: distinct clinicopathologic meanings[J]. *Hepatology*. (2011) 53:810–20. doi: 10.1002/hep.24127

17. Tian Y, Li F, Du L, Peng D, Yang Z, Li J, et al. Fermented fruits ameliorate obesity by controlling food intake and regulating lipid metabolism in high-fat dietary mice. *J Funct Foods*. (2024) 114:106072. doi: 10.1016/j.jff.2024.106072

18. Cao S, Yang L, Xie M, Yu M, Shi T. Peanut-natto improved obesity of high-fat diet mice by regulating gut microbiota and lipid metabolism. *J Funct Foods*. (2024) 112:105956. doi: 10.1016/j.jff.2023.105956

19. Zhao M, Wang B, Li L, Zhao W. Anti-obesity effects of dietary fibers extracted from flaxseed cake in diet-induced obese mice. *Nutrients*. (2023) 15:1718. doi: 10.3390/nu15071718

20. Wang B, Yu H, He Y, Wen L, Gu J, Wang X, et al. Effect of soybean insoluble dietary fiber on prevention of obesity in high-fat diet fed mice via regulation of the gut microbiota. *Food Funct*. (2021) 12:7923–37. doi: 10.1039/D1FO00078K

21. Sun YS, Qu W. Dietary Apigenin promotes lipid catabolism, thermogenesis, and browning in adipose tissues of HFD-fed mice. *Food Chem Toxicol*. (2019) 133:110780. doi: 10.1016/j.fct.2019.110780

22. Li J, Shen SG, Han CF, Liu ST, Zhang LL, Chen N, et al. Nostoc flagelliforme capsular polysaccharides from different culture conditions improve hyperlipidemia and regulate intestinal flora in C57BL/6J mice to varying degrees. *Int J Biol Macromol*. (2022) 202:224–33. doi: 10.1016/j.ijbiomac.2022.01.034

23. Isken F, Klaus S, Osterhoff M, Pfeiffer AF, Weickert MO. Effects of long-term soluble vs. insoluble dietary fiber intake on high-fat diet-induced obesity in C57BL/6J mice. *J Nutr Biochem*. (2010) 21:278–84. doi: 10.1016/j.jnutbio.2008.12.012

24. Fang D, Wang D, Ma G, Ji Y, Zheng H, Chen H, et al. *Auricularia polytricha* noodles prevent hyperlipemia and modulate gut microbiota in high-fat diet fed mice. *Food Sci Hum Well*. (2021) 10:431–41. doi: 10.1016/j.fshw.2021.04.005

25. Ou X, Chen J, Li B, Yang Y, Liu X, Xu Z, et al. Multiomics reveals the ameliorating effect and underlying mechanism of aqueous extracts of *polygonatum sibiricum* rhizome on obesity and liver fat accumulation in high-fat diet-fed mice. *Phytomedicine*. (2024) 132:155843. doi: 10.1016/j.phymed.2024.155843

26. Ge Y, Qiu H, Zheng J. Physicochemical characteristics and anti-hyperlipidemic effect of polysaccharide from BaChu mushroom (*Helvella leucopus*). *Food Chem X*. (2022) 15:100443. doi: 10.1016/j.fochx.2022.100443

27. Xu N, Ren Z, Zhang J, Song X, Gao Z, Jing H, et al. Antioxidant and anti-hyperlipidemic effects of mycelia zinc polysaccharides by *Pleurotus eryngii* var. tuoliensis. *Int J Biol Macromol*. (2017) 95:204–14. doi: 10.1016/j.ijbiomac.2016.11.060

28. Sun B, Huang Z, Xiao Y, Zhang F, Pan L, Yu L, et al. β-Glucan from *Lyophyllum decastes* regulates gut microbiota and plasma metabolites in high-fat diet-induced obese mice. *J Funct Foods*. (2024) 116:106166. doi: 10.1016/j.jff.2024.106166

29. Wu Y, Zhang Y, Huang S, Xie W, Huang G, Zou Y, et al. Anti-obesity effects of the high molecular weight *Cordyceps militaris* polysaccharide CMP40 in high-fat diet mice. *Food Biosci*. (2024) 60:104467. doi: 10.1016/j.fbio.2024.104467

30. Stefan N, Häring HU, Cusi K. Non-alcoholic fatty liver disease: causes, diagnosis, cardiometabolic consequences, and treatment strategies. *Lancet Diabetes Endo*. (2019) 7:313–24. doi: 10.1016/s2213-8587(18)30154-2

31. Du L, Lü H, Chen Y, Yu X, Jian T, Zhao H, et al. Blueberry and blackberry Anthocyanins ameliorate metabolic syndrome by modulating gut microbiota and short-chain fatty acids metabolism in high-fat diet-fed C57BL/6J mice. *J Agric Food Chem*. (2023) 71:14649–65. doi: 10.1021/acs.jafc.3c04606

32. Liu X, Wang Y, Cao Y, Zhou H, Xia Q, Lu S. Ougan (*Citrus suavissima* Hort. Ex Tanaka) pomace dietary fibers alleviate high fat diet-induced obesity in mice by regulating intestinal microbiota. *Food Biosci*. (2024) 62:104997. doi: 10.1016/j.fbio.2024.104997

33. Yang C, Xu Z, Deng Q, Huang Q, Wang X, Huang F. Beneficial effects of flaxseed polysaccharides on metabolic syndrome via gut microbiota in high-fat diet fed mice. *Food Res Int*. (2020) 131:108994. doi: 10.1016/j.foodres.2020.108994

34. Belcheva A, Irrazabal T, Robertson SJ, Streutker C, Maughan H, Rubino S, et al. Gut microbial metabolism drives transformation of MSH2-deficient colon epithelial cells. *Cell*. (2014) 158:288–99. doi: 10.1016/j.cell.2014.04.051

35. Yue SJ, Wang WX, Zhang L, Liu J, Feng WW, Gao H, et al. Anti-obesity and gut microbiota modulation effect of Astragalus polysaccharides combined with Berberine on high-fat diet-fed obese mice. *Chin J Integr Med*. (2021) 29:617–25. doi: 10.1007/s11655-021-3303-z

36. Cordain L, Eaton S, Sebastian A, Mann N, Lindeberg S, Watkins B, et al. Origins and evolution of the Western diet: health implications for the 21st century1, 2. *Am J Clin Nutr*. (2005) 81:341–54. doi: 10.1093/ajcn.81.2.341

37. Wang JH, Kim BS, Han K, Kim H. Ephedra-treated donor-derived gut microbiota transplantation ameliorates high fat diet-induced obesity in rats. *Int J Environ Res Public Health*. (2017) 14:555. doi: 10.3390/ijerph14060555

38. Chang S, Cui X, Guo M, Tian Y, Xu W, Huang K, et al. Insoluble dietary Fiber from pear pomace can prevent high-fat diet-induced obesity in rats mainly by improving the structure of the gut microbiota. *J Microbiol Biotechnol*. (2017) 27:856–67. doi: 10.4014/jmb.1610.10058

39. Zhang J, Wang S, Wang J, Liu W, Gong H, Zhang Z, et al. Insoluble dietary Fiber from soybean residue (Okara) exerts anti-obesity effects by promoting hepatic mitochondrial fatty acid oxidation. *Foods*. (2023) 12:2081. doi: 10.3390/foods12102081

40. Nie Y, Luo F, Wang L, Yang T, Shi L, Li X, et al. Anti-hyperlipidemic effect of rice bran polysaccharide and its potential mechanism in high-fat diet mice. *Food Funct*. (2017) 8:4028–41. doi: 10.1039/c7fo00654c

41. Xie Y, Pei F, Liu Y, Liu Z, Chen X, Xue D. Fecal fermentation and high-fat diet-induced obesity mouse model confirmed exopolysaccharide from *Weissella cibaria* PFY06 can ameliorate obesity by regulating the gut microbiota. *Carbohydr Polym*. (2023) 318:121122. doi: 10.1016/j.carbpol.2023.121122

42. Chen J, Mao D, Yong Y, Li J, Wei H, Lu L. Hepatoprotective and hypolipidemic effects of water-soluble polysaccharidic extract of *Pleurotus eryngii*. *Food Chem*. (2012) 130:687–94. doi: 10.1016/j.foodchem.2011.07.110

43. Peng M, Wang C, Gao Z, Fu F, Li G, Su D, et al. 'Daidai' physiological premature fruit drop relieves obesity in high-fat-diet-fed mice via modulating lipid metabolism and gut microbiota. *Food Biosci*. (2024) 61:104713. doi: 10.1016/j.fbio.2024.104713

44. Magne F, Gotteland M, Gauthier L, Zazueta A, Pesoa S, Navarrete P, et al. The Firmicutes/Bacteroidetes ratio: a relevant marker of gut Dysbiosis in obese patients? *Nutrients*. (2020) 12:1474. doi: 10.3390/nu12051474

45. Li R, Xue Z, Li S, Zhou J, Liu J, Zhang M, et al. Mulberry leaf polysaccharides ameliorate obesity through activation of brown adipose tissue and modulation of the gut microbiota in high-fat diet fed mice. *Food Funct*. (2022) 13:561–73. doi: 10.1039/D1FO02324A

46. Tian M, Li D, Ma C, Feng Y, Hu X, Chen F. Barley leaf insoluble dietary Fiber alleviated dextran sulfate sodium-induced mice colitis by modulating gut microbiota. *Nutrients*. (2021) 13:846. doi: 10.3390/nu13030846

47. Ney LM, Wipplinger M, Grossmann M, Engert N, Wegner VD, Mosig AS. Short chain fatty acids: key regulators of the local and systemic immune response in inflammatory diseases and infections. *Open Biol*. (2023) 13:230014. doi: 10.1098/rsob.230014

48. Zhu X, Zhang X, Gao X, Yi Y, Hou Y, Meng X, et al. Effects of inulin propionate ester on obesity-related metabolic syndrome and intestinal microbial homeostasis in diet-induced obese mice. *ACS Omega*. (2020) 5:12865–76. doi: 10.1021/acsomega.0c00649

49. Kaakoush NO. Insights into the role of Erysipelotrichaceae in the human host. *Front Cell Infect Microbiol*. (2015) 5:84. doi: 10.3389/fcimb.2015.00084

50. Zou T, Xie F, Liang P, Chen J, Wang Z, Du M, et al. Polysaccharide-rich fractions from *Enteromorpha prolifera* improve hepatic steatosis and gut barrier integrity in high-fat diet-induced obese mice linking to modulation of gut microbiota. *Biomed Pharmacother*. (2023) 157:114034. doi: 10.1016/j.biopha.2022.114034

51. Jiang C, Xie C, Li F, Zhang L, Nichols RG, Krausz KW, et al. Intestinal farnesoid X receptor signaling promotes nonalcoholic fatty liver disease. *J Clin Invest*. (2014) 125:386–402. doi: 10.1172/jci76738

52. Cho S, Song N, Choi JY, Shin A. Effect of citric acid cycle genetic variants and their interactions with obesity, physical activity and energy intake on the risk of colorectal Cancer: results from a nested case-control study in the UK biobank. *Cancer*. (2020) 12:2939. doi: 10.3390/cancers12102939

53. Jiao W, Sang Y, Wang X, Wang S. Metabonomics and the gut microbiome analysis of the effect of 6-shogaol on improving obesity. *Food Chem*. (2023) 404:134734. doi: 10.1016/j.foodchem.2022.134734

54. Zapata RC, Singh A, Pezeshki A, Chelikani PK. Tryptophan restriction partially recapitulates the age-dependent effects of total amino acid restriction on energy balance in diet-induced obese rats. *J Nutr Biochem*. (2018) 65:115–27. doi: 10.1016/j.jnutbio.2018.12.006

55. Ji J, Zhang S, Yuan M, Zhang M, Tang L, Wang P, et al. Fermented *Rosa Roxburghii* TrattJuice alleviates high-fat diet-nducedHyperlipidemia in rats by modulating gut microbiota and metabolites. *Front Pharmacol*. (2022) 13:883629. doi: 10.3389/fphar.2022.883629

Frontiers in Nutrition

Explores what and how we eat in the context of health, sustainability and 21st century food science

A multidisciplinary journal that integrates research on dietary behavior, agronomy and 21st century food science with a focus on human health.

Discover the latest Research Topics

See more →

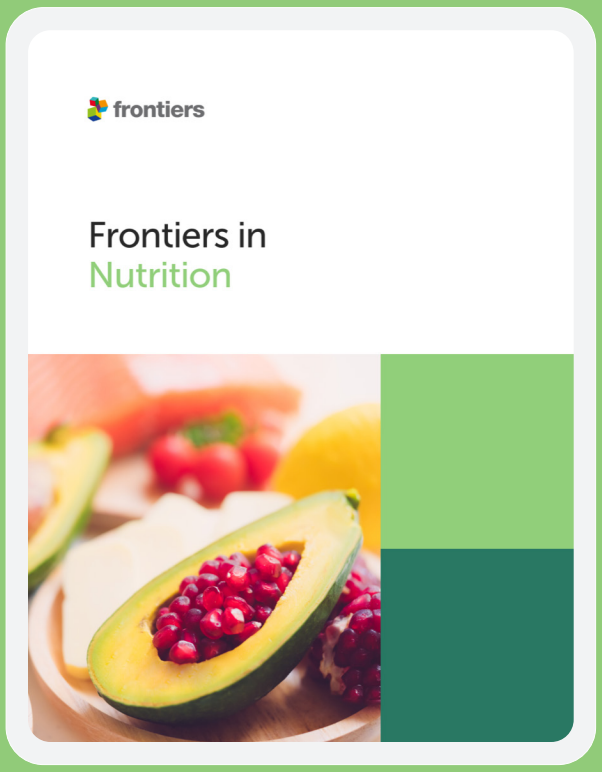

Frontiers

Avenue du Tribunal-Fédéral 34
1005 Lausanne, Switzerland
frontiersin.org

Contact us

+41 (0)21 510 17 00
frontiersin.org/about/contact